Design and Synthesis of Small-Molecule Inhibitors Targeting the SCF^{SKP2} E3 Ligase and the MDMX-p53 Interaction for Cancer Therapy

Andrew Eric Shouksmith

This thesis is submitted to Newcastle University for the degree of Doctor of Philosophy

September 2014

Declaration

The work described in this thesis was conducted between October, 2010 and September, 2014 in the Medicinal Chemistry Laboratories, Bedson Building, Northern Institute for Cancer Research, Newcastle University, Newcastle-upon-Tyne, UK, NE1 7RU and in the Cancer Structural Biology Laboratories, Paul O'Gorman Building, Northern Institute for Cancer Research, Newcastle University, Newcastle-upon-Tyne, UK, NE2 4HH.

All of the research described in this thesis is original and does not incorporate any material or concepts previously published or presented by other authors except where due reference is given in the text.

No part of this thesis has been previously submitted for a degree or other qualification at any other university or academic institution.

Acknowledgements

Heartfelt gratitude goes to my supervisors Prof. Roger Griffin, Prof. Bernard Golding, Dr Ian Hardcastle and Dr Céline Cano. Your guidance and knowledge have always been invaluable. It was a real pleasure to be your student and thank you for giving me the opportunity.

I also wish to thank the many great people I have had the chance to work with in chemistry as we strived for our PhDs together; Tristan Reuillon, Annalisa Bertoli, Nick Martin, Bian Zhang, Honorine Lebraud, Santosh Adhikari, James Pickles and Amy Heptinstall. Thanks also to the post doctorates I have had the joy to work with. As well as being great mentors, you have been awesome friends; Dr Sarah Cully, Dr Lauren Molyneux, Dr David Turner, Dr Steph Myers, Dr Chris Matheson, Dr Ruth Bawn, Dr Stephen Hobson, Dr Suzannah Harnor, Dr Claire Wilson, Dr Tom Gale, Dr Kate Smith, Dr Benoit Carbain and Dr Tim Blackburn. Special thanks go to Dr Duncan Miller; your knowledge, guidance and patience helped me not only to improve my practical chemistry expertise, but also to understand the principles of medicinal chemistry. You were always a great friend and an extremely talented supervisor and I wish you all the best for the future.

Massive thanks go to Dr Karen Haggerty and Carlo Bawn for your friendship over these four years. You kept our labs from descending into a barren wasteland with no chemicals or working machinery and I will always be grateful for that.

At the Paul O'Gorman (POG) Building, I want to first thank Prof. David 'Herbie' Newell for his infectiously boundless enthusiasm for drug discovery and for always being there for guidance and support throughout this PhD. I also want to thank the many talented people who have supervised the structural biology for their guidance on the progression of both the projects I have worked on; Prof. Martin Noble, Prof. Jane Endicott, Prof. John Lunec, Prof. Deborah Tweddle, Dr Elaine Willmore and Prof. Steve Wedge.

Although I worked in the POG for just two months, the people I worked with were some of the friendliest, wittiest and considerate people anyone could ever hope to share

a lab with. You made my time there unforgettable and I thank you all for that; Dr Judith Reeks, Dr Richard Heath, Dr Mathew Martin, Dr Julie Tucker, Dr Martyna Pastok, Svitlana Korolchuk, Dr Will Stanley, Bailey Massa, Stephen Hallett, Judith Unterlass, Dr Martin Day, Dr Regina Mora Vidal, Gesa Junge and Dr Sari Alhasan. Special thanks go to Dr Claire Jennings; you taught me the fundamental knowledge and skills of structural biology. Your patience with me was otherworldly, considering how little I knew when I started. You were an inspirational mentor and friend and I will miss working with you and learning from you. Good luck with everything you do.

Special acknowledgements also go to Laura Evans, Dr Yan Zhao and Dr Judith Reeks for running the biochemical assays for every compound I synthesised. I also want to acknowledge the crystallography master Dr Arnaud Basle; I know I was not the most naturally talented student in crystallography but you helped me to set up over 11,000 crystallisation conditions within one month and I thank you for that.

I wish to thank Cancer Research UK for providing the funding for my PhD and the EPSRC National Mass Spectrometry Service at the University of Wales (Swansea) for mass spectrometric determinations.

Finally, to those who have always been there for me: mum, dad, Mike, Vick, Merryn, Monty, Uncle Dave, Auntie Pam, Simon, Foz, Lewis and Jordan. Your belief in me, support, guidance and understanding enabled me to get as far in life as I have done.

To all those mentioned here, this thesis is dedicated to you.

Abstract

The SKP1-Cullin1-F-box (SCF) E3 ligases promote the ubiquitination and proteasome-mediated degradation of regulatory proteins. Subunits of the SCF complex have shown oncogenic activity, including the F-box protein S-phase Kinase-associated Protein 2 (SKP2). The SCF^{SKP2} E3 ligase targets several cell cycle negative regulators, e.g. p27, enabling replicative immortality. The only marketed drug that targets the ubiquitin-proteasome system is Bortezomib (*Velcade*; Millenium Pharmaceuticals) (**15**), which is used to treat multiple myeloma, but has numerous side effects, as the result of targeting a proteasome involved in the regulation of multiple proteins. Targeting an F-box protein is an attractive solution because the F-box protein defines E3 ligase selectivity and each E3 ligase regulates fewer proteins. To date, no small molecule targeting an F-box protein has entered clinical trials. A recently reported compound, (((3-(2,2-dimethyltetrahydro-2*H*-pyran-4-yl)-4-phenylbutyl)amino)methyl)-*N*,*N*-dimethylaniline (**16a**), has shown evidence to suggest it inhibits the SCF^{SKP2} ligase. The synthesis of **16a** (diastereoisomeric mixture) was completed at Newcastle University and growth inhibitory activity was confirmed in HeLa cells using a sulforhodamine B assay.

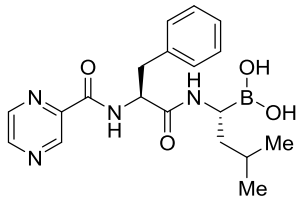

15

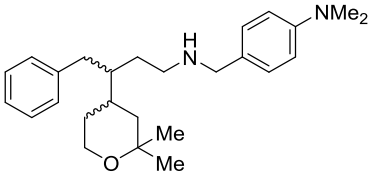

16a

Both enantiomers of *N*,*N*-dimethyl-4-(((4-phenyl-3-(tetrahydro-2*H*-pyran-4-yl)butyl)amino)methyl)aniline (**68a**) were synthesised, in one of the first documented enantioselective syntheses of a molecule of this chemotype, and demonstrated similar growth inhibitory activity in HeLa cells to each other and to the racemate, suggesting the compounds have a non-specific mechanism of action.

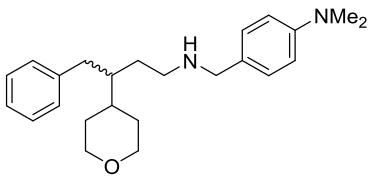

68a

ID	HeLa GI_{50} (µM)
68a	27 ± 4
(*S*)-68a	33 ± 4
(*R*)-68a	29 ± 2

Murine double minute 2 (MDM2) and its structurally related homologue MDMX (MDM4) negatively regulate the protein level and transcriptional activity of the tumour suppressor p53. Overexpression of MDM2 and MDMX has been observed in multiple human cancers and is associated with cell immortality.

Co-crystallisation of the p53-MDM2 and p53-MDMX complexes showed that three p53 residues (F19, W23 and L26) are critical to the formation of these dimers and small-molecule inhibitors function by competitively blocking the p53-binding sites on MDM2 or MDMX. Several small-molecule MDM2 inhibitors have entered clinical trials; however, no small-molecule MDMX inhibitor has reached the same stage. A recently discovered series of 2,4-disubstituted thiazoles have shown modest potency against MDM2 and MDMX. *In silico* modelling suggested the compounds interacted with the p53-binding domains in both proteins and extensive SAR studies around 4-(2-((4-fluorobenzyl)amino)thiazol-4-yl)benzene-1,2-diol (**59a**) were conducted. This series was extended to include benzenoid and pyrrole-based compounds, including 2'-(4-chlorophenoxy)-3'-((4-fluorophenyl)amino)-[1,1'-biphenyl]-4-ol (**138c**) and 2-(4-chlorobenzyl)-1-(4-chlorophenyl)-5-(4-fluorophenyl)-1*H*-pyrrole-3-carboxylic acid (**220c**). All three chemotypes demonstrated low micromolar activity against MDMX and MDM2 by ELISA.

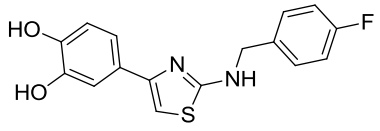

59a

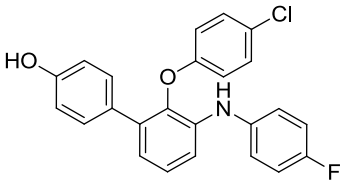

138c

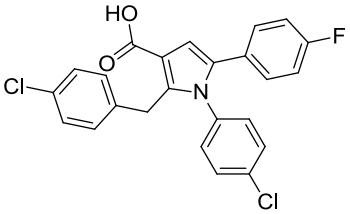

220c

ID	MDMX IC_{50} (µM)	MDM2 IC_{50} (µM)
59a	24.7	12.1
138c	19.0	23.2
220c	14.6	11.2

Current efforts are focussing on potentiating MDMX potency in each of the above chemotypes and trialling various co-crystallisation conditions so as to understand the molecules' binding mechanism and guide rational drug design.

Abbreviations

Table i: Amino acids

Full Name	3-Letter Code	1-Letter Code
Alanine	Ala	A
Arginine	Arg	R
Asparagine	Asn	N
Aspartic acid	Asp	D
Cysteine	Cys	C
Glutamine	Gln	Q
Glutamic acid	Glu	E
Glycine	Gly	G
Histidine	His	H
Isoleucine	Ile	I
Leucine	Leu	L
Lysine	Lys	K
Methionine	Met	M
Phenylalanine	Phe	F
Proline	Pro	P
Serine	Ser	S
Threonine	Thr	T
Tryptophan	Trp	W
Tyrosine	Tyr	Y
Valine	Val	V

Table ii: Elements and Groups

Element or Group	Definition
H	Hydrogen
C	Carbon
O	Oxygen
N	Nitrogen
P	Phosphorus
S	Sulfur
B	Boron

F	Fluorine
Cl	Chlorine
Br	Bromine
Al	Aluminium
Li	Lithium
Na	Sodium
K	Potassium
Mg	Magnesium
Si	Silicon
Ti	Titanium
Fe	Iron
Ni	Nickel
Cu	Copper
Zn	Zinc
Ru	Ruthenium
Ag	Silver
Pd	Palladium
Ce	Cerium
Mn	Manganese
Tb	Terbium
Me	Methyl (CH_3)
Et	Ethyl (CH_2CH_3)
Pr	*n*-Propyl ($CH_2CH_2CH_3$)
^{i}Pr	*iso*-Propyl ($CH(CH_3)_2$)
^{t}Bu	*tert*-Butyl ($C(CH_3)_3$)
Hex	*n*-Hexyl ($CH_2CH_2CH_2CH_2CH_2CH_3$)
Cy	Cyclo
Ph	Phenyl (C_6H_5)
Bn	Benzyl (CH_2Ph)
TMS	Trimethylsilyl ($Si(CH_3)_3$)
TIPS	Triisopropylsilyl ($Si(CH)_3(CH_3)_6$)
TBS	*tert*-Butyldimethylsilyl ($SiC(CH_3)_3(CH_3)_2$)
Ac	Acetyl
Alk	Alkyl

Ar	Aryl

Table iii: Units of Measurement

Symbol	Definition
h	Hour
min	Minute
s	Second
m	Metre
mm	Millimetre (10^{-3} m)
µm	Micrometre (10^{-6} m)
nm	Nanometre (10^{-9} m)
Å	Angstrom (10^{-10} m)
L	Litre
mL	Millilitre (10^{-3} L)
µL	Microlitre (10^{-6} L)
nL	Nanolitre (10^{-9} L)
Hz	Hertz
MHz	Megahertz (10^{3} Hz)
M	Molar (mol L^{-1})
mM	Millimolar (10^{-3} M)
µM	Micromolar (10^{-6} M)
nM	Nanomolar (10^{-9} M)
mP	Millipolarisation unit
^{o}C	Degrees Celsius
Bar	Bar
Atm	Atmosphere
K_i	Dissociation constant
g	Grams
mg	Milligrams (10^{-3} g)
Mol	Moles
Da	Daltons (g mol^{-1})
%	Percent

Table iv: Miscellaneous

A	AML	Acute Myeloid Leukaemia
	ATP	Adenosine triphosphate
	ABCG2	ATP-binding cassette subfamily G member 2
	ADME	Absorption, distribution, metabolism, excretion
	Akt	Protein kinase B
	AR	Androgen receptor
	ARF	Alternate reading frame
	aq	Aqueous
B	Bcl	B-cell lymphoma
	Bax	Bcl-2-associated X
	BRCA	BReast CAncer (gene or protein)
	B-TrCP	Beta-transducin repeat-containing protein
	BAD	Bcl-2-associated death
	BuLi	Butyllithium
	Boc_2O	Di-*tert*-butyldicarbonate
	$B_2(Pin)_2$	Bis(pinacolato)diboron
	Boc	*tert*-Butoxycarbonyl
	BSA	Bovine serum albumin
C	CAM	Cell-to-cell adhesion molecule
	CRC	Colorectal cancer
	CML	Chronic myelogenous leukaemia
	CTCL	Cutaneous T-cell lymphoma
	CCR5	C-C chemokine receptor type 5
	CAD	Computer-aided design
	Cul	Cullin
	Cks1	Cyclin kinase subunit 1
	CDK	Cyclin-dependent kinase
	CSC	Cancer stem cell
	CYP450	Cytochrome P450
	c	Calculated
	CSA	Camphor sulfonic acid
	COOT	Crystallographic Object-Oriented Toolkit

	CCP4	Collaborative Computational Project 4
	CO_2	Carbon dioxide
D	d	Doublet
	DNA	Deoxyribonucleic acid
	DHFR	Dihydrofolate reductase
	DCM	Dichloromethane
	DMF	*N*,*N*-Dimethylformamide
	DMSO	Dimethylsulfoxide
	DMAP	*N*,*N*-Dimethylaminopyridine
	DIPA	Diisopropylamine
	DIBAL-H	Diisobutylaluminium hydride
	DTP	Developmental therapeutics program
	DePPICT	Design of protein-protein interaction inhibitors for cancer therapy
	DMP	Dess-Martin periodinane
	de	Diastereoisomeric excess
	dr	Diastereoisomeric ratio
	DMC	Dimethylcarbonate
	dppf	1,1'-Bis(diphenylphosphino)ferrocene
	dtbpf	1,1'-Bis(di-*tert*-butylphosphino)ferrocene
	DoM	Directed-*ortho*-metallation
	DHP	Dihydropyran
	DSF	Differential scanning fluorimetry
	DTT	Dithiothreitol
	DAD	Diode array detector
E	EGFR	Epidermal growth factor receptor
	EtOAc	Ethyl acetate
	Et_2O	Diethyl ether
	EtOH	Ethanol
	EC	Effective concentration
	E_{max}	Maximum effective concentration
	ELISA	Enzyme-linked immunosorbent assay
	ee	Enantiomeric excess
	Equiv.	Equivalent

F	FDA	Food and Drugs Administration
	FBxW7	F-box/WD repeat-containing protein 7
	FP	Fluorescence polarisation
	FRET	Fluorescence resonance energy transfer
	FPLC	Flash performance liquid chromatography
	FTIR	Fourier transform infrared
G	GIST	Gastrointestinal stromal tumour
	G1/2	Growth phase 1 or 2 (cell cycle)
	GI	Growth inhibition
	GST	Glutathione S-transferase
H	HPV	Human papilloma virus
	HCC	Hepatocellular carcinoma
	HDAC	Histone deacetylase
	HTS	High-throughput screening
	h	Humanised
	HIV	Human immunodeficiency virus
	H-bond	Hydrogen bond
	HAUSP	Herpes virus-associated ubiquitin-specific protease
	HPLC	High performance liquid chromatography
	HTRF	Homogeneous time-resolved fluorescence
	HWE	Horner-Wadsworth-Emmons
	HMPA	Hexamethylphosphoramide
	HMDS	Hexamethyldisilazide
	HD	Halogen dance
	HEPES	2-[4-(2-hydroxyethyl)piperazin-1-yl]ethanesulfonic acid
	HRP	Horseradish peroxidase
	HRMS	High resolution mass spectrometry
I	IND	Investigational new drug
	IC	Inhibitory concentration
	IR	Infrared or ionising radiation
	IPTG	Isopropyl-β-D-thiogalactoside
	IV	Intravenous
L	LTT	Ligand-targeted therapy
	LD	Lethal dose

	LRR	Leucine-rich repeat
	LC-MS	Liquid chromatography mass spectrometry
	LDA	Lithium diisopropylamide
	LE	Ligand efficiency
	LipE	Lipophilic efficiency
	LB	Lysogeny broth
M	m	Multiplet
	MBC	Metastatic breast cancer
	MM	Multiple myeloma
	MTC	Medullary thyroid carcinoma
	MeOH	Methanol
	MeCN	Acetonitrile
	MDM2/X	Murine double minute 2/X
	mTOR	Mammalian target of rapamycin
	MoAB	Monoclonal antibody
	MEF	Mouse embryonic fibroblast
	Ms	Mesyl/methanesulfonyl
	MCL-1	Myeloid cell leukaemia 1
	MDR	Multidrug resistance
	MTS	3-(4,5-Dimethylthiazol-2-yl)-5-(3-carboxymethoxyphenyl)-2-(4-sulfophenyl)-2*H*-tetrazolium
	mRNA	Messenger ribonucleic acid
	*m*CPBA	*meta*-Chloroperbenzoic acid
	MW	Microwave
	m	*meta*
	mHBS	Modified HEPES buffer solution
	MWCO	Molecular weight cut-off
N	NSCLC	Non-small cell lung cancer
	NMR	Nuclear magnetic resonance
	NDA	New drug application
	NAE	Need8 activating enzyme
	NF	Nuclear factor
	NCI	National Cancer Institute
	NIH	National Institute of Health

	ND	Not determined
	NA	Not active
	NBS	*N*-bromosuccinimide
	NoLS	Nuclear localisation signal
	NICR	Northern Institute for Cancer Research
O	*o*	*Ortho*
	o/n	Overnight
P	p	Protein/phosphorylated
	p	*Para*
	P	Partition coefficient
	PDGF	Platelet-derived growth factor
	PPI	Protein-protein interaction
	PI3K	Phosphatidylinositol-3-kinase
	PTEN	Phosphatase and tensin homologue
	PDB	Protein Data Bank
	*p*TSA	*para*-Toluenesulfonic acid
	PBS	Phosphate-buffered saline
	PMA	Phosphomolybdic acid
	PMB	*para*-Methoxybenzyl
	pRB	Retinoblastoma protein
Q	qPCR	Quantitative polymerase chain reaction
R	RNA	Ribonucleic acid
	RGD	Arginine-glycine-aspartate
	RING	Really interesting new gene
	RoC	Regulator of Cullins
	RBX	RING-box protein
	RT	Room temperature
	Rac or ±	Racemic
	RLU	Relative luminescence units
	RPM	Revolutions per minute
	RCF	Relative centrifugal force
S	s	Singlet
	SKP	S-phase kinase-associated protein
	SCF	SKP1-cullin-F-box

	SAR	Structure-activity relationship
	STAT3	Signal transducer and activator of transcription 3
	SRB	Sulforhodamine B
	S_NAr	Nucleophilic aromatic substitution
	SDS-PAGE	Sodium dodecylsulfate polyacrylamide gel electrophoresis
	SOB	Super-optimal broth
T	TK	Tyrosine kinase
	THF	Tetrahydrofuran
	THP	Tetrahydropyran
	TFE	2,2,2-Trifluoroethanol
	tPSA	Topological polar surface area
	Tf	Trifluoromethanesulfonyl
	TAD	Transactivation domain
	TR	Time-resolved
	TFA	Trifluoroacetic acid
	TCA	Trichloroacetic acid
	Temp.	Temperature
	TBAF	Tetra-*n*-butylammonium fluoride
	TMEDA	*N*,*N*,*N'*,*N'*-Tetramethylethylenediamine
	T_m	Melting temperature
	TBS-Tween	Tris-buffered saline Tween
	TB	Terrific broth
	TLC	Thin layer chromatography
U	UV	Ultraviolet
	Ub	Ubiquitin
	UPS	Ubiquitin-proteasome system
V	VEGF	Vascular endothelial growth factor
	VEGFR	Vascular endothelial growth factor receptor
	VLS	Virtual ligand screening
W	WT	Wild-type
	WST	Water-soluble tetrazolium salt

Contents

Chapter One: Introduction

1.1 Characteristics of Cancer

Cancer is the leading cause of death worldwide, responsible for over 7.6 million deaths (13% of all deaths) in 2008, with the death toll expected to reach more than 11 million by 2030.[1] The disease stems from changes to the genome within a cell. Mutations in the DNA sequence lead to the production of oncogenes with a dominant gain in function and tumour-suppressor genes with a loss of function.[2] This produces cells with defects in the regulatory circuits controlling cell proliferation and homeostasis. Most, if not all, cancer cell genotypes are the manifestation of six cellular alterations thought to be essential for malignant growth, termed the 'Hallmarks of Cancer' (**Figure 1**).[3, 4] Each capability and its functional significance are explained below:

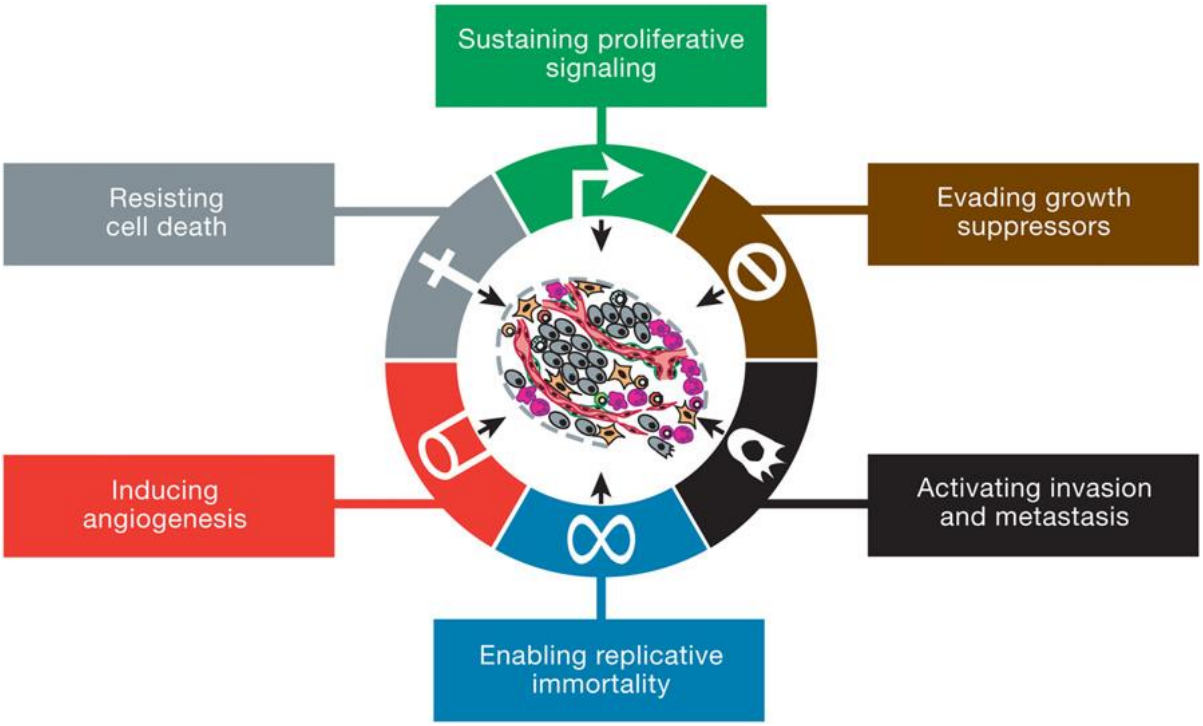

Figure 1: The hallmarks of cancer[4]

1. Sustaining proliferative signalling

Cells require mitogenic growth signals before they can move from a dormant state into an active proliferative state. However, many oncogenes act by mimicking the action of these growth signals, so the dependence of cancer cells on exogenous growth stimulation is lower than that of normal cells.[4]

2. Evading growth suppressors

Within a normal tissue, soluble growth inhibitors and immobilised inhibitors embedded in the extracellular matrix and on the surface of nearby cells work to maintain cellular quiescence and tissue homeostasis. Anti-proliferative signals are channelled through the retinoblastoma protein (pRb), p107 and p130. In cancer cells the pRb pathway is disrupted, causing uncontrolled cell division that is insensitive to growth suppressors.[4, 5]

3. Resisting cell death

One of the most significant natural defences against tumour development is programmed cell death (apoptosis)[4, 5] and acquired resistance to apoptosis is being supported by ever increasing evidence as a hallmark of most, if not all, cancers.[4, 5, 6] Once triggered, apoptosis occurs in a precisely choreographed sequence of steps, in which the cell membrane degrades, the cytoplasmic and nuclear skeletons break down, the cytosol is extruded, the chromosomes degrade and the nucleus fragments.[7] The p53 tumour-suppressor protein facilitates apoptosis by upregulating the expression of the pro-apoptotic Bcl-2 protein Bax. Mutation of the p53 gene, which produces the functionally inactive p53 protein, is seen in almost 50% of human cancers.[8, 9, 10]

4. Enabling replicative immortality

Many mammalian cells can only undergo a limited number of divisions before entering senescence.[11] Disabling the pRb and p53 proteins enable the cells to continue multiplying for a finite number of doublings until they enter a second senescence state termed ‘crisis’, characterised by mass cell death and the occasional emergence of a cell (1 in 10^7) which has limitless replicative potential, a process termed immortalisation.[12] Most tumour cell types grown in culture appear immortalised, indicating that limitless replicative potential is a phenotype which is acquired *in vivo* and is essential for the development of the cancer cells’ malignant growth.[11]

5. **Inducing angiogenesis**

All cells require oxygen and nutrients to function and survive. Once a new tissue is formed, the formation of new blood vessels (angiogenesis) is carefully coordinated.[3, 4] Despite the need for blood vessels to provide nutrients, proliferating cells have no intrinsic ability to induce blood vessel growth. To progress to larger sizes, neoplasias must develop angiogenic capability and the experimental evidence highlighting the significance of sustained angiogenesis in tumours is profound.[13, 14, 15]

6. **Activating invasion and metastasis**

All types of cells possess proteins which bind the cells to their surroundings, including the cell-to-cell adhesion molecules (CAMs).[3] These proteins are altered in cells possessing invasive or metastatic capabilities. The most widely studied is E-cadherin, a CAM expressed ubiquitously in epithelial cells. The function of this protein is disrupted in the majority of epithelial cancers, meaning primary tumours can spawn cells capable of invading adjacent tissues and travelling to distant sites.[16] Invasive tumours are the cause of 90% of human cancer deaths.[17] If E-cadherin is forcibly expressed in cultured cancer cells, this impairs their invasive and metastatic phenotypes, whereas interference of E-cadherin enhances both phenotypes, meaning the functional elimination of E-cadherin is a key step in the acquisition of metastasis.[18]

1.2 Causes of Cancer

There are over 200 types of cancer, all with their own triggers which cause sufficient damage to a cell's genome to make it cancerous, but the most significant causes of cancer are summarised below:

1. **Carcinogens:** Cancer-causing chemicals, e.g. tobacco smoke, which has been shown to be a major cause of lung cancer.[1, 19, 20, 21]

2. **Age:** When cells divide they must precisely replicate their genetic sequence in the new cell being made. In approximately one in 10^7 base pair replications, an error will occur, which is normally corrected by DNA-repairing enzymes.[22] If this fails to happen, the replicative error will be passed on to the daughter cell. Multiple replicative errors produce oncogenes, but this process takes a long time, which explains why most cancers are more common in older people.

3. **Genetic predisposition:** Some people are born with genetic mutations that increase their chances of developing a particular cancer, e.g. women born with mutations in the *BRCA1* or *BRCA2* genes are statistically more likely to develop breast cancer.[23]

4. **Lifestyle choices:** Obesity, smoking, excessive alcohol and the consumption of certain foods, e.g. red and processed meat, have all been linked to an increased risk of cancer.[24]

5. **Radiation:** UV radiation from the sun has been shown to increase the risk of developing a melanoma and nuclear radiation has been linked to a rise in several cancer types, e.g. leukaemia.[25]

6. **Viral and bacterial infections:** Viruses can cause the genetic damage to a cell that lead to it becoming malignant, e.g. human papilloma virus (HPV) has been shown to increase the risk of cervical cancer.[26] *Helicobacter pylori* has been linked to the onset of several cancers, e.g. stomach cancer.[27]

1.3 Treatments for Cancer

Various forms of oncological treatments exist, the most fundamental of which is to surgically remove the tumour and an area of healthy tissue surrounding it to prevent a recurrence at that site. If removal of the entire tumour is impossible, as much of it will be removed as possible so as to alleviate any pain, airway obstruction or bleeding. While this treatment can be effective for treating benign or pre-metastatic tumours, those which have spread beyond the primary tumour site cannot often be targeted.

Radiation therapy uses high-energy X-rays, proton or neutron beams to damage the DNA of cancer cells to elicit single- or double-strand breaks, causing the cell either to die or senesce. Radiation can be applied externally, using a beam of radiation, or internally where a source of radioactivity is implanted in the body near the tumour site. However, radiation therapy is considered a ‘local’ form of treatment and so cannot be used to effectively treat metastatic tumours. It can also cause DNA damage to the surrounding healthy cells, potentially leading to relapse in the long term.

1.3.1 Chemotherapy

Chemotherapy is one of the most widely used forms of cancer therapy. Various classes of chemotherapeutic agents have been used, a short summary of which is given below:

1. **Mustard agents:** One of the first groups of chemicals found to have anticancer activity and examples include mechlorethamine (**1**) and cyclophosphoramide (**2**). The drugs are alkylating agents and bind covalently to purine bases in DNA and cross-link strands which induce apoptosis.[28, 29]

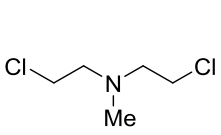

1

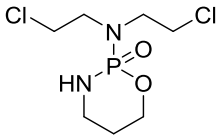

2

2. **Antimetabolites:** Chemicals which inhibit the action of a metabolite responsible for normal cell function. Examples include purine analogues, e.g. 6-thioguanine (**3**),[30] pyrimidine analogues, e.g. 5-fluorouracil (5-FU) (**4**)[31] and antifolates, e.g. methotrexate (**5**), a competitive inhibitor of dihydrofolate reductase (DHFR), an enzyme essential for purine biosynthesis.[29]

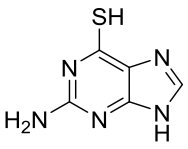

3

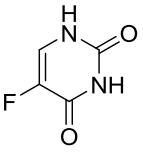

4

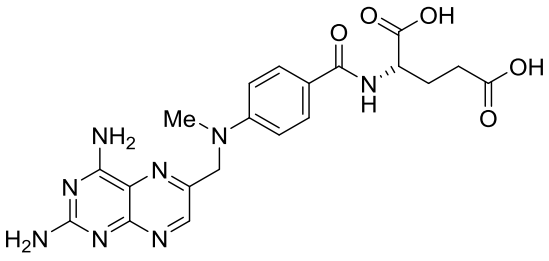

5

3. **Vinca alkaloids:** Naturally occurring chemicals produced in the common periwinkle plant (*Vinca rosea*). Examples include vincristine (**6**) and vinblastine (**7**) and they function as antimitotic agents.[32] They inhibit microtubule polymerisation, which is a fundamental process in the metaphase of mitosis, and induce cell cycle arrest.[33, 34]

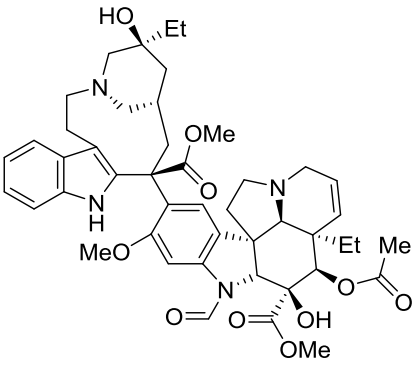

6

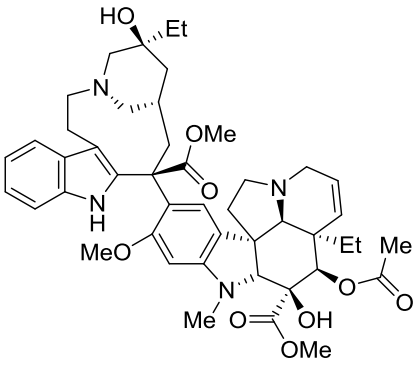

7

4. **Taxanes and camptothecins:** Plant-derived antimitotic agents, like the vinca alkaloids. Taxanes promote the formation of irregularly structured microtubule bundles that cannot form the mitotic spindles required to separate the chromosomes during the anaphase of mitosis, promoting cell cycle arrest. Camptothecin (**8**) and its analogues inhibit Type I topoisomerases, which are critical for the unwinding of DNA from the histones during prophase.[34]

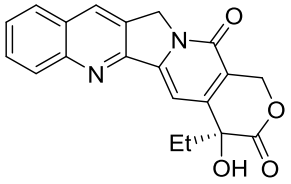

8

5. **Platinum-containing drugs:** Examples include *cis*-platin (**9**) and carboplatin (**10**) and they function by forming intrastrand cross-links by binding covalently to two neighbouring guanines. This causes a significant bending in the DNA helix, sufficient to inhibit DNA synthesis and induce apoptosis.[35, 36, 37]

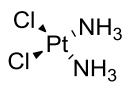

9

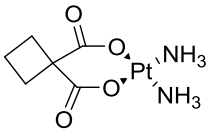

10

Cytotoxic chemotherapy has shown potent activity against a range of cancer types and the ability to affect tumours in multiple sites of the body gives it an advantage over surgery and radiation therapy. However, all the agents listed suffer from the onset of

resistance which reduces their efficacy. Many have poor selectivity towards cancer cells and therefore produce adverse reactions in patients, commonly including nausea, vomiting, fatigue and alopecia, but some side effects can be severe, e.g. peripheral neuropathy, cardiotoxicity and bone marrow toxicity, which can lead some patients to abstain from taking their medication. To reduce the side effects, drugs are now being developed which are tailored to patients' individual circumstances.

1.3.2 Targeted Therapy

Targeted therapy refers to a new generation of cancer drugs designed to alter the biological function of a specific protein which has been shown to play a fundamental role in the growth or progression of the tumour. These drugs have enhanced selectivity towards tumour cells and therefore promise reduced patient toxicity compared with cytotoxics. However, the compounds are less versatile because they are only effective in cancers which depend upon the protein or pathway being targeted. Most solid tumours, which comprise 90% of human cancers, are the manifestation of multiple genetic mutations and so a drug which targets a single cellular pathway may not have a strong efficacious effect.[38] Similar to chemotherapy, the impact of targeted therapies on tumours is reduced by the build-up of resistance. The design of drugs capable of targeting multiple pathways, as well as combination therapy in which several drugs with different modes of action are used to combat the same tumour, can overcome these problems and various forms of targeted therapy exist (**Figure 2**).

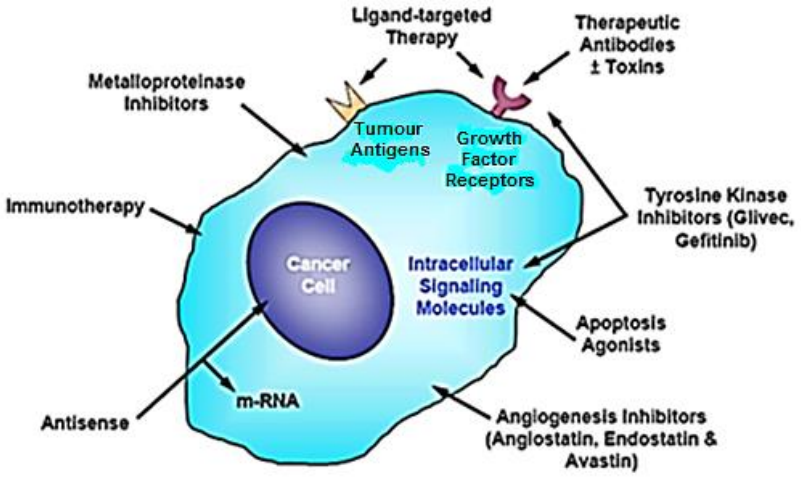

Figure 2: Different types of targeted therapy; adapted from[38]

1.3.2.1 Antibody-targeted Therapy

Monoclonal antibodies (MoAbs) (i.e. antibodies which recognise only one type of antigen and are produced by identical immune cells) are well tolerated and effective against a range of human malignancies. Anticancer agents can be conjugated to MoAbs, improving their selectivity and the versatility of those unable to be administered alone.[38] The agents which can be attached include small-molecule drugs and toxins. The high tolerance for antibodies is due to the often simple conversion of non-human antibodies, e.g. murine antibody, to human or humanised formats not recognised as foreign by the immune system. However, this mode of therapy does have drawbacks; success of treatment critically depends on the choice of antigen to target. The antigen must be present on most, if not all of the cancer cells to ensure selectivity and prevent a subpopulation of antigen-negative cells from developing. Antigens which shed from the cell membrane and travel in the blood stream are not optimal targets, as higher doses of the antibody will be required to clear the circulating antigen before it reaches the cancer cells. Penetrance of solid tumours is also a problem due to various barriers, e.g. the vascular epithelium, and the fact solid tumours are often heterogeneous means that targeting them completely is difficult.[38] Despite this, several antibodies have been approved for anticancer therapy (**Table 1**).

Table 1: Therapeutic antibodies approved by the US FDA for cancer treatment[38]

Monoclonal Antibody	Target	Indication	Product	Year	Corporate Sponsor
Trastuzumab (Herceptin)	HER2/neu	Metastatic breast cancer	Humanised	1998	Genentech
Gemtuzumab-ozogamicin (Mylotarg)	CD33	AML	Humanised	2000	Wyeth Laboratories
Bevacizumab (Avastin)	VEGF	Metastatic CRC; NSCLC	Humanised	2004	Genentech

AML, acute myeloid leukaemia; CRC, colorectal cancer; NSCLC, non-small cell lung cancer; VEGF, vascular endothelial growth factor

Herceptin is a genetically engineered MoAb that inhibits proliferation of cells overexpressing the HER2 oncoprotein, which is seen in 25-30% of breast cancers and has been associated with aggressive cell growth.[38] Humanisation of Herceptin reduces the immunogenicity seen when using murine MoAb therapy. Avastin targets the VEGF signal protein, which plays a key role in establishing angiogenesis. This makes Avastin a versatile medication, as VEGF inhibition has been shown to be an effective treatment for solid tumours, various leukaemias and haematological cancers.

1.3.2.2 Ligand-targeted Therapy

Ligand-targeted therapy (LTT) involves the conjugation of an anticancer drug to a molecule capable of recognising an antigen or receptor expressed uniquely or overexpressed on cancer cells relative to healthy cells. This allows for the selective delivery of higher concentrations of a drug to cancer cells that otherwise would cause unwanted toxicity to the patient.[38, 39] This makes LTT similar to antibody-targeted therapy, but whereas antibodies can be used as anticancer agents in their own right, LTT

encompasses all molecules that can act as carriers of cytotoxic drugs, e.g. liposomes and nano-particles (**Table 2**).[39] One reason for the onset of resistance in chemotherapy is the use of suboptimal doses of a drug to combat the tumour, due to the risk of toxicity at higher concentrations. LTT allows for high concentrations to be administered in a safer manner to the patient, thereby reducing the chances of resistance build-up and early relapse.[38, 39]

The success of this treatment is dependent on the choice of antigen to target, similar to antibody-targeted therapy. The antigen must have a high density on the target cell and the cancer cells cannot have too high a heterogeneity in their antigens, as this could affect the selectivity of the carrier.[38] Antigens which shed from the cell and circulate in the bloodstream also do not make optimal targets. Compared with antibodies, non-antibody carriers are often readily available, inexpensive to manufacture and simple to store and handle.[39] However, they can have worse selectivity profiles; the RGD (arginine-glycine-aspartate) and transferrin ligands have been shown to bind to non-target tissues.[38, 39, 40] Folate, which has also been used as a carrier, is found naturally in body fluids and the natural folate competes with the targeted therapy for the antigen. Antibodies have an advantage over other carriers in that they can have cytotoxic properties themselves, allowing for a potential synergy with the bound chemotherapeutic, as the tumour cell can be targeted via two different mechanisms.

Table 2: Non-antibody carriers used in LTT[39]

Ligand	Target	Indication
RGD	Cellular adhesion molecules	Solid tumours
Folate	Folate receptor	Cancer cells overexpressing the folate receptor
Transferrin	Transferrin receptor	Cancer cells overexpressing the transferrin receptor

1.3.2.3 Targeted Therapy with Small Molecules

This modern form of chemotherapy provides molecular level-based anticancer medicine with greater selectivity for cancer cells over normal cells, significantly reducing the frequency and severity of side effects that patients experience. Hit compounds (i.e. molecules which demonstrate activity against a pre-determined target) are identified in a molecular screen and the structures are meticulously altered to enhance and improve the pharmacological properties and selectivity profile to produce a drug candidate (**Table 3**).

Table 3: Small-molecule targeted cancer therapies[38, 41]

Drug	Target	Indication	Year of FDA Approval	Corporate Sponsor
Imatinib (Glivec)[42]	Bcr-Abl, c-Kit, PDGF receptor, ARG kinase	CML, GIST	2001	Novartis
Gefitinib (Iressa)[43]	EGFR TK	NSCLC	2003	AstraZeneca
Erlotinib (Tarceva)[44]	EGFR TK	NSCLC	2005	Genentech
Lapatinib (Tyverb)[45]	ErbB1 (EGFR) and ErbB2 TK	MBC	2007	GlaxoSmithKline
Bortezomib (Velcade)[46]	26S proteasome	MM	2003	Millennium Pharmaceuticals
Sorafenib (Nexavar)[47]	b-Raf and c-Raf kinase	HCC	2007	Bayer AG
Vandetanib (Caprelsa)[48]	VEGFR	MTC	2011	AstraZeneca
Vorinostat (Zolinza)[49, 50]	HDACs	CTCL	2006	Merck

PDGF, platelet-derived growth factor; CML, chronic myelogenous leukaemia; GIST, gastrointestinal stromal tumour; EGFR, epidermal growth factor receptor; TK, tyrosine kinase; NSCLC, non-small cell lung cancer; MBC, metastatic breast cancer; MM, multiple myeloma; HCC, hepatocellular carcinoma; VEGFR, vascular endothelial growth factor receptor; MTC, medullary thyroid carcinoma; HDAC, histone deacetylase; CTCL, cutaneous T-cell lymphoma

The advantage of small-molecule targeted therapies having significantly reduced side effects than previous chemotherapies is also a limitation in that the drugs can only be used to treat cancers possessing a specific overexpressed or amplified protein. Imatinib has shown dramatic results in CML patients, but clinical trials on related protein targets in different cancers showed greatly reduced efficacy, highlighting the importance of target expression over pathway activation.[38] Gefitinib treatment has shown noticeable tumour regression in only 10-30% of NSCLC patients, despite the near universal presence of EGFR kinase. This can be explained by the presence of transporter proteins, e.g. ABCG2, which remove foreign agents from the cell and have high affinities for tyrosine kinase receptor inhibitors such as Gefitinib.[38, 43] Variable expression levels and polymorphisms of these transporters amongst different cultures and races can influence the responses observed in individual patients. Targeted therapies are also not immune to the occurrence of side effects. Uncommon but serious side effects of Gefitinib treatment include interstitial lung disease and skin toxicity.[38]

1.3.2.4 Protein-Protein Interaction Inhibitors

Protein-protein interactions (PPIs) play a crucial role in many cellular processes and inhibition of these interactions is an important method for investigating the cell-signalling pathways critical to cellular function.[51] This makes PPI inhibitors desirable agents for anticancer therapy. Combinatorial chemistry, high-throughput screening (HTS) and structure-based rational design methodologies have all produced promising small-molecule inhibitors of PPIs. One example is the *cis*-imidazoline-based Nutlin family, which were optimised to selectively inhibit the *h*MDM2-p53 interaction. Nutlin-3a (**11**) inhibits this PPI with an IC_{50} of 90 nM and activates the p53 pathway, promoting cell cycle arrest, apoptosis and reducing tumour cell proliferation *in vivo*.[52] A close analogue, RG7112 (**12**), has now been advanced to clinical development, with evidence suggesting the compound activates p53 signalling in human tumour xenografts.[53]

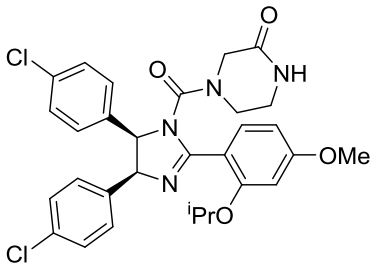

11

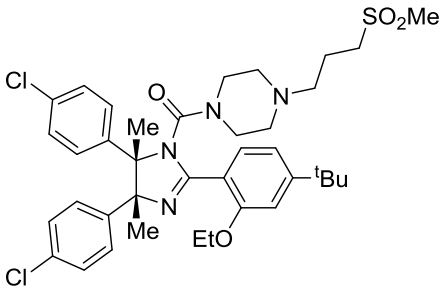

12

Currently, the only marketed PPI inhibitor is Maraviroc (Celsentri; Pfizer) (**13**), an antiretroviral modulator of the CCR5 receptor, found on the surface of white blood cells. This receptor has high binding affinity for several HIV strains and is important for entry of the virus into the cell. Maraviroc has been shown to significantly reduce the levels of HIV RNA found in human cells.[51, 54]

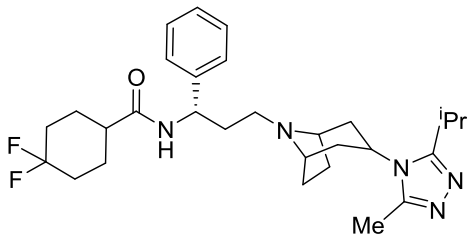

13

To efficiently bind to a protein's surface, a small molecule must cover an area of 800-1100 Å^2 whilst complimenting sufficiently the often poorly defined hydrophobic and hydrophilic domains of a flat or near-flat surface. Consequently, many of the potential PPI inhibitors entering clinical trials are larger and more lipophilic than the currently marketed binding inhibitors of a protein with a relatively smaller substrate, e.g. ATP.[51]

1.4 The Drug Development Process

The full drug development process, starting from the identification and validation of a target, e.g. a protein, to the approval and marketing of a drug, takes 10-15 years and costs $800 million to $1 billion. It can be split into four main stages:

1. **Pre-drug discovery**
2. **Drug discovery**
3. **Drug trials**
4. **Drug approval**

The following tables outline the various sub-stages associated with each of the four main steps in the drug development process, to explain what was done prior to these projects commencing, what the aims of these project were, and what will be done following discovery of a drug candidate (**Tables 4-7**).

Table 4: Objectives in the pre-drug discovery process

Task	Description
Disease Identification	Identify the target disease and the underlying cause of the condition (i.e. which genes are altered and how, the proteins they encode, how those proteins function and how they affect the patient).
Target Identification	Decide which biochemical pathway or receptor is to be targeted and develop a hypothesis for the mechanism of treatment (e.g. to inhibit a PPI crucial to cell transformation).
Target Validation	Use *in vitro* and animal-based studies to confirm the chosen target is critical to the onset of the disease and can be affected by the use of a drug or gene-silencing.
Hit Identification	Employ combinatorial chemistry, HTS or computer-aided design (CAD) with 3D modelling software to identify compounds or pharmacophores which appear crucial for activity against the chosen target, then evaluate the feasibility of producing the compound and further derivatives.
Hit Validation	Fully characterise the hit compounds' chemical structures and confirm the biological activity observed in the initial screen. The latter may involve isolated protein assays with dose-response studies, NMR evaluation or co-crystallisation of the hit compound with the target.

Table 5: Objectives in the drug discovery process	
Task	**Description**
Hit-to-Lead	Structurally optimise hit compounds to optimise their pharmacological properties, e.g. potency and selectivity for the target. Structural analogues are screened against the target and the data suggests further changes which can be made. Compounds demonstrating significant activity against the target are called 'leads'.
Lead Optimisation	Novel compounds demonstrating high potency are optimised to produce a drug candidate. Compounds will be screened across various cell lines to see if potency and selectivity are maintained. Potential routes of formulation, administration and metabolism are considered.

Table 6: Objectives in the drug trials process	
Task	**Description**
Pre-Clinical Trials	Conduct *in vitro* and *in vivo* studies to determine if a drug candidate is safe to trial in humans. Evaluate the acute and sustained toxicity in non-human animals (often one rodent, one non-rodent). Dose at increasingly high levels to induce toxicity and determine a lethal dose (LD). Dose at levels which give a therapeutic value over short and long periods to analyse long-term use toxicity. Assess how a drug may be absorbed, distributed, metabolised and excreted in animals (ADME properties).
IND Application	Investigational New Drug (IND) application submitted to the Food and Drugs Administration (FDA) to allow human exposure to a drug candidate.
Phase I Clinical Trials	Evaluates the pharmacokinetic (ADME) properties of a drug in 20-80 healthy volunteers over a one-year period, costing $100,000-$1 million. Conduct single-dose, dose-escalation and short-term repeated dose studies to determine any side effects with increased dosing and initial evidence of drug efficacy.
Phase II Clinical Trials	Assess a drug's effectiveness at treating a particular condition or disease and side effect profile in 100-300 volunteers over a two-year period, costing $10-100 million. Compare findings to those of rival compounds or placebos.
Phase III Clinical Trials	Confirm the effectiveness and safety of a drug within a large population, involving 1000-3000 volunteers over a 3-4-year period in multiple sites (nationally and internationally) and costing $10-500 million. Compare

	findings to those of rival compounds or placebos, at various doses and trialling various routes of administration.

Table 7: Objectives in the drug approval process

Task	Description
NDA	New Drug Application (NDA) submitted to the FDA for approval to market a drug. Supply sufficient evidence that the drug is safe and effective, that the benefits outweigh the risks, that the proposed labelling is appropriate and that manufacturing methods and controls maintain the drug's identity, strength, quality and purity.
Phase IV Clinical Trials	After gaining approval to market a drug, further studies are done to evaluate a drug's benefits and side effects when used more widely over greater time periods.

1.4.1 SKP2 Hit Identification Criteria

The Lipinski Rules of Five[55, 56] describe the criteria to maximise the oral activity of a candidate drug by successfully balancing aqueous solubility with cell-permeability *in vivo*:

- Molecular mass ≤ 500 g/mol
- clogP ≤ 5
- Number of H-bond donors ≤ 5
- Number of H-bond acceptors ≤ 10

There are many properties to consider for a lead compound before classifying it as such and different drug discovery programs prioritise different properties to optimise, depending on the drug's mode of action and administration. In this project, the priority characteristics to optimise were molecular mass, calculated partition coefficient (clogP), potency, solubility and topological polar surface area (tPSA). The significances of these properties are described below.

1. **Potency**

A measurement of drug activity expressed as the concentration of drug required to elicit a pharmacological response of pre-defined intensity. The response intensifies with increasing concentrations of the drug until a point is reached at which higher doses do

not affect the response; this is the maximal effective/inhibitory concentration (E_{max}). The drug concentration at which the response is 50% E_{max} is the half-maximal effective/inhibitory concentration (EC_{50} or IC_{50}) and potency refers to this value. Drugs with higher potency require lower quantities to achieve a therapeutic outcome, which often correlates with reduced side effects.[57]

2. **Partition coefficient (P)**

A measurement of drug lipophilicity, defined as the ratio of concentrations of a drug between two immiscible solvents at equilibrium. The two solvents are often deionised water and octan-1-ol. High lipophilicity correlates with extensive metabolism high clearance and reduced target selectivity.

3. **Aqueous solubility**

A drug must have sufficient solubility to dissolve in blood plasma and the desired solubility range for a particular drug depends on its potency and cell permeability. Low aqueous solubility correlates with poor absorption and a delayed therapeutic effect.[58]

4. **Molecular mass**

Most marketed drugs have a molecular mass below 500 g/mol. Larger molecules diffuse slower through cell membranes resulting in a delayed therapeutic response.

5. **Topological polar surface area (tPSA)**

Quantifies the polarity of a drug (measured in $Å^2$) by calculating the sum of all polar atom surfaces (usually oxygens, nitrogens and their attached hydrogens) and predicts a drug's transport properties. High polarity correlates with accelerated clearance and a poor pharmacological response.

In the case of the projects described herein, the criteria defining a suitable PPI inhibitor lead compound designed for intravenous (IV) administration are as follows:

- Potency: ≤ 100 nM
- Selectivity: ≥ 100-fold
- LogP: ≤ 5
- Solubility: ≥ 50 µM
- Molecular mass: ≤ 500 g/mol
- tPSA: 75-100 $Å^2$

Chapter Two: Project SKP2

2.1 The SCF E3 Ubiquitin Ligases

The SKP1-Cullin1-F-box (SCF) E3 ligases are the largest family of E3 ubiquitin ligases and regulate many cellular processes by promoting the ubiquitination of regulatory proteins, e.g. cell cycle regulators and transcription factors, targeting them for proteasome-mediated degradation or otherwise affecting their function/activity.[59]

Ubiquitination of a substrate is a multi-step process (**Figure 3**). Ubiquitin-activating enzyme E1 coordinates to ubiquitin through use of ATP and transfers it to ubiquitin-conjugating enzyme E2. The SCF ligase E3 recognises and coordinates to the protein substrate and catalyses ubiquitin transfer from E2 to the protein. Ubiquitin is conjugated to a protein by an isopeptide link formed between the carboxy group of the *C*-terminal glycine residue of ubiquitin and the ε-amino group of a lysine residue within the substrate. This process can be repeated to assemble polyubiquitin chains by conjugating the carboxy group of the *C*-terminal glycine residue of the new ubiquitin molecule to the ε-amino group of one of seven internal lysines within the preceding ubiquitin. The fate of the ubiquitinated substrate depends on the type of isopeptide linkage formed; K48-linked polyubiquitination targets the substrate for proteasome-mediated degradation, but K63-linked or monoubiquitination alters the protein's function and its interactions with other proteins etc.[60]

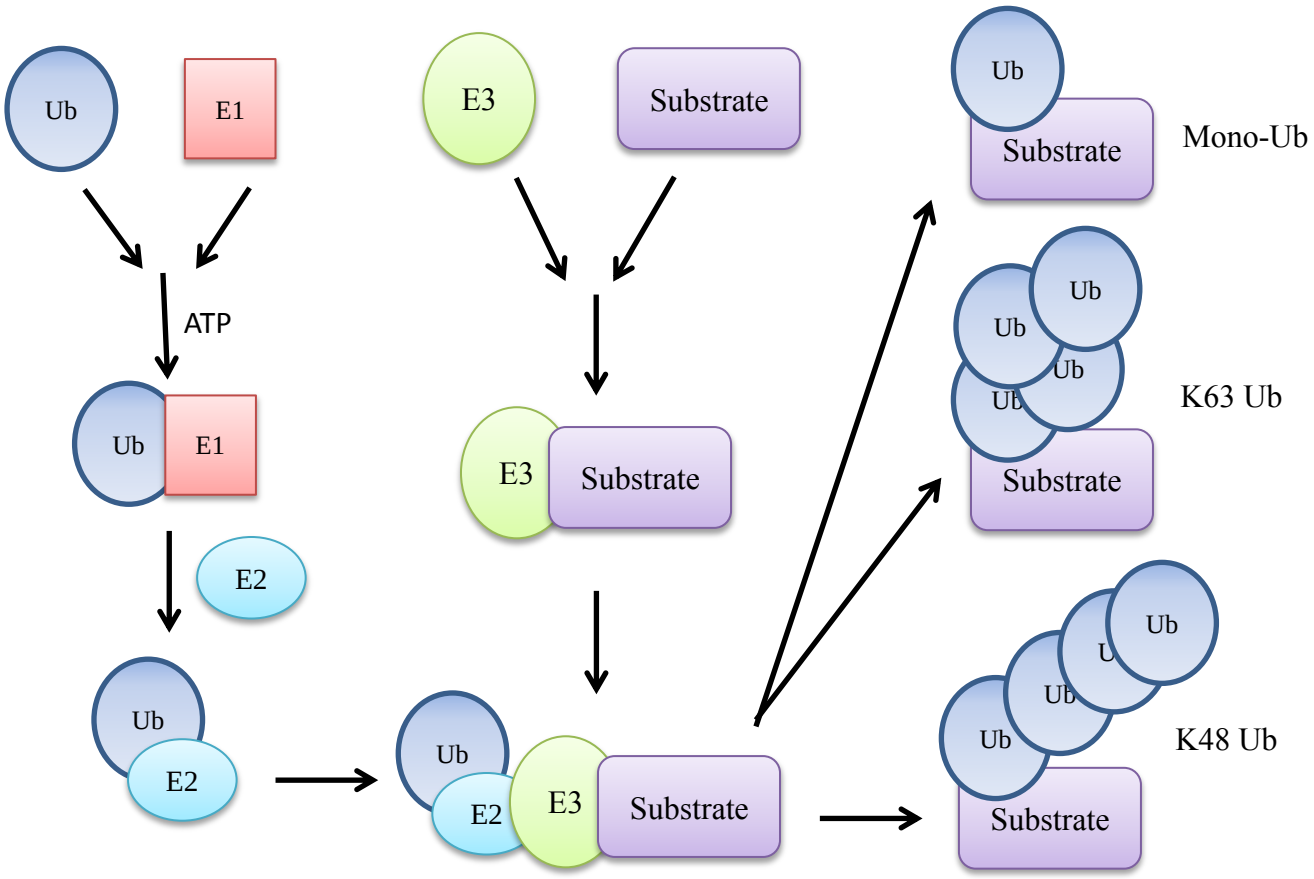

Figure 3: Protein ubiquitination pathway (Ub, ubiquitin); adapted from[60]

The SCF E3 ligases are multi-subunit complexes consisting of adaptor proteins, cullins, RING finger proteins and F-box (receptor) proteins (**Figure 4**). Crystal structures of SCF complexes reveal the cullins are scaffold proteins, which bind the adaptor and F-box proteins at its *N*-terminus and the RING finger proteins at its *C*-terminus.[59] Seven cullins are known in the human genome (Cul-1, -2, -3, -4A, -4B, -5 and -7) and all are involved in the coordination of different F-box proteins. The RING finger proteins coordinate to E2 enzymes and facilitate ubiquitin transfer to the substrate. Two RING finger proteins are known in the human genome, RBX1 (RoC1) and RBX2 (RoC2), both of which have been shown to be functionally non-redundant in mouse-knockout studies.[59, 61] SKP1 is an adaptor protein found in several SCF complexes and links the cullin with the F-box protein.[59]

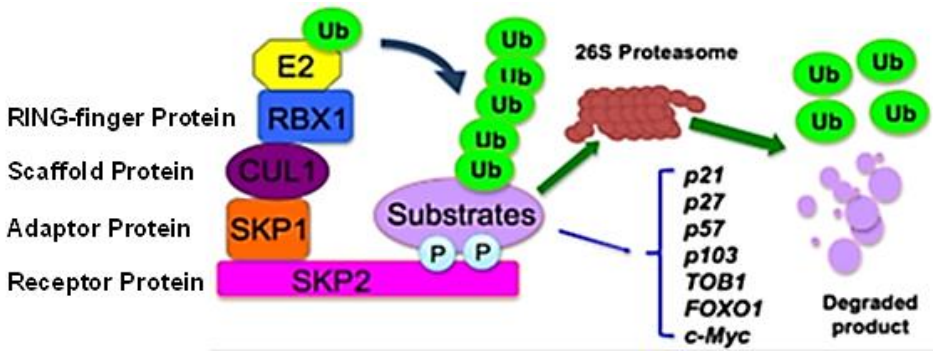

Figure 4: The SCF^{SKP2} E3 Ligase; adapted from[62]. Ubiquitin (Ub) is transferred from an E2 enzyme to a substrate that is bound to SKP2. The substrate must be phosphorylated before SKP2 can bind to it (P = phosphate). Once ubiquitinated, the substrate is degraded by the 26S proteasome with the release of ubiquitin. Substrates of SKP2 include p21, p27, p57, p103, TOB1, FOXO1 and c-Myc

F-box proteins are the substrate-recognising subunits that determine the selectivity of an SCF complex. One F-box protein can recognise multiple substrates, some of which have opposite biological functions, e.g. cell cycle suppressors and promoters. Whether a particular substrate will be targeted or not depends on the cell's internal environment, highlighting the significance of SCF complexes in determining the life and death of a cell. In the human genome there are 69 F-box proteins,[63] each of which binds to the adaptor protein via its F-box domain, and are classed into one of three categories depending on the nature of the binding domain that links them to the substrate.[59] Those which have WD40 domains (i.e. domains consisting of a 40-amino acid motif ending in a tryptophan-aspartic acid dipeptide) are called FBXWs, those with domains consisting of leucine-rich repeats are called FBXLs and those which have other diverse domains are called FBXOs. To date, three F-box proteins have been well studied: Fbxw7,[64] β-TrCP[65] and SKP2.[59, 65, 66]

2.2 SCF E3 Ubiquitin Ligases as Anticancer Targets

Several subunits of the SCF complex have demonstrated oncogenic activity; of the seven cullin scaffold proteins, Cul-1 is overexpressed in 40% of lung cancers and Cul-4A is overexpressed in breast cancer, HCC and mesotheliomas. Cul-4A overexpression is associated with cell cycle progression in breast cancer cells resulting in poor prognosis and Cul-4A knockdown by siRNA causes accumulation of cell cycle suppressors p21 and p27, inducing G1 cell cycle arrest.[59]

SCF-mediated ubiquitination must be activated by the coordination of a ubiquitin-like protein, Nedd8 activating enzyme (NAE), to the cullins of the SCF ligase; a process termed neddylation. This forms an isopeptide bond between the *C*-terminal glycine residue of Nedd8 and the ε-amino group of a conserved cullin lysine residue. Inhibitors of neddylation, e.g. MLN4924 (**14**), induce many SCF substrates, including p27, which can promote cell cycle arrest and cell death (**Figure 5**). This evidence suggests the significance of targeting Nedd8 as a form of cancer treatment.[67]

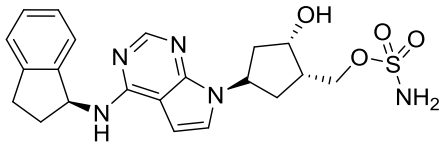

14

The accessory protein cyclin kinase subunit 1 (Cks1) is essential for efficient SKP2-mediated degradation of p27, as evidenced by the slow proliferation of p27 in Cks1-knockout mice. Cks1 levels have been shown to correlate positively with those of SKP2 and inversely with those of p27. As a result, Cks1 overexpression has been linked with tumour aggressiveness and a poor prognosis in several cancers including colorectal carcinoma.[68]

RBX1 is overexpressed in several human tumours including lung cancer. Knockdown of RBX1 by siRNA triggers a DNA damage response and subsequent G2/M cell cycle arrest, senescence and apoptosis. RBX2 is also overexpressed in several human cancers giving a poor prognosis. The RING finger proteins exert E3 ubiquitin ligase activity and promote the degradation of multiple cell cycle regulators including p27 and c-Jun.[61] RBX2 siRNA silencing induces cancer cell apoptosis and sensitisation to chemotherapeutics and radiation. This evidence suggests the significance of the RING finger proteins as anticancer targets.[59]

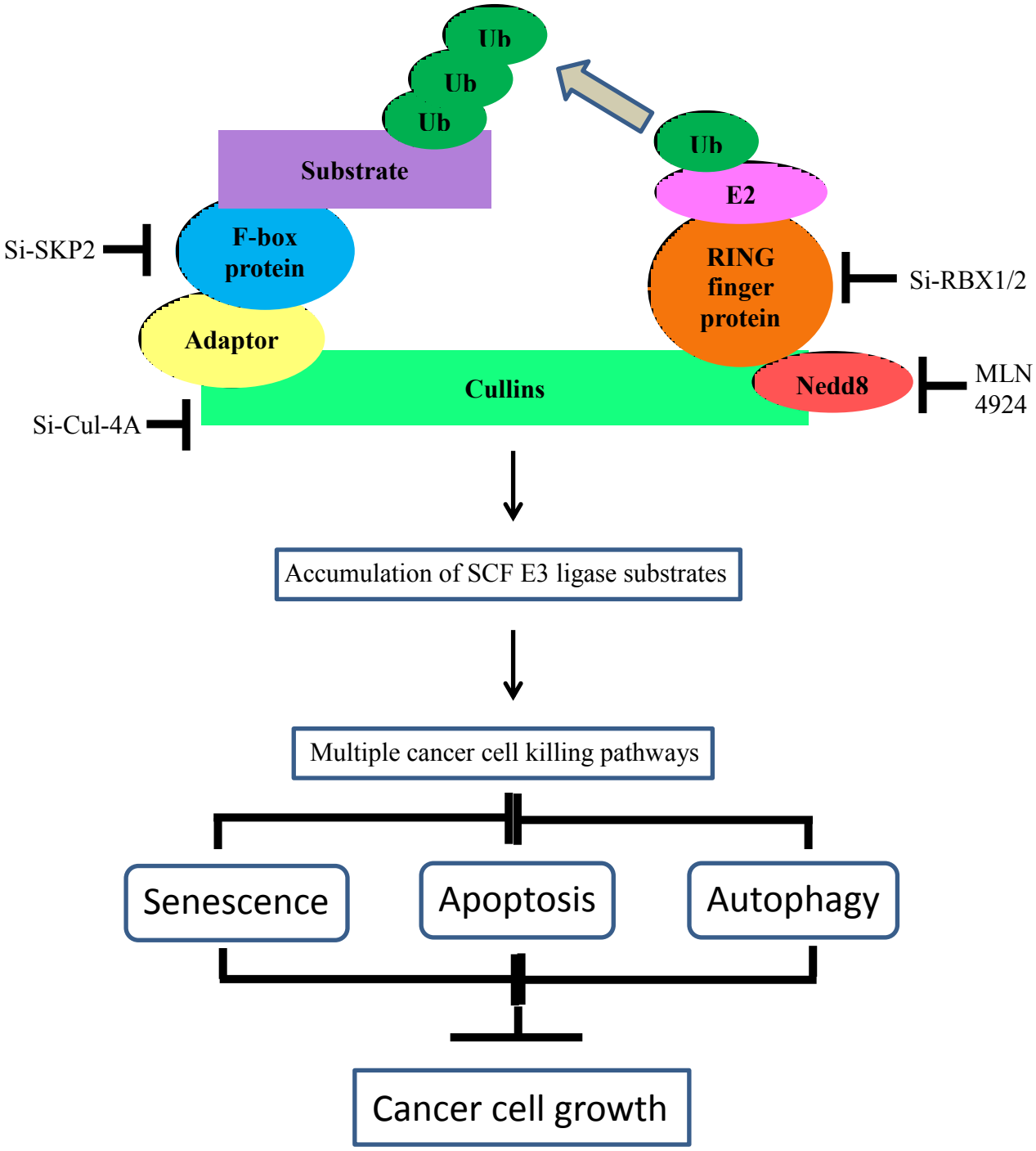

Figure 5: Targeting the SCF E3 ligases to trigger multiple cancer cell killing mechanisms[59]

2.2.1 Targeting the F-Box Protein SKP2 for Cancer Therapy

The SCF^{SKP2} E3 ligase recognises and targets several cell cycle negative regulators, e.g. p21, p27, p57 and p130.[69] Oncogenic SKP2 increases ubiquitination of these proteins and enables replicative immortality.[63] Reduced p27 levels are common in many human cancers, being associated with an aggressive phenotype and poor prognosis.[70, 71] In

multiple myeloma (MM), clinical studies show patients with low p27 expression have a shorter survival period compared to those with high p27 expression on high-dose chemotherapy.[72] SKP2 is overexpressed in several human cancers, giving a poor prognosis in gastric, colon, prostate and breast cancers. Xenografts of breast cancer cells with high SKP2 levels in mice grow faster than xenografts expressing low SKP2 levels. In mouse knock-out models, disruption of SKP2 alone does not induce cellular senescence, but SKP2-null environments or siRNA silencing of SKP2 does induce senescence and inhibits cell growth in melanoma, oral cancer, glioblastoma and lung cancer. SKP2-null mice are still viable and do not show an increased incidence of cancer. This evidence suggests that pharmacological inhibitors of SKP2 activity would be of therapeutic value for cancer therapy.[73] Several protein regulators of SKP2 have been discovered, many of which are down-regulated or inactivated in cancer cells (**Figure 6**). Their mechanisms of action on the activity of SKP2 are discussed below:

1. **PI3K/Akt**

Phosphatidylinositol-3-kinases (PI3Ks) regulate many cellular functions including cell growth, proliferation, differentiation and signal transduction. Akt is an important regulator of cell growth and survival, which is able to inhibit or promote apoptosis through the regulation of several signaling pathways including Bcl-2-Associated-Death (BAD), caspase-9 and mTOR. Studies in which the PI3K/Akt pathway has been disrupted report reduced SKP2 protein expression, coupled with increased p27 levels.[62]

2. **PTEN**

Phosphatase and tensin homolog (PTEN) is a tumour suppressor protein which functions as a negative regulator of the PI3K/Akt pathway and is frequently inactivated in several human cancers, e.g. prostate cancer. PI3K/Akt signaling is up-regulated by 30-50% in prostate cancer cells, often due to PTEN inactivation, but restoration of PTEN activity inhibits the growth of PTEN-null prostate cancer xenografts in mice.[62] PTEN regulates the oncogenic activity of SKP2 in prostate cancer cells. DU145 cells with down-regulated PTEN function showed a PTEN/Akt-dependent regulation of SKP2 activity, with an inverse correlation observed between PTEN levels and SKP2 expression.[62]

3. Androgen and AR

The androgen receptor (AR) is a ligand-activated transcription factor which, upon binding to androgen, undergoes phosphorylation and relocates to the nucleus where it interacts with DNA, initiating gene transcription and subsequently promoting cell growth. The AR has been implicated in all stages of prostate carcinogenesis including initiation, proliferation and treatment resistance, partly through regulation of SKP2 by inhibiting its degradation.[62] SKP2 in turn serves as an effector of the AR by promoting cell proliferation independent of AR activity. Androgen expression has been shown to promote G1 cell cycle arrest in prostate cancer cells through reduction of SKP2 expression and induction of p27 in an AR-dependent manner.[62]

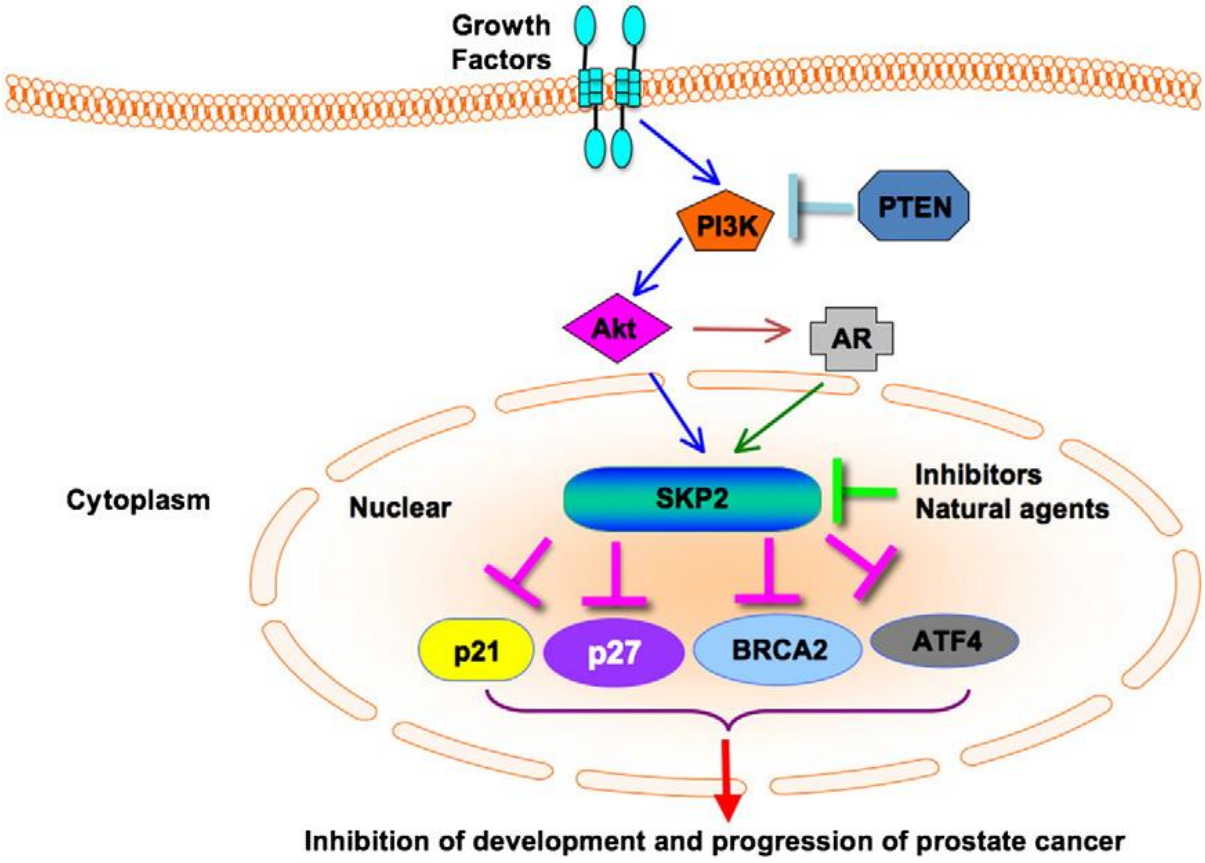

Figure 6: The cross-communication between the PI3K/Akt, PTEN and AR pathways and their combined regulation of SKP2 activity.[62]

4. MYCN

MYCN is a member of the MYC family of transcription factors and is frequently amplified in human neuroblastomas.[74, 75] Half of neuroblastomas are considered high risk (survival rates under 40%) and all instances with amplified MYCN fall into this

category, being associated with rapid disease progression and metastasis.[74, 76] SKP2 levels are higher in neuroblastomas where MYCN is amplified than when it is not. In one study, SKP2 expression was 2- to 9.5-fold higher in MYCN-amplified cancer cells than in cells showing no MYCN amplification and this SKP2 activation was independent of mitogenic signalling.[76] This evidence shows that MYCN is another important regulator of SKP2 activity in neuroblastomas.

Currently, the only marketed drug that targets the ubiquitin-proteasome system (UPS) is bortezomib (Velcade; Millenium Pharmaceuticals) (**15**),[46] which is used to treat multiple myeloma (MM). Myeloma cells are up to 1000-fold more susceptible to apoptosis in the presence of **15** than normal cells *in vitro*, due to the inhibition of nuclear factor-κB (NF-κB), a transcription factor crucial to the pathogenesis of many inflammatory and neoplastic diseases.[46, 77]

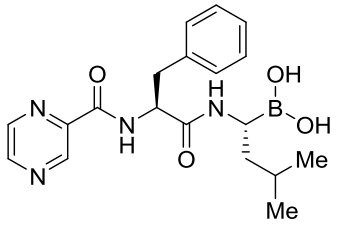

15

The boronic acid group in **15** interacts irreversibly with and inhibits the action of the 26S proteasome (**Figure 7**), which is responsible for the degradation of multiple pre-ubiquitinated targets, including p27.[46] In normal cells, NF-κB, which exists as a dimer of p50 and p65, is bound to an inhibitory protein, IκB, which keeps it inactive. In cancer cells, the 26S proteasome activates NF-κB by catalysing the destruction of IκB and the generation of p50 from its inactive precursor p105. NF-κB then enters the nucleus where it helps the cancer cells to survive and proliferate. Inhibition of the 26S proteasome keeps NF-κB inactivated by IκB and blocks cell proliferation.

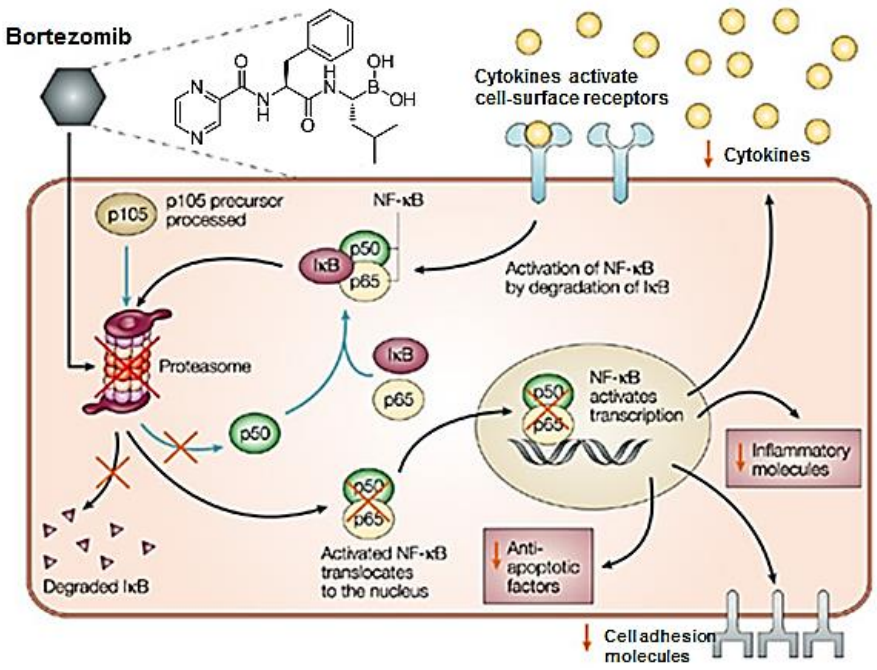

Figure 7: The mechanism of action of **15**. By inhibiting the 26S proteasome (red cross), and therefore the activation of NF-κB (orange crosses), **15** suppresses the growth of myeloma cells; adapted from[46]

Bortezomib has numerous side effects, including peripheral neuropathy, as the result of targeting a proteasome involved in the regulation of many proteins with diverse cellular functions.[46] Targeting the F-box protein of an SCF E3 ligase is an attractive therapeutic approach, as the F-box protein defines E3 ligase selectivity and each E3 ligase has fewer target proteins than the 26S proteasome. This means that targeting a specific E3 ligase pathway would have reduced patient toxicity.

To date, no small molecule targeting an F-box protein has entered clinical trials. [78]

2.3 (((3-(2,2-Dimethyltetrahydro-2*H*-pyran-4-yl)-4-phenylbutyl)amino)methyl)-*N*,*N*-dimethylaniline: An SCF^{SKP2} Ligase Inhibitor

(((3-(2,2-Dimethyltetrahydro-2*H*-pyran-4-yl)-4-phenylbutyl)amino)methyl)-*N*,*N*-dimethylaniline (**16a**) was identified as an inhibitor of HeLa cell growth in an *in vitro* reconstituted system containing the cyclin E, CDK2, SKP2, SKP1, Cul-1, RBX1 and cellular extract from vehicle-treated HeLa cells (**Figure 8**).[78] This system could ubiquitinate ^{35}S-labelled *in vitro*-transcribed and -translated p27 and was adapted to a high-throughput format to screen compound libraries. The screen analysed labelled p27 levels (Lanes 1 and 4) and levels of its polyubiquitinated form (Lane 2). In the presence of 30 µM **16a** (Lane 3), ubiquitination was inhibited. Addition of excess SKP2/SKP1/Cul-1/RBX1 (SCF^{SKP2} complex) restored ubiquitination both in the absence of **16a** (Lane 5) and in its presence (Lane 6).

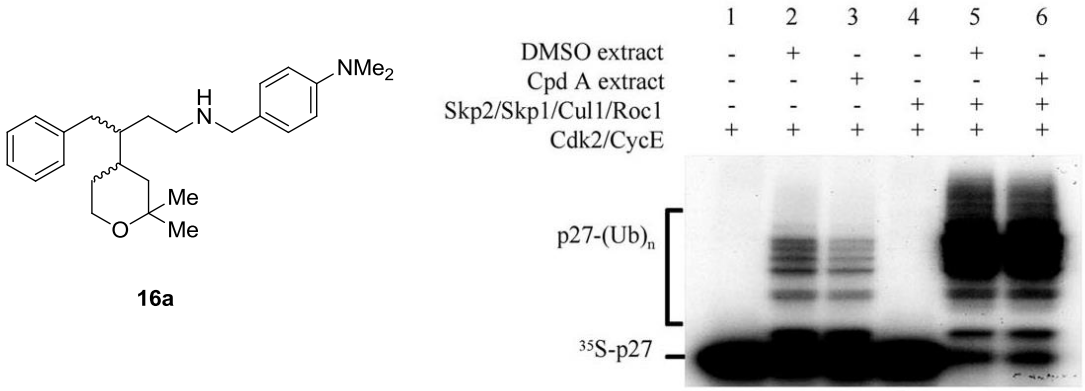

Figure 8: The *in vitro* reconstituted system used to identify HeLa cell growth inhibitors[78] (Cpd A = **16a**; Roc 1 = RBX1)

In a subsequent experiment (**Figure 9**), HeLa cells were arrested in the S-phase and exposed to either a vehicle, 30 µM **16a** or 10 µM proteasome inhibitor MG132 (**17**) for 16 h, then treated with cycloheximide to inhibit protein biosynthesis. Compounds **16a** and **17** extended the half-life of p27 and phosphorylated p27 compared with vehicle-treated cells.

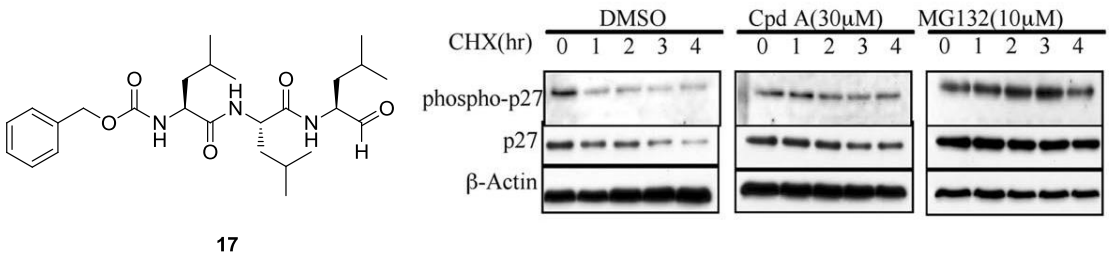

17

Figure 9: Western blots reveal **16a** (Cpd A) and **17** (MG132) extend the half-life of p27 and phosphorylated p27. β-Actin serves as a loading control.[78]

In WT mouse embryonic fibroblast (MEF) cells, 5 μM **16a** increased p21, p27 and p57 levels. In $p27^{-/-}$ cells, it increased p21 and p57 levels and in $SKP2^{-/-}$ cells it had no effect on these proteins' levels (**Figure 10**).[78] This evidence suggests **16a** inhibits the action of SKP2, as the only cells in which **16a** had no detectable effect were those in which the SKP2 had been removed.

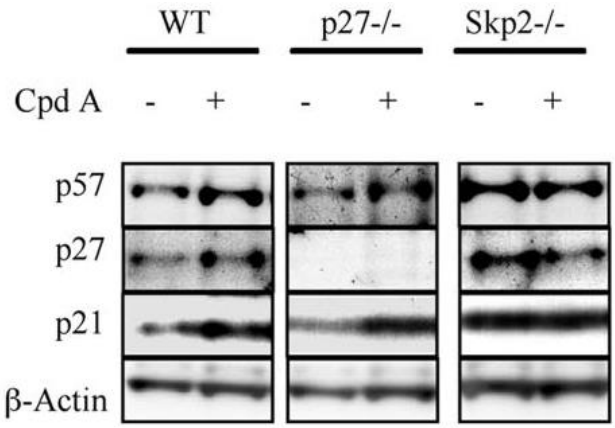

Figure 10: WT, $P27^{-/-}$ and $SKP2^{-/-}$ MEF cells exposed to 5 μM **16a** (Cpd A) for 24 h before Western blot analysis[78]

WT MEFs showed a dose-dependent reduction in viability upon treatment with **16a** (**Figure 11**). $SKP2^{-/-}$ and $p27^{-/-}$ cells showed greater resistance to the increasing doses of **16a**, with only a small drop in viability recorded compared to vehicle-treated cells.

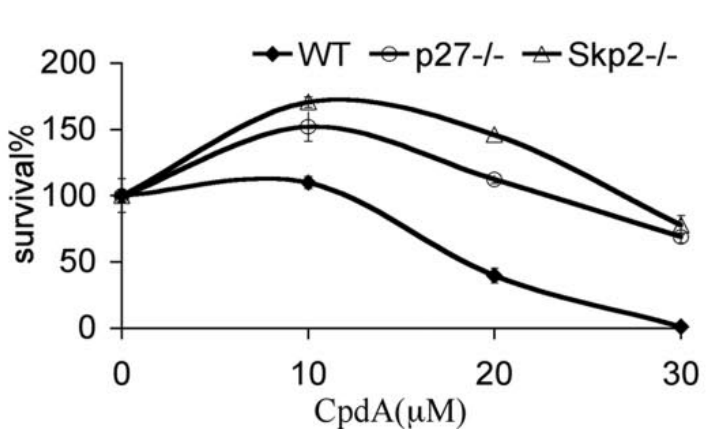

Figure 11 WT, $P27^{-/-}$ and $SKP2^{-/-}$ MEF cells treated with a vehicle or increasing concentrations of **16a** (Cpd A) for 24 h before assessment of cell viability using a WST-1 assay.[78]

RPMI 8226 myeloma cells treated with **16a** or bortezomib (**15**) showed increased levels of p21, p27 and p57 but **15**-treated cells also showed increased levels of β-catenin (an $SCF^{\beta\text{-}TrCP}$ substrate) and c-Jun (an SCF^{Fbxw7} substrate). All MM cell lines treated with **16a** showed a dose-dependent fall in viability, with IC_{50} values ranging from 4.2 ± 0.2 μM for U266 cells to 13.2 ± 1.4 μM for NCI-H929 cells.[78] RPMI 8226 cells treated with **16a** underwent cell cycle arrest at the G_0/G_1 phases, showing a dose-dependent rise in apoptosis, as measured by a correlational rise in positive staining by annexin V.[78]

Melphalan (**18**)-resistant RPMI 8226 and U266 cells showed sensitivity towards **16a** with similar IC_{50} values to their non-melphalan-resistant analogues. Doxorubicin (**19**)-resistant RPMI 8226 and MM1.S cells also displayed sensitivity towards **16a**, demonstrating that **16a** could be used to treat myelomas which have become resistant to currently used medication (**Table 8**).

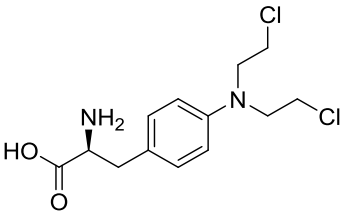

18

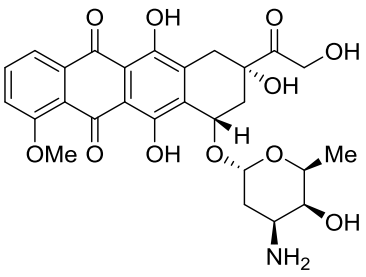

19

Table 8: Comparison of IC_{50} values obtained with various MM cell lines and their drug-resistant counterparts upon treatment with **16a**[a]

Parental Cell Line	16a IC_{50} (μM)	Drug-Resistant Cell Line	16a IC_{50} (μM)
RPMI 8226	8.0 ± 1.1	RPMI 8226/LR5	6.3 ± 1.0
		RPMI 8226/Dox40	8.5 ± 0.9
U266	4.2 ± 0.2	RPMI 8226/LR6	4.3 ± 0.8
MM1.S	5.4 ± 0.4	MM1.RL	5.4 ± 0.7
ANBL-6	10.0 ± 0.4	ANBL-6/B7R	8.0 ± 0.3

(a) Cells were cultured with **16a** for 72 h and cell viability determined using a WST-1 assay. Data represent average IC_{50} plus or minus SD from triplicate assays.

Compound **16a** demonstrated enhanced activity against RPMI 8226 cells when combined with bortezomib (**15**), possibly due to the combined inhibition of protein ubiquitination and of the degradation of proteins which have been ubiquitinated.[78] This suggests that **15** and **16a** could be used synergistically to enhance the accumulation of SCF^{SKP2} substrates.

2.4 Aims of the SKP2 Project

The aim of this project was to design and synthesise a novel, potent antitumour agent targeting the SKP2 pathway, using **16a** for structure-activity studies. The compound was synthesised using the route described by McKenna (**Scheme 1**),[79] and its growth-inhibitory activity *in vitro* was confirmed in HeLa cells using a sulfohodamine B (SRB) assay. Its structure was modified to optimise potency, measured by the half-maximal inhibitory concentration of HeLa cell growth (GI_{50}), and other pharmacokinetic properties including clogP and tPSA.

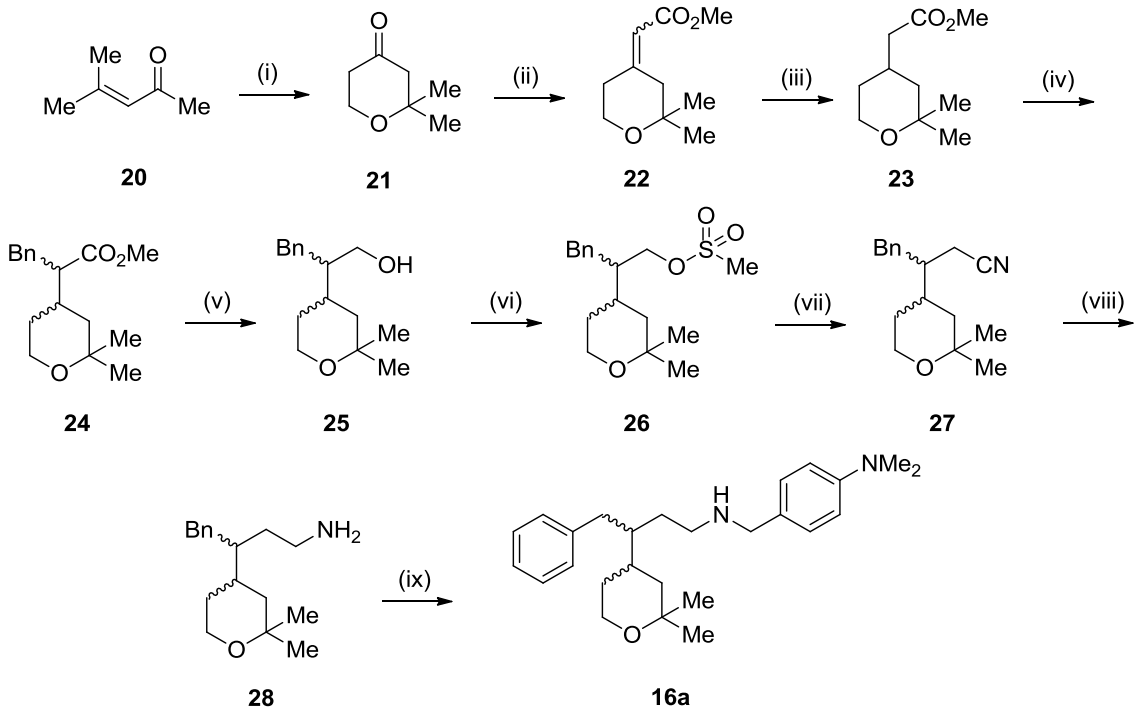

Scheme 1: Literature synthesis of **16a**;[79] (i) CH_2O, Amberlyst-15; (ii) $(MeO)_2(O)PCH_2CO_2Me$, NaH, THF; (iii) H_2, Pd/C, EtOAc; (iv) $^{i}Pr_2NH$, *n*-BuLi, THF, BnBr; (v) DIBAL-H, DCM; (vi) MsCl, $^{i}Pr_2NEt$, DCM; (vii) NaCN, DMF, 100 ^{o}C; (viii) $LiAlH_4$, THF; (ix) 4-(*N*,*N*-dimethylamino)benzaldehyde, $MgSO_4$, DCM; $NaBH_4$, MeOH

Compound **16a** had a suitable molecular mass for a drug candidate (394 g/mol) but had a high clogP (5.8) and low tPSA (24.5 $Å^2$) and potency in myeloma cells. It also had two chiral centres, although it was unknown whether one diastereoisomer was responsible for the observed activity in myeloma and HeLa cells. Determining the significance of the two stereogenic centres in **16a** was another aim of this project. The proposed structural modifications to **16a** for SAR studies are displayed below (**Figure 12**).

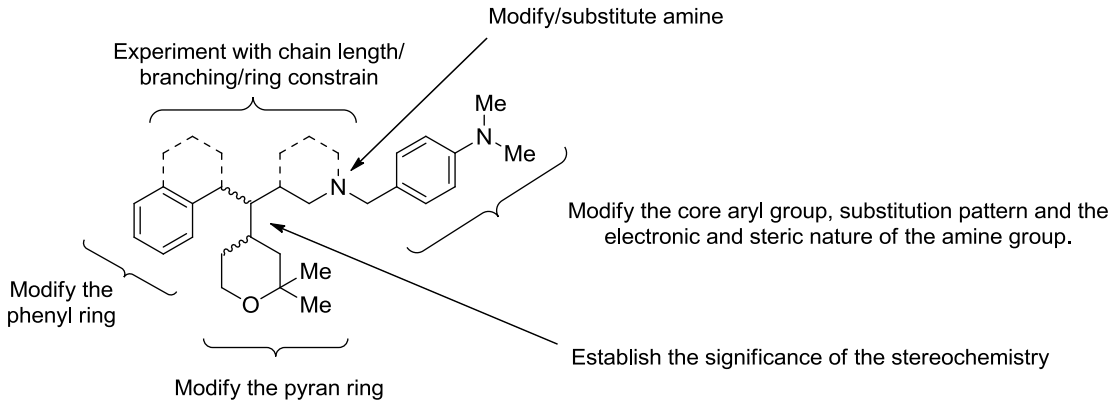

Figure 12: Proposed structural modifications to **16a**

2.5 Competitor Compounds Targeting the SCF^{SKP2} E3 Ligase Pathway

2.5.1 Inhibitors of the SKP2-Cks1-p27 Trimer

Wu *et al.* recently described the identification of several selective inhibitors of the PPI between p27 and the SKP2-Cks1 complex.[80] *In silico* interrogation of the published SKP2-Cks1-p27 crystal structure identified a p27 binding pocket formed at the SKP2-Cks1 interface (**Figure 13**). This pocket was flanked by amino acids SKP2-R294, SKP2-Y346, Cks1-R44 and Cks1-Q52, which were shown to be essential for p27 binding and ubiquitination, interacting with p27-*p*T187 and p27-E185.

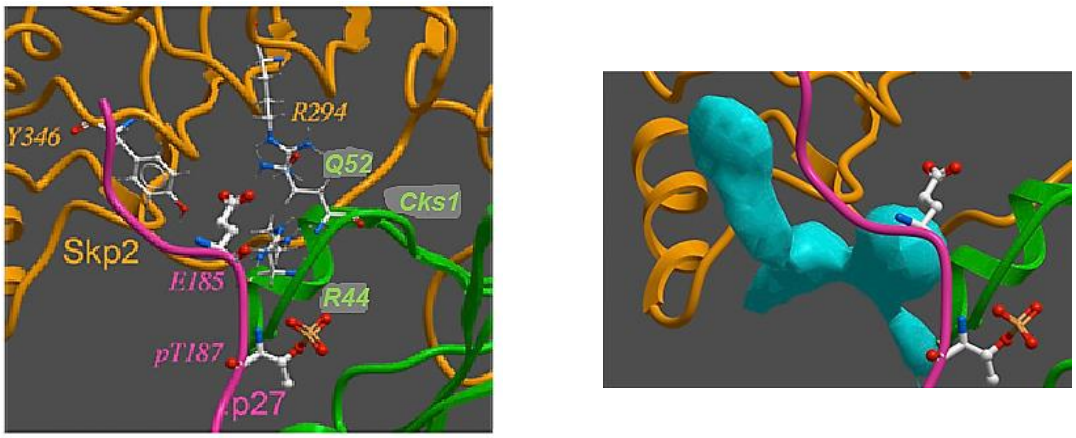

A) **B)**

Figure 13: A) Crystal structure of SKP2 (orange), Cks1 (green) and phosphorylated p27 (purple); **B)** *In silico* binding pocket (blue) identified upon removal of p27. Images created using ICM-PocketFinder (Molsoft, La Jolla, CA, USA); adapted from[80]

Virtual ligand screening (VLS) of 315,000 diverse compounds identified 202 hit molecules, of which 96 were selected, based on their calculated binding scores and Lipinski properties. *In vitro* ubiquitination assays of these 96 compounds identified **29**, **30**, **31** and **32** as modest inhibitors of p27 ubiquitination with good selectivity for non-SKP2-p27 interfaces (**Figure 14**).

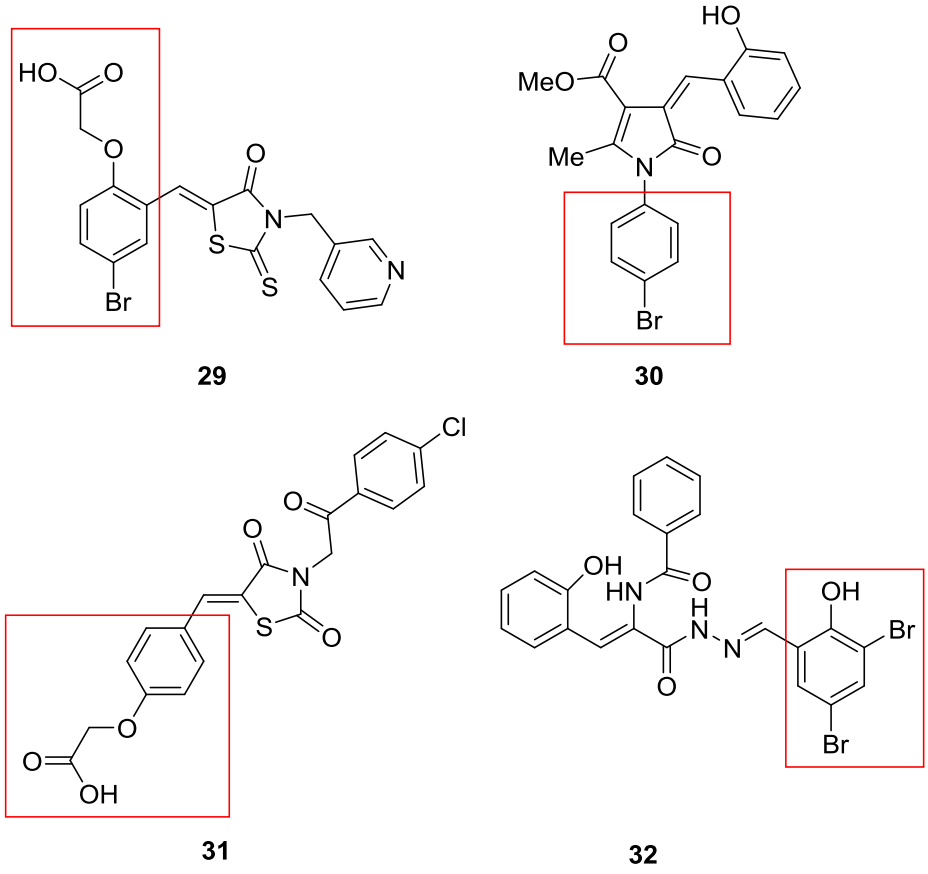

Figure 14: The initial hit compounds identified by *in vitro* screening for selective SKP2-p27 inhibitors. Active groups, thought to be responsible for the observed activity, are shown in the red boxes.[80]

In silico modelling of **29** in the p27 binding domain predicted electrostatic interactions with Cks1-Q52 and/or hydrogen bonding to Cks1-R44 or SKP2-R344 (**Figure 15a**). *In silico* modelling of **30** predicted cation-π interactions with SKP2-R294 and/or hydrogen bonding to Cks1-R44 (**Figure 15b**).

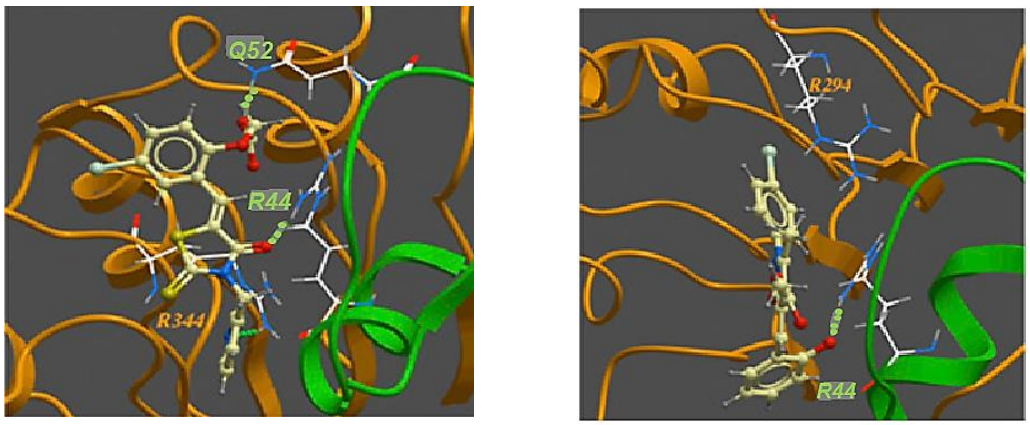

A) **B)**

Figure 15: A) Predicted lowest energy conformation of **29** in the p27 binding domain of the SKP2 (orange)-Cks1 (green) interface. Key residues thought to be involved in binding are highlighted. Electrostatic interactions and hydrogen bonds are shown as dotted lines; **B)** Predicted lowest energy conformation of **30** in the p27 binding domain of the SKP2 (orange)-Cks1 (green) interface. Images created using ICM-PocketFinder (Molsoft, La Jolla, CA, USA); adapted from[80]

Compounds **31** and **32** were thought to have similar binding modes to **29** and **30** respectively and this hypothesis was supported when *in vitro* screening of analogues lacking the chemical moieties thought to be responsible for these interactions (shown in red boxes) exhibited no inhibition of p27 ubiquitination with WT SKP2 and Cks1 (**Figure 16**).

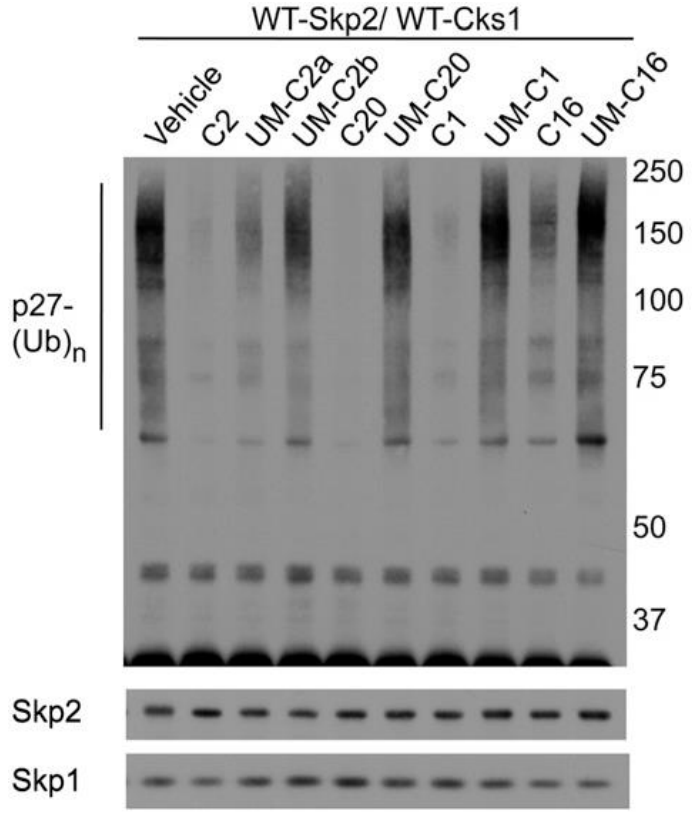

Figure 16: Ubiquitination assays treated either with a vehicle (0.1 % DMSO), 50 µM each inhibitor (**29** (C1), **30** (C2), **31** (C16) or **32** (C20)) or 50 µM analogous unmatched compound (UM) lacking proposed active groups (shown in red boxes in Figure 14)[80]

The significance of the interaction between Cks1-Q52 and the carboxy groups of **29** and **31** was confirmed when these compounds showed activity against WT SKP2 and WT Cks1 but lacked activity with WT SKP2 and Q52L-Cks1 mutants. The fact that Cks1-Q52 was significant for the binding of p27 inidicated that compounds **29** and **31** could be potent inhibitors of the SKP2-p27-cks1 trimer.

To assess the ability of each compound to inhibit p27 ubiquitination in cells, the metastatic melanoma cell line 501 MeI was treated with either a vehicle (0.1% DMSO) or a 10 µM solution of each inhibitor. Levels of p27 were elevated in the presence of these compounds, compared with the vehicle, in a dose-dependent manner (**Figure 17**).

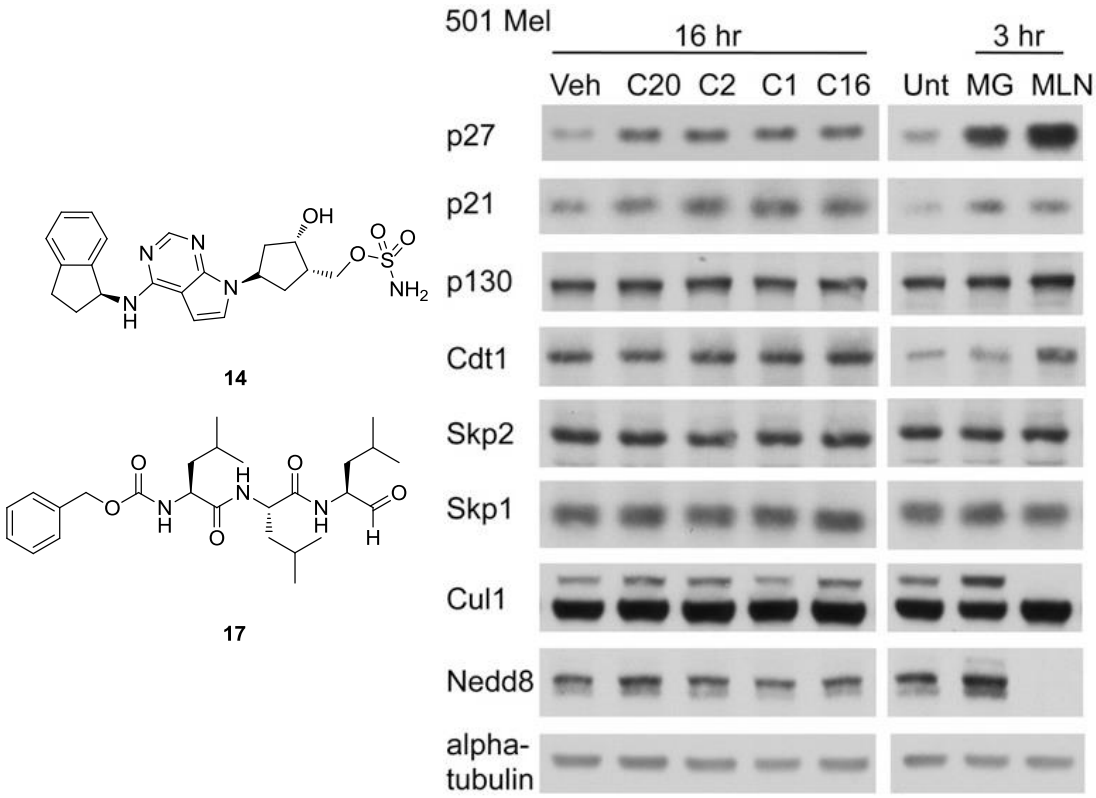

Figure 17: Protein induction assay, immunoblotting for steady-state levels of SKP2 substrates (p27, p21, p130 and Cdt), SKP2, SKP1, Cul1 and Nedd8 in 501 MeI cells, with loading normalised to α-tubulin. Cells treated either with a vehicle (0.1% DMSO), 10 µM each inhibitor (**29** (C1), **30** (C2), **31** (C16) or **32** (C20)), 10 µM MG-132 (**17**) (MG) or 400 nM MLN-4924 (**14**) (MLN). Unt, untreated cells[80]

In 501 MeI cells treated with a vehicle (0.1% DMSO) or 10 µM each inhibitor and subsequently exposed to cycloheximide, cells treated with the vehicle reported a p27 half-life of 1 h but cells treated with one of the SKP2 ligase inhibitors gave p27 half-lives ranging from 3 to > 5 h. Protein levels of SKP2 and SKP1 remained constant, showing that these inhibitors function by increasing the half-lives of SKP2 substrates, without affecting levels of the SCF complex.[80]

These compounds represent some of the first small-molecule inhibitors of SKP2-mediated p27 degradation, which have been shown to function specifically by inhibiting formation of the SKP2-Cks1-p27 trimer. The identified compounds have been shown to induce p27 levels, both in *in vitro* and *in vivo* experiments, establishing a proof of principle for the selective targeting of SCF^{SKP2} as a novel treatment for a variety of cancers.

2.5.2 Inhibitors of the SKP2-SKP1 Interaction

A series of chromone-based small molecules were identified, by high-throughput *in silico* screening[81] and subsequent SAR analysis, to suppress activity of the SCF^{SKP2} E3 ligase and trigger p53-independent cellular senescence and apoptosis.[82] Using HiPCDock software, over 120,000 compounds were screened, of which 25 were predicted to bind with SKP2. One of these compounds (**26a**) was subsequently shown to bind to SKP2 *in vivo* and inhibit the SKP2-SKP1 interaction, thus attenuating E3 ligase activity.

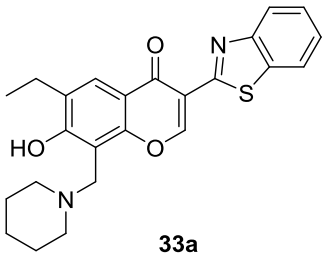

33a

Structural analysis of the SCF^{SKP2} complex (**Figure 18**)[83] had revealed the SKP2 protein interacts directly with SKP1 via its F-box domain. Along the SKP2-SKP1 interface, several residues were shown to contribute significantly to this binding interaction and were termed hot-spot residues. The authors concluded from their hot spot analysis that 19 SKP2 residues made direct contact with SKP1, forming two distinct pocket-like regions.[82] Pocket 1 was located at the *N*-terminus of SKP2, within the F-box motif, and included residues W97, F109, E116, K119 and W127. Pocket 2 was close to the SKP2 *C*-terminus, formed by the leucine-rich repeat (LRR) region and several residues from the F-box.

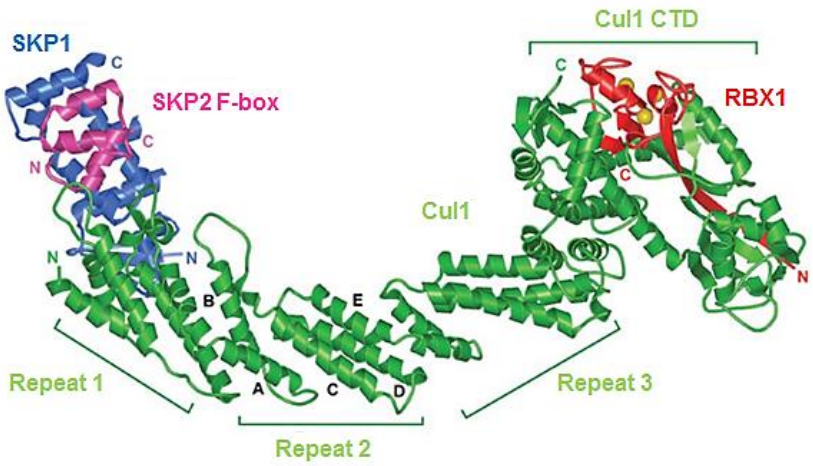

Figure 18: Quaternary structure of the SCF^{SKP2} complex, with the SKP2, SKP1, Cul-1 and RBX-1 proteins coloured in magenta, blue, green and red respectively. Labels A-E represent the 5 α-helices which make up a repeat unit in the cullin protein and three such repeats exist; adapted from[83]

Modelling of **33a** in these binding regions of SKP2 indicated efficient binding in pocket 1 (**Figure 19**). The benzothiazole ring was predicted to make polar contacts and aromatic stacking interactions with W97. The chromone moiety was extended through a pocket, formed by residues D98 and W127, and was predicted to make hydrogen bonds or hydrophobic/aromatic interactions with these amino acids. The ethyl group extended into the region where SKP1 normally bound, therefore inhibiting the interaction with SKP2 and its natural substrate. Finally, the piperidine ring was shown to interact closely with D98 and W127 and so was also essential for binding.[82]

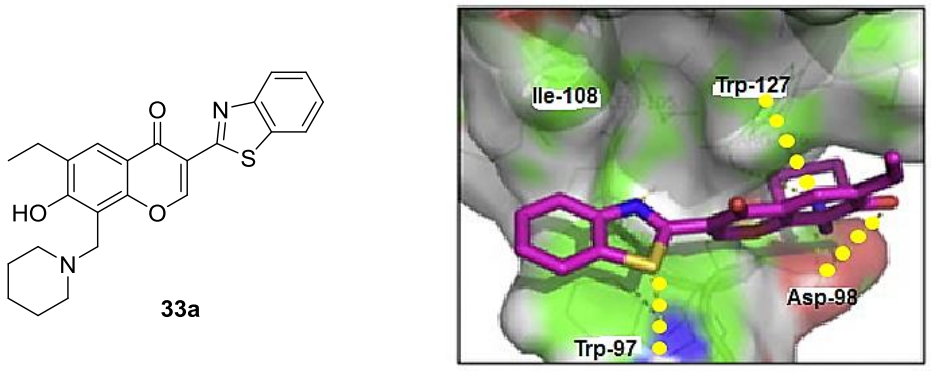

Figure 19: Predicted docking of **33a** in pocket 1 of the SKP2 protein. Yellow dashed lines represent hydrogen bonds between **33a** and the protein. Residues in green form hydrogen bonds/hydrophobic/aromatic stacking interactions with compound **33a**.[82]

In agreement with modelling predictions, analogues of **33a** in which the benzothiazole was replaced by a smaller thiazole ring (**33n** and **33o**) lost all binding affinity (**Table 9**) but the isosteric benzimidazole (**33j**) retained activity. Removal of the ethyl group (**33b**) abolished potency, in agreement with the hypothesis that the ethyl group was projecting into the SKP1-binding region and was thus preventing SKP1 from binding. Attempts to insert groups at the 2-position of the chromone scaffold were detrimental to potency (**33k**, **33l** and **33m**). The 4-chromone scaffold could be replaced by a 2-chromone and retain affinity (**33f**), which was predicted to be due to the molecule adopting a different binding conformation. In support of this theory, the ethyl group was no longer essential for activity in the 2-chromone series, as it was shown by modelling that the piperidine ring was occupying the space thought to be where the ethyl group binds in the 4-chromone series. In the 4-chromone series, the piperidine ring was found to be essential, with ring-opened and substituted ring systems abrogating potency (**33e**, **33g**, **33h** and **33i**). The model had predicted that the piperidine ring occupied a channel formed by residues D98 and W127, and was also in close proximity to R126, therefore substituted derivatives would not be tolerated. Site-directed mutagenesis revealed that **33a** could not inhibit binding between SKP2 W97A or D98A mutants with SKP1, highlighting the importance of these two residues in binding to **33a**.

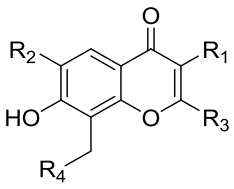

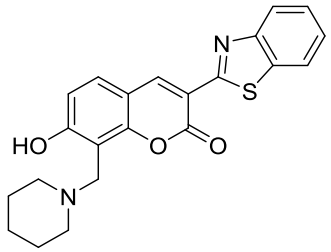

33f

Table 9: SAR studies of compound **26** and its derivatives[82]

ID	R_1	R_2	R_3	R_4	Activity
33a	Benzothiazole	Et	H	-N$(CH_2)_5$	***ACTIVE***
33b	Benzothiazole	H	H	-N$(CH_2)_5$	Inactive
33c	Benzothiazole	H	Me	-N$(CH_2)_6$	Inactive
33d	Benzothiazole	H	Me	-N$(CH_2)_4$	Inactive
33e	Benzothiazole	H	Me	4-*N*-Me-piperazine	Inactive
33f	See above for structure				***ACTIVE***
33g	Benzothiazole	H	Me	2-Me-piperidine	Inactive
33h	Benzothiazole	Et	H	4-Olamine-piperazine	Inactive
33i	Benzothiazole	Et	H	-NEt_2	Inactive
33j	Benzimidazole	Et	H	-N$(CH_2)_5$	***ACTIVE***
33k	Benzothiazole	Et	CO_2Et	-N$(CH_2)_5$	Inactive
33l	Benzothiazole	*n*-Pr	Me	4-*N*-Me-piperazine	Inactive
33m	Benzothiazole	Et	Me	-N$(CH_2)_5$	Inactive
33n	4-Me-thiazole	Et	H	-N$(CH_2)_4$	Inactive
33o	4-Me-thiazole	Et	H	3-Piperidin-3-ylpyridine	Inactive

In vitro binding assays revealed 5 µM **33a** could completely inhibit the SKP2-SKP1 interaction and a similar observation was made *in vivo*, with **33a** impeding this interaction in a dose-dependent manner (**Figure 20a**). *In vivo* p27 ubiquitination assays revealed **33a** inhibited SKP2-mediated p27 ubiquitination and induced p27 and p21 expression in prostate cancer cells (**Figure 20b**).

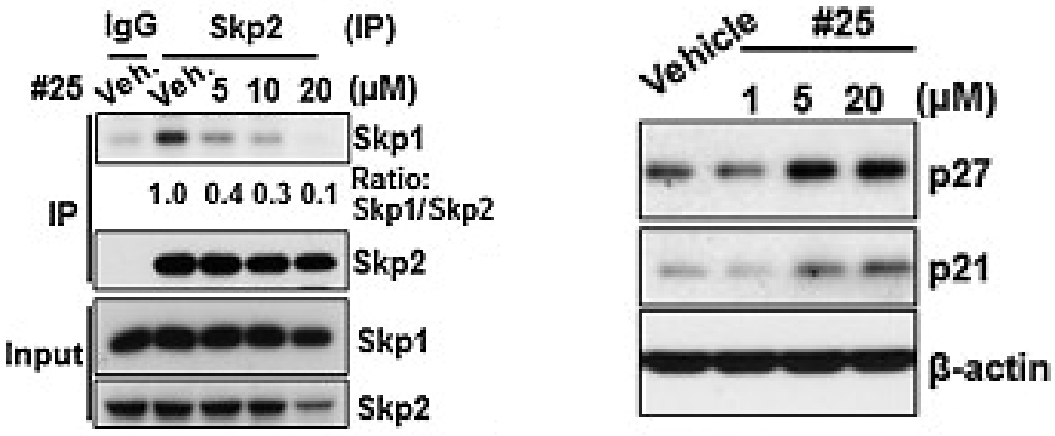

A) **B)**

Figure 20: A) *In vivo* SKP2-SKP1 binding assay with or without #25 (**33a**) in PC3 cells; **B)** Treatment of PC3 cells with either a vehicle or **26** for 24 h before harvesting by immunoblotting assay[82]

Compound **33a** inhibited SKP2-mediated ubiquitination of known SKP2 substrates, including p27, p21 and Akt, however it showed no inhibiting effects on ubiquitination mediated by other SCF E3 ligases, including Fbw-7 and β-TrCP. Consequently, levels of c-Jun, MCL-1 (both Fbw-7 substrates), Snail and IκBα (both β-TrCP substrates) were unaffected upon treatment with **33a**. Compound **33a** was also shown to significantly reduce cell viability in PC3 cells, in contrast to normal prostate PNT1A cells, where cell viability was only slightly affected (**Figure 21**).

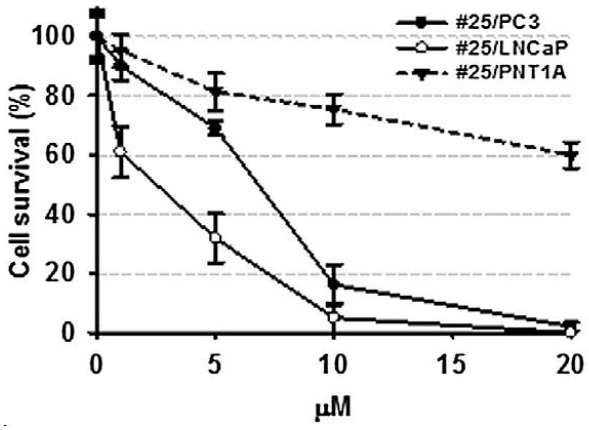

Figure 21: Prostate cancer PC3 and LNCaP cells and normal prostate PNT1A cells were treated with various doses of #25 (**33a**) before analysis by cell survival assay[82]

Compound **33a** caused cell-cycle arrest at the G2/M phase of the cell cycle, an effect that was attenuated in SKP2-silenced cells. The evidence from these studies conclude that **33a** can suppress cell viability of prostate cancer cells by inhibiting SKP2-mediated ubiquitination of cell cycle regulators, including p27, without affecting levels of other E3 ligase substrates and with only limited cytotoxicity in healthy prostate cells.

2.5.3 Inhibitors of the SKP2-Cks1 Interaction

The cyclin-dependent kinase regulatory subunit 1 (Cks1) is an adaptor protein required for p27 ubiquitination by SCF^{SKP2}. In order for p27 to be recognised and targeted for ubiquitination, it must first be phosphorylated at T187, either by CDK2/cyclin E or CDK2/cyclin A. Cks1 binds the CDK/cyclin complex, phosphorylated p27 and SKP2 proteins together (**Figure 22**), therefore disruption of the interaction between SKP2 and Csk1 should prevent p27 ubiquitination and induce p27 expression.

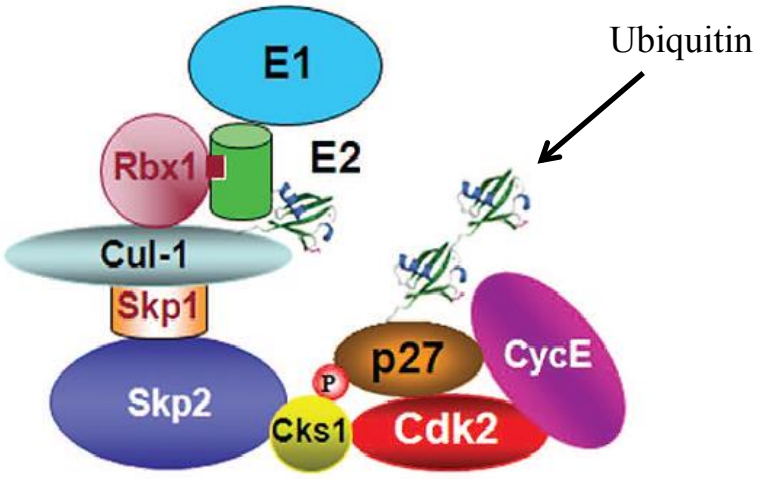

Figure 22: Schematic of the SCF^{SKP2}-dependent ubiquitination of p27 *in vitro*[84]

In an AlphaScreen assay of 3,125 compounds supplied by the National Cancer Institute (NCI) and the National Institutes of Health (NIH) Developmental Therapeutics Program (DTP), 45 were identified as potential inhibitors of the SKP2-Cks1 interaction. Further testing of these hits in an *in vitro* p27 ubiquitination assay revealed 12 compounds with the ability to inhibit p27 ubiquitination. Two of these compounds (**34** and **35**) were investigated further, as they were among the most potent inhibitors of p27 ubiquitination but were also structurally related.[84] The authors did stress that, while both compounds are known to possess antitumour activity, their mechanism of action remains elusive.[85]

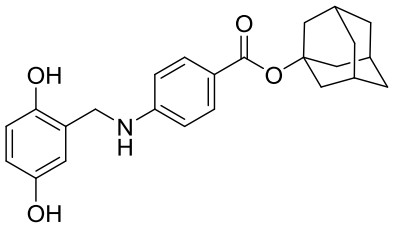

34

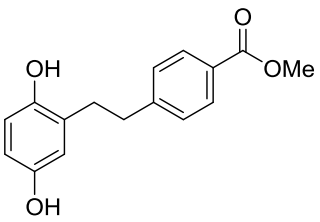

35

SAR analysis on **34** revealed that oxidation to the quinone (**36**) retained activity but monomethylation of either of the hydroxy groups (**37** and **38**) was detrimental to potency (**Table 10**). However, screening the lone quinol (**39**) or quinone fragment (**40**) also gave no activity in the SKP2-Cks1 AlphaScreen assay, implying that it was due to the compound's specific structure rather than the quinol or quinone warhead that was responsible for the observed inhibitory activity.[84]

Table 10: SAR analysis of SKP2-Cks1 Inhibitors[84]

ID	Structure	SKP2-Cks1 IC_{50} (μM)	p27 Ubiquitination IC_{50} (μM)
34	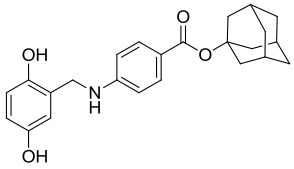	36 ± 6	30
35	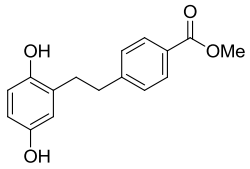	76 ± 7	80
36	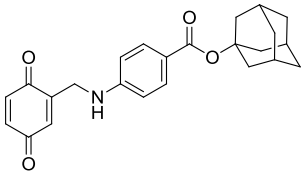	71 ± 4	15
37	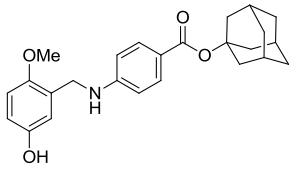	1090 ± 189	> 300
38	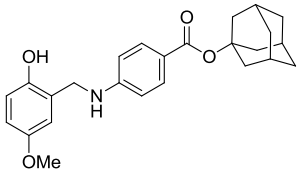	8311 ± 1458	> 300
39	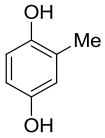	434 ± 40	> 300
40	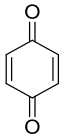	626 ± 66	> 300

Compounds **34** and **35** gave GI_{50} values of 12.8 and 18.5 μM respectively in leukaemia K562 cells and, in the NCI 60 cell lines, returned average GI_{50} values of 1.25 and 7.97 μM respectively. While the authors did concede this wide-ranging activity may be due to inhibition of tyrosine kinases, the evidence provided in these aforementioned assays suggests the compounds may also be involved in preventing p27 ubiquitination via inhibition of the SKP2-Cks1 interaction.

2.5.4 Salinomycin as an Inhibitor of STAT3

Salinomycin (**41**) is isolated from *Streptomyces albus* and has been widely used as an agricultural antibiotic. Koo *et al*. described the cytotoxic properties of **41**; this compound selectively targets cancer stem cells (CSCs) in breast, colorectal, lung and gastric cancer, as well as osteosarcoma and leukaemia.[86] CSCs are a subpopulation of cancer cells possessing genetic alterations which confer drug resistance and disease relapse.

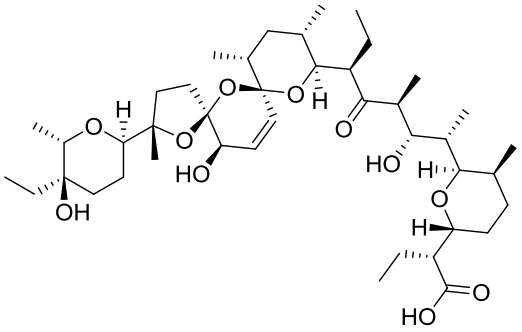

41

Compound **41** induced growth inhibition in human ovarian adrenocarcinoma OVCAR-8 cells, as well as the multidrug-resistant NCI/ADR-RES and DXR cell lines (**Figure 23a**). The latter two cell lines had previously demonstrated resistance to a range of chemotherapeutic agents, including doxorubicin (**Figure 23b**), and were shown to have higher levels of multidrug resistance protein 1 (MDR-1) than the non-drug-resistant OVCAR-8 cells.

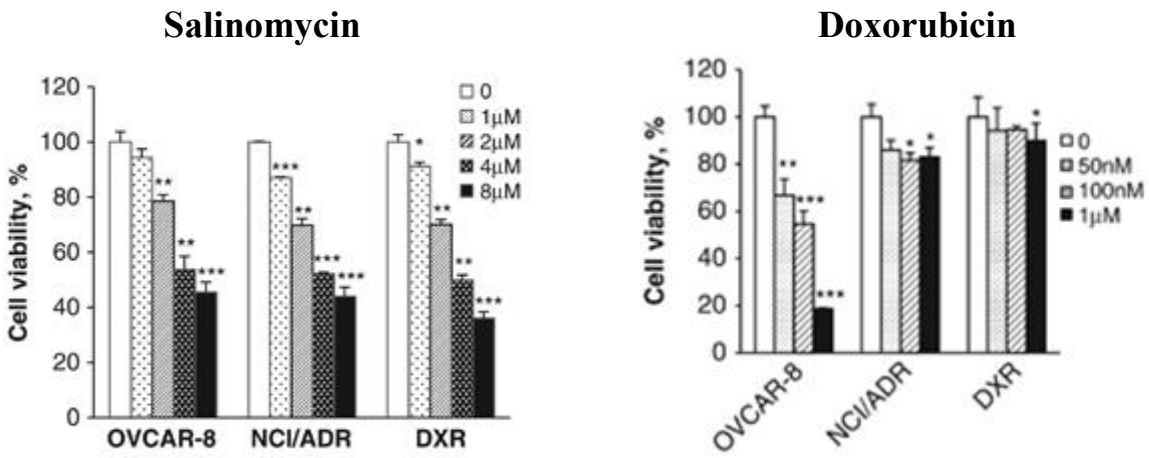

A) **B)**

Figure 23: A) Treatment of OVCAR-8, NCI/ADR and DXR cell lines with various concentrations of **41** over 72 h and monitoring of cell growth inhibition by MTS assay. Data are average values of triplicate measurements, with error bars representing standard deviations. **P* <0.05, ***P* < 0.005 and ****P* < 0.0005; **B)** Treatment of OVCAR-8, NCI/ADR and DXR cell lines with various concentrations of doxorubicin over 72 h and monitoring of cell growth inhibition by MTS assay. Data are average values of triplicate measurements, with error bars representing standard deviations. **P* <0.05, ***P* < 0.005 and ****P* < 0.0005[86]

Compound **41**'s mechanism of action involves the downregulation of SKP2 and it was observed that levels of p27 conversely accumulated on treatment with **41** in all three cell lines (**Figure 24a**). SKP2 degradation was enhanced in cells transfected with si-SKP2 and treated with **41**, but any **41**-induced cell cycle arrest was attenuated in si-p27 cells. In DXR cells, quantitative PCR (qPCR) revealed the levels of SKP2 mRNA reduced by 43% following treatment with **41**, compared with control cells (**Figure 24b**). In the presence of MG132 (**17**), **41**-induced SKP2 downregulation was impeded, suggesting **41** reduces SKP2 levels via a proteasomal pathway.

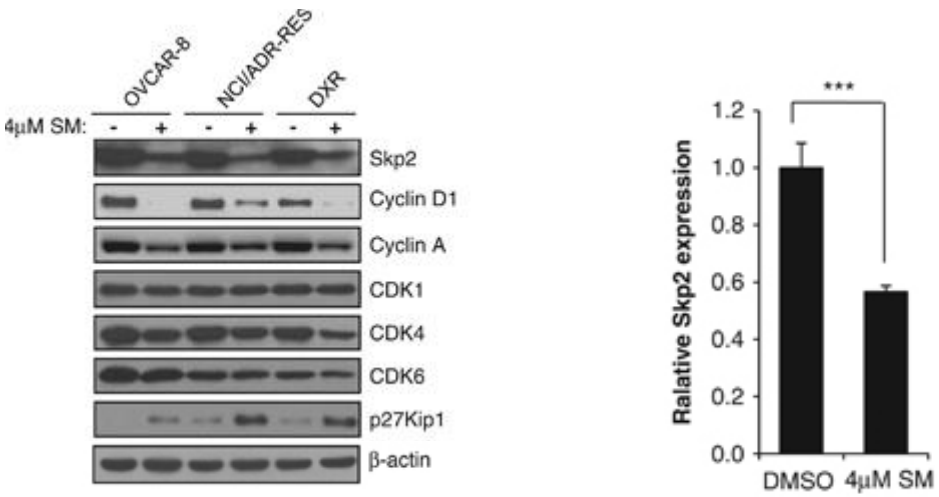

A) **B)**

Figure 24: A) Cells treated with or without 4 μM **41** for 24 h before immunoblot analysis; **B)** DXR cells treated with or without 4 μM **41** for 24 h before determination of SKP2 mRNA by qPCR. ****P* < 0.0005[86]

The mechanism of action of **41** is currently unclear, but it has been shown to inhibit the activity of signal transducer and activator of transcription 3 (STAT3), and with it, decrease levels of known STAT3-target genes, including SKP2. STAT3 is a transcription activator protein which mediates the expression of several genes involved in cell growth and apoptosis. Known STAT3-specific inhibitors, e.g. S3I-201 (**42**)[87], reduced DXR cell viability in a dose- and time-dependent manner similar to that seen upon treatment with **41** (**Figure 25**). Compound **42** also reduced the levels of SKP2 and increased levels of p27. Activation of STAT3, using DXR cells transfected with constitutively active STAT3 (CA-STAT3), attenuated SKP2-downregulation and p27-upregulation mediated by **41**, further establishing **41** as a novel of inhibitor of STAT3 for cancer therapy.

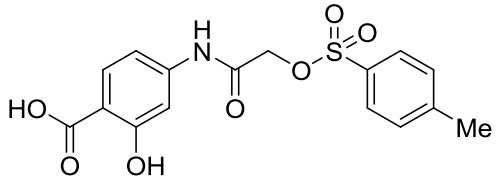

42

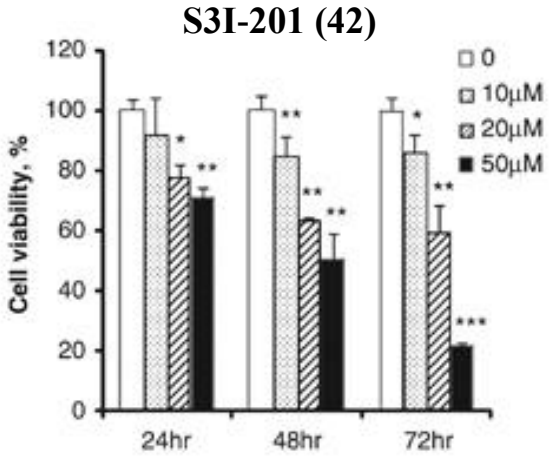

Figure 25: Treatment of DXR cells with increasing concentration of **42** for 24 h and cell viability was measured using MTS assay. Data are average values of triplicate measurements, with error bars representing standard deviations. *P <0.05, **P < 0.005 and ***P < 0.0005[86]

Chapter Three: Project MDMX

3.1 The p53 Tumour Suppressor

Murine double minute X (MDMX), also known as MDM4, interacts with and inhibits the activity of the p53 protein, a tumour suppressor which maintains genomic stability and protects against malignant transformations by inducing cell cycle arrest, apoptosis and senescence in response to cellular stress.[10, 88, 89] The p53 protein is activated in response to oncogenic transformations, extrinsic stress and viral infections and in most cancers the p53 pathway is disrupted.[90, 91] In approximately 50% of cancers the p53 gene is mutated and in the remaining tumours the genes which regulate the p53 pathway are mutated.[91] The latter scenario may include deletion or inactivation of the p53 positive regulator Alternate Reading Frame (ARF) or overexpression of the p53 negative regulators MDM2 and MDMX.[92]

3.2 MDM2

MDM2 is a member of the RING E3 ubiquitin ligase family and promotes proteasome-mediated degradation of p53.[92] MDM2 acts as a molecular scaffold to position p53 and ubiquitin-carrying E2 enzymes in sufficiently close proximity to enable ubiquitin transfer to p53, where it is subsequently degraded.[92] Overexpression of MDM2 inhibits p53-mediated cell cycle arrest and apoptosis and in 30% of human osteogenic sarcomas and soft tissue sarcomas, MDM2 is overexpressed by gene amplification.[10, 89] Hyperactivation due to silencing of ARF expression also leads to p53 inactivation and MDM2 has been an attractive anticancer target for over 20 years.[10]

Binding between the MDM2 and p53 *N*-termini has been explored by X-ray crystallography.[93, 94, 95] Amino acids 15-29 of p53 are a highly conserved region known as Box I or the p53 Transactivation Domain (TAD). Binding between MDM2 and p53 is largely hydrophobic; p53-F19 and p53-W23 are positioned face-to-face on the same side of the α-helix and, like p53-L26, point towards a cleft on the surface of MDM2. These three amino acids become surrounded by the following MDM2 residues: L54, L57, I61, M62, Y67, V75, F86, F91, V93, I99, Y100 and I103. Additionally, intermolecular hydrogen bonds between the following amino acids stabilise the

interaction: p53-F19 with MDM2-Q72, p53-W23 with MDM2-L54 and p53-N29 with MDM2-Y100. In total, 13 residues in the MDM2-p53 binding domain are critically important for a strong interaction between the two proteins but p53 residues F19, L22, W23 and L26 appear fundamental to this binding mechanism (**Figure 26**).[93]

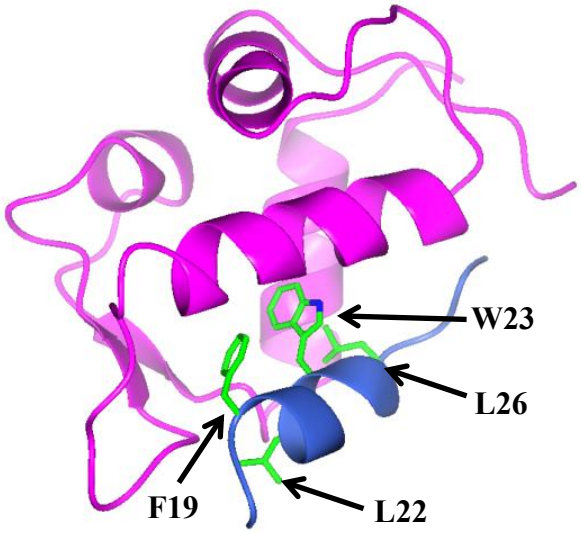

Figure 26: X-ray crystal structure of MDM2 (magenta) bound to p53 (blue). The p53 residues F19, L22, W23 and L26 are highlighted (green). Image created using COOT with CCP4mg plug-in (resolution, 2.6 Å; PDB: 1YCR)[95]

cis-Imidazoline Nutlin-2 (**43**) dissociates the p53-MDM2 complex by competitively blocking the p53-binding sites on MDM2 crucial for a successful interaction (**Figure 27**).[89] Small molecules disrupting this complex can reactivate p53, stimulating *in vivo* tumour regression. Nutlin-3a (**11**) and RG7112 (**12**) sensitise tumour cells to chemotherapy and inhibit the growth of human tumour xenografts in nude mice.[4, 52, 53, 96]

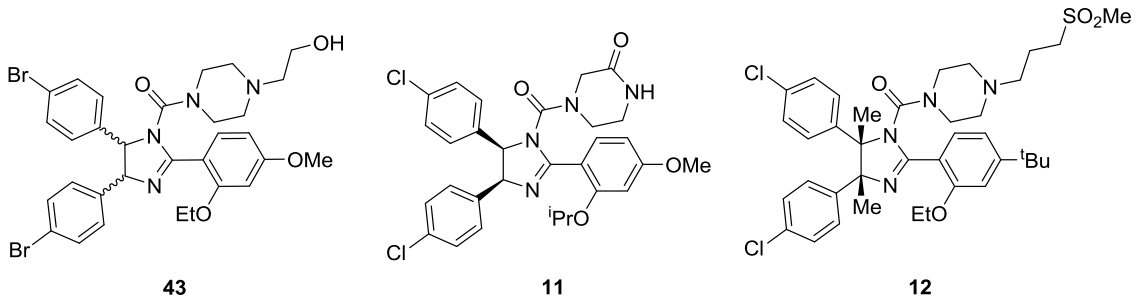

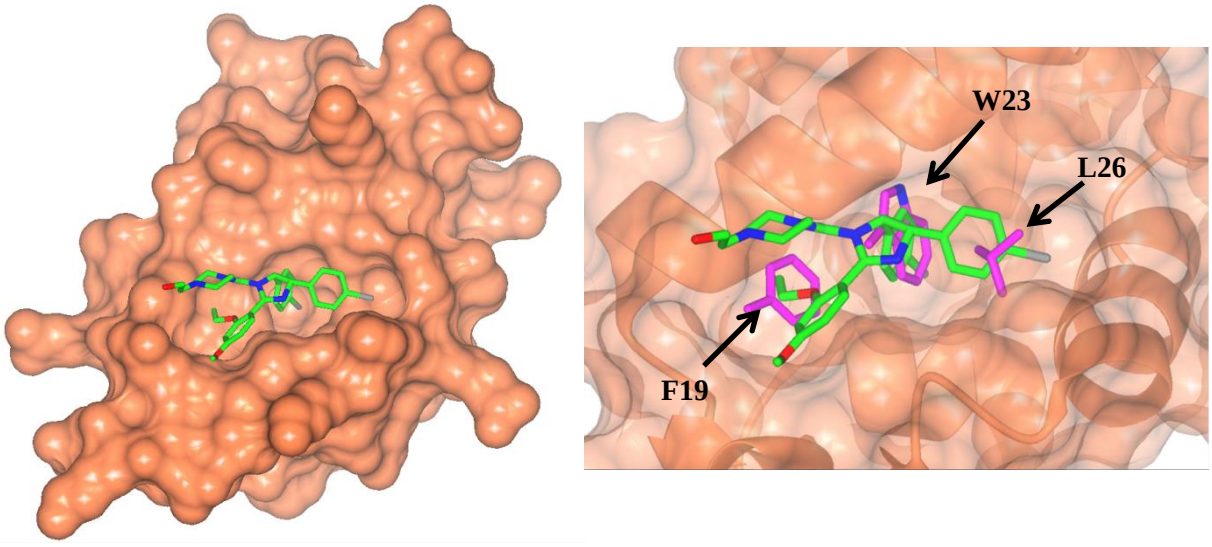

A) **B)**

Figure 27: A) X-ray structure of Nutlin-2 (green) bound to MDM2 (coral); **B)** Same image zoomed in. The MDM2 surface has been made partially transparent. The p53 residues F19, W23 and L26 are overlaid (magenta). Images created using COOT with CCP4mg plug-in (resolution, 2.3 Å; PDB: 1RV1).[52]

3.3 MDMX

MDMX is a negative regulator of p53 with high homology to MDM2, especially in the p53-binding domain.[10, 88, 89, 97, 98] MDMX overexpression has been discovered in a variety of tumour cell lines, most notably 80% of adult pre-B lymphoblastic leukaemia, 60-65% of retinoblastomas, 50% of hepatocellular carcinomas, 50% of head and neck cancers, 25% of bladder cancers, 20% of breast, lung and colon cancers and 14% of melanomas.[10, 89, 92, 99]

Genetic studies show that MDM2 and MDMX perform non-redundant functions to keep p53 inactivated during embryogenesis and later development.[92] MDMX-knockout mice die *in utero* despite the presence of MDM2.[10, 90] Overexpression of MDM2 and MDMX is mutually exclusive in cancer cells, suggesting that transformation of just one of these

proteins is sufficient to inactivate p53 and initiate carcinogenesis.[89] MDMX knockdown leads to p53-dependent growth arrest and apoptosis in breast carcinoma and retinoblastoma cell lines, which suggests that, in the absence of changes to other p53 regulatory proteins, MDMX-dependent inhibition of p53 is essential for tumourigenesis.[92] Despite high structural homology between MDM2 and MDMX, most small-molecule inhibitors of the p53-MDM2 interaction fail to strongly inhibit p53-MDMX binding.[89] Nutlins cannot induce apoptosis in cancer cells with increased MDMX levels, showing a 40-fold weaker equilibrium binding constant (K_i) for MDMX than for MDM2.[89, 91]

MDMX and MDM2 are negative regulators of p53 activity but MDMX does not have intrinsic E3 ligase activity and does not promote p53 degradation.[10] Instead, MDMX binds to MDM2 via their *C*-terminal RING domains, forming a heterodimer with enhanced E3 ligase activity relative to monomeric or homodimeric MDM2.[10] Quantitative analysis of normal human fibroblasts and mammary epithelial cells suggests endogenous MDMX levels are approximately 10-20% of those of MDM2.[92] The high binding affinity of the MDM2 RING domain for that of MDMX suggests most MDMX exists as a heterodimer with MDM2 in normal cells. Immunoprecipitation of MCF-7 breast cancer cells (MDMX overexpressed) indicate that the MDM2:MDMX heterodimer is the predominant complex. No MDMX homodimers have been observed.[92]

MDM2 requires only ubiquitin and E1 or E2 enzymes to catalyse p53 ubiquitination *in vitro*.[92] However, MDM2-mediated inhibition of p53 is inadequate in the absence of MDMX as evidenced by the embryonic lethality or postnatal induction of cell cycle arrest and apoptosis in mice.[92] When MDMX is absent, higher concentrations of MDM2 are required to maximise the formation of homodimers to elicit an equivalent effect. The data conclude that, while MDM2 can successfully ubiquitinate and degrade p53, the presence of MDMX and the formation of heterodimers augments E3 ligase activity and reduces the concentration of MDM2 required for efficient p53-degradation.[92]

Mice which overexpressed MDMX developed tumours earlier than a control group of mice which did not express MDMX.[99] Out of 75 mice overexpressing MDMX, twenty (27%) developed tumours during an 18-month observation period, four of which had more than one type of tumour. MDMX levels were higher in the cancer tissues relative

to the normal tissues, suggesting that overexpression of MDMX contributes to a tumour phenotype.[99] The mice which overexpressed MDMX showed reduced MDMX levels in spleen samples following exposure to ionising radiation (IR). This is essential to induce MDM2 self-degradation and MDM2-mediated degradation of MDMX to elicit a p53 DNA damage response (**Figure 28**). However, p53 levels were less stabilised in these spleen samples compared with those of WT mice, suggesting that MDMX overexpression diminished the p53 response following IR. High MDMX levels could therefore affect the efficacy of radiotherapy in cancer patients.[99]

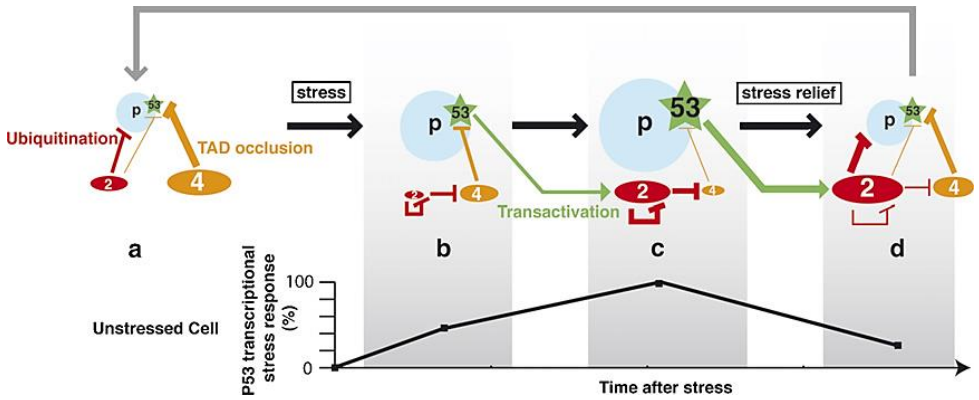

Figure 28: The roles of MDM2 and MDMX in mediating the p53 response; (a) In unstressed cell, p53 levels are kept low (MDM2-mediated degradation) and inactive (MDMX-mediated TAD domain blocking). (b) Initial stress response: MDM2 stops targeting p53 and degrades itself and MDMX. (c) Maximum p53 activation initiates DNA repair/cell-cycle arrest and increases MDM2 levels (green arrow), enhancing MDMX degradation. (d) Stress response complete: MDM2 targets p53 again, MDMX levels rise and p53 levels fall. The cell can now re-enter the cell cycle (grey arrow). In this diagram, p53 stability is represented as a blue circle and its activity as a green star. MDM2 and MDMX are represented as red and orange ovals respectively.[93]

Studies of the deubiquitinating enzyme Herpes Virus-Associated Ubiquitin-Specific Protease (HAUSP) explain how MDM2 switches from ubiquitinating p53 in unstressed cells to targeting itself and MDMX following DNA damage.[93] HAUSP interacts with and stabilises MDM2, MDMX and p53. When cells are unstressed, the Death Domain-Associated Protein (Daxx) associates with MDM2 and HAUSP forming a trimer, which reduces the autoubiquitination of MDM2, allowing it to target p53. DNA damage disrupts the trimer resulting in increased MDM2 degradation and subsequent p53 stabilisation.

Ten of the thirteen residues in the MDM2-p53 binding domain which are critically important for a strong interaction are conserved in MDMX. Additionally, MDM2 and MDMX possess a flexible 'lid', composed of residues 16-24 in both proteins. This region regulates binding between either proteins with p53 but it does not share a conserved homology.[92, 93] This suggests the p53-MDM2 and p53-MDMX interfaces have subtle but distinctive differences. MDMX possesses a P95-S96-P97 motif at the end of the α-helical domain in the p53 binding site, which is absent in MDM2.[92] It has been proposed that the proline residues shift the α-helical section of MDMX, relative to MDM2, and make the p53-binding site in MDMX shallower and less accessible to small molecules.[92] The shallower binding site of MDMX and the contrasting amino acid sequence which makes up residues 16-24 could explain why MDM2 inhibitors do not have the same efficacy against MDMX.[10, 92] However, the p53 residues F19, W23 and L26 appear fundamental to the interaction with MDM2 and MDMX and it is these residues which MDMX inhibitors will be designed to mimic (**Figure 29**).

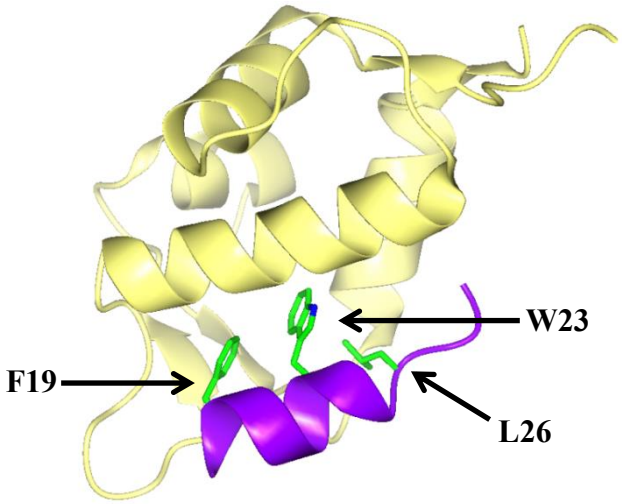

Figure 29: X-ray structure of MDMX (yellow) bound to p53 (purple). The p53 residues F19, W23 and L26 are highlighted (green). Image created using COOT with CCP4mg plug-in (resolution, 1.9 Å; PDB: 3DAB).[100]

3.4 Aims of the MDMX Project

The aim of this research project was to design and synthesise a novel inhibitor of the MDMX-p53 interaction. A series of 2-amino-4-substituted thiazoles with modest activity against MDMX and MDM2, including **44a**, were identified in a screen of several hundred compounds. The molecule was structurally altered with the aim of improving potency against MDMX and achieving selectivity over MDM2. An EU-funded Framework Program 6 initiative set up between various institutions, including Newcastle University and Siena Biotech, termed DePPICT (Design of Protein-Protein Interaction Inhibitors for Cancer Therapy), financed the program.

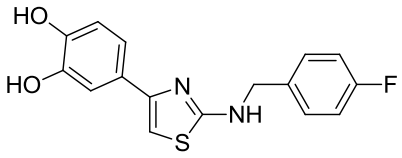

44a

The compound had moderate ligand efficiency (LE) (MDM2, 0.31; MDMX, 0.29) and a low molecular weight (377.3 Da), making it a suitable hit compound. The catechol ring, 2-aminothiazole scaffold and 4-fluorobenzyl substituent were all modified to construct SARs (**Figure 30**).

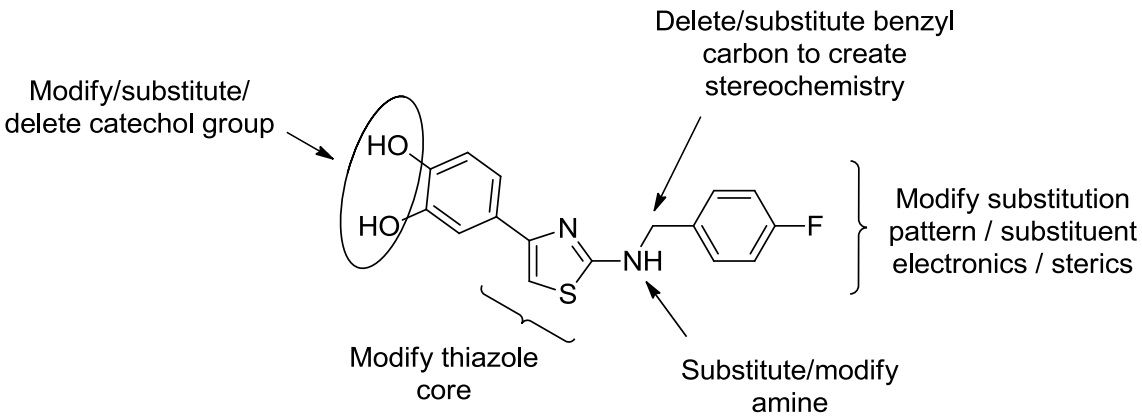

Figure 30: Structural modifications made to the 2-aminothiazole scaffold

As well as potency against MDMX (IC_{50} < 10 nM) a suitable drug candidate needed to have high LE and lipophilic efficiency (LipE). LE is a parameter which measures compound potency relative to molecular mass and is calculated by dividing the pIC_{50} by the number of non-hydrogen atoms in the compound. LipE measures compound potency relative to lipophilicity and is calculated by subtracting the clogP or $clogD_{7.4}$ value from the pIC_{50}. In this project, a drug candidate needed to have a LE value of at least 0.30 and a LipE value of at least 5.0.

The catechol moiety, 2-aminothiazole ring and benzyl methylene group were all potential sites of metabolism. Catechols are often glucuronidated *in vivo* to produce polar compounds which are easily excreted (**Scheme 2**). They can also be oxidised by cytochrome P450 (CYP450) enzymes to give *ortho*-quinones which are highly electrophilic Michael acceptors with potential genotoxicity. Two-amino thiazoles have demonstrated hepatotoxicity *in vivo* in previous drug discovery projects due to oxidation of the heterocycle to a thiourea.[112, 113] Benzyl methylene carbons are a well-characterised area of CYP450-mediated oxidation to give hemi-aminals, which can fragment to give aldehydes.

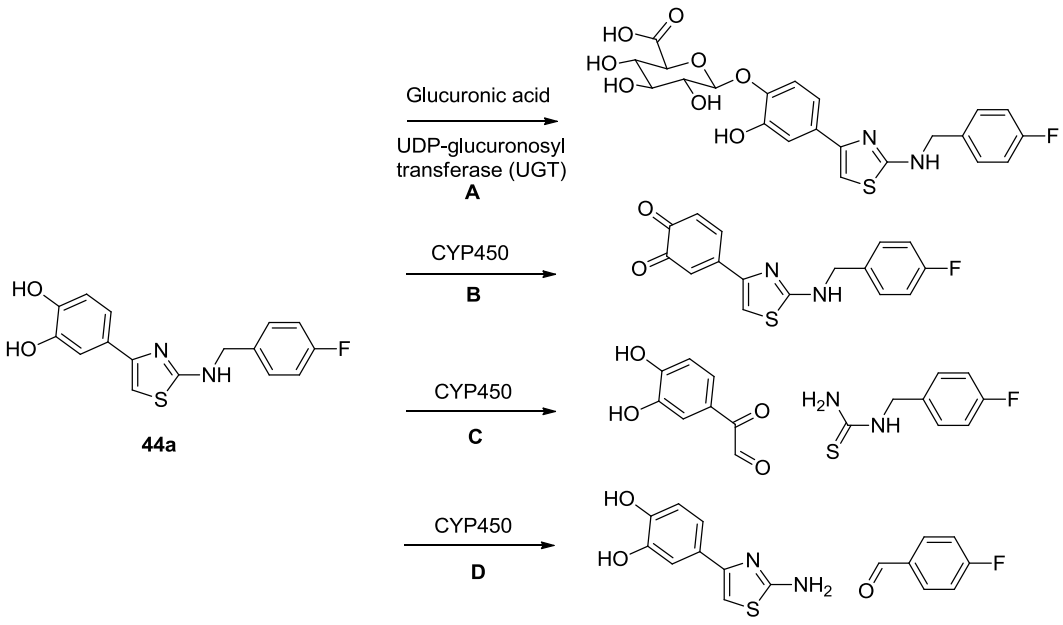

Scheme 2: Potential metabolic pathways for 44**a**, including glucuronidation (**A**) and CYP450-mediated oxidation to give an *ortho*-quinone (**B**), thiourea (**C**) and aldehyde (**D**)

Desirable lead compounds produced in this project had to therefore possess suitable metabolic resistance and not produce potentially toxic metabolites. Preliminary work conducted at Newcastle University (E. Bulatov, MPhil 2009-10) investigated whether the catechol ring could be substituted for more metabolically stable groups and retain activity (**Table 11**).[114] The significance of the halogen substituent for improving target activity was also investigated (**Table 12**).[114]

Table 11: ELISA inhibition data for thiazoles **44a-44j**[114] (conducted by Dr Yan Zhao at the NICR)

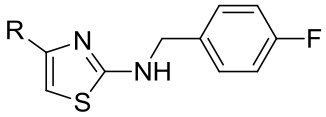

ID	R	MDMX IC_{50} (μM)[a]	MDM2 IC_{50} (μM)[b]	Ratio (MDMX : MDM2)
44a	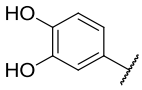	24.7	12.1	0.49
44b		650 ± 150	260 ± 35	0.40
44c	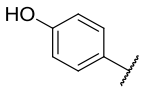	64 ± 7	17 ± 5	0.27
44d	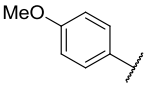	351 ± 19	93 ± 24	0.26
44e	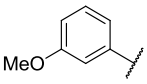	919 ± 81	468 ± 175	0.51
44f	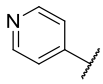	200 ± 3	115 ± 28	0.58
44g	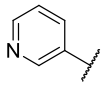	909 ± 62	859 ± 273	0.94
44h	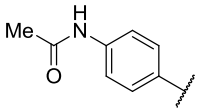	677	38	0.06
44i	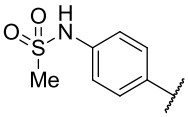	200 ± 40	110 ± 30	0.55
44j	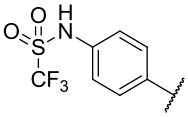	5.7 ± 1	11 ± 2	1.93

(a) $n = 2$; (b) $n = 3$

Elimination of the 3-hydroxy substituent (**44c**) had little effect on MDM2 and MDMX affinity, but elimination of the 3- and 4-hydroxy groups (**44b**) abolished potency against both targets. The fact that methylation of the 4-hydroxy group also abrogated activity against both proteins (**44d**) suggested the hydroxy group was functioning as a hydrogen bond donor but not an acceptor. Pyridyl rings (**44f** and **44g**) were equally inactive to the

benzene ring with no 4-hydroxy group present. Replacement of the 4-hydroxy group with isosteric hydrogen bond donors (**44h** and **44i**) reduced activity against both proteins, but substitution for a trifluoromethylsulfonamide (**44j**) afforded a 4-fold increase in MDMX-activity **44a**. The fact that the methylsulfonamide (**44i**) was less active than **44j** suggested substituent size and acidity were the key determinants of activity.

Table 12: ELISA inhibition data for thiazoles **44c** and **44j-44q**[114] (conducted by Dr Yan Zhao at the NICR)

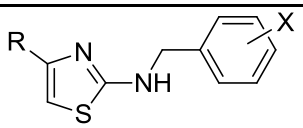

ID	R	X	MDMX IC_{50} (μM)[a]	MDM2 IC_{50} (μM)[b]	Ratio (MDMX : MDM2)
44c	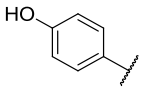	4-F	64 ± 7	17 ± 5	0.49
44k	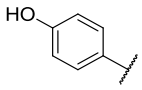	H	150 ± 20	77 ± 22	0.51
44l	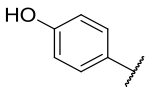	4-Cl	32 ± 9	5.6 ± 1.3	0.18
44m	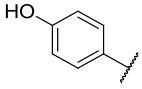	4-Br	20 ± 5	6.9 ± 1.2	0.35
44n	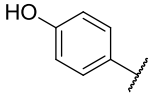	3-Cl	270 ± 91	36 ± 3	0.13
44o	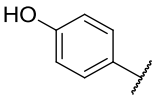	3-Br	192 ± 9	44 ± 5	0.23
44j	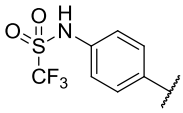	4-F	5.75 ± 1	11 ± 2	1.93
44p	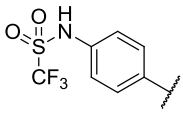	4-Cl	17 ± 4	6.2 ± 2	0.36
44q	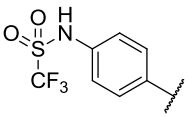	4-Br	6.0 ± 1	5.5 ± 4	0.92

(a) $n = 2$; (b) $n = 3$

para-Halogenated rings (**44a**, **44l**, **44m**, **44j**, **44p** and **44q**) improved potency against both proteins compared to the unsubstituted ring (**44k**). The difference in activity between different halogens was small, suggesting their electronics were more important than their steric bulk. p*ara*-Substituted rings were more active against both proteins than their *meta*-substituted derivatives (**44l** vs. **44n** and **44m** vs. **44o**) but it was clear that the substituent at the *para*-position of the 4-aryl group was more significant for determining potency than the halogen.

3.5 Literature Compounds with Moderate MDMX Inhibitory Activity

There are three strategies to inhibit the oncogenic activity of MDMX, the first of which is to reduce MDMX levels to increase p53 activity. Down-regulation of MDMX mRNA has been shown to activate p53 and induce cell cycle arrest *in vitro*. However, improvements to the delivery of RNA-interfering agents to solid tumours must be made before this is considered a viable treatment option.[92] A second approach is to target the proteins involved in the transcription and translation of MDMX. The transcription factors c-Ets-1 and Elk-1 have been described as key regulators of these processes[101] but they are general transcriptional co-activators and any attempt to deregulate their activity would likely have off-target effects.[92]

A third approach is to target the MDMX protein, either by enhancing MDMX proteolysis pathways or inhibiting those which prevent MDMX degradation. Targeting the MDMX-HAUSP interaction could be an effective cancer therapy[92, 93] but proving this method results in potent antitumour activity is difficult, as HAUSP has multiple substrates, so any observed therapeutic benefit may not originate from inhibition of MDMX.[92] Targeting the interaction between MDMX and MDM2 is another potential therapeutic strategy. The two proteins are linked via their RING domains but the RING-RING interaction would be difficult to drug because crystal structures reveal it lacks a defined catalytic site or any hydrophobic pocket into which a small molecule could bind.[92, 102] Small-molecule inhibition of the p53-MDMX interaction is an attractive approach to cancer therapy. MDMX is a negative p53 regulator so disrupting this interaction should restore p53-mediated cell cycle arrest and apoptosis.[92] The subtle structural differences between MDM2 and MDMX necessitate the design of small molecules that specifically target the MDMX-p53 interaction, as potent inhibitors of the

MDM2-p53 interaction show comparatively reduced efficacy.[89, 91]The following sections review literature attempts to disrupt the MDMX-p53 interaction.

3.5.1 SJ-172550

High-throughput screening of more than 200,000 compounds at the St. Jude Research Hospital, TN, US, with the aim of finding novel small-molecule inhibitors of the MDMX-p53 interaction, identified over 1,000 active compounds. Dose-response assays on all compounds in MDMX, *h*MDMX and *h*MDM2, and Weri-1 cell-based assays (MDMX amplified), identified SJ-172550 (**45**), as the first small-molecule MDMX inhibitor.[91]

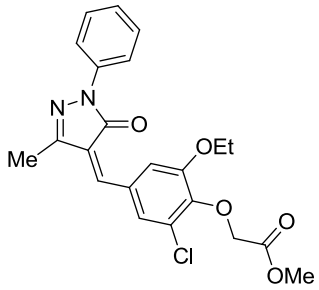

45

Compound **45** was found to bind reversibly with MDMX to inhibit p53 binding, with an IC_{50} of 4.3 µM against WT p53 in *in vitro* assays. Isobologram experiments in which **45** and Nutlin-3a (**11**) were incubated with Weri-1 retinoblastoma cells indicated an additive inhibitory effect on cell growth. In a separate experiment, Weri-1 and RB355 retinoblastoma cell lines and ML-1 leukaemia cells (WT p53) were exposed to 20 µM **45** for 20 h before analysis by immunofluorescence (**Figure 31a**). Cells exposed to **45** demonstrated modest accumulation of p53 compared with vehicle-treated cells, though not to the same extent as cells exposed to **11** or ionising radiation (IR). Apoptosis was induced in **45**-treated cells in a p53-dependent manner (**Figure 31b**)

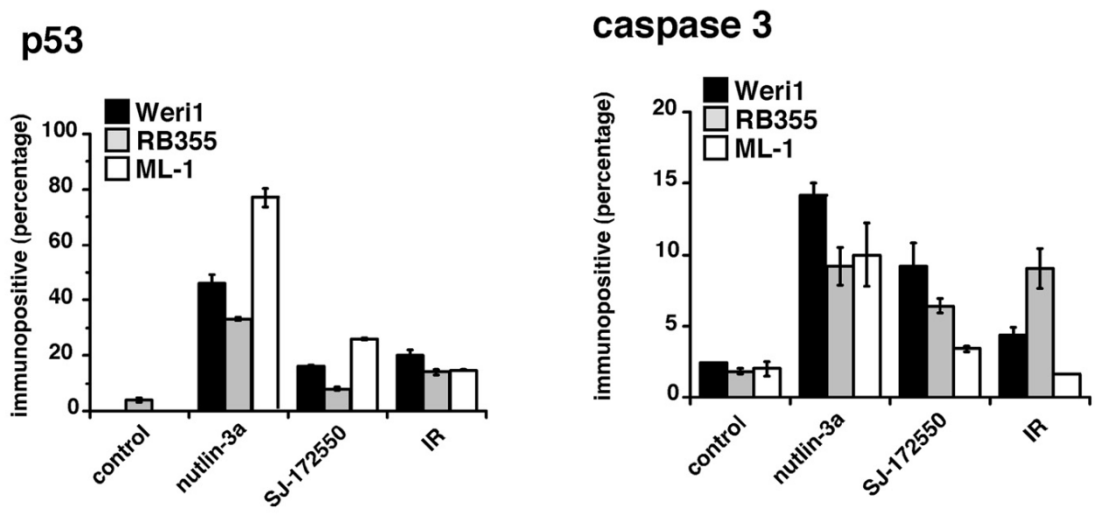

A) **B)**

Figure 31: A) p53 induction on exposure of Weri-1, RB355 and ML-1 cells to DMSO (control), 5 µM Nutlin-3a (**11**), 20 µM SJ-172550 (**45**) or IR. **B)** caspase-3-mediated apoptosis in Weri-1, RB355 and ML-1 cells exposed to DMSO (control), 5 µM Nutlin-3a (**11**), 20 µM SJ-172550 (**45**) or IR.[91]

A reduction in potency was observed for **45** against several MDMX mutants (**Table 13**). Some mutants (e.g. H54F) were predicted to displace **45** without affecting peptide binding while other mutations (e.g. M53L) were predicted to make the p53 binding domain of MDMX more structurally similar to that of MDM2, therefore reducing **45** potency without affecting that of **11**. Compound **45** is the first small molecule to inhibit the MDMX-p53 interaction and establish a proof of principle that this effect can induce apoptosis in cancer cell lines.

Table 13: IC_{50} values obtained for binding of WT p53, Nutlin-3a (**11**) and SJ-172550 (**45**) to several MDMX mutants[91]

Inhibitor	**MDMX Mutation**							
	WT	**M53L**	**H54F**	**Q58D**	**M61F**	**Y66I**	**Q71K**	**QUAD**
p53 peptide (µM)	1.4	2.3	1.4	1.3	2.4	15.7	12.4	38.9
11 (µM)	29.5	12.8	69.1	43.4	>400	22.3	ND	ND
45 (µM)	4.3	14.7	12.7	8.3	9.6	7.0	ND	ND

WT, wild-type; QUAD, quadruple mutant (P95H, S96R, P97K and R103Y); ND, not determined

Published data on the mechanism of action of **45** has shown that MDMX can exist in various conformations, which differ in affinity for p53 and small molecules.[103] Compound **45** binds covalently to MDMX-C76 and it is possible that non-reducing

conditions cause a conformational shift in the MDMX protein which exposes C76.[103] Nucleophilic attack of the cysteine thiol on the β-carbon of the ene-amide functionality in **45** was predicted to be major binding mechanism and saturation of this group to give **46** reduced MDMX inhibitory activity 30-fold (**Figure 32**).

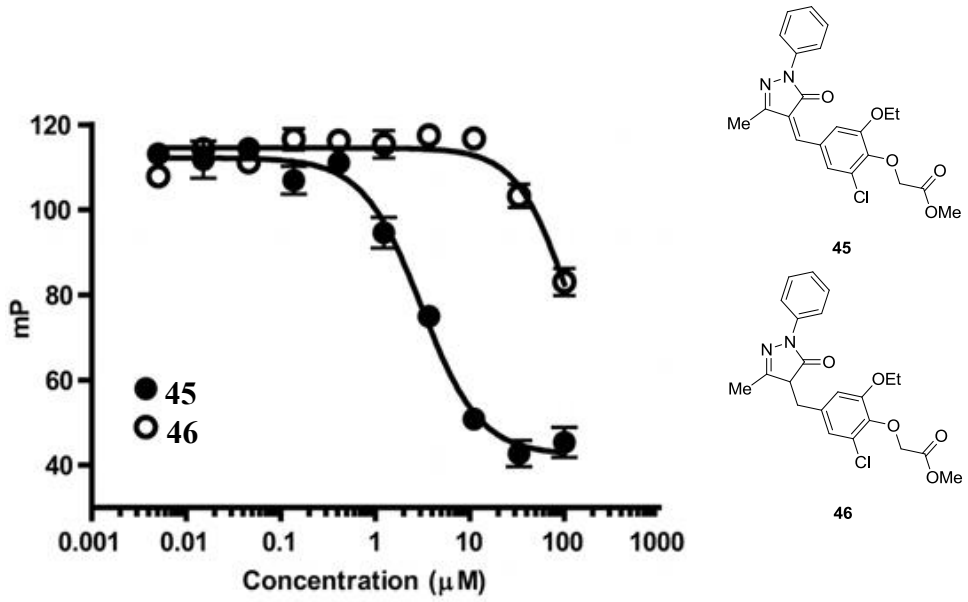

Figure 32: FP assay measuring MDMX-p53 inhibition by **45** (IC_{50}, 3 μM) and **46** (IC_{50} > 100 μM).[103] mP, milli-polarisation units

Compound **45** showed 10-fold reduced activity against a C77V MDM2 mutant compared with inhibition of WT MDM2, suggesting that **45** is not a competitive inhibitor of MDMX but instead causes a conformational change that reduces p53 affinity.[103]

3.5.2 Imidazole-based MDMX Inhibitors

Several published imidazole-based MDM2 inhibitors have demonstrated moderate MDMX inhibitory activity (**Table 14**).[104] The published data explained how the significant structural differences between the two proteins prevented a dual inhibitory effect being observed and this data could therefore be used to develop a potent MDMX inhibitor.

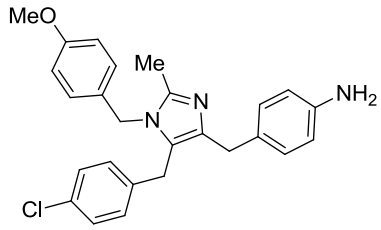

47

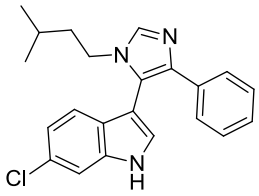

48

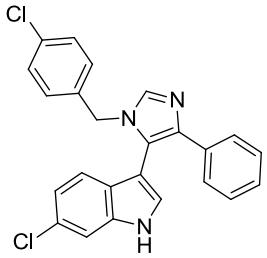

49

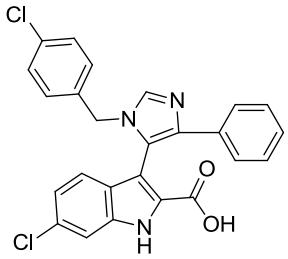

50

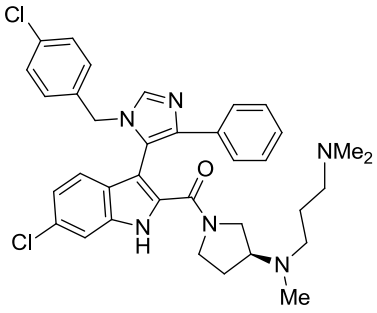

51

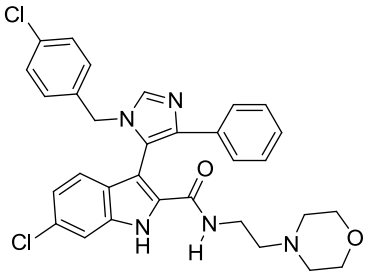

52

Table 14: MDM2 and MDMX inhibitory activity of imidazole-based compounds[104]

	MDM2		MDMX	
	IC_{50} (μM)	**K_i (nM)**	**IC_{50} (μM)**	**K_i (μM)**
47	3.40	ND	ND	ND
48	0.90	ND	ND	ND
49	0.20	ND	ND	ND
50	1.71	916	44.5	36
51	0.19	109	19.7	11
52	0.03	ND	19.0	ND

ND, not determined

Molecular modelling revealed that positioning a planar aromatic ring within Van der Waals proximity to the MDM2-V93 side chain gave appropriate substitution vectors for accessing the p53-F19, p53-W23 and p53-L26 binding pockets of MDM2. These vectors would stem from three consecutive atoms on the core aromatic ring (**Figure 33**).

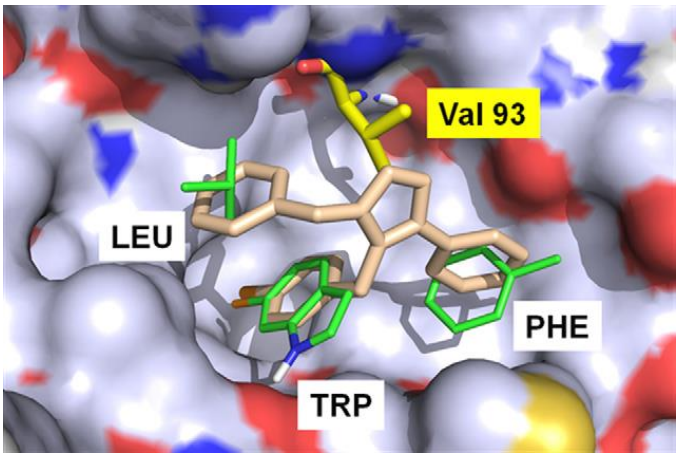

Figure 33: Molecular scaffold model in which a 5-membered aromatic core (beige), positioned near MDM2-V93 (yellow), directs three branching substituents into the key p53-binding pockets of MDM2. The side chains of p53-F19, p53-W23 and p53-L26 are overlaid (green)[104]

In early compounds, a *p*-chlorobenzyl ring was used to access the p53-W23 pocket. The significance of the chloro group was observed from peptide-based MDM2 inhibitors, in which a chloro-substituted aromatic ring enhanced binding potency by filling the p53-W23 pocket more than the unsubstituted ring.[104, 105] Additional benzylic substituents were attached either side of the *p*-chlorobenzyl ring on an imidazole scaffold and docking studies indicated a tight fit in the MDM2 protein. TR-FRET analysis of **47** gave an IC_{50} of 3.4 μM (*cf*. Table 12) and modelling this compound in the MDM2 domain suggested that potency could be enhanced by exploiting the hydrogen bond between the NH of p53-W23 and the backbone carbonyl of MDM2-L54. The *p*-chlorobenzyl ring was substituted for a 6-chloroindole (**Figure 34**).[104, 105]

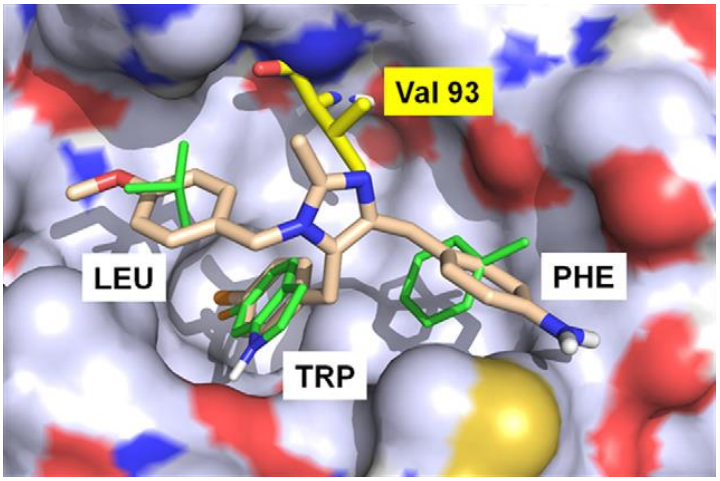

Figure 34: Binding model of **47** (beige) in the p53 binding domain of MDM2. The side chains of p53-F19, p53-W23 and p53-L26 are overlaid (green)[104]

Modelling also suggested that a phenyl ring bound directly to the imidazole scaffold would better occupy the p53-F19 pocket than one bound via a methylene linker. Analysis of the p53-L26 pocket revealed it was of predominantly hydrophobic character so it was decided to replace the 4-methoxy group. Compounds **48** and **49** were synthesised and were found to be 4- and 17-fold more potent than **47** respectively by TR-FRET analysis. The isobutyl substituent in **48** mimiced exactly the p53-L26 side chain but the 4-chlorobenzyl group in **49** gave better occupancy of the pocket.

Introducing hydrophilic groups at the 2-position of the 6-chloroindole ring was predicted to point into solvent. Compounds **50**, **51** and **52** were synthesised and the latter improved MDM2 inhibition to 30 nM by TR-FRET analysis. Compound **52** also demonstrated micromolar inhibition of growth in SJSA-1 cells (MDM2 amplified). The crystal structure of **52** with MDM2 confirmed the morpholine chain does not interact with any MDM2 residue but instead folds onto the imidazole ring (**Figure 35**).[104] The amide carbonyl of **52** forms water-mediated hydrogen bonds with MDM2 residues K51, F55 and Q59. In addition, the chlorobenzyl moiety makes an aromatic stacking interaction with MDM2-H96. This interaction is what gives these molecules selectivity for MDM2 over MDMX; the latter has a proline residue in place of the histidine and all compounds in this series were much less active against MDMX.[104]

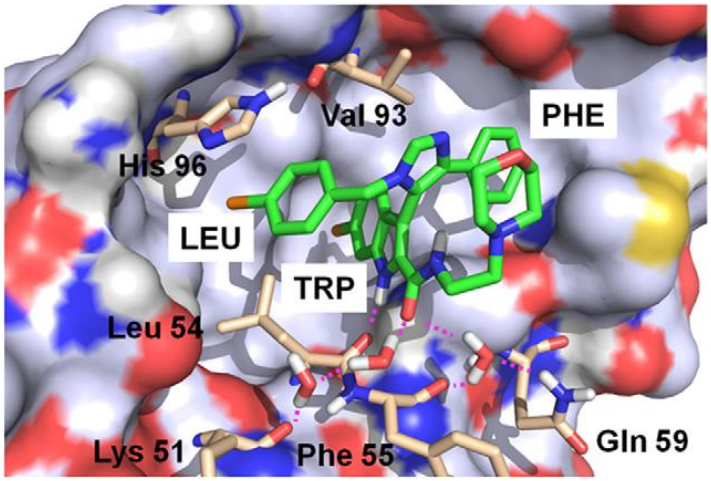

Figure 35: Crystal structure of **52** (green) in the p53 binding domain of MDM2. The side chains of residues which interact with **52** are shown (beige). Hydrogen bonds are shown as pink dots (resolution, 1.9 Å; PDB code: 4DIJ)[104]

Analysis by Popowicz of compound **51** interacting with MDMX confirmed the 6-chloroindole occupies the p53-W23 pocket, with the indole NH forming a hydrogen bond with the carbonyl of MDMX-M53 (**Figure 36**).[106] However, the plane of the 5-chloroindole ring is shifted 0.63 Å more towards the p53-L26 pocket compared with the p53-W23 substituent. The 4-chlorobenzyl ring of **51** occupies the p53-L26 pocket and the phenyl ring fills the p53-F19 pocket, but the plane of this ring is almost perpendicular to that of the p53-F19 ring.[106] Other known interactions include a hydrogen bond (3.29 Å) between the amide carbonyl of **51** and the MDMX-H54 Nδ atom. The dimethylamino side-chain folds over the p53-F19 pocket and shields the hydrophobic region, made up of MDMX residues M61 and Y66, from solvent.[106]

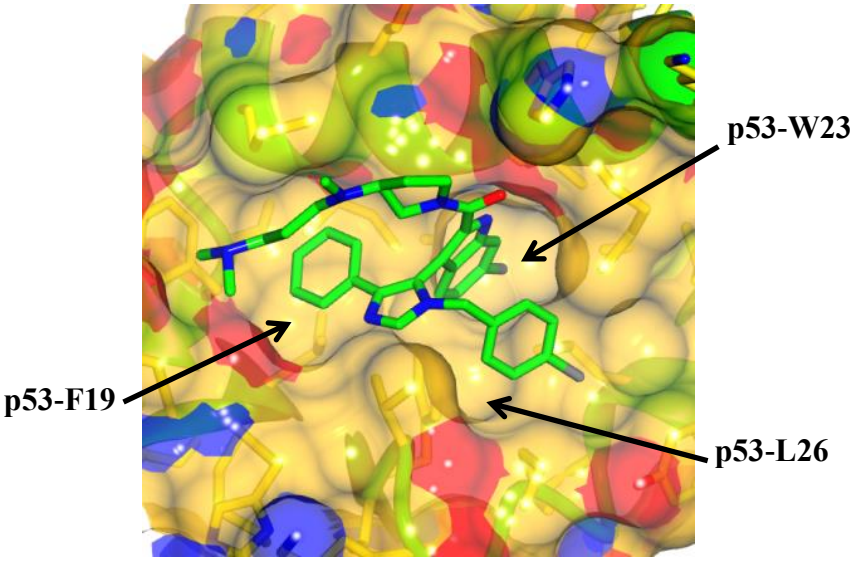

Figure 36: Crystal structure of **51** (green) in the p53 binding domain of MDMX (yellow). The p53 binding subpockets F19, W23 and L26 are highlighted. Image modified using CCP4mg (resolution, 1.5 Å; PDB code: 3LBJ)[106]

Compound **51** binds to MDMX by an induced fit. To accommodate the chloro ligand on the indole ring the MDMX-L56 side-chain retracts by 0.81 Å. Other residues forced to move include MDMX-M53 (0.71 Å), MDMX-L98 (0.69 Å) and MDMX-L102 (1.14 Å). The structural differences between the **51**-MDMX and the p53-MDMX complexes are energetically unfavourable and explain the reduced potency of **51** against MDMX compared with MDM2.[106]

3.5.3 Diaryl- and Triaryl-Pyrroles as MDM2 and Dual MDM2/MDMX Inhibitors

Developed at Newcastle University, a screen of 800 compounds obtained from the Cancer Research UK screening collection, using a MDM2-p53 ELISA assay, identified pyrrole **53a** as a moderately active MDM2-p53 inhibitor.[107] Compound **53a** demonstrated dose-dependent inhibition of MDM2 and induction of p53 by Western blotting. A screen of 96 structurally similar compounds under similar conditions identified pyrroles **53b-53l**, with MDM2 inhibition all < 10 μM (**Table 15**).

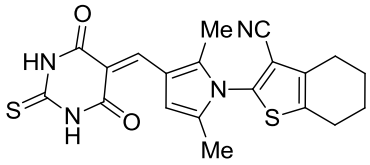

53a

Table 15: SARs for pyrrole barbiturates **53a-53l** against MDM2[107]

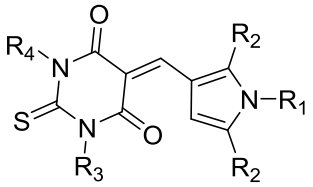

ID	R^1	R^2	R^3	R^4	MDM2 IC_{50} (μM)
53a	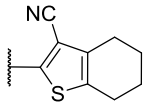	Me	H	H	12.3 ± 1.5
53b	4-ClPh	Me	H	H	0.72 ± 0.10
53c	4-ClPh	Me	H	Ph	3.30 ± 0.70
53d	4-ClPh	Ph	H	H	0.12 ± 0.02
53e	4-ClPh	Ph	H	Ph	0.23 ± 0.04
53f	4-ClPh	Ph	H	3-ClPh	0.16 ± 0.02
53g	4-ClPh	Ph	3,4-diMePh	Ph	0.26 ± 0.04
53h	4-ClPh	Ph	Me	Me	Insoluble
53i	4-BrPh	Me	Ph	Ph	0.20 ± 0.02
53j	4-MePh	Me	H	Ph	8.40 ± 0.90
53k	4-MePh	Me	H	H	4.70 ± 0.20
53l	4-EtO_2CPh	Ph	H	H	0.70 ± 0.02

Compounds with an aromatic ring at R^1 that was *para*-substituted by chloro (**53b-53g**), bromo (**53i**) or ethoxylcarbonyl (**53l**) were the most potent. Pyrroles with 2,5-diphenyl substituents (**53d-53e**) were 5-10-fold more active than the analogous 2,5-dimethyl pyrroles (**53b-53c**) and any substitution on the barbiturate ring reduced activity.

Compound **52d** was the most potent pyrrole identified and was selected for further SAR analysis (**Table 16**). The *N*-4-aryl substituent significantly affected potency, with active compounds possessing only electron-withdrawing groups at this position, including

chloro, bromo, cyano and nitro. Substitution on the barbiturate ring was met with a loss in potency or had no effect on potency, however thiobarbiturates generally had superior activity than the corresponding oxobarbiturates. Pyrrole **53d** also demonstrated low micromolar activity against MDMX. *N*-alkylation of the barbiturate ring had a more detrimental effect on MDMX activity than for MDM2 and alkylation also reduced the aqueous solubility of these compounds.[107]

Table 16: SARs for pyrroles **53d** and **53m-53z** against MDM2 and MDMX[107]

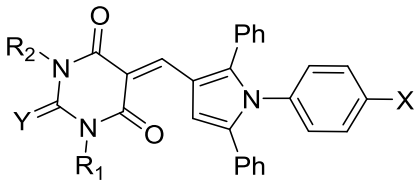

ID	R^1	R^2	X	Y	MDM2 IC_{50} (μM)[a]	MDMX IC_{50} (μM)[a]
53d	H	H	Cl	S	0.12 ± 0.02	4.2 ± 1.2
53m	H	H	Cl	O	0.30 ± 0.03	ND
53n	H	H	Br	O	0.18 ± 0.07	ND
53o	H	H	OMe	O	1.9 ± 0.3	13 ± 7
53p	H	H	*t*-Bu	O	1.9 ± 0.3	ND
53q	H	H	CN	O	4.7 ± 1.9	7.0 ± 3.0
53r	H	H	CN	S	0.20 ± 0.07[d]	0.90 ± 0.42
53s	H	H	NO_2	O	0.15 ± 0.06	0.68 ± 0.18
53t	H	H	NO_2	S	0.17 ± 0.09[d]	0.63 ± 0.12
53u	Et	Et	Cl	S	0.30 ± 0.12[c]	ND
53v	Et	Et	Br	O	0.89 ± 0.04	74%[b]
53w	Et	Et	Br	S	0.26 ± 0.05	ND
53x	Me	H	Cl	S	0.11 ± 0.02[d]	28 ± 23
53y	Me	H	Br	O	0.34 ± 0.08	35 ± 20
53z	Me	H	Br	S	0.073 ± 0.002	ND

(a) *n* = 3; (b) % inhibition at 50 μM; (c) *n* = 6; (d) *n* = 4; ND, not determined

A series of 2-alkyl-1,5-diarylpyrroles were designed to further probe the SAR for MDM2 and MDMX inhibition (**Table 17**). All attempts to replace the 2-aryl group with an alkyl group caused a large drop in potency against MDM2 and an even more

substantial reduction in MDMX potency, which was independent of the position of the barbiturate ring.[107]

Table 17: SARs for pyrroles **54a-54g** against MDM2 and MDMX[107]

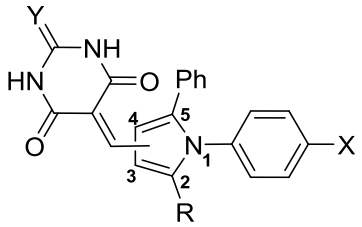

ID	Regioisomer	R	X	Y	MDM2 IC_{50} (μM)[a]	MDMX IC_{50} (μM)[b]
54a	Mixture	Me	Cl	O	> 1	ND
54b	4	*t*-Bu	Br	S	0.76 ± 0.27[c]	963
54c	4	*t*-Bu	Cl	S	1.1 ± 0.7[c]	1684
54d	3	CyPr	Cl	S	1.6 ± 1.7	3486
54e	3	CyPr	Br	S	1.6 ± 1.6	3428
54f	4	CyPr	Cl	S	2.1 ± 2.7	4916
54g	4	CyPr	Br	S	2.2 ± 2.7	5322

(a) *n* = 3; (b) *n* = 1; (c) *n* = 4; ND, not determined

Binding modes for selected pyrroles were generated by superpositioning the pyrrole on top of the imidazole-based inhibitors **50** and **51** in the crystal structures[106] of these compound with MDM2 (pdb: 3LBK) and MDMX (pdb: 3LBJ) respectively, and removing the original ligand (**Figure 37**).[107] For **53d**, the *N*-4-chlorophenyl ring occupies the p53-W23 pocket in MDM2 and MDMX, overlaying with the 6-chloroindole ring of **50** and **51**. The 5-phenyl ring of **53d** occupies the p53-F19 pocket, overlaying well with the 1-phenyl ring of **50** and **51**, and the 2-phenyl ring of **53d** accommodates the p53-L26 pocket. The barbiturate ring projects into solvent, suggesting this group functions as a hydrophilic cap.[107]

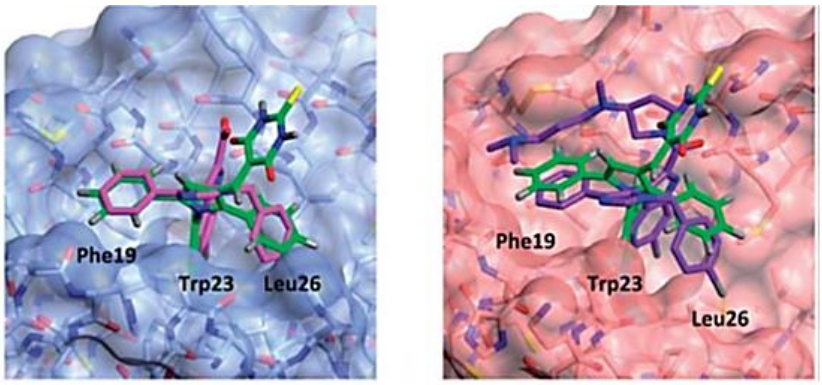

A) **B)**

Figure 37: A) Modelled binding of **53d** (green) overlaid with **50** (magenta) in MDM2 (blue) (pdb: 3LBK); **B)** Modelled binding of **53d** (green) overlaid with **51** (purple) in MDMX (pink) (pdb: 3LBJ). Hotspot p53 residues F19, W23 and L26 are highlighted. Image created using COOT with CCP4mg plug-in.[107]

When pyrrole **54c** was modelled in MDM2 and MDMX, the *tert*-butyl group was placed in the p53-F19 pocket in both proteins, with the 5-phenyl ring projecting into the p53-L26 pocket. In this series the 5-phenyl ring no longer made a well-defined interaction with the p53-L26 pocket. This would explain the loss of activity observed against MDM2 and MDMX for the 2-alkylpyrrole series.

Cell-based assay data suggested the pyrroles were non-specific MDM2 and MDMX binders.[107] Compounds **53d**, **53r**, **53t** and **53x** were equally growth inhibitory in SJSA-1 osteosarcoma cells (MDM2 amplified, WT p53) and SN40R2 cells (MDM2 amplified, mutant p53), suggesting a non-specific mechanism of action (**Table 18**). Nutlin-3a (**11**) only possessed activity in the SJSA-1 cells. The pyrroles were also equipotent in MRK-NU-1 breast cancer cells (MDMX amplified, WT p53), despite large potency differences against MDM2 and MDMX in the ELISA.

Table 18: Growth inhibitory activity for pyrroles **53d**, **53r**, **53t** and **53x** in SJSA-1, SN40R2 and MRK-NU-1 cell lines[107]

	GI_{50} (μM)[a]		
ID	**SJSA-1**	**SN40R2**[b]	**MRK-NU-1**
53d	2.3 ± 0.2	2.8 ± 0.6	2.3 ± 0.3
53r	5.1 ± 0.9	5.9 ± 0.3	6.1 ± 0.7
53t	4.7 ± 1.0	5.2 ± 0.4	4.9 ± 0.6
53x	5.5 ± 0.6	6.3 ± 0.4	7.0 ± 1.0

(a) n = 3; (b) p53-null

Compound **53d** induced p53 in SJSA-1 cells at 5 μM by Western blotting but not in A2780/CP70 ovarian carcinoma cells (mutant p53). These results demonstrated a p53-dependent response to **53d** in cells, however the growth inhibitory data in Table 16 suggested this was not the only effect the pyrroles had in cells.[107]

3.5.4 Pyrrolidone Inhibitors of MDM2 and MDMX

Several pyrrolidone-based MDM2 inhibitors synthesised at the School of Pharmacy, Shanghai were found to possess moderate MDMX affinity.[108] Structure-based screening of the Specs molecular database and fluorescence polarisation (FP) analysis identified nine hit compounds with MDM2 inhibitory activity below 100 μM, six of which shared a pyrrolidone scaffold. The most potent compounds (**55a** and **56**) had IC_{50} values below 1 μM.

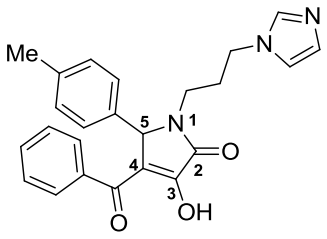

55a
K_i (MDM2) = 0.78 μM

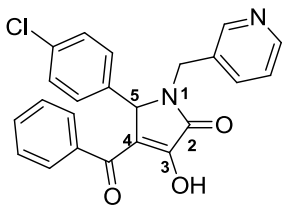

56
K_i (MDM2) = 0.57 μM

Modelling studies of **55a** and **56** with MDM2 revealed primarily hydrophobic interactions, with the *N*-, 5- and 4- substituents occupying the p53-F19, p53-W23 and

p53-L26 binding pockets respectively (**Figure 38**). The compounds also formed a hydrogen bond with MDM2-G16 via the acetophenone carbonyl oxygen.

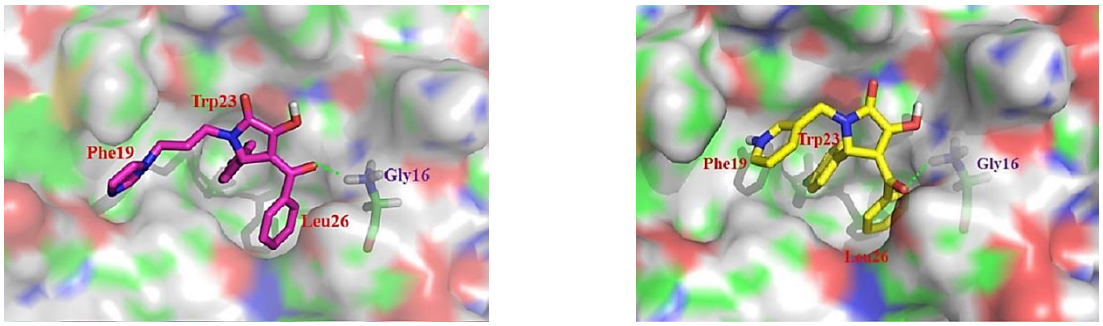

A) **B)**

Figure 38: A) Binding mode of **55a** (purple) and **B) 56** (yellow) in MDM2. Hydrogen bonds are shown as green dotted lines. The p53 binding pockets F19, W23 and L26 are highlighted, as is the key hydrogen bond-forming residue MDM2-G16[108]

The aqueous solubility of **55a** was superior to that of **56** and therefore the former was selected for hit optimisation against MDM2. Several of the most active compounds identified from SAR analysis against MDM2 were also screened against MDMX (**Table 19**). The nature of the 3-substituent significantly affected potency, with compounds **55d** and **55i** exhibiting more potent MDMX inhibition than Nutlin-3a, but the structurally similar compound **55c** was 15-fold less active.

Table 19: SARs of selected pyrrolidones against MDM2 and MDMX[108]

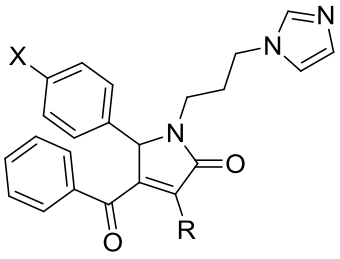

ID	R	X	MDM2 K_i (μM)[a]	MDMX K_i (μM)[a]
55a	OH	Me	0.78	Not tested
55b	OH	Br	0.29	NA
55c	OEt	Br	0.69	38.91
55d	O^{i}Pr	Br	0.26	2.68
55e	O$(CH_2)_4$Me	Br	0.34	NA
55f	O$(CH_2)_3$Me	Br	0.47	NA
55g	OCyHex	Br	0.49	17.93
55h	OBn	Br	2.07	NA
55i	O$(CH_2)_2$OMe	Br	1.34	2.11
55j	O$(CH_2)_2$Me	Br	6.97	9.32
55k	NH_2	Br	0.048	NA
55l[b]	NH(*R*)-1-phenylethyl	Br	0.15	NA
Nutlin-3a (11)	-	-	0.23	5.86

(a) FP assay; (b) Specifically the *R*,*R*-diastereomer; the *R*,*S*-diastereomer was inactive against MDM2 and not tested against MDMX; NA, not active

Compound **55d** gave dose-dependent increases in MDMX, p21 and p53 levels in MCF-7 breast cancer cells after 24 h, although it had no effect on the activity of phosphorylation-p53 (p-p53) (**Figure 39**). From this research, several novel pyrrolidone-based inhibitors were identified as potent MDM2 inhibitors with activity in MDMX-overexpressing cell lines that was superior to that of Nutlin-3a.

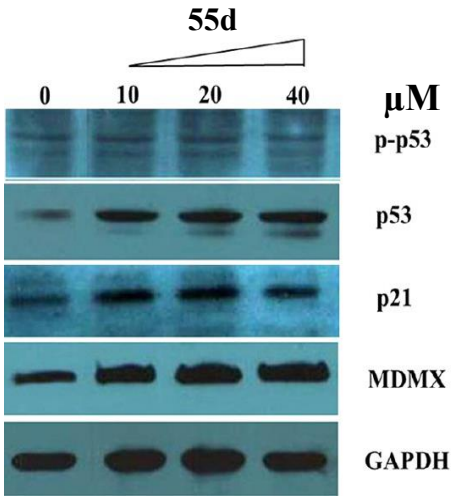

Figure 39: Dose-dependent induction of p53, p21 and MDMX in MCF-7 cells by **55d** after 24 h detected by Western blotting[108]

3.6 Potent Dual MDM2 and MDMX Inhibitors

3.6.1 Indolyl-Hydantoin MDM2 and MDMX Dual Inhibitors

High-throughput screening at the Roche Research Centre, NJ, US, identified several indolyl-hydantoin compounds with potent dual inhibitory activity of MDM2 and MDMX (**Table 20**).[109]

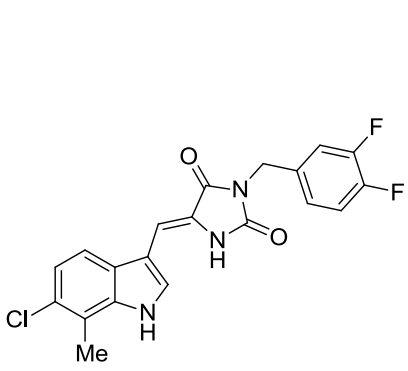

57

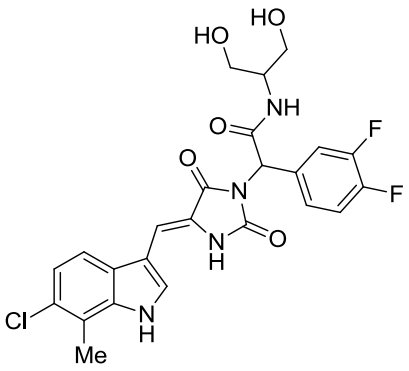

58

Table 20: TR-FRET inhibition data for **57**, **58** and Nutlin-3a against MDM2 and MDMX[109]

Inhibitor	MDM2-p53 IC_{50} (μM)	MDMX-p53 IC_{50} (μM)
57	0.033	0.041
58	0.017	0.024
Nutlin-3a (11)	0.019	9

Co-crystallisation of **57** with MDMX revealed a structure composed of two molecules of **57** and two molecules of MDMX, arranged as a pair of dimers (**Figure 40**).[109] For each molecule of **57**, the indolyl-hydantoin moiety occupies the p53-F19 pocket of one MDMX protein, while the difluorophenyl ring occupies the p53-W23 pocket of the second. Extensive aromatic π-stacking between the two indolyl-hydantoin scaffolds stabilises the complex, extending to include both MDMX-Y63 side chains, forming a four-level π-sandwich.

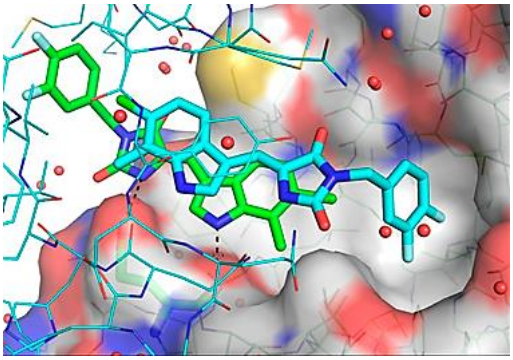

Figure 40: Crystal structure of two molecules of **57** (cyan and green) in the p53 binding domain of two MDMX proteins. One protein is shown in surface rendition (carbon, white; oxygen, red; nitrogen, blue; sulfur, yellow), the other as a stick figure (same colour scheme except carbons are cyan). In the cyan-coloured **57**, the indolyl-hydantoin moiety is occupying the p53-F19 pocket of the stick-figure MDMX, while the difluorophenyl ring is occupying the p53-W23 pocket of the surface-rendition protein. The green-coloured **57** binds in the reverse mode (resolution, 1.8 Å; PDB code: 3U15)[109]

Co-crystallisation of **57** with MDM2 revealed the analogous homodimeric structure (resolution, 2.8 Å, PDB code: 3VBG).[109] Compound **57** demonstrated potent MDM2 and MDMX inhibition *in vitro* but had poor aqueous solubility. Addition of hydrophilic groups to the methylene carbon yielded **58**, which was more active than **57** against both targets and had enhanced aqueous solubility.[109] Compound **58** penetrated MCF-7 breast cancer cells and stabilised p53, increased levels of its transcription targets p21 and MDM2, and induced apoptosis. Immunoprecipitation of p53 or MDMX from **58**-treated MCF-7 cells confirmed these observations were the result of inhibition of the p53-MDMX and -MDM2 interactions. When the cells were treated with Nutlin-3a, a lower apoptotic response resulted.[109]

The indolyl-hydantoins therefore represent the first small-molecule dual inhibitors of the MDM2- and MDMX-p53 interactions, demonstrating nanomolar activity against

both proteins *in vitro* and inducing apoptosis in various cell lines overexpressing either protein or both. These compounds exhibit high potency without any substituent occupying the p53-L26 pocket of the protein target, which may explain why the compounds are similarly active against both proteins, as it is in this p53-binding pocket that the structures of MDM2 and MDMX are most diverse. However, the unorthodox binding mode of the compounds complicates SARs and limits the development of these compounds as a lead series.

3.6.2 Stapled α-Helical Peptides as Potent Dual Inhibitors of MDM2 and MDMX

Stapled peptide **59** is a selective dual inhibitor of MDM2 and MDMX with nanomolar potency against both targets and can activate p53-mediated tumour suppression in multiple MDM2- and MDMX-overexpressing cancer xenografts.[110]

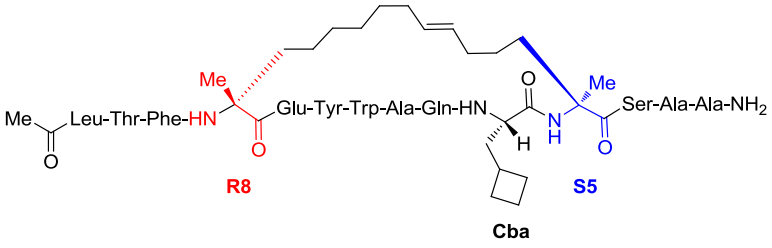

59

Peptide **59** was created at Hoffman-La Roche by modification of the natural p53 peptide to make it stable to administration by IV and bind with greater affinity than the natural peptide.[110] Taking influence from the recently reported sequence enhancements described for linear phage display peptide (pDI) Ac-L^{17}TFEHYWAQLTS^{28}-NH_2,[90, 98] **59** was formed by the inclusion of an 11-carbon linker between two α-methylated alanine residues. Peptide **59** possessed high binding affinity for MDM2 and MDMX, with K_i inhibition values of 0.9 and 6.8 nM respectively, which was more potent than competitor peptides, e.g. SAH-p53-8,[111] and for Nutlin-3a (**Table 21**). The negative control ATSP-7342, in which the Phe^{19} residue was mutated to Ala^{19} was comparatively inactive against both targets.

Table 21: SARs of various stapled and non-stapled peptides against MDM2 and MDMX with Nutlin-3a as a reference[110]

	Residue Sequence[a]																		
ATSP#	**14**	**15**	**16**	**17**	**18**	**19**	**20**	**21**	**22**	**23**	**24**	**25**	**26**	**27**	**28**	**29**	**30**	**K_i (MDM2) (nM)**	**K_i (MDMX) (nM)**
1800	Q	S	Q	Q	T	F	R8[b]	N	L	W	R	L	L	S5[b]	Q	N		25.9	105.7
3648				L	T	F	E	H	Y	W	A	Q	L	T	S			14.6	47.4
3900				L	T	F	R8[b]	H	Y	W	A	Q	L	S5[b]	S			1.0	18.3
4641				L	T	F	R8[b]	A	Y	W	A	Q	L	S5[b]	S			4.9	34.3
6935				L	T	F	R8[b]	E	Y	W	A	Q	L	S5[b]	S			1.2	8.0
7041				L	T	F	R8[b]	E	Y	W	A	Q	Cba	S5[b]	S	A	A	0.9	6.8
7342				L	T	A	R8[b]	E	Y	W	A	Q	Cba	S5[b]	S	A	A	536	> 1000
Nutlin-3a																		52.3	> 1000

(a) Each sequence begins with an acetyl group (Ac-) and ends with an amino group (-NH_2); (b) R8 and S5 are the linker residues. ATSP-3648 is not a stapled peptide

Peptide **59** had greater potency and aqueous solubility compared to prototype peptides such as ATSP-3900, mainly due to replacing His^{21} in 3900 with Glu^{21} in **59**. Modification of Leu^{26} to the unnatural Cba amino acid and adding the Ala^{29}-Ala^{30} *C*-terminus further augmented binding affinity against both proteins.

Conformational studies of **59** indicated it was approximately 70% α-helical in solution at pH 7.0. The greater α-helical nature of **59** compared to earlier peptides, e.g. 3900, has been used to explain the improved cell penetration efficiency and the corresponding increase in potency of **59** against MDM2 and MDMX. The crystal structure of **59** bound to humanised zebrafish MDMX (15-106, L46V/V95L) confirmed the Phe^{19} and Trp^{23} side-chains occupied the expected sub-pockets in MDMX, with the Cba residue interacting in the Leu^{26} sub-pocket (**Figure 41**).[110]

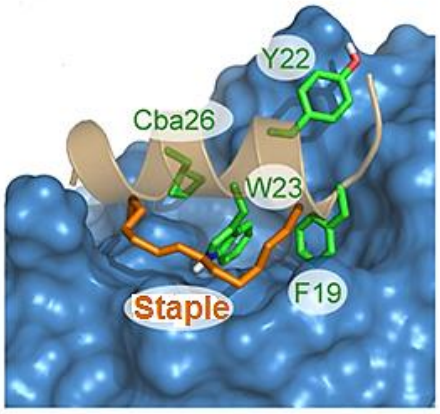

Figure 41: X-ray structure of peptide **59** (brown) interacting with humanised zebrafish MDMX (blue). Residues which make interactions with the protein, including the staple olefin, are highlighted in green and orange respectively (resolution, 1.7 Å; PDB code: 4N5T).[110]

Compound **59**-Y22 makes multiple Van der Waals contacts with MDMX-Q66, -R67, -Q68, -H69, -V89 and -K90, as well as water-mediated hydrogen bonds with Nε of MDMX-K90 and Nδ1 of MDMX-H69. The staple is also well accommodated in the MDMX protein and forms multiple Van der Waals contacts with MDMX-K47, -M50, -H51, -G54, -Q55 and -M58.

Peptide **59** was shown to reduce the levels of MDM2-p53 and MDMX-p53 in MCF-7 cells at 10 μM, in comparison to a DMSO control, following analysis by Western blotting after 4 h incubation. Peptide **59** induced p53 in a dose-dependent manner in MCF-7 and SJSA-1 cell lines, as well as p53 target genes, including p21 and MDM2, that was comparable to that observed with Nutlin-3a in SJSA-1 cells and superior to that seen in MCF-7 cells. Induction of p53 was only observed in cell lines which expressed WT p53; treatment of MDA-MB-435 and SW480 cell lines (p53 mutants) with **59** resulted in no induction of p53 target genes and no reduction in cell viability, as measured by MTT assay (**Figure 42**).

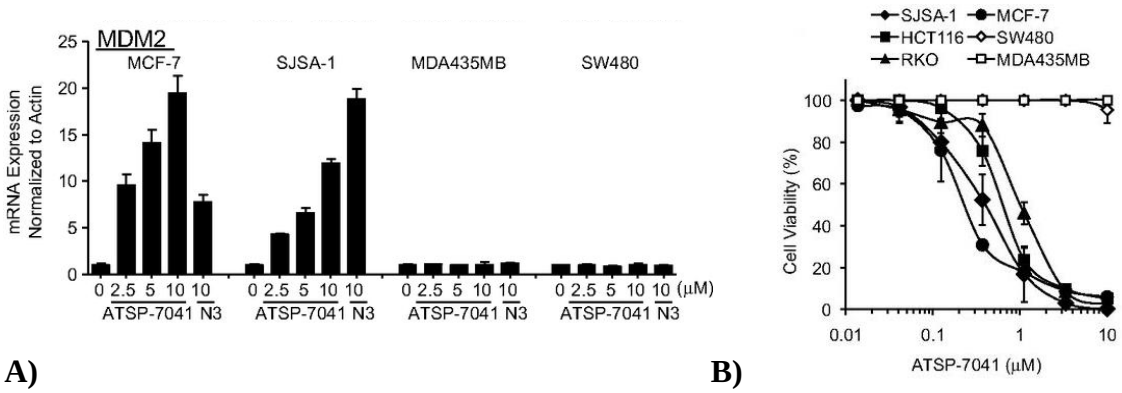

A) **B)**

Figure 42: A) Treatment with varying concentrations of **59** causes dose-dependent induction of MDM2 in MCF-7 and SJSA-1 cell lines but not in p53 mutant MDA-MB-435 or SW480 cell lines. Cells were incubated with 2.5, 5.0 or 10.0 μM **59** or 10.0 μM Nutlin-3a (N3) for 24 h before measuring MDM2 mRNA levels by qPCR, expressed as fold increase. **B)** Treatment with **59** causes a fall in viability of SJSA-1, MCF-7, HCT-116 and RKO cell lines, but has no effect on the viability of p53 mutant MDA-MB-435 or SW480 cell lines.[110]

Peptide **59** could be readily formulated for IV administration and a plasma pharmacokinetic profile was compiled in mouse, rat and cynomolgus monkey. Exposure to **59** increased in a dose-dependent manner in all species, with durable plasma half-lives of 1.5, 2.1 and 18.3 h in mouse, rat and monkey respectively and suitably low clearance.[110] The data indicated the potential to achieve efficacious exposure levels of **59** at therapeutic doses in man, highlighting the ongoing success of stapled peptides in the design of potent dual MDM2 and MDMX inhibitors.

Chapter Four: SKP2 Results and Discussion

4.1 Synthesis of 16a, 68a and their Derivatives

Owing to the high cost of 2,2-dimethyldihydro-2*H*-pyran-4(3*H*)-one (**21**), the *des*-dimethyl derivative *N*,*N*-dimethyl-4-(((4-phenyl-3-(tetrahydro-2*H*-pyran-4-yl)butyl)amino)methyl)aniline (**68a**) was synthesised first. Horner-Wadsworth-Emmons (HWE) olefination of pyranone **60** with trimethyl phosphonoacetate gave ester **61** in excellent yield. Hydrogenation of alkene 61 was examined under a range of conditions, starting with the literature approach, using hydrogen over Pd/C in ethyl acetate,[79] which gave ester **62** in 70% yield. Hydrogenation was also accomplished using a 'H-cube' hydrogenation reactor. However, for larger scale reactions, multiple hydrogenations were necessary because the catalyst cartridges could support no more than 300 mg samples. Transfer hydrogenation using ammonium formate and Pd/C proceeded to completion at 90 ^{o}C in half the time required to achieve full conversion using the H-cube and ester **62** was also isolated in superior yield.

Deprotonation of **62** with LDA followed by addition of benzyl bromide gave **63**. Reduction of the ester to give **64** was initially attempted using DIBAL-H, as described in the literature synthesis,[79] but no product could be isolated. Subsequent reductions using lithium aluminium hydride gave **64** in quantitative yield. Treatment of **64** with methanesulfonyl chloride gave mesylate **65** in high yield. Mesylation was found to be more high-yielding than tosylation, achieving full conversion more rapidly and with lower equivalents of the sulfonyl chloride required. Nitrile **66** was obtained upon heating **65** with sodium cyanide in DMF.

Reduction of nitrile **66** was achieved in good yield using lithium aluminium hydride to give amine **67**. This transformation was also achieved by hydrogenation using the H-cube with a Raney nickel catalyst. The nitrile was hydrogenated cleanly and the amine was isolated with no need for purification, giving this method an advantage over reduction with lithium aluminium hydride. However, similar problems with scale-up to those encountered when hydrogenating ester **61**, and the need for longer reaction times and specialised conditions, meant that reduction with lithium aluminium hydride was the preferred method.

Reductive amination of **67** with 4-(*N*,*N*-dimethylamino)benzaldehyde, followed by addition of sodium borohydride, gave pyran **68a**. This synthetic route was repeated for the formation of **16a**, using a commercially available sample of pyranone **21**. Compound **16a** was synthesised in overall yields of up to 58% over eight steps (**Scheme 3**). The diastereoisomeric ratio was 5:2 by ^{1}H NMR analysis, which is in agreement with the 3:1 ratio reported in the published synthesis.[79]

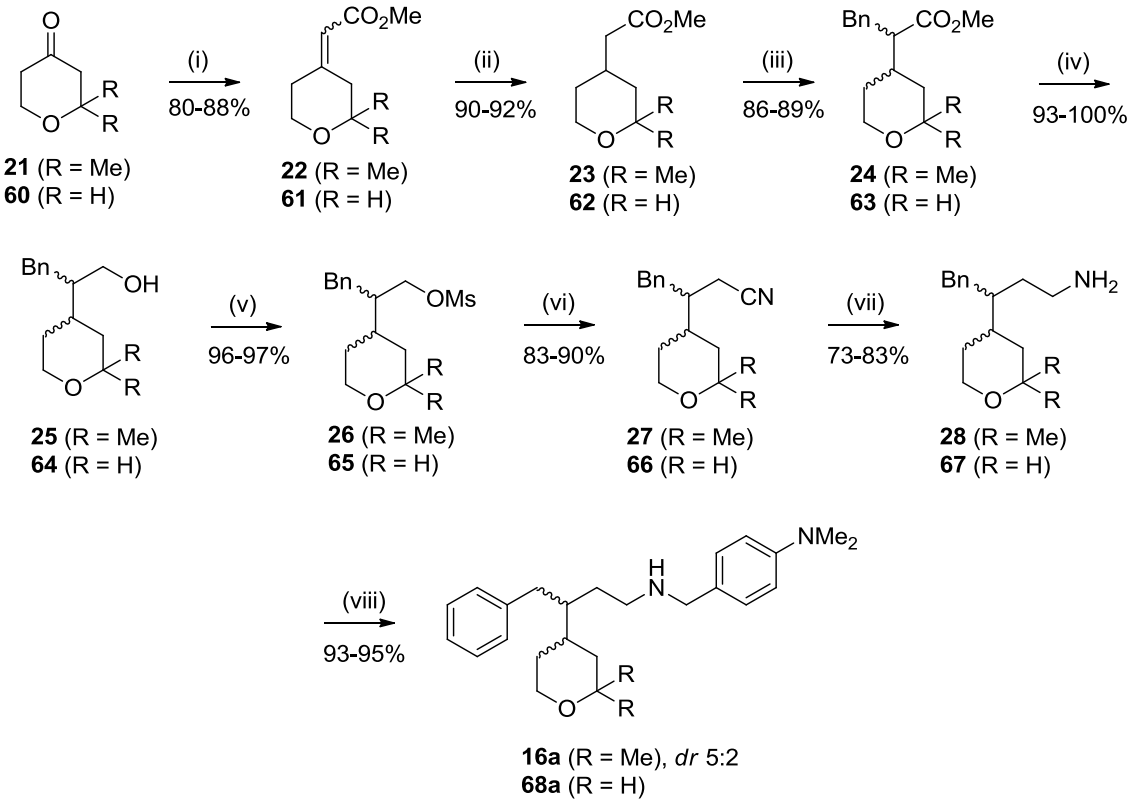

Scheme 3: (i) $(MeO)_2(O)PCH_2CO_2Me$, NaH, THF, 0 ^{o}C-RT, 20 h; (ii) NH_4HCO_2, 10% Pd/C, MeOH, 0-90 ^{o}C, 90 min; (iii) $^{i}Pr_2NH$, *n*-BuLi, THF, -78 ^{o}C, 1 h; BnBr, THF, 30 ^{o}C, o/n; (iv) $LiAlH_4$, THF, 0 ^{o}C, 2 h; (v) MsCl, $^{i}Pr_2NEt$, DCM, RT, 2 h; (vi) NaCN, DMF, 100 ^{o}C, 7 h; (vii) $LiAlH_4$, THF, 0 ^{o}C, 3 h; (viii) 4-(*N*,*N*-dimethylamino)benzaldehyde, $MgSO_4$, DCM, RT, 4 h; $NaBH_4$, MeOH, RT, 1 h

To explore initial structure-activity relationships (SARs), amines **28** and **67** were reacted with various benzaldehyde derivatives under analogous conditions to those shown in Scheme 3. The corresponding analogues in the *gem*- and *des*-dimethylpyran series were synthesised to compare cellular activities. To synthesise regioisomer **16c** (*cf.* Table 23), the required aldehyde **70** needed to be synthesised. Oxidation of alcohol **69** using manganese(IV) oxide gave a complex mixture of products. However, oxidation using Dess-Martin periodinane (DMP) gave **70** in 54% yield. Subsequent reductive amination of amine **28** gave **16c** (**Scheme 4**).

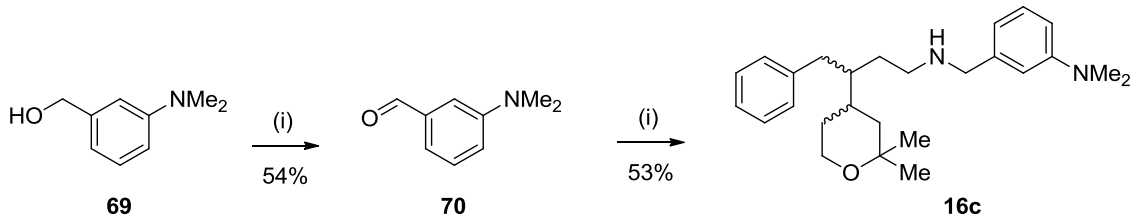

Scheme 4: (i) DMP, DCM, RT, 1 h; (ii) **28**, $MgSO_4$, DCM, RT, 4 h; $NaBH_4$, MeOH, RT, 1 h

Amines **28** and **67** were also reacted with acyl chlorides and sulfonyl chlorides, giving high yields of the corresponding amides and sulfonamides (**Scheme 5**).

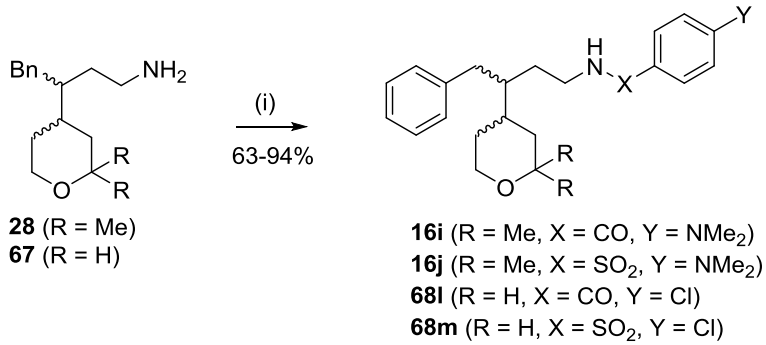

Scheme 5: (i) Appropriate acyl or sulfonyl chloride, Et_3N or $^iPr_2NEt$, DCM, RT, 1-2 h

To synthesise sulfonamide **16j**, the required sulfonyl chloride **73** was not available commercially. Treating bis(trimethylsilyl)sulfate with *N*,*N*-dimethylaniline (**71**) gave sulfonic acid **72**, which was converted to **73** using phosphorus(V) chloride (**Scheme 6**).

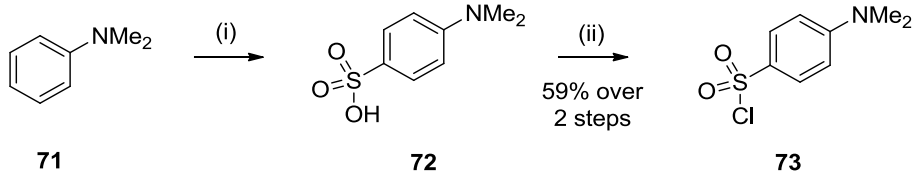

Scheme 6: (i) $(SiMe_3)_2SO_4$, 170 ^oC, 1 h; (ii) PCl_5, DCM, 0 ^oC-RT, 20 h

The secondary amines of **16a** and **68e** were methylated by means of Eschweiler-Clarke reactions using formic acid and formaldehyde, to give **74a** and **74b**, respectively (**Scheme 7**).

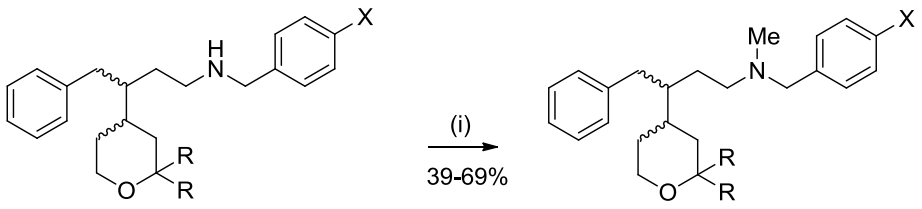

16a (R = Me, X = NMe_2)
68e (R = H, X = Cl)

74a (R = Me, X = NMe_2)
74b (R = H, X = Cl)

Scheme 7: (i) 37% aq. H_2CO, 95% aq. HCO_2H, EtOH, 40 ^oC, 90 min

To synthesise azide **68i**, reductive amination of 4-nitrobenzaldehyde with amine **67** gave **68g**, which was hydrogenated to aniline **68h**. Oxidation of **68h** with sodium nitrite in HCl, followed by addition of sodium azide at 0 ^oC, generated **68i** (**Scheme 8**).

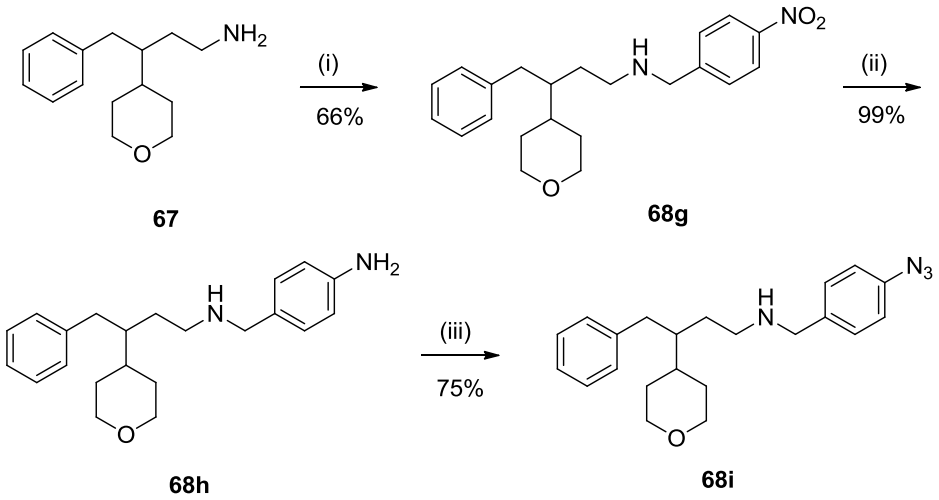

Scheme 8: (i) 4-Nitrobenzaldehyde, $MgSO_4$, DCM, RT, 4 h; $NaBH_4$, MeOH, RT, 1 h; (ii) H_2, Raney Ni, MeOH, RT/1 atm, 3 h; (iii) $NaNO_2$, 5 M HCl, 0 ^oC, 40 min, dark; NaN_3, 0 ^oC-RT, 2.5 h, dark

4.2 Improving the Aqueous Solubility of 16a

Several of the compounds synthesised so far were relatively lipophilic [clog*P* values ranged from 3.0 (**68k**) to 7.1 (**16d**), *cf.* Tables 23 and 24]. In an effort to reduce lipophilicity but retain cellular activity, the tetrahydropyran ring of **16a** was replaced with a morpholino group (**80**). The synthetic route to **80** was shorter than the synthesis of **16a**, potentially allowing for the rapid synthesis of analogues (**Scheme 9**).

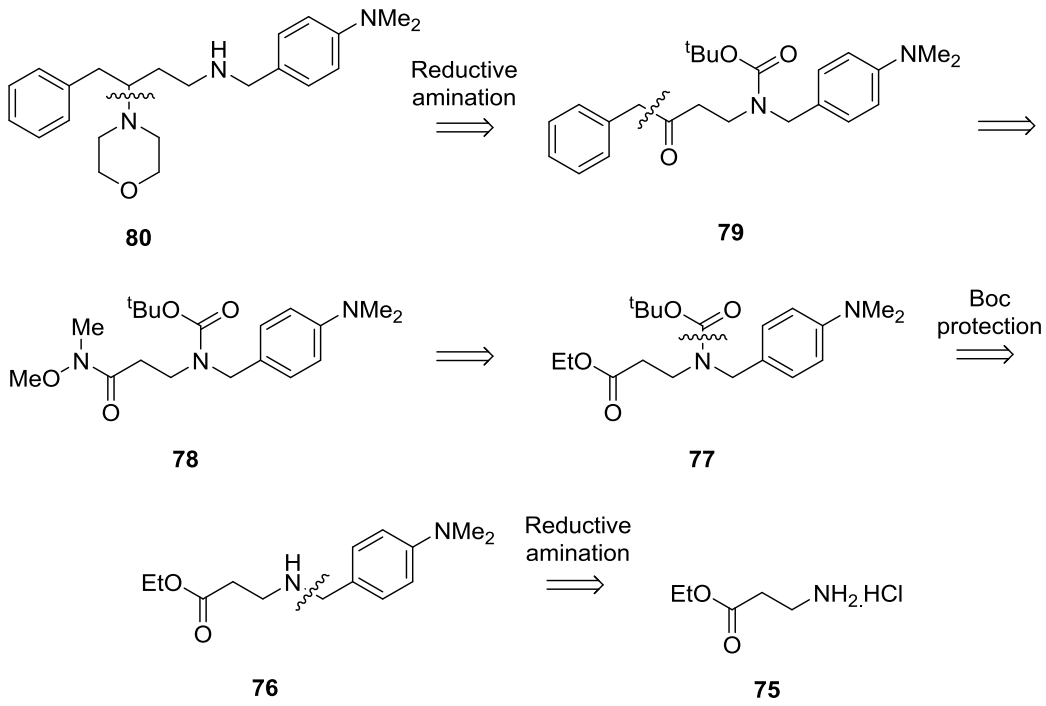

Scheme 9: Retrosynthetic analysis of morpholine **80**

Reductive amination of 4-(*N*,*N*-dimethylamino)benzaldehyde with β-alanine ethyl ester hydrochloride (**75**) in DMF and acetic acid gave amine **76**. Work-up of the crude reaction mixture was difficult due to the high aqueous solubility of **76**, meaning that multiple extractions were needed to recover the product. Protection of the amino group was accomplished using di-*tert*-butyl dicarbonate (Boc_2O) (**Scheme 10**).

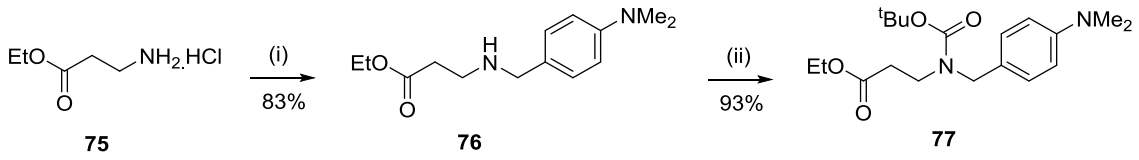

Scheme 10: (i) 4-(*N*,*N*-Dimethylamino)benzaldehyde, $NaB(OAc)_3H$, AcOH, DMF, RT, 4 h; (ii) Boc_2O, DCM, 0 ^oC-RT, 1 h

It was found that **77** could be synthesised from **75** without needing to isolate **76**. Addition of 4-(*N*,*N*-dimethylamino)benzaldehyde to neutralised **75** in THF gave **76** upon addition of sodium borohydride in methanol. Removal of the solvent followed by addition of Boc_2O gave **77**. While the yield of **77** was poorer (21%) than that achieved

by the procedure in Scheme 10 (77%), the less laborious work-up and purification meant it was the preferred procedure for the formation of this intermediate.

Weinreb amide **78** was isolated in 61% yield following reaction of *N*,*O*-dimethylhydroxylamine hydrochloride with **77** in the presence of ^{i}PrMgCl (**Scheme 11**). Conversion was poor when the reaction was conducted at 0 ^{o}C due to competing side reactions. Reducing the temperature to -20 ^{o}C minimised these side reactions and increasing the equivalents of *N*,*O*-dimethylhydroxylamine and ^{i}PrMgCl accelerated the reaction to give **78** within 1 h in almost quantitative yield. Treatment of **78** with BnMgCl at 0 ^{o}C gave a 1:2 mixture of ketone **79** and carbamate **81** by LC-MS. The latter was presumably formed by deprotonation and fragmentation of **78** to give **81** and acrylamide **82**, which were not isolated (**Scheme 11**).

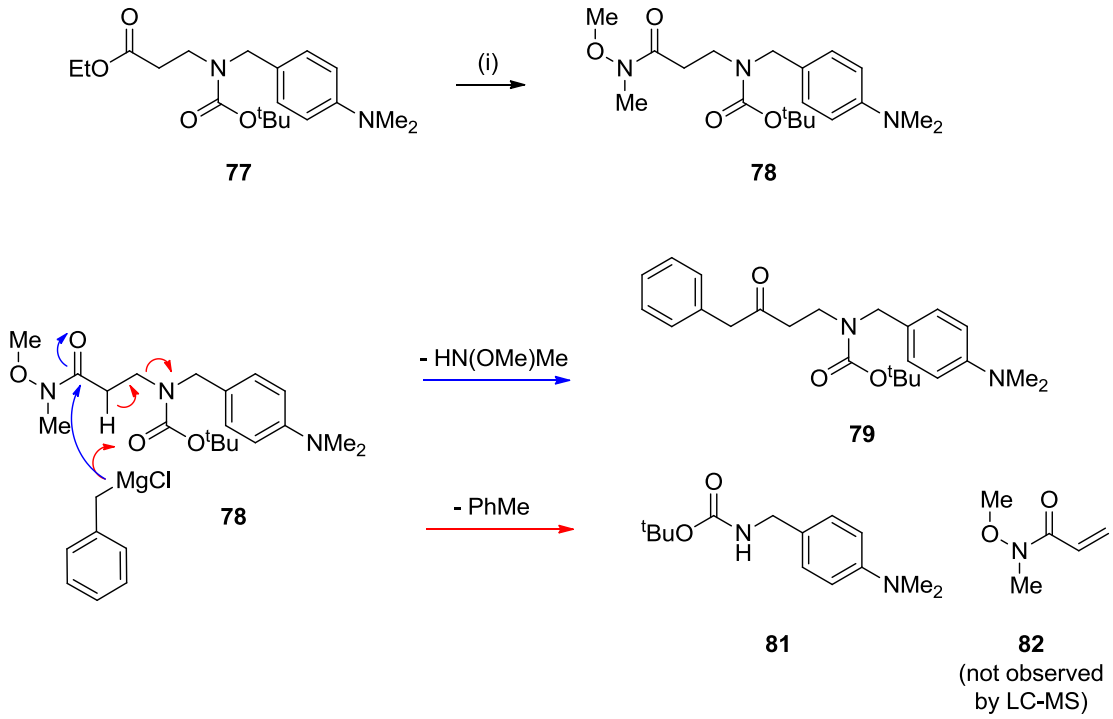

Scheme 11: Conversion of **77** to **78** and competing nucleophilic addition (blue arrow) to give **79** and elimination (red arrow) to give **81** and **82**; (i) HN(OMe)Me.HCl, ^{i}PrMgCl, THF, -20 °C, 1 h

No reaction was observed at -78 ^{o}C, whilst allowing the reaction mixture to warm slowly to room temperature gave a 1:1 mixture of **79** and **81**. Imamoto had previously described the use of $CeCl_3$ for accomplishing the addition of organometallic compounds to Weinreb amides with acidic α-protons.[115] Transmetallation of BnMgCl with $CeCl_3$, followed by addition of **78**, resulted in no reaction, but when $CeCl_3$ was mixed with **78**

followed by addition of BnMgCl, full conversion was achieved within 30 min at 0 °C, with no observed formation of **81** (**Scheme 12**).

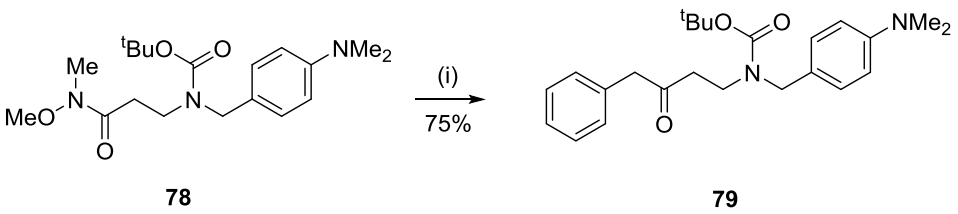

78 **79**

Scheme 12: (i) $CeCl_3$, THF, RT, 1 h; BnMgCl, THF, 0 °C, 30 min

Attempts to react ketone **79** with morpholine proved unsuccessful, showing poor conversion by LC-MS (**Table 22**). The steric bulk of the benzyl and carbamate groups presumably hindered access to the ketone carbonyl group. The relatively low nucleophilicity of morpholine compared to other secondary amines also reduced the rate of reaction.

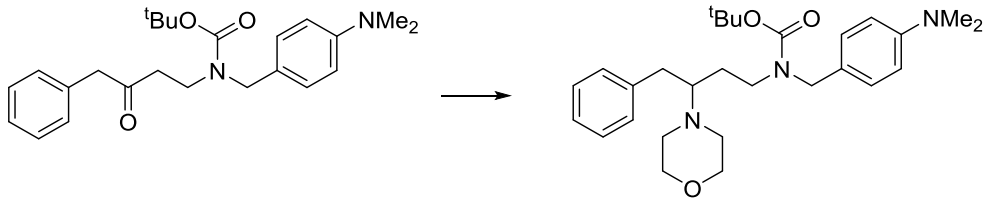

Table 22: Conditions applied to the reductive amination of **79** with morpholine[a]

Attempt	Reducing Agent	Solvent	Temp. (^{o}C)	Additional Reagents	Results
1	$NaB(OAc)_3H$	DMF	25-90	AcOH[c]	No product
2	$NaBH_4$	DCM, MeOH[b]	25	$MgSO_4$[d]	No product
3	$NaB(OAc)_3H$	THF	25	$Ti(O^iPr)_4$[e]	No product
4[f]	$NaB(OAc)_3H$	PhMe	140	AcOH[c]	No product

(a) **79** (100-180 mg, 1.0 equiv.), morpholine (1.0-5.0 equiv.) and reducing agent (1.2-2.0 equiv.) at 0.5-1.0 M; (b) DCM removed before addition of MeOH and $NaBH_4$; (c) 1% (v/v); (d) Anhydrous, excess; (e) 1.5 equiv.; (f) Dean-Stark set-up

Reduction of amide **78** with lithium aluminium hydride gave aldehyde **84**. Employing Katritzky's protocol for the synthesis of tertiary amines,[116, 117] carbamate **83** was obtained by reaction of **84** with morpholine in the presence of 1*H*-benzotriazole, followed by addition of BnMgCl. Removal of the Boc group with TFA proceeded quantitatively at room temperature to give **80** in 15% overall yield over five steps (**Scheme 13**).

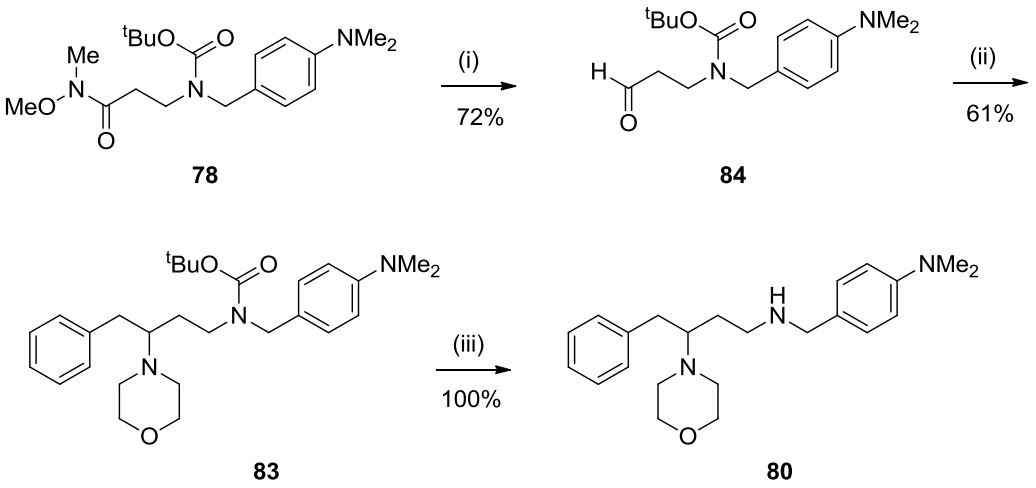

Scheme 13: (i) $LiAlH_4$, THF, 0 °C, 1 h; (ii) morpholine, 1*H*-benzotriazole, 3 Å MS, DCM, RT, 3 h; BnMgCl, THF, 0 °C, 1 h; (iii) TFA, DCM, RT, 1 h

4.3 Inhibition Data for 16a, 68a and their Derivatives

Compounds **16a** and **68a** were assessed for their ability to inhibit cell growth in a sulforhodamine B (SRB) assay using HeLa cervical cancer cells (**Figure 43**). Both compounds demonstrated growth-inhibitory activity, with **16a** giving a GI_{50} of 16 ± 1 µM and **68a** giving a GI_{50} of 27 ± 4 µM. Compound **16a** was the more potent, bringing cell density below that of the pre-treatment level. All derivatives were analysed for cell growth-inhibitory activity in the SRB assay (**Tables 23** and **24**). The procedure for the SRB assay is described in Chapter 7.2.

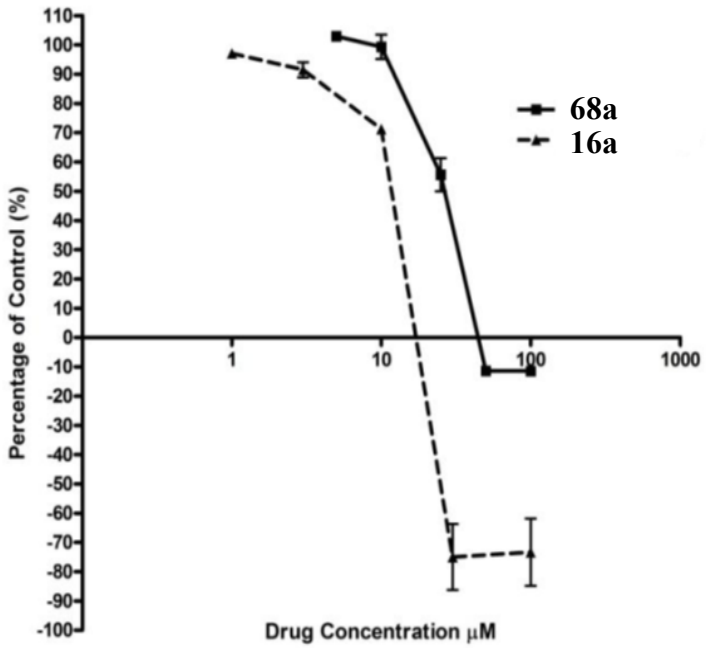

Figure 43: Inhibition of HeLa cell growth by **16a** and **68a** in a SRB assay (conducted by Laura Evans at the NICR)

Table 23: HeLa SRB assay for inhibitors **16a-16j** (conducted by Laura Evans at the NICR)

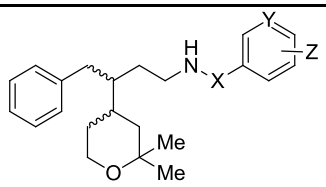

ID[a]	X	Y	Z	HeLa GI_{50} (μM)[b]
16a[c]	CH_2	CH	4-NMe_2	16 ± 1
16b	CH_2	CH	H	17 ± 3
16c	CH_2	CH	3-NMe_2	18 ± 2
16d	CH_2	CH	4-^{i}Pr	5.8 ± 1.1
16e	CH_2	CH	4-Cl	11 ± 4
16f	CH_2	CH	4-CN	36 ± 2
16g	CH_2	CH	4-OMe	29 ± 7
16h	CH_2	N	4-NMe_2	40 ± 3
16i	CO	CH	4-NMe_2	53 ± 7
16j	SO_2	CH	4-NMe_2	35 ± 2

(a) Diastereoisomers (*dr*, 5:2); (b) n = 3; (c) Compound tested as the free base. Dihydrochloride salt was similarly active at 13 ± 0 μM

All compounds in the *gem*-dimethylpyran series (**16a-16j**) were active against HeLa cell growth with **16d**, possessing a 4-isopropyl substituent, displaying superior potency to

16a. Unsubstituted analogue **16b** and regioisomer **16c** had similar potency to **16a**, suggesting that the dimethylamino group was not essential for cellular activity. Replacing the 4-NMe_2 group with a cyano (**16f**) or a methoxy substituent (**16g**) afforded a 2-fold loss in activity in each case. Introduction of a pyridyl ring (**16h**), as well as substituting an amide (**16i**) or sulfonamide (**16j**) for the methylene group of **16a**, reduced HeLa cell growth inhibition. However, none of these structural changes had a significant effect on activity, although interestingly, the most active compounds were also the most lipophilic [clog*P* 7.1 (**16d**); 6.4 (**16e**); clog*P* values for **16a**-**16c** and **16f**-**16j** were in the range 4.9-5.8], possibly due to improved cell penetration. Methylation of the secondary amine (**74a**) did not significantly affect potency, giving a GI_{50} value of 31 ± 3 μM, suggesting the amine NH was not involved in binding to the protein.

Table 24: HeLa SRB assay for pyrans **68a**-**68m** and morpholine **80** (conducted by Laura Evans at the NICR)

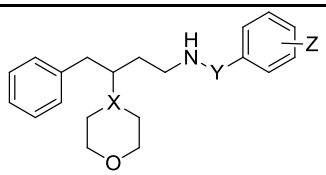

ID[a]	X	Y	Z	HeLa GI_{50} (μM)[b]
68a	CH	CH_2	4-NMe_2	27 ± 4
68b	CH	CH_2	4-$N(CH_2)_4$	8 ± 1
68c	CH	CH_2	4-CF_3	16 ± 1
68d	CH	CH_2	4-SMe	17 ± 1
68e	CH	CH_2	4-Cl	18 ± 1
68f	CH	CH_2	4-F	45 ± 1
68g	CH	CH_2	4-NO_2	47 ± 5
68h	CH	CH_2	4-NH_2	> 100
68i	CH	CH_2	4-N_3	17 ± 2
68j	CH	CH_2	4-$N(Me)CH_2CH_2OH$	33 ± 2
68k	CH	CH_2	4-SO_2Me	> 100
68l	CH	CO	4-Cl	37 ± 3
68m	CH	SO_2	4-Cl	30 ± 1
80	N	CH_2	4-NMe_2	40 ± 5

(a) Racemates; (b) $n = 3$

In the *des*-dimethyl series (**68a**-**68m**), 4-pyrrolidinyl (**68b**), 4-trifluoromethyl (**68c**), 4-methylthio (**68d**) and 4-chloro (**68e**) ligands improved HeLa cell growth-inhibitory

activity relative to **68a**. Comparison between **68a** and **68e** with the *gem*-dimethyl analogues (**16a** and **16e**) showed that the latter had marginally superior growth-inhibitory activity. Reducing 4-nitro (**68g**) to 4-amino (**68h**) or oxidising methylthio to methylsulfone (**68k**) abolished potency. These compounds were also the least lipophilic [clog*P* 3.4 (**68h**) and 3.0 (**68k**), as opposed to clog*P* 4.1-5.5 for the remaining compounds] supporting the hypothesis that compound activity depended on cell permeability. Replacing the methylene linker with an amide or sulfonamide and retaining the 4-chloro substituent (**68l** and **68m**, respectively) gave compounds of similar potency to **68a**. Compound **80** was 2-fold less active than **16a**, but had reduced lipophilicity [clog*P* 4.1 (**80**) and 5.8 (**16a**)] and the carbamate precursor **83** was similarly potent to **16a**, giving a GI_{50} of 20 ± 4 μM. Methylation of the secondary amine (**74b**) did not significantly affect potency, giving a GI_{50} value of 23 ± 2 μM.

4.4 Synthesis of Novel Pyran-4-ones

The high cost of pyranone **21** and the lack of commercially available 2,2-disubstituted pyranone analogues necessitated the development of a general procedure for the synthesis of pyranones for SAR studies.

4.4.1 Formation from Mesityl Oxide (20)

Following the published methodology,[79] refluxing mesityl oxide (**20**) in aqueous formaldehyde failed to form β-hydroxyenone **85**, giving no observable reaction by LC-MS, even after prolonged heating (**Scheme 14**). Subsequently, no cyclisation to pyranone **21** was observed upon addition of Amberlyst-15 resin to the crude material.

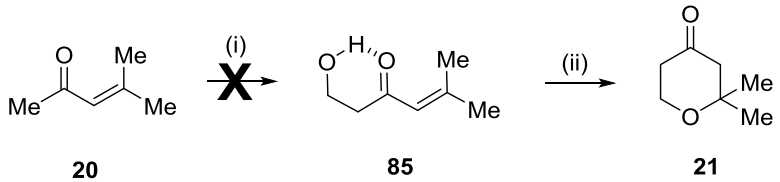

20 **85** **21**

Scheme 14: (i) 37% aq. H_2CO, 165 ^oC, 2 h; (ii) Amberlyst-15, $CHCl_3$, RT[79]

Using conditions described by Colonge,[118] **20** was successfully reacted with ethyl formate in the presence of sodium hydride to give 1,3-dicarbonyl **86** (**Scheme 15**). Cyclisation in the presence of mercury(II) sulfate and sulfuric acid gave

dihydropyranone **87** in 39% yield (^{1}H NMR analysis) after heating for several days, but the product was difficult to purify.

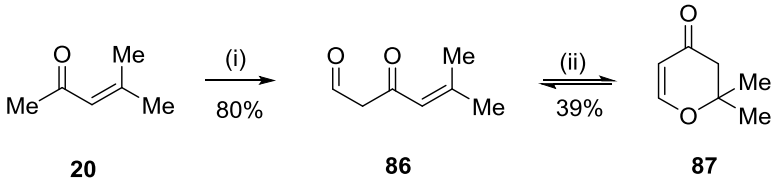

Scheme 15: (i) HCO_2Et, NaH, Et_2O, 0-10 ^oC, 24 h; (ii) $HgSO_4$, 10% aq. H_2SO_4, 100 ^oC, 48 h

The low yield in the cyclisation could be due to an unfavourable equilibrium so that full conversion of **86** could not be achieved. The low yield and the use of a toxic mercuric salt made this synthesis of **21** less attractive. It was found that cyclisation could be achieved using *p*TSA in place of mercury(II) sulfate,[119] but full conversion could still not be achieved. Alternative synthetic methods for a general synthesis of **21** and other 2,2-disubstituted pyranone derivatives were therefore investigated.

Deprotonation of **20** using LDA followed by addition of trioxane gave no reaction by LC-MS, even after warming to room temperature. However, it was shown that LDA did deprotonate **20**, as ^{1}H NMR analysis of the product from a D_2O-quenched reaction proved the incorporation of one atom of deuterium (**Scheme 16**).

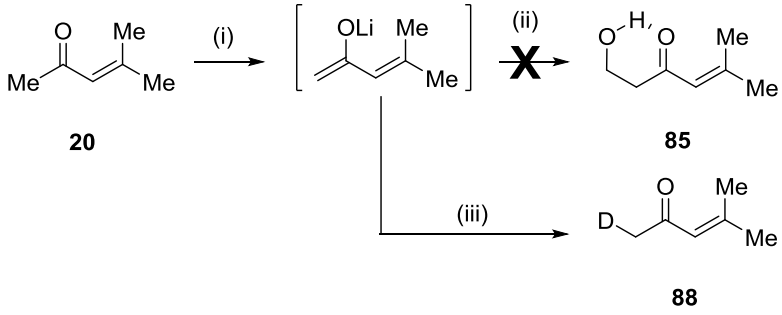

Scheme 16: (i) $^iPr_2NH$, *n*-BuLi, Et_2O, -78 ^oC, 24 h; (ii) $(H_2CO)_3$, Et_2O, -78-33 ^oC, 24 h; (iii) D_2O, Et_2O, -78 ^oC-RT

Using the procedure described by Yamamoto, trioxane was added neat to aluminium complex **90**, which was prepared *in situ* from trimethylaluminium (**89**) and 2,6-diphenylphenol (**Scheme 17**).[120] The high oxophilicity of aluminium(III) causes the trioxane to fragment into individual formaldehyde molecules and the Lewis acidity of

the aluminium centre potentiates the electrophilicity of formaldehyde by withdrawing electron density from the carbonyl carbon.[120] However, addition of the enolate of **20** to aluminium complex **91** at -78 °C resulted in no reaction (^{1}H NMR analysis), even after warming to room temperature.

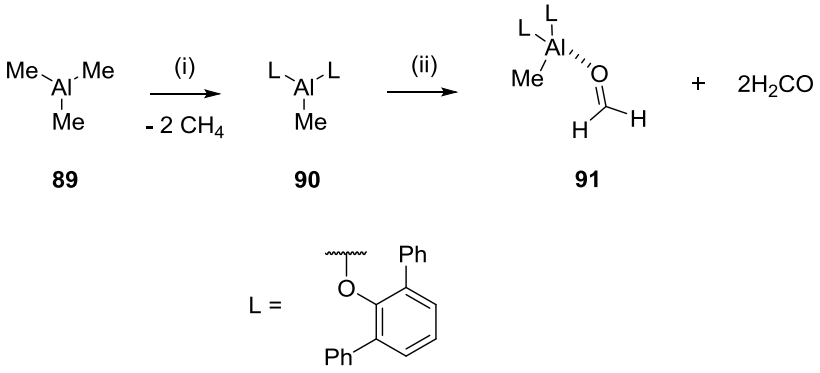

Scheme 17: (i) 2,6-Diphenylphenol (2.0 equiv.), DCM, RT, 1 h; (ii) $(H_2CO)_3$, DCM, 0 °C, 1 h

4.4.2 Formation of 1-Hydroxy-5-methylhex-4-en-3-one (85)

Starting from 3-hydroxypropionitrile (**92**), high-yielding silylation of the alcohol was followed by reaction with 2-methyl-1-propenylmagnesium bromide (**Scheme 18**).[121] However, the desired enone **94** did not form under these conditions.

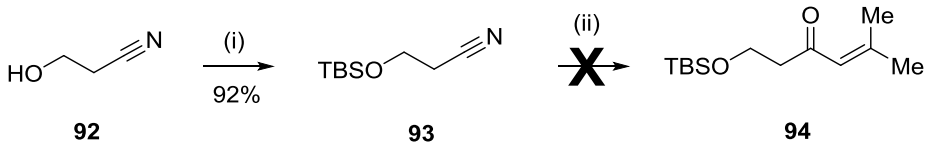

Scheme 18: (i) TBSCl, imidazole, DCM, 0 °C-RT, 5 h; (ii) $Me_2CCHMgBr$, THF, 0 °C, 2 h; NH_4Cl, RT

^{1}H NMR analysis of the crude material showed that *tert*-butyldimethylsilylalcohol (^{t}BuMe$_2$SiOH) was the predominant species present. It was possible that the Grignard reagent behaved as a base and eliminated ^{t}BuMe$_2$SiOH, forming 2-methylpropene (**95**) and acrylonitrile (**96**) (**Scheme 19**). These low-boiling side products would have been lost during concentration of the crude material *in vacuo*, explaining the absence of their corresponding peaks in the ^{1}H NMR spectrum.

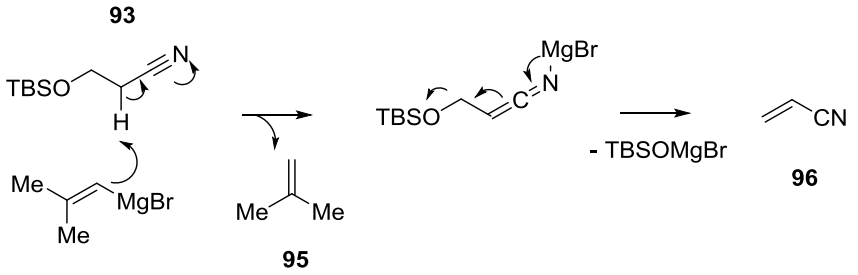

Scheme 19: Proposed elimination of 2-methylpropene (**95**) and acrylonitrile (**96**) initiated by 2-methyl-1-propenylmagnesium bromide

To reduce the basicity of the organometallic reagent, 2-methyl-1-propenylmagnesium bromide was transmetallated to the corresponding organocopper reagent (**Scheme 20**). Upon addition of **93**, no reaction occurred, as shown by ^{1}H NMR analysis after stirring at room temperature for 24 h.

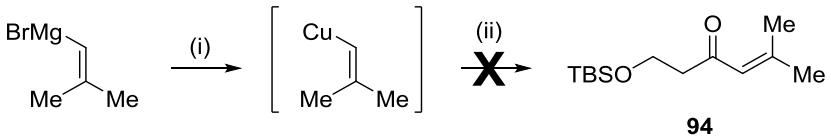

Scheme 20: (i) CuCl, THF, 0 ^{o}C-RT, 1 h; (ii) **93**, THF, RT, 24 h; NH_4Cl, RT

Following the procedure by Fry, nitrile **93** was coupled with 2-chloropropane in the presence of $FeCl_3$ to give the isopropylnitrilium salt **97** with enhanced electrophilicity at the nitrile carbon (**Scheme 21**).[122] Reaction of **97** with 2-methyl-1-propenylmagnesium bromide gave enone **94**, as shown by ^{1}H NMR analysis. However, the purification was difficult and the yield was low. A similar result was obtained upon reaction of **97** with the corresponding organocopper reagent (*cf*. Scheme 20).

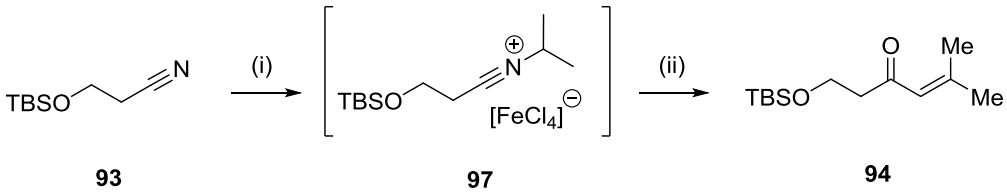

Scheme 21: (i) 2-Chloropropane, $FeCl_3$, 0-50 ^{o}C, o/n; (ii) $Me_2CCHMgBr$ or Me_2CCHCu, THF, 0 ^{o}C-RT, 6-16 h; NH_4Cl, RT

4.4.3 Formation of Dihydropyran-4-ones by Cycloaddition

Huang and Rawal had synthesised 2,2-disubstituted dihydropyran-4-ones by reacting ketones with diene **98**, with pyranone **87** reportedly being synthesised in 40% yield using acetone (**Scheme 22**).[123] 2-Butanol was found to be the optimal solvent for the cyclisation, as it resulted in negligible diene alcoholysis when compared to water or other simple alcohols.[123] The solvent needed to be protic, as it formed a hydrogen bond with the carbonyl oxygen, enhancing the electrophilicity of the ketone. When this reaction was attempted under the described conditions, no observable quantities of **87** could be isolated and diene **98** rapidly converted to enone **100** at room temperature (^{1}H NMR analysis). 2-Butanol was subsequently used in catalytic amounts in acetone but this reaction was slower and diene **98** was still subject to alcoholysis. Replacing 2-butanol with TFE (pK_a 12.4) was expected to accelerate the reaction and reduce alcoholysis. However, replacing 2-butanol with TFE gave no obvious advantage, with most of **98** being alcoholysed at room temperature within 1 h (^{1}H NMR analysis). Based on the possibility that conversion of **98** to **100** was mediated by adventitious water, acetone and 2-butanol were rigorously dried by distillation over calcium hydride. This reduced alcoholysis of **98**, but no cyclisation product **99** was detected by ^{1}H NMR analysis after 30 h at room temperature. Despite considerable efforts to repeat the claims of Huang and Rawal, no trace of pyranone **87** was obtained.

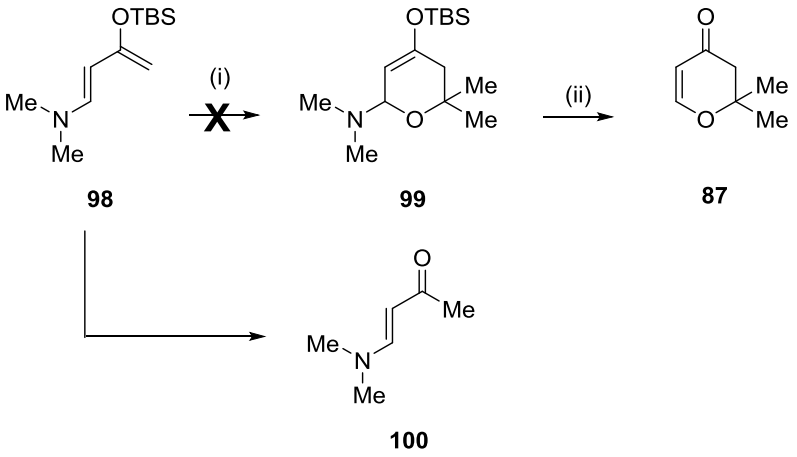

98 **99** **87** **100**

Scheme 22: Me_2CO, 2-BuOH, RT, 30 h; (ii) AcCl, Et_2O, -78 ^oC[123]

4.5 Finding the Minimum Pharmacophore of 16a

In the *gem*-dimethylpyran series, deletion of the dimethylamino group (*cf.* Table 23, **16b**) did not affect potency and indeed, substitution of the benzylamino substituent for a carbamate (**101**), synthesised by treatment of amine **28** with Boc_2O (**Scheme 23**), produced a similarly active species (**Table 25**).

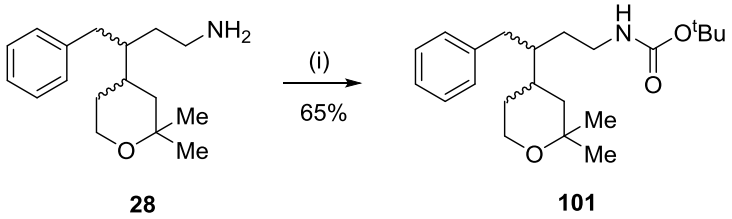

Scheme 23: (i) Boc_2O, DCM, 0 °C-RT, o/n

Removal of the *gem*-dimethyl group had no significant impact on cellular potency (*cf.* Table 24, **68a** and **68e**) and deletion of the tetrahydropyran ring (**109**) also retained activity in HeLa cells (**Table 25**). Compound **109** was synthesised from ester **103**, obtained *via* HWE olefination of benzaldehyde (**102**) with triethyl 2-phosphonopropionate (**Scheme 24**).

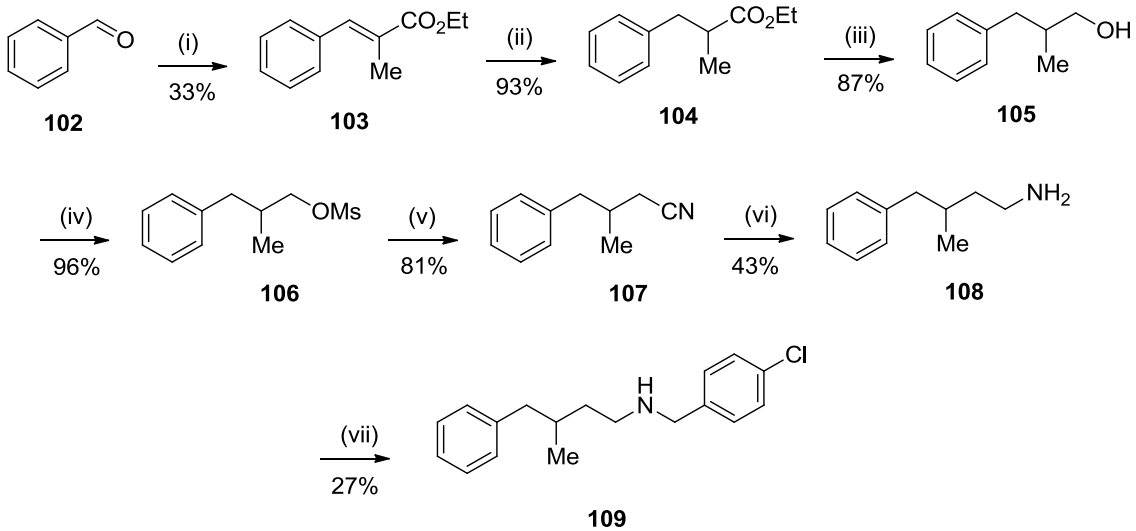

Scheme 24: (i) $(EtO)_2(O)PCH(Me)CO_2Et$, NaH, THF, 0-30 °C 48 h; (ii) NH_4HCO_2, 10% Pd/C, MeOH, 0-90 °C, 90 min; (iii) $LiAlH_4$, THF, 0 °C, 2 h; (iv) $MeSO_2Cl$, $^iPr_2NEt$, DCM, RT, 2 h; (v) NaCN, DMF, 100 °C, 7 h; (vi) H_2, Raney Ni, 60 bar, 70 °C, 24 h; (vii) 4-chlorobenzaldehyde, $MgSO_4$, DCM, RT, 4 h; $NaBH_4$, MeOH, RT, 1 h

Further simplification to compound **111**, synthesised by reductive amination of 4-chlorobenzaldehyde with isopentylamine (**110**) (**Scheme 25**), abrogated activity in HeLa cells. Several intermediates (**63**, **66** and **67**) in the synthesis of **68a** were also evaluated and found to be inactive (**Table 25**).

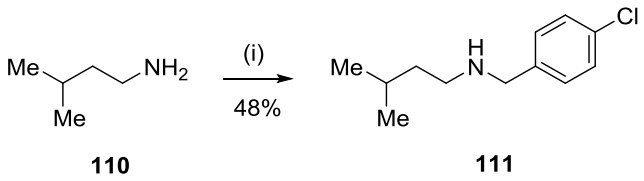

110 **111**

Scheme 25: (i) 4-Chlorobenzaldehyde, $MgSO_4$, DCM, RT, 4 h; $NaBH_4$, MeOH, RT, 1 h

Table 25: HeLa SRB assay for fragment derivatives of **16a** and **68e**[a] (conducted by Laura Evans at the NICR)

ID[b]	Structure	HeLa GI_{50} (µM)[c]
101	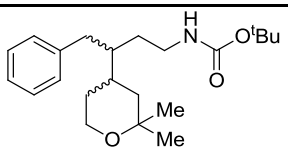	35 ± 2
67	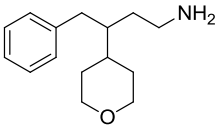	> 100
66	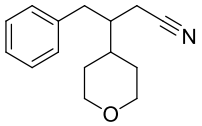	> 100
63	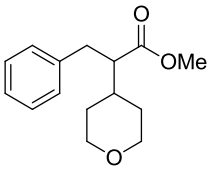	> 100
109	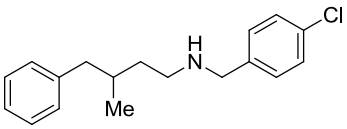	16 ± 1
111	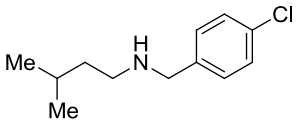	> 100

(a) Compound **16a** HeLa GI_{50}, 16 ± 1 µM and compound **68e** HeLa GI_{50}, 18 ± 1 µM; (b) Racemates or diastereoisomers (*dr*, 5:2); (c) $n = 3$

Substitution of the tetrahydropyran ring by a methyl group (**109**) retained activity but replacement of both the pyran and phenyl ring by methyl groups (**111**) abolished potency, suggesting that the phenyl ring was important for cell toxicity, although this modification was accompanied by a decrease in lipophilicity. The intermediates **63**, **66** and **67** possessed no growth-inhibitory activity, suggesting with reference to compounds **67** and **111**, that structure **109** is the minimum pharmacophore.

4.6 Synthesis of the Enantiomers of 68a

It was of interest to determine if **16a** demonstrated stereoselectivity in HeLa cells, as this would provide evidence of a specific binding interaction with a receptor. The enantiomers of **68a** were selected, as the racemate was similarly active to **16a** in HeLa cells and the absence of the *gem*-dimethyl group meant that **68a** had only one chiral centre. Separation of the enantiomers of **68a** by chiral HPLC was unsuccessful, necessitating the development of an enantioselective route.

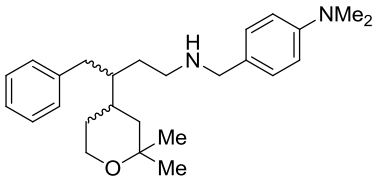

16a

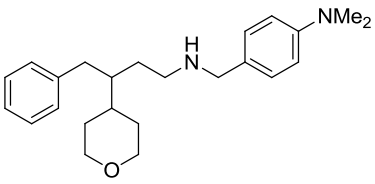

(±)-68a

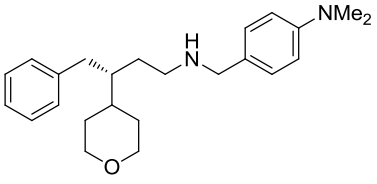

(*R*)-68a

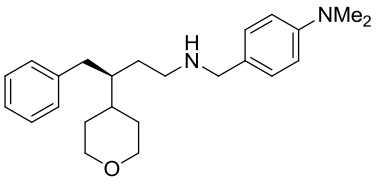

(*S*)-68a

Starting from pyranone **60**, HWE olefination and transfer hydrogenation yielded ester **62**. Hydrolysis with lithium hydroxide provided carboxylic acid **112** and treatment with pivaloyl chloride and (*R*)- or (*S*)-4-benzyloxazolidin-2-one, gave oxazolidinones ***(R)*-113** and ***(S)*-113**, respectively (**Scheme 26**).

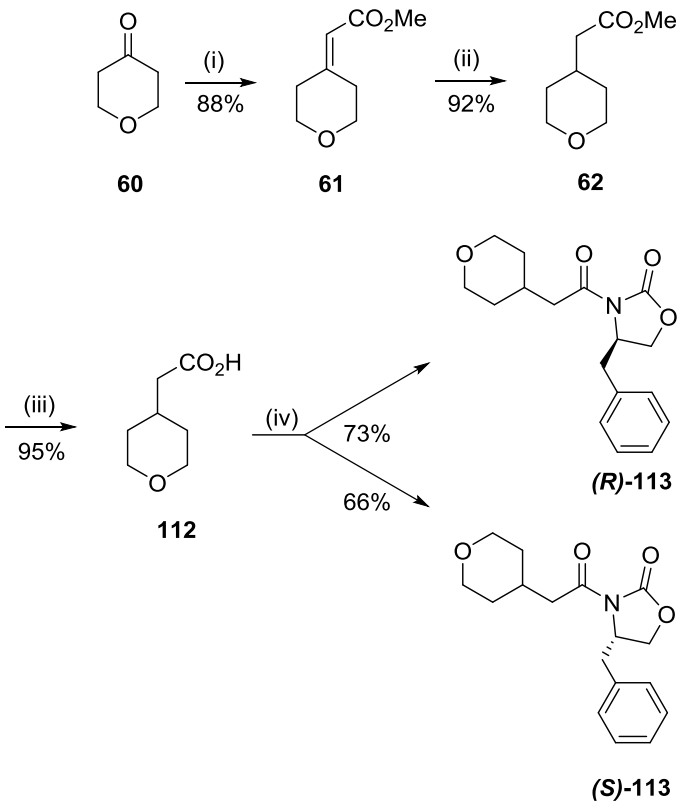

Scheme 26: (i) $(MeO)_2(O)PCH_2CO_2Me$, NaH, THF, 0 ^oC-RT, 20 h; (ii) NH_4HCO_2, 10% Pd/C, MeOH, 0-90 ^oC, 90 min; (iii) $LiOH.H_2O$, 50% THF, H_2O, 60 ^oC, 2 h; (iv) ^tBuCOCl, Et_3N, THF, 0 ^oC, 45 min; (*R*)- or (*S*)-4-benzyloxazolidin-2-one, LiCl, THF, RT, 16 h

Using Evans' methodology,[124] enolate formation with LDA in the presence of HMPA prior to addition of benzyl bromide, gave **(*R*,*R*)-114** and **(*S*,*S*)-114** in > 98% *de*. Removal of the chiral auxiliary to give alcohols **(*R*)-64** and **(*S*)-64** proved surprisingly difficult. Reduction of **(*S*,*S*)-114** with lithium borohydride failed to yield **(*S*)-64**, instead yielding amide **(*S*,*S*)-115**, as a result of borohydride attack on the *endo*-carbonyl group of the oxazolidin-2-one (**Scheme 27**).

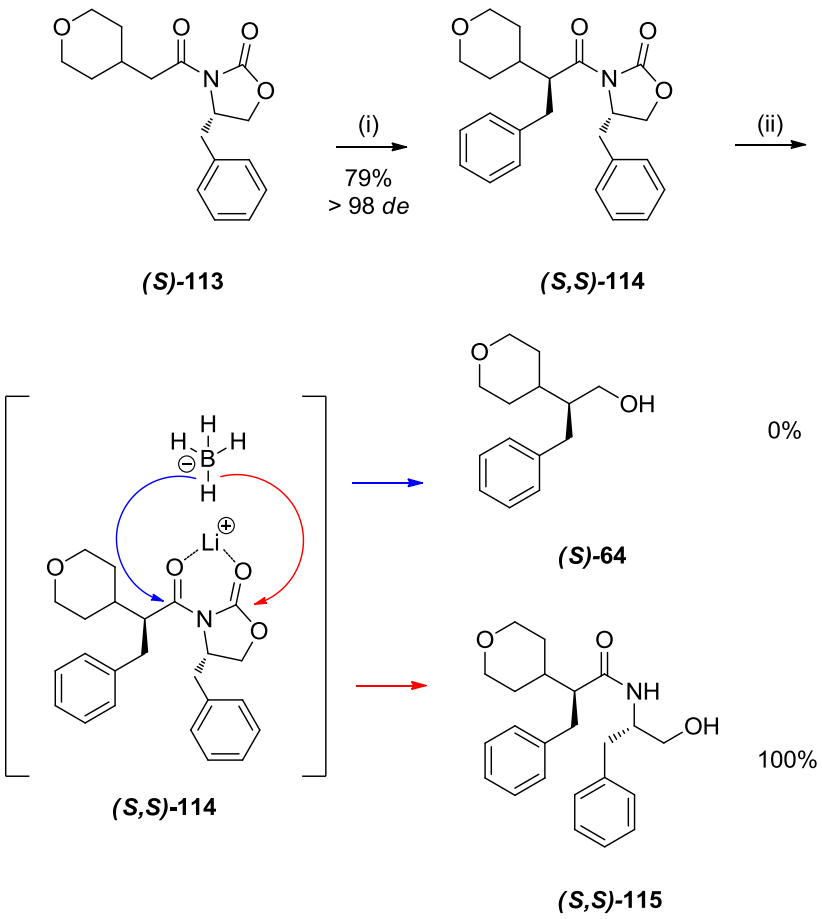

Scheme 27: Competing borohydride attack on the *exo* (blue arrow) and *endo* carbonyls of **(*S*,*S*)-114**; (i) $^{i}Pr_2NH$, *n*-BuLi, HMPA, THF, 0 to -78 ^{o}C, 1 h; BnBr, THF, -78 ^{o}C, 6 h; (ii) $LiBH_4$ (2.0 M in THF), THF, 40 ^{o}C, 1 h

Palomo had described the use of sodium borohydride in water as a convenient method for the reduction of chiral auxiliaries to the corresponding alcohols.[125] However, these conditions resulted in only partial conversion to **(*S*,*S*)-115** when applied to **(*S*,*S*)-114** and none of the desired alcohol was formed. Kanomata had described the use of sodium methoxide in an excess of dimethyl carbonate (DMC) as a facile method for cleaving sterically demanding chiral auxiliaries to the corresponding methyl esters.[126] Attack by methoxide on the *endo*-carbonyl would generate DMC as a by-product, but if DMC was already present in excess, the equilibrium would shift to minimise this reaction and form only the *exo*-product (**Scheme 28**).[126]

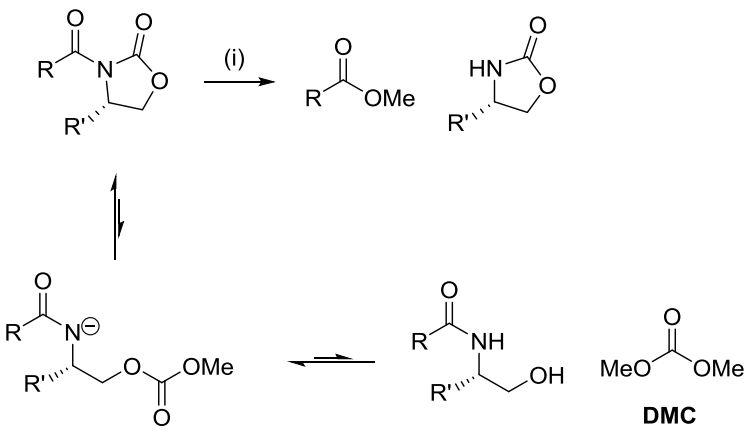

Scheme 28: (i) NaOMe, DMC, RT-50 ^{o}C[126]

When these conditions were applied to **(*S*,*S*)-114**, amide **(*S*,*S*)-115** was obtained as the sole product. Success was achieved by switching from lithium borohydride to either lithium aluminium hydride solution or triethylborohydride (superhydride) solution.[127] At -78 ^{o}C, **(*S*,*S*)-114** was converted to a mixture of **(*S*)-64** and **(*S*,*S*)-115** upon warming to room temperature. Lithium aluminium hydride gave a 1:1 ratio of the products whilst superhydride generated a 3:1 ratio of **(*S*)-64** and **(*S*,*S*)-115** by LC-MS. Removal of the auxiliaries using superhydride gave **(*R*)-64** and **(*S*)-64** in 41% yield. Mesylation, substitution with sodium cyanide, reduction with lithium aluminium hydride and reductive amination with 4-(*N*,*N*-dimethylamino)benzaldehyde gave enantiomer **(*R*)-68a** or **(*S*)-68a** (**Scheme 29**).

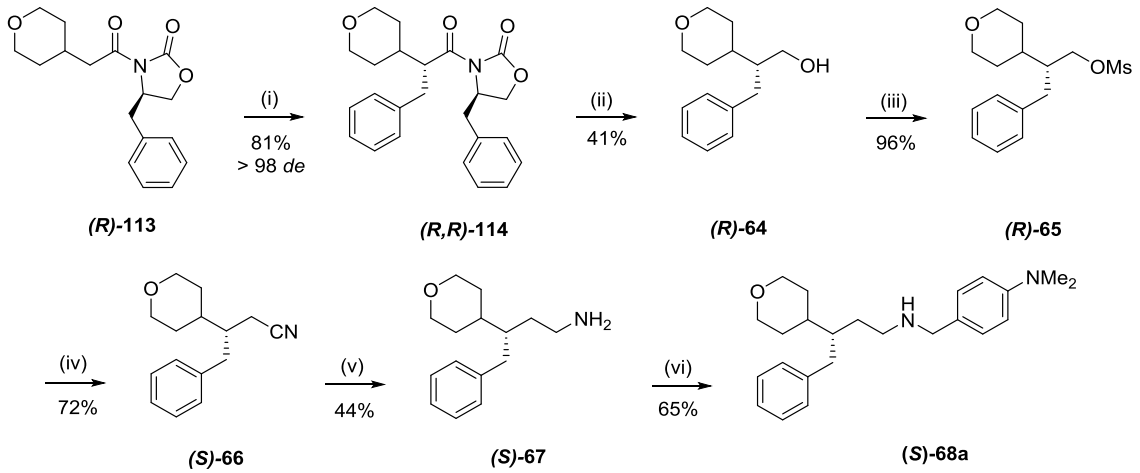

A)

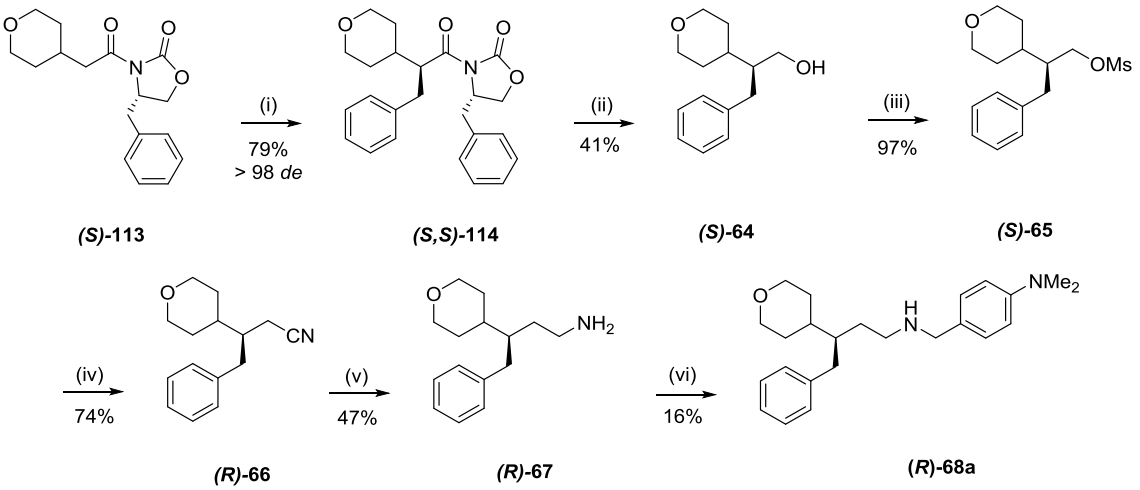

B)

Scheme 29: A) Synthesis of **(*S*)-68a**; **B)** synthesis of **(*R*)-68a**; (i) $^{i}Pr_2NH$, *n*-BuLi, HMPA, THF, 0 to -78 ^{o}C, 1 h; BnBr, THF, -78 ^{o}C, 6 h; (ii) $LiBEt_3H$, Et_2O, -78 ^{o}C-RT, o/n; (iii) MsCl, $^{i}Pr_2NEt$, DCM, RT, 2 h; (iv) NaCN, DMF, 100 ^{o}C, 7 h; (v) $LiAlH_4$, THF, 0 ^{o}C, 3 h; (vi) 4-(*N*,*N*-dimethylamino)benzaldehyde, $MgSO_4$, DCM, RT, 4 h; $NaBH_4$, MeOH, RT, 1 h

Chiral HPLC on intemediates **(*R*)-67** and **(*S*)-67** revealed both compounds were present in ≥ 99% *ee* (± 1%) when compared to a sample of the racemate (**Figure 44**). Enantiomers **(*R*)-68a** and **(*S*)-68a** were analysed by the HeLa cell-based SRB assay (**Table 26**). Both enantiomers and the racemate were equipotent in HeLa cells, suggesting a non-stereoselective mechanism of cellular toxicity.

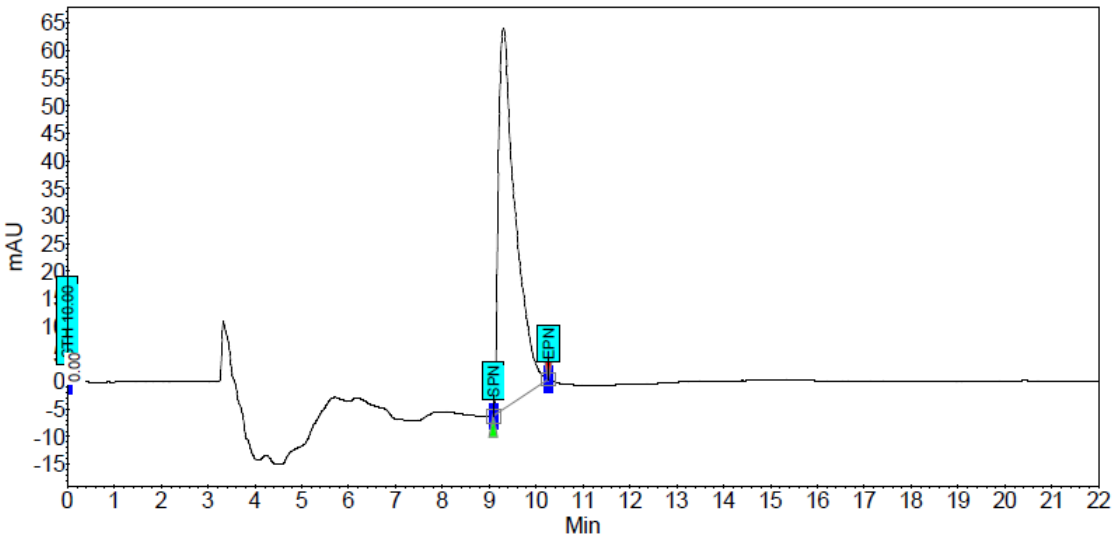

A)

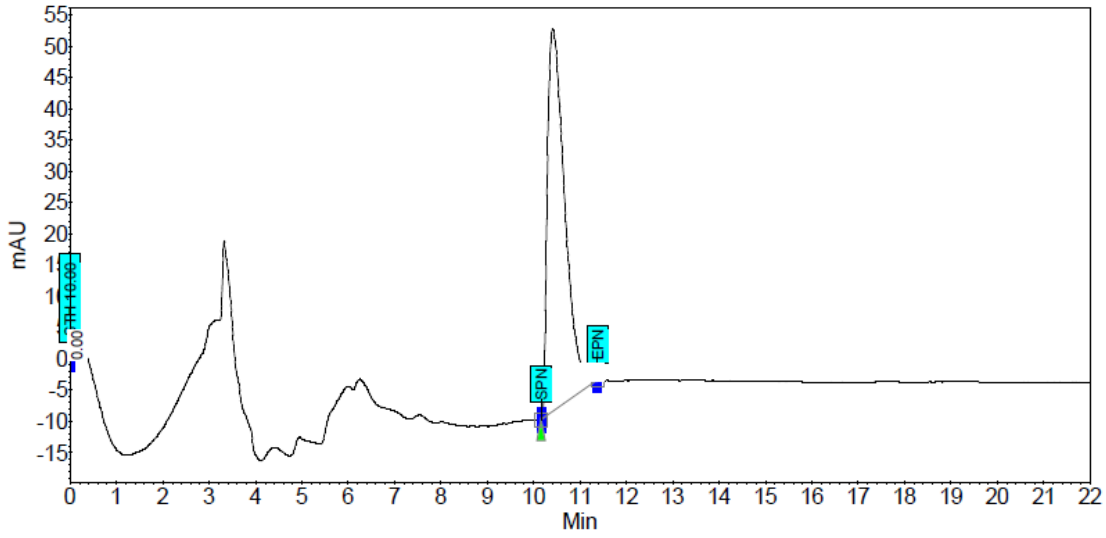

B)

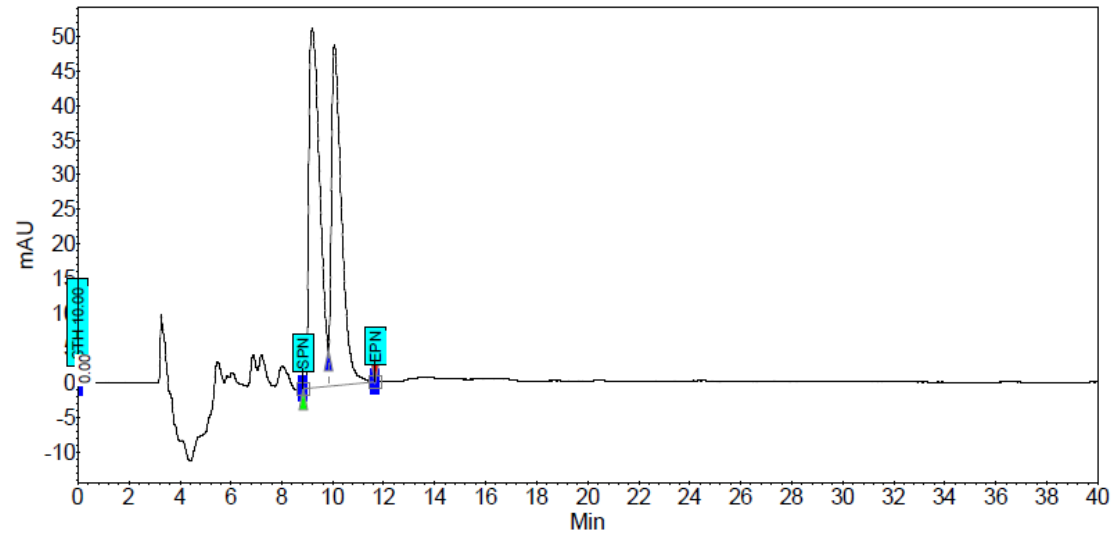

C)

Figure 44: Chiral HPLC results for **A) (*S*)-67**; **B) (*R*)-67** and **C)** (±)-**67** (conducted by Dr Karen Haggerty in the Medicinal Chemistry Laborotories)

Table 26: HeLa cell-based assay for compound **68a** enantiomers[a] (conducted by Laura Evans at the NICR)

ID	HeLa GI_{50} (μM)[b]
***(S)*-68a**	33 ± 4
***(R)*-68a**	29 ± 2

(a) ±-**68a** HeLa GI_{50}, 27 ± 4 μM; (b) n = 3

4.7 Conclusion

In conclusion, an efficient and versatile synthesis of the first-reported small-molecule inhibitor of the SCF^{SKP2} complex, **16a**, was completed and growth-inhibitory activity was confirmed in HeLa cells using an SRB assay. Removal of the *gem*-dimethyl group from the pyran ring of **16a** did not significantly affect potency in HeLa cells and modification of the 4-(*N*,*N*-dimethylamino)benzyl substituent also did not improve activity in either the *gem*- or *des*-dimethylpyran series. Replacing the pyran ring with a morpholino ring (**80**) reduced compound lipophilicity without seriously affecting activity but complete removal of the pyran ring (**109**) had a similar effect. There was a trend observed between lipophilicity and growth-inhibitory activity, with the most lipophilic compounds, **16d** and **16e**, being the most active and the least lipophilic compounds, **68h** and **68k**, being inactive. **(*R*)-** and **(*S*)-68a** were synthesised using an enantioselective route featuring Evans' chiral auxiliaries. Both enantiomers and the racemate were equipotent in HeLa cells, suggesting that these cytotoxic compounds have a non-specific mechanism of action yet to be defined.

Chapter Five: MDMX Results and Discussion

5.1 The 1,3-Disubstituted Benzenoid MDMX Inhibitors

Docking of thiazole **44a** in the MDMX binding site indicated that a substituent branching from the thiazole nitrogen atom could potentially make hydrophobic interactions within the p53-W23 subpocket (**Figure 45**).

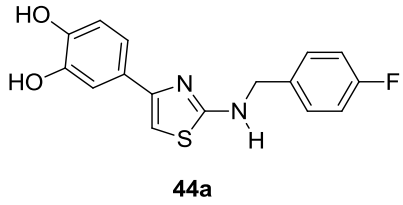

44a

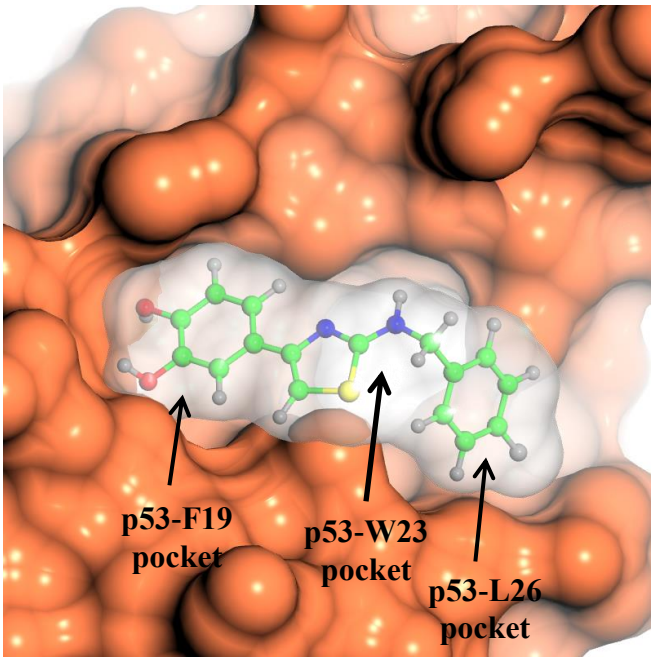

Figure 45: Model of thiazole **44a** interacting with the p53-binding site of MDMX (coral). Compound colour scheme: carbon = green; hydrogen = grey, small; fluorine = grey, large; oxygen = red; nitrogen = blue; sulfur = yellow. The p53-W23 binding pocket is the area of white indicated by the arrow. Image created using COOT with CCP4mg plug-in.

Substitution at the thiazole nitrogen would form a reactive thiazolium salt so the thiazole scaffold was replaced by a benzene ring, allowing for multiple derivatives to be rapidly synthesised for developing SARs (**Scheme 30**).

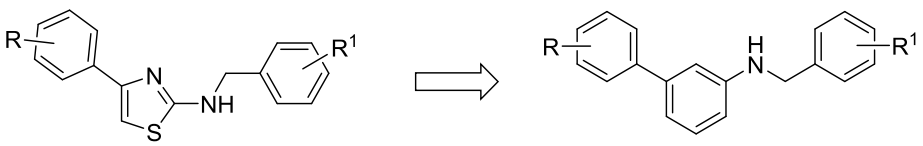

Scheme 30: Scaffold-hop from a 2,4-disubstituted thiazole to a 1,3-disubstituted benzene ring

Initial target compounds were based on hit compounds synthesised in the thiazole series, to examine whether the SARs in the benzenoid series differed significantly. Starting from 3-aminobenzeneboronic acid (**116**), Suzuki coupling with 4-bromophenol in the presence of $Pd(PPh_3)_4$, gave aniline **117a** in 26% yield after heating at 100 ^oC for 22 h. Optimisation of the conditions found that $Pd(dtbpf)Cl_2$ was a superior catalyst and gave a faster and cleaner conversion compared with $Pd(PPh_3)_4$ and $Pd(dppf)Cl_2$ (**Table 27**). Combined with microwave irradiation instead of conventional heating, full conversion could be achieved within 20 min at 120 ^oC.

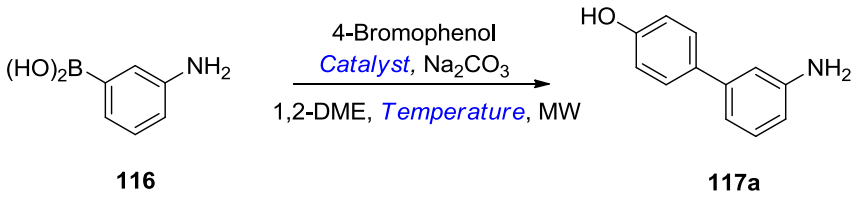

116 **117a**

Table 27: Optimisation of temperature and catalyst in the Suzuki coupling between boronic acid **116** and 4-bromophenol[a]

Catalyst	Temp. (^oC)	% Conversion[b]
$Pd(PPh_3)_4$	40	1.6
$Pd(PPh_3)_4$	60	8.2
$Pd(PPh_3)_4$	80	9.6
$Pd(PPh_3)_4$	100	11.5
$Pd(PPh_3)_4$	120	16.8
$Pd(PPh_3)_4$	140	17.5
$Pd(dppf)Cl_2$	140	31.8
$Pd(dtbpf)Cl_2$	140	70.0

(a) **116** (48 mg, 1.2 equiv.), 4-bromophenol (1.0 equiv.), catalyst (5.0 mol%), 2 M aq. Na_2CO_3 (2.0 equiv.), 1,2-DME (3.2 mL); (b) After 5 min by LC-MS

The optimised Suzuki coupling conditions were used to couple **116** with several aryl bromides in moderate to excellent yields. All reactions achieved full conversion of the aryl bromide within 20 min at 120 ^oC. Reductive amination of 4-fluorobenzaldehyde with **117a** to **117d** yielded the target compounds **118a** to **118d** respectively (**Scheme 31**).

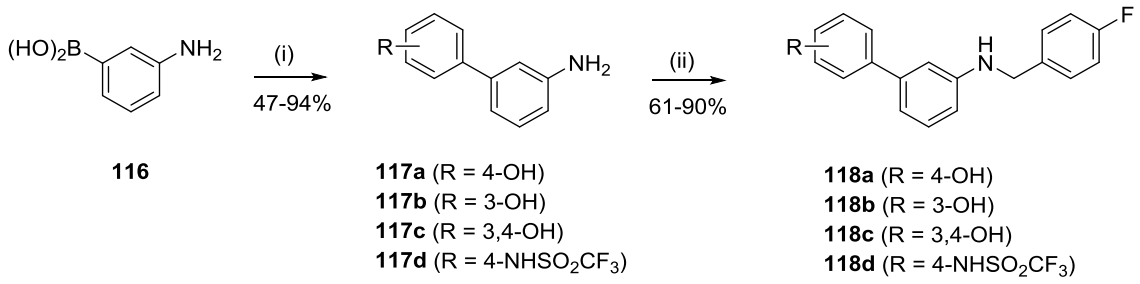

116

117a (R = 4-OH)
117b (R = 3-OH)
117c (R = 3,4-OH)
117d (R = 4-$NHSO_2CF_3$)

118a (R = 4-OH)
118b (R = 3-OH)
118c (R = 3,4-OH)
118d (R = 4-$NHSO_2CF_3$)

Scheme 31: (i) Aryl bromide, Pd(dtbpf)Cl_2, Na_2CO_3, 1,2-DME, 120 ^oC, MW, 20 min; (ii) 4-fluorobenzaldehyde, $MgSO_4$, THF, RT, 4 h; $NaBH_4$, MeOH, RT, 1 h

For the synthesis of **117d**, the desired aryl bromide (**120**) was not commercially available. Triflation of 4-bromoaniline (**119**) using triflic anhydride (Tf_2O) with Hünig's base gave **120** in high yield (**Scheme 32**).

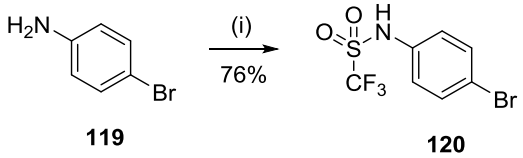

119 **120**

Scheme 32: (i) Tf_2O, $^iPr_2NEt$, DCM, 0 ^oC-RT, 30 min; 2.5 M NaOH, MeOH (1:3), RT, 3 h

The 1,4-disubstituted regioisomer **118e** was obtained by Suzuki coupling of aryl bromide **120** with 4-aminobenzeneboronic acid pinacol ester under previously optimised conditions (*cf.* Scheme 31), followed by reductive amination of 4-fluorobenzaldehyde with **117e** (**Scheme 33**).

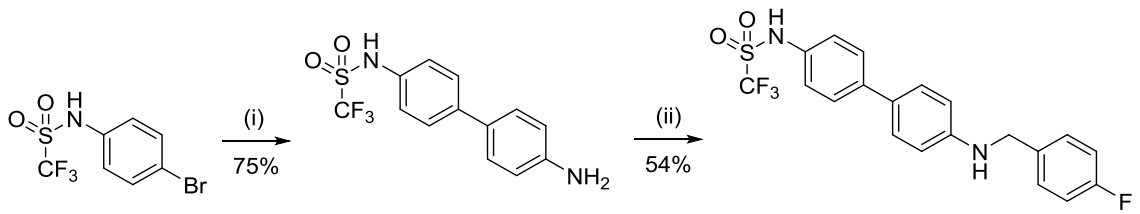

120 **117e** **118e**

Scheme 33: (i) 4-Aminobenzeneboronic acid pinacol ester, Pd(dtbpf)Cl_2, Na_2CO_3, 1,2-DME, 120 ^oC, MW, 20 min; (ii) 4-fluorobenzaldehyde, $MgSO_4$, THF, RT, 4 h; $NaBH_4$, MeOH, RT, 1 h

Compounds **118a-118e** were screened against MDMX and MDM2 using an enzyme-linked immunosorbent assay (ELISA) (**Table 28**).

Table 28: ELISA data for 1,3-disubstituted benzene derivatives **118a-118e** (conducted by Dr Yan Zhao at the NICR)

ID	Structure	MDMX IC_{50} (μM)[a]	MDM2 IC_{50} (μM)[b]	Ratio (MDMX: MDM2)	LE[c]	LipE[c,d]
118a	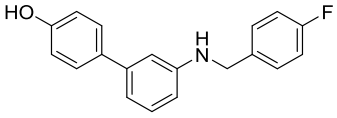	41.3	48.3	1.17	0.27	+ 1.70
118b	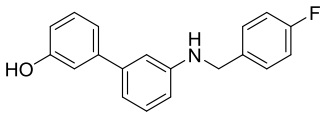	208	71.0	0.34	0.23	+ 0.99
118c	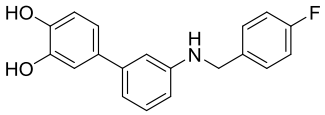	64.7	35.0	0.54	0.25	+ 2.15
118d	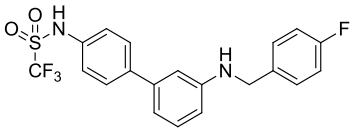	61.2	49.8	0.81	0.20	+ 0.73
118e	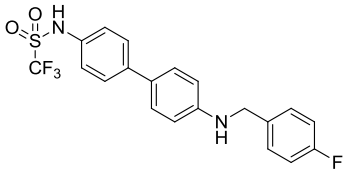	48.9	59.9	1.22	0.20	+ 0.87

(a) n = 2; (b) n = 1; (c) With respect to MDMX; (d) LipE = pIC_{50} – $clogD_{7.4}$ (clogD values from StarDrop)

A benzenoid scaffold was tolerated, with compounds **118a, 118c**, **118d** and **118e** showing modest activity against MDMX. All compounds demonstrated low selectivity for MDMX or MDM2 but the selectivity profiles were dependent on the molecular scaffold (*cf.* Table 20, **44a**, **44c** and **44j**). Compound **44c** showed 5-fold greater MDM2 potency over MDMX but the corresponding benzenoid compound (**118a**) was equipotent against both proteins. With a *p*-hydroxy group, activity against MDMX or MDM2 was moderate, but a *m*-hydroxy group reduced MDMX potency 5-fold in the benzenoid series (**118b**). A 3,4-catechol restored potency (**118c**) suggesting the *p*-hydroxy group was making a favourable interaction with the protein. Most of the corresponding benzenoid and thiazole compounds were similarly active against both

proteins (1.5 to 4-fold difference in activities). However, compound **44j** was 10-fold more active against MDMX than the corresponding benzenoid compound **118d**. When the 4-fluorobenzylamino substituent was *para* to the 4-*N*-sulfonamidobenzene ring (**118e**), affinity for MDMX and MDM2 was not affected relative to the 1,3-disubstituted derivative (**118d**). It is possible that the 4-fluorobenzylamino moiety was either not making any significant contact with the protein or the binding pocket was sufficiently large to accommodate either regioisomer.

Future SARs were limited to 1,3-disubstituted benzenoid compounds due to the structural similarity of the 1,4-disubstituted compound to benzidine (**121**), a potent human bladder carcinogen.

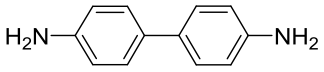

121

The SAR data in Table 28 highlighted the significance of a *p*-OH or *p*-$NHSO_2CF_3$ group for potent inhibition of MDMX or MDM2, an observation previously made in the 2,4-disubstituted thiazole series. However, phenols display metabolic instability *in vivo* (*cf.* Scheme 2) and the trifluoromethylsulfonamide significantly increased molecular weight and lipophilicity, necessitating alternative functionalities. Several alternative substituents had been tested in the thiazole series, facilitating comparisons with the benzenoid series (**Table 29**). Reductive amination of 4-fluorobenzaldehyde with aniline **122** gave boronic ester **123**. Compounds **118f-118h**, **118j** and **118k** were synthesised *via* Suzuki coupling with **123** and the appropriate aryl bromide (**Scheme 34**).

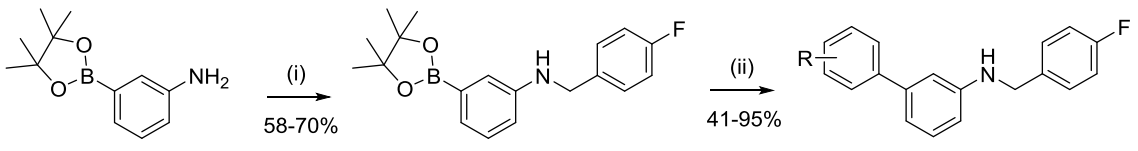

122 **123**

118f (R = 4-$NHSO_2Me$)
118g (R = 4-NH_2)
118h (R = 3-NH_2)
118j (R = 3-OMe)
118k (R = 4NHCOMe)

Scheme 34: (i) 4-Fluorobenzaldehyde, $MgSO_4$, THF, RT, 4 h; $NaBH_4$, MeOH, RT, 1 h; (ii) appropriate aryl bromide, $Pd(dtbpf)Cl_2$, Na_2CO_3, 1,2-DME, 120 ^oC, MW, 20 min

Compound **118i** was synthesised by reductive amination of 4-fluorobenzaldehyde with aniline hydrochloride **117f** (**Scheme 35**).

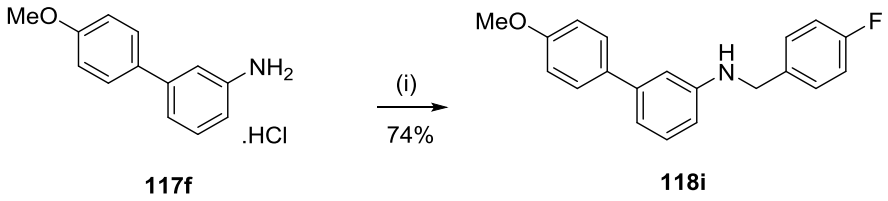

117f **118i**

Scheme 35: (i) 4-Fluorobenzaldehyde, $NaB(OAc)_3H$, DMF, AcOH, RT, 24 h

Compounds **118l**, **118m** and **118o** were synthesised by reductive amination of 4-fluorobenzaldehyde with anilines **117g**, **117h** and **117i** (**Scheme 36**).

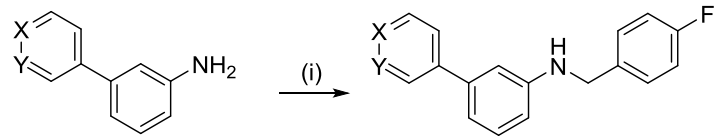

117g (X = Y = CH)
117h (X = CH, Y = N)
117i (X = N, Y = CH)

118l (X = Y = CH)
118m (X = N, Y = CH)
118o (X = CH, Y = N)

Scheme 36: (i) 4-Fluorobenzaldehyde, $MgSO_4$, THF, RT, 4 h; $NaBH_4$, MeOH, RT, 1 h

For the synthesis of **118n**, aryl bromide **125** was prepared from neutralised 4-bromopyridine hydrochloride (**124**) by oxidising with *m*CPBA, followed by Suzuki coupling with **123** (**Scheme 37**).

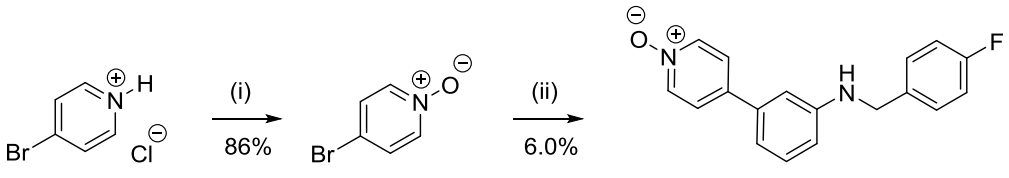

124 **125** **118n**

Scheme 37: (i) NaOH (aq.), RT, 20 min; *m*CPBA, Et_2O, RT, 3 h; (ii) **123**, $Pd(dtbpf)Cl_2$, Na_2CO_3, 1,2-DME, 120 ^oC, MW, 45 min

Table 29: ELISA data for 1,3-disubstituted benzene derivatives **118f-118o** (conducted by Dr Yan Zhao at the NICR)

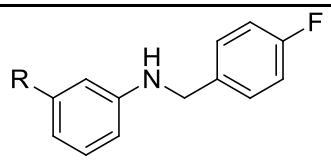

ID	R	MDMX IC_{50} (μM)[a]	MDM2 IC_{50} (μM)[b]	Ratio (MDMX : MDM2)	LE[c]	LipE[c,f]
118f	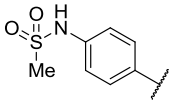	13%[e]	913	-	-	-
118g	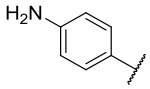	419	496	1.18	0.21	+ 0.39
118h	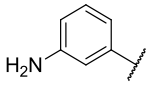	688	205	0.30	0.20	0.14
118i	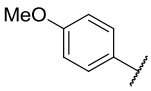	25%[e]	20%[d]	-	-	-
118j	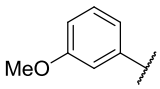	1002	10%[d]	-	0.18	- 0.35
118k	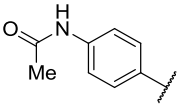	197	588	2.98	0.20	+ 0.69
118l	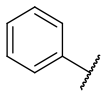	14%[e]	697	-	-	-
118m	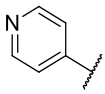	41%[e]	29%[d]	-	-	-
118n	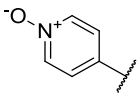	33%[d]	25%[d]	-	-	-
118o	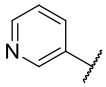	1000	34%[d]	-	0.20	+ 0.44

(a) *n* = 2; (b) *n* = 1; (c) With respect to MDMX; (d) 200 μM; (e) 1 mM; (f) LipE = $pIC_{50} - clogD_{7.4}$ (clogD values from StarDrop)

The presence of a *p*-hydroxy or *p*-trifluoromethylsulfonamido group (*cf.* Table 28, **118a**, **118c**, **118d** and **118e**) was essential for activity against MDMX and MDM2. Removal of the hydroxy proton by methylation (**118i**) or replacing with an *N*-oxide

(**118n**) or unsubstituted phenyl ring (**118l**) or pyridyl ring (**118m** and **118o**) abolished activity, supporting the hypothesis that the hydroxy group was interacting favourably with the protein. Replacing the trifluoromethylsulfonamido group with a methylsulfonamido substituent (**118f**) abolished target activity, as did replacing the hydroxy group with an isosteric amino group (**118g**), suggesting that a relatively acidic proton at the 4-position was needed for potency. All *m*-substituted derivatives (**118h, 118j** and **118o**) were equally or less active than the corresponding *p*-substituted compounds against MDMX. However, none of these compounds improved MDMX or MDM2 potency over **118a**, **118c**, **118d** or **118e**.

5.2 The Disubstituted Pyridyl MDMX Inhibitors

Pyridyl scaffolds were investigated, as they should also have allowed access to the p53-W23 binding pocket of MDMX but would reduce lipophilicity without compromising molecular weight (**Scheme 38**).

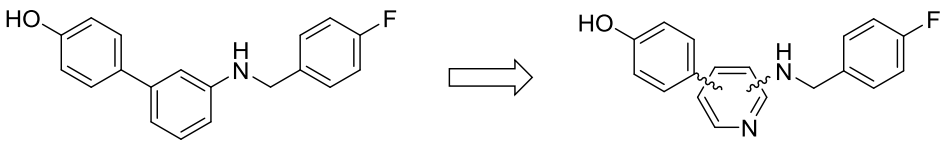

118a

Scheme 38: Scaffold-hop from a benzene to a pyridyl scaffold

Starting from pyridines **126a**, **126b** and **126c**, Suzuki coupling with 4-hydroxybenzeneboronic acid followed by reductive amination of 4-fluorobenzaldehyde gave 4- and 5-pyridyls **128a** and **128b**, but not **128c** (**Scheme 39**).

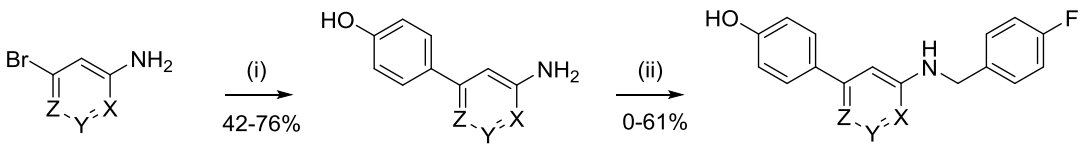

126a (X = N, Y = Z = CH)
126b (X = Z = CH, Y = N)
126c (X = Y = CH, Z = N)

127a (X = N, Y = Z = CH)
127b (X = Z = CH, Y = N)
127c (X = Y = CH, Z = N)

128a (X = N, Y = Z = CH), 12%
128b (X = Z = CH, Y = N), 61%
128c (X = Y = CH, Z = N), 0%

Scheme 39: (i) 4-Hydroxybenzeneboronic acid, $Pd(dtbpf)Cl_2$, Na_2CO_3, 1,2-DME, 120 ^oC, MW, 30-150 min; (ii) 4-fluorobenzaldehyde, $MgSO_4$, THF, RT, 4 h; $NaBH_4$, MeOH, RT, 1 h

Difficulties with achieving full conversion and purification contributed to the poor yields obtained compared with the benzenoid series. Longer reaction times, increased equivalents of catalyst and boronic acid in the Suzuki couplings and increased equivalents of 4-fluorobenzaldehyde in the reductive aminations were necessary to achieve suitable conversion. The low reactivity of aminopyridines **127a**, **127b** and **127c** relative to the corresponding anilines was due to conjugation of the amino nitrogen lone pair into a comparatively electron-deficient aromatic ring. The reactivity of pyridine **127b** was moderate, giving 61% yield of **128b**, but the lower reactivity of pyridines **127a** and **127c** meant only 12% yield of **128a** was obtained. Aminopyridine **128c** was not obtained under these conditions.

Starting from pyridine **126c**, coupling with 4-fluorobenzoyl chloride in the presence of pyridine gave amide **130**. It was observed by LC-MS that some **130** reacted further with 4-fluorobenzoyl chloride to form imide **129**. Quenching the reaction with methanolic sodium hydroxide converted **129** to **130**. Suzuki coupling with 4-hydroxybenzeneboronic acid, followed by reduction of the amide using lithium aluminium hydride gave **128c**, with no reduction of the pyridyl ring observed (**Scheme 40**).

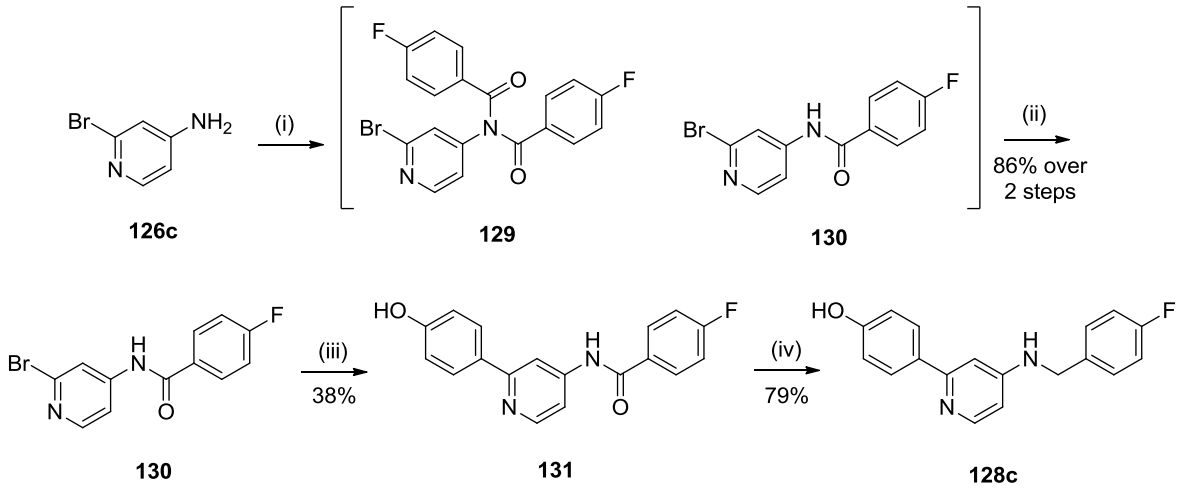

Scheme 40: (i) 4-Fluorobenzoyl chloride, pyridine, MeCN, RT, o/n; (ii) 2.5 M NaOH, MeOH (1:3), RT, 15 min; (iii) 4-hydroxybenzeneboronic acid, $Pd(dtbpf)Cl_2$, Na_2CO_3, 1,2-DME, 120 ^oC, MW, 1 h; (iv) $LiAlH_4$, THF, 0 ^oC-RT, 6 h

Oxidation of **128b** to pyridine-*N*-oxide **128d** with *m*CPBA was unsuccessful due to problems with purifying the product from the 3-chlorobenzoic acid impurity (**Scheme**

41). The high aqueous solubility of **128d** meant that the product could not be separated from the 3-chlorobenzoic acid into an organic and aqueous layer, despite numerous extractions of the aqueous layer. Compound **128d** was synthesised *via* reductive amination of 4-fluorobenzaldehyde with aniline **126b** to give **132**. This compound was oxidised with *m*CPBA to give **133** and Suzuki coupling with 4-hydroxybenzeneboronic acid gave **128d** with no deprotection of the *N*-oxido group observed (**Scheme 41**). Pyridyl compounds **128a**, **128b**, **128c** and **128d** were analysed by ELISA (**Table 30**).

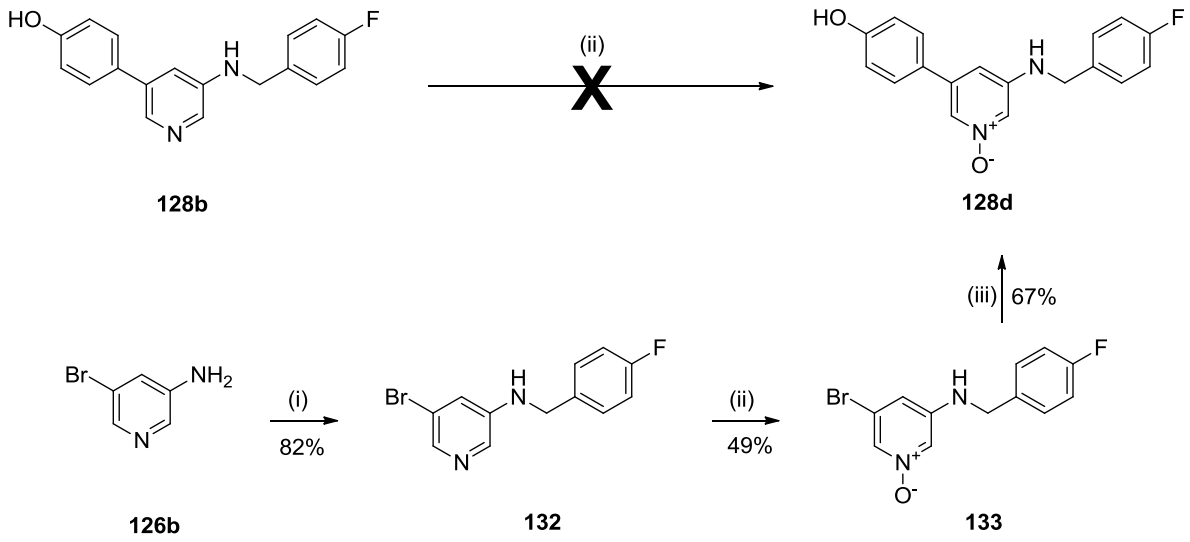

Scheme 41: (i) 4-Fluorobenzaldehyde, $MgSO_4$, THF, RT, 4 h; $NaBH_4$, MeOH, RT, 1 h; (ii) *m*CPBA, DCM, 0 ^oC-RT, 30 min; (iii) 4-hydroxybenzeneboronic acid, $Pd(dtbpf)Cl_2$, Na_2CO_3, 1,2-DME, 120 ^oC, MW, 1 h

Table 30: ELISA data for pyridyl derivatives **128a**, **128b**, **128c**, **128d** and **131**(conducted by Dr Yan Zhao at the NICR)

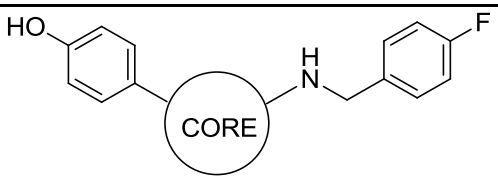

ID	Scaffold / Structure	MDMX IC_{50} (µM)[a]	MDM2 IC_{50} (µM)[b]	Ratio (MDMX : MDM2)	LE[c]	LipE[c,e]
128a	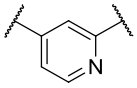	574	303	0.53	0.20	+ 1.17
128b	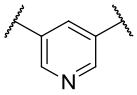	552	459	0.83	0.20	+ 1.23
128c	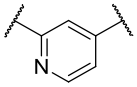	17%[d]	128	-	-	-
128d	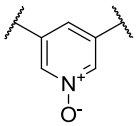	212	50.0	0.24	0.22	+ 1.46
131	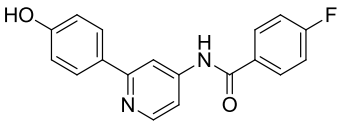	467	11%[d]	-	0.20	+ 0.39

(a) $n = 2$; (b) $n = 1$; (c) With respect to MDMX; (d) 200 µM; (e) LipE = $pIC_{50} - clogD_{7.4}$ (clogD values from StarDrop)

A large drop in MDMX and MDM2 activity was observed relative to the benzenoid scaffold (*cf.* Table 28, **118a**), with compounds **128a** and **128b** being 13-14-fold less active against MDMX and **128c** being so inactive that only a percentage inhibition value could be recorded. Compound **128d** partially restored potency against MDMX and totally restored activity against MDM2 relative to **118a**. The results showed that an electron-deficient scaffold was detrimental to MDMX and MDM2 potency. The increase in activity observed with **128d** also showed that substitution at the 5-position of the scaffold was tolerated and could be investigated in future SAR studies.

5.3 The 1,2,3-Trisubstituted Benzenoid MDMX Inhibitors

Published MDM2 inhibitors, e.g. RG7112,[53] and MDMX inhibitors, e.g. Novartis-101,[104] used chloride-substituted aromatic rings to access the p53-W23 pocket. To see if such a group would be tolerated in the benzenoid series, trisubstituted benzene derivatives were designed (**Figure 46**).

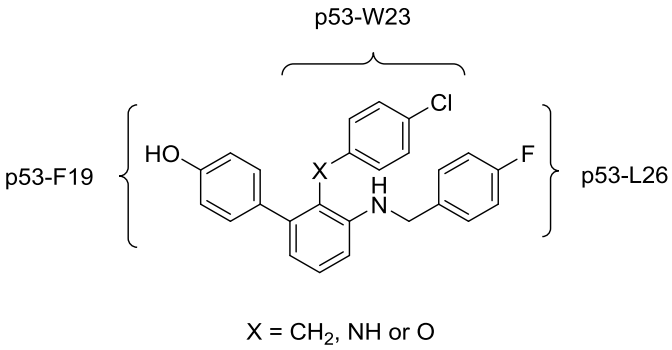

Figure 46: 1,2,3-Trisubstituted benzenoid derivatives with predicted binding mode in MDMX and MDM2

The proposed synthesis of phenol **138a** started with Ullman coupling of 2-bromo-6-nitrophenol (**134**) with 1-chloro-4-iodobenzene to give biaryl ether **135a**. Suzuki coupling with 4-hydroxybenzeneboronic acid would give **136a** and reduction of the nitro group followed by reductive amination of 4-fluorobenzaldehyde would give **138a** (**Scheme 42**).

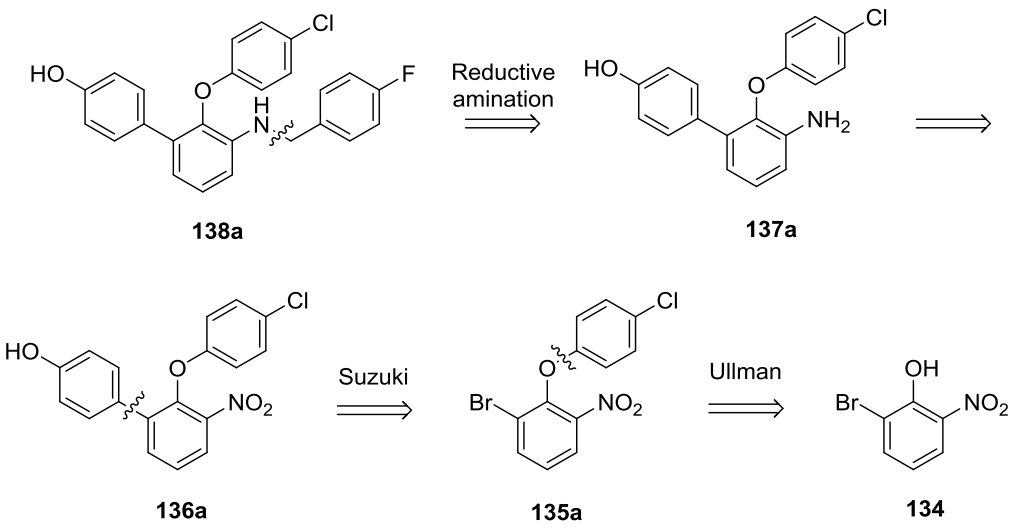

Scheme 42: Retrosynthesis of **138a**

Buchwald had previously described conditions for the efficient formation of biaryl ethers where the aryl halide or phenol were flanked by *o*-substitutents.[128] Heating **134** and 1-chloro-4-iodobenzene at 80 ^{o}C in DMSO with tripotassium phosphate, CuI and 2-picolonic acid gave 25-30% conversion to **135a** after 24 h. Microwave irradiation at 140 ^{o}C and tripling the loading of CuI and 2-picolinic acid did not improve this result. The poor conversion was possibly due to inactivation of the phenol by the *o*-nitro substituent. The authors only cited phenols and aryl iodides flanked by *o*-methyl and *o*-methoxy groups,[128] therefore it is possible that the steric hinderance of the bromo and nitro groups further reduced the reactivity of **134**.

Starting from 3-bromo-2-fluoronitrobenzene (**139**), nucleophilic aromatic substitution with 4-chlorophenol in DMF gave **135a** in excellent yield. Suzuki coupling with 4-hydroxybenzeneboronic acid gave phenol **136a**, with similar yields obtained compared to the 1,3-disubstituted benzenoid series. It was found that the success of this reaction depended on irradiation time and reaction concentration; irradiation for longer than 30 min at 120 ^{o}C or having a concentration above 0.5 M resulted in significant de-chlorination of the product. Iron-mediated reduction of the nitro group gave aniline **137a** at 50 ^{o}C. Subsequent nitro reductions found that the temperature could be reduced to 30 ^{o}C, with full conversion after 2 h. Attempts to reduce the nitro group using Pd/C or Ru/C resulted in significant de-chlorination. Reductive amination of 4-fluorobenzaldehyde gave **138a** in 34% yield (**Scheme 43**). Poor conversion of **137a** was observed by LC-MS even with increased equivalents of 4-fluorobenzaldehyde. Refluxing at 70 ^{o}C overnight did not have any significant effect. This was possibly due to the steric hinderance of the 4-chlorophenoxy substituent hindering access to the aniline nitrogen. Hosseinzadeh had described the use of TFE in reductive aminations, giving substantially accelerated reactions compared with conventional solvents.[129] Using TFE in place of THF gave full conversion to the imine without need for a drying agent and improved yields of the desired amines by at least two-fold.

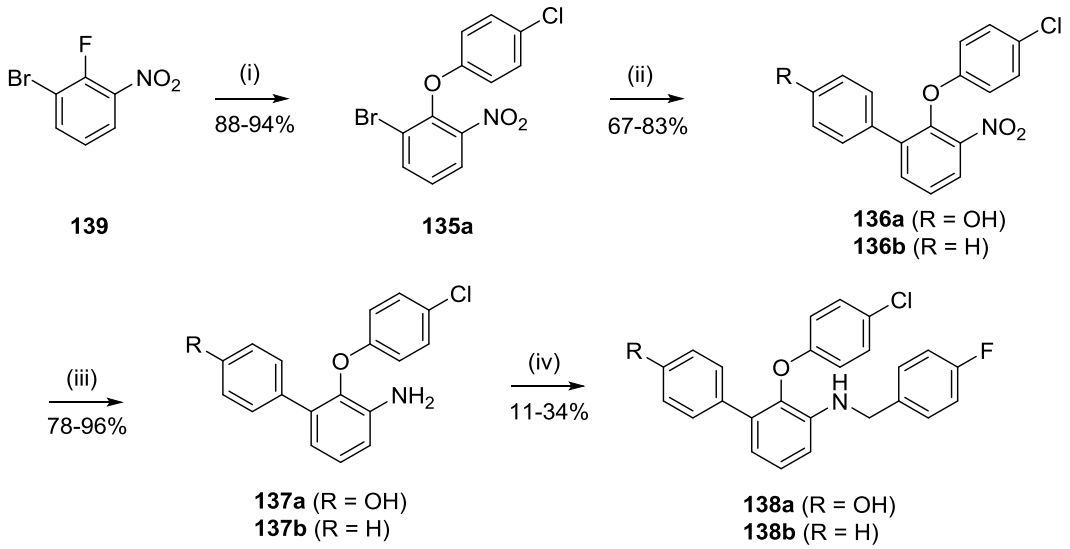

Scheme 43: (i) 4-Chlorophenol, K_2CO_3, DMF, 120 ^oC, MW, 20 min; (ii) 4-hydroxybenzeneboronic acid or phenylboronic acid, Pd(dtbpf)Cl_2, Na_2CO_3, 1,2-DME, MW, 20 min; (iii) Fe, AcOH, 50 ^oC, MW, 1 h; (iv) 4-fluorobenzaldehyde, $MgSO_4$, THF, RT, o/n; $NaBH_4$, MeOH, RT, 1 h

Compounds **138c**, **138d**, **138e** and **138f** were also synthesised from anilines **137a** and **137b**. Buchwald coupling of the appropriate aryl bromide proceeded in moderate to high yields with Pd_2dba_3 and XPhos proving an effective catalyst (**Scheme 44**).

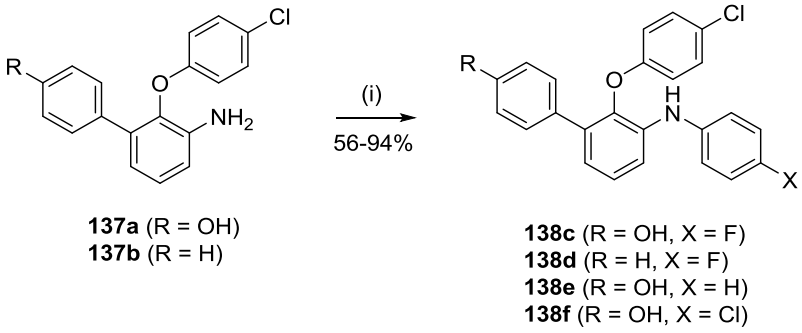

Scheme 44: (i) 1-Bromo-4-fluorobenzene or 1-bromo-4-chlorobenzene or bromobenzene, Pd_2dba_3, XPhos, K_2CO_3, MeCN, 120 ^oC, MW, 3 h

To determine whether a 4-chlorophenoxy substituent was of optimal length to access the p53-W23 binding pocket, compounds **138g** and **138h** were synthesised with a 4-chlorobenzoxyl substituent. Starting from **134**, coupling of 4-chlorobenzyl bromide in acetonitrile gave **135b** in high yield. Suzuki coupling, nitro group reduction and either Buchwald coupling or reductive amination gave **138g** or **138h** respectively (**Scheme 45**). Compounds **138a-138h** were screened using an ELISA (**Table 31**).

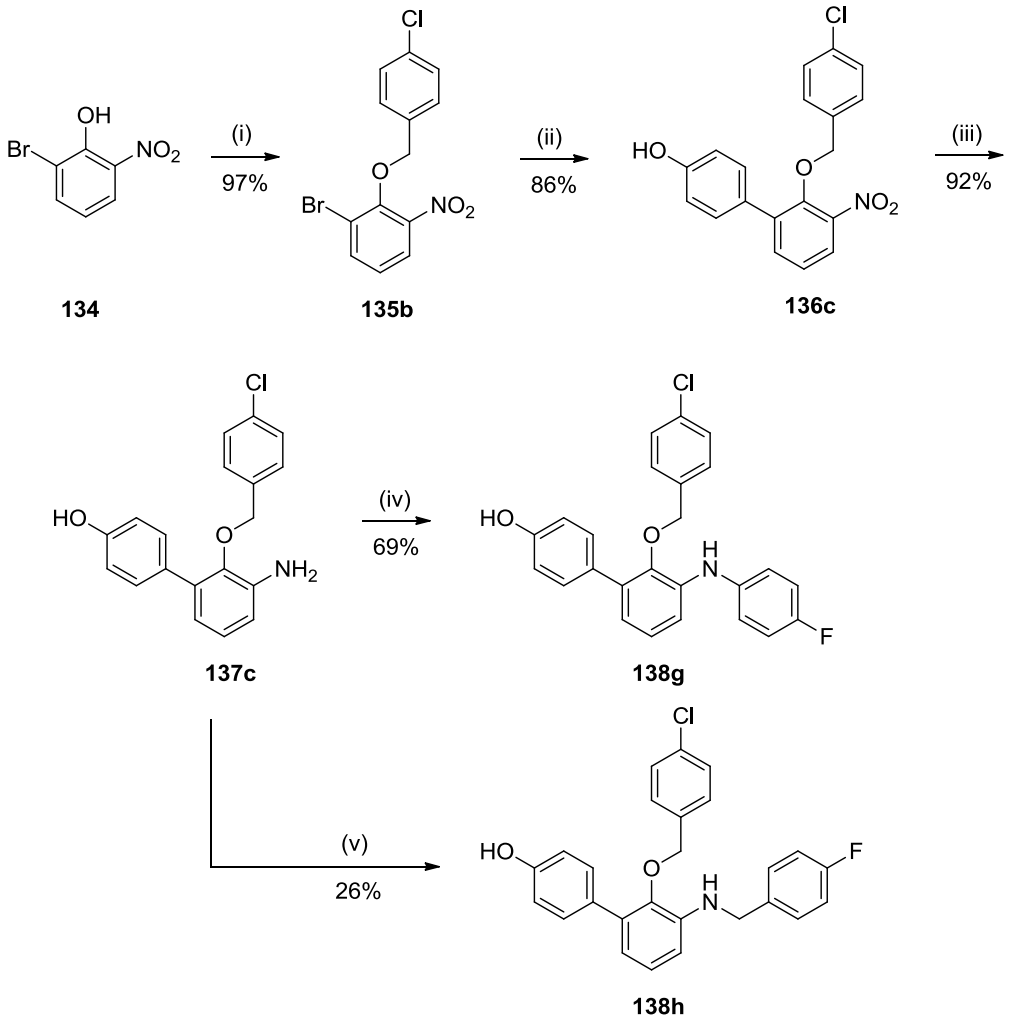

Scheme 45: (i) 4-Chlorobenzyl bromide, K_2CO_3, MeCN, 80 ^oC, MW, 90 min; (ii) 4-hydroxybenzeneboronic acid, Pd(dtbpf)Cl_2, Na_2CO_3, 1,2-DME, MW, 20 min; (iii) Fe, AcOH, 50 ^oC, MW, 1 h; (iv) 1-bromo-4-fluorobenzene, Pd_2dba_3, XPhos, K_2CO_3, MeCN, 120 ^oC, MW, 3 h; (v) 4-fluorobenzaldehyde, $MgSO_4$, THF, RT, o/n; $NaBH_4$, MeOH, RT, 1 h

Table 31: ELISA data for 1,2,3-trisubstituted benzene derivatives **138a-138h** (conducted by Dr Yan Zhao at the NICR)

ID	Structure	MDMX IC_{50} (μM)[a]	MDM2 IC_{50} (μM)[b]	Ratio (MDMX : MDM2)	LE[c]	LipE[c,e]
138a	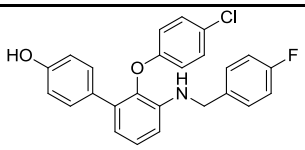	79.0	135	1.71	0.19	- 0.30
138b	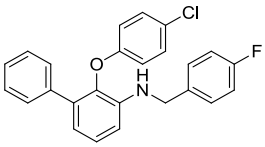	22%[d]	5%[d]	-	-	-
138c	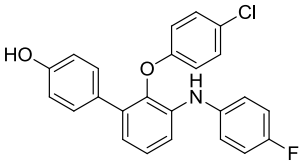	19.0	23.2	1.22	0.22	- 1.51
138d	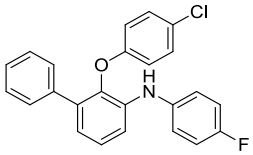	19%[d]	5%[d]	-	-	-
138e	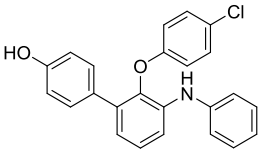	28.9	15.9	0.55	0.22	- 1.72
138f	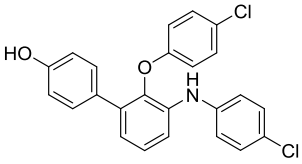	33.0	81.0	2.45	0.21	- 2.28
138g	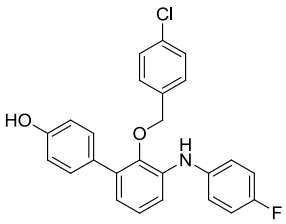	41.0	36.0	0.88	0.20	- 1.93
138h	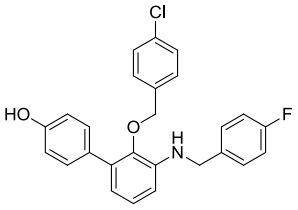	126	37%[d]	-	0.17	- 0.68

(a) $n = 2$; (b) $n = 1$; (c) With respect to MDMX; (d) 200 μM; (e) LipE = $pIC_{50} - clogD_{7.4}$ (clogD values from StarDrop)

Compound **138a** had similar activity against MDMX to the corresponding analogue with no 4-chlorophenoxy ring (*cf*. Table 28, **118a**), indicating that the 4-chlorophenoxy group was tolerated and could be optimised to improve potency. Compound **138c** was the most active compound, with removal of the methylene linker in **138a** improving MDMX potency 4-fold and MDM2 potency 6-fold. Having a methylene linker between the 4-chlorophenyl ring and the oxygen (**138g**) gave a 2-fold drop in MDMX activity relative to **138c**. Compound **138h**, with two methylene linkers, saw a cumulative fall in potency against both protein targets. This is possibly because the shorter compounds could accommodate the p53 binding domain of MDMX and MDM2 more efficiently. Removing the fluoro group (**138e**) or replacing it with a chloro group (**138f**) did not significantly affect MDMX activity, although **138f** was 3-fold less active against MDM2 than **138c**. Removal of the *p*-hydroxy group abolished potency against both proteins (**138b** and **138d**).

5.3.1 Investigating the Binding Mode of the 1,2,3-Trisubstituted Benzenoid Series

The structural nature of the compounds synthesised thus far potentially enabled binding to MDMX in different orientations (**Figure 47**).

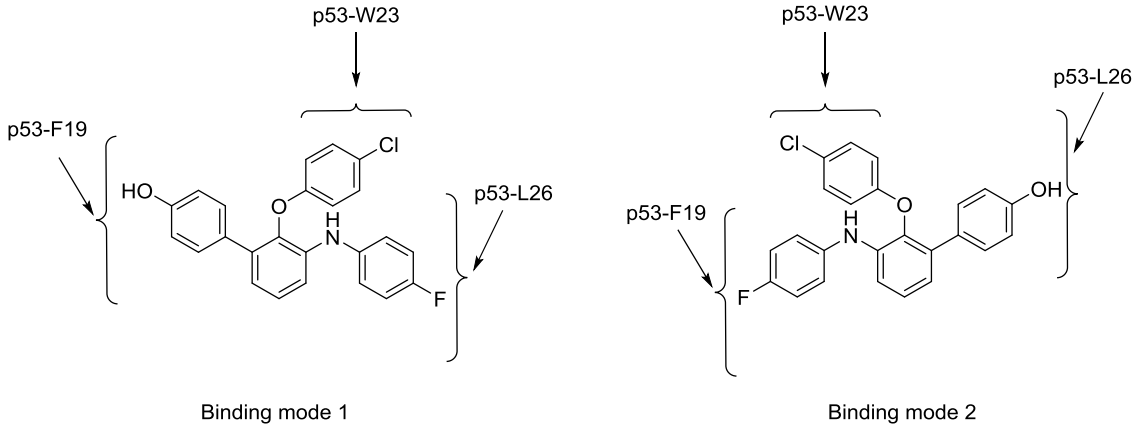

Figure 47: Two possible binding orientations of the 1,2,3-trisubstituted benzenoid compounds in the p53 binding domains of MDM2 and MDMX

Modelling of thiazole **44a** in the MDMX binding pocket had indicated that a sub-pocket, present in the p53-F19 pocket, could be accessed by substitution at the 2-position of the catechol ring (**Figure 48**). Since the binding orientation of the

compounds was ambiguous, substitution at the 2-position of the catechol ring and the 4-fluorophenyl ring was investigated.

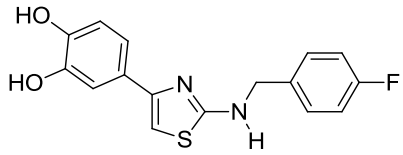

44a

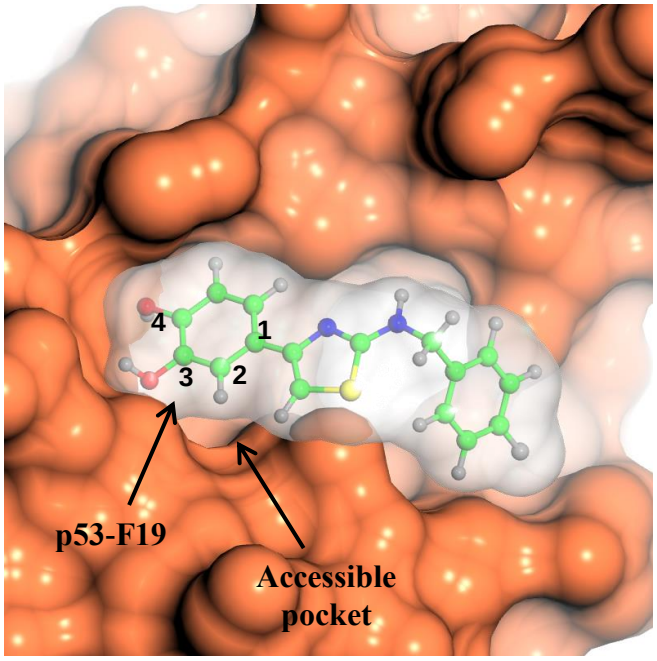

Figure 48: Model of thiazole **44a** interacting with the p53-binding site of MDMX (coral). Compound colour scheme: carbon = green; hydrogen = grey, small; fluorine = grey, large; oxygen = red; nitrogen = blue; sulfur = yellow. Image created using COOT with CCP4mg plug-in.

Derivatives of **138c** were synthesised possessing a 2-methyl or 2-chloro group on either the 4-fluorophenyl or 4-hydroxyphenyl ring. Methyl and chloro substituents were selected as these groups would not significantly affect the electron density of the ring to which they were attached. Using aniline **137a**, compounds **138i** and **138j** were synthesised by Buchwald coupling of 2-bromo-5-fluorotoluene or 1-bromo-2-chloro-4-fluorobenzene, respectively (**Scheme 46**).

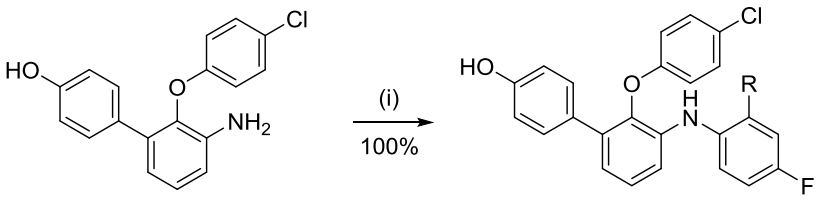

137a

138i (R = Me)
138j (R = Cl)

Scheme 46: (i) 2-Bromo-5-fluorotoluene or 1-bromo-2-chloro-4-fluorobenzene, Pd_2dba_3, XPhos, K_2CO_3, MeCN, 120 ^oC, MW, 3 h

Initial attempts to synthesise **138k** and **138l** began with borylation of **135a** using the conditions described by Imanishi.[130, 131] When **135a** was heated in 1,4-dioxane with bis(pinacolato)diboron ($B_2(pin)_2$) and $(PPh_3)_2PdCl_2$ it was completely consumed. However, ^{1}H NMR analysis revealed that approximately 50% of product **140** had coupled with **135a** to give dimer **141**. Despite attempts to optimise the yield of **140**, significant dimerisation could not be avoided (**Table 32**). Using Pd(dppf)Cl_2.DCM in place of $(PPh_3)_2PdCl_2$ increased the levels of dimerisation. Increasing the equivalents of $B_2(pin)_2$ and reducing the reaction temperature both failed to reduce dimerisation so other synthetic routes were investigated.

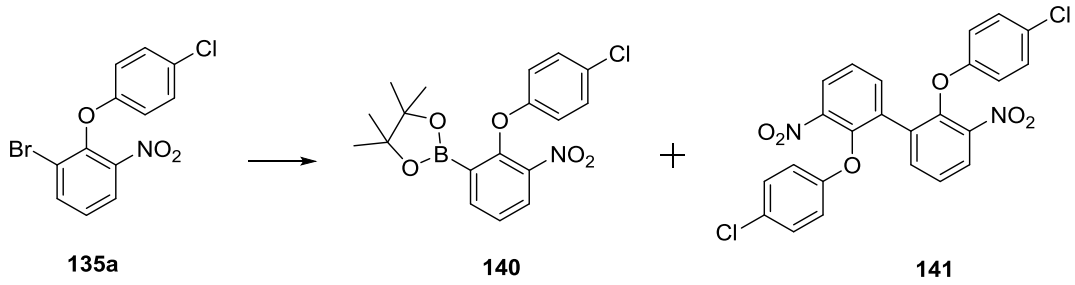

Table 32: Conditions applied to minimise dimerisation of **140**[a]

Entry	Catalyst	$B_2(pin)_2$ equiv.	Temp. (^{o}C)/time	140:141 ratio	Results
1	$(PPh_3)_2PdCl_2$	1.2	90, o/n	1:1	**140** isolated in 29% yield (impure)
2	Pd(dppf)Cl_2. DCM	1.2	90, o/n	1:5	No product isolated
3	$(PPh_3)_2PdCl_2$	2.0	80, 4 h	1:1	No product isolated
4[b]	$(PPh_3)_2PdCl_2$	2.0	90, 20 min	2:3	No product isolated

(a) **140** (50 mg, 1.0 equiv.), catalyst (5.0 mol%), KOAc (2.0 equiv.) 1,4-dioxane (0.5 M); (b) Microwave irradiation instead of conventional heating

Goodacre had described the successful borylation of 3-bromo-2-fluoronitrobenzene (**139**).[132] Under the described conditions, boronate ester **142** was synthesised with just 5-10% dimerisation (^{1}H NMR analysis). Using $(PPh_3)_2PdCl_2$ in place of Pd(dppf)Cl_2.DCM eliminated dimerisation completely. However, reducing the quantity of $B_2(pin)_2$ from 1.5 to 1.2 equivalents increased dimerisation.

Nucleophilic aromatic substitution with 4-chlorophenol resulted in complete deborylation of the product (**Scheme 47**).

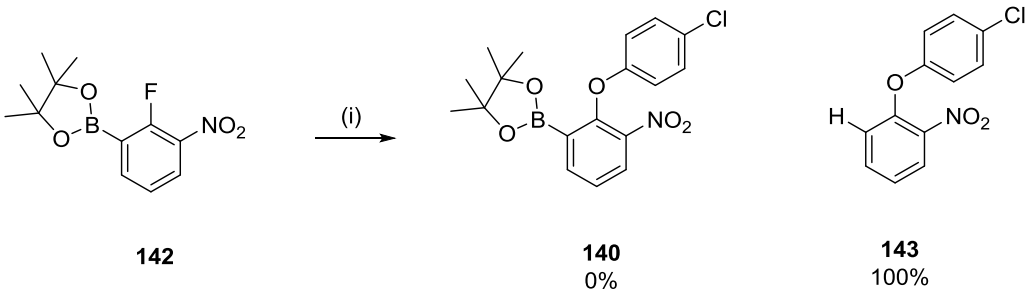

142 **140** 0% **143** 100%

Scheme 47: (i) 4-Chlorophenol, K_2CO_3, DMF, 120 ^oC, MW, 20 min

Suzuki coupling of **142** with 4-bromo-3-methylphenol or 4-bromo-3-chlorophenol gave **144a** and **144b** respectively (**Scheme 49**). Subsequent nucleophilic aromatic substitution found that increased equivalents of 4-chlorophenol were necessary to minimise competing dimerisation of the starting materials. Using **144b**, four equivalents of 4-chlorophenol gave a mixture of **136e** and dimer **145** (**Scheme 48**).

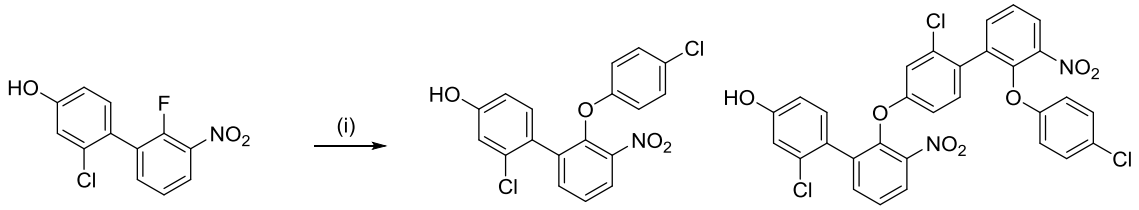

144b **136e** **145**

Scheme 48: (i) 4-Chlorophenol (4 equiv.), K_2CO_3, DMF, 120 ^oC, MW, 40 min (**136e**:**145** ratio = 5:1)

Using six equivalents of 4-chlorophenol minimised formation of **145** and gave biaryl ethers **136d** and **136e** in 83 and 82% yield respectively. Iron-mediated reduction of the nitro groups at 30 ^oC gave anilines **137d** and **137e** and Buchwald coupling gave final compounds **138k** and **138l** (**Scheme 49**). Compounds **138i-138l** and intermediates **136d-136e** and **137d-137e** were analysed by ELISA (**Table 33**).

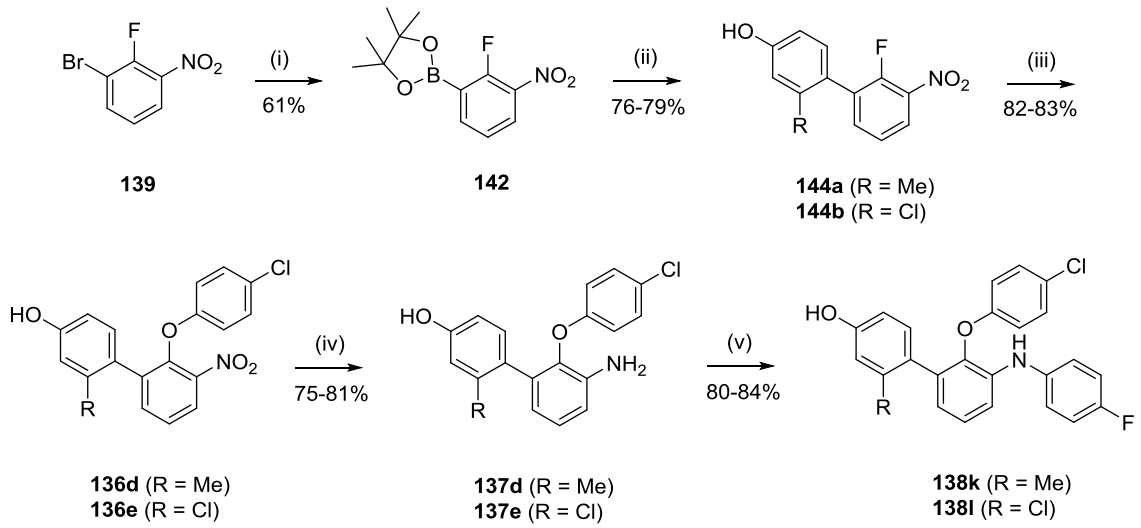

Scheme 49: (i) $B_2(pin)_2$, $(PPh_3)_2PdCl_2$, KOAc, 1,4-dioxane, DMSO, 90 ^oC, 15 h; (ii) 4-bromo-3-methylphenol or 4-bromo-3-chlorophenol, $Pd(dtbpf)Cl_2$, Na_2CO_3, 1,2-DME, MW, 20 min; (iii) 4-chlorophenol, K_2CO_3, DMF, 120 ^oC, MW, 30 min; (iv) Fe, AcOH, 30 ^oC, 2 h; (v) 1-bromo-4-fluorobenzene, Pd_2dba_3, XPhos, K_2CO_3, MeCN, 120 ^oC, MW, 3 h

Table 33: ELISA data for 1,2,3-trisubstituted benzene derivatives **138i-138l** and their intermediates (conducted by Dr Yan Zhao at the NICR)

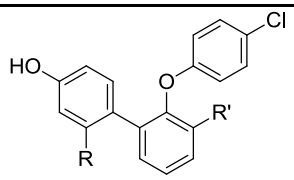

ID	R	R'	MDMX IC_{50} (μM)[a]	MDM2 IC_{50} (μM)[a]	Ratio (MDMX : MDM2)	LE[b]	LipE[b,d]
138i	H	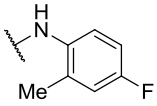	40.2	137	3.41	0.20	- 2.19
138j	H	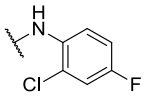	42%[c]	44%[c]	-	-	-
138k	Me	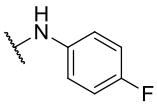	49.0	43.0	0.88	0.20	- 2.28
138l	Cl	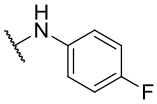	23.7	52.9	2.23	0.21	- 2.13
136d	Me	NO_2	43%[c]	51.5	-	-	-
136e	Cl	NO_2	54.5	20.1	0.37	0.23	- 1.24
137d	Me	NH_2	33%[c]	99.1	-	-	-
137e	Cl	NH_2	58.4	56.6	0.97	0.25	+ 0.54

(a) n = 1; (b) With respect to MDMX; (c) 200 μM; (d) LipE = $pIC_{50} - clogD_{7.4}$ (clogD values from StarDrop)

Methylation at the 2-position of the 4-fluorophenyl ring (**138i**) and 4-hydroxyphenyl ring (**138k**) reduced potency for MDMX 2-fold compared to the non-methylated analogue (*cf.* Table 31, **138c**). Chlorination on the 4-fluorophenyl ring (**138j**) abolished activity against both proteins but the 2-chlorophenol derivative (**138l**) had similar activity to **138c**. With no fluorophenyl substituent, intermediates with a 2-methylphenol ring (**136d** and **137d**) were completely inactive against MDMX, but the corresponding 2-chlorophenol compounds (**136e** and **137e**) had modest MDMX activity. Coupling of the 4-fluorophenyl ring greatly increased the activity of the 2-methylphenol intermediate **137d** and doubled the potency of the 2-chlorophenol compound **137e** against MDMX. The data suggest that a 2-chloro ligand on the phenol ring was making

a favourable interaction, possibly in the binding domain highlighted in Figure 48, as intermediates with a 2-chlorophenol ring were active, whereas the corresponding 2-methylphenol compounds were not. Attaching the 4-fluorophenyl ring improved binding affinity in both derivatives, generating similarly active compounds. This could be because the 4-fluorophenyl ring affected the binding orientation of the compounds, so that any substituent at the 2-position of the phenol ring no longer made a favourable interaction with the protein.

5.3.1.1 Interchanging the Hydroxy and Fluoro Groups of 138c

SAR studies had shown that the *p*-hydroxy group was important for binding potency against MDMX and MDM2. It was of interest to synthesise analogues with the fluoro and hydroxy groups of active compounds interchanged to investigate the binding orientation of the trisubstituted benzenoid compounds (**Figure 49**). If the compounds had one fixed binding orientation in the target protein, interchanging the position of these groups should abolish target potency.

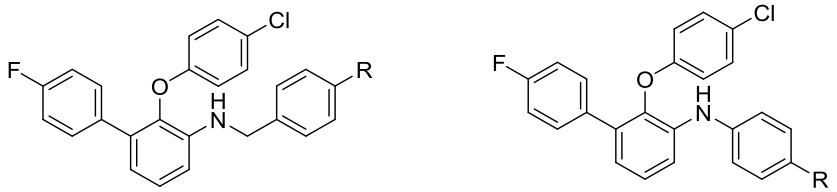

138m (R = OH)
138n (R = $NHSO_2CF_3$)

138o (R = OH)
138p (R = $NHSO_2CF_3$)

Figure 49: New targets to investigate the binding orientation of the trisubstituted benzenoid compounds with the fluoro and hydroxy substituents interchanged

Starting from **135a**, Suzuki coupling with 4-fluorobenzeneboronic acid and iron-mediated nitro reduction gave aniline **137f** as the precursor to compounds **138m-138p** (**Scheme 50**).

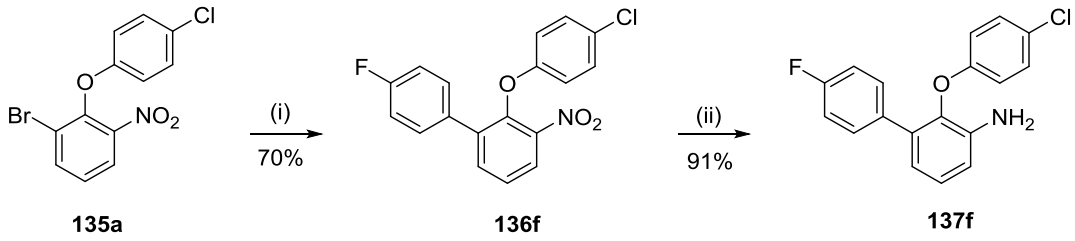

Scheme 50: (i) 4-Fluorobenzeneboronic acid, $Pd(dtbpf)Cl_2$, Na_2CO_3, 1,2-DME, 120 ^oC, MW, 20 min; (ii) Fe, AcOH, 40 ^oC, 2 h

The attempted synthesis of **138m** and the synthesis of **138n** proceeded *via* reduction of the corresponding amides. Trial amide couplings with 3-bromo-2-methylaniline (**146**) and methyl 4-methoxybenzoate resulted in no reaction following irradiation at 120 ^oC (LC-MS analysis). However, addition of ^{i}PrMgCl.LiCl to this reaction at room temperature led to rapid conversion to amide **147a** and these conditions were also effective with ethyl 4-hydroxybenzoate to give **147b**. Suzuki coupling with 4-fluorobenzeneboronic acid and reduction of the amide with lithium aluminium hydride gave **149a** but not **149b** (**Scheme 51**). Compound **147b** was taken forward to the Suzuki coupling without purification to give **148b** in 93% yield from **146**.

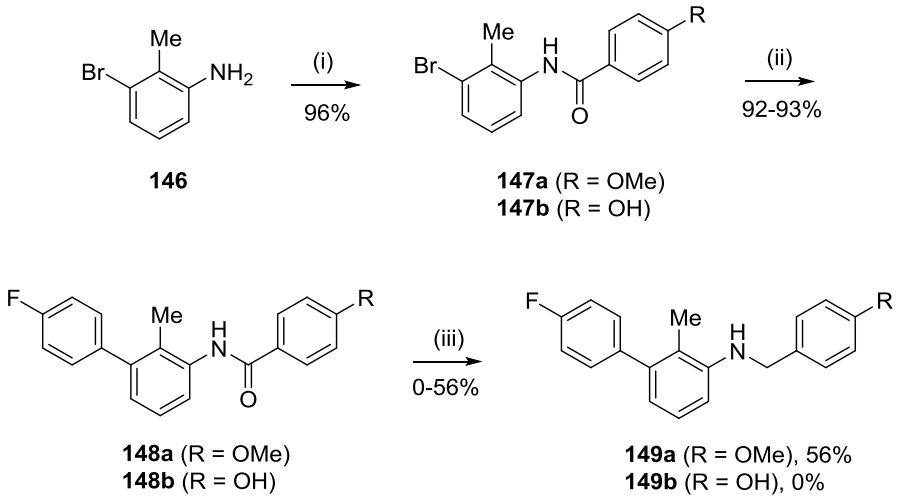

Scheme 51: (i) Methyl 4-methoxybenzoate or ethyl 4-hydroxybenzoate, ^{i}PrMgCl.LiCl (5.0 equiv.), 1,2-DME, RT, 30 min; (ii) 4-fluorobenzeneboronic acid, $Pd(dtbpf)Cl_2$, Na_2CO_3, 1,2-DME, 120 ^oC, MW, 20 min; (iii) $LiAlH_4$, THF, 0 ^oC-RT, 48 h

Attempts to demethylate **149a** using boron tribromide failed to yield **149b** due to rapid debenzylation of the product (**Scheme 52**). For this reason, target compounds **149b** and **138m** were abandoned.

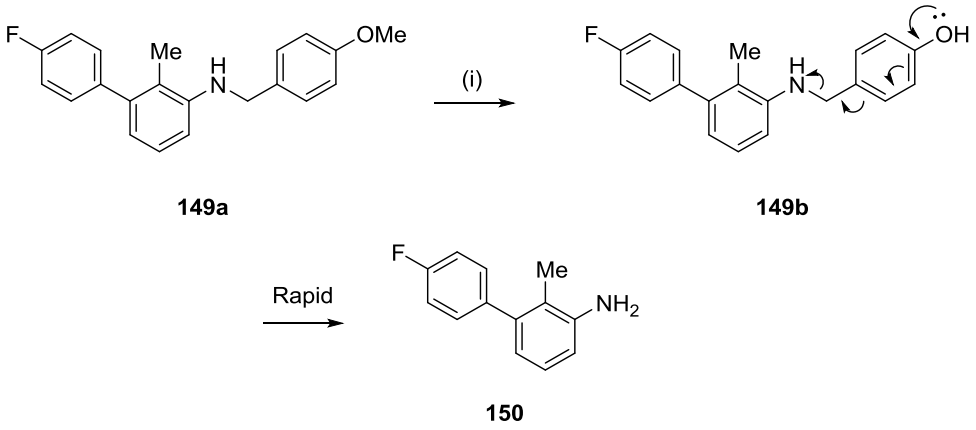

Scheme 52: (i) BBr_3, DCM, 0 ^{o}C-RT, o/n

The amide coupling conditions in Scheme 51 were similarly effective for coupling ethyl 4-hydroxybenzoate, ester **153** or methyl 4-methoxybenzoate with aniline **137f** to give amides **151a**, **151b** or **151c**, respectively (**Scheme 53**).

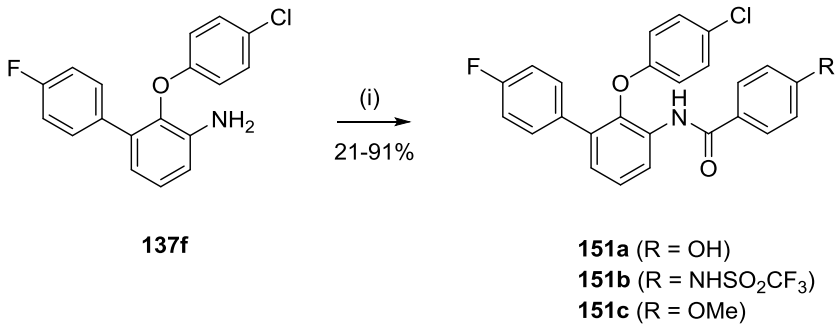

Scheme 53: (i) Ethyl 4-hydroxybenzoate or **153** or methyl 4-methoxybenzoate, ^{i}PrMgCl.LiCl, 1,2-DME, RT, 30 min

Attempts to reduce the amide of **151b** or **151c** using lithium aluminium hydride failed to yield **138n** or **138q**, respectively, so these compounds were synthesised *via* reductive amination of the required aldehydes. Starting from methyl 4-aminobenzoate (**152**), sulfonylation with Tf_2O gave ester **153**. Reduction of the ester was accomplished using DIBAL-H to afford alcohol **154** and oxidation with DMP gave aldehyde **155** (**Scheme 54**).

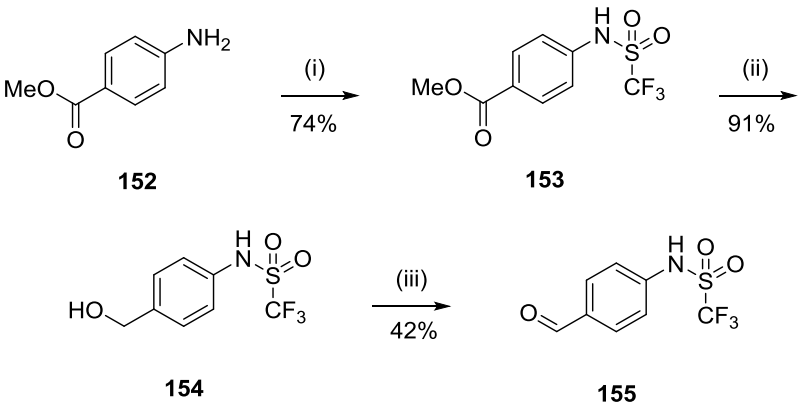

Scheme 54: (i) Tf_2O, NEt_3, DCM, RT, 90 min; 2.5 M aq. NaOH, MeOH (1:3), RT, 40 min; (ii) DIBAL-H, PhMe, -78 ^{o}C-RT, o/n; (iii) DMP, DCM, RT, 2 h

Reductive amination of either aldehyde **155** or 4-anisaldehyde with **137f** in TFE gave target compounds **138n** and **138q**, respectively (**Scheme 55**).

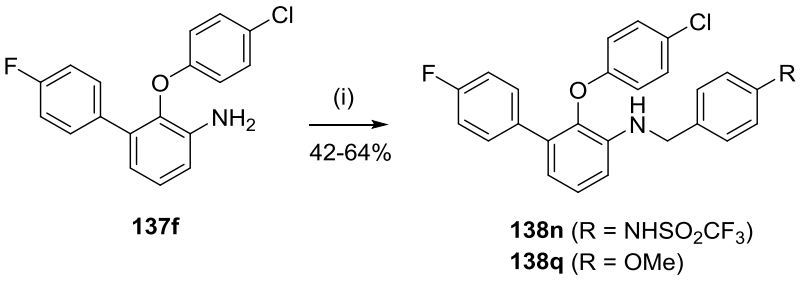

Scheme 55: (i) **155** or 4-anisaldehyde, TFE, 40 ^{o}C, o/n; $NaBH_4$, TFE, RT, 1 h

Attempted Buchwald coupling of 4-bromophenol or aryl bromide **120** with **137f** to synthesise **138o** and **138p**, respectively gave no reaction after 3 h at 120 ^{o}C. Verkade had postulated that chelation of the phenoxide (or sulfonamide) anion to the palladium inhibited oxidative addition to the C-Br bond.[133] Verkade had identified lithium hexamethyldisilazide (LiHMDS) as a suitable base when protic functional groups were present in the aryl halide, suggesting that migration of a trimethylsilyl group from the base to the anion would act as an *in situ* protecting group, preventing coordination to the palladium.[133] However, attempts to couple **137f** with 4-bromophenol under these conditions resulted in poor conversion and no product was isolated. Coupling of **137f** with 4-bromoanisole isolated **138r** and demethylation with boron tribromide gave **138o** (**Scheme 56**).

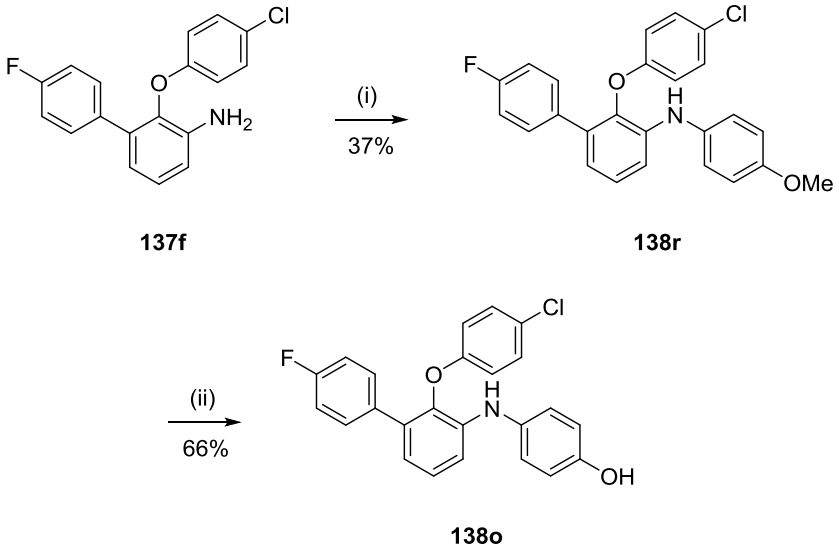

Scheme 56: (i) 4-Bromoanisole, Pd_2dba_3, XPhos, K_2CO_3, MeCN, 120 ^oC, MW, 3 h; (ii) BBr_3, DCM, 0 ^oC-RT, 2 h

To synthesise **138p**, aniline **137f** was coupled with 1-bromo-4-nitrobenzene. Using acetonitrile produced a mixture of by-products but switching to toluene[134, 135] gave **138s** in 87% yield. Reduction of the nitro group was accomplished with iron in glacial acetic acid and sulfonylation was achieved selectively on the terminal amino group of **138t** using Tf_2O to give **138p** in 35% yield (**Scheme 57**). The steric bulk of the 4-chlorophenoxy substituent blocked access to the secondary amino group of **138t**. No base was required to achieve full conversion, possibly due to the secondary amino group acting as a base. Compounds **138n-138p** and several intermediates were screened by ELISA against MDMX and MDM2 (**Table 34**).

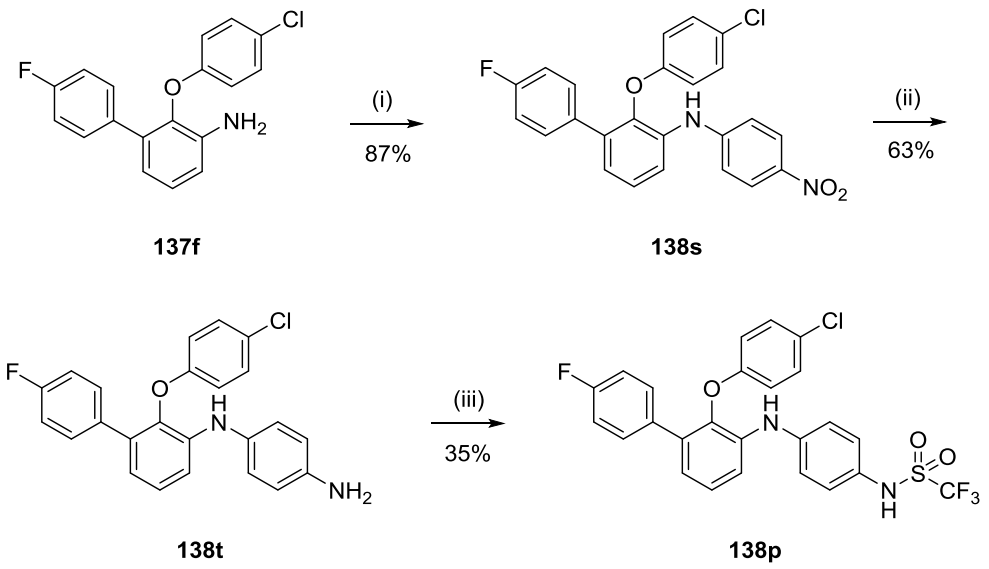

Scheme 57: (i) 1-Bromo-4-nitrobenzene, Pd_2dba_3, XPhos, K_2CO_3, PhMe, 120 ^oC, 15 h; (ii) Fe, AcOH, 50 ^oC, o/n; (iii) Tf_2O, DCM, 0 ^oC, 10 min

Table 34: ELISA data for 1,2,3-trisubstituted benzene derivatives **138n-138r**, **138t**, **148a**, **148b**, **149a** and **151a-151c** (conducted by Dr Yan Zhao at the NICR)

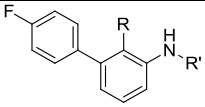

ID	R	R'	MDMX IC_{50} (μM)[a]	MDM2 IC_{50} (μM)[a]	Ratio (MDMX : MDM2)	LE[b]	LipE[b,d]
138n	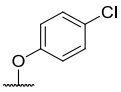	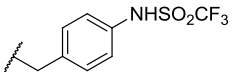	5.23	10.0	1.91	0.20	+ 0.36
138o	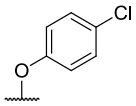	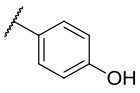	19.2	3.82	0.20	0.22	- 1.51
138p	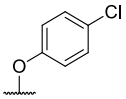	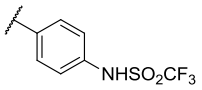	6.45	10.5	1.63	0.20	- 1.48
138q	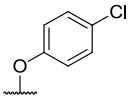	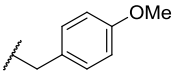	34%[c]	0%[c]	-	-	-
138r	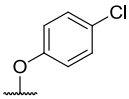	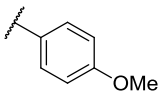	198	1517	7.66	0.17	- 3.09
138t	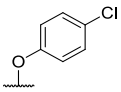	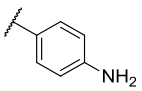	33.9	96.2	2.84	0.21	- 0.41
148a	Me	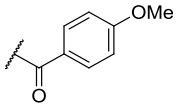	1.1%[c]	16%[c]	-	-	-
148b	Me	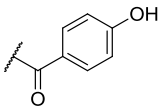	20%[c]	25%[c]	-	-	-
149a	Me	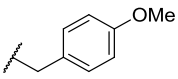	0%[c]	0%[c]	-	-	-
151a	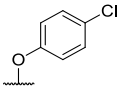	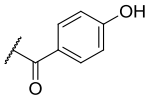	22.0	69.8	3.17	0.21	- 0.97
151b	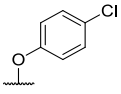	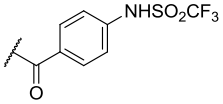	107	13.5	0.13	0.14	- 2.10
151c	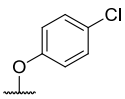	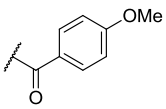	43%[c]	21%[c]	-	-	-

(a) *n* = 1; (b) With respect to MDMX; (c) 200 μM; (d) LipE = pIC_{50} – $clogD_{7.4}$ (clogD values from StarDrop)

Interchanging the fluoro and hydroxy (or trifluoromethylsulfonamido) substituents had no detrimental effect on activity against MDMX or MDM2, with **138n** and **138p** becoming the first trisubstituted benzenoid compounds with an IC_{50} below 10 μM against MDMX. There was a notable similarity in SARs between this series of compounds and those in which the fluoro and hydroxy groups were in opposite positions (*cf*. Table 31). A hydrogen bond donor was essential for activity; removing the methyl group from **138r** afforded a 10-fold gain in activity against MDMX and a 400-fold increase in MDM2 activity (**138o**). Compounds **138q**, **148a**, **149a** and **151c** were completely inactive against both proteins. The aniline (**138t**) was two-fold less active against MDMX than **138o** and five-fold less potent than the sulfonylated derivative (**138p**). Compound **148b** was inactive against both proteins despite the presence of a hydroxy group. The corresponding derivative with a 4-chlorophenoxy group (**151a**) did have activity against MDMX and MDM2, highlighting the significance of this substituent for potency.

5.3.2 Optimising the Drug-like Properties of 138c

Single digit micromolar MDMX inhibitors had now been identified with a key hydrogen bond donor on one side of a 4-chlorophenoxy substituent. Compound **138n** had 4-fold greater potency against MDMX than **138c**, possibly related to the increased lipophilicity of **138n** (**Table 35**). This suggested that the increased activity of **138n** was the result of increased hydrophobic interactions rather than the interaction of a functional group with the protein. A more detailed SAR around the hydroxyphenyl ring in **138c** had also been compiled compared with the trifluoromethylsulfonamide in **138n**. For these reasons, **138c** was selected as the lead compound for further optimisation.

Table 35: Comparison of active compounds **138c** and **138n**

ID	Structure	MW (g/mol)	clogP[a]	clogD$_{7.4}$[b]	MDMX IC$_{50}$ (μM)[c]	MDM2 IC$_{50}$ (μM)[c]	LE[d]
138c	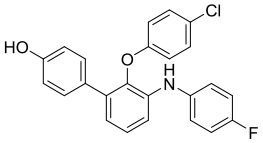	405	7.5	6.2	19.0	23.2	0.223
138n	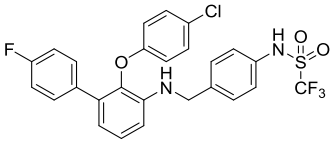	550	8.8	4.9	5.23	10.0	0.196

(a) Values from ChemDraw; (b) Values from StarDrop; (c) *n* = 1; (d) With respect to MDMX

5.3.2.1 Synthesis of 3-Hydroxyheterocycles 183a and 183b

Replacing the hydroxyphenyl ring of **138c** with a 3-hydroxyisoxazole or a 3-hydroxypyrazole was predicted to increase aqueous solubility, as they both have greater polarity than a hydroxyphenyl ring. SAR studies around the hydroxyphenyl ring had indicated a trend between the acidity of the hydrogen bond donor at the *para*-position and target potency. 3-Hydroxyisoxazoles are approximately 10,000-fold more acidic (pK_a 5-6) than phenols (pK_a 10.0) and 3-hydroxypyrazoles are also more acidic than phenols,[136, 137] so it was predicted that this ring substitution would enhance target potency (**Figure 50**).

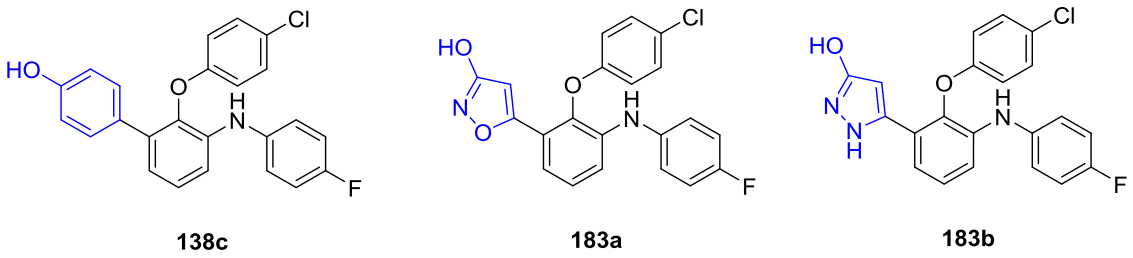

Figure 50: Replacing the hydroxyphenyl ring in **138c** with a 3-hydroxyisoxazole (**183a**) or 3-hydroxypyrazole (**183b**)

5-Aryl-3-hydroxyisoxazoles and the corresponding pyrazoles can be synthesised by a 5-*endo-dig* cyclisation of the intermediate derived from the reaction between a propiolate

ester and hydroxylamine or hydrazine respectively.[138] Sonogashira coupling of methyl propiolate and subsequent cyclisation with hydroxylamine would complete synthesis of the 3-hydroxyisoxazole (**Scheme 58**).

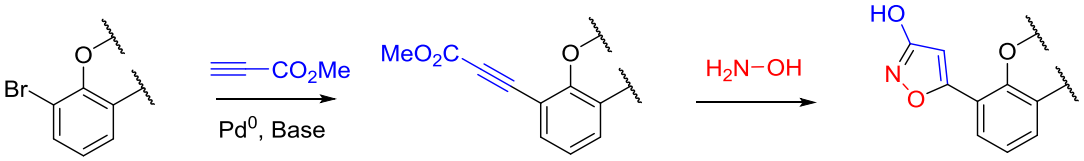

Scheme 58: Synthesis of a 3-hydroxyisoxazole ring *via* Sonogashira coupling and 5-*endo*-*dig* cyclisation

Optimisation of Sonogashira coupling conditions used 4-bromoanisole (**156**) as a coupling partner. Standard coupling conditions with methyl propiolate gave the desired methyl 4-methoxyphenylpropiolate (**157**) in 7% isolated yield when the reaction was conducted in THF (**Table 36**). Attempts in 1,4-dioxane, acetonitrile and DMF were comparatively less clean than with THF (LC-MS analysis). The low yield was possibly due to the poor reactivity of 4-bromoanisole, the relatively high electron density of which would have slowed the rate of oxidative addition of palladium across the C-Br bond, and the poor reactivity of methyl propiolate. Sonogashira has described high-yielding couplings of aryl bromides using electron-rich phosphine ligands, explaining that the high electron density of the catalyst accelerated oxidative addition across the C-Br bond.[139] However, when $(PPh_3)_2PdCl_2$ was replaced by catalysts possessing strongly electron-donating ligands (Table 36, entries 5-7), all reactions gave poor conversion by LC-MS and produced several unidentified impurities.

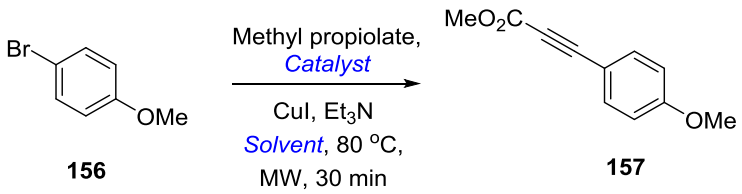

Table 36: Attempted optimisation of the Sonogashira coupling of 4-bromoanisole (**156**) with methyl propiolate[a]

Entry	Catalyst	Solvent	% Yield[b]
1	$(PPh_3)_2PdCl_2$	THF	7
2	$(PPh_3)_2PdCl_2$	1,4-Dioxane	0
3	$(PPh_3)_2PdCl_2$	MeCN	0
4	$(PPh_3)_2PdCl_2$	DMF	0
5	$Pd(dtbpf)Cl_2$	THF	0
6	$(MeCN)_2PdCl_2$, P^tBu_3	THF	0
7	$(PhCN)_2PdCl_2$, P^tBu_3	THF	0

(a) **156** (200 mg, 1.0 equiv.), methyl propiolate (1.5 equiv.), catalyst (5.0 mol%), ligand (10.0 mol%), CuI (5.0 mol%) and Et_3N (3.0 equiv.) at 0.3 M; (b) Isolated yield

Sonogashira coupling of **156** with TMS-acetylene, in the presence of $(PhCN)_2PdCl_2/P^tBu_3$ and CuI gave just 10% isolated yield of **159**, following desilylation with potassium carbonate. Finke has described the use of $ZnCl_2$ as a co-catalyst in Sonogashira couplings in place of CuI, explaining that $ZnCl_2$ did not facilitate homocoupling of the acetylene substrate (**Scheme 59**).[140] This meant that larger catalytic amounts of $ZnCl_2$ could be used without the risk of homocoupling occurring.

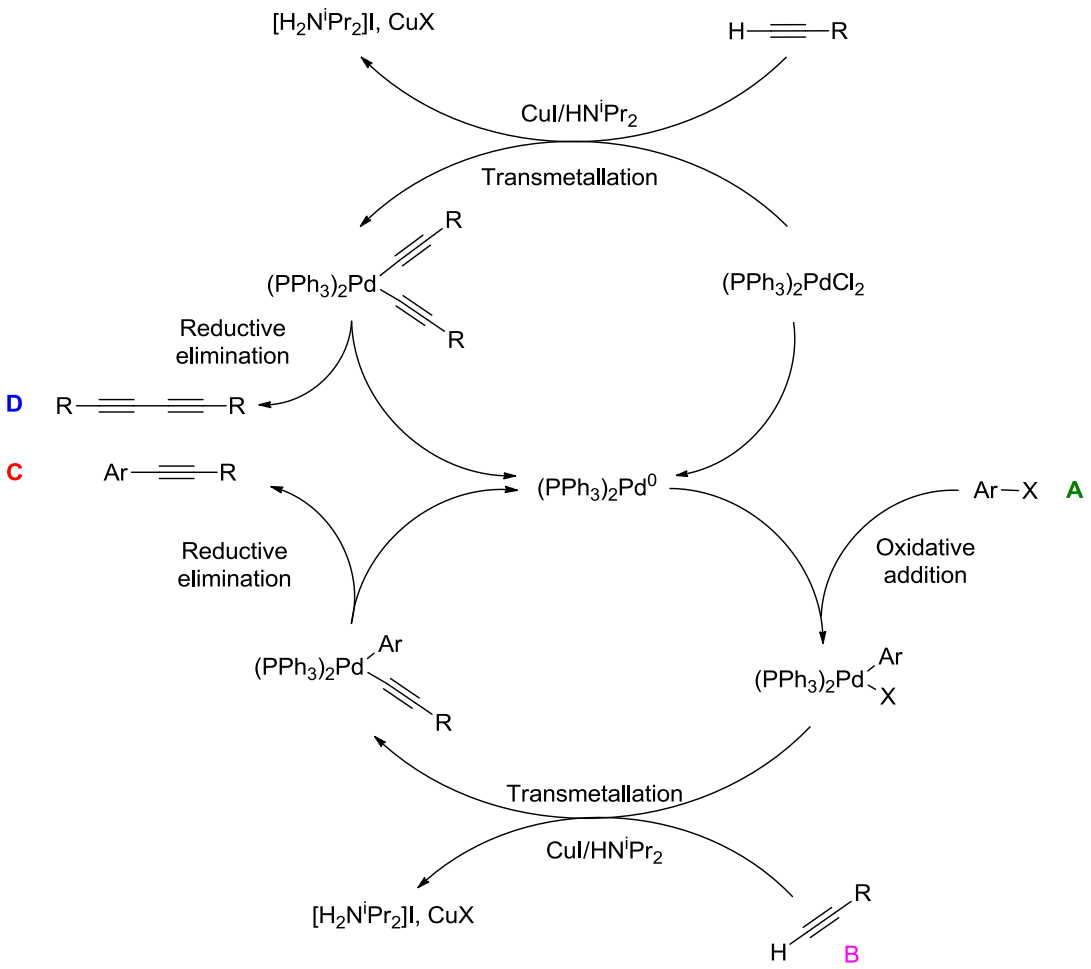

Scheme 59: Sonogashira coupling with an aryl halide (**A**) and a terminal alkyne (**B**) to give a substituted alkyne (**C**) and potential homocoupling to give a conjugated acetylene (**D**).[141]

Coupling **156** with TMS-acetylene using $ZnCl_2$ gave full conversion of the aryl bromide in under 3 h. Under the same conditions with CuI, full conversion was not achieved until after 24 h and a greater number of impurities were produced. Subsequent desilylation with TBAF gave **159** in 68-80% yield (**Scheme 60**).

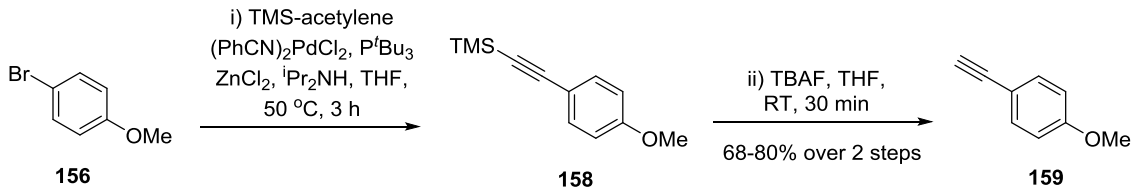

Scheme 60: Optimised Sonogashira coupling conditions

Deprotonation of **159** with LDA, followed by addition of methyl chloroformate, gave propiolate ester **157** in 68% overall yield. Formation of the 3-hydroxyisoxazole ring followed the procedure outlined by Iwai, using hydroxylamine hydrochloride in aqueous base.[138] The reaction mechanism involves addition to the propiolate ester carbonyl carbon by the amino group of hydroxylamine to give hydroxamic acid **160**. A *5-endo-dig* cyclisation forms isoxazol-3(2*H*)-one **161a** and subsequent tautomerisation completes the transformation (**Scheme 61**). Theoretical studies of the tautomeric equilibria of 3-hydroxyisoxazoles have revealed that the enol tautomer (**162a**) predominates over the oxo form (**161a**) in aqueous solution.[142]

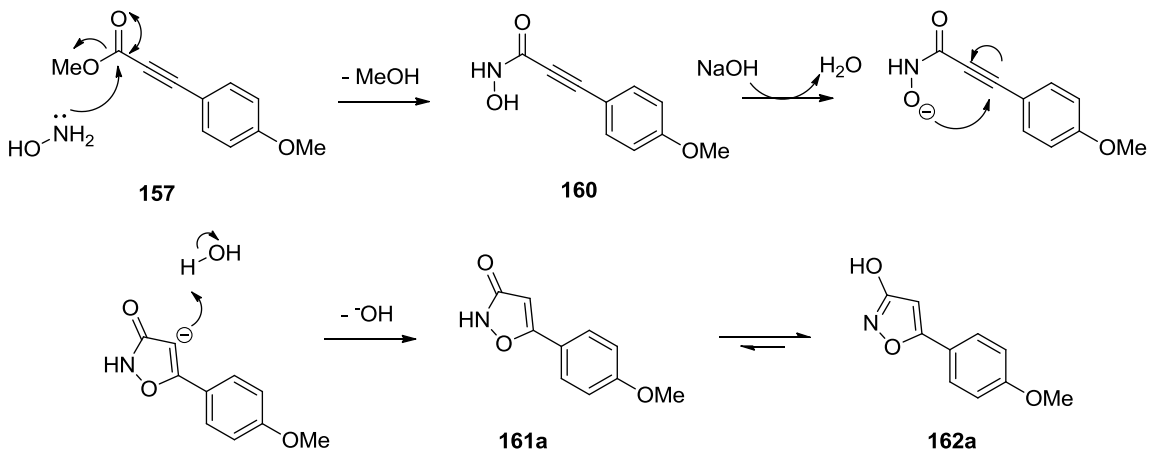

Scheme 61: Reaction mechanism for the formation of isoxazole **162a** from ester **157**

Cyclisation of **160** at room temperature gave **162a** in 35% yield. ^{1}H NMR analysis indicated incomplete cyclisation of hydroxamic acid **160**. One impurity had an identical mass and a similar ^{1}H NMR spectrum to the product, suggesting it was the regioisomeric isoxazole **162b**. This was predicted to form when hydroxylamine attacked ester **157** by conjugate addition instead of 1,2-addition (**Scheme 62**). The resulting α,β-unsaturated ester **163b** would then undergo a base-mediated *5-exo-trig* cyclisation to form **162b**.

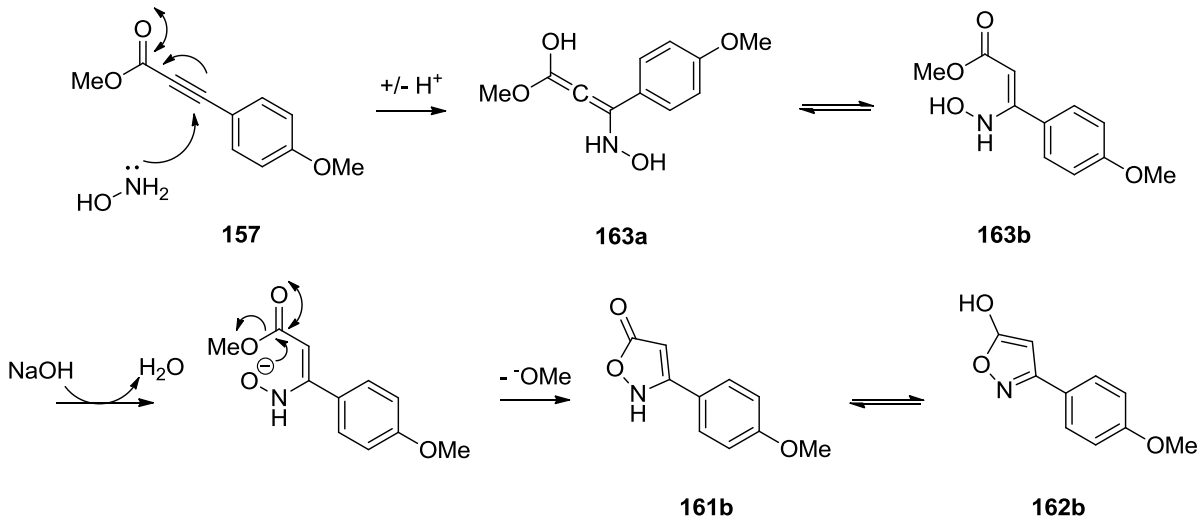

Scheme 62: Proposed mechanism for the formation of **162b**

Cyclisation at 0 ^{o}C instead of at room temperature gave full conversion to a mixture of isoxazole **162a** and hydroxamic acid **160**. None of the regioisomeric isoxazole **162b** was observed and subsequent heating fully converted **160** to **162a** in 93% yield (**Scheme 63**).

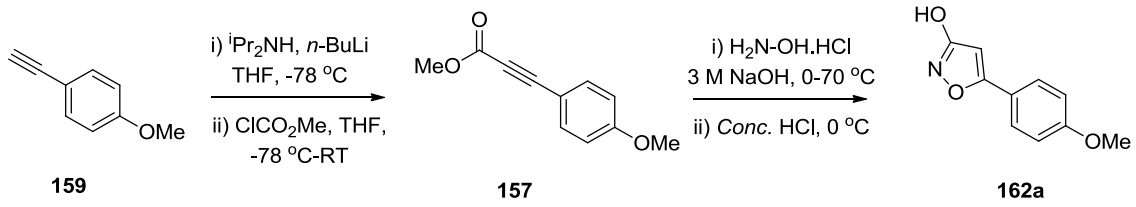

Scheme 63: Final reaction conditions for the formation of ester **157** and isoxazole **162a**

When the optimised Sonogashira coupling conditions were applied to aryl bromide **135a**, multiple impurities were generated. Using conditions described by Shimada, aryl bromide **139** was coupled with TIPS-acetylene using CuI to give **164** in excellent yield after 1 h at 70 ^{o}C.[143] Analogous coupling with $ZnCl_2$ gave no conversion after the same time period. Aromatic substitution with 4-chlorophenol generated an impurity which was identified by ^{1}H NMR analysis as the de-silylated biaryl ether **165**. The crude material was therefore mixed with TBAF to complete formation of **165**. Tin-mediated reduction of the nitro group proceeded quantitatively to **166**, but Buchwald coupling using conditions previously described for compound **138c** (*cf.* Scheme 44), gave an

indistinguishable mass of impurities (**Scheme 64**). It was clear that the terminal acetylene group was not compatible with the coupling conditions.

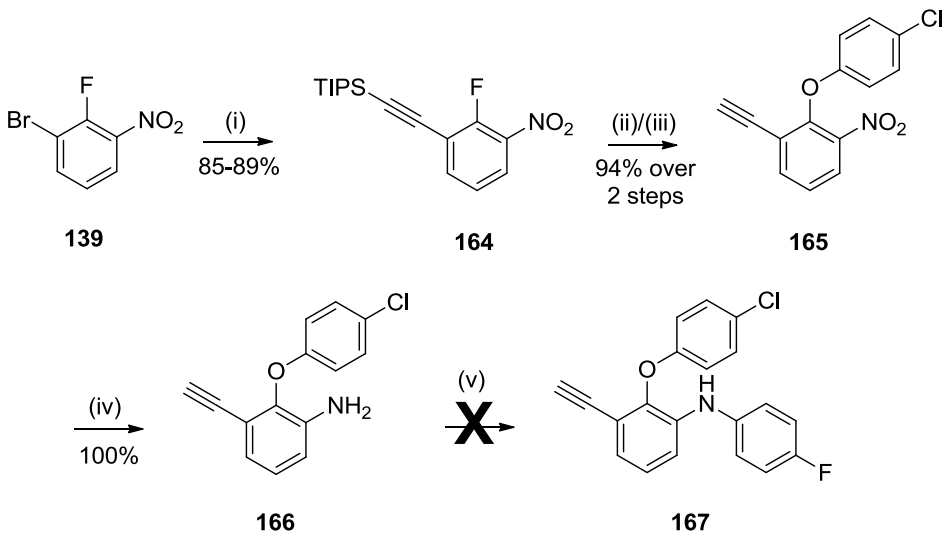

Scheme 64: (i) TIPS-acetylene, $(PPh_3)_2PdCl_2$, CuI, $^iPr_2NH$, THF, 70 ^oC, 1 h; (ii) 4-chlorophenol, K_2CO_3, MeCN, 90 ^oC, MW, 1 h; (iii) TBAF, THF, RT, 30 min; (iv) $SnCl_2.2H_2O$, EtOH, 70 ^oC, 30 min; (v) 1-bromo-4-fluorobenzene, Pd_2dba_3, XPhos, K_2CO_3, MeCN, 120 ^oC, MW, 3 h

The terminal acetylene group of **165** was therefore converted to the 3-hydroxyisoxazole. Formation of propiolate ester **168** proceeded in high yield, but formation of isoxazole **169** proceeded in a poor yield of 28%. The major impurity was phenol **170**, formed by displacement of 4-chlorophenoxide by the excess sodium hydroxide (**Scheme 65**).

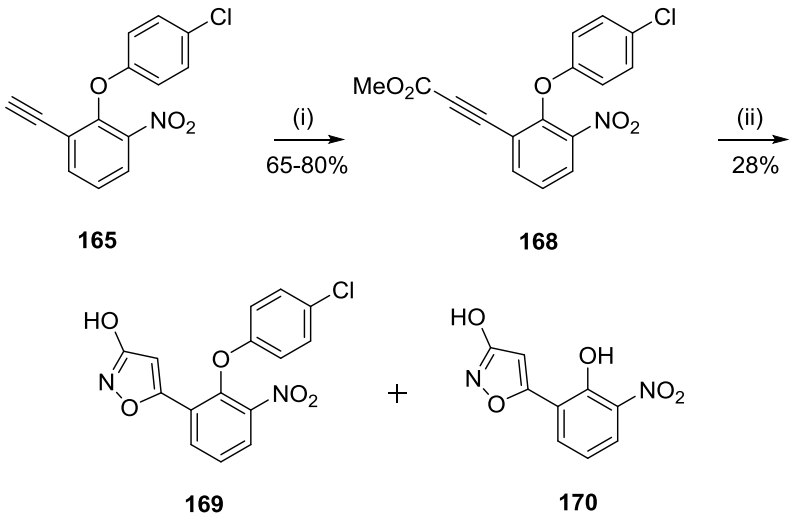

Scheme 65: (i) $^iPr_2NH$, *n*-BuLi, THF, -78 ^oC; $ClCO_2Me$, THF, -78 ^oC-RT; (ii) H_2N-OH.HCl, 3 M aq. NaOH, 0-70 ^oC; *Conc*. HCl, 0 ^oC

Reduction of the nitro group of **169** proceeded as before; however, Buchwald coupling generated several impurities and purification was unable to isolate sufficient material for complete characterisation and screening. Buchwald coupling of aniline **171** with an excess of 1-bromo-4-fluorobenzene did not prove to be scaleable due to the generation of multiple impurities. This was possibly the result of dimerisation of the starting material and further coupling of **172** and **171** (**Scheme 66**).

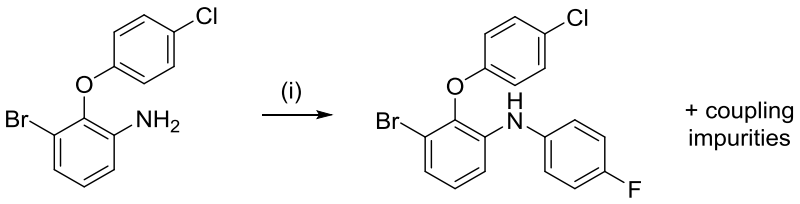

171 **172**

Scheme 66: (i) 1-Bromo-4-fluorobenzene (10 equiv.), Pd_2dba_3, XPhos, K_2CO_3, MeCN, 120 ^oC, MW, 3 h

Coupling of **171** with 4-fluoroaniline gave compound **173**. A large excess of 4-fluoroaniline was used to prevent dimerisation of **171**. However, column chromatographic purification could achieve only partial separation from the excess of 4-fluoroaniline, and the purity of **173** never exceeded 70% (^{1}H NMR analysis). Attempts to convert **173** to aryl iodide **174** were unsuccessful and generated only impurities (**Scheme 67**).

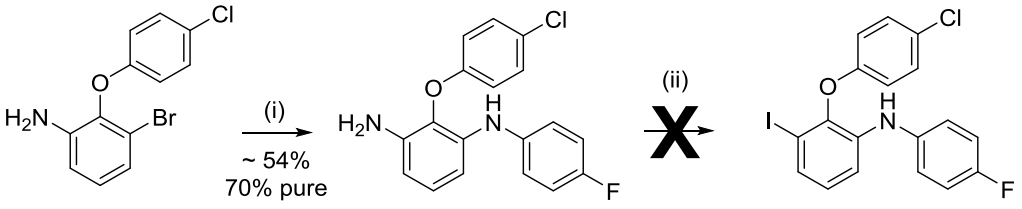

171 **173** **174**

Scheme 67: (i) 4-Fluoroaniline, Pd_2dba_3, XPhos, K_2CO_3, MeCN, 120 ^oC, MW, 3 h; (ii) KI, $NaNO_2$, AcOH, CSA, RT, dark

Buchwald coupling of aryl bromide **135a** with 4-fluoroaniline gave side-product **175** (^{1}H NMR analysis) (**Scheme 68**). This was possibly due to the electron-withdrawing influence of the nitro group facilitating substitution at the aryl chloride, as this reaction was not observed when coupling 4-fluoroaniline with **171** under analogous conditions.

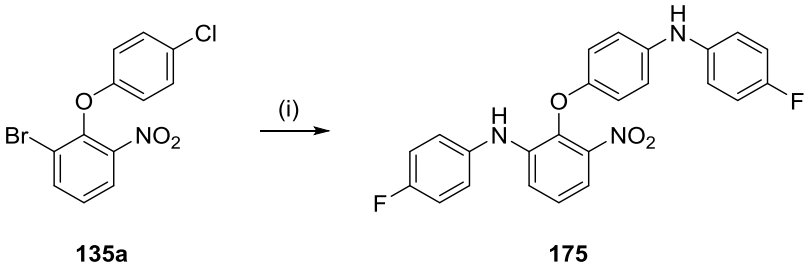

Scheme 68: (i) 4-Fluoroaniline, Pd_2dba_3, XPhos, K_2CO_3, MeCN, 120 ^oC, MW, 3 h

Acetylene **165** was treated with *n*-BuLi before mixing with TIPS-chloride to give **176** and reduction of the nitro group gave aniline **177**. Using sodium *tert*-butoxide in place of potassium carbonate, Buchwald coupling of **177** gave the desired product **178** in high yield. Removal of the TIPS group with TBAF gave acetylene **167** (**Scheme 69**).

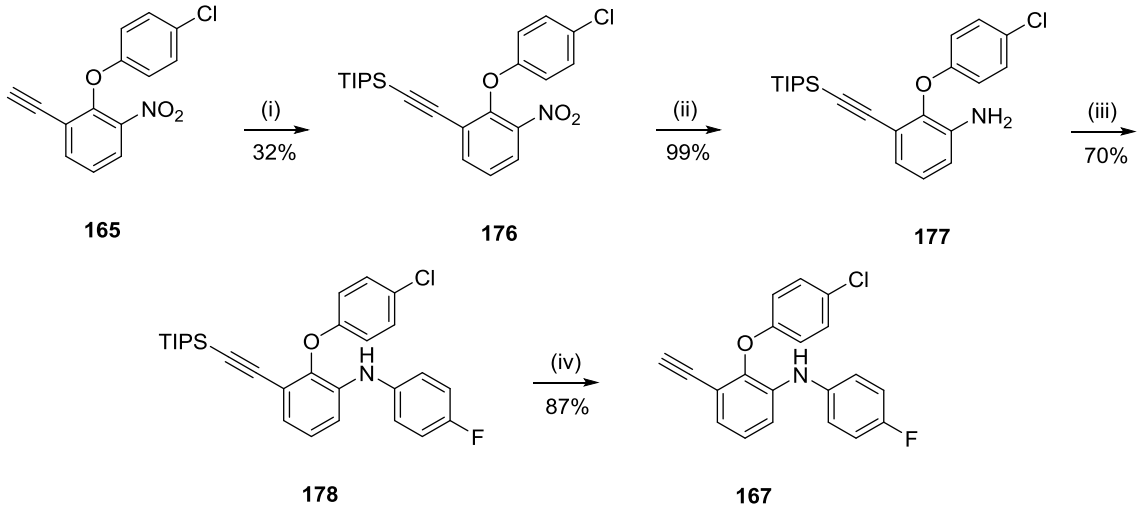

Scheme 69: (i) *n*-BuLi, THF, -78 ^oC, 15 min; TIPSCl, THF, RT, 2 h; (ii) $SnCl_2.2H_2O$, EtOH, 70 ^oC, 15 min; (iii) 1-bromo-4-fluorobenzene, Pd_2dba_3, XPhos, NaO^tBu, MeCN, 120 ^oC, MW, 3 h; (iv) TBAF, THF, RT, 20 min

Treatment of **167** with LDA followed by methyl chloroformate generated carbamate **179** on a 20 mg scale reaction, with acylation occurring on the acetylene and aniline nitrogen. However, this result was not reproducible, with carbamate **180** being the only product isolated on a 250 mg scale with increased equivalents of LDA and methyl chloroformate (**Scheme 70**).

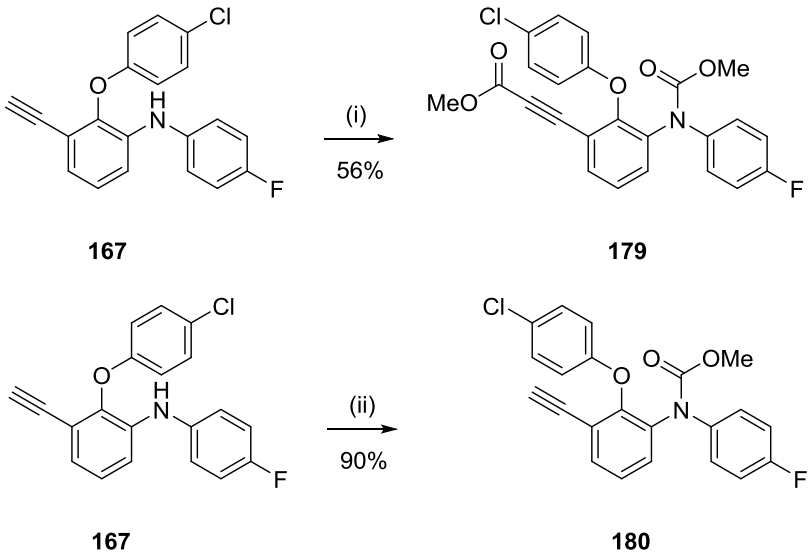

Scheme 70: (i) **167** (20 mg, 1.0 equiv.), $^{i}Pr_2NH$ (1.1 equiv.), *n*-BuLi (1.1 equiv.), THF (1.9 mL), -78 ^{o}C to RT to -78 ^{o}C, 20 min; $ClCO_2Me$ (1.1 equiv.), THF, -78 ^{o}C-RT; (ii) **167** (250 mg, 1.0 equiv.), $^{i}Pr_2NH$ (1.3 equiv.), *n*-BuLi (1.3 equiv.), THF (13.3 mL), -78 ^{o}C to RT to -78 ^{o}C, 20 min; $ClCO_2Me$ (2.5 equiv.), THF, -78 ^{o}C-RT

Carbamate **180** was converted to aniline **167** by refluxing in sodium hydroxide. Protection of the aniline nitrogen with Boc_2O, followed by acylation of the terminal acetylene using LDA and methyl chloroformate, gave ester **182**. Ring-closure with hydroxylamine and quenching with concentrated HCl simultaneously formed the isoxazole ring and removed the Boc group to give **183a**. Treating **182** with hydrazine hydrate formed **183b** (**Scheme 71**).

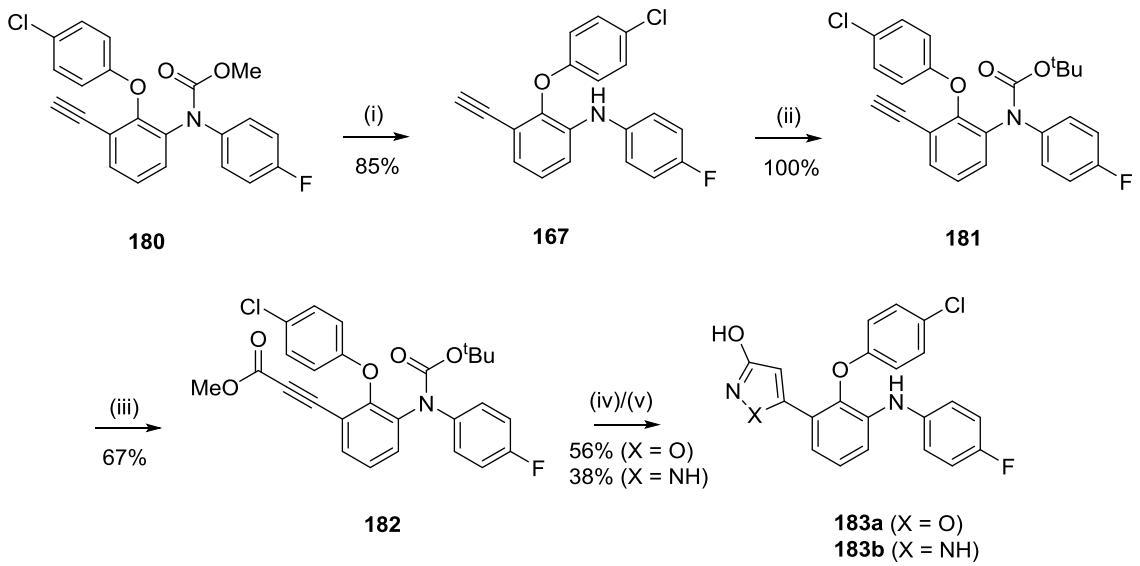

Scheme 71: (i) 2 M aq. NaOH, MeOH (1:1), 70 ^{o}C, 8 h; (ii) Boc_2O, DMAP, MeCN, 50 ^{o}C, 3 h; (iii) $^{i}Pr_2NH$, *n*-BuLi, THF, -78 ^{o}C to 0 ^{o}C to -78 ^{o}C, 20 min; $ClCO_2Me$, THF, -78 ^{o}C-RT, 20 min; (iv) H_2N-OH.HCl, NaOH, 0-60-0 ^{o}C, 4 h; *Conc*. HCl, 0-50 ^{o}C, 1 h; (v) H_2N-$NH_2.H_2O$, 0-60-0 ^{o}C; *Conc*. HCl, 0-50 ^{o}C, 1 h

5.3.2.2 Formation of Triazole 185 and Carboxylic Acid 187

Huisgen-style cycloaddition of acetylene **166** with TMS-azide and catalytic $CuSO_4.5H_2O$ and sodium ascorbate did not proceed beyond 70% conversion (LC-MS analysis) and adding more $CuSO_4$ and sodium ascorbate only produced impurities. Cycloaddition of acetylene **181** using CuI also did not reach full conversion and produced more impurities than the reaction using $CuSO_4$ and sodium ascorbate. The incomplete conversion was possibly due to chelation of the copper to the aniline and triazole nitrogen atoms, preventing further catalysis from occurring. With an excess of $CuSO_4$ and sodium ascorbate, acetylene **181** was converted to triazole **184** (**Table 37**). Removal of the Boc group with TFA gave triazole **185** (**Scheme 72**).

Table 37: Optimisation of the cycloaddition of acetylenes **166** and **181** with TMS-azide[a]

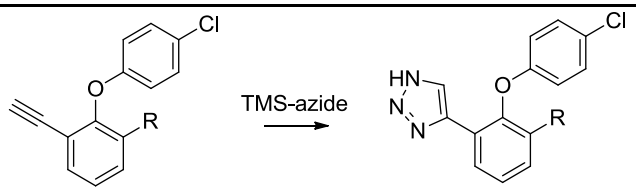

Entry	ID	R	Cu source (equiv.)	Reducing agent (equiv.)	Solvent	Temp. (^{o}C)	Results
1	**166**	NH_2	$CuSO_4.5H_2O$ (5 mol%)	Sodium ascorbate (10 mol%)	EtOH, H_2O (1:1)	25	No product
2	**181**	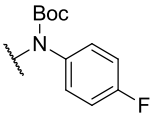	CuI (20 mol%)	-	DMF, MeOH (9:1)	100	No product
3	**181**	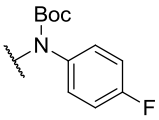	$CuSO_4.5H_2O$ (2.0)	Sodium ascorbate (3.0)	EtOH, H_2O (1:1)	25	**184** formed, 73% yield

(a) **166** or **181** (35-100 mg, 1.0 equiv) and TMS-azide (2.0 equiv.) at 0.5 M

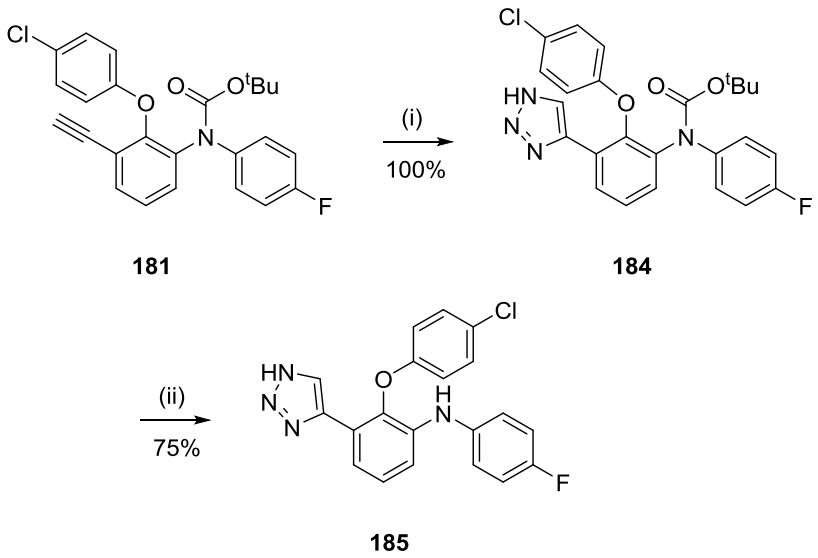

181 **184** **185**

Scheme 72: (i) TMS-azide, $CuSO_4.5H_2O$, sodium ascorbate, 50% H_2O, EtOH, 50 ^{o}C, o/n; (ii) 17% TFA, DCM, RT, 1 h

Hydrolysis of ester **182** with lithium hydroxide gave carboxylic acid **186** and removal of the Boc group with TFA generated **187** (**Scheme 73**). Treatment of **182** with TFA removed the Boc group to give propiolate ester **188**. All carboxylic acids, triazoles, 3-hydroxyisoxazoles and the corresponding pyrazoles were subsequently screened by ELISA against MDMX and MDM2 (**Table 38**).

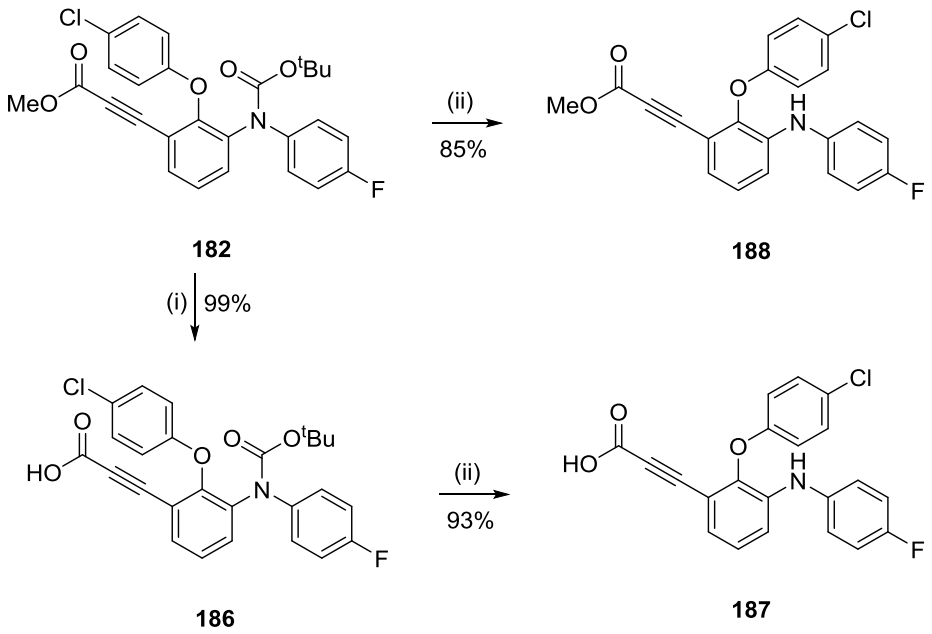

Scheme 73: (i) LiOH.H_2O, 50% THF, H_2O, 60 ^oC, 2 h; (ii) 17% TFA, DCM, RT, 1 h

Table 38: ELISA data for 1,2,3-trisubstituted benzene derivatives **183a**, **183b** and **184-187** (conducted by Dr Yan Zhao at the NICR)

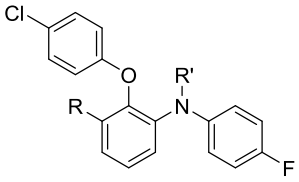

ID	R	R'	MDMX IC_{50} (μM)[a]	MDM2 IC_{50} (μM)[a]	Ratio (MDMX : MDM2)	LE[b]	LipE[b,c]
183a	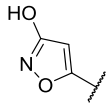	H	30.3	29.1	0.96	0.221	- 0.61
183b	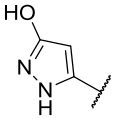	H	27.9	25.0	0.90	0.223	- 0.08
184	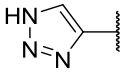	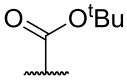	67.8	73.7	1.09	0.168	- 1.24
185	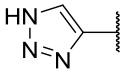	H	29.1	39.3	1.35	0.230	+ 0.02
186	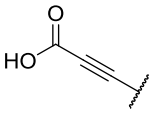	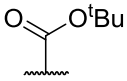	104	46.9	0.45	0.161	+ 1.92
187	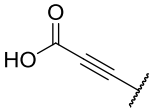	H	77.3	47.3	0.61	0.209	+ 2.09

(a) n = 1; (b) With respect to MDMX; (c) LipE = pIC_{50} – $clogD_{7.4}$ (clogD values from StarDrop)

Replacing the hydroxyphenyl ring of **138c** with a 3-hydroxyisoxazole (**183a**), 3-hydroxypyrazole (**183b**) or a 1,2,3-triazole (**185**) did not compromise potency against MDMX or MDM2. None of the compounds increased potency relative to **138c** (*cf.* Table 31) against either protein but they did significantly improve LipE. Only compounds possessing an acidic hydrogen bond donor motif had any activity against MDMX or MDM2. Propiolate esters **179** and **188** and acetylenes **167** and **178** were all weaker inhibitors (IC_{50} > 160 μM) against both targets. Compound **169** gave an IC_{50} of 237 μM against MDMX and only 31% inhibition at 200 μM against MDM2, despite the

presence of a 3-hydroxyisoxazole moiety. Compounds with carbamate-protected anilines (**179, 184** and **186**) were less active than their unprotected analogues.

5.3.2.3 Replacing the 4-Chlorophenoxy Ring with a 6-Chloroindol-3-yl Ring

Imidazole-based MDM2 inhibitors have described the 6-chloroindol-3-yl ring as an optimal substituent for binding into the p53-W23 pocket.[104] The 6-chloroindole ring exploits the hydrogen bond formed between the indole NH of tryptophan and the carbonyl oxygen of MDM2-L54. The crystal structure of compound **50** with MDMX has shown the 6-chloroindol-3-yl ring makes an analogous interaction with MDMX-M53 (**Figure 51**).[106]

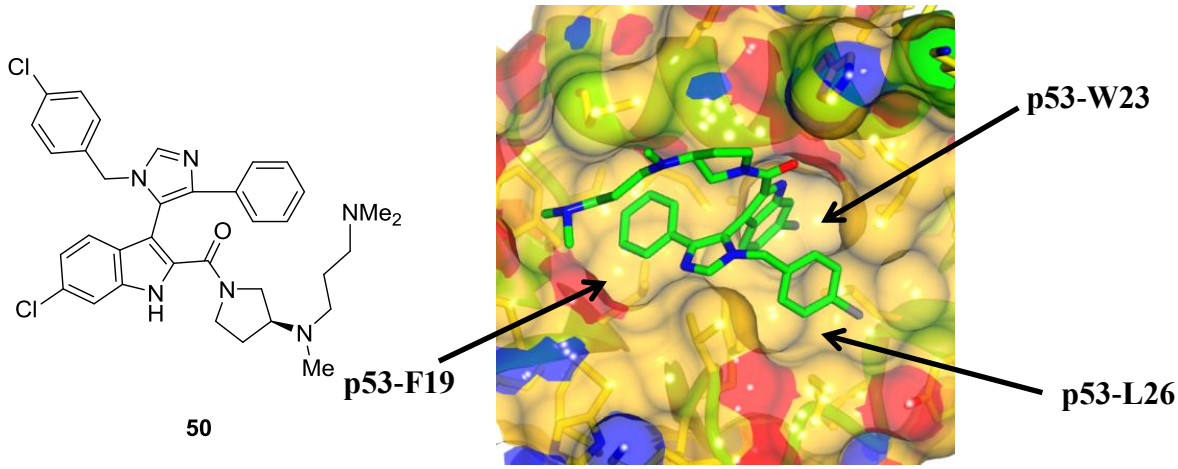

Figure 51: Crystal structure of **50** (green) in the p53 binding domain of MDMX (yellow). The p53 binding subpockets F19, W23 and L26 are highlighted. Image modified using CCP4mg (resolution, 1.5 Å; PDB code: 3LBJ)[106]

It was of interest to see if replacing the 4-chlorophenoxy substituent in the 1,2,3-trisubstituted benzenoid series with a 6-chloroindol-3-yl ring, could afford a similar enhancement in activity against MDMX and MDM2 (**Figure 52**).

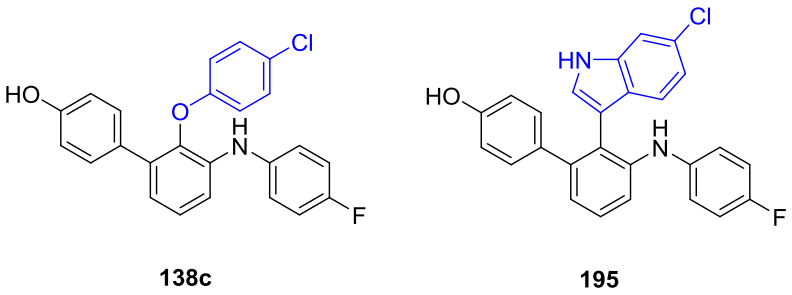

Figure 52: Replacing the 4-chlorophenoxy group in **138c** with a 6-chloroindol-3-yl ring (**195**)

The proposed synthesis of **195** started from 2-bromo-3-nitroanisole (**189**). Suzuki coupling with an indolyl substituent, followed by demethylation and sulfonylation would form triflate **192**. Suzuki coupling with 4-hydroxybenzeneboronic acid, reduction of the nitro group and Buchwald coupling with 1-bromo-4-fluorobenzene completes the synthesis (**Scheme 74**).

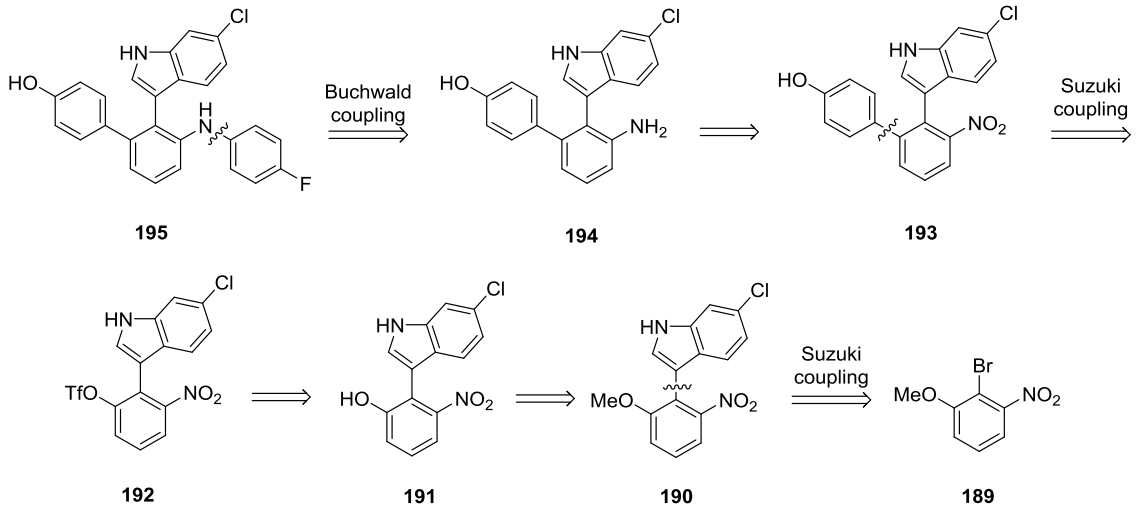

Scheme 74: Retrosynthesis of indole **195**

Starting from 6-chloroindole (**199**), silylation using TIPS-chloride with *n*-BuLi formed **200** in high yield. An attempt was made to synthesise boronic ester **201** directly following the synthesis described by Del Grosso using B-chlorocatecholborane (**196**).[144] In the presence of aluminium chloride, the chloro group from B-chlorocatecholborane-triethylamine adduct **197** is abstracted, forming borenium cation **198** that poorly nucleophilic indoles will attack at *C*-3 (**Scheme 75**).[144]

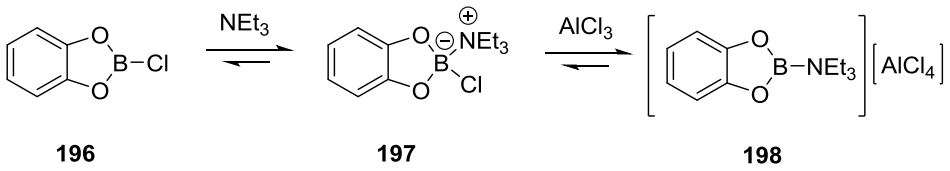

Scheme 75: The formation of borenium cation **102** by halide abstraction with aluminium chloride[144]

However, under these conditions, no reaction was observed between indole **200** and **198** even after heating at 50 ^{o}C. The authors had reported that *N*-silylated indoles were inadequately nucleophilic due to the negligible electron donation to the indole ring by the silyl group. Only indoles substituted on nitrogen by electron-donating substituents, e.g. alkyl groups, were sufficiently reactive.[144]

Bromination of **200** using *N*-bromosuccinimide (NBS) proceeded in excellent yield and regioselectively at *C*-3 (NMR analysis) to give **202** (**Scheme 76**).

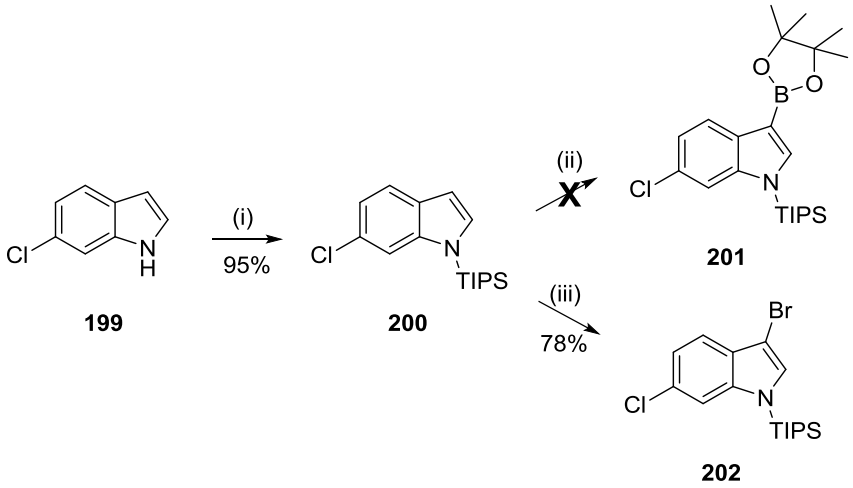

Scheme 76: (i) *n*-BuLi, THF, -78 ^{o}C, 1 h; TIPSCl, THF, -78 ^{o}C-RT, 1 h; (ii) **198**, $AlCl_3$, Et_3N, DCM, 0 ^{o}C; Et_3N, pinacol, RT-50 ^{o}C; (iii) NBS, THF, -78 ^{o}C, 2 h

Borylation of **202** using $B_2(pin)_2$ gave **201**, but only in 23% yield. Yang had previously described a high-yielding synthesis of 3-indolylboronic acids from the corresponding 3-bromoindoles *via* halogen-lithium exchange and addition of a trialkylborate followed by hydrolysis to the desired boronic acid (**Scheme 77**).[145]

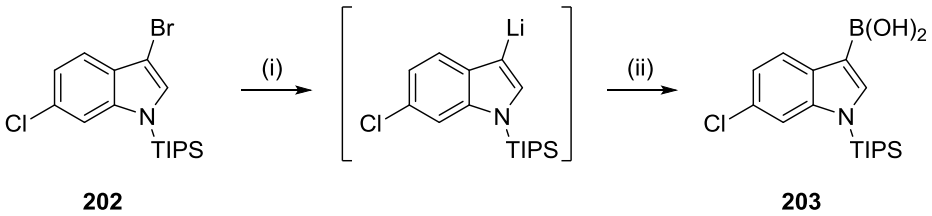

202 **203**

Scheme 77: (i) *n*-BuLi, THF, -78 °C; (ii) $B(O^iPr)_3$, THF, -78 °C; 50% MeOH, H_2O, -78 °C-RT[145]

Bromoindole **202** underwent complete halogen-lithium exchange upon treatment with *n*-BuLi within 5 min at -78 °C. Addition of triisopropylborate gave a 5:2 ratio of boronic acid **203** and indole **200** (LC-MS analysis). However, isolation of the pure product resulted in rapid deborylation to **200** (^{1}H NMR analysis). Halogen-lithium exchange followed by addition of methoxyboronic acid pinacol ester (MeOB(pin)) gave a 2:1 ratio of **201** and **200** but the product could be isolated in pure form without any degradation observed. Reducing the equivalents of MeOB(pin) from three to two gave a **201:200** ratio of 1:6. Increasing the equivalents of MeOB(pin) from three to six restored the **201:200** ratio to 2:1 (**Table 39**).

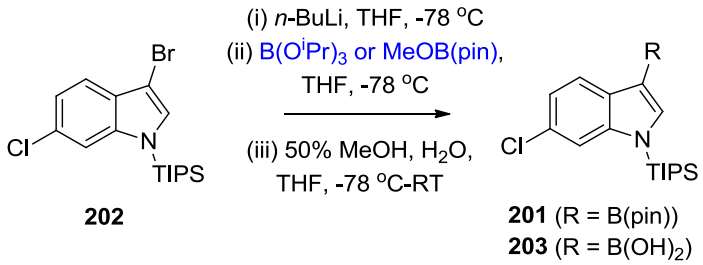

202

201 (R = B(pin))
203 (R = $B(OH)_2$)

Table 39: Optimisation of the borylation of **202** *via* halogen-lithium exchange

Entry	Borate (equiv.)	Target product	Product:200 Ratio[a]	Results
1	$B(O^iPr)_3$ (3.0)	**203**	5:2	Product not isolated
2	MeOB(pin) (3.0)	**201**	2:1	**201** isolated, 56% yield.
3	MeOB(pin) (2.0)	**201**	1:6	Product not isolated
4	MeOB(pin) (6.0)	**201**	2:1	Product not isolated

(a) LC-MS UV trace

Borylation of anisole **189** with $B_2(pin)_2$ and $(PPh_3)_2PdCl_2$ proceeded to > 90% conversion by LC-MS with low levels of homocoupling observed. Replacing $(PPh_3)_2PdCl_2$ with $Pd(dppf)Cl_2$.DCM produced a greater number of impurities, as did switching from 1,4-dioxane to DMF or DMSO. Increasing the equivalents of $(PPh_3)_2PdCl_2$ accelerated the reaction but also increased the levels of homocoupling. Increasing the equivalents of $B_2(pin)_2$ enhanced the reaction rate but homocoupling remained at low levels (**Table 40**).

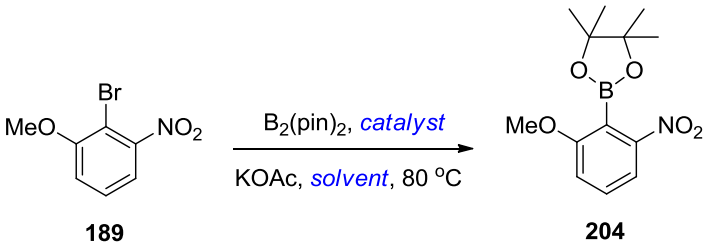

189 **204**

Table 40: Optimisation of the borylation of anisole **189**[a]

Entry	Catalyst (mol%)	Solvent	B_2Pin_2 Equiv.	Results
1	$(PPh_3)_2PdCl_2$ (3.0)	1,4-Dioxane	1.5	No product.
2	$Pd(dppf)Cl_2$.DCM (3.0)	1,4-Dioxane	1.5	No product.
3	$(PPh_3)_2PdCl_2$ (3.0)	DMF	1.5	No product.
4	$(PPh_3)_2PdCl_2$ (3.0)	DMSO	1.5	No product.
5	$(PPh_3)_2PdCl_2$ (5.0)	1,4-Dioxane	1.5	No product.
6	$(PPh_3)_2PdCl_2$ (3.0)	1,4-Dioxane	2.0	**201** isolated, 78% yield.

(a) **189** (100 mg, 1.0 equiv.) and KOAc (3.0 equiv.) at 0.5 M for at least 24 h by conventional heating

Suzuki coupling of **202** and **204** resulted in total deborylation of **204** within 30 min at 120 °C with no observed product formation. Switching from $Pd(dtbpf)Cl_2$to $Pd(PPh_3)_4$ had no effect on the level of deborylation under similar conditions. Reducing the temperature to 80 °C and heating conventionally significantly reduced deborylation and formed the desired product **205** (^{1}H NMR analysis). However, difficulties with purification from the excess of boronic ester **204** meant that the product could not be isolated in pure form and the yield was poor. Reducing the equivalents of $Pd(dtbpf)Cl_2$slowed the rate of the reaction and did not affect the levels of deborylation observed (**Table 41**).

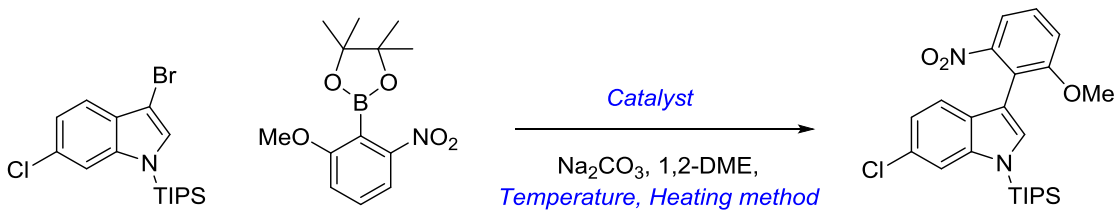

202 **204** **205**

Table 41: Optimisation of the Suzuki coupling between **202** and **204**[a]

Entry	Catalyst (mol%)	Heating method	Temp. (^{o}C)	Time (min)	Results
1	$Pd(dtbpf)Cl_2$ (5.0)	MW	120	30	No product
2	$Pd(PPh_3)_4$ (5.0)	MW	120	30	No product
3	$Pd(dtbpf)Cl_2$ (5.0)	Conventional	120	30	No product
4	$Pd(dtbpf)Cl_2$ (5.0)	Conventional	80	180	**205** isolated, ~35% yield (80% purity)
5	$Pd(dtbpf)Cl_2$ (1.5)	Conventional	80	180	No product

(a) **202** (30 mg, 1.0 equiv.), **204** (1.5 equiv.), 2 M aq. Na_2CO_3 (2.0 equiv.) at 0.2 M

It was becoming clear that facile debromination and deborylation, both of the indole substituent and the benzenoid scaffold, were severely abrogating yields, both in the formation of these coupling partners and in the subsequent attempt to join them together by Suzuki coupling. An alternative coupling strategy was therefore needed and it was decided to investigate nucleophilic aromatic substitution.

5.3.2.4 Replacing the 4-Chlorophenoxy Ring with a 6-Chloroindol-3-yl Ring by the S_NAr Reaction

There are no reported examples of nucleophilic aromatic substitutions in which an indole attacking at the *C*-3 position is the nucleophile. There are literature examples of stabilised carbanion nucleophiles being used in this transformation such as 1,3-dicarbonyls[146, 147] or 9*H*-fluorene anions,[148] with high yields being obtained.

Reaction of indole **199** with PMB-chloride in DMF gave **206** in high yield (**Scheme 78**). An electron-donating protecting group was selected to increase the indole's nucleophilicity.

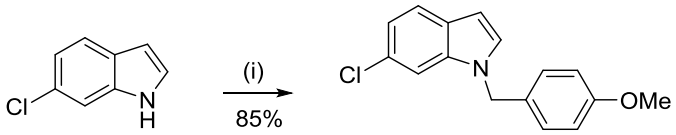

199 **206**

Scheme 78: (i) PMB-Cl, NaH, DMF, 80 ^{o}C, 2 h

2-Fluoronitrobenzene (**207**) was selected as a model system. Attempts to couple indole **199** or **206** with **207** using microwave-assisted irradiation in acetonitrile at 120 ^{o}C gave no reaction after 2 h.

Indole **199** was deprotonated using either *n*-BuLi, sodium hydride or methylmagnesium chloride (MeMgCl) before addition of **207**. The *n*-BuLi and sodium hydride reactions did not proceed at 0 ^{o}C or room temperature, but at 60 ^{o}C reacted to give the *N*-arylated product **208** with 100% regioselectivity over the desired *C*-3-arylated indole **209** (**Scheme 79**). This was not unexpected, as the ionic indole salts formed from deprotonation with a lithium or sodium base would predominatly react *via* the more electronegative nitrogen atom instead of the *C*-3 carbon.The reaction using MeMgCl did not proceed even when heated to 80 ^{o}C, most likely due to the increased covalent character of the indole Grignard reagent, which rendered the indole less reactive towards electrophiles than the corresponding lithium or sodium salts.

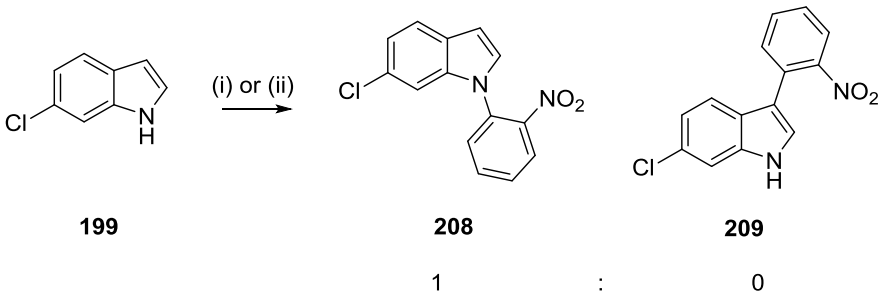

Scheme 79: (i) *n*-BuLi, THF, 0 °C; **207**, THF, 0-60 °C; (ii) NaH, THF, RT; **207**, THF, RT-60 °C

Transmetallation of *n*-BuLi with anhydrous $ZnCl_2$ or CuCl, generating an organozincate or organocopper reagent respectively, was done prior to addition of **207**. However, no reaction was observed after heating both reactions at 80 °C (**Table 42**).

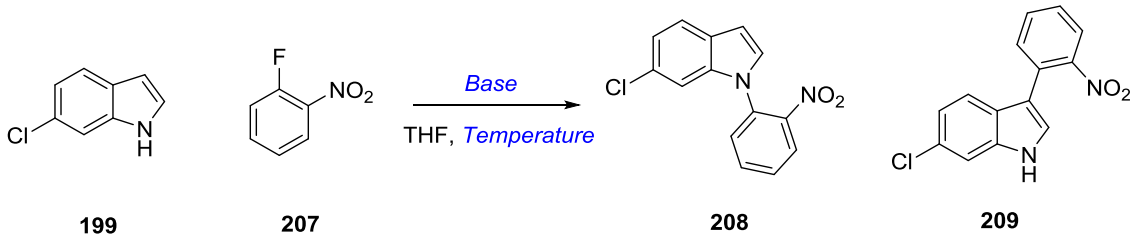

Table 42: Attempts made to react indole **199** with aryl fluoride **207** by S_NAr[a]

Entry	Base	Temp. (°C)	Results
1	*n*-BuLi[b]	0-60	**208** isolated, 68% yield
2	NaH[c]	0-60	**208** isolated, 84% yield
3	MeMgCl[d]	0-80	No reaction
4	*n*-BuLi[b], then $ZnCl_2$[e]	0-80	No reaction
5	*n*-BuLi[b], then CuCl	0-80	No reaction

(a) **199** (100 mg, 1.0 equiv.), **207** (1.0 equiv.), *n*-BuLi, MeMgCl, $ZnCl_2$, CuCl (1.1 equiv.) or NaH (2.0 equiv.) at 0.3 M; (b) 2.5 M in hexanes; (c) 60% in mineral oil; (d) 3.0 M in THF; (e) pre-dried at 150 °C

Indole **206** was brominated at *C*-3 to give **210** (**Scheme 80**).

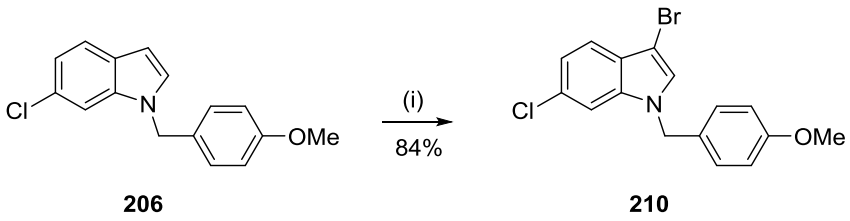

206 **210**

Scheme 80: (i) NBS, THF, -78 ^{o}C, 2 h

Bromoindole **210** was treated with either *n*-BuLi or MeMgCl at 0 ^{o}C before addition of excess **207**. Bromine-lithium exchange went to completion within 30 min (LC-MS analysis) and gave a 1:1 mixture of **206** and the desired product **211** upon addition of **207**, with the latter being isolated in 53% yield. The analogous reaction with MeMgCl failed to undergo magnesium-bromine exchange and no reaction occurred with **207**. Conducting the reactions with *n*-BuLi at -78 ^{o}C hindered bromine-lithium exchange and subsequent addition of **207** gave only a mixture of **206** and **210**. Halogen-lithium exchange at 0 ^{o}C, followed by addition of **207** at -20 ^{o}C formed **206** as the major product and various impurities. However, if **207** was added at 0 ^{o}C or room temperature, **211** was the predominant product formed. Reducing the equivalents of **207** did not affect product distribution, indicating reaction temperature to be a key variable in the success of this reaction (**Table 43**). This is the first documented aromatic substitution using an indol-3-yl carbanion as the nucleophile. Halogen-lithium exchange and the subsequent S_NAr reaction can be completed within one hour at 0 ^{o}C without the need for a palladium catalyst. This reaction offers a novel procedure for the rapid formation of 3-arylindoles using inexpensive reagents and with fewer variables to optimise relative to organometallic coupling reactions.

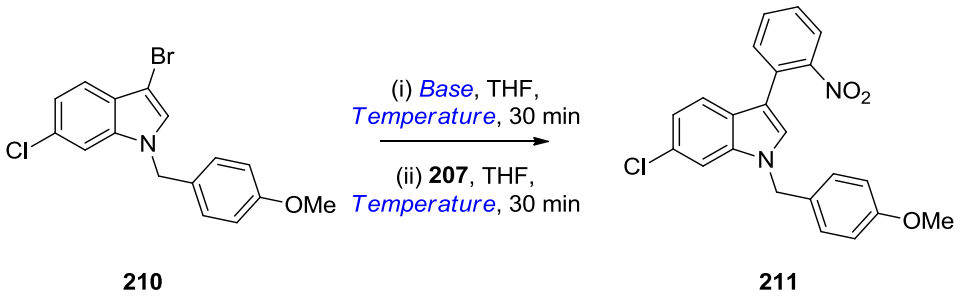

210 **211**

Table 43: Optimisation of the conditions for halogen-metal exchange and S_NAr with **207**[a]

Entry	Base	Equiv. of 207	Temp. for step (i) (°C)	Temp. for step (ii) (°C)	Results
1	*n*-BuLi[b]	2.0	0-RT	0	**211** isolated, 53% yield
2	MeMgCl[c]	2.0	0-RT	0	No reaction
3	*n*-BuLi[b]	2.0	-78	-78	**210** major product
4	*n*-BuLi[b]	2.0	0	-78	**210** major product
5	*n*-BuLi[b]	2.0	0	-20	**210** major product
6	*n*-BuLi[b]	2.0	0-RT	RT	**211** major product
7	*n*-BuLi[b]	1.5	0	0	**211** major product

(a) **210** (50-100 mg, 1.0 equiv.) and *n*-BuLi or MeMgCl (1.1 equiv.) at 0.4 M; (b) 2.5 M in hexanes; (c) 3.0 M in THF

Indole **199** was also reacted with Boc_2O to give indole **212** (**Scheme 81**). The Boc-group was investigated for the S_NAr reaction to see what effect an electron-withdrawing protecting group would have on the stability of the *C*-3 carbanion and the ratio of S_NAr product to de-bromination product observed.

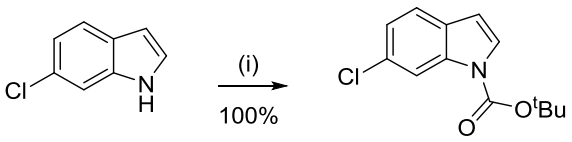

199 **212**

Scheme 81: (i) Boc_2O, DMAP, MeCN, 50 °C, 3 h

Under previous conditions (*cf.* Scheme 80), bromination of **212** achieved only partial conversion and additional NBS formed an inseparable mixture of the 3-bromo- and 2,3-

dibromoindole products **213** and **214**, respectively. Replacing THF with DMF, heating to 60 ^{o}C and reducing the excess of NBS resulted in a faster reaction that gave **213** as the major product (**Table 44**).

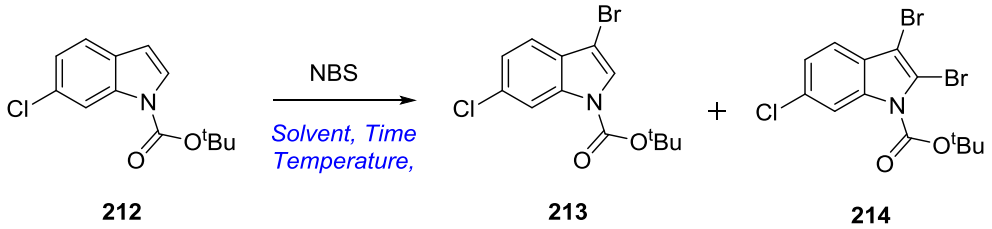

Table 44: Optimisation of the bromination of **212**[a]

Entry	NBS Equiv.	Solvent	Temp. (^{o}C)	Time (h)	213:214 Ratio[b]	Results
1	2.5	THF	25	24	3:2	**213** yield 47%, **214** yield 25%
2	1.1	THF	60	2	> 95:5	Incomplete reaction
3	1.1	DMF	60	2	> 95:5	**213** isolated, 86% yield

(a) **212** (50-300 mg, 1.0 equiv.) at 1.0 M; (b) LC-MS UV trace

Reaction of **213** with *n*-BuLi followed by addition of **207** produced a greater number of impurities than the reaction with indole **210** and none of the desired S_NAr product. A similar number of impurities were generated when the lithiated species was quenched with deionised water in place of **207**. It is possible that the Boc-protected 3-lithioindole was undergoing ring-opening to give acetylene **215** (**Scheme 82**). This is known to happen when the indole nitrogen is conjugated with electron-withrawing groups, including carbonyls. [149]

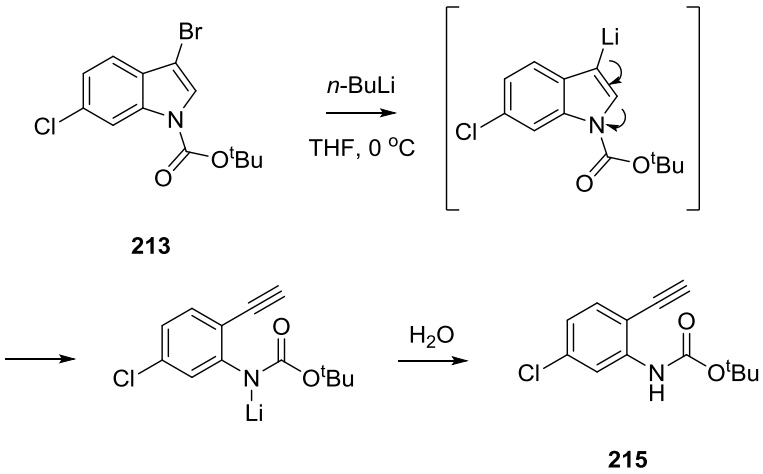

Scheme 82: Proposed ring-opening of **213** upon treatment with *n*-BuLi to give **215**[149]

From these experiments, it was clear that:

1. *N*-Boc-protected 3-bromoindoles were less stable towards lithiation than the corresponding *N*-PMB-protected indoles.

2. *N*-PMB-protected indoles undergo lithium-bromine exchange to completion within 30 min at 0 °C and reaction with aryl fluoride **207** at 0 °C or room temperature forms the desired product **211**. Lower temperatures result in increased de-bromination.

Bromine-lithium exchange with **210** followed by addition of 3-bromo-2-fluoronitrobenzene (**139**) at 0 °C produced a mixture of four species: **210**, de-brominated indole **206**, aryl fluoride **207** and unreacted **139** (**Scheme 83**). None of the desired S_NAr product was formed. The fact some of **210** remained suggested that the 3-lithioindole had abstracted bromine from **139** to give **207**, instead of substituting for fluoride. The remaining 3-lithioindole would be protonated upon quenching to give **206**.

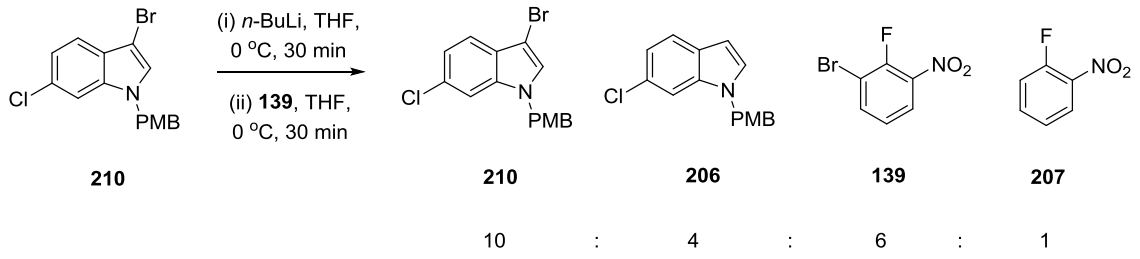

Scheme 83: Attempted S_NAr reaction between **210** and **139**, the subsequent products identified and their approximate ratio (^1H and ^{19}F NMR analysis)

The bromine substituent of **139** was therefore inhibiting the ability of the 3-lithioindole to undergo S_NAr. Suzuki coupling of **139** with the appropriate boronic acid would therefore allow the S_NAr reaction to proceed, as previously with **207**, to give **217** (**Scheme 84**). Reduction of the nitro group and Buchwald coupling of **218** with 1-bromo-4-fluorobenzene, followed by removal of all protecting groups, was predicted to give the target compound **195**. However, due to the problems already encountered in this synthesis, it was decided to investigate other targets of interest.

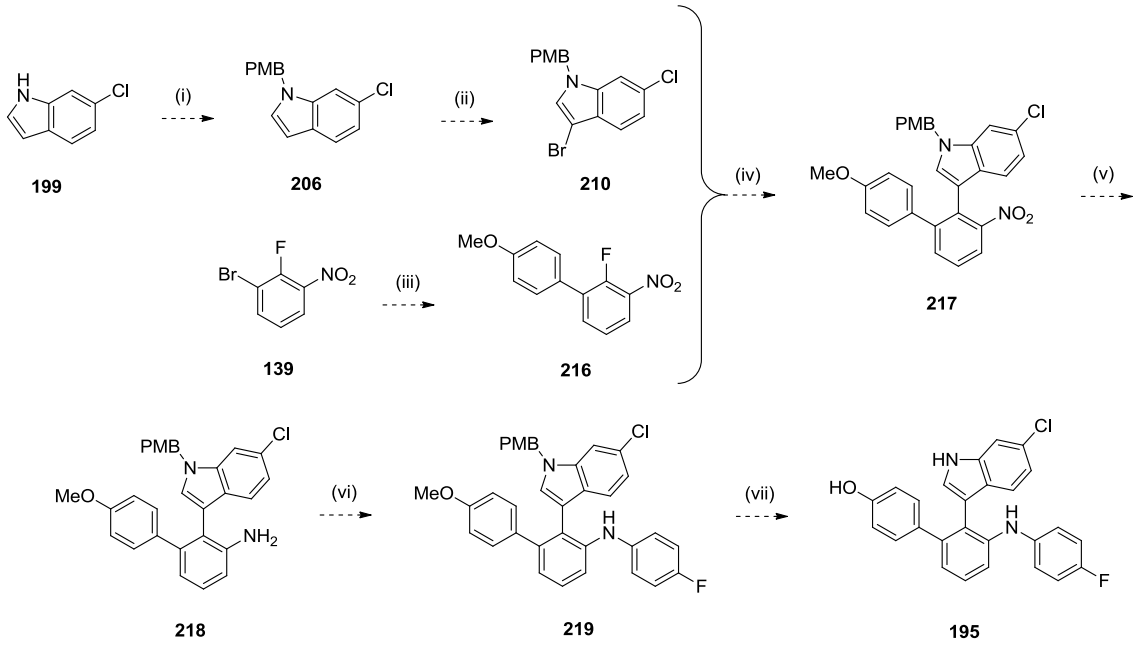

Scheme 84: Proposed route to indole **195** (i) PMB-Cl, NaH, DMF, 80 °C; (ii) NBS, THF, -78 °C; (iii) 4-methoxybenzeneboronic acid, $Pd(dtbpf)Cl_2$, Na_2CO_3, 1,2-DME, 120 °C, MW; (iv) *n*-BuLi, THF, 0 °C; (v) $SnCl_2.2H_2O$, EtOH, 70 °C; (vi) 1-bromo-4-fluorobenzene, Pd_2dba_3, XPhos, NaO^tBu, MeCN, 120 °C, MW; (vii) Removal of PMB and phenoxymethyl group

5.3.3 Addition of Water-Solubilising Groups to the Benzenoid Scaffold

During lead optimisation of the benzenoid series of MDMX inhibitors, optimisation of the corresponding pyrrole-based inhibitors at Newcastle University (S. Adhikari, PhD 2012-2015) had found that having a carboxy group at the 3-position of the pyrrole scaffold (**220c**) enhanced potency against MDMX and MDM2 relative to the unsubstituted pyrrole **220a** (**Table 45**). The carboxy group could obviously make a favourable interaction with the protein, a hypothesis supported by the fact that the corresponding methyl ester (**220b**) was inactive.

Table 45: ELISA data for pyrroles **220a-220c** (conducted by Dr Yan Zhao at the NICR)

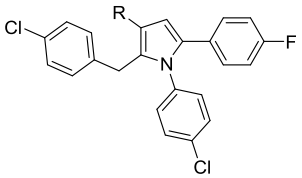

ID	R	MDMX IC_{50} (μM)	MDM2 IC_{50} (μM)
220a	H	198[a]	38.3%[a,d]
220b	CO_2Me	189[a]	24.8%[a,d]
220c	CO_2H	14.6[c]	11.2[b]

(a) n = 1; (b) n = 2; (c) n = 3; (d) 200 μM

It was of interest to determine whether addition of the same functionality would achieve a similar increase in potency in the benzenoid series. Starting from 4-fluoro-3-nitrobenzoic acid (**221**), regioselective bromination with NBS in concentrated H_2SO_4 afforded aryl bromide **222**. Nucleophilic aromatic substitution with 4-chlorophenol, Suzuki coupling with 4-hydroxybenzeneboronic acid and tin-mediated nitro reduction gave the desired intermediates **223**, **224** and **225**, respectively in moderate to high yields, but Buchwald coupling failed to give target **226** (**Scheme 85**). It was clear that the failure of this reaction was due to the carboxy group, as coupling of the same aryl bromide to aniline **137a** (*cf.* Scheme 44), which has no carboxy group, proceeded in greater than 80% yield under the same conditions.

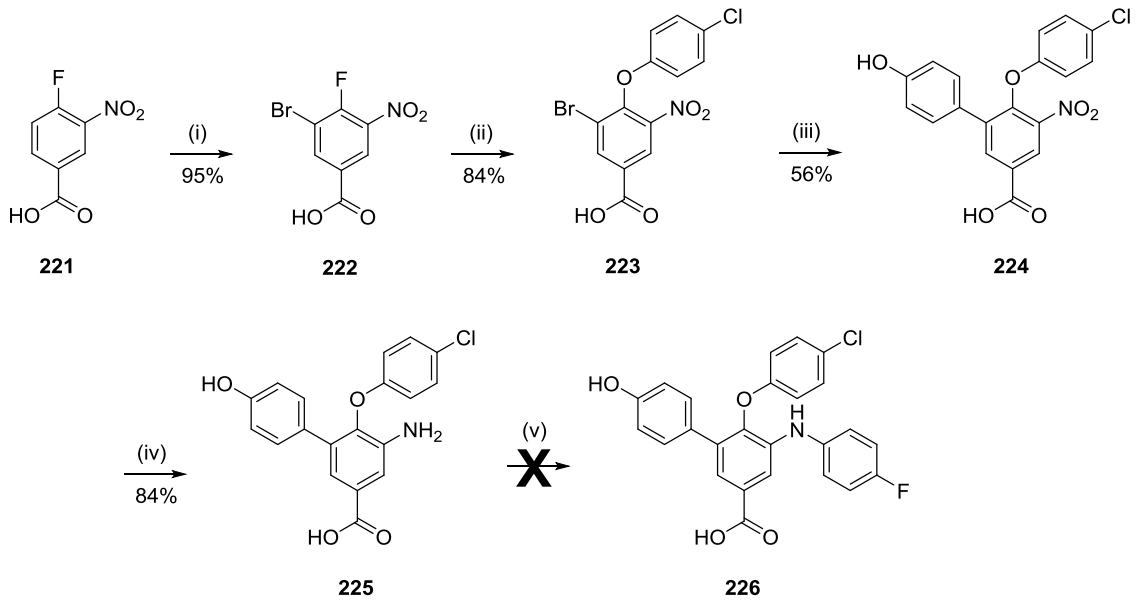

Scheme 85: (i) NBS, *conc.* H_2SO_4, 80 ^oC, 3 h; (ii) 4-chlorophenol, K_2CO_3, MeCN, 90 ^oC, MW, 45 min; (iii) 4-hydroxybenzeneboronic acid, Pd(dtbpf)Cl_2, Na_2CO_3, 1,2-DME, 120 ^oC, MW, 20 min; (iv) $SnCl_2.2H_2O$, EtOH, 70 ^oC, 20 min; (v) 1-bromo-4-fluorobenzene, Pd_2dba_3, XPhos, NaO^tBu, MeCN, 120 ^oC, MW, 4 h

Aryl ether **223** was esterified under acidic conditions to give ester **227** in near quantitative yield. It was later found that the bromination, S_NAr and esterification could all be done without the need for chromatographic purification. Suzuki coupling and nitro reduction proceeded as before to give **228** and **229**, respectively. Buchwald coupling gave aniline **230** in high yield and hydrolysis of the ester with lithium hydroxide gave **226**. The ester of **230** was also reduced to give alcohol **231** using DIBAL-H (**Scheme 86**). Compounds **226**, **230** and **231** were screened by ELISA (**Table 46**).

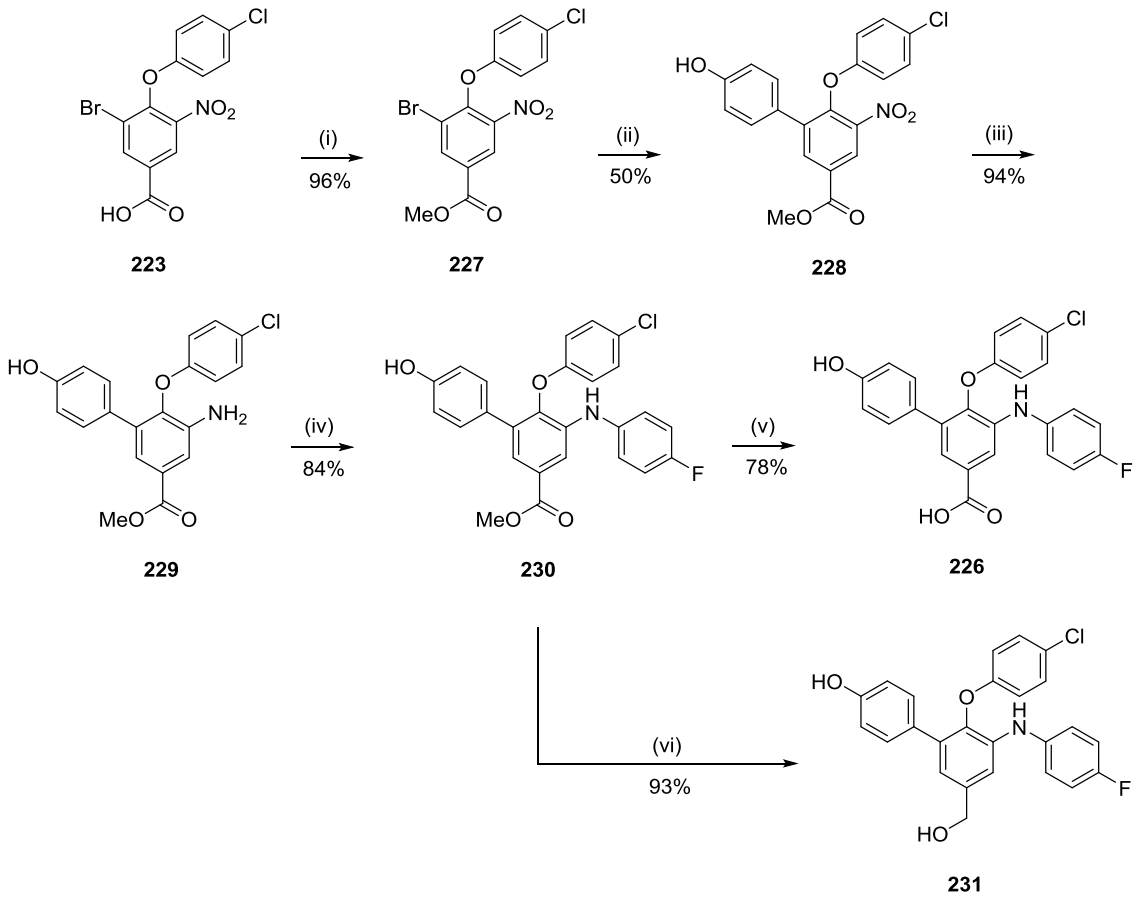

Scheme 86: (i) MeOH, *conc.* H_2SO_4, 80 ^oC, 1 h; (ii) 4-hydroxybenzeneboronic acid, Pd(dtbpf)Cl_2, Na_2CO_3, 1,2-DME, 120 ^oC, MW, 20 min; (iii) $SnCl_2.2H_2O$, EtOH, 70 ^oC, 20 min; (iv) 1-bromo-4-fluorobenzene, Pd_2dba_3, XPhos, K_2CO_3, MeCN, 120 ^oC, MW, 3 h; (v) LiOH.H_2O, 50% THF, H_2O, 60 ^oC, o/n; (vi) DIBAL-H, THF, -78 ^oC-0 ^oC, 4 h

Table 46: ELISA data for 1,2,3,5-tetrasubstituted benzene derivatives **226**, **230** and **231**(conducted by Dr Yan Zhao at the NICR)

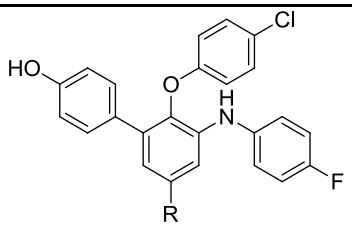

ID	R	MDMX IC_{50} (µM)[a]	MDM2 IC_{50} (µM)[a]	Ratio (MDMX : MDM2)	LE[b]	LipE[b,c]
226	CO_2H	29.1	3.23	0.11	0.194	+ 1.85
230	CO_2Me	45.6	94.7	2.08	0.180	- 1.64
231	CH_2OH	22.8	11.4	0.50	0.205	- 0.52

(a) n = 1; (b) With respect to MDMX; (c) LipE = pIC_{50} – $clogD_{7.4}$ (clogD values from StarDrop)

Addition of carboxy and hydroxymethyl groups to the 5-position of the benzenoid scaffold was tolerated with both protein targets. Compounds **226** and **231** were similarly potent to parent compound **138c** (*cf.* Table 31), but ester **230** was half as active. None of the compounds was more active against MDMX than **138c**, but **226** and **231** did have improved LipE. Ester **230** was four-fold less potent than **138c** against MDM2, but **231** was twice as active and **226** was eight-fold more potent and almost ten-fold selective for MDM2.

5.3.3.1 Homologation of the Carboxy Group of 226

The carboxy group of **226** was homologated to investigate whether this would allow the functionality to make a better interaction with the protein. Attempts to reduce aryl acid **223** using sodium borohydride and iodine[150] generated a large number of impurities and using borane-THF only went to 30% conversion (LC-MS analysis). However, ester **227** was reduced to alcohol **232** using DIBAL-H. Initial attempts to form nitrile **234** involved sulfonylation with methanesulfonyl chloride followed by reaction with sodium cyanide in acetonitrile.[151] However, stirring at 60 ^{o}C gave no conversion of mesylate **233**. Repeating the cyanation in DMF generated a large number of unidentifiable impurities. When the mesylation and cyanation were repeated at 0 ^{o}C on a 50 mg scale of **232**, clean conversion of the alcohol to a single product was observed (^{1}H NMR analysis). It was later found that the product isolated was benzyl chloride **235**, formed by displacement of the mesylate in **233** with chloride (**Scheme 87**). Compound **235** did not react with sodium cyanide at room temperature (**Table 47**).

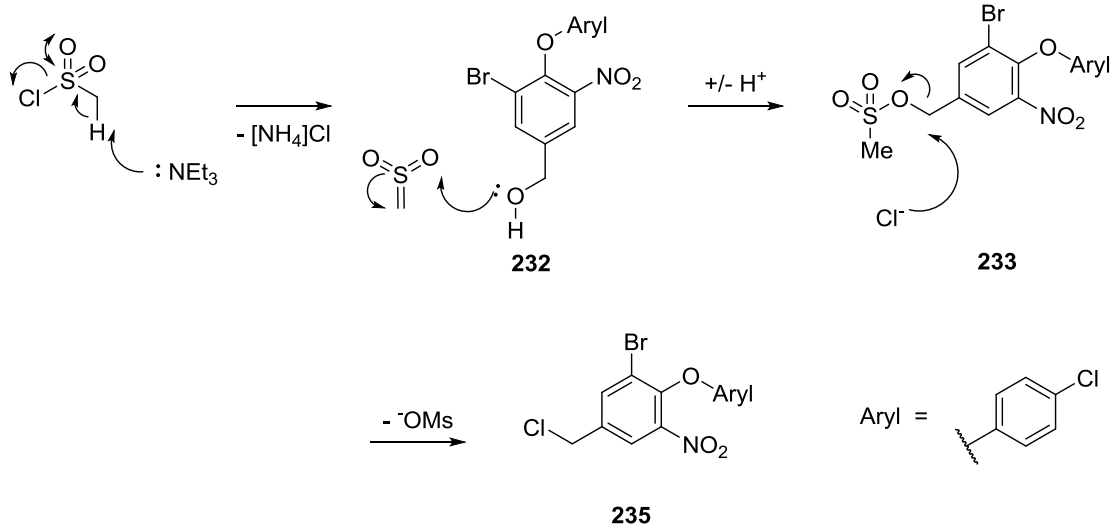

Scheme 87: Mesylation of alcohol **232** followed by displacement with chloride to give **235**

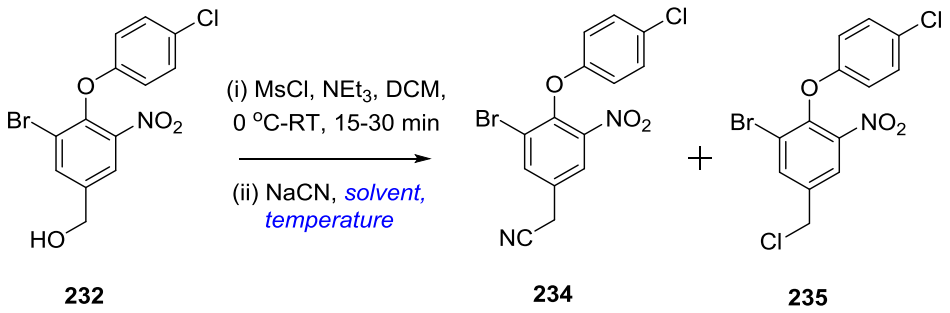

232 **234** **235**

Table 47: Optimisation of the mesylation/cyanation of **232** using sodium cyanide[a]

Entry	NaCN Formulation	NaCN Equiv.	Solvent[b]	Temp. (°C)[b]	Results
1	Powder	1.1	MeCN	25-60	**235** only product
2	Powder	1.1	DMF	0-25	**235** only product
3	0.15 M in DMF	1.1	DMF	0-25	**235** only product
4	0.15 M in DMF	1.5	DMF	0-25	**235** only product

(a) **232** (200 mg, 1.0 equiv.), MsCl (1.1 equiv.), Et_3N (1.5 equiv.) at 0.5 M for the mesylation and 0.2 M for the cyanation; (b) With respect to the cyanation

Alcohol **232** was reacted with methanesulfonic anhydride (Ms_2O), in place of mesyl chloride, giving mesylate **233**. Cyanation followed the procedure described by Soli using TMS-cyanide and TBAF in acetonitrile.[152] In this reaction, TBAF reacts with TMS-cyanide (**236**) to form pentavalent silicon species **237** that is the nucleophilic source of cyanide (**Scheme 88**).[152]

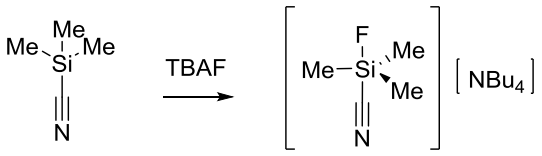

236 **237**

Scheme 88: Coordination of fluoride to TMS-cyanide (**236**) to give pentavalent silicon complex **237**[152]

When mesylate **233** was mixed with TMS-cyanide and TBAF, LC-MS showed full conversion to the desired product after 30 min at room temperature. Conducting the reaction at 0 °C produced fewer impurities and nitrile **234** was obtained in 29% yield.

An Arndt-Eistert homologation was also trialled using 3-nitrobenzoic acid (**238**) as a model system. Reaction with thionyl chloride formed the desired acid chloride and

subsequent treatment with TMS-diazomethane gave diazoketone **239** within 2 h. No conversion was observed upon treating **239** with methanol in the presence of catalytic $PhCO_2Ag$, even after prolonged heating. However, when stoichiometric quantities of $PhCO_2Ag$ were added, conversion to the homologated ester **240** was observed and the product was isolated in 27% yield (**Scheme 89**).

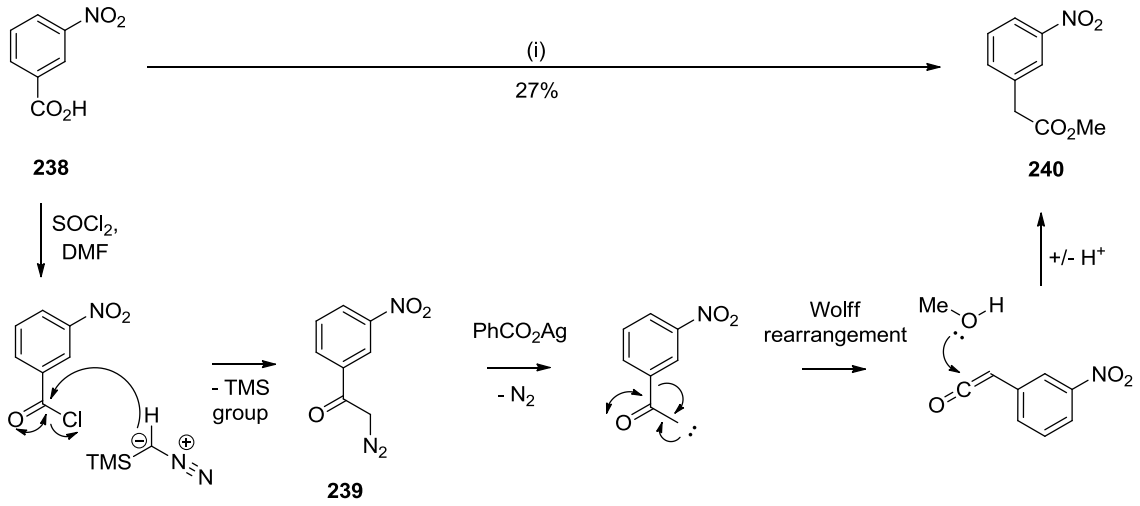

Scheme 89: (i) $SOCl_2$, DMF, THF, 0 ^oC-RT, 5 h; $TMSCHN_2$, Et_3N, 60% THF, MeCN, 0 ^oC, 2 h; $PhCO_2Ag$, MeOH, Et_3N, RT

Although Arndt-Eistert homologation did produce **240**, the yield was no better than that obtained with benzyl alcohol **232** using Ms_2O and substituting with cyanide. While the yield for the mesylation/cyanation procedure was poor, it was scaleable (**Table 48**).

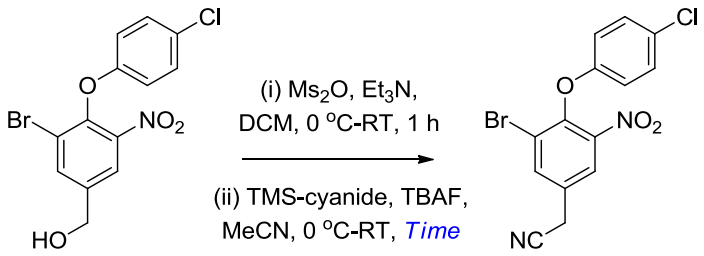

232 **234**

Table 48: Optimisation of the mesylation/cyanation of **232** using TMS-cyanide and TBAF[a]

Entry	Cyanation time (min)	Results
1	15	**234** isolated, 16% yield.
2	90	**234** isolated, 29-33% yield.

(a) **232** (100-1000 mg, 1.0 equiv.), Ms_2O (1.5 equiv.), Et_3N (1.5 equiv.), TMS-cyanide (1.5 equiv.), TBAF (1.5 equiv.) at 0.5 M for the mesylation and 0.2 M for the cyanation

Suzuki coupling of **234** with 4-hydroxybenzeneboronic acid followed by tin-mediated reduction of the nitro group gave aniline **242**. However, Buchwald coupling gave a large number of unidentifiable impurities, which were not observed with aniline substrates in which the cyanomethyl group was absent (*cf.* Scheme 44). Despite this, aniline **243** was isolated in 4.3% yield and hydrolysis in aqueous sodium hydroxide successfully gave homologated acid **244** (**Scheme 90**).

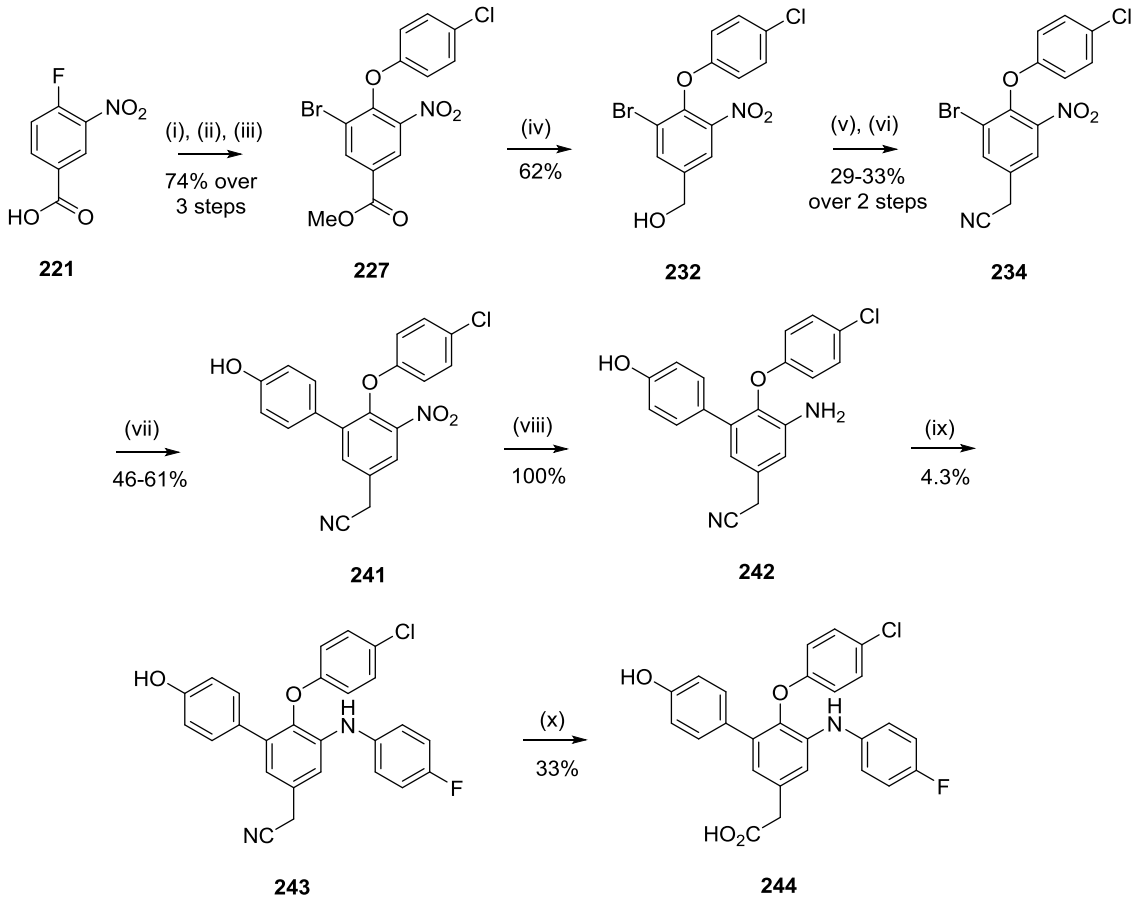

Scheme 90: (i) NBS, *conc.* H_2SO_4, 80 ^oC, 3 h; (ii) 4-chlorophenol, K_2CO_3, MeCN, 90 ^oC, MW, 45 min; (iii) MeOH, *conc.* H_2SO_4, 80 ^oC, 1 h; (iv) DIBAL-H, THF, -78-0 ^oC, 4 h; (v) Ms_2O, Et_3N, DCM, 0 ^oC-RT, 1 h; (vi) TMS-cyanide, TBAF, MeCN, 0 ^oC-RT, 90 min; (vii) 4-hydroxybenzeneboronic acid, $Pd(dtbpf)Cl_2$, Na_2CO_3, 1,2-DME, 120 ^oC, MW, 20 min; (viii) $SnCl_2.2H_2O$, EtOH, 70 ^oC, 20 min; (ix) 1-bromo-4-fluorobenzene, Pd_2dba_3, XPhos, K_2CO_3, MeCN, 120 ^oC, MW, 3 h; (x) 15% aq. NaOH, 130 ^oC, o/n

The low yields in the cyanation of **232** may have been due to unwanted side reactions by other substituents on the benzenoid scaffold, e.g. the bromo or nitro groups. These functionalities were consequently transformed, e.g. by Suzuki coupling of the aryl bromide or reduction of the nitro group (**Scheme 91**). Nitro reduction was found to proceed in excellent yields with zinc powder in acetic acid. Mesylation and cyanation reactions were then attempted on alcohols **249** and **250** to see if they afforded any improvement in yield over the same reaction with alcohol **232** (**Table 49**).

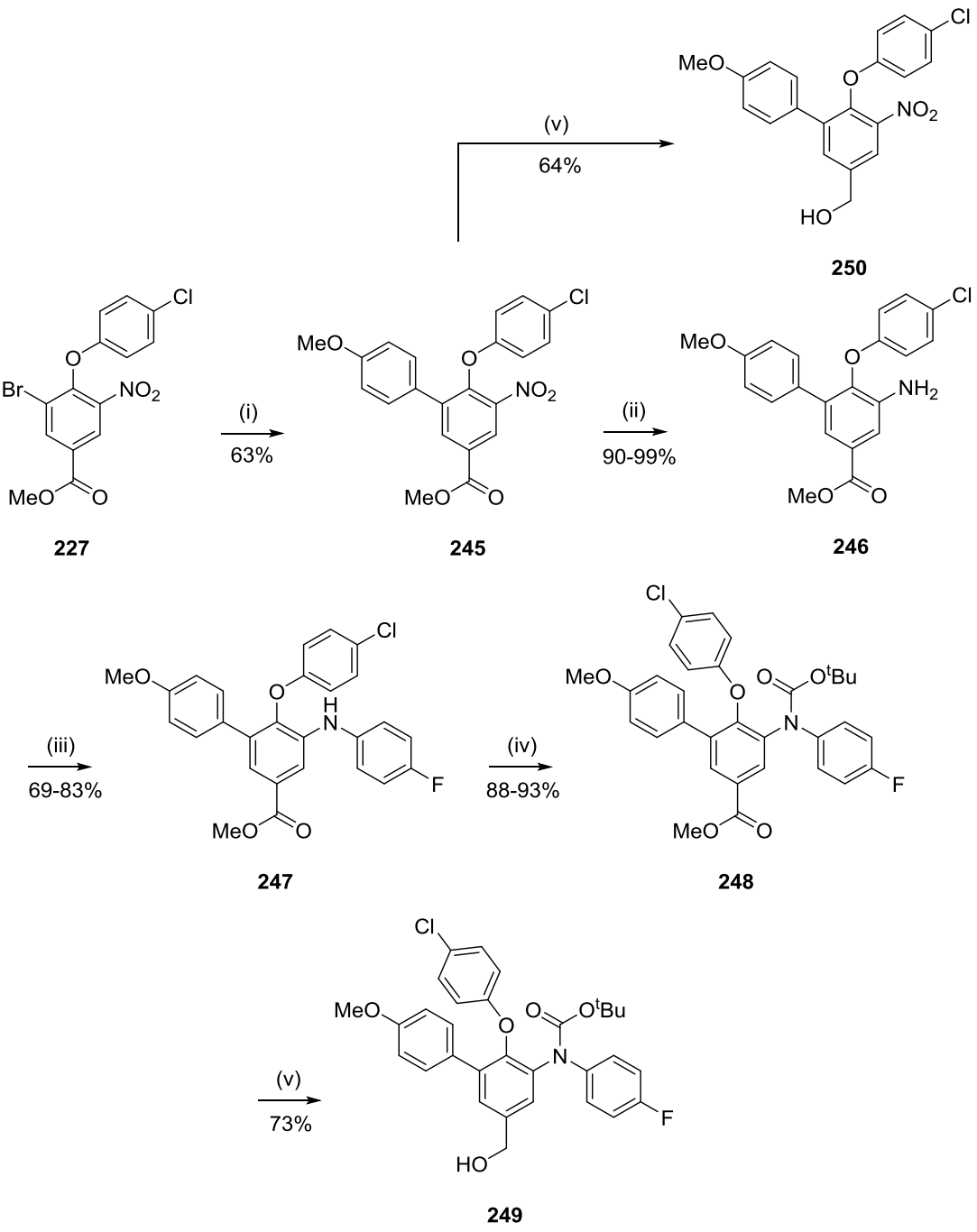

Scheme 91: (i) 4-Methoxybenzeneboronic acid, $Pd(dtbpf)Cl_2$, Na_2CO_3, 1,2-DME, 120 ^oC, MW, 20 min; (ii) Zn, AcOH, RT 1 h; (iii) 1-bromo-4-fluorobenzene, Pd_2dba_3, XPhos, K_2CO_3, MeCN, 120 ^oC, MW, 3 h; (iv) Boc_2O, DMAP, MeCN, 50 ^oC, 3 h; (v) DIBAL-H, THF, -78-0 ^oC, 4 h

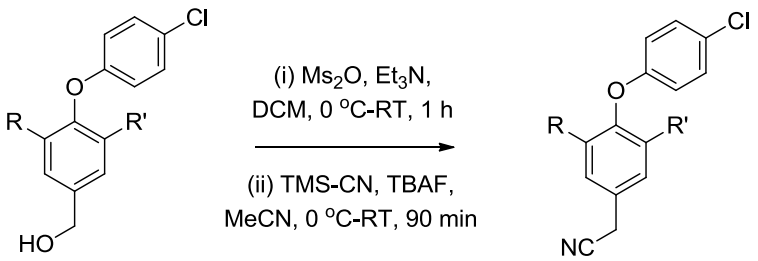

Table 49: Mesylation and cyanation on alcohols **249** and **250**

Alcohol	R	R'	Nitrile	Yield (%)[a]
249	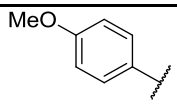	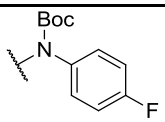	**249a**	4.3
250	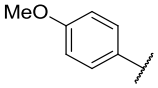	NO_2	**250a**	21

(a) Isolated yield

The bromo and nitro substituents were not responsible for the low yields recorded for the cyanation of mesylate **233**, as the mesylation and cyanation of alcohols **249** and **250** gave even poorer yields of their respective nitriles **249a** and **250a**.

5.3.3.2 Carboxylic Acid Regioisomers of 226

It was of interest to explore attaching the carboxy group of **226** at different positions on the benzenoid scaffold to determine if one of the regioisomers afforded the same enhancement in activity seen in the pyrrole series (*cf.* Table 45). Synthesis of the 1,2,3,4-tetrasubstituted compound **258** started from aryl bromide **139**. Reduction of the nitro group and Boc-protection of the aniline would give a directed *ortho* metalation (DoM) group (**253**) allowing for insertion of the carboxy group at the 4-position of the benzenoid scaffold (**254**) (**Scheme 92**).[153]

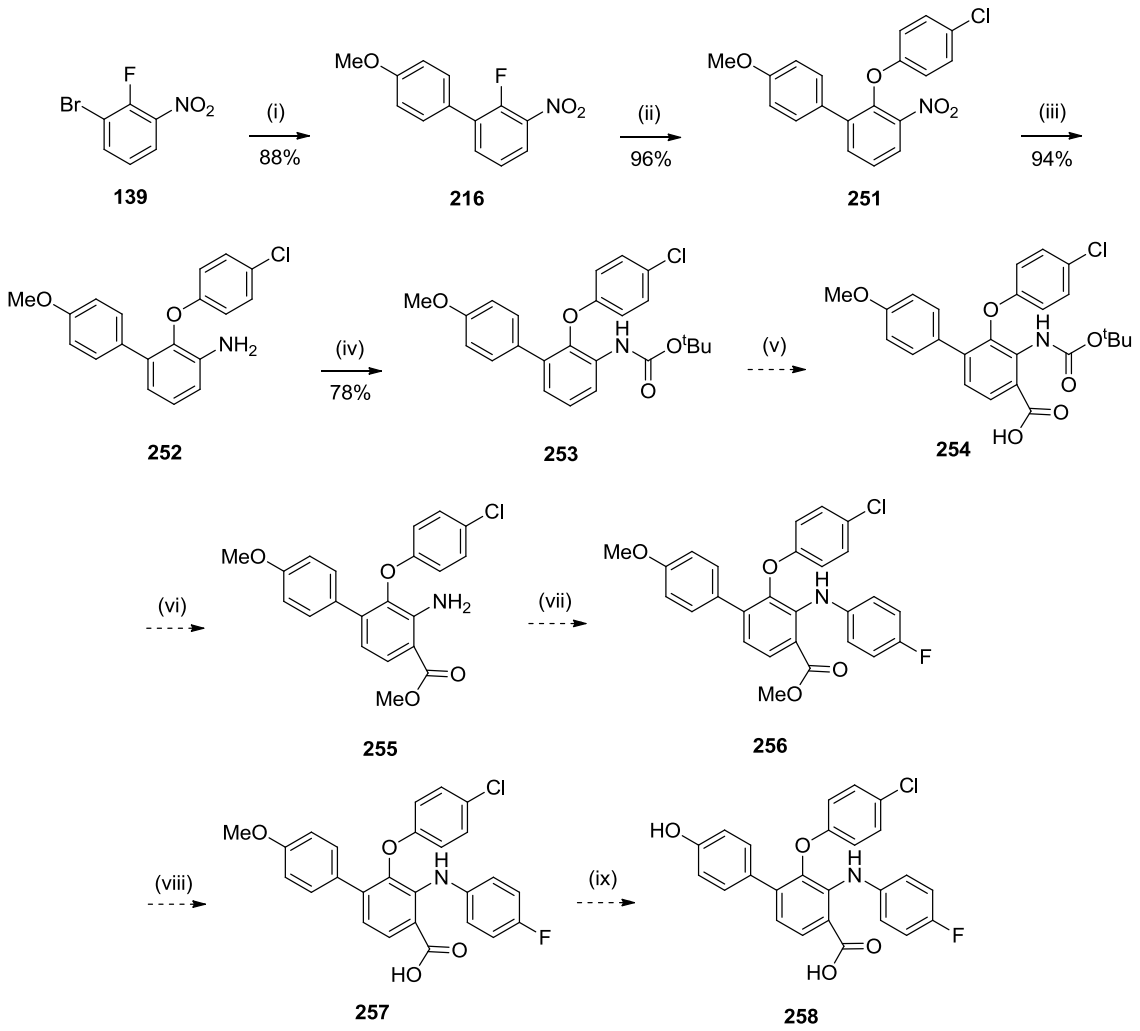

Scheme 92: (i) 4-Methoxybenzeneboronic acid, $Pd(dtbpf)Cl_2$, Na_2CO_3, 1,2-DME, 120 ^oC, MW, 1 h; (ii) 4-chlorophenol, K_2CO_3, MeCN, 90 ^oC, MW, 1 h; (iii) $SnCl_2.2H_2O$, EtOH, 70 ^oC, 30 min; (iv) Boc_2O, DMAP, MeCN, 50 ^oC, 3 h; NaOH, 33% THF, MeOH, RT, 1 h; (v) organolithium base; $CO_{2(s)}$; (vi) mineral acid, MeOH; (vii) 1-bromo-4-fluorobenzene, Pd_2dba_3, XPhos, K_2CO_3, MeCN, 120 ^oC, MW; (viii) $LiOH.H_2O$, 50% THF, H_2O, 60 ^oC; (ix) BBr_3, DCM, 0 ^oC

Suzuki coupling of **139** with 4-methoxybenzeneboronic acid gave **216** in 88% yield. Nucleophilic aromatic substitution and tin-mediated nitro reduction also proceeded in high yields to obtain aniline **252**. The nitro reduction was later found to give similarly high yields when conducted in the presence of zinc powder in glacial acetic acid. Boc-protection using excess Boc_2O and catalytic DMAP gave only the di-Boc-protected species **259** in 71% yield. However, it was later found that this compound could be converted to the desired mono-Boc-protected compound **253** by treatment with sodium hydroxide. Subsequent repeats of this synthesis deliberately allowed formation of di-

Boc-protected aniline **259** before mixing the crude material with sodium hydroxide to give **253** in 78% overall yield (**Scheme 93**).

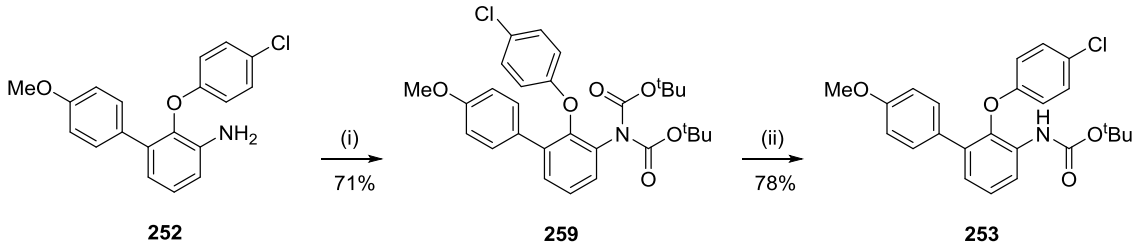

Scheme 93: (i) Boc_2O, DMAP, MeCN, 50 °C, 3 h; (ii) NaOH, 33% THF, MeOH, RT, 1 h

Treating **253** with *n*-BuLi and *N,N,N',N'*-tetramethylethylenediamine (TMEDA) at -78 °C for 2 h, followed by quenching with solid CO_2 gave a 1:3 mixture of **254** and **253**. However, deprotonation with *n*-BuLi and TMEDA at 0 °C, or using *sec*-BuLi in place of *n*-BuLi gave superior conversion to **254** (**Table 50**). Due to time constraints, full completion of the synthesis of **258** could not be achieved.

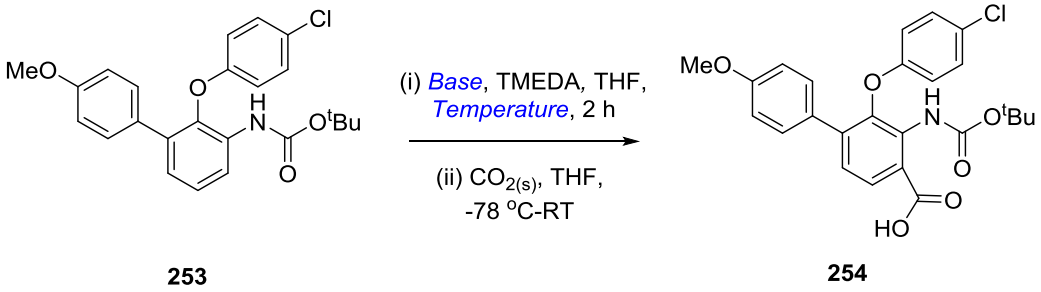

Table 50: Optimisation of the DoM reaction with carbamate **253**[a]

Entry	Base	Step (i) Temp. (°C)	253:254 Ratio[b]
1	*n*-BuLi[c]	-78	3:1
2	*n*-BuLi[c]	0	1:7
3	*sec*-BuLi[d]	-78	1:7

(a) **253** (30 mg, 1.0 equiv.), TMEDA (2.1 equiv.) and solid CO_2 (excess) at 0.1 M; (b) LC-MS UV trace; (c) 2.5 M in hexanes; (d) 1.4 M in cyclohexane

5.4 The 2,4-Disubstituted Thiazole MDMX Inhibitors

Preliminary SAR studies on the thiazole-based MDMX inhibitors had already been conducted at Newcastle University (E. Bulatov, MPhil 2009-10).[114] Thiazole **44j** displayed single-digit micromolar activity against MDMX and MDM2 in an ELISA. The fact that the 5-position of the thiazole scaffold had never been investigated in SAR studies meant that superior potency against MDMX could potentially be achieved. It had also been shown in the benzenoid series that truncation of the amino substituent increased MDMX potency 4-fold and MDM2 potency 6-fold (*cf.* Table 31, **138a** *vs.* **138c**). It was therefore of interest to investigate whether truncation of the 4-fluorobenzylamino group in **44j** and the corresponding phenol **44c** would improve target activity. Thiazole **44r** was synthesised by heating 2-bromo-4'-hydroxyacetophenone (**260**) and 4-fluorophenylthiourea (**261**) in ethanol (**Scheme 94**).

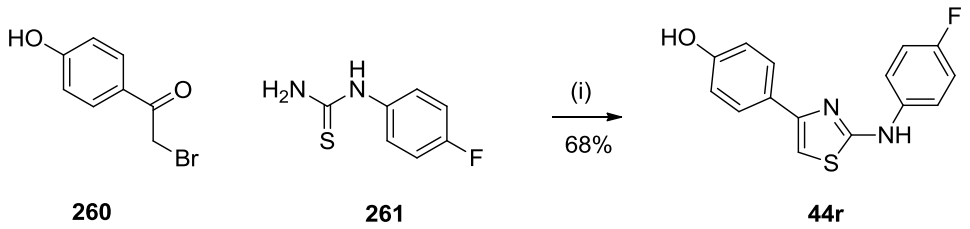

260 **261** **44r**

Scheme 94: (i) EtOH, 70 ^{o}C, MW, 5 min

Thiazole **44s** was synthesised from 4-aminoacetophenone (**262**). Sulfonation with Tf_2O gave trifluoromethylsulfonamide **263**. Bromination of the α-carbon using pyridinium tribromide in acetic acid gave a 7:3 mixture of bromoketone **264** and di-bromoketone **265** (^{1}H NMR analysis). Irradiation of this mixture with **261** gave thiazole **44s** in 37% yield, with the di-bromoketone **265** not participating in the reaction (**Scheme 95**).

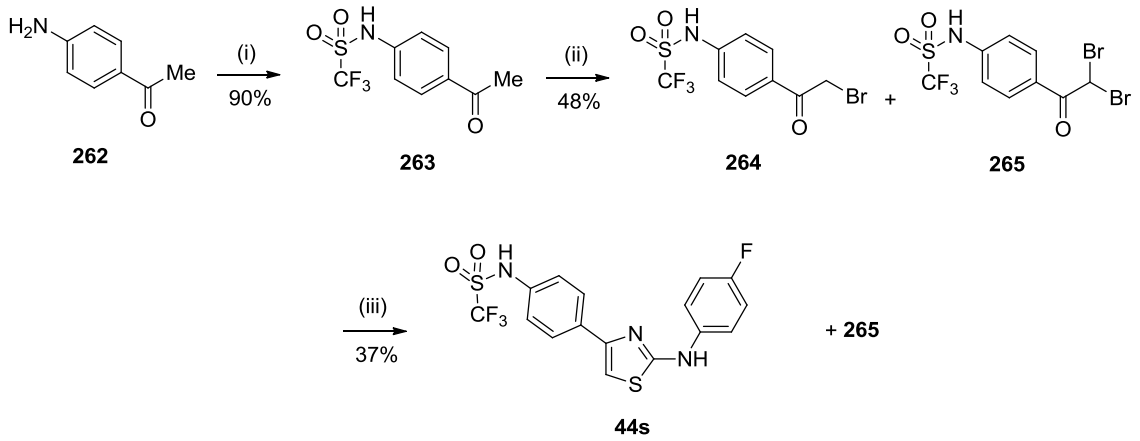

Scheme 95: (i) Tf_2O, $^{i}Pr_2NEt$, DCM, 0 ^{o}C-RT, 5 h; 3M NaOH, H_2O (1:3), RT, o/n; (ii) pyridinium tribromide, AcOH, RT, 2 h; (iii) **261**, EtOH, 70 ^{o}C, MW, 15 min

Only phenol, catechol and trifluoromethylsulfonamide analogues had demonstrated activity against MDMX or MDM2. Indazoles have been used as bioisosteres for phenols and catechols, giving similar or greater potency against a biological target while also being more stable towards metabolism.[154]

Starting from 2-amino-5-bromo-1,3-thiazole hydrobromide (**266**), coupling with 4-fluorobenzoyl chloride in DCM gave amide **267** in 36% yield. Using THF in place of DCM resulted in a much slower reaction and using DMF generated multiple impurities. Acetonitrile gave rapid conversion, generated fewer impurities, and afforded amide **267** in 92% yield following quenching with methanolic sodium hydroxide (**Table 51**).

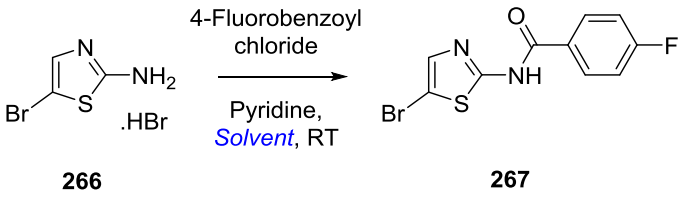

Table 51: Optimisation of the coupling of thiazole **266** with 4-fluorobenzoyl chloride[a]

Entry	Solvent	Results
1	DCM	**267** isolated, 36% yield
2	THF	Slow, incomplete reaction
3	DMF	Multiple impurities generated
4	MeCN	**267** isolated, 92% yield.

(a) **266** (50 mg, 1.0 equiv.), 4-fluorobenzoyl chloride (1.5 equiv.) and pyridine (3.0 equiv.) at 0.3 M

Following the procedure described by Stanetty, amide **267** was converted to the 4-bromo regioisomer **268** upon treatment with LDA in a halogen 'dance' (HD) reaction.[155] The mechanism of the HD reaction is shown in **Scheme 96**. Following deprotonation of the amide NH by one equivalent of strong base to give **267a**, a second equivalent deprotonates at the 4-position of the thiazole to give di-lithiated species **267b**, which can undergo halogen-lithium exchange with another **267a**. This generates a mixture of *des*-bromothiazole **269a** and 4,5-dibromothiazole **270a**. These two species can react with each other to generate a mixture of the starting thiazole **267b** and the desired 4-bromothiazole **268a**. Depending on when the reaction is quenched, four products can potentially be isolated: (**267**, **268**, **269** and **270**).[155, 156]

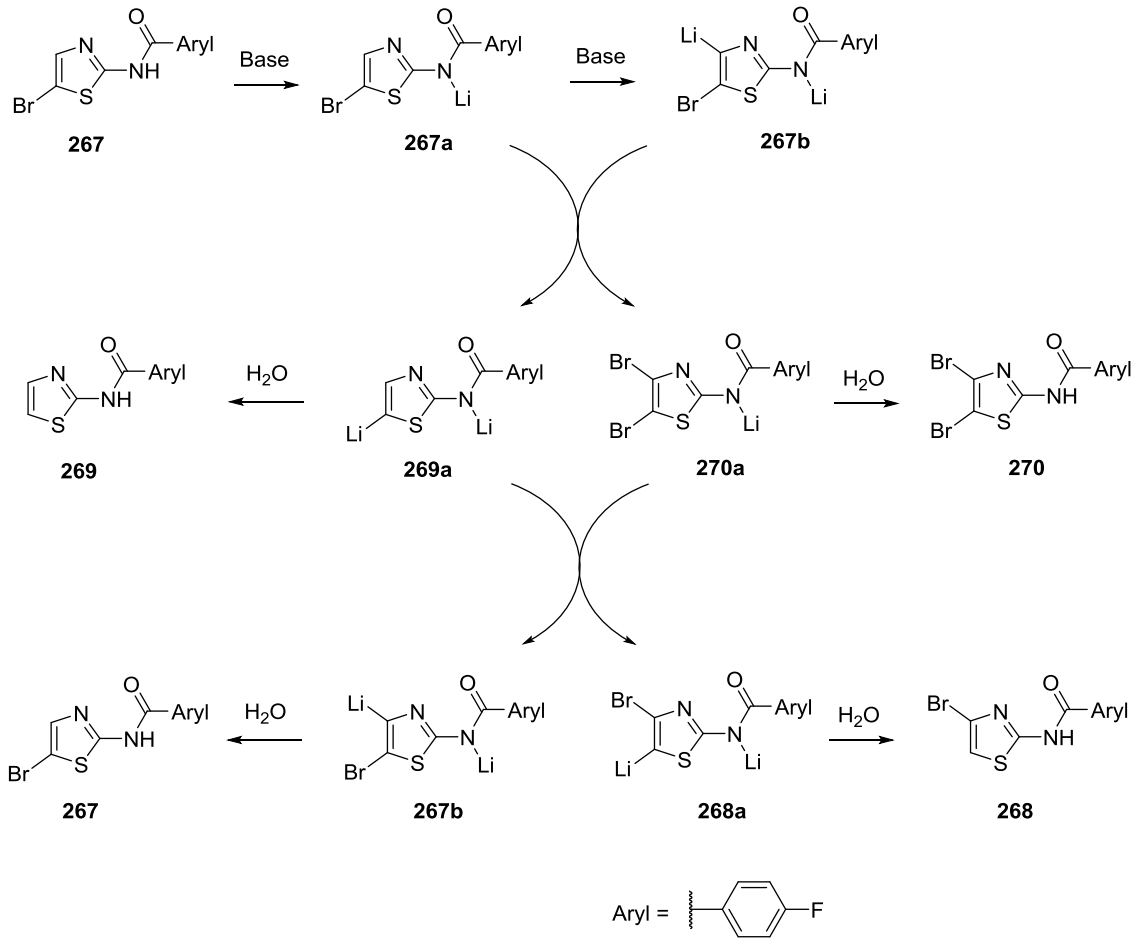

Scheme 96: Mechanism of the HD reaction on 2-aminothiazoles[155, 156]

The HD reaction could also allow for addition of various groups to the 5-position of the thiazole scaffold by replacing water as the quenching agent with electrophilic species, e.g. haloalkanes or aldehydes.[155]

5-Bromo-1*H*-indazole (**271**) was coupled with $B_2(pin)_2$ in the presence of Pd(dppf)Cl_2.DCM to give **272**. Suzuki coupling of **272** with thiazole **268** resulted in no conversion; however, protection of **272** with 3,4-dihydro-2*H*-pyran (DHP), followed by Suzuki coupling with **268**, gave thiazole **274** in 78% yield. Following THP deprotection to give indazole **275**, attempts to reduce the amide with lithium aluminium hydride were hindered by the insolubility of **275** in organic solvents (**Scheme 97**).

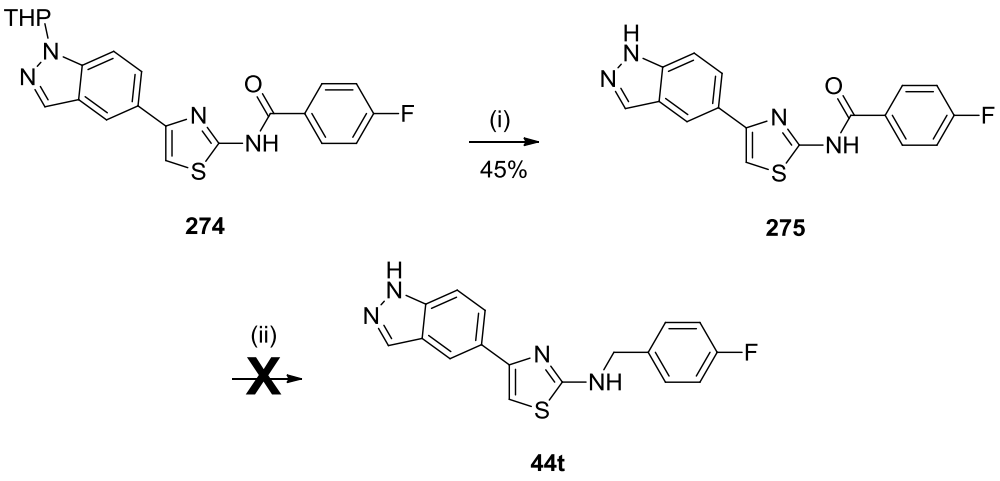

Scheme 97: (i) 1 M HCl, MeOH, 50 ^{o}C, o/n; (ii) $LiAlH_4$, THF, 0-60 ^{o}C, 24 h

Reduction of indazole **274** with lithium aluminium hydride gave **276**. This intermediate had greater organic solubility than **275** and the THP ring was removed in dilute HCl, yielding indazole **44t** (**Scheme 98**), which was analysed by ELISA against MDMX and MDM2 (**Table 52**).

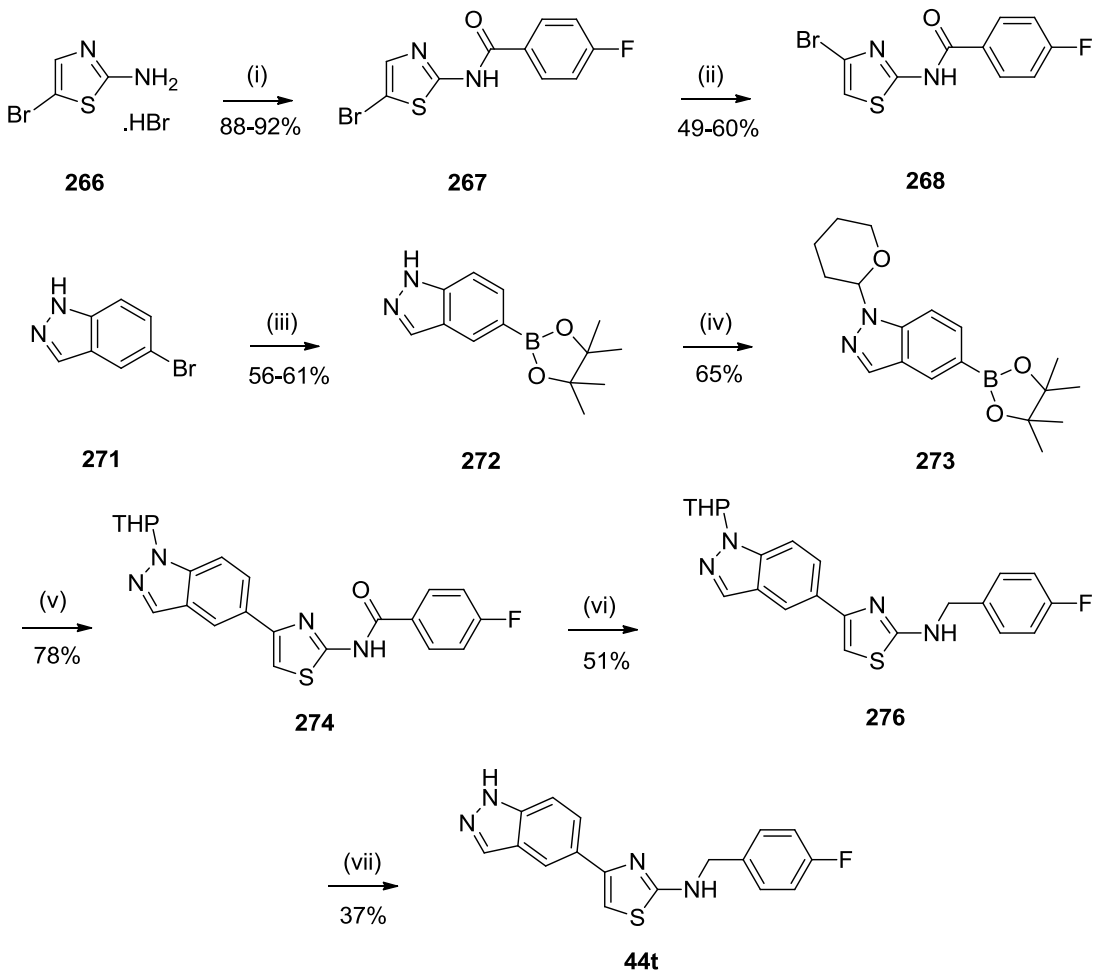

Scheme 98: (i) 4-Fluorobenzoyl chloride, pyridine, MeCN, RT, 1 h; (ii) $^{i}Pr_2NH$, *n*-BuLi, THF, -78-0 ^{o}C, 30 min; H_2O, 0 ^{o}C-RT, o/n; (iii) $B_2(pin)_2$, $Pd(dppf)Cl_2$.DCM, KOAc, DMF, 90 ^{o}C, 15 h; (iv) DHP, *p*TSA, DCM, RT, 2 h; (v) **268**, $Pd(dtbpf)Cl_2$, Na_2CO_3, 1,2-DME, 120 ^{o}C, MW, 40 min; (vi) $LiAlH_4$, THF, 0-60 ^{o}C, 24 h; (vii) 1 M HCl, MeOH, 50 ^{o}C, o/n

Table 52: ELISA data for thiazoles **44r**-**44t and 276** (conducted by Dr Yan Zhao at the NICR)

ID	Structure	MDMX IC_{50} (μM)[a]	MDM2 IC_{50} (μM)[a]	Ratio (MDMX : MDM2)	LE[b]	LipE[b,d]
44r	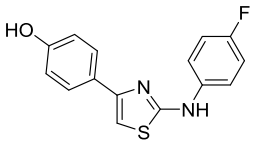	52.7	8.30	0.16	0.293	+ 0.60
44s	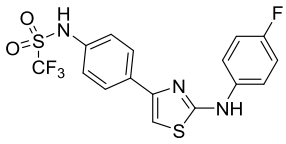	16.7	21.3	1.28	0.242	+ 0.09
44t	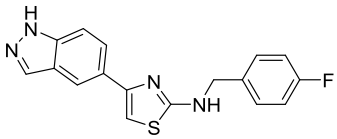	64.0	34.4%[c]	-	0.248	+ 1.59
276	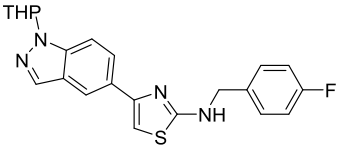	90.0	38.6%[c]	-	0.185	- 0.49

(a) n = 1; (b) With respect to MDMX; (c) 200 μM; (d) LipE = pIC_{50} – $clogD_{7.4}$ (clogD values from StarDrop)

Truncation of the amino substituent (**44r** and **44s**) did not enhance MDMX or MDM2 activity over the corresponding truncated benzenoid compounds (*cf.* Table 31, **138c**). Compound **44s** had 3-fold weaker MDMX activity and 2-fold weaker MDM2 activity compared to the homologated derivative (*cf.* Table 20, **44j**). Thiazole **44r** was equipotent against MDMX and 2-fold more active against MDM2 than the homologated analogue (*cf.* Table 20, **44c**) and was one of the most ligand efficient compounds synthesised. Indazole **44t** had equivalent MDMX activity to **44c**, meaning the indazole was a suitable isosteric replacement for the phenol against MDMX. However, indazoles **44t** and **276** were inactive against MDM2. Due to its relatively high MDMX and MDM2 potency and low $cLogD_{7.4}$ (+ 3.07), compound **44j** was selected for co-crystallisation trials with MDMX and MDM2 (*cf.* Chapter 6.1). 4-Fluorobenzylamine (**277**) was reacted with benzoyl isothiocyanate, giving full conversion to **278** and cleavage with potassium carbonate gave *N*-(4-fluorobenzyl)thiourea (**279**). Cyclisation with α-bromoketone **264** (*cf.* Scheme 95) gave **44j** (**Scheme 99**).

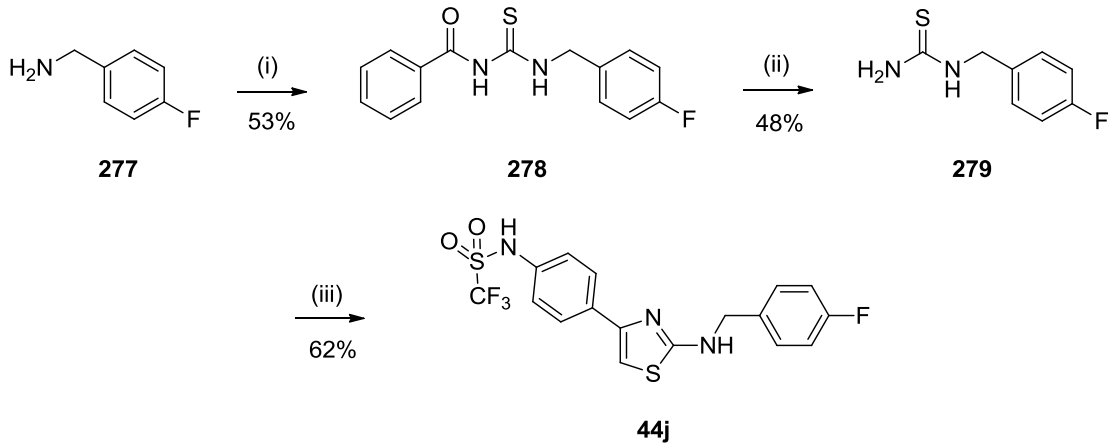

Scheme 99: (i) Benzoyl isothiocyanate, DCM, 0 ^{o}C-RT, 1 h; (ii) K_2CO_3, MeOH, RT, o/n; (iii) **264**, EtOH, 70 ^{o}C, MW, 30 min

5.5 The 1,2,3,5-Tetrasubstituted Pyrrole MDMX Inhibitors

The pyrrole series had produced some of the most potent MDMX inhibitors.[107] However, a significant drawback of the pyrrole compounds was their low solubility in both aqueous and organic solvents. The presence of a barbituric or thiobarbituric acid ring increased compound lipophilicity and previous attempts to remove the ring (e.g. by replacement with malonamide derivatives) had resulted in a loss of activity against both targets. Subsequent analysis (S. Adhikari, PhD 2012-15) had found that insertion of a methylene linker between the pyrrole scaffold and the 2-phenyl ring granted increased organic solubility. Compounds with a methylene linker were less active against MDMX and MDM2 than the corresponding truncated compounds. However, the barbituric acid ring could be replaced with a carboxy group (**220c**), giving compounds of similar activity to the most active compounds in the benzenoid and thiazole series (**Table 53**).

Table 53: ELISA data for pyrroles **220a-220f**[a] (conducted by Dr Yan Zhao at the NICR)

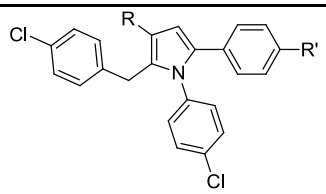

ID	R	R'	MDMX IC_{50} (μM)	MDM2 IC_{50} (μM)	Ratio (MDMX : MDM2)	LE[e]	LipE[e,g]
220a	H	F	198[b]	38.3%[b,f]	-	0.188	- 3.33
220b	CO_2Me	F	189[b]	24.8%[b,f]	-	0.165	- 3.19
220c	CO_2H	F	14.6[d]	11.2[c]	0.77	0.221	+ 1.47
220d	CH_2OH	F	49.5%[b,f]	17.1%[b,f]	-	-	-
220e	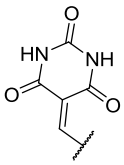	F	4.51[b]	3.54[b]	0.78	0.198	+ 0.36
220f	CO_2H	H	7.88[b]	14.7[b]	1.87	0.241	+ 1.70

(a) Synthesised by S. Adhikari; (b) *n* = 1; (c) *n* = 2; (d) *n* = 3; (e) With respect to MDMX; (f) 200 μM; (g) LipE = $pIC_{50} - clogD_{7.4}$ (clogD values from StarDrop)

1,2,5-Trisubstituted pyrroles were inactive against MDMX or MDM2 (**220a**). However, incorporation of a carboxy group at the 3-position (**220c**) enhanced potency against both proteins, similar to that obtained with the barbituric acid (**220e**). The fact that methyl ester **220b** was inactive highlighted the importance of the carboxy group, suggesting that this group was making a favourable interaction with the protein. Alcohol **220d** also had no potency against either protein, suggesting that the acidity of **220c** was significant, hinting that the carboxy group may be positioned in a predominantly basic region of the protein. Removal of the fluoro substituent (**220f**) doubled MDMX activity compared to **220c**, giving one of the most ligand efficient compounds in this series.

5.5.1 Synthesis of 220c and Regioisomer 220g

4-Chlorophenylacetyl chloride (**280**) was reacted with Meldrum's acid, followed by treatment with ethanol to give β-ketoester **281**. Deprotonation of **281** with sodium hydride followed by addition of 2'-bromo-4-fluoroacetophenone gave 1,4-diketone **282a**. Paal-Knorr condensation of **282a** with 4-chloroaniline in acetic acid afforded pyrrole **283a**, which was hydrolysed using aqueous sodium hydroxide to give **220c** (**Scheme 100**).

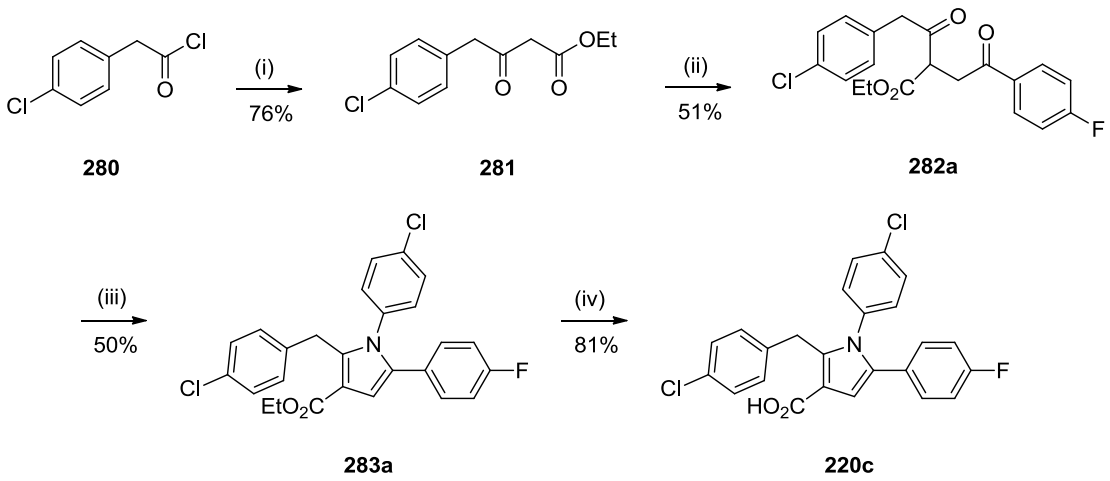

Scheme 100: (i) Meldrum's acid, pyridine, DCM, 0 ^{o}C-RT, 4 h; EtOH, 100 ^{o}C, 2 h; (ii) NaH, THF, 0 ^{o}C, 20 min; 2'-bromo-4-fluoroacetophenone, THF, 0 ^{o}C-RT, 3 h; (iii) 4-chloroaniline, AcOH, 170 ^{o}C, MW, 12 min; (iv) NaOH, 75% MeOH, H_2O, 90 ^{o}C, 3 h

It was also of interest to determine whether placing the carboxy group at the 4-position of the pyrrole scaffold would improve activity. Starting from acid chloride **280**, reaction with a mixture of MeLi and CuI gave ketone **284** quantitatively. Bromination of **284** was complicated by the fact that two different α-carbons could potentially be brominated. Following the procedure described by Lee, bromination of ketone **284** using an excess of NBS in acetonitrile generated a mixture of **285** and **286** (^{1}H NMR analysis), with **285** being the major product.[157] ^{1}H NMR analysis also showed that some starting material had been dibrominated to 1,3-dibromoketone **287**. Subsequent heating with additional NBS led to full consumption of **285** and **286** to give a 3:1 ratio of **287** and 1,3,3-tribrominated ketone **288**. Following the procedure described by Choi, treatment of the crude material with hydrobromic acid and acetone gave **286** in 49-55% yield (**Scheme 101**).[158]

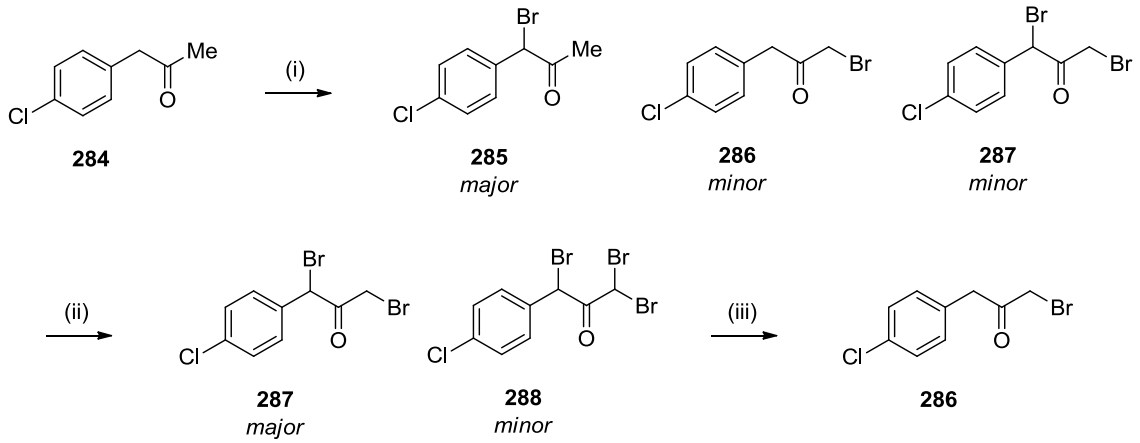

Scheme 101: Non-selective bromination of ketone **284**,[157] followed by selective de-bromination to give α-bromoketone **286**.[158] (i) NBS (2.2 equiv.), *p*TSA, MeCN, 100 ^{o}C, o/n; (ii) NBS (1.0 equiv.), *p*TSA, MeCN, 100 ^{o}C, 1 h; (iii) Me_2CO, AcOH, 45% HBr in AcOH, RT, o/n

Bromoketone **286** was reacted with ethyl 3-(4-fluorophenyl)-3-oxopropanoate in the presence of sodium hydride to give 1,4-diketone **282b**. Paal-Knorr condensation of the latter with 4-chloroaniline gave **283b**, which was hydrolysed with sodium hydroxide to give pyrrole **220g** (**Scheme 102**). Pyrroles **283b** and **220g** were analysed using a HTRF assay (*cf*. Chapter 6.2).

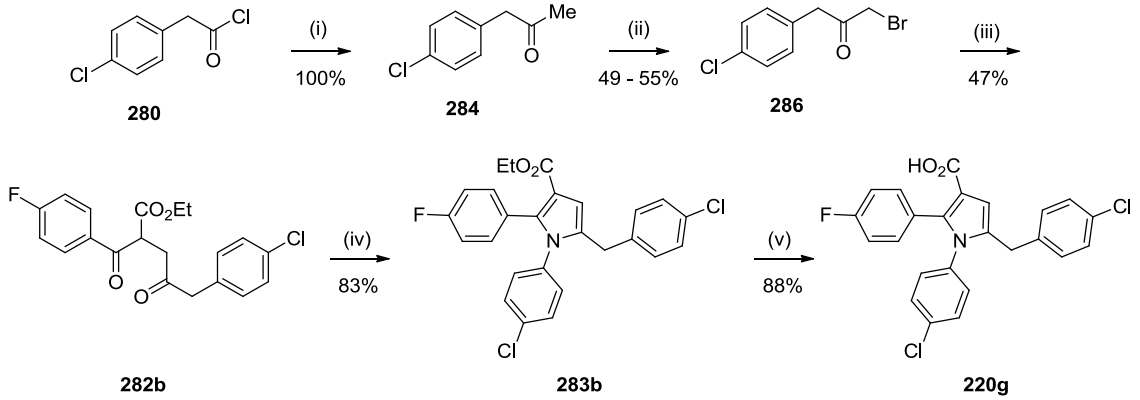

Scheme 102: (i) MeLi, CuI, Et_2O, 0 to -78 ^{o}C, 45 min; (ii) NBS, *p*TSA, MeCN, 100 ^{o}C, 3 h; Me_2CO, AcOH, 45% HBr in AcOH, RT, o/n; (iii) ethyl 3-(4-fluorophenyl)-3-oxopropanoate, NaH, THF, 0 ^{o}C-RT, 8 h; (iv) 4-chloroaniline, AcOH, 170 ^{o}C, MW, 12 min; (v) NaOH, 75% MeOH, H_2O, 90 ^{o}C, 3 h

5.6 Conclusion

Several 1,3-disubstituted benzenoid compounds (**118a-118d** and **118f-118o**) were synthesised and MDMX and MDM2 inhibitory activity was confirmed using an ELISA. The majority of the active compounds had similar activity to the corresponding thiazole-based derivatives, and in both series, only compounds possessing acidic hydrogen bond donating functionalities, e.g. phenols or trifluoromethylsulfonamides, were active against MDMX or MDM2. 1,3-Disubstituted pyridyl scaffolds were considerably less active than the corresponding benzenoid compounds. Introduction of a 2-(4-chlorophenoxy) substituent in the benzenoid series was tolerated against MDMX and MDM2, with truncation of the 4-fluorobenzyl substituent enhancing potency against both proteins (Table 31, **138a** *vs.***138c**).

Substitution by methyl or chloro at the 2-position of the 4-fluorophenyl ring abrogated activity against both proteins but substitution by the same groups at the 2-position of the 4-hydroxyphenyl ring of **138c** was tolerated (**138k** and **138l**). The fluoro and hydroxy groups of **138c** could be interchanged without compromising activity against either target, suggesting the compounds could adopt alternative binding modes (**138o**). The 4-hydroxyphenyl ring of **138c** could be replaced with a 3-hydroxyisoxazole (**183a**), 3-hydroxypyrazole (**183b**) or 1,2,3-triazole (**185**) and retain potency. Attempts to replace the 4-chlorophenoxy group of **138c** with a 6-chloroindol-3-yl ring were unsuccessful, but did achieve the first documented example of an S_NAr reaction using a 3-lithioindole to synthesise **211**. Addition of small functionalities, e.g. a carboxy group, to the 5-position of the benzenoid scaffold was tolerated against MDMX and MDM2. However, attempts to measure the activity of the homologated derivative (**244**) using an HTRF assay gave inconclusive results. Addition of small functionalities to the 4-position of the benzenoid scaffold in place of the 5-position is ongoing.

In the thiazole series, truncation of the 4-fluorobenzyl substituent did not achieve the increase in target potency observed in the benzenoid series. The 4-hydroxyphenyl ring of **44c** could be substituted by an indazole (**44t**) without compromising activity against MDMX or MDM2. In the pyrrole series, compounds **220c** and **220g** were synthesised regioselectively. Pyrrole **220c** had already been analysed using an ELISA; however, attempts to evaluate the potency of **220g** using an HTRF assay gave inconclusive results, possibly due to the poor solubility of **220g**.

Chapter Six: MDMX and MDM2 Structural Biology

6.1 Protein Crystallography of Benzenoid and Thiazole-based Inhibitors of MDMX and MDM2

Crystal structures of MDMX have been reported where the protein is interacting with various substrates, including p53 (**Figure 53**)[100] and imidazole-based small molecules,[104, 106] but no crystal structure was available for any small-molecule Newcastle inhibitor bound to MDMX.

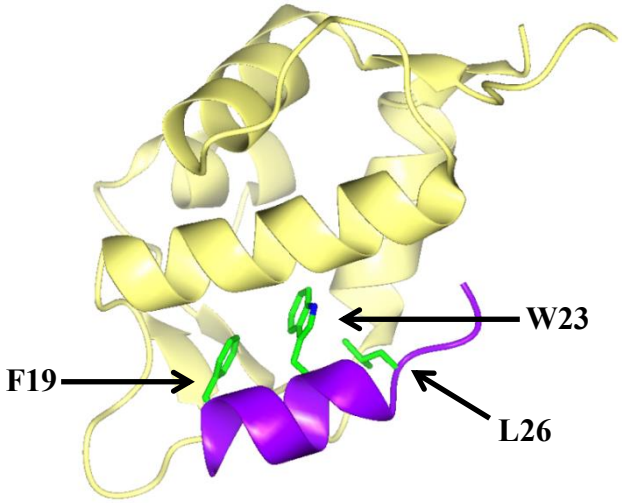

Figure 53: X-ray structure of MDMX (yellow) bound to p53 (purple). The p53 residues F19, W23 and L26 are highlighted (green). Image created using COOT with CCP4mg plug-in (resolution, 1.9 Å; PDB: 3DAB).[100]

MDMX is a 490-amino acid protein with an overall 34.0% sequence identity to MDM2.[159] At the N-terminal end of both proteins is the p53-binding domain, which is the most conserved region, at 53.6% sequence identity. The Really Interesting New Gene (RING) domain is located at the C-terminus and is essential for heterodimerisation between MDMX and MDM2, sharing 53.2% sequence identity between the two proteins. The C-terminus also contains the nucleolar localisation signal (NoLS), which encodes the ability of the protein to localise to the nucleolus (**Figure 54**).

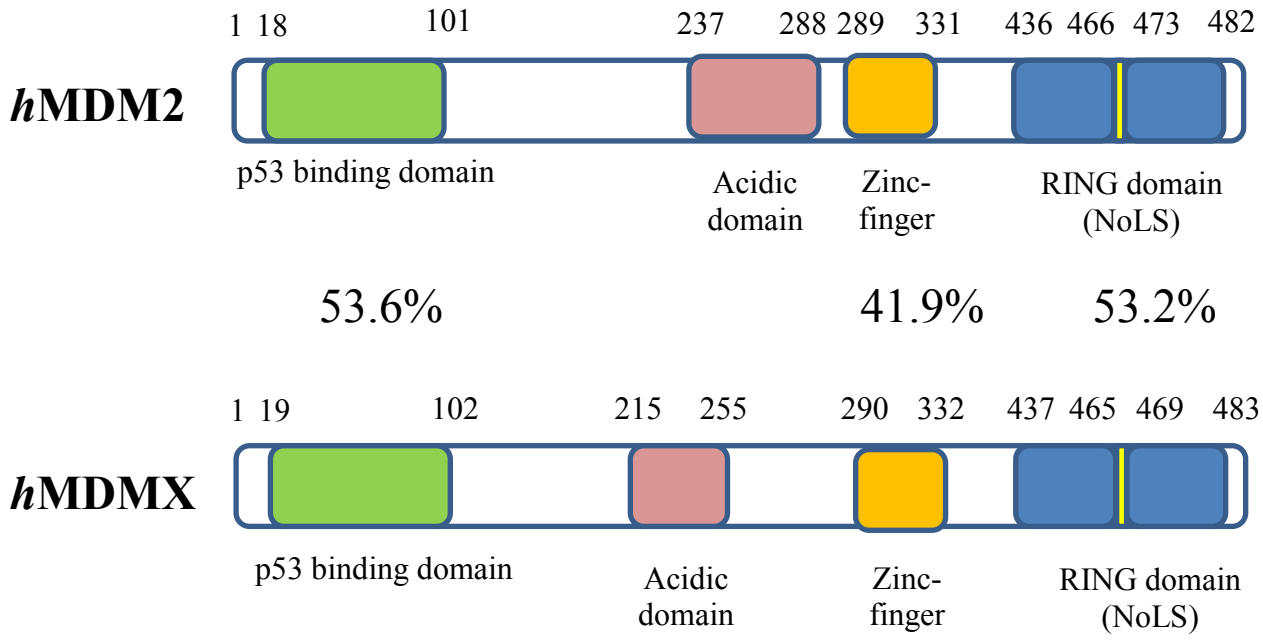

Figure 54: The primary sequence of *h*MDM2 and *h*MDMX. The numbers along the top of the proteins show the lengths of key domains and the percentages refer to sequence identity of the regions they are situated between.[160]

Crystal structures of MDM2 with various substrates have also been obtained, including p53[95] and several members of the isoindolinone series developed at Newcastle.[159] Co-crystals of isoindolinones with MDM2 were difficult to acquire, as usually compounds need to have high binding affinity to stabilise the protein sufficiently for crystallisation to occur.[159] However, compound WK298 (**51**), an MDM2 inhibitor with only moderate potency against MDMX, was successfully crystallised with MDMX (**Figure 55**),[106] suggesting that MDMX may be more amenable to crystallisation.

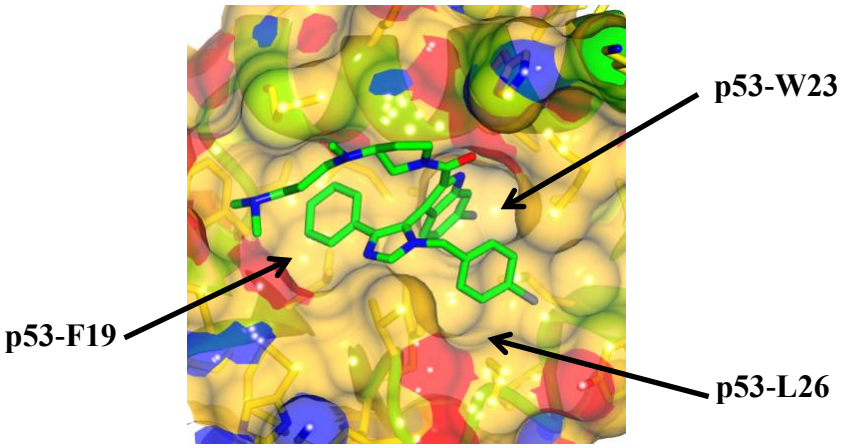

Figure 55: Crystal structure of **51** (green) in the p53 binding domain of MDMX (yellow). The p53 binding subpockets F19, W23 and L26 are highlighted. Image modified using CCP4mg (resolution, 1.5 Å; PDB code: 3LBJ)[106]

To guide rational drug design, a co-crystal of a small molecule in either the benzenoid, thiazole or pyrrole series with MDMX was necessary and a two-month placement in the structural biology laboratories at Newcastle University aimed to achieve this. Five compounds from the benzenoid and thiazole series were selected for co-crystallisation trials (**Table 54**). Compounds were selected based on having moderate MDMX inhibitory activity in the ELISA, a low clog$D_{7.4}$ and structural diversity.

Table 54: Benzenoid and thiazole-based inhibitors selected for co-crystallisation trials with MDMX and MDM2

ID	Structure	MDMX IC_{50} (μM)	MDM2 IC_{50} (μM)	Ratio (MDMX : MDM2)	$clogD_{7.4}$[d]
44j	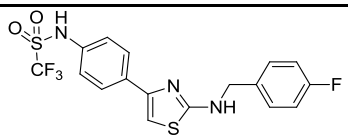	5.75[b]	11.3[b]	1.97	+ 3.07
118c	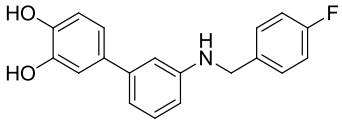	64.7[a]	35.0[a]	0.54	+ 2.04
185	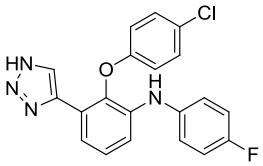	29.1[a]	39.3[a]	1.35	+ 4.52
226	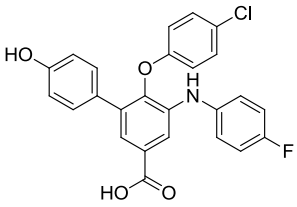	29.1[a]	3.23[b]	0.11	+ 2.69
244	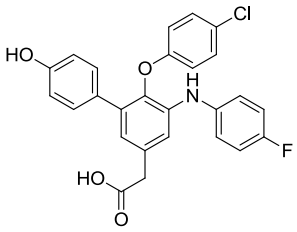	Unknown[c]	Unknown[c]	-	+ 2.79

(a) $n = 1$; (b) $n = 2$; (c) Not tested in ELISA; (d) Values from StarDrop

The most active thiazole-based MDMX inhibitor was selected (**44j**) as more potent compounds are generally more likely to crystallise with their target protein. From the benzenoid series, a mixture of di-, tri- and tetra-substituted compounds were selected. Despite not being analysed by ELISA, compound **244** was selected due to its relatively low $clogD_{7.4}$ value and its structural similarity to compound **226**, for which an ELISA value had been measured.

6.1.1 Expression and Purification of MDMX and MDM2

Co-crystallisation had been achieved with MDM2 and isoindolinone-based inhibitors[159] so MDM2 was also expressed and purified as a control. Conditions that had been previously used to crystallise isoindolinones with MDM2 were also tested to determine whether they would be as effective at crystallising a benzenoid or thiazole-based compound with MDMX. Three MDM2 and MDMX constructs were selected for co-crystallisation trials, each encompassing the p53-binding domain. Constructs were selected based on previous knowledge of their ease of expression and handling and success at crystallising compounds reported in the literature (**Table 55**).

Table 55: Constructs of MDMX and MDM2 used for co-crystallisation trials

Protein	Construct	Amino acid range	Mutations
MDMX	1	18-111	-
MDMX	2	22-111	-
MDMX	3	26-111	-
MDM2	1	17-125	K51A
MDM2	2	17-109	E69A/K70A
MDM2	3	17-125	E69A/K70A

Recombinant MDMX and MDM2 constructs were expressed in *E. coli* Rosetta(DE3)pLys S and BL21(DE3) pLys S strains, respectively, by insertion of the pre-cloned DNA coding for each construct into the pGEX-6P-1 vector (**Figure 56**).

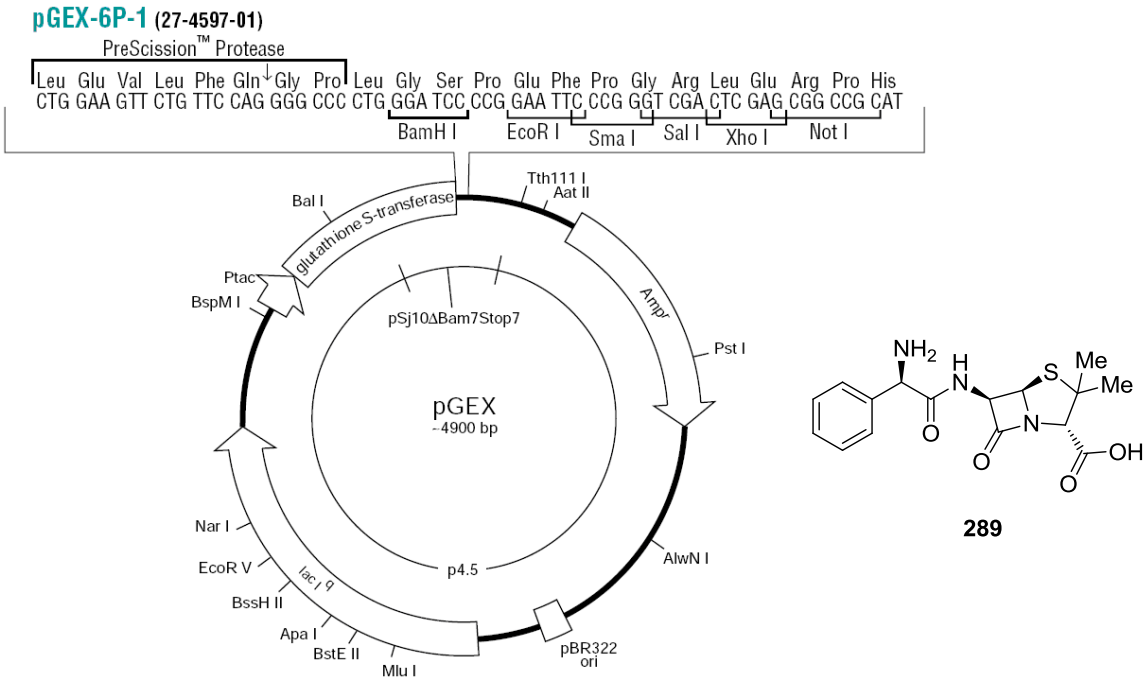

Figure 56: The pGEX-6P-1 expression vector, showing the genes for ampicillin (**289**) resistance (Amp^{r}), the GST protein tag (glutathione S-transferase), the cleavage codon (PreScission^{TM} Protease) and the *lac* operon (lac I ^{q})[161]

The pGEX-6P-1 plasmid contains a series of genes essential for targeted protein expression. In addition to a gene conferring its resistance to ampicillin (**289**), the plasmid also possesses genes encoding for a glutathione S-transferase (GST) protein tag to assist separation of the desired protein construct from the cellular media following expression. A 3C viral protease cleavage site was also present to cleave specifically the GST-tag from the MDMX and MDM2 sequence. MDMX and MDM2 expression is induced by addition of isopropyl-β-D-thiogalactoside (IPTG) (**290**) that binds to the lac repressor to relieve repression of the lac promoter to permit binding of *E. coli* RNA polymerase and gene transcription (**Figure 57**).

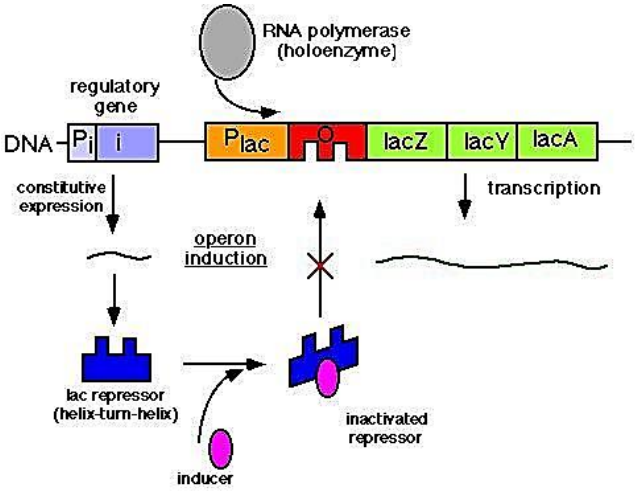

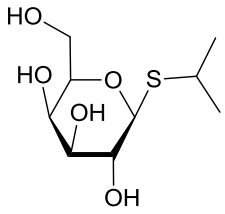

290

Figure 57: The *lac* operon mechanism: RNA polymerase binds to the promoter gene (P_{lac}) and transcribes the genes lacZ, lacY and LacA. Normally, the *lac* repressor binds to the *lac* operator (O), preventing RNA polymerase from binding to P_{lac} when lactose is absent. When an inducer, e.g. IPTG (**290**), binds to the repressor, it can no longer bind to the operator, allowing for continued transcription of lacZ, lacY and lacA, promoting the metabolism of lactose.[162]

Full details of the expression and purification of recombinant GST-MDM2 and GST-MDMX are given in Chapters 7.4 and 7.5. Following separation of the expressed protein from the *E. coli* with lysozyme, incubation with glutathione-agarose and filtration separated the protein from the cellular extract. The protein was eluted in 1 mL samples by washing with mHBS buffer, pH 7.4, containing 25 mM glutathione. Protein concentration was determined for each 1 mL fraction (Nanodrop 2000, Thermo Scientific) and an SDS-PAGE was also run on the crude protein (**Figure 58**).

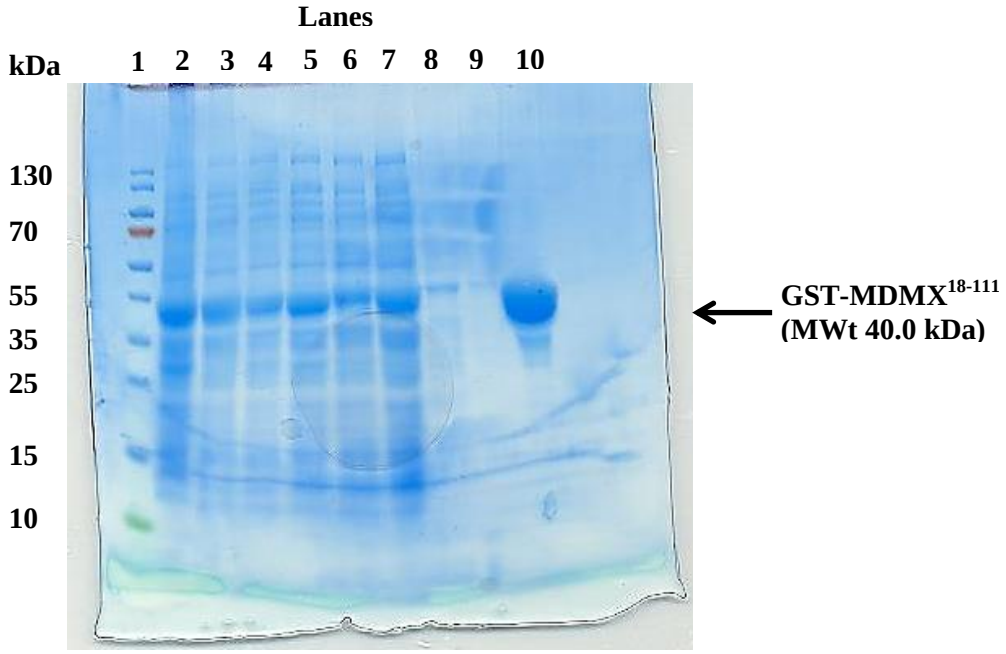

Figure 58: SDS-PAGE (12% acrylamide) of crude GST-MDMX fractions (constructs 1-3). The position of GST-MDMX$^{18-111}$ (lane 10) is highlighted. Lane 1, MWt marker; lane 2, GST-MDMX$^{18-111}$ total cell; lane 3, GST-MDMX$^{18-111}$ cell-free extract; lane 4, GST-MDMX$^{22-111}$ total cell; lane 5, GST-MDMX$^{22-111}$ cell-free extract, lane 6, GST-MDMX$^{26-111}$ total cell; lane 7, GST-MDMX$^{26-111}$ cell-free extract; lanes 8-9, GST-MDMX$^{18-111}$ washes with mHBS buffer, pH 7.4; lane 10, GST-MDMX$^{18-111}$ fraction 3

Fractions containing the desired protein were pooled and incubated overnight at 4 ^{o}C with 1 mg/mL 3C protease (50:1 (w/v) protein:3C protease). This step cleaved the GST tag from the desired protein. The protein was purified by size exclusion chromatography on a Superdex 75 HR 26/600 column (GE Healthcare), equilibrated with mHBS buffer (**Figure 59**).

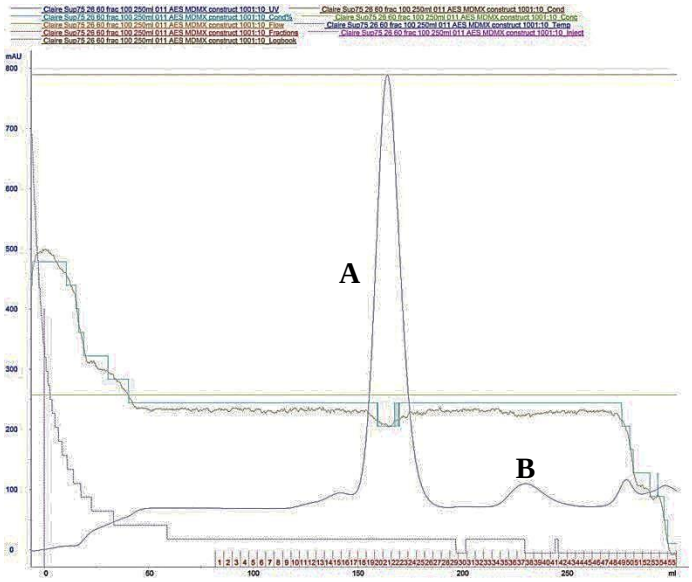

Figure 59: Size exclusion chromatograph of MDMX$^{18\text{-}111}$ following 3C digest. MDMX is well resolved from the GST tag. **A)** GST tag (MWt 26.9 kDa); **B)** MDMX$^{18\text{-}111}$ (MWt 11.0 kDa)

Purification gave protein of sufficient purity for structural studies, as determined by SDS-PAGE analysis (**Figure 60**). Pure protein fractions were pooled, concentrated by ultrafiltration and stored at -80 ^{o}C.

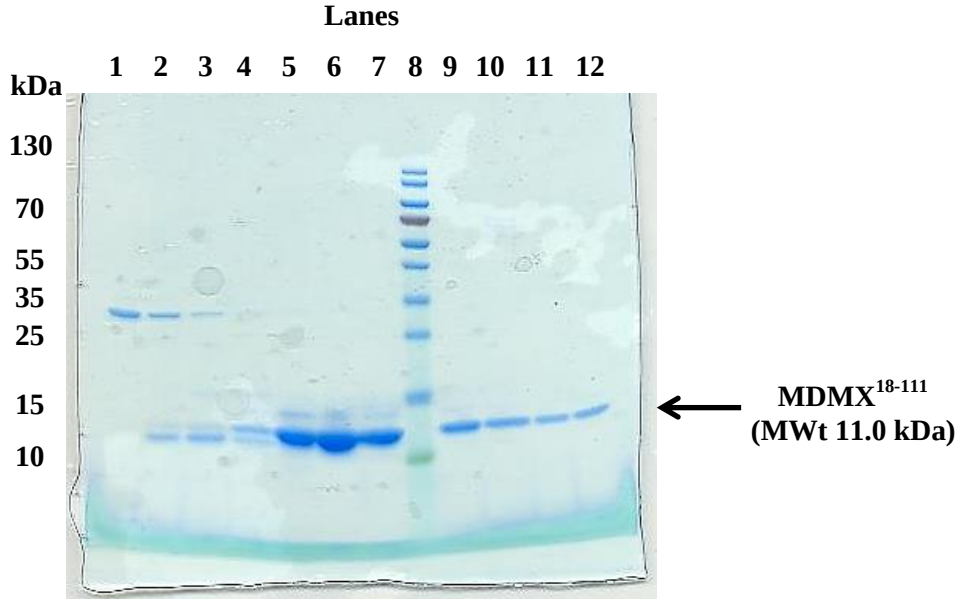

Figure 60: SDS-PAGE (16% acrylamide) of purified MDMX$^{18\text{-}111}$ fractions. The position of the MDMX protein is highlighted. Similar results were obtained for MDMX constructs 2-3 and MDM2 constructs 1-3. Lanes 1-7 and 9-12, column fractions; lane 8, MWt marker

6.1.2 Crystallisation Trials of MDMX and MDM2 Constructs 1-3 with Benzenoid and Thiazole-based Inhibitors

MDM2 construct 2 (*cf.* Table 55) did not express readily and gave a reduced mass of pure protein following gel filtration, so was used in a more focussed library of screens. Supplies of compound **244** were limited so crystallisation trials with this compound used MDMX$^{18\text{-}111}$ and MDMX$^{22\text{-}111}$ only.

Selected inhibitors were incubated overnight at 4 ^{o}C with the concentrated protein in a 3:2 ratio (inhibitor:protein). Competitor compound RO-2443 (**57**), for which the crystal structure with both proteins was already known,[109] was used as a control.

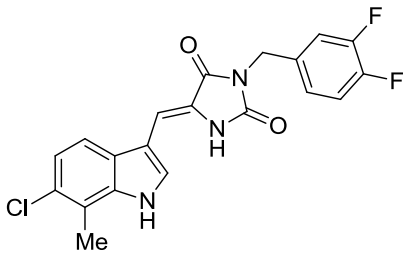

57

Protein-inhibitor complexes were concentrated to between 5 and 10 mg/mL (Nanodrop 2000, Thermo Scientific) (**Table 56**). Complexes of MDMX were more difficult to concentrate than the corresponding MDM2 complexes. Precipitation was observed with all benzenoid inhibitors, which precluded reaching the desired concentration range in some cases. No precipitation was observed for any of the MDM2 complexes. Compounds **57** and **44j** did not precipitate when mixed with either MDMX or MDM2.

Table 56: Protein-inhibitor concentrations for co-crystallisation trials

Protein	Construct	Inhibitor	Complex Concentration (mg/mL)[a,b]
MDMX	1	44j	5.4
		118c	4.3
		185	4.6
		226	3.5
		244	4.1
		57	7.9
	2	44j	12.0
		118c	3.4
		185	4.2
		226	5.2
		244	2.2
		57	5.5
	3	44j	6.9
		118c	3.1
		185	2.9
		226	2.4
		57	3.7
MDM2	1	44j	10.4
		118c	7.6
		185	11.5
		226	13.3
		57	4.2
	2	44j	3.7
		118c	2.4
		185	3.1
		226	-[c]
		57	-[c]
	3	44j	9.5
		118c	14.7
		185	16.2
		226	15.5
		57	4.8

(a) Nanodrop 2000 (Thermo Scientific); (b) Average of 3 readings; (c) Insufficient protein available

Full details of the preparation of each protein construct for crystallography are given in Chapter 7.6. Two screens were used to find appropriate conditions for co-crystallisation:

ammonium sulfate ($AmSO_4$) (Qiagen) and JCSG+ (Molecular Dimensions). Screening solutions were arranged in a 96-well format, with each well differing in precipitants, pH range, salts and buffers. Complexes and screening solutions were combined in 2-subwell 96-well crystallisation trays using a Mosquito® robot and the sitting drop method. Each complex and screening solution was mixed in sub-wells in a 1:1 and 2:1 ratio (complex:screen). Plates were stored at 4 ^{o}C in a Rikagu Minstrel tray hotel for a maximum period of 8 weeks. Images were taken of each sub-well at set time points to monitor crystal formation (**Figure 61**).

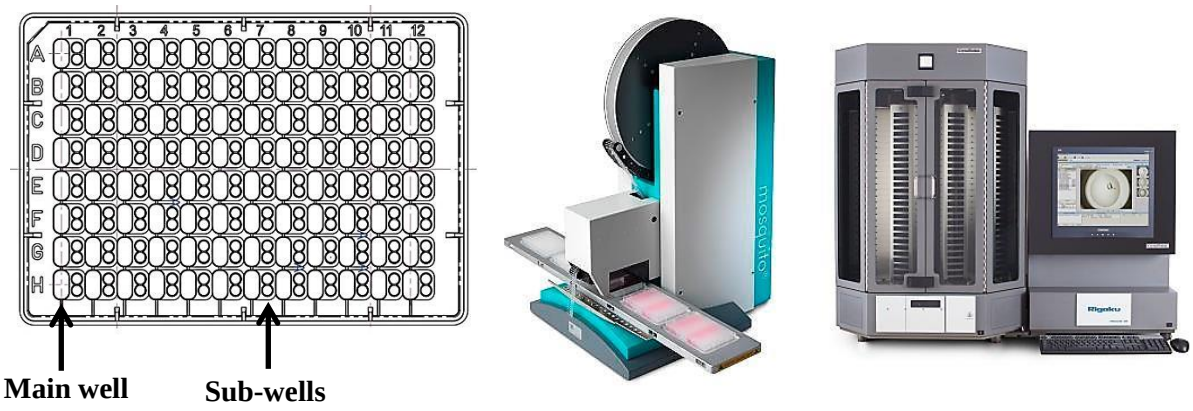

Figure 61: A) 2-subwell 96-well tray used for co-crystallisation trials; **B)** Mosquito® robot; **C)** Rikagu Minstrel tray hotel

A total of 30 protein-inhibitor complexes were prepared using MDMX and MDM2 constructs 1-3. Each complex was screened using $AmSO_4$ and JCSG+ in 2-subwell 96-well trays, giving a total of 384 crystallisation conditions trialled for each complex. Overall, more than 11,000 conditions were trialled in an attempt to crystallise MDMX or MDM2 with a benzenoid or thiazole-based inhibitor.

6.1.3 Crystal Formation and Data Collection

Crystals were obtained for compound **226** with MDM2 construct 3; however, the crystals were too small to be suitable for data collection (**Figure 62**). Work is ongoing to optimise crystallisation conditions for this complex. The conditions which resulted in crystal formation differed only in the salt used (**Table 57**).

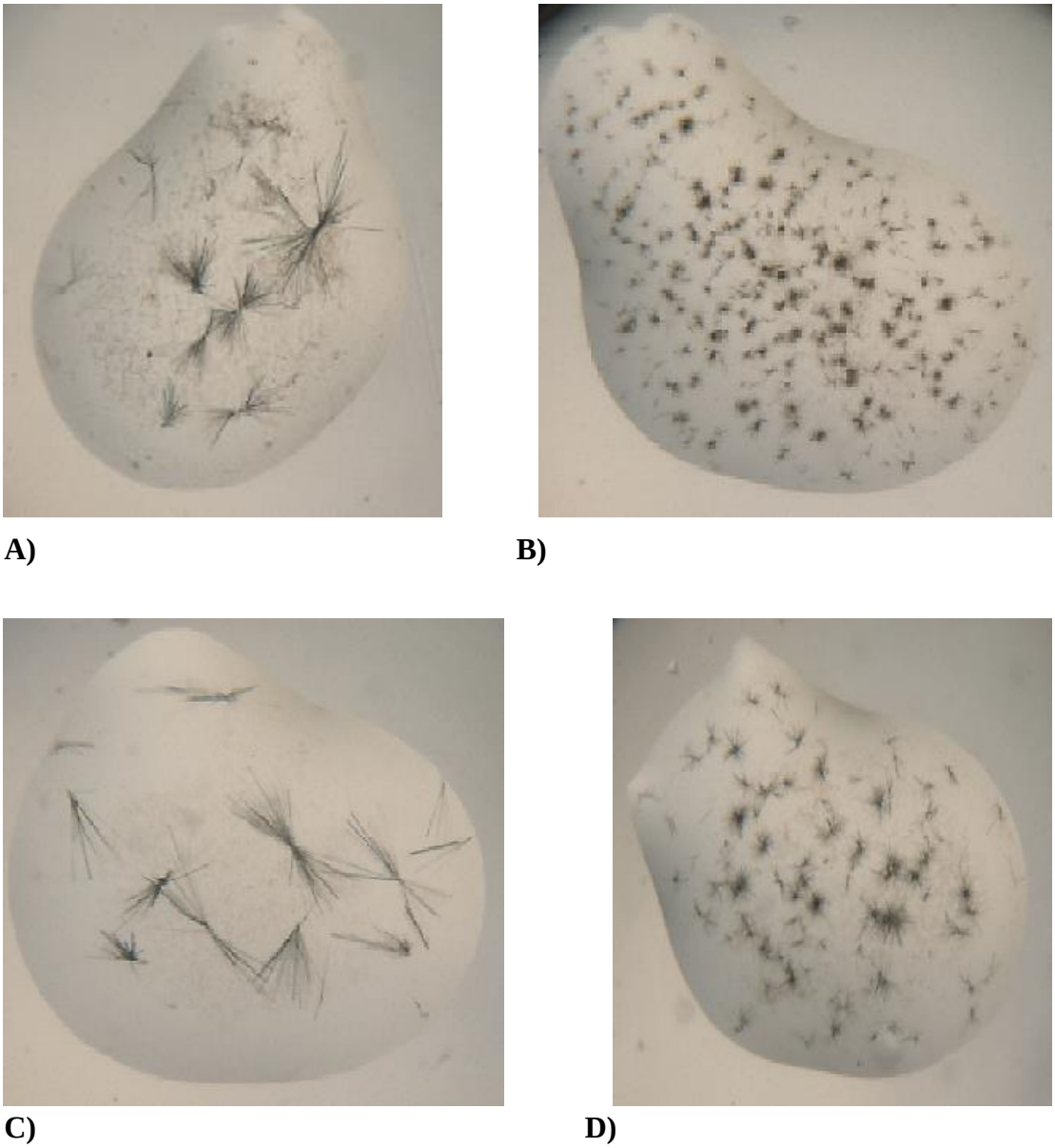

A) **B)**

C) **D)**

Figure 62: Small crystals obtained for MDM2 construct 3 with **226** in a JCSG+ screen

Table 57: Crystallisation conditions for Figure 62, A-D

Well	Complex	Conc. (mg/mL)[a,b]	Screen	Complex : Screen ratio	Salt	Polymer	Buffer (pH)
A	MDM2 c3-**226**	15.5	JCSG+	2:1	-	25% (w/v) PEG 3350	0.1 M Bis-tris (5.5)
B	MDM2 c3-**226**	15.5	JCSG+	2:1	0.2 M NaCl	25% (w/v) PEG 3350	0.1 M Bis-tris (5.5)
C	MDM2 c3-**226**	15.5	JCSG+	2:1	0.2 M Li_2SO_4	25% (w/v) PEG 3350	0.1 M Bis-tris (5.5)
D	MDM2 c3-**226**	15.5	JCSG+	2:1	0.2 M NH_4OAc	25% (w/v) PEG 3350	0.1 M Bis-tris (5.5)

(a) Nanodrop 2000 (Thermo Scientific); (b) Average of 3 readings

6.2 Measuring the Potency of Benzenoid, Thiazole- and Pyrrole-based MDMX Inhibitors by Homogeneous Time-Resolved Fluorescence

All compounds screened against MDMX or MDM2 had been assessed using an enzyme-linked immunosorbent assay (ELISA) (*cf.* Chapter 7.3). This assay provided repeatable potency values, but limited supplies of the desired antibody and a comparatively long testing period for each compound necessitated a higher throughput assay. Discrepancies between inhibition data for competitor compounds in the ELISA and what had been previously reported in the literature also cast doubt on the ability of the ELISA to accurately compare potencies of the Newcastle inhibitors with the competitor compounds (**Table 58**).

Table 58: Comparison of IC_{50} values for known MDMX inhibitors recorded at Newcastle and in the literature

ID	Structure	Literature MDMX K_i/IC_{50} (µM)	Newcastle MDMX K_i/IC_{50} (µM)[a]	Fold Difference
WK-298 (51)[104]	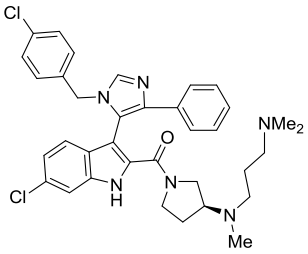	19.7[b]	Not tested	-
52[104]	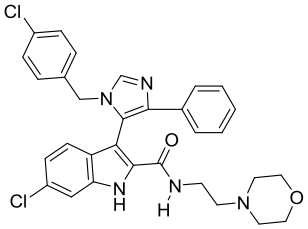	19.0[b]	139[e]	7.3
55d[108]	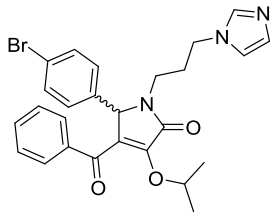	2.68[c]	0%[f,h]	-
RO-2443 (57)[109]	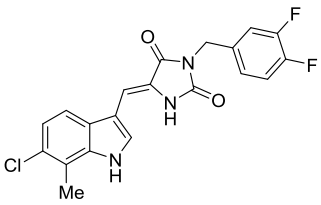	0.041[b]	10.6[g]	259
RO-5963 (58)[109]	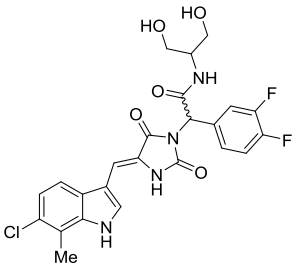	0.024[b]	20.2[d]	842

(a) ELISA; (b) TR-FRET assay; (c) FP assay; (d) *n* = 1; (e) *n* = 2; (f) *n* = 3; (g) *n* = 4; (h) 200 µM

Homogeneous time-resolved fluorescence (HTRF) evaluates compound potency by the measurement of fluorescence resonance energy transfer (FRET). FRET is the transfer of energy between two fluorophores (a donor and an acceptor), which can only occur when

the fluorophores are in sufficiently close proximity. Excitation of the donor triggers the transferral of energy to the acceptor, which in turn emits energy at a specific wavelength; this wavelength is the variable detected to measure binding affinity. In HTRF, there is a time delay of 50-150 µs between excitation of the donor and the measurement of FRET, so as to allow for the clearance of short-lived background fluorescence that would complicate the results. HTRF acceptors emit a far longer-lived fluorescence when engaged in the FRET process.

In the assays conducted at Newcastle, GST-tagged MDMX$^{22\text{-}111}$ was mixed with fluorescein-coupled IP3 peptide (Ac-16-MPRFMDYWQGLN-27-NH_2).[163, 164] IP3 is a p53-mutant sequence with enhanced affinity for MDMX and MDM2 over the authentic p53 sequence (16-QETFSDLWKLLP-27)[98, 164] and fluorescein was the acceptor fluorophore. In addition, a terbium (Tb)-labelled anti-GST antibody was coordinated to the GST-MDMX fusion protein and functioned as the donor fluorophore.

In the absence of a small-molecule inhibitor, excitation of the terbium would lead to energy transfer to the fluorescein, which would in turn emit FRET. Coordination of an inhibitor to MDMX, in place of IP3, would mean the two fluorophores were not sufficiently close for FRET to occur. More potent MDMX inhibitors would give a reduced FRET readout (**Figure 63**).

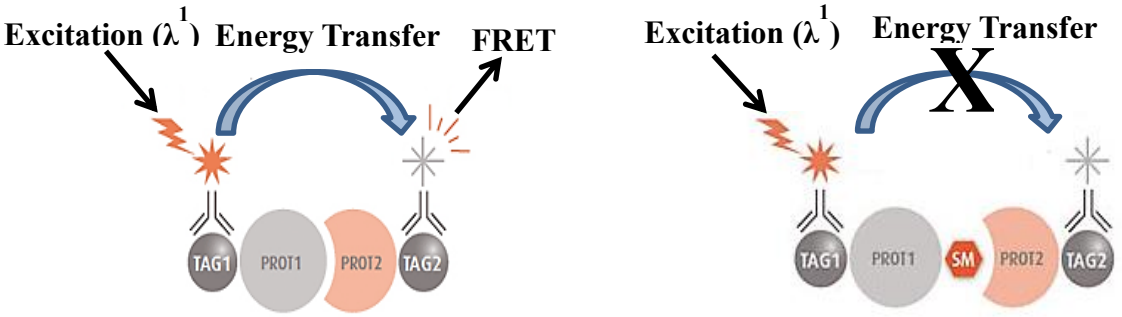

A) **B)**

Figure 63: A) In the absence of an inhibitor, excitation of the donor (terbium) bound to the GST (TAG1) causes energy transfer to the fluorescein (TAG2), which in turn emits FRET; **B)** In the presence of an inhibitor (SM), MDMX (PROT1) and IP3 (PROT2) can no longer bind and the two fluorophores are not close enough for FRET to occur.[165, 166]

The advantages of the HTRF assay over the ELISA were that no washing steps were required, speeding up the analytical process. HTRF could also be adapted to a 384-well plate format, meaning multiple inhibitors could be tested simultaneously using minute quantities of protein and fluorophore.

Full details of the HTRF assay are given in Chapter 7.7. Twelve Newcastle inhibitors in the benzenoid, thiazole and pyrrole series were screened against $MDMX^{22\text{-}111}$ to compare the IC_{50} values obtained to those acquired by ELISA, including **44j**, **118c**, **185**, **226** and **244** (*cf*. Table 54). Compounds were selected for HTRF based on having moderate activity against MDMX by ELISA (IC_{50} of 1-80 µM), or not having been measured for potency before in any assay, and having as low a $clogD_{7.4}$ as possible (**Table 59**). Four competitor compounds were selected to compare the potency of these compounds in the HTRF assay with those reported in the literature. These were WK-298 (**51**) (synthesised in house), RO-2443 (**57**) (synthesised in house), p53 17-30, N30F (kindly donated by David Lane, A*Star, Singapore) and p53 17-27 (Astex, UK).

Table 59: Newcastle MDMX inhibitors selected for HTRF analysis in addition to **44j**, **118c**, **185**, **226** and **244**

ID	Structure	MDMX IC_{50} (µM)	MDM2 IC_{50} (µM)	Ratio (MDMX : MDM2)	$clogD_{7.4}$[c]
118d	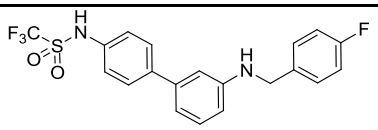	61.2[a]	49.8[a]	0.81	+ 3.48
118e	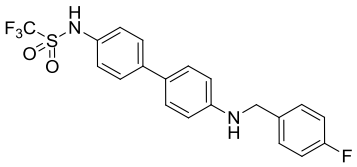	48.9[a]	59.9[a]	1.22	+ 3.44
187	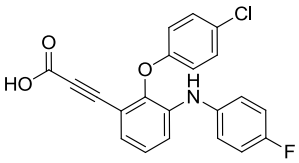	77.3[a]	47.3[a]	0.61	+ 2.02
44r	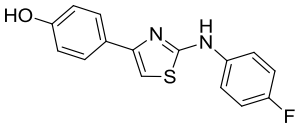	52.7[a]	8.30[a]	0.16	+ 3.68
44s	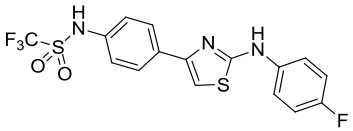	16.7[a]	21.3[a]	1.28	+ 4.69
283b	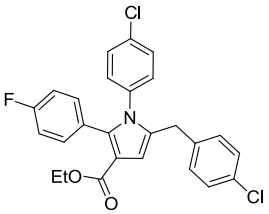	Unknown[b]	Unknown[b]	-	+ 7.23
220g	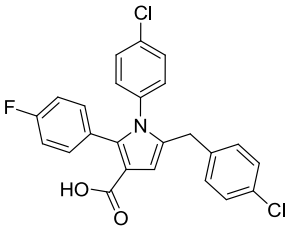	Unknown[b]	Unknown[b]	-	+ 3.37

(a) n = 1; (b) Not tested in ELISA; (c) Values from StarDrop

As the benzenoid series had been explored the most extensively, more compounds were selected from this series than from the thiazoles and pyrroles, and involved a mixture of di-, tri- and tetrasubstituted derivatives. Compounds were arranged in a 384-well plate at 10 concentrations varying on a semi-log scale (**Figure 64**). Positions 21-22 in each

row were positive controls (GST-MDMX, IP3-fluorescein and DMSO) and positions 23-24 in each row were negative controls (IP3-fluorescein in DMSO and buffer).

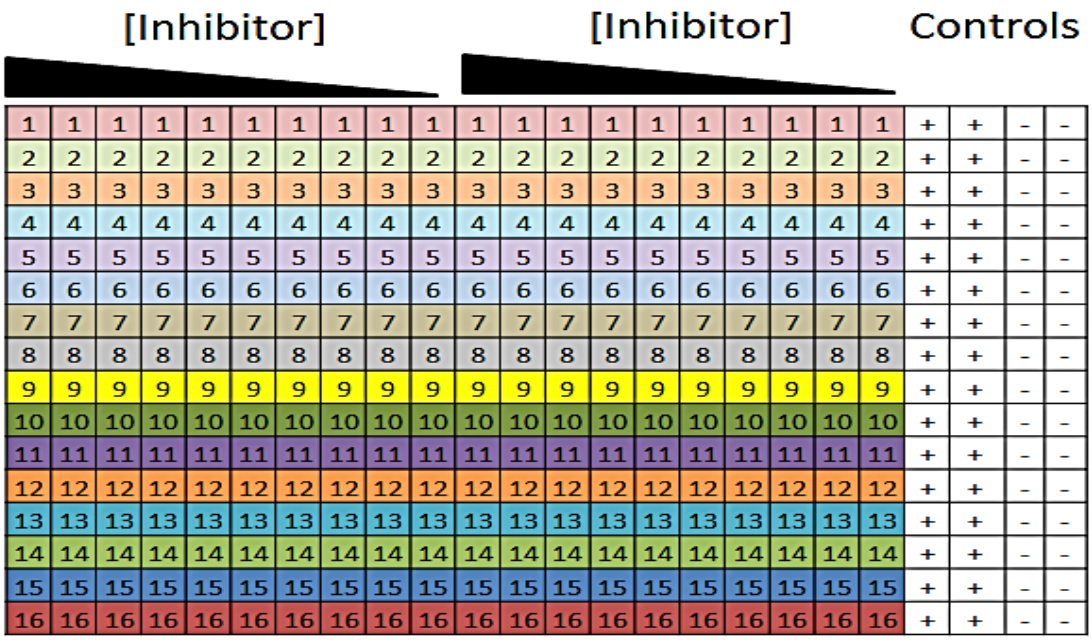

1	1	1	1	1	1	1	1	1	1	1	1	1	1	1	1	1	1	1	1	+	+	-	-
2	2	2	2	2	2	2	2	2	2	2	2	2	2	2	2	2	2	2	2	+	+	-	-
3	3	3	3	3	3	3	3	3	3	3	3	3	3	3	3	3	3	3	3	+	+	-	-
4	4	4	4	4	4	4	4	4	4	4	4	4	4	4	4	4	4	4	4	+	+	-	-
5	5	5	5	5	5	5	5	5	5	5	5	5	5	5	5	5	5	5	5	+	+	-	-
6	6	6	6	6	6	6	6	6	6	6	6	6	6	6	6	6	6	6	6	+	+	-	-
7	7	7	7	7	7	7	7	7	7	7	7	7	7	7	7	7	7	7	7	+	+	-	-
8	8	8	8	8	8	8	8	8	8	8	8	8	8	8	8	8	8	8	8	+	+	-	-
9	9	9	9	9	9	9	9	9	9	9	9	9	9	9	9	9	9	9	9	+	+	-	-
10	10	10	10	10	10	10	10	10	10	10	10	10	10	10	10	10	10	10	10	+	+	-	-
11	11	11	11	11	11	11	11	11	11	11	11	11	11	11	11	11	11	11	11	+	+	-	-
12	12	12	12	12	12	12	12	12	12	12	12	12	12	12	12	12	12	12	12	+	+	-	-
13	13	13	13	13	13	13	13	13	13	13	13	13	13	13	13	13	13	13	13	+	+	-	-
14	14	14	14	14	14	14	14	14	14	14	14	14	14	14	14	14	14	14	14	+	+	-	-
15	15	15	15	15	15	15	15	15	15	15	15	15	15	15	15	15	15	15	15	+	+	-	-
16	16	16	16	16	16	16	16	16	16	16	16	16	16	16	16	16	16	16	16	+	+	-	-

Figure 64: Layout of the 384-well plate used for the HTRF assay. Numbers refer to the 16 compounds analysed, including controls; (+) = positive control, (-) = negative control

Individual compounds and DMSO were dispensed into each well using an Echo® 550 liquid handler (Labcyte). Following incubation with the Tb-linked antibody, FRET detection was measured using a PHERAstar *FS* microplate reader (**Figure 65**).

A) **B)**

Figure 65: A) Echo® 550 liquid handler (Labcyte) **B)** PHERAstar *FS* microplate reader

Data points of the FRET readouts for each compound at the ten concentrations were tabulated, giving a Z' value of 0.44. IC_{50} values for the two p53 peptides and for WK-

298 were similar to the literature values.[98, 104] However, there was a larger than 100-fold discrepancy between the IC_{50} recorded for RO-2443 and that presented in the literature.[109] None of the Newcastle inhibitors returned a measurable IC_{50}, either because of no observed inhibition of FRET or because inhibition did not reach a plateau concentration (**Figure 66**).

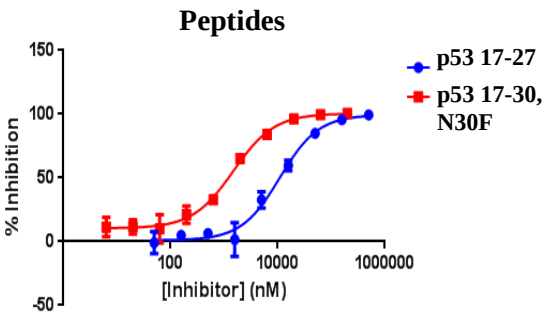

Peptide	MDMX IC_{50} (µM)
p53 17-27	11.0
p53 17-30, N30F	1.49

A)

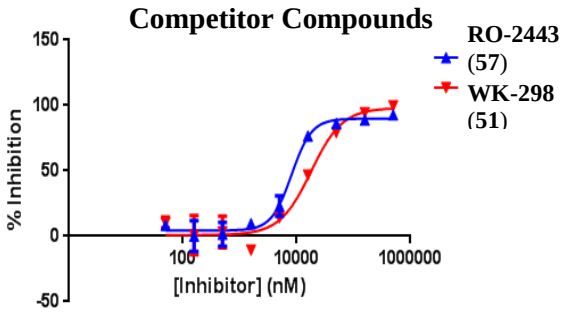

Literature Compound	MDMX IC_{50} (µM)
RO-2443	8.16
WK-298	17.9

B)

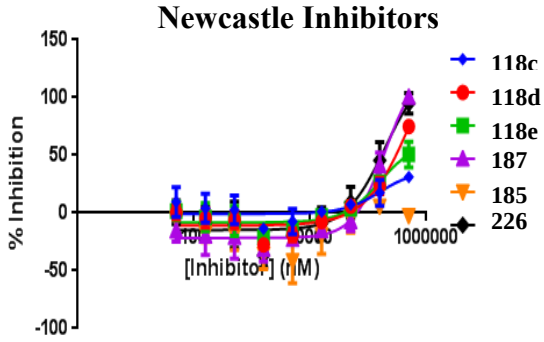

C)

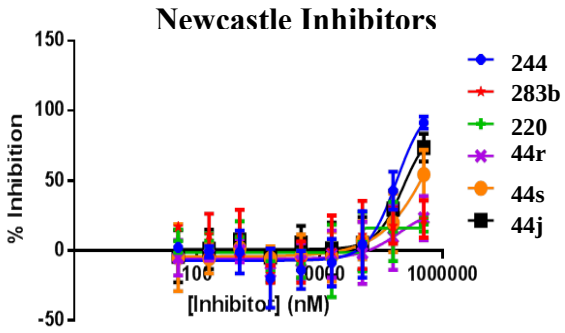

D)

Figure 66: A) HTRF assay results for p53 17-30, N30F (David Lane, A*Star, Singapore) and p53 17-27 (Astex, UK); **B)** HTRF assay results for RO-2443 (**57**) and WK-298 (**51**); **C)** HTRF assay results for Newcastle inhibitors **118c**, **118d**, **118e**, **185**, **187** and **226**; **D)** HTRF assay results for Newcastle inhibitors **44r**, **44s**, **44j**, **220g**, **283b** and **244**

Compound **185** showed negligible activity despite being moderately potent by ELISA (29.3 µM). In contrast, compounds **187** and **226** gave high percentage inhibition, but were similarly active to **185** in the ELISA. Compounds **244** and **44j** also gave high percentage inhibition. Generally, compounds with lower $clogD_{7.4}$ values were more

active in the HTRF assay, suggesting that poor compound solubility was preventing accurate comparison between the activities determined in this assay with those of the ELISA.

6.3 Analysing MDMX Stabilisation by Benzenoid, Thiazole- and Pyrrole-based Inhibitors using Fluorescence-based Thermal Shift

Thermal shift, also known as Differential Scanning Fluorimetry (DSF), is a denaturation assay for hit identification.[167, 168] It provides an estimate of ligand-binding affinity by measuring the change in the unfolding transition temperature (ΔT_m) of a protein in the presence of a ligand, relative to the unfolding temperature in the absence of a ligand (the apoprotein). Protein unfolding is monitored using a dye which fluoresces in hydrophobic environments but is quenched in polar environments, e.g. water. As the protein unfolds, the dye binds to the exposed hydrophobic regions of the protein resulting in an increase in fluorescence (**Figure 67**).

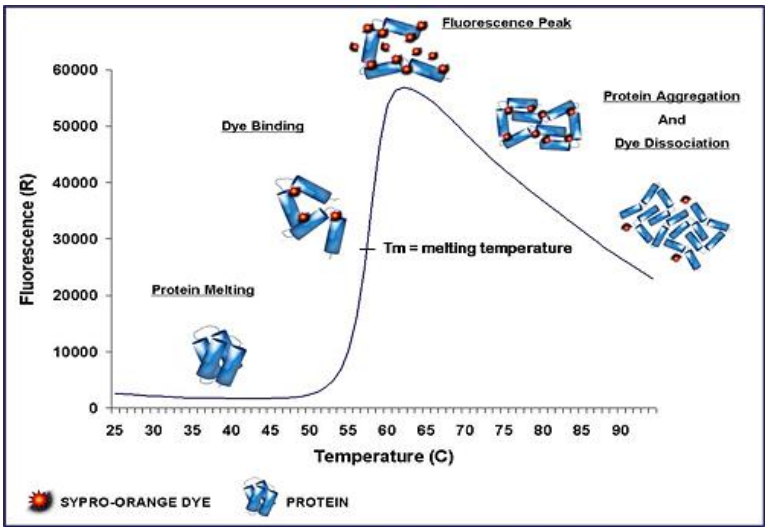

Figure 67: DSF graph showing how fluorescence intensity increases with protein denaturation, exposing the dye SYPRO orange.[169]

DSF is a high-throughput, rapid method for screening compounds, requiring low quantities of protein. However, DSF should not be used as the sole method for hit identification. Two different compounds with equal affinity for the same protein may give different T_m values, as binding is dependent on multiple factors, including enthalpy and entropy.[168] Compounds which stabilise a protein significantly often bind more

entropically (e.g. through hydrophobic interactions) and these modes of binding can compete with each other and complicate the results obtained.

Full details of the DSF assay are given in Chapter 7.8. Twenty-nine benzenoid, thiazole- and pyrrole-based compounds were screened, in addition to five competitor compounds and peptides: p53 17-30, N30F (David Lane, A*Star, Singapore), WK-298 (**51**), RO-2443 (**57**), RO-5963 (**58**) and RG7388 (**291**).[170] All compounds were screened against MDMX$^{18\text{-}111}$, MDMX$^{22\text{-}111}$ and MDMX$^{26\text{-}111}$, using a 384-well plate format, in the presence of SYPRO orange dye. Plates were heated from 25-95 ^{o}C at 3 ^{o}C/min and the differences in melting temperature in the presence of a ligand relative to the apoprotein (ΔT_m) for each MDMX construct are shown in **Tables 60-62**.

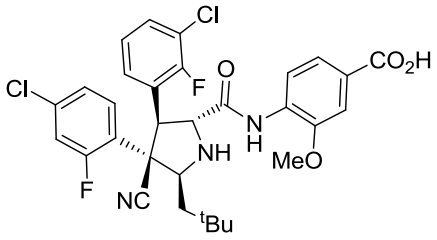

291

Table 60: ΔT_m values observed for benzenoid, thiazole- and pyrrole-based inhibitors against MDMX$^{18\text{-}111}$ (T_m, apoprotein = 55.9 ^{o}C)

Inhibitor[a]	ΔT_m 1 (^{o}C)[b]	ΔT_m 2 (^{o}C)[b]	ΔT_m 3 (^{o}C)[b]	Average ΔT_m (^{o}C)[b]
118b	-0.1	-0.2	-0.1	-0.1
118c	-0.2	0.6	-0.3	0.0
118d	-0.2	0.0	-1.3	-0.5
118i	0.0	0.2	-0.1	0.0
118l	-0.1	-0.1	0.0	-0.1
118m	-0.1	0.1	0.0	0.0
118o	-0.3	0.4	0.0	0.0
118e	-0.3	-0.2	0.0	-0.2
128b	-0.5	0.1	-0.2	-0.2
137b	-0.1	0.1	-0.1	0.0
138c	-0.2	-0.3	-0.2	-0.2

138d	-0.9	0.5	0.0	-0.1
138i	-0.2	-0.1	-0.1	-0.1
138j	0.6	0.3	0.3	0.4
151a	0.5	0.3	0.3	0.4
183a	-1.0	0.5	-0.3	-0.3
185	-0.3	0.3	0.2	0.1
186	0.3	-0.1	0.2	0.1
187	-1.7	-0.5	-2.6	-1.6
226	-15.5	0.0	-13.0	-9.5
231	0.8	0.2	0.5	0.5
244	-0.4	-0.2	-0.7	-0.4
44j	-2.9	-1.0	-0.9	-1.6
44r	0.4	0.3	0.4	0.4
44s	-0.8	-0.9	-0.9	-0.9
44t	-0.1	-0.2	0.0	-0.1
220c	0.1	0.1	0.0	0.0
283b	-0.1	0.0	0.0	0.0
220g	-0.1	-0.1	-0.5	-0.2
p53 17-30, N30F	1.2	0.9	3.4	1.8
RO-2443	0.1	0.2	0.2	0.2
RO-5963	0.1	0.2	0.3	0.2
RG7388	-0.3	-0.4	-0.4	-0.4
WK-298	1.0	0.6	0.7	0.8

(a) Benzenoid inhibitor numbers are written in black, thiazole-based inhibitors are in green and pyrrole-based compounds are in blue; (b) Boxes that are coloured green signify protein stabilisation by at least +0.5 ^{o}C and boxes in red signify destabilisation by at least -0.5 ^{o}C

Several compounds were destabilising to MDMX$^{18\text{-}111}$, giving an average change in melting temperature (ΔT_m) below that of the apoprotein. Compounds which strongly destabilised the protein all possessed acidic functional groups. The most potent destabilising compound was **226**, with a benzoic acid substituent, but the corresponding benzyl alcohol **231** had a stabilising effect. This observation was also seen in the thiazole series, where compounds **44j** and **44s**, which both have trifluoromethylsulfonamide groups, reduced melting temperature but the analogous

phenol **44r** did not. The pyrrole series did not affect melting temperature, even though two possessed acidic functional groups (**220c** and **220g**).

Table 61: ΔT_m values observed for benzenoid, thiazole- and pyrrole-based inhibitors against MDMX[22-111] (T_m, apoprotein = 55.0 °C)

Inhibitor[a]	ΔT_m 1 (°C)[b]	ΔT_m 2 (°C)[b]	ΔT_m 3 (°C)[b]	Average ΔT_m (°C)[b]
118b	-0.2	-0.5	0.1	-0.2
118c	0.1	0.5	0.6	0.4
118d	-0.2	-1.3	-0.7	-0.7
118i	0.5	0.1	0.3	0.3
118l	-0.3	0.0	0.3	0.0
118m	0.5	0.0	0.1	0.2
118o	-0.3	0.2	0.0	0.0
118e	0.0	-0.5	-0.3	-0.3
128b	-0.5	0.2	0.2	-0.1
137b	-0.3	0.1	0.0	-0.1
138c	-0.1	0.3	0.2	0.1
138d	-0.5	-0.1	0.2	-0.2
138i	0.2	0.0	-0.1	0.0
138j	0.3	0.2	0.5	0.3
151a	0.3	0.4	0.7	0.5
183a	-0.4	0.2	0.3	0.0
185	-0.3	0.3	0.5	0.2
186	0.1	-0.8	0.4	-0.1
187	-0.2	-1.0	-0.2	-0.5
226	-0.9	-0.1	0.4	-0.2
231	0.2	0.4	0.4	0.3
244	-1.2	-0.6	-0.5	-0.8
44j	0.0	-0.2	0.0	-0.1
44r	1.0	0.3	0.5	0.6
44s	0.1	0.2	0.4	0.3
44t	0.2	0.0	0.2	0.1

220c	-0.6	-0.1	0.1	-0.2
283b	-0.2	-0.1	0.0	-0.1
220g	0.0	0.1	-0.3	-0.1
p53 17-30, N30F	2.3	1.2	2.4	1.9
RO-2443	0.2	0.3	0.0	0.2
RO-5963	0.8	0.6	0.2	0.5
RG7388	-0.2	0.0	0.0	-0.1
WK-298	2.1	2.2	2.3	2.2

(a) Benzenoid inhibitor numbers are written in black, thiazole-based inhibitors are in green and pyrrole-based compounds are in blue; (b) Boxes that are coloured green signify protein stabilisation by at least +0.5 ^{o}C and boxes in red signify destabilisation by at least -0.5 ^{o}C

Three compounds on average destabilised MDMX$^{22\text{-}111}$: **118d**, **187** and **244**. Similar to MDMX$^{18\text{-}111}$, these compounds all possessed acidic functional groups. Thiazole **44r** and RO-5963 gave a mildly stabilising effect on melting temperature that was not observed with MDMX$^{18\text{-}111}$.

Table 62: ΔT_m values observed for benzenoid, thiazole- and pyrrole-based inhibitors against MDMX$^{26\text{-}111}$ (T_m, apoprotein = 53.7 ^{o}C)

Inhibitor[a]	**ΔT_m 1 (^{o}C)**[b]	**ΔT_m 2 (^{o}C)**[b]	**ΔT_m 3 (^{o}C)**[b]	**Average ΔT_m (^{o}C)**[b]
118b	-0.3	-0.5	-0.5	-0.4
118c	0.0	0.5	0.1	0.2
118d	-0.4	0.2	-0.4	-0.2
118i	-0.2	-0.3	0.2	-0.1
118l	-0.5	-0.7	-0.5	-0.6
118m	-0.1		0.2	0.1
118o	-0.9	-0.1	-0.1	-0.4
118e	0.5	0.3	-0.8	0.0
128b	-0.7	-0.3	-0.2	-0.4
137b	-0.5	0.6	-0.3	-0.1
138c	-0.4	-0.8	-0.4	-0.5
138d	-0.6	-0.2	-0.7	-0.5

138i	-0.7	-0.5	-0.4	-0.5
138j	0.2	0.3	0.0	0.2
151a	0.1	0.0	0.0	0.0
183a	-0.3	0.9	-0.4	0.1
185	-0.7	0.3	-0.1	-0.2
186	0.9	1.2	0.6	0.9
187	-0.8	1.0	-0.5	-0.1
226	-1.0	-8.7	-0.4	-3.4
231	-0.5	-0.1	0.4	-0.1
244	0.2	0.4	-0.5	0.0
44j	0.3	0.2	-0.3	0.1
44r	0.4	0.7	0.4	0.5
44s	-0.3	-0.7	-0.4	-0.4
44t	-0.7	0.0	-0.5	-0.4
220c	-0.7	0.1	-0.1	-0.2
283b	-0.4	-0.2	-0.2	-0.3
220g	-0.4	-0.3	-0.7	-0.5
p53 17-30, N30F	1.1	1.9	1.8	1.6
RO-2443	-0.6	-0.4	-0.1	-0.3
RO-5963	-0.4	-0.3	1.2	0.1
RG7388	-1.0	-1.0	-0.5	-0.8
WK-298	2.3	1.1	0.6	1.3

(a) Benzenoid inhibitor numbers are written in black, thiazole-based inhibitors are in green and pyrrole-based compounds are in blue; (b) Boxes that are coloured green signify protein stabilisation by at least +0.5 ^{o}C and boxes in red signify destabilisation by at least -0.5 ^{o}C

More compounds destabilised MDMX$^{26\text{-}111}$ than had been observed for MDMX$^{18\text{-}111}$ and MDMX$^{22\text{-}111}$ and some of these, e.g. **118l**, did not possess acidic functional groups. Compound **226** was the most destabilising compound and compound **186** gave a reproduceable yet significant stabilising effect. RG7388 destabilised this construct, but p53 17-30, N30F and WK-298 stabilised it.

6.4 Conclusion

Three MDMX and three MDM2 constructs were successfully expressed in *E. coli* Rosetta(DE3)pLys S and BL21(DE3) pLys S strains and purified using size exclusion chromatography. Attempts were made to crystallise five benzenoid and thiazole-based compounds, **44j**, **118c**, **185**, **226** and **244**, and control compound **57**, with these six constructs, trialling over 11,000 conditions with $AmSO_4$ and JCSG+ screens. Needle-like crystals were observed for **226** with MDM2 construct 3 in several wells with similar conditions, but the crystals were too small for data collection. Optimisation of these crystallisation conditions is ongoing. Twelve benzenoid, thiazole- and pyrrole-based compounds were assessed for potency against $MDMX^{22-111}$ using an HTRF assay with fluorescein-coupled IP3 peptide. However, none of the compounds returned a measurable IC_{50}, either due to weak FRET inhibition or because inhibition never reached a plateau concentration. Twenty-nine benzenoid, thiazole- and pyrrole-based compounds were also screened against $MDMX^{18-111}$, $MDMX^{22-111}$ and $MDMX^{26-111}$ using a DSF assay. Compounds with strongly acidic functional groups, e.g. carboxy or trifluoromethylsulfonamido groups, often destabilised the construct relative to the apoprotein, with **226** being the most strongly destabilising compound against $MDMX^{18-111}$ and $MDMX^{26-111}$. Most compounds did not affect the melting temperature of any MDMX construct by more than 1 ^{o}C.

Chapter Seven: Experimental

7.1 Computer Software

All chemical structures were drawn and values for clogP were calculated using ChemDraw Ultra v12.0 (PerkinElmer Informatics). Chemical reaction conditions were sourced, where possible, from Reaxys (Elsevier) and SciFinder (Chemical Abstracts Service). Values for ligand efficiency (LE), lipophilic efficiency (LipE) and $clogD_{7.4}$ were calculated using StarDrop (Optibrium). ^{1}H, ^{13}C and ^{19}F NMR data were analysed using TopSpin v3.2 (Bruker). Crystallographic Object-Orientated Toolkit (COOT) (Paul Emsley, Cambridge) with CCP4mg plug-in (Martin Noble, Oxford) was used for the construction of molecular models.

7.2 SKP2 Sulforhodamine B Assay

SRB assays were undertaken by Laura Evans at the Northern Institute for Cancer Research (NICR) and followed the procedure described by Skehan.[171] Pre-cultured stocks of HeLa cervical cancer cells were seeded (2,000 cells per well) in a tissue culture-treated 96-well plate (Corning) and left to attach overnight. All compounds were screened on a log scale at 0.01, 0.03, 0.1, 0.3, 1, 3, 10, 30 and 100 µM. Compounds were suspended in 100% DMSO to 100 mM, when solubility allowed, and stored at -20 ^{o}C. Final compound concentrations added to each well were in 100 µL medium, 0.5% DMSO and each concentration was replicated in 6 wells. After treatment, cells were incubated for 72 h at 37 ^{o}C, 5% CO_2. DMSO only was used as a negative control and a day 0 plate was fixed and stained on the day of drug treatment to correct for cell growth overnight. Cells were fixed by adding cold 50% (w/v) aqueous trichloroacetic acid (TCA) (25 µL, per well) and incubating at 4 ^{o}C for 1 h. The wells were washed with deionised water and stained with 0.4% (w/v) sulforhodamine B (SRB) (100 µL per well) at room temperature for 30 min. Unbound dye was removed using 1% (v/v) acetic acid and left to dry in air at room temperature overnight. Bound dye was solubilised using 10 mM Tris buffer, pH 9.5 (100 µL per well) and optical density measured using a spectrophotometric plate reader (Model 680, Microplate reader, Bio-Rad) at 570 nm.

Cell growth inhibition was calculated using GraphPad Prism Version 6.0 software (GraphPad Software Inc.). Readings were corrected for one day cell growth and the percentage growth inhibition relative to the DMSO-only control determined for each

concentration. GI_{50} values were calculated using a plot of concentration versus percentage of DMSO-only control on a standard point-to-point gradient with 1,000 segments.

7.3 MDMX-p53 and MDM2-p53 Enzyme-linked Immunosorbent Assay

ELISA assays were undertaken by Dr Yan Zhao at the Northern Institute for Cancer Research (NICR). *In vitro*-translated full-length MDMX and MDM2 (MDMX-IV and MDM2-IV) constructs were prepared by mixing the following components together at 0 ^{o}C, heating at 30 ^{o}C for 2 h and storing at -20 ^{o}C overnight (**Table 63**).

Table 63: Composition of the *in vitro* transcription/translation reaction mixture to prepare MDMX and MDM2 proteins for the ELISA

	MDM2	**MDMX**
Component	**Volume (µL)**	**Volume (µL)**
T7 buffer	80	80
T7 polymerase	40	40
Amino acid mix, Complete[a]	80	40
Rnasin	40	40
Plasmid DNA[b]	160	40
Sterile H_2O	750	760
Reticulocyte lysate	1000	1000

(a) 1 mM each of the 20 essential amino acids; (b) 1 mg/mL

Compounds were dissolved to 2 mM in 100% DMSO and plated out in 10 µL aliquots into a clear, non-coated 96-well plate (Nunc, Thermo Scientific). DMSO alone was used as a negative control. Nutlin-3a was used as a positive control for MDM2, tested in triplicate at final concentrations 50, 100 and 200 nM (starting concentrations of 1, 2 and 10 µM). IP3 peptide was used as a positive control for MDMX, tested in triplicate at final concentrations of 0.5, 2 and 10 µM (starting concentrations of 10, 40 and 200 µM). MDM2-IV (or MDMX-IV) (800 µL) was added to phosphate-buffered saline (PBS) (20 mL), mixed and plated out in 190 µL aliquots to each well of the clear 96-well plate. The plate was left to stand at room temperature (no shaking) for 20 min.

A 100 µg/mL PBS aliquot of biotinylated IP3 peptide (IP3: Ac-16-MPRFMDYWQGLN-27-NH_2) (200 µL) was added to PBS (20 mL), mixed and distributed in 200 µL aliquots to each well of a Streptavidin-coated 96-well plate (Wallac) and stored on a shaking platform at 4 ^oC for 1 h. The contents of the plate were discarded and the plate was washed with PBS (3 × 200 µL per well). The MDMX/2-compound mixtures were transferred to the b-IP3-Streptavidin plate, which was incubated at 4 ^oC on a shaking platform for 90 min.

The contents of the plates were discarded and the plate was washed with PBS (3 × 200 µL per well). Primary mouse monoclonal anti-MDM2 antibody (MDM2 Ab-5, Calbiochem) (100 µL) was added to TBS-Tween (50 mM Tris, pH 7.5, 150 mM NaCl, 0.05% Tween 20 nonionic antibody) (20 mL) and mixed. This was repeated for MDMX Ab-5 (BETHYL(A300-287A)) (10 µL) in TBS-Tween (20 mL). Antibody solutions were transferred to the analogous protein-containing wells and incubated at room temperature on a platform shaker for 1 h. The primary antibody was discarded from the plates, which were washed with TBS-Tween (3 × 200 µL per well). Goat anti-mouse HRP-conjugated antibody (Dako) (for MDM2) or goat anti-rabbit HRP-conjugated antibody (Dako) (for MDMX) (10 µL) was mixed with TBS-Tween (20 mL) and aliquots (200 µL) were added to each well of the plate, which was incubated at room temperature on a platform shaker for 45 min. The contents of the plates were discarded. TBS-Tween (200 µL per well) was added, the plate was shaken briefly and the contents discarded. TBS-Tween (200 µL per well) was added, the plate was shaken vigorously on a platform shaker for 5 min and the contents discarded. This process was repeated twice with TBS-Tween (200 µL per well each time), shaking the plate vigorously for 10 and 15 min respectively before discarding the contents.

Bound HRP activity was measured by enhanced chemiluminescence (ECL, Amersham Biosciences) using the oxidation of luminol to generate a quantifiable light signal. The luminol and enhancer were injected into each well and the relative luminescence units (RLU) measured over 30 s using a Berthold MicroLumat-Plus LB 96 V microplate luminometer. The percentage MDM2/X inhibition at a given concentration was calculated using **Equation 1** and IC_{50} was calculated using a plot of % MDM2/X inhibition versus concentration.

% MDM2/X inhibition = RLU (compound-treated sample) ÷ RLU (DMSO controls) x 100%.

Equation 1

7.4 Expression of Recombinant GST-MDMX and GST-MDM2 in *E. coli*

Recombinant MDMX pGEX-6P-1 expression vector plasmids were transformed into competent Rosetta(DE3)pLys S (Novagen) *E. coli*, whilst recombinant MDM2 pGEX-6P-1 plasmids were transformed into competent BL21(DE3) pLys S *E. coli* (Novagen) (*cf.* Table 64). Competent cells (50 µL) were incubated on ice with plasmid DNA (1 µL, ~100 ng) for 30 min before being heatshocked at 42 ^{o}C for 30 s and then cooled on ice for 2 min. The cells were recovered by adding SOB media (200 µL) before incubating at 37 ^{o}C and 200 RPM for 1 h. The transformed cells (200 µL) were then spread onto LB-agar supplemented with 100 µg/mL ampicillin and 34 µg/mL chloramphenicol, before being incubated at 37 ^{o}C overnight. Single transformed colonies were incubated into LB-media (for the expression of recombinant MDM2) (10 mL) or TB-media (for the expression of recombinant MDMX) (10 mL), with both media supplemented with 100 µg/mL ampicillin and 34 µg/mL chloramphenicol. These starter cultures were incubated at 37 ^{o}C and 200 RPM overnight and then inoculated into a 5 L wide-neck Erlenmeyer flask containing LB-media (1 L) or TB-media (1 L) for the expression of MDM2 and MDMX respectively. The expression media was supplemented with 50 µg/mL ampicillin and 34 µg/mL chloramphenicol. The inoculated media was incubated at 37 ^{o}C with shaking at 160 RPM until the cultures had grown to an OD_{600} in the range 0.6-1.0, at which point the media were supplemented with 0.2 mM IPTG. The incubation temperature and shaking speed was reduced to 20 ^{o}C and 100 RPM, respectively, overnight before harvesting the cells by centrifugation at 5,000 RPM for 10 min at 4 ^{o}C (Rotor JLA 8.1, Beckman Coulter). Cell pellets resulting from 1 L of culture were suspended in ice-cooled mHBS buffer (30 mL) containing one solubilised protease inhibitor tablet (Roche). The resuspended cells were flash-frozen in liquid nitrogen or dry ice and then stored at -80 ^{o}C.

7.5 Purification of Recombinant GST-MDMX and GST-MDM2

Frozen cells were defrosted and treated with 25 mg/mL lysozyme (400 µL), 10 mg/mL RNase A (200 µL), 2 mg/mL DNase I (200 µL) and 2 M $MgCl_2$ (100 µL), whilst being kept on ice. The cell suspension was sonicated on ice at 30% amplitude (15 times, 20 s on/40 s off) before being centrifuged at 20,000 RPM for 1 h at 4 ^{o}C (Rotor JA 25.50, Beckman Coulter). The supernatant was retained and incubated with pre-equilibrated glutathione Sepharose 4B GST affinity resin (GE Healthcare) whist being mixed on a motorised roller at 4 ^{o}C overnight. The incubated resin was poured into an empty gravity column (bed volume *circa* 2 mL) and then washed with mHBS buffer (2 × 50 mL) to remove *E. coli* contaminants. The GST-bound protein was eluted from the column in 1 mL fractions using mHBS buffer, pH 7.4 containing 25 mM glutathione. Protein concentrations were determined using a Nanodrop 2000 (Thermo Scientific) by UV absorbance at 280 nm and protein-containing fractions were pooled. GST was cleaved by mixing with 3C protease (stock at 1 mg/mL, cleavage ratio 1:50 3C:GST-fusion) and purified by size-exclusion chromatography on an Äkta FPLC system using a HiLoad 26/600 Superdex 75 column (mHBS, isocratic gradient, 4 mL/min, UV absorbance 280 nm). Protein-containing fractions were analysed by SDS-PAGE (*cf.* Chapter 7.9.3), before concentrating fractions containing purified MDMX or MDM2 by ultrafiltration using an Allegra^{TM} 25R centrifuge (Beckman Coulter).

7.6 Protein Preparation for Crystallography

Following purification, MDMX and MDM2 were concentrated by ultrafiltration using 15 mL Amicon Ultra 3 kDa columns (3 kDa MWCO, Millipore), centrifuged at 5,000 RCF and 4 °C. During ultrafiltration, protein concentration was determined using a Nanodrop 2000 (Thermo Scientific) according to protein construct molecular weights and extinction coefficients (*cf.* Table 64). Once concentration values could be ascertained, a suitable amount of protein was incubated overnight at 4 ^{o}C with selected inhibitors at a 1.5-fold excess. The inhibitors had been previously resuspended to 20 mM in 100% DMSO. The incubated protein-inhibitor mixture was then concentrated using either 15 mL or 4 mL Amicon Ultra 3 kDa columns (3 kDa MWCO) until a protein concentration of 3-10 mg/mL had been achieved.

The concentrated protein was used to set up 2-subwell 96-well crystallisation trays after dispensing reservoir solutions from commercially available ammonium sulfate ($AmSO_4$) (Qiagen) and JCSG+ screen (Molecular Dimensions) deep-well blocks. The protein-inhibitor complex (100 nL and 200 nL drops) was mixed with the reservoir solution (100 nL) using a Mosquito® robot to dispense sitting drops. The plates were sealed and stored in a Rikagu Minstrel tray hotel at 4 ^{o}C until seven time-points had been imaged over an eight-week period.

7.7 GST-MDMX$^{22\text{-}111}$ Homogeneous Time-resolved Fluorescence Assay

Compounds were dissolved to 20 mM in 100% DMSO and plated out into a black, low volume, low binding, round-bottom 384-well plate (Corning) using an Echo® 550 liquid handler (Labcyte). Each well was backfilled with DMSO to a volume of 250 nL. The peptides p53 17-27 (Pamela Williams, Astex, UK) and p53 17-30, N30F (David Lane, A*Star, Singapore), RO-2443 (synthesised in house) and WK-298 (synthesised in house) were used as control compounds. Each compound was screened at 10 concentrations using a semi-log scale starting at 500 µM, except for p53 17-30, N30F, which started at 200 µM. Each concentration was tested in duplicate. Each well was charged with 500 nM fluorescein-labelled IP3 peptide in buffer A (50 mM Tris, pH 7.5, 100 mM NaCl, 100 µg/mL bovine serum albumin (BSA) and 1 mM dithiothreitol (DTT)) containing 4.2% DMSO (6 µL) (final concentration 300 nM) followed by 25 nM GST-MDMX 22-111 in buffer A (4 µL) (final concentration 10 nM). The final concentration of DMSO in each well was 5%. Positive controls contained IP3 peptide, GST-MDMX and DMSO. Negative controls contained IP3 peptide and DMSO with buffer A replacing the protein. The plate was incubated on a shaking platform at room temperature for 1 h. To each well was added 20 nM LanthaScreen® Tb-anti-GST antibody (Life Technologies) in buffer B (50 mM Tris, pH 7.5, 100 mM NaCl and 100 µg/mL BSA) (10 µL) (final concentration 10 nM) and the plate was incubated on a shaking platform at room temperature for 45 min.

The homogeneous time-resolved fluorescence (HTRF) ratio was measured using a PheraStar FS microplate reader (donor excitation at 337 nm, donor emission at 490 nm, acceptor emission at 520 nm). The HTRF ratio was calculated using **Equation 2** and converted to a percentage inhibition using **Equation 3**. IC_{50} values were calculated with GraphPad Prism Version 6.0 software (GraphPad Software Inc.), using a plot of log

inhibitor concentration versus percentage inhibition with the data fitted to a sigmoidal dose-response curve.

$$\text{HTRF ratio} = \text{FRET } \lambda \div \text{acceptor emission } \lambda \times 10{,}000$$

Equation 2

$$\%\ \text{Inhibition (compound X)} = [(\text{positive control FRET } \lambda - \text{compound X FRET } \lambda)] \div \text{positive control FRET } \lambda \times 100\%$$

Equation 3

7.8 MDMX Thermal Shift (Differential Scanning Fluorimetry) Assay

Compounds were dissolved to 20 mM in 100% DMSO and plated out (45 nL per well) in a MicroAmp® optical 384-well plate (Life Technologies) using an Echo® 550 liquid handler (Labcyte). Echo dispensing was designed to test each compound and control in triplicate, with a total reaction volume of 15 µL/well to give a final inhibitor concentration of 60 µM. Test reactions contained 30 µM MDMX, SYPRO orange (1:1000, 5 X stock), 4% DMSO and mHBS buffer to bring the reaction volume to 15 µL/well. Positive control reactions were performed using the same conditions and selected compounds: RG-7388 (synthesised in house), p53 17-30, N30F (David Lane, A*Star, Singapore), RO-2443 (synthesised in house), RO-5963 (synthesised in house) and WK-298 (synthesised in house). Negative control reactions were set up without MDMX or without DMSO (mHBS was used as a replacement in both instances). Once dispensed, the plates were centrifuged at 1,250 RCF for 5 min at 4 ^{o}C and heated from 25-95 ^{o}C at 3 ^{o}C/min using a ViiA™ 7 Real-Time PCR System (Applied Biosystems).

T_m values were calculated using an Excel-based DSF analysis Transformation tool downloaded from *ftp://ftp.sgc.ox.ac.uk/pub/biophysics* (Frank Neisen, SGC, Oxford). Data was compiled using GraphPad Prism Version 6.0 software (GraphPad Software Inc.).

7.9 General Biology Procedures and Reagents

7.9.1 MDMX and MDM2 protein constructs

Genes encoding human MDMX and MDM2 were cloned into pGEX-6P-1 to yield several GST-MDMX and GST-MDM2 constructs (**Table 64**).

Table 64: MDMX and MDM2 protein constructs used

Protein	Construct	Amino Acid Range	Molecular Weight (g mol $^{-1}$)	Extinction Coefficient (M^{-1} cm^{-1})[a]	Mutations
MDMX	1	18-111	11070.9	7450	None
MDMX	2	22-111	10617.4	7450	None
MDMX	3	26-111	10204.9	7450	None
MDM2	1	17-125	12874.7	10430	K51A
MDM2	2	17-109	11067.9	10430	E69A/K70A
MDM2	3	17-125	12816.7	10430	E69A/K70A

(a) Measured at 280 nm in H_2O

7.9.2 Culture media protein buffer and stock solutions

The compositions of the culture media and stock solutions are provided in **Table 65.**

Table 65: Culture media protein buffer and stock solutions

Solution	Components (quantities)	Additional Information
Lysogeny broth (LB)	Tryptone (10 g), yeast extract (5 g), NaCl (10 g) in distilled water (1 L)	Autoclaved at 121 ^{o}C for 20 min before use
Terrific broth (TB)	Enzymatic casein digest (12 g), yeast extract (24 g), potassium phosphate, dibasic, anhydrous (9.4 g), potassium phosphate, monobasic, anhydrous (2.2 g) in distilled water (1 L) and glycerol (4 mL)	Autoclaved at 121 ^{o}C for 20 min before use
mHBS buffer[a]	5 M NaCl (20 mL), 1 M DTT (5 mL) and 1 M HEPES, pH 7.4 (20 mL) in distilled water (955 mL)	Vacuum filtered through a 0.4 µM membrane and degassed *in vacuo* for 10 min before use
IPTG (100 mM)	DTT (1 g) in distilled water (42 mL)	Filter sterilised and stored at -20 ^{o}C
Glutathione (20 mM)	Glutathione (307 mg) in mHBS (50 mL)	pH adjusted to 7.4 with aqueous NaOH before use
Ampicillin	Dissolved in distilled water to 50 mg/mL	Stored at -20 ^{o}C
Chloramphenicol	Dissolved in 100% ethanol to 34 mg/mL	Stored at -20 ^{o}C

(a) Final concentrations of NaCl, DTT and HEPES were 100 mM, 5 mM and 20 mM respectively

7.9.3 Sodium Dodecyl Sulfate Polyacrylamide Gel Electrophoresis

SDS-PAGE was used for protein identification, estimation of sample impurity and semi-quantitative analysis. Pre-cast 12-well 12% or 16% acrylamide gels (RunBlue) were used with SDS-PAGE running buffer (25 mM Tris, pH 9.5, 192 mM glycine, 0.1% SDS) (1 L). Samples (2.5-15 µL) were mixed with SDS-PAGE loading buffer (0.25% (w/v) bromophenol blue, 0.5 M DTT, 50% (v/v) glycerol, 10% (w/v) sodium dodecyl sulfate (SDS) and 0.25 M Tris-Cl, pH 6.8) (5 µL per sample) and made up to 20 µL with distilled water, then denatured at 100 ^{o}C for 5 min before loading onto the gel. PageRuler pre-stained protein ladder (170-10 kDa, Thermo Scientific) (7.5 µL) was also used (**Figure 68**). Electrophoresis was carried out at 180 V and the gel was subsequently stained with Instant Blue.

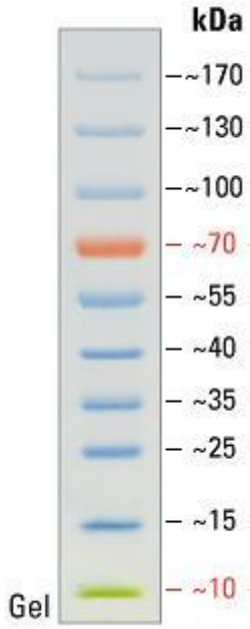

Figure 68: PageRuler pre-stained protein ladder (170-10 kDa, Thermo Scientific)

7.10 Chemicals and solvents

Chemicals were purchased from Sigma Aldrich Chemical Company, Alfa Aesar, Fluorochem, Apollo Scientific, Frontier Scientific, TCI UK, ChemBridge and Acros Organics. Reactions were routinely performed under an atmosphere of nitrogen, employing anhydrous solvents, including DCM, methanol, ethanol, DMF, TFE, acetone, 2-butanol, 1,4-dioxane, DMSO, toluene, α,α,α-TFT, acetonitrile, 1,2-DME,

diethyl ether and THF purchased from Sigma Aldrich Chemical Company in SureSeal bottles. Diisopropylamine (DIPA), 2-butanol and acetone were distilled over calcium hydride or potassium hydroxide and butyllithium was titrated using a quantitative analytical solution purchased from Aldrich, containing 1.0 M 2-propanol in toluene with 0.2% 1,10-phenanthroline. Bottles of lithium aluminium hydride were purchased from Aldrich, as a 1.0 M or 2.0 M solution in anhydrous THF, and inspected by eye to be clear with little or no traces of sediment present before use. All hydrogenation reactions except transfer hydrogenations and those performed with tin(II) chloride, iron or zinc powder were performed in a 'H-cube' hydrogenation reactor supplied by ThalesNano Inc. 10% Pd/C and Raney Nickel CatCarts® were purchased from ThalesNano Inc., Product ID: THS 01111 and THS 01112 respectively. All uses were logged and CatCarts® were flushed with IPA after each use. All microwave-assisted reactions were performed in an Initiator Sixty Biotage apparatus with a robotic samples bed, using 'Hold Temperature' mode in all cases. Reactions were irradiated at 2.45 GHz, with temperatures able to reach 250 ^{o}C and pressures able to reach 20 bar.

7.11 Chemistry Analytical Techniques

Proton (^{1}H), carbon (^{13}C) and fluorine (^{19}F) nuclear magnetic resonance (NMR) experiments were conducted on a Bruker Avance 500 (^{1}H at 500 MHz, ^{13}C at 125 MHz and ^{19}F at 470 MHz). Chemical shifts (δ) are quoted in parts per million (ppm), referenced to the appropriate deuterated solvent used, and coupling constants (*J*) are quoted in Hertz (Hz). The deuterated solvents used were chloroform-d (99.8 atom% D), methanol-d_4 (99.8 atom% D) or DMSO-d_6 (99.9 atom% D) purchased from Sigma Aldrich Chemical Company, unless otherwise specified. Multiplicities are given as singlet (s), doublet (d), triplet (t), quartet (q), multiplet (m), broad (br) or a combination of these and correspond to those observed in the spectrum rather than those predicted to be observed. Liquid chromatography-mass spectrometry (LC-MS) was conducted on a Waters Acquity UPLC system with PDA and ELSD, using an Acquity UPLC BEH C18 column measuring 1.7 µm, 2.1 x 50 mm. The mobile phase consisted of either 0.1% (v/v) formic acid in water or 0.1% (v/v) formic acid in acetonitrile. Gradients were measured over two minutes with a flow rate of 0.6 mL/min and an injection volume of 2 µL. Mass spectrometry was conducted using a Waters SQD with ESCi source in ES mode. Capillary voltage was 3 kV, cone voltage was 30 V, source temperature was 150 ^{o}C, desolvation temperature was 450 ^{o}C, desolvation gas was used at a rate of 800 L/h

and cone gas was used at a rate of 50 L/h. Analytical high performance liquid chromatography (HPLC) was used to provide an estimate of compound purity and was conducted on an Agilent 1200 HPLC system with a diode array detector (DAD) monitoring wavelengths at 210, 230, 254, 280, 310 and 340 nm. Chromatography was performed on a 4.6 x 150 mm Waters XTerra RP18 5 µm column with a mobile phase consisting of either 0.1% (v/v) aqueous ammonia in acetonitrile or 0.1% (v/v) aqueous formic acid in acetonitrile. Gradient programs were run over 25 min (5-100% acetonitrile) followed by column clean-up and equilibrium at a flow rate of 1.0 mL/min. A HPLC in acidic and basic media was recorded for each compound that was screened and the lowest measured percentage purities are quoted. Chiral HPLC was used to determine the enantiomeric excess and was conducted on a Daicel Chiralpak AD-H 250 x 4.6 mm i.d., 5 µm (Chiral Technologies Europe, Illkirch, France).

Infrared (IR) spectra were recorded on a Bio-Rad FTS 3000MX diamond ATR as a neat sample or on an Agilent Technologies Cary 630 FTIR Spectrometer with Diamond ATR accessory (Agilent Technologies, Santa Clara, California, USA) as a neat sample. Ultraviolet (UV) spectra were recorded in ethanol on a U-2800A Spectrophotometer or a Hitachi U-2900 UV-Visible Spectrophotometer (Hitachi High-Technologies Corporation, Tokyo, Japan), using Hitachi UV Solutions 2.0 software, in Hellma 100-QG 10 mm synthetic quartz glass cuvettes (matched pair). Optical rotations were recorded on a PolAAr 3001 Automatic Polarimeter (Optical Activity Ltd., Cambridgeshire, UK). High resolution mass spectrometry (HRMS) was performed using a Thermofisher LTQ Orbitrap XL Finnigan or a MAT95 or MAT900 by the EPSRC National Mass Spectrometry Service Centre, Grove Building, Swansea University, Singleton Park, Swansea, Wales, UK, SA2 8PP. Melting points were recorded on a Stuart SMP40 Automatic Melting Point VWR® and are uncorrected. Combustion analysis was conducted at the Chemical Analytical Services, Newcastle University, using a CARLO ERBA 1108 elemental analyser system controlled with CE Eager 200 software and calibrated with Acetanilide Organic Analytical Standard. Samples were weighed using a certified Mettler MX5 Microbalance. Confidence limits are < 0.3% for solids and < 0.5% for liquids and oils.

7.11.1 Chromatography

Thin Layer Chromatography (TLC) was conducted on Merck silica gel $60F_{254}$ and NH_2F_{254} on aluminium sheets. All sheets were dried after use and visualised using short wave (254 nm) and long wave (365 nm) UV light and/or using an appropriate staining agent, including potassium permanganate, ninhydrin, ammonium molybdate, phosphomolybdic acid (PMA), iodine, iron(III) chloride, 50% sulfuric acid in distilled water and anisaldehyde. Column chromatography was carried out either under medium pressure using Davisil silica gel 40-63µ 60Å from Fisher Scientific or from Fluorochem or on a Biotage SP4 purification system. GraceResolv Silica Cartridges, Grace Reveleris Amino Cartridges or Grace Reveleris C18 Cartridges (Grace Discovery Sciences, Lokeren, Belgium) or Agilent Si50 cartridges were used. Semi-preparative HPLC was performed using an Agilent 1200 system equipped with preparative pumps, fraction collector, autosampler and diode array detector (DAD), with an Agilent ChemStation data system. Samples were run on a 21.2 x 250 mm Phenomenex Luna 5 µm C8(2) (S/No. 313467-1) column, with a mobile phase consisting of either: (A) 0.1% (v/v) aqueous formic acid in acetonitrile or (B) 0.1% (v/v) aqueous ammonia in acetonitrile, running at the specified flow rate.

7.12 General Procedures
7.12.1 SKP2

A) 4-(((3-(2,2-Dimethyltetrahydro-2*H*-pyran-4-yl)-4-phenylbutyl)amino)methyl)-*N*,*N*-dimethylaniline (16a)[78, 79]

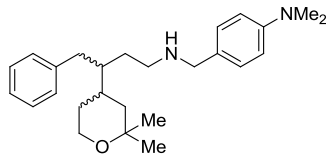

4-(*N*,*N*-dimethylamino)benzaldehyde (154 mg, 1.03 mmol) was added to a solution of amine **28** (200 mg, 0.86 mmol) and excess anhydrous magnesium sulfate in DCM (4.3 mL) and the reaction was stirred at room temperature. After 18 h, the reaction was filtered, washing with DCM (20 mL), and concentrated *in vacuo*. The oil was dissolved in methanol (4.1 mL) before gradual addition of sodium borohydride (127 mg, 3.35 mmol). After 1 h, the reaction was quenched with distilled water (10 mL) and partitioned with EtOAc (2 × 20 mL). Organic fractions were washed with brine (20 mL), dried ($MgSO_4$), filtered and concentrated *in vacuo*. Chromatography (silica, 20% EtOAc, DCM, followed by 2% c. $NH_{3(aq)}$/MeOH, DCM) afforded a yellow oil. The oil was partitioned between brine (10 mL) and DCM (3 × 10 mL), dried (Na_2SO_4) and concentrated *in vacuo* to give **16a**, as an inseparable mixture of diastereoisomers (*dr* = 5:2), as a yellow oil (293 mg, 93%); R_f = 0.49 (silica, 2% c. $NH_{3(aq)}$/MeOH, DCM); UV λ_{max} (EtOH/nm) 263.0; IR ν_{max}/cm^{-1} 2926 (C-H), 2854 (C-H), 2801 (C-H), 1614, 1521, 1452, 1344, 1228, 1162, 1085, 946, 803, 737, 699; ^{1}H δ/ppm (500 MHz, $CDCl_3$) 1.11 (2.2H, s, Alk-C*H*$_3$ (major)), 1.13 (0.9H, s, Alk-C*H*$_3$ (minor), 1.20 (2.2H, s, Alk-C*H*$_3$ (major)), 1.22 (0.9H, s, Alk-C*H*$_3$ (minor), 1.22-1.29 (1H, m, Alk-H (major and minor)), 1.34-1.43 (2H, m, Alk-H (major and minor)), 1.43-1.50 (2H, m, Alk-H (major and minor)), 1.50-1.61 (2H, br, m, Alk-H (major and minor)), 1.67-1.80 (1H, m, Alk-H (major and minor)), 2.40 (1H, dd, *J* = 8.3 and 13.6 Hz, Alk-H (major and minor)), 2.48-2.61 (2H, m, CH_2*C*H_2NH (major and minor)), 2.68 (1H, dd, *J* = 5.4 and 13.6 Hz, Alk-H (major and minor)), 2.92 (6H, s, N(*C*H_3)$_2$ (major and minor)), 3.56-3.63 (1H, m, Alk-H), 3.61 (1.4H, s, NH*C*H_2Ar (major)), 3.63 (0.5H, s, NH*C*H_2Ar (minor)) 3.69-3.74 (1H, m, Alk-H (major and minor)), 6.66-6.71 (2H, m, Ar-H (major and minor)), 7.09-7.15 (4H, m, Ar-H (major and minor)), 7.15-7.20 (1H, m, Ar-H (major and minor)), 7.23-7.29 (2H, m, Ar-H (major and minor)); ^{13}C δ/ppm (125 MHz, $CDCl_3$) 21.8, 29.4, 29.6,

30.0, 31.9, 32.9, 33.1, 37.2, 39.5, 39.8, 40.7, 42.9, 43.0, 46.9, 53.0, 61.9, 71.8, 112.7, 125.8, 128.3, 129.1, 129.2, 141.5, 149.9; LC-MS (ESI+) *m/z* = 395.2 $[M+H]^+$; HRMS calcd. for $C_{26}H_{39}N_2O$ $[M+H]^+$ 395.3057, found 395.3060; Analytical HPLC: 95.2%

B) 4-(Dimethylamino)-*N*-(3-(2,2-dimethyltetrahydro-2*H*-pyran-4-yl)-4-phenylbutyl)benzamide (16i)[79]

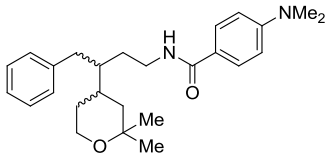

4-(*N*,*N*-dimethylamino)benzoyl chloride (105 mg, 0.57 mmol) was added to a solution of amine **28** (90 mg, 0.34 mmol) and triethylamine (80 µL, 58.1 mg, 0.57 mmol) in DCM (2.0 mL) and the reaction was stirred at room temperature. After 90 min, the reaction was partitioned with distilled water (10 mL) and DCM (3 × 10 mL). Organic layers were washed with 1 M HCl (2 × 10 mL), brine (10 mL), dried ($MgSO_4$), filtered and concentrated *in vacuo*. Chromatography (silica, 18% EtOAc, DCM) afforded **16i** as an inseparable mixture of diastereoisomers (*dr* = 5:2), as a white solid (87 mg, 63%); R_f = 0.29 (silica, 20% EtOAc, DCM); UV λ_{max} (EtOH/nm) 300.0; IR ν_{max}/cm^{-1} 3316 (N-H), 2970 (C-H), 2928 (C-H), 2860 (C-H), 1737 (C=O), 1606, 1545, 1511, 1445, 1364, 1296, 1233, 1202, 1130, 1071, 946, 828, 737, 700; ^1H δ/ppm (500 MHz, $CDCl_3$) 1.17 (3H, s, Alk-C*H*$_3$ (major and minor)), 1.23 (3H, s, Alk-C*H*$_3$ (major and minor)), 1.28-1.30 (1H, m, Alk-H (major and minor)), 1.36-1.72 (7H, m, Alk-H (major and minor)), 1.82-1.85 (1H, m, Alk-H (major and minor)), 2.45 (1H, dd, *J* = 8.9 and 13.6 Hz, Alk-H (major and minor)), 2.75 (1H, dd, *J* = 4.9 and 13.6 Hz, Alk-H (major and minor)), 3.01 (6H, s, N(*CH*$_3$)$_2$ (major and minor)), 3.34-3.40 (2H, m, CH_2*CH*$_2$NH (major and minor)), 3.58-3.67 (1H, m, Alk-H (major and minor)), 3.73-3.79 (1H, m, Alk-H (major and minor)), 5.65-5.68 (1H, m, N*H* (major and minor)), 6.64 (2H, d, *J* = 9.0 Hz, Ar-H (major and minor)), 7.17-7.22 (3H, m, Ar-H (major and minor)), 7.29 (2H, t, *J* = 7.6 Hz, Ar-H (major and minor)), 7.56 (2H, d, *J* = 8.9 Hz, Ar-H (major and minor)); ^{13}C δ/ppm (125 MHz, $CDCl_3$) 21.9, 29.4, 29.5, 30.1, 30.2, 31.9, 33.0, 33.4, 37.1, 38.0, 39.7, 40.0, 40.1, 42.8, 42.9, 61.8, 71.8, 111.0, 121.4, 125.9, 128.2, 128.5, 129.1, 141.1, 152.4; LC-MS (ESI+) *m/z* = 409.5 $[M+H]^+$; HRMS calcd. for $C_{26}H_{36}N_2O_2$ $[M+H]^+$ 409.2850, found 409.2851; Analytical HPLC: 95.1%

C) 4-(((3-(2,2-Dimethyltetrahydro-2*H*-pyran-4-yl)-4-phenylbutyl)(methyl)amino)methyl)-*N*,*N*-dimethylaniline (74a)

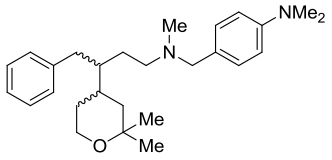

Formic acid (95%, 32 µL, 0.74 mmol) was added to a solution of amine **16a** (60 mg, 0.15 mmol) in ethanol (0.72 mL) at 40 ^{o}C and stirred for 30 min. Formaldehyde (37%, 31 µL, 0.41 mmol) was added and the solution was stirred for 90 min before cooling to room temperature and quenching with 10% NaOH (1 mL). The reaction was partitioned with DCM (3 × 10 mL) and distilled water (10 mL). Organic layers were washed with brine (10 mL), dried ($MgSO_4$), filtered and concentrated *in vacuo*. Chromatography (silica, 0-10% MeOH, DCM) afforded **74a** as an inseparable mixture of diastereoisomers (*dr* = 5:2), as a yellow gum (24 mg, 39%); R_f = 0.41 (silica, 10% MeOH, DCM); UV λ_{max} (EtOH/nm) 260.0; IR ν_{max}/cm^{-1} 2926 (C-H), 2855 (C-H), 2785 (C-H), 1614, 1521, 1453, 1345, 1229, 1185, 1162, 1084, 947, 858, 803, 737, 699; ^{1}H δ/ppm (500 MHz, $CDCl_3$) 1.07 (2.3H, s, Alk-C*H*$_3$ (major)), 1.11 (0.8H, s, Alk-C*H*$_3$ (minor)), 1.20 (2.4H, s, Alk-C*H*$_3$ (major)), 1.21 (0.9H, s, Alk-C*H*$_3$ (minor)), 1.21-1.25 (1H, m, Alk-H), 1.36-1.47 (5H, m, Alk-H (major and minor)), 1.58 (2H, m, Alk-H (major and minor)), 1.71 (1H, m, Alk-H (major and minor)), 2.10 (3H, s, N-C*H*$_3$ (major and minor)), 2.27-2.45 (3H, m, Alk-H (major and minor)), 2.61-2.70 (1H, m, Alk-H (major and minor)), 2.93 (6H, s, N(C*H*$_3$)$_2$ (major and minor)), 3.33 (2H, s, Alk-H (major and minor)), 3.58 (1H, dt, Alk-H, *J* = 2.5 and 12.0 Hz (major and minor)), 3.70-3.76 (1H, m, Alk-H (major and minor)), 6.67-6.69 (2H, m, Ar-H (major and minor)), 7.10-7.13 (4H, m, Ar-H (major and minor)), 7.15-7.18 (1H, m, Ar-H (major and minor)), 7.24-7.27 (2H, m, Ar-H (major and minor)); ^{13}C δ/ppm (125 MHz, $CDCl_3$) 21.8, 29.5, 29.7, 31.9, 32.8, 37.0, 37.2, 39.4, 39.7, 40.7, 42.6, 43.0, 54.5, 61.9, 71.8, 112.5, 125.7, 128.3, 129.1, 130.2; LC-MS (ESI+) *m/z* = 409.5 $[M+H]^+$; HRMS calcd. for $C_{27}H_{40}N_2O$ $[M+H]^+$ 409.3213, found 409.3212; Analytical HPLC: 95.1%

D) 4-(((4-Phenyl-3-(tetrahydro-2*H*-pyran-4-yl)butyl)amino)methyl)aniline (68h)

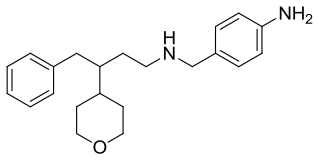

Amine **68g** (286 mg, 0.78 mmol) was dissolved in methanol (15.6 mL) and hydrogenated in a H-cube hydrogen reactor at atmospheric temperature and pressure, flow rate 1 mL/min. After 3 h, the reaction was concentrated *in vacuo* to afford **68h** as a white solid (261 mg, 99%); R_f = 0.27 (silica, 10% MeOH, DCM); m.p. decomposed; UV λ_{max} (EtOH/nm) 248.0; IR ν_{max}/cm^{-1} 3320 (N-H), 2935 (C-H), 2841 (C-H), 1638, 1557, 1439, 1390, 1277, 1222, 1193, 1125, 1107, 873, 780, 738, 700; ^{1}H δ/ppm (500 MHz, $CDCl_3$) 1.46-1.66 (8H, m, Alk-H), 1.78-1.82 (1H, m, N*H*), 2.34 (1H, dd, PhC*H*$_2$-Alk, *J* = 8.1 and 13.5 Hz), 2.49-2.55 (1H, m, AlkC*H*$_2$-NH), 2.58-2.64 (1H, m, AlkC*H*$_2$-NH), 2.71 (1H, dd, PhC*H*$_2$-Alk, *J* = 5.4 and 13.8 Hz), 3.27-3.31 (2H, m, C*H*$_2$-O), 3.67-3.73 (4H, m, ArN*H*$_2$ and HN-C*H*$_2$Ar), 3.94-3.96 (2H, m, C*H*$_2$-O), 6.61 (2H, d, Ar-H, *J* = 7.0 Hz), 7.11 (2H, d, Ar-H, *J* = 7.5 Hz), 7.14 (2H, d, Ar-H, *J* = 7.2 Hz), 7.18 (1H, t, Ar-H, *J* = 7.3 Hz), 7.25-7.27 (2H, m, Ar-H); ^{13}C δ/ppm (125 MHz, $CDCl_3$) 27.4, 29.5, 31.0, 37.2, 37.7, 42.9, 44.5, 50.4, 68.3, 115.1, 126.1, 128.5, 129.0, 131.0, 140.7, 146.9; LC-MS (ESI+) *m/z* = 339.4 $[M+H]^+$; HRMS calcd. for $C_{22}H_{31}ON_2$ $[M+H]^+$ 339.2431, found 339.2433; Analytical HPLC: 96.3%

E) *N*-(4-Azidobenzyl)-4-phenyl-3-(tetrahydro-2*H*-pyran-4-yl)butan-1-amine (68i)

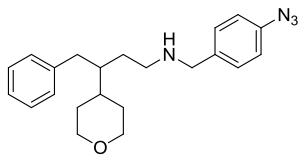

Aniline **68h** (100 mg, 0.30 mmol) was suspended in 5 M HCl (1.2 mL) in darkness and cooled to 0 ^{o}C. Sodium nitrite (28 mg, 0.40 mmol) in distilled water (0.8 mL, 0.5 M) was added dropwise over 2 min. After 40 min, sodium azide (85 mg, 1.3 mmol) was carefully added and the reaction was stirred for 30 min then allowed to reach room temperature. After 2 h the reaction was diluted with distilled water (1 mL) and quenched with saturated aqueous $NaHCO_3$ to pH 9. The reaction was partitioned using EtOAc (10 mL) and brine (10 mL), dried (Na_2SO_4), filtered and concentrated *in vacuo*.

Chromatography (silica, 0-5% MeOH, DCM) afforded **68i** as a yellow solid (84 mg, 75%); R_f = 0.28 (silica, 5% MeOH, DCM); UV λ_{max} (EtOH/nm) 252.5; IR ν_{max}/cm^{-1} 2927 (C-H), 2842 (C-H), 2749 (C-H), 2103 (N≡N, strong), 1604, 1507, 1454, 1281, 1124, 1091, 1013, 824, 739, 700; ^{1}H δ/ppm (500 MHz, $CDCl_3$) 1.46-1.58 (7H, m, Alk-H), 1.75 (1H, m, N*H*), 2.34 (1H, dd, PhC*H*$_2$, *J* = 7.9 and 13.7 Hz), 2.46-2.51 (1H, m, AlkC*H*$_2$-NH), 2.55-2.61 (1H, m, AlkC*H*$_2$-NH), 2.72 (1H, dd, PhCH_2, *J* = 4.8 and 13.7 Hz), 3.27-3.32 (2H, m, C*H*$_2$-O), 3.73 (2H, s, HN-C*H*$_2$Ar), 3.95-3.98 (2H, m, C*H*$_2$-O), 6.97 (2H, d, Ar-H, *J* = 8.3 Hz), 7.11 (2H, d, Ar-H, *J* = 7.7 Hz), 7.17-7.20 (1H, m, Ar-H), 7.24-7.27 (2H, m, Ar-H), 7.33 (2H, d, Ar-H, *J* = 8.2 Hz); ^{13}C δ/ppm (125 MHz, $CDCl_3$) 28.1, 29.58, 29.64, 37.3, 37.9, 42.9, 45.4, 50.7, 68.3, 119.4, 126.1, 128.5, 129.0, 130.9, 140.3, 140.8; LC-MS (ESI+) *m/z* = 365.4 $[M+H]^+$; HRMS calcd. for $C_{22}H_{29}ON_4$ $[M+H]^+$ 365.2336, found 365.2338; Analytical HPLC: 97.5%

F) Ethyl 3-((4-dimethylamino)benzyl)amino)propanoate (76)

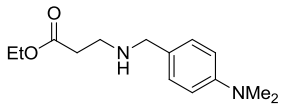

Sodium triacetoxyborohydride (2.84 g, 13.4 mmol) was added to a solution of β-alanine ethyl ester hydrochloride (2.06 g, 13.4 mmol) (**75**) in DMF (16.8 mL) and glacial acetic acid (0.34 mL). After 10 min, 4-(*N*,*N*-dimethylamino)benzaldehyde (1.00 g, 6.70 mmol) in DMF (16.8 mL, 0.4 M) was added dropwise over 3 min and the solution was stirred at room temperature. After 5 h, the reaction was partitioned with brine (100 mL), saturated aqueous $NaHCO_3$ (100 mL) and diethyl ether (10 × 20 mL), dried ($MgSO_4$), filtered and concentrated *in vacuo*. Chromatography (silica, 0-10% MeOH, DCM) afforded **76** as a yellow oil (1.39 g, 83%); R_f = 0.31 (silica, 5% MeOH, DCM); UV λ_{max} (EtOH/nm) 302.0 and 257.0; IR ν_{max}/cm^{-1} 2801 (C-H), 1730 (C=O), 1615, 1522, 1445, 1346, 1213, 1164, 1121, 946, 806; ^{1}H δ/ppm (500 MHz, $CDCl_3$) 1.25 (3H, t, $CO_2CH_2CH_3$, *J* = 7.2 Hz) 1.63 (1H, s, br, N*H*), 2.52 (2H, t, C*H*$_2$, *J* = 6.5 Hz), 2.89 (2H, t, C*H*$_2$, *J* = 6.5 Hz), 2.93 (6H, s, N(C*H*$_3$)$_2$) 3.71 (2H, s, HN-C*H*$_2$Ar), 4.13 (2H, q, $CO_2CH_2CH_3$, *J* = 7.1 Hz) 6.69-6.72 (2H, m, Ar-H), 7.17-7.20 (2H, m, Ar-H); ^{13}C δ/ppm (125 MHz, $CDCl_3$) 14.2, 34.8, 40.8, 44.4, 53.3, 60.4, 112.8, 128.2, 129.0, 149.9, 172.8; LC-MS (ESI+) *m/z* = 251.4 $[M+H]^+$; HRMS calcd. for $C_{14}H_{23}N_2O_2$ $[M+H]^+$ 251.1754, found 251.1756

G Ethyl 3-((*tert*-butoxycarbonyl)(4-(dimethylamino)benzyl)amino)propanoate (77)

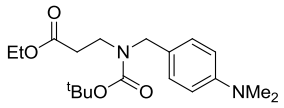

Method 1:

Amine **76** (1.39 g, 5.53 mmol) was added to a solution of Boc_2O (1.33 g, 6.08 mmol) in DCM (12 mL) at 0 ^oC and stirred for 5 min before warming to room temperature. After 1 h, the reaction was partitioned between saturated aqueous $NaHCO_3$ (20 mL) and DCM (3 × 10 mL). Organic layers were washed with brine (10 mL), dried (Na_2SO_4), filtered and concentrated *in vacuo*. Chromatography (silica, 0-15% EtOAc, hexane) afforded **77** as a pale yellow oil (1.80 g, 93%); R_f = 0.32 (silica, 20% EtOAc, hexane); UV λ_{max} (EtOH/nm) 302.5 and 258.5; IR ν_{max}/cm^{-1} 2976 (C-H), 2934 (C-H), 2805 (C-H), 1732 (C=O), 1688, 1614, 1522, 1464, 1409, 1364, 1243, 1156, 1107, 1045, 1019, 946, 885, 802, 772; ^1H δ/ppm (500 MHz, $CDCl_3$) 1.24 (3H, t, $CO_2CH_2CH_3$, J = 7.2 Hz), 1.48 (9H, s, $C(CH_3)_3$), 2.47-2.52 (2H, m, CH_2), 2.93 (6H, s, $N(CH_3)_2$), 3.39-3.46 (2H, m, CH_2), 4.10 (2H, q, $CO_2CH_2CH_3$, J = 7.2 Hz), 4.35 (2H, s, BocN-CH_2Ar), 6.68-6.70 (2H, m, Ar-H), 7.12 (2H, m, br, Ar-H); ^{13}C δ/ppm (125 MHz, $CDCl_3$) 14.2, 28.5, 40.7, 60.4, 79.8, 112.7, 126.1, 128.5, 129.0, 150.0; LC-MS (ESI+) *m/z* = 351.4 $[M+H]^+$; HRMS calcd. for $C_{19}H_{31}N_2O_4$ $[M+H]^+$ 351.2278, found 351.2276

Method 2:

4-(*N*,*N*-dimethylamino)benzaldehyde (3.49 g, 23.4 mmol) was added to a solution of β-alanine ethyl ester hydrochloride (3.00 g, 19.5 mmol) (**75**), sodium acetate trihydrate (3.18 g, 23.4 mmol) and excess anhydrous magnesium sulfate in THF (66 mL) and stirred at room temperature. After 24 h, the reaction was filtered and concentrated *in vacuo*, then dissolved in ethanol (55 mL) and mixed carefully with sodium borohydride (2.21 g, 58.5 mmol). After 30 min, the reaction was cooled to 0 ^oC and quenched with ice-cooled distilled water (10 mL). The solution was concentrated to a small volume *in vacuo* and partitioned with diethyl ether (4 × 20 mL). Organic layers were washed with brine (20 mL), dried ($MgSO_4$), filtered and concentrated *in vacuo*. The oil was dissolved in DCM (50 mL), washed with saturated aqueous $NaHCO_3$ (6 × 20 mL), brine (20 mL), dried ($MgSO_4$), filtered and concentrated *in vacuo*. The oil was dissolved in anhydrous DCM (31.5 mL), cooled to 0 ^oC and mixed with Boc_2O (3.15 g, 14.4 mmol). After 1 h, the reaction was partitioned with distilled water (2 × 20 mL), washed with brine (20

mL), dried ($MgSO_4$), filtered and concentrated *in vacuo*. Chromatography (silica, 0-5% EtOAc, DCM) afforded **77** as a yellow oil (1.44 g, 21%); *Analysis data as above*

H) *tert*-Butyl 4-(dimethylamino)benzyl-(3-(methoxy(methyl)amino)-3-oxopropyl)carbamate (78)

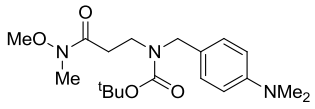

Isopropylmagnesium chloride (2 M in THF, 15.8 mL, 31.6 mmol) was added dropwise to a suspension of *N,O*-dimethylhydroxylamine hydrochloride (1.54 g, 15.8 mmol) in THF (42 mL) at -20 ^oC. After 20 min, ester **77** (1.38 g, 3.94 mmol) was added and the reaction was stirred at -20 ^oC. After 1 h, the reaction was quenched with saturated aqueous NH_4Cl (20 mL) and stirred at -20 ^oC for 5 min. The reaction was partitioned between distilled water (10 mL) and diethyl ether (4 × 20 mL). Organic layers were washed with brine (50 mL), dried (Na_2SO_4), filtered and concentrated *in vacuo* to afford **78** as a yellow oil (1.34 g, 93%); R_f = 0.33 (silica, 15% EtOAc, DCM); UV λ_{max} (EtOH/nm) 302.5 and 258.5; IR ν_{max}/cm^{-1} 2972 (C-H), 2932 (C-H), 2800 (C-H), 1686 (C=O), 1660 (C=O), 1614, 1522, 1462, 1409, 1364, 1244, 1160, 1130, 992, 946, 886, 802, 773; ^1H δ/ppm (500 MHz, $CDCl_3$) 1.48 (9H, s, C(CH_3)$_3$), 2.58-2.66 (2H, m, CH_2), 2.92 (6H, s, N(CH_3)$_2$), 3.15 (3H, s, NCH_3), 3.42-3.47 (2H, m, CH_2), 3.63 (3H, s, OCH_3), 4.36 (2H, s, BocN-CH_2Ar), 6.68-6.69 (2H, m, Ar-H), 7.15 (2H, m, Ar-H); LC-MS (ESI+) *m/z* = 366.4 $[M+H]^+$

I) *tert*-Butyl 4-(dimethylamino)benzyl-(3-oxo-4-phenylbutyl)carbamate (79)

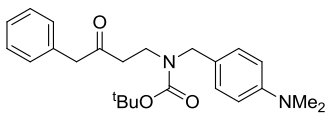

Cerium trichloride heptahydrate (608 mg, 1.63 mmol) was heated to 140 ^oC *in vacuo* for 2 h then cooled to 0 ^oC and suspended in THF (9.5 mL). The suspension was warmed to room temperature with vigorous stirring. After 4 h, amide **78** (567 mg, 1.55 mmol) was added and the reaction was stirred at room temperature. After 1 h, the reaction was cooled to 0 ^oC and benzylmagnesium chloride (2 M in THF, 1.17 mL, 2.34 mmol) was added dropwise. After 30 min, the reaction was quenched with 10% acetic acid (5 mL)

and partitioned between distilled water (5 mL) and diethyl ether (10 mL). The organic layer was washed with distilled water (2 × 10 mL) and the aqueous layer was extracted with diethyl ether (3 × 20 mL). The organic layer was washed with brine (20 mL), dried ($MgSO_4$), filtered and concentrated *in vacuo*. Chromatography (C18, 70-80% MeOH, H_2O) afforded **79**, which was dissolved in DCM (10 mL) and partitioned with distilled water (10 mL), washed with brine (2 × 20 mL), dried ($MgSO_4$), filtered and concentrated *in vacuo* to afford **79** as a yellow oil (464 mg, 75%); R_f = 0.29 (silica, 100% DCM); UV λ_{max} (EtOH/nm) 302.0 and 259.5; IR ν_{max}/cm^{-1} 2976 (C-H), 1684 (C=O), 1614, 1522, 1463, 1414, 1364, 1243, 1161, 946, 873, 802, 771, 733, 699; ^1H δ/ppm (500 MHz, $CDCl_3$) 1.45 (9H, s, C(C*H*$_3$)$_3$), 2.58-2.69 (2H, m, C*H*$_2$), 2.93 (6H, s, N(C*H*$_3$)$_2$), 3.33-3.41 (2H, m, C*H*$_2$), 3.64 (2H, m, PhC*H*$_2$-CO), 4.28 (2H, s, BocN-C*H*$_2$Ar), 6.66-6.68 (2H, m, Ar-H), 7.09 (2H, m, br, Ar-H), 7.15 (2H, d, Ar-H, *J* = 7.3 Hz), 7.24-7.27 (1H, m, Ar-H), 7.30-7.33 (2H, m, Ar-H); ^{13}C δ/ppm (125 MHz, $CDCl_3$) 28.5, 40.7, 40.9, 41.8, 50.1, 79.7, 112.6, 126.1, 127.0, 128.7, 129.1, 129.4, 134.0, 150.0, 155.6, 207.1; LC-MS (ESI+) *m/z* = 397.5 $[M+H]^+$

J) *tert*-Butyl 4-(dimethylamino)benzyl-(3-oxopropyl)carbamate (84)

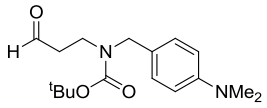

Lithium aluminium hydride (2 M in THF, 0.81 mL, 1.62 mmol) was added dropwise to a solution of amide **78** (454 mg, 1.24 mmol) in THF (35 mL, 35 mM) at 0 °C. After 1 h, the reaction was quenched with sodium bisulfate (694 mg, 5.78 mmol) in distilled water (25 mL, 0.2 M) and warmed to room temperature. The reaction was partitioned with distilled water (20 mL) and EtOAc (2 × 10 mL). Organic layers were washed with brine (20 mL), dried ($MgSO_4$), filtered and concentrated *in vacuo*. Chromatography (silica, 0-5% EtOAc, DCM) afforded **84** as a colourless oil (273.6 mg, 72%); ^1H δ/ppm (500 MHz, $CDCl_3$) 1.48 (9H, s, br, C(C*H*$_3$)$_3$), 2.51-2.60 (2H, m, C*H*$_2$), 2.93 (6H, s, N(C*H*$_3$)$_2$), 3.46-3.48 (2H, m, C*H*$_2$), 4.34 (2H, s, br, BocN-C*H*$_2$Ar), 6.68-6.70 (2H, m, Ar-H), 7.11 (2H, m, br, Ar-H); LC-MS (ESI+) *m/z* = 307.4 $[M+H]^+$

K) *tert*-Butyl 4-(dimethylamino)benzyl-(3-morpholino-4-phenylbutyl)carbamate (83)

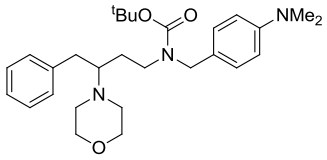

Morpholine (96 µL, 96 mg, 1.10 mmol) was added to a mixture of 1*H*-benzotriazole (217 mg, 1.82 mmol), aldehyde **84** (280 mg, 0.91 mmol) and 3 Å molecular sieves (600 mg) in DCM (3.8 mL) and stirred at room temperature. After 16 h, the reaction was filtered and concentrated *in vacuo*, then partitioned with DCM (15 mL) and 2 M NaOH (2 × 10 mL) followed by distilled water (2 × 10 mL). The aqueous layer was extracted with DCM (2 × 10 mL) and the organic layer was washed with brine (20 mL), dried ($MgSO_4$), filtered and concentrated *in vacuo*, then dissolved in THF (5.5 mL) and cooled to 0 ^oC. Benzylmagnesium chloride (2 M in THF, 0.91 mL, 1.82 mmol) was added dropwise and the reaction was warmed to room temperature. After 24 h, the reaction was partitioned with 2 M NaOH (2 × 10 mL) followed by distilled water (3 × 10 mL). The aqueous layer was extracted with diethyl ether (2 × 10 mL) and the organic layer was washed with brine (10 mL), dried ($MgSO_4$), filtered and concentrated *in vacuo*. Chromatography (silica, 2-50% EtOAc, DCM) afforded **83** as a yellow oil (254 mg, 61%); R_f = 0.29 (20% EtOAc, DCM); UV λ_{max} (EtOH/nm) 258.5; IR ν_{max}/cm^{-1} 2930 (C-H), 2851 (C-H), 2810 (C-H), 1684 (C=O), 1614, 1522, 1453, 1414, 1364, 1233, 1152, 1115, 947, 880, 802, 733, 699; ^1H δ/ppm (500 MHz, DMSO-d_6, 130 ^oC) 1.39 (9H, s, C(C*H*$_3$)$_3$), 1.43-1.48 (1H, m, Alk-H), 1.49-1.56 (1H, m, Alk-H), 1.60-1.66 (1H, m, Alk-H), 2.41 (1H, dd, PhC*H*$_2$-Alk, *J* = 8.2 and 13.3 Hz), 2.56-2.58 (2H, m, Alk-H), 2.63-2.66 (1H, m, Alk-H), 2.91-2.94 (7H, m, N(C*H*$_3$)$_2$ and Alk-H), 3.04-3.09 (1H, m, Alk-H), 3.20-3.25 (1H, m, Alk-H), 3.52-3.59 (4H, m, C*H*$_2$-O and BocN-C*H*$_2$Ar), 4.18-4.27 (2H, m, C*H*$_2$-O), 6.70 (2H, d, Ar-H, *J* = 8.6 Hz), 7.04 (2H, d, Ar-H, *J* = 8.2 Hz), 7.18-7.19 (3H, m, Ar-H), 7.26-7.29 (2H, m, Alk-H); ^{13}C δ/ppm (125 MHz, DMSO-d_6, 130 ^oC) 27.9, 28.0, 28.1, 40.2, 63.5, 66.8, 112.3, 125.6, 125.8, 128.1, 128.5, 129.1, 149.7; LC-MS (ESI+) *m/z* = 468.6 $[M+H]^+$; Analytical HPLC: 93.7%

L) *N*,*N*-Dimethyl-4-(((3-morpholino-4-phenylbutyl)amino)methyl)aniline (80)

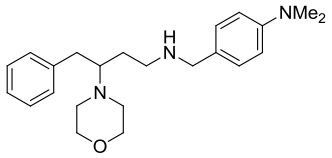

Trifluoroacetic acid (0.7 mL) was added to a solution of carbamate **83** (100 mg, 0.21 mmol) in DCM (0.7 mL, 0.3 M) and stirred at room temperature. After 1 h, the reaction was concentrated *in vacuo* and quenched with saturated aqueous $NaHCO_3$ (10 mL). The solution was partitioned with EtOAc (2 × 10 mL) and the organic layer was washed with brine (10 mL), dried ($MgSO_4$), filtered and concentrated *in vacuo* to afford **80** as a brown oil (77 mg, 100%); R_f = 0.43 (silica, 10% MeOH, DCM); UV λ_{max} (EtOH/nm) 263.5; IR ν_{max}/cm^{-1} 3418 (N-H), 2923 (C-H), 2852 (C-H), 2813 (C-H), 1677, 1614, 1526, 1454, 1354, 1197, 1168, 1113, 1065, 945, 798, 700; ^{1}H δ/ppm (500 MHz, $CDCl_3$) 1.24-1.27 (1H, m, Alk-H), 1.52-1.57 (1H, m, Alk-H), 2.02-2.09 (1H, m, Alk-H), 2.31 (1H, dd, Alk-H, *J* = 10.8 and 12.9 Hz), 2.45-2.49 (2H, m, Alk-H), 2.66-2.71 (1H, m, Alk-H), 2.72-2.77 (1H, m, Alk-H), 2.92-3.01 (9H, m, $N(CH_3)_2$ and Alk-H), 3.12-3.15 (1H, m, Alk-H), 3.54-3.59 (4H, m, Alk-H), 3.67 (1H, d, Alk-H, *J* = 13.1 Hz), 4.10 (1H, d, Alk-H, *J* = 12.8 Hz), 6.69 (2H, d, Ar-H, *J* = 8.9 Hz), 7.08 (2H, d, Ar-H, *J* = 7.5 Hz), 7.18-7.23 (3H, m, Ar-H), 7.26-7.29 (2H, m, Ar-H); ^{13}C δ/ppm (125 MHz, $CDCl_3$) 24.3, 31.0, 34.1, 40.3, 47.7, 51.1, 66.9, 69.0, 112.5, 126.5, 128.7, 129.1, 130.3, 138.9, 151.0; LC-MS (ESI+) *m/z* = 368.6 $[M+H]^+$; HRMS calcd. for $C_{23}H_{34}ON_3$ $[M+H]^+$ 368.2696, found 368.2699; Analytical HPLC: 95.4%

M) Methyl 2-(dihydro-2*H*-pyran-4-(3*H*)-ylidene) acetate (61)

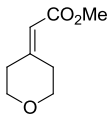

Sodium hydride (60% in mineral oil, 390 mg, 9.75 mmol) was suspended in THF (35 mL) and cooled to 0 ^oC. Trimethyl phosphonoacetate (1.52 mL, 9.36 mmol), dissolved in THF (7 mL, 1.3 M), was added dropwise. After 40 min, pyranone **60** (1.00 g, 7.80 mmol), in THF (7 mL, 1.1 M), was added dropwise and the flask was warmed to room temperature. After 19 h the reaction was quenched with saturated aqueous NH_4Cl (10 mL). The precipitate was removed by filtration and the layers were separated. The

aqueous layer was extracted with diethyl ether (2 × 20 mL) and the organic layer was dried ($MgSO_4$), filtered and concentrated *in vacuo*. Chromatography (silica, 5-50% Et_2O, DCM) afforded **61** as a pale yellow oil (1.27 g, 88%); R_f = 0.75 (silica, 33% EtOAc, hexane); UV λ_{max} (EtOH/nm) 225.5; IR ν_{max}/cm^{-1} 2953 (C-H), 2847 (C-H), 1712 (C=O), 1652, 1435, 1387, 1250, 1201, 1174, 1147, 1096, 1029, 987, 852, 683; ^1H δ/ppm (500 MHz, $CDCl_3$) 2.31-2.34 (2H, m, C*H*$_2$), 2.99-3.01 (2H, m, C*H*$_2$), 3.69 (3H, s, CO_2CH_3), 3.73 (2H, t, C*H*$_2$-O, *J* = 5.6 Hz), 3.76 (2H, t, C*H*$_2$-O, *J* = 5.5 Hz), 5.68 (1H, m, C*H*CO_2Me); ^{13}C δ/ppm (125 MHz, $CDCl_3$) 31.1, 37.5, 51.0, 68.5, 69.1, 114.1, 157.6, 166.8; LC-MS (ESI+) *m/z* = 157.2 $[M+H]^+$

N) Methyl 2-(tetrahydro-2*H*-pyran-4-yl) acetate (62)

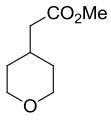

Ester **61** (1.30 g, 7.06 mmol) was dissolved in methanol (7 mL) and cooled to 0 ^oC. 10% Pd/C (226 mg, 2.12 mmol) was added, followed by methanol (55 mL). Ammonium formate (2.23 g, 35.3 mmol) was added portion-wise and the flask was heated to 80 ^oC. After 90 min the reaction was cooled to room temperature and filtered through celite, giving **62** as a pale yellow oil (1.21 g, 92%); R_f = Spot not observed by UV or stains; UV λ_{max} (EtOH/nm) No distinguished peak; IR ν_{max}/cm^{-1} 2920 (C-H), 2842 (C-H), 1733 (C=O), 1437, 1363, 1271, 1244, 1168, 1136, 1092, 1015, 984, 854, 814, 701; ^1H δ/ppm (500 MHz, $CDCl_3$) 1.28-1.37 (2H, m, C*H*$_2$), 1.60-1.64 (2H, m, C*H*$_2$), 1.96-2.05 (1H, m, C*H*), 2.24 (2H, d, C*H*$_2CO_2Me$, *J* = 7.1 Hz), 3.39 (2H, td, C*H*$_2$-O, *J* = 11.8 and 2.2 Hz), 3.66 (3H, s, CO_2CH_3), 3.91-3.94 (2H, m, C*H*$_2$-O); ^{13}C δ/ppm (125 MHz, $CDCl_3$) 32.2, 32.7, 41.2, 51.5, 67.7, 172.8; LC-MS (ESI+) *m/z* = 159.1 $[M+H]^+$; HRMS calcd. for $C_8H_{15}O_3$ $[M+H]^+$ 159.1016, found 159.1013

O) Methyl 3-phenyl-2-(tetrahydro-2*H*-pyran-4-yl)propanoate (63)

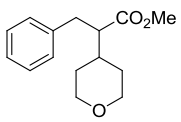

Diisopropylamine (1.00 mL, 7.08 mmol) was dissolved in THF (4 mL) and cooled to -78 ^oC. Butyllithium (2.36 M, 3.00 mL, 7.08 mmol) was added dropwise over 15 min.

The flask was allowed to reach room temperature over 40 min and cooled to -78 ^{o}C. Ester **62** (1.20 g, 6.44 mmol) was dissolved in THF (13 mL, 0.5 M) and added dropwise. The solution was stirred at -78 ^{o}C for 90 min before dropwise addition of benzyl bromide (0.92 mL, 1.32 g, 7.73 mmol) as a solution in THF (3 mL, 2.6 M) and warmed to room temperature. After 21 h, the reaction was quenched with saturated aqueous NH_4Cl (10 mL) and the layers were separated. The organic layer was washed with saturated aqueous NH_4Cl (10 mL) and the aqueous layer was extracted with EtOAc (10 mL). Organic layers were washed with brine (20 mL), dried ($MgSO_4$), filtered and concentrated *in vacuo*. Chromatography (silica, 0-20% Et_2O, hexane) afforded **63** as a pale yellow oil (1.58 g, 89%); R_f = 0.57 (silica, 33% EtOAc, hexane); UV λ_{max} (EtOH/nm) 258.5; IR ν_{max}/cm^{-1} 2949 (C-H), 2842 (C-H), 1730 (C=O), 1496, 1441, 1365, 1236, 1161, 1092, 1017, 985, 882, 842, 745, 699; ^{1}H δ/ppm (500 MHz, $CDCl_3$) 1.41-1.54 (3H, m, Alk-H), 1.73-1.77 (1H, m, Alk-H), 1.82-1.90 (1H, m, Alk-H), 2.51-2.56 (1H, m, Alk-H), 2.84 (1H, dd, Alk-H, *J* = 10.5 and 13.5 Hz), 2.91 (1H, dd, Alk-H, *J* = 5.0 and 13.6 Hz), 3.34-3.42 (2H, m, *CH*$_2$-O), 3.52 (3H, s, OC*H*$_3$), 3.96-4.02 (2H, m, *CH*$_2$-O), 7.14 (2H, d, Ar-H, *J* = 7.3 Hz), 7.19 (1H, t, Ar-H, *J* = 7.4 Hz), 7.27 (2H, t, Ar-H, *J* = 7.4 Hz); ^{13}C δ/ppm (125 MHz, $CDCl_3$) 30.7, 30.9, 35.4, 37.7, 51.2, 53.7, 67.9, 126.4, 128.4, 128.7, 139.3, 174.8; LC-MS (ESI+) *m/z* = 249.3$[M+H]^+$; Analytical HPLC: 98.8%

P) (±)-3-Phenyl-2-(tetrahydro-2*H*-pyran-4-yl)propan-1-ol (64)

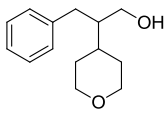

Lithium aluminium hydride (2 M in THF, 3.20 mL, 6.40 mmol) was added dropwise over 1 min to a solution of ester **63** (1.57 g, 5.68 mmol) in THF (12 mL, 0.5 M) at 0 ^{o}C. After 90 min, the solution was warmed to room temperature and quenched with saturated aqueous Rochelle salt (10 mL). The layers were separated and the aqueous layer was extracted with EtOAc (2 × 20 mL). The organic layer was washed with brine (20 mL), dried ($MgSO_4$), filtered and concentrated *in vacuo* to give **64** as an oil (1.42 g, 100%); R_f = 0.33 (silica, 50% EtOAc, hexane); UV λ_{max} (EtOH/nm) 259.5; IR ν_{max}/cm^{-1} 3427 (O-H), 2932 (C-H), 2845 (C-H), 1602, 1495, 1454, 1387, 1267, 1244, 1142, 1087, 1031, 1016, 995, 980, 921, 870, 838, 742, 699; ^{1}H δ/ppm (500 MHz, $CDCl_3$) 1.14 (1H, t, C*H*, *J* = 5.1 Hz), 1.46-1.55 (2H, m, C*H*$_2$), 1.63-1.68 (3H, m, C*H*$_2$ and O*H*), 1.74-1.81

(1H, m, C*H*), 2.55 (1H, dd, Ph-CH_2, *J* = 9.5 and 13.6 Hz), 2.78 (1H, dd, Ph-CH_2, *J* = 5.1 and 13.6 Hz), 3.36-3.41 (2H, m, CH_2-O), 3.52-3.62 (2H, m, CH_2-OH), 3.99-4.02 (2H, m, CH_2-O), 7.18-7.21 (3H, m, Ar-H), 7.27-7.30 (2H, m, Ar-H); ^{13}C δ/ppm (125 MHz, $CDCl_3$) 30.3, 30.4, 34.3, 35.7, 47.6, 61.8, 68.4, 126.0, 128.5, 129.0, 141.0; LC-MS (ESI+) *m/z* = 221.3 $[M+H]^+$; HRMS calcd. for $C_{14}H_{21}O_2$ $[M+H]^+$ 221.1536, found 221.1536

(*R*)- and (*S*)-3-Phenyl-2-(tetrahydro-2H-pyran-4-yl)propan-1-ol ((*R*)- and **(*S*)-64)**

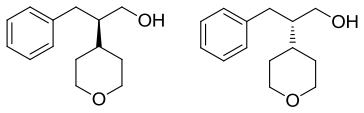

Lithium triethylborohydride (1 M in THF, 5.0 equiv.) was added dropwise over 1-2 min to a solution of either (*R*,*R*)- or (*S*,*S*)-oxazolidin-2-one **(*R*,*R*)-114** (1.86 g, 4.73 mmol) or ***(S,S)*-114** (1.57 g, 4.00 mmol) in diethyl ether (28 mL, 0.2 M) at -78 ^{o}C and stirred overnight, allowing the reaction to reach room temperature. Saturated aqueous NH_4Cl (10 mL) was added dropwise at room temperature, followed by 3 M NaOH (20 mL), and the layers were separated. The organic layer was washed with 3 M NaOH (10 mL) and distilled water (10 mL) and the aqueous layer was extracted with diethyl ether (10 mL). The organic layer was washed with brine (10 mL), dried ($MgSO_4$), filtered and concentrated *in vacuo*. Chromatography (silica, 60% Et_2O, petrol) afforded (*R*)-enantiomer **(*R*)-64** and (*S*)-enantiomer **(*S*)-64** as yellow oils (453 mg, 41% and 380 mg, 41% respectively). Analytical data equivalent to ***(±)*-64**; $[\alpha]_D^{21.4}$ +16.1^{o} (*R*) (*c* 0.87 in EtOH), $[\alpha]_D^{21.2}$ -16.0^{o} (*S*) (*c* 0.84 in EtOH)

Q) 3-Phenyl-2-(tetrahydro-2*H*-pyran-4-yl)propylmethanesulfonate (65)

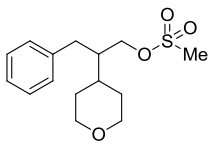

Methanesulfonyl chloride (487 µL, 721 mg, 6.29 mmol) was added dropwise to a solution of alcohol **64** (1.42 g, 5.72 mmol) and diisopropylethylamine (1.50 mL, 1.11 g, 8.58 mmol) in DCM (20.5 mL) at 0 ^{o}C and warmed to room temperature. After 90 min, the reaction was partitioned with distilled water (2 × 20 mL), 1 M HCl (2 × 10 mL) and

brine (20 mL). The organic layer was dried ($MgSO_4$), filtered and concentrated *in vacuo* to give **65** as a brown solid (1.82 g, 97%); R_f = 0.38 (silica, 50% EtOAc, hexane); m.p. 66-68 ^oC; UV λ_{max} (EtOH/nm) 258.5; IR ν_{max}/cm^{-1} 3017 (C-H), 2899 (C-H), 2841 (C-H), 1467, 1344, 1248, 1173, 1136, 1089, 974, 924, 820, 747, 699; ^1H δ/ppm (500 MHz, $CDCl_3$) 1.43-1.54 (2H, m, Alk-H), 1.65-1.73 (2H, m, Alk-H), 1.75-1.89 (2H, m, Alk-H), 2.54 (1H, dd, PhC*H*$_2$, *J* = 9.8 and 13.8 Hz), 2.88 (1H, dd, PhC*H*$_2$, *J* = 5.1 and 14.2 Hz) 2.91 (3H, s, SO_2CH_3), 3.37-3.42 (2H, m, C*H*$_2$-O), 4.01-4.03 (2H, m, C*H*$_2$-O), 4.06 (1H, dd, C*H*$_2$-OMs, *J* = 4.7 and 9.9 Hz), 4.16 (1H, dd, C*H*$_2$-OMs, *J* = 4.2 and 9.8 Hz), 7.16-7.18 (2H, m, Ar-H), 7.21-7.24 (1H, m, Ar-H), 7.29-7.32 (2H, m, Ar-H); ^{13}C δ/ppm (125 MHz, $CDCl_3$) 30.2, 30.3, 33.9, 35.6, 37.0, 45.0, 68.1, 68.7, 126.5, 128.7, 129.0, 139.5; LC-MS (ESI+) *m/z* = 299.3 $[M+H]^+$; HRMS mass not observed

R) *(±)*-4-Phenyl-3-(tetrahydro-2*H*-pyran-4-yl)butanenitrile (66)

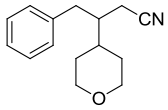

Sodium cyanide (297 mg, 6.06 mmol) was added to a solution of sulfonate **65** (1.80 g, 5.51 mmol) in DMF (11.5 mL) at room temperature and heated to 100 ^oC. After 7 h, the reaction was cooled to room temperature and partitioned with diethyl ether (5 × 15 mL) and distilled water (10 mL). The organic layer was washed with distilled water (5 × 10 mL) and brine (20 mL), dried ($MgSO_4$), filtered and concentrated *in vacuo* to give **66** as a brown solid, which could be taken forward without further purification (1.27 g, 90%). Chromatography (silica, 10% EtOAc, hexane) afforded pure **66** as a colourless oil; R_f = 0.42 (silica, 33% EtOAc, hexane); UV λ_{max} (EtOH/nm) 258.5; IR ν_{max}/cm^{-1} 2945 (C-H), 2916 (C-H), 2856 (C-H), 2242 (C≡N), 1600, 1493, 1452, 1420, 1247, 1139, 1095, 1024, 984, 887, 856, 748, 703; ^1H δ/ppm (500 MHz, $CDCl_3$) 1.41-1.52 (2H, m, Alk-H), 1.66-1.69 (1H, m, Alk-H), 1.74-1.83 (3H, m, Alk-H), 2.20 (1H, dd, Alk-H, *J* = 5.1 and 17.0 Hz), 2.31 (1H, dd, Alk-H, *J* = 4.1 and 17.0 Hz), 2.49 (1H, dd, Alk-H, *J* = 10.1 and 13.8 Hz), 3.01 (1H, dd, Alk-H, *J* = 4.2 and 13.7 Hz), 3.40-3.45 (2H, m, *CH*$_2$-O), 4.02-4.06 (2H, m, *CH*$_2$-O), 7.17-7.19 (2H, m, Ar-H), 7.23-7.26 (1H, m, Ar-H), 7.31-7.34 (2H, m, Ar-H); ^{13}C δ/ppm (125 MHz, $CDCl_3$) 18.1, 30.2, 30.3, 36.4, 37.5, 42.6, 67.9, 118.5, 126.7, 128.8, 129.0, 139.0; LC-MS (ESI+) *m/z* = 230.3 $[M+H]^+$; HRMS calcd. for $C_{15}H_{20}NO$ $[M+H]^+$ 230.1539, found 230.1542; Analytical HPLC: 99.5%

(*R*)- and (*S*)-4-Phenyl-3-(tetrahydro-2*H*-pyran-4-yl)butanenitrile ((*R*)- and **(*S*)-66)**

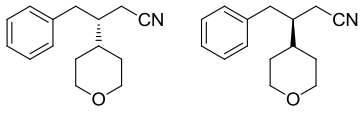

General procedure R i): Using either (*R*)- or (*S*)-mesolate **(*R*)-65** or **(*S*)-65** (569 mg, 1.91 mmol and 479 mg, 1.61 mmol respectively), chromatography (silica, 10-30% EtOAc, hexane) afforded **(*S*)-** or **(*R*)-66** as colourless oils (316 mg, 72% and 274 mg, 74% respectively). Analytical data equivalent to ***(±)*-66**; $[\alpha]_D^{22.1}$ -55.4^o (*R*) (*c* 1.01 in EtOH), $[\alpha]_D^{22.5}$ +55.4^o (*S*) (*c* 1.01 in EtOH)

S) (±)-4-Phenyl-3-(tetrahydro-2*H*-pyran-4-yl)butan-1-amine (67)

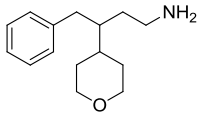

Nitrile **66** (100 mg, 0.44 mmol) was dissolved in ethanol (22.7 mL) and hydrogenated using an H-cube over a Raney Nickel CatCart® at 50 bar, 70 ^{o}C, at 1 mL/min. After 17 h, the solvent was removed *in vacuo* to give **67** as a colourless oil (74 mg, 73%); R_f = 0.13 (silica, 20% MeOH, DCM); UV λ_{max} (EtOH/nm) 259.5; IR ν_{max}/cm^{-1} 3385 (N-H), 3320 (N-H), 2929 (C-H), 2843 (C-H), 1601, 1494, 1453, 1387, 1243, 1090, 1014, 982, 841, 739, 699; ^{1}H δ/ppm (500 MHz, $CDCl_3$) 1.31-1.38 (4H, m, Alk-H), 1.44-1.64 (7H, m, Alk-H, N*H*$_2$ and H_2O), 2.44 (1H, dd, PhC*H*$_2$, *J* = 7.8 and 13.6 Hz), 2.59-2.72 (3H, m, PhC*H*$_2$ and AlkC*H*$_2$NH$_2$), 3.30-3.37 (2H, m, C*H*$_2$-O), 3.97-4.02 (2H, m, C*H*$_2$-O), 7.14-7.15 (2H, m, Ar-H), 7.17-7.20 (1H, m, Ar-H), 7.26-7.29 (2H, m, Ar-H); ^{13}C δ/ppm (125 MHz, $CDCl_3$) 29.5, 29.8, 34.4, 37.4, 40.5, 42.7, 68.5, 125.8, 128.3, 129.0, 141.5; LC-MS (ESI+) *m/z* = 234.3 $[M+H]^+$; HRMS calcd. for $C_{15}H_{23}NO$ $[M+H]^+$ 234.1852, found 234.1852; Analytical HPLC: 93.3%

(*R*)- and (*S*)-4-Phenyl-3-(tetrahydro-2*H*-pyran-4-yl)butan-1-amine ((*R*)- and **(*S*)-67)**

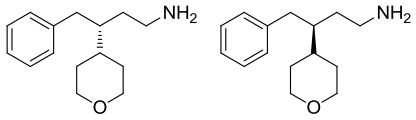

Lithium aluminium hydride (2 M in THF, 1.4 equiv.) was added dropwise to a solution of either (*R*)- or (*S*)-nitrile **(*R*)-** or **(*S*)-66** (264 mg, 1.15 mmol and 316 mg, 1.38 mmol respectively) in THF (0.2 M) at 0 ^{o}C and stirred at room temperature. After 15 h, the reaction was quenched with distilled water (0.26 mL), 3 M NaOH (0.26 mL) and more distilled water (0.78 mL). The reaction was filtered through celite, washing with DCM (20 mL), and concentrated *in vacuo*. Chromatography (silica, 10% MeOH, EtOAc) afforded **(*R*)-** and **(*S*)-67** as yellow oils (132 mg, 47% and 148 mg, 44% respectively). Analytical data equivalent to ***(±)*-67**; $[\alpha]_D^{23.5}$ +9.6^{o} (*R*) (*c* 1.02 in EtOH), $[\alpha]_D^{23.3}$ -9.0^{o} (*S*) (*c* 1.03 in EtOH)

T) 3-(2,2-Dimethyltetrahydro-2*H*-pyran-4-yl)-4-phenylbutan-1-amine (28)[79]

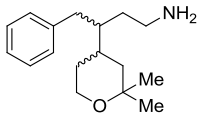

Lithium aluminium hydride (2 M in THF, 3.45 mL, 6.90 mmol) was added dropwise to a solution of nitrile **27** (1.27 g, 4.93 mmol) in THF (24 mL) at 0 ^{o}C and stirred at room temperature. After 15 h, the reaction was quenched with distilled water (0.26 mL), 3 M NaOH (0.26 mL) and more distilled water (0.78 mL). The reaction was filtered through celite, washing with DCM (20 mL), and concentrated *in vacuo*. Chromatography (silica, 0-30% MeOH/DCM) afforded **28** as an inseparable mixture of diastereoisomers (*dr* = 5:2), as a yellow oil (1.07 g, 83%); R_f = 0.17 (silica, 10% MeOH, DCM); UV λ_{max} (EtOH/nm) 207.5; IR ν/cm^{-1} 3371 (N-H), 3290 (N-H), 2970 (C-H), 2927 (C-H), 2858 (C-H), 1583, 1494, 1453, 1364, 1285, 1203, 1084, 1014, 857, 737, 699; ^{1}H δ/ppm (500 MHz, $CDCl_3$) 1.15 (3H, s, Alk-C*H*$_3$ (major and minor)), 1.22 (2H, s, Alk-C*H*$_3$ (major)), 1.23 (1H, s, Alk-C*H*$_3$ (minor)), 1.23-1.25 (2H, m, Alk-H (major and minor)), 1.28-1.51 (6H, m, Alk-H (major and minor)), 1.53-1.60 (1H, m, Alk-H (major and minor)), 1.73-1.81 (1H, m, Alk-H (major and minor)), 2.40 (0.8H, dd, C*H*$_2$Ph, *J* = 8.5 and 13.6 Hz (major)), 2.46 (0.3H, dd, C*H*$_2$Ph, *J* = 8.5 and 13.6 Hz (minor)), 2.57-2.67 (2H, m,

C*H*$_2$CH$_2$NH$_2$ (major and minor)), 2.72 (1H, dd, C*H*$_2$Ph, *J* = 5.8 and 13.7 Hz (major and minor)), 3.63 (1H, td, C*H*$_2$-O, *J* = 2.6 and 12.2 Hz (major and minor)), 3.73-3.79 (1H, m, C*H*$_2$-O (major and minor)), 7.14 (2H, d, Ar-H, *J* = 7.3 Hz (major and minor)), 7.19 (1H, t, Ar-H, *J* = 7.5 Hz (major and minor)), 7.26-7.29 (2H, m, Ar-H (major and minor)); ^{13}C δ/ppm (125 MHz, $CDCl_3$) 29.5, 29.8, 34.5, 37.4, 37.5, 40.6, 42.7, 68.5, 125.8, 128.3, 129.0, 141.5; LC-MS (ESI+) *m/z* = 234.3 $[M+H]^+$; HRMS cald. for $C_{17}H_{28}NO$ $[M+H]^+$ 262.2165, found 262.2164

U) 2-(Tetrahydro-2*H*-pyran-4-yl)acetic acid (112)

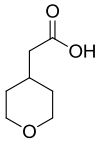

Lithium hydroxide monohydrate (6.37 g, 152 mmol), as a solution in distilled water (79.5 mL, 1.9 M), was added to a solution of methyl ester **62** (1.20 g, 7.59 mmol) in THF (79.5 mL, 0.1 M) at room temperature in air and stirred at 60 ^{o}C for 90 min. The reaction was cooled to room temperature, acidifed to pH 0 with 1 M HCl and partitioned with EtOAc (20 mL). The aqueous layer was extracted with EtOAc (20 mL) and the organic layer was washed with brine (20 mL), dried ($MgSO_4$), filtered and concentrated *in vacuo* to give **112** as a yellow solid (1.04 g, 95%); R_f = 0.26 (silica, 80% EtOAc, petrol); m.p. 56-60 ^{o}C; UV λ_{max} (EtOH/nm) No distinguished peak; IR ν_{max}/cm^{-1} 2934 (C-H), 2914 (br) (O-H), 2841 (C-H), 1703 (C=O), 1640, 1444, 1411, 1303, 1279, 1233, 1173, 1132, 1086, 1018, 981, 916, 885, 855; ^{1}H δ/ppm (500 MHz, $CDCl_3$) 1.37 (2H, qd, C*H*$_2$CH, *J* = 4.3 and 12.0 Hz), 1.67-1.70 (2H, m, C*H*$_2$CH), 1.98-2.07 (1H, m, C*H*), 2.30 (2H, d, C*H*$_2$CO$_2$H, *J* = 7.1 Hz), 3.42 (2H, td, C*H*$_2$-O, *J* = 1.9 and 12.0 Hz), 3.95-3.98 (2H, m, C*H*$_2$-O), 10.88 (1H, s, br, CO$_2$*H*); ^{13}C δ/ppm (125 MHz, $CDCl_3$) 31.8, 32.6, 41.0, 67.7, 177.8; LC-MS (ESI+) *m/z* = 143.1 $[M-H]^-$; HRMS calcd. for $C_7H_{11}O_3$ $[M-H]^-$ 143.0714, found 143.0718

V) (*R*)- and (*S*)-4-Benzyl-3-(2-(tetrahydro-2*H*-pyran-4-yl)acetyl)oxazolidin-2-one ((*R*)- and (*S*)-113)

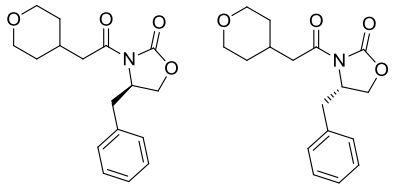

Triethylamine (2.07 mL, 1.50 g, 14.8 mmol) was added to a solution of pyran **112** (1.07 g, 7.42 mmol) in THF (31.0 mL, 0.2 M) at room temperature, stirred for 10 min and then cooled to 0 ^{o}C before addition of pivaolyl chloride (1.09 mL, 1.07 g, 8.90 mmol). After 30 min at 0 ^{o}C, lithium chloride (0.5 M in THF, 17.8 mL, 8.90 mmol) was added, followed by either (*R*)-(+)- or (*S*)-(-)-4-benzyloxazolidin-2-one (1.58 g, 8.90 mmol) and the reaction was stirred at room temperature for 20 h. The reaction was partitioned with EtOAc (20 mL) and 1 M HCl (20 mL), the organic layer was washed with 1 M HCl (2 × 20 mL), 1 M K_2CO_3 (3 × 20 mL) and the acidic aqueous layer was extracted with EtOAc (20 mL). The organic layer was washed with brine (10 mL), dried ($MgSO_4$), filtered and concentrated *in vacuo*. Chromatography (silica, 30% EtOAc, petrol) afforded either **(*R*)-113** or **(*S*)-113** as white solids (1.59 g, 66% and 1.72 g, 73% respectively); R_f = 0.29 (silica, 30% EtOAc, petrol); m.p. 102-104 ^{o}C; $[\alpha]_D^{24.5}$ -83.3^{o} (*R*) (*c* 1.02 in EtOH), $[\alpha]_D^{24.1}$ +92.1^{o} (*S*) (*c* 1.01 in EtOH); UV λ_{max} (EtOH/nm) 205.0; IR ν_{max}/cm^{-1} 2948 (C-H), 2912 (C-H), 2832 (C-H), 1760 (C=O), 1687 (C=O), 1395, 1354, 1279, 1211 (C-O), 1141, 1092, 1053, 984, 850, 765, 697; ^{1}H δ/ppm (500 MHz, $CDCl_3$) 1.36-1.47 (2H, m, OCH_2CH_2CH), 1.67-1.73 (2H, m, OCH_2CH_2CH), 2.11-2.20 (1H, m, $CHCH_2CO$), 2.76 (1H, dd, CH_2CO, *J* = 9.7 and 13.4 Hz), 2.84 (1H, dd, $PhCH_2$, *J* = 7.0 and 16.7 Hz), 2.95 (1H, dd, $PhCH_2$, *J* = 6.6 and 16.7 Hz), 3.30 (1H, dd, CH_2CO, *J* = 3.3 and 13.3 Hz), 3.41-3.47 (2H, m, CH_2-O), 3.95-3.98 (2H, m, CH_2-O), 4.16-4.23 (2H, m, CH_2OCON), 4.66-4.70 (1H, m, CHN), 7.21(2H, d, Ar-H, *J* = 7.0 Hz), 7.28-7.30 (1H, m, Ar-H), 7.32-7.36 (2H, m, Ar-H); ^{13}C δ/ppm (125 MHz, $CDCl_3$) 31.4, 32.8, 38.0, 42.2, 55.2, 66.3, 67.8, 67.9, 127.4, 129.0, 129.4, 135.2, 153.5, 171.8; LC-MS (ESI+) *m/z* = 304.4 $[M+H]^+$; HRMS calcd. for $C_{17}H_{22}O_4N$ $[M+H]^+$ 304.1543, found 304.1546

***N*-Benzyl-3-(2,2-dimethyltetrahydro-2*H*-pyran-4-yl)-4-phenylbutan-1-amine (16b)**

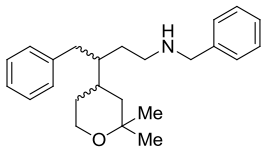

General Procedure A: Using amine **28** (212 mg, 0.81 mmol) and benzaldehyde (0.10 mL, 0.10 g, 0.97 mmol), chromatography (silica, 20% EtOAc, DCM followed by 2% $NH_{3(aq)}$, MeOH) afforded **16b**, as an inseparable mixture of diastereoisomers (*dr* = 5:2), as a yellow oil (171 mg, 60%); R_f = 0.39 (silica, 5% $NH_{3(aq)}$/MeOH, DCM); IR ν_{max}/cm^{-1} 3025 (C-H), 2970 (C-H), 2927 (C-H), 2855 (C-H), 1602, 1494, 1453, 1364, 1285, 1202, 1085, 1029, 963, 909, 857, 733, 697; ^{1}H δ/ppm (500 MHz, $CDCl_3$) 1.11 (2.4H, s, Alk-C*H*$_3$ (major)), 1.13 (0.7H, s, Alk-C*H*$_3$ (minor)) 1.21 (2.2H, s, Alk-C*H*$_3$ (major)), 1.22 (0.8H, s, Alk-C*H*$_3$ (minor)) 1.23-1.29 (2H, m, Alk-H (major and minor)), 1.34-1.62 (6H, m, Alk-H (major and minor)), 1.70-1.79 (1H, m, N*H* (major and minor)), 2.41 (1H, dd, Alk-H, *J* = 8.2 and 13.7 Hz (major and minor)), 2.50-2.61 (2H, m, CH_2CH_2NH (major and minor)), 2.68 (1H, dd, Alk-H, *J* = 5.6 and 13.7 Hz (major and minor)), 3.58-3.63 (1H, m, Alk-H (major and minor)), 3.70 (1.4H, s, NHC*H*$_2$Ar (major)), 3.72 (0.5H, s, NHC*H*$_2$Ar (minor)) 3.75-3.78 (1H, m, Alk-H (major and minor)), 7.12 (2H, d, Ar-H, *J* = 8.2 Hz (major and minor)), 7.16-7.19 (1H, m, Ar-H (major and minor)), 7.23-7.32 (2H, m, Ar-H (major and minor)); ^{13}C δ/ppm (125 MHz, $CDCl_3$) 21.8, 29.4, 29.7, 30.3, 31.9, 33.0, 33.2, 37.2, 37.3, 39.5, 39.8, 42.8, 43.0, 47.4, 53.8, 61.9, 71.8, 125.8, 127.0, 128.2, 128.3, 128.4, 129.1, 141.0; LC-MS (ESI+) *m/z* = 352.2 $[M+H]^+$; HRMS calcd. for $C_{24}H_{34}NO$ $[M+H]^+$ 352.2635, found 352.2626; Analytical HPLC: 95.7%

3-(((3-(2,2-Dimethyltetrahydro-2*H*-pyran-4-yl)-4-phenylbutyl)amino)methyl)-*N*,*N*-dimethylaniline (16c)

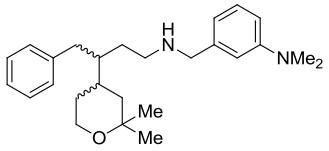

General Procedure A: Using amine **28** (100 mg, 0.38 mmol) and 3-(*N*,*N*-dimethylamino)benzaldehyde (69 mg, 0.46 mmol), chromatography (silica, 20% EtOAc, DCM followed by 10% MeOH, DCM) afforded **16c**, as an inseparable mixture

of diastereoisomers (*dr* = 5:2), as a yellow oil (71 mg, 53%); R_f = 0.40 (silica, 10% MeOH, DCM); UV λ_{max} (EtOH/nm) 302.5 and 256.0; IR ν_{max}/cm^{-1} 2970 (C-H), 2927 (C-H), 2856 (C-H), 2804 (C-H), 1602, 1495, 1453, 1363, 1230, 1204, 1116, 1085, 997, 961, 857, 738, 697; ^{1}H δ/ppm (500 MHz, $CDCl_3$) 1.11 (2.2H, s, Alk-C*H*$_3$ (major)), 1.13 (0.8H, s, Alk-C*H*$_3$ (minor)), 1.21 (2.3H, s, Alk-C*H*$_3$ (major)), 1.22 (0.7H, s, Alk-C*H*$_3$ (minor)), 1.23-1.29 (1H, m, Alk-H (major and minor)), 1.35-1.61 (7H, m, Alk-H (major and minor)), 1.72-1.79 (1H, m, N*H* (major and minor)), 2.42 (1H, dd, PhC*H*$_2$-Alk, *J* = 8.3 and 13.7 Hz (major and minor)), 2.52-2.63 (2H, m, Alk*CH*$_2$NH (major and minor)), 2.68 (1H, dd, Ph*CH*$_2$-Alk, *J* = 5.5 and 13.8 Hz (major and minor)), 2.94 (6H, s, ArN(C*H*$_3$)$_2$ (major and minor)), 3.57-3.63 (1H, m, *CH*$_2$-O (major and minor)), 3.67 (1.4H, s, HN*CH*$_2$Ar (major)), 3.69 (0.4H, s, HN*CH*$_2$Ar (minor)) 3.71-3.78 (1H, m, *CH*$_2$-O (major and minor)), 6.61-6.67 (3H, m, Ar-H (major and minor)), 7.11-7.13 (2H, m, Ar-H (major and minor)), 7.16-7.19 (2H, m, Ar-H (major and minor)), 7.24-7.27 (2H, m, Ar-H (major and minor)); ^{13}C δ/ppm (125 MHz, $CDCl_3$) 21.8, 29.4, 29.7, 30.3, 31.9, 32.9, 33.1, 37.2, 37.3, 39.4, 39.8, 40.7, 42.8, 43.0, 47.3, 47.4, 54.3, 61.9, 71.8, 111.4, 112.4, 116.5, 125.8, 128.3, 129.1, 141.5, 150.8; LC-MS (ESI+) *m/z* = 395.5 $[M+H]^+$; Analytical HPLC: 95.4%

3-(2,2-Dimethyltetrahydro-2*H*-pyran-4-yl)-*N*-(4-isopropylbenzyl)-4-phenylbutan-1-amine (16d)[79]

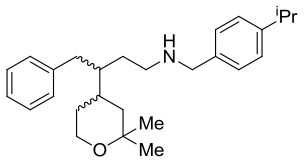

General Procedure A: Using amine **28** (200 mg, 0.77 mmol) and 4-isopropylbenzaldehyde (0.14 mL, 0.16 g, 0.92 mmol), chromatography (silica, 20% EtOAc, DCM followed by 5% $NH_{3(aq)}$/MeOH, DCM) eluted **16d**, as an inseparable mixture of diastereoisomers (*dr* = 5:2), as a yellow oil (47 mg, 16%); R_f = 0.37 (silica, 5% $NH_{3(aq)}$/MeOH, DCM); IR ν_{max}/cm^{-1} 3026 (C-H), 2960 (C-H), 2927 (C-H), 2865 (C-H), 2818 (C-H), 1602, 1495, 1454, 1364, 1203, 1086, 818, 737, 699; ^{1}H δ/ppm (500 MHz, $CDCl_3$) 1.10 (2.3H, s, Alk-C*H*$_3$ (major), 1.12 (0.8H, s, Alk-C*H*$_3$ (minor)), 1.20 (2.5H, s, Alk-C*H*$_3$ (major), 1.22 (0.9H, s, Alk-C*H*$_3$ (minor)), 1.25 (3H, s, ArCH(C*H*$_3$)$_2$ (major and minor)), 1.26 (3H, s, ArCH(C*H*$_3$)$_2$ (major and minor)), 1.25-1.28 (2H, m, Alk-H (major and minor)), 1.36-1.62 (7H, m, Alk-H (major and minor)), 1.72-1.79 (1H,

m, N*H* (major and minor)), 2.41 (1H, dd, Alk-H, *J* = 8.5 and 13.7 Hz (major and minor)), 2.50-2.61 (2H, m, CH_2CH_2NH (major and minor)), 2.67 (1H, dd, Alk-H, *J* = 5.6 and 13.6 Hz (major and minor)), 2.89 (1H, hep, Alk-H, *J* = 6.9 Hz, $ArCH(CH_3)_2$ (major and minor)), 3.58-3.63 (1H, m, Alk-H (major and minor)), 3.68 (1.5H, s, $NHCH_2Ar$ (major)), 3.70 (0.5H, s, $NHCH_2Ar$ (minor)), 3.72-3.78 (1H, m, Alk-H (major and minor)), 7.11 (2H, d, Ar-H, *J* = 7.4 Hz (major and minor)), 7.16-7.18 (5H, m, Ar-H (major and minor)), 7.24-7.27 (2H, m, Ar-H (major and minor)); ^{13}C δ/ppm (125 MHz, $CDCl_3$) 21.8, 24.0, 29.4, 29.7, 30.3, 31.9, 32.9, 33.1, 33.8, 37.2, 39.5, 39.8, 42.8, 43.0, 47.4, 53.7, 61.9, 71.8, 125.8, 126.4, 128.1, 128.3, 129.1, 137.7, 141.5, 147.6; LC-MS (ESI+) *m/z* = 394.2 $[M+H]^+$; HRMS calcd. for $C_{27}H_{40}NO$ $[M+H]^+$ 394.3104, found 394.3091; Analytical HPLC: 99.8%

_N_-(4-Chlorobenzyl-3-(2,2-dimethyltetrahydro-2_H_-pyran-4-yl)-4-phenylbutan-1-amine (16e)[79]

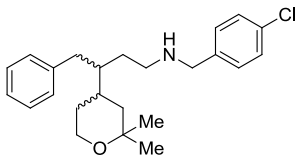

General Procedure A: Using amine **28** (212 mg, 0.81 mmol) and 4-chlorobenzaldehyde (137 mg, 0.97 mmol), chromatography (silica, 20% EtOAc, DCM followed by 5% $NH_{3(aq)}$/MeOH, DCM) afforded **16e**, as an inseparable mixture of diastereoisomers (*dr* = 5:2), as a yellow oil (80 mg, 26%); R_f = 0.34 (silica, 5% $NH_{3(aq)}$/MeOH, DCM); IR ν_{max}/cm^{-1} 2970 (C-H), 2929 (C-H), 2857 (C-H), 1601, 1491, 1453, 1365, 1285, 1202, 1086, 1015, 962, 801, 738, 699; ^1H δ/ppm (500 MHz, $CDCl_3$) 1.12 (2.5H, s Alk-C*H*$_3$ (major)), 1.14 (0.8H, s Alk-C*H*$_3$ (minor)) 1.21 (2.2H, s Alk-C*H*$_3$ (major)), 1.23 (0.7H, s Alk-C*H*$_3$ (minor)) 1.23-1.29 (2H, m, Alk-H (major and minor)), 1.34-1.61 (6H, m, Alk-H (major and minor)), 1.73-1.80 (1H, m, N*H* (major and minor)), 2.40 (1H, dd, Alk-H, *J* = 8.6 and 13.7 Hz (major and minor)), 2.46-2.60 (2H, m, CH_2CH_2NH (major and minor)), 2.68 (1H, dd, Alk-H, *J* = 5.9 and 13.7 Hz (major and minor)), 3.58-3.64 (1H, m, Alk-H (major and minor)), 3.65 (1.4H, s, $NHCH_2Ar$ (major)), 3.67 (0.5H, s, $NHCH_2Ar$ (minor)) 3.71-3.79 (1H, m, Alk-H(major and minor)), 7.11 (2H, d, Ar-H, *J* = 8.2 Hz (major and minor)), 7.17-7.20 (3H, m, Ar-H (major and minor)), 7.25-7.28 (4H, m, Ar-H (major and minor)); ^{13}C δ/ppm (125 MHz, $CDCl_3$) 21.8, 29.4, 29.7, 30.4, 31.9, 33.0, 33.3, 37.3, 39.5, 39.8, 42.8, 43.0, 47.5, 53.2,

53.4, 61.9, 71.8, 125.8, 128.3, 128.5, 129.0, 129.4, 132.6, 138.9, 141.5; LC-MS (ESI+) *m/z* = 386.2 $[M+H]^+$; HRMS calcd. for $C_{24}H_{33}{}^{35}ClNO$ $[M+H]^+$ 386.2245, found 386.2236; Analytical HPLC: 97.4%

4-(((3-(2,2-Dimethyltetrahydro-2*H*-pyran-4-yl)-4-phenylbutyl)amino)methyl)benzonitrile (16f)

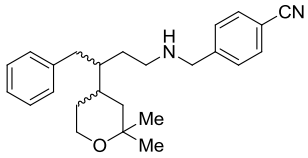

General Procedure A: Using amine **28** (100 mg, 0.38 mmol) and 4-formylbenzonitrile (61 mg, 0.46 mmol), chromatography (silica, 10-50% EtOAc, DCM) afforded **16f**, as an inseparable mixture of diastereoisomers (*dr* = 5:2), as a yellow oil (82 mg, 64%); R_f = 0.17 (silica, 50% EtOAc, DCM); UV λ_{max} (EtOH/nm) 279.0 and 268.0; IR ν_{max}/cm^{-1} 2926 (C-H), 2857 (C-H), 2228 (C≡N), 1608, 1494, 1453, 1365, 1204, 1084, 1041, 857, 817, 738, 699; ^{1}H δ/ppm (500 MHz, $CDCl_3$) 1.12 (2.2H, s, Alk-C*H*$_3$ (major)), 1.14 (0.9H, s, Alk-C*H*$_3$ (minor)), 1.21 (2.3H, s, Alk-C*H*$_3$ (major)), 1.23 (0.8H, s, Alk-C*H*$_3$ (minor)), 1.26-1.29 (1H, m, Alk-H (major and minor)), 1.35-1.59 (8H, m, Alk-H (major and minor)), 1.73-1.80 (1H, m, N*H* (major and minor)), 2.39 (1H, dd, Alk-H, *J* = 8.7 and 13.7 Hz (major and minor)), 2.46-2.57 (2H, m, CH_2*CH*$_2$NH (major and minor)), 2.70 (1H, dd, Alk-H, *J* = 5.5 and 13.7 Hz (major and minor)), 3.61 (1H, t, Alk-H, *J* = 12.1 Hz (major and minor)), 3.73 (1.6H, s, NH*CH*$_2$Ar (major)), 3.75 (0.5H, s, NH*CH*$_2$Ar (minor)), 3.76-3.79 (1H, m, Alk-H (major and minor)), 7.11 (2H, d, Ar-H, *J* = 7.2 Hz (major and minor)), 7.16-7.19 (1H, m, Ar-H (major and minor)), 7.24-7.27 (2H, m, Ar-H (major and minor)), 7.35-7.38 (2H, m, Ar-H (major and minor)), 7.58 (2H, d, Ar-H, *J* = 8.2 Hz (major and minor)); ^{13}C δ/ppm (125 MHz, $CDCl_3$) 21.8, 29.4, 29.7, 30.5, 31.9, 33.1, 33.4, 37.4, 39.5, 39.9, 42.8, 42.9, 47.7, 53.4, 61.8, 71.8, 110.7, 119.0, 125.9, 128.3, 128.6, 129.0, 132.2, 141.4, 146.1; LC-MS (ESI+) *m/z* = 377.4 $[M+H]^+$; Analytical HPLC: 95.8%

3-(2,2-Dimethyltetrahydro-2*H*-pyran-4-yl)-*N*-(4-methoxybenzyl)-4-phenylbutan-1-amine (16g)[79]

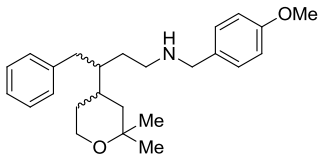

General Procedure A: Using amine **28** (100 mg, 0.38 mmol) and 4-anisaldehyde (56 µL, 62.7 mg, 0.46 mmol), chromatography (silica, 10-20% EtOAc, DCM followed by 10% MeOH, Et_2O) afforded **16g**, as an inseparable mixture of diastereoisomers (*dr* = 5:2), as a colourless oil (69 mg, 53%); R_f = 0.39 (silica, 10% MeOH, Et_2O); UV λ_{max} (EtOH/nm) 275.0; IR ν_{max}/cm^{-1} 2930 (C-H), 2856 (C-H), 1584, 1511, 1453, 1379, 1243, 1179, 1084, 1037, 822, 737, 699; ^1H δ/ppm (500 MHz, $CDCl_3$) 1.12 (2.3H, s, Alk-C*H*$_3$ (major)), 1.13 (0.8H, s, Alk-C*H*$_3$ (minor)), 1.21 (2.3H, s, Alk-C*H*$_3$ (major)), 1.22 (0.8H, s, Alk-C*H*$_3$ (minor)), 1.23-1.29 (1H, m, Alk-H (major and minor)), 1.33-1.60 (8H, m, Alk-H (major and minor)), 1.73-1.76 (1H, m, N*H* (major and minor)), 2.40 (1H, dd, *J* = 8.5 and 13.7 Hz, Alk-H (major and minor)), 2.48-2.59 (2H, m, CH_2CH_2NH (major and minor)), 2.66 (1H, dd, Alk-H, *J* = 5.7 and 13.6 Hz (major and minor)), 3.58-3.61 (1H, m, Alk-H (major and minor)), 3.63 (1.7 H, s, NHC*H*$_2$Ar (major)), 3.65 (0.5 H, s, NHC*H*$_2$Ar (minor)), 3.72-3.79 (4H, m, Alk-H and OC*H*$_3$ (major and minor)), 6.85 (2H, d, Ar-H, *J* = 8.6 Hz (major and minor)), 7.11 (2H, d, Ar-H, *J* = 7.3 Hz (major and minor)), 7.16-7.19 (3H, m, Ar-H (major and minor)), 7.25-7.28 (2H, m, Ar-H (major and minor)); ^{13}C δ/ppm (125 MHz, $CDCl_3$) 21.8, 29.4, 29.7, 30.3, 30.4, 31.9, 32.9, 33.1, 37.2, 37.3, 39.5, 39.8, 42.9, 43.0, 47.4, 53.3, 55.3, 61.9, 71.8, 113.8, 125.8, 128.3, 129.1, 129.2, 132.5, 141.5, 158.6; LC-MS (ESI+) *m/z* = 382.5 $[M+H]^+$; Analytical HPLC: 98.8%

5-(((3-(2,2-Dimethyltetrahydro-2*H*-pyran-4-yl)-4-phenylbutyl)amino)methyl)-*N*,*N*-dimethylpyridin-2-amine (16h)

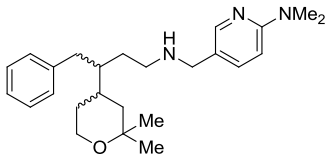

General Procedure A: Using amine **28** (100 mg, 0.38 mmol) and 6-(*N*,*N*-dimethylamino)nicotinaldehyde (69 mg, 0.46 mmol), chromatography (silica, 5% MeOH, Et_2O followed by 20% MeOH, EtOAc) afforded **16h**, as an inseparable mixture of diastereoisomers (*dr* = 5:2), as a dark yellow oil (63 mg, 47%); R_f = 0.33 (silica, 10% MeOH, DCM); UV λ_{max} (EtOH/nm) 253.5; IR ν_{max}/cm^{-1} 2926 (C-H), 2856 (C-H), 1608, 1559, 1511, 1453, 1398, 1364, 1318, 1208, 1178, 1085, 1015, 958, 858, 806, 738, 700; ^1H δ/ppm (500 MHz, $CDCl_3$) 1.11 (2.2H, s, Alk-C*H*$_3$ (major)), 1.12 (0.7H, s, Alk-C*H*$_3$ (minor)), 1.20 (2.2H, s, Alk-C*H*$_3$ (major)), 1.22 (2.2H, s, Alk-C*H*$_3$ (minor)), 1.25-1.27 (1H, m, Alk-H (major and minor)), 1.34-1.59 (7H, m, Alk-H (major and minor)), 1.71-1.77 (1H, m, N*H* (major and minor)), 2.39 (1H, dd, Ph*CH*$_2$-Alk, *J* = 8.4 and 13.7 Hz (major and minor)), 2.46-2.58 (2H, m, Alk*CH*$_2$-NH (major and minor)), 2.67 (1H, dd, Ph*CH*$_2$-Alk, *J* = 5.3 and 13.7 Hz (major and minor)), 3.07 (6H, s, Ar-N(C*H*$_3$)$_2$ (major and minor)), 3.56 (1.6H, s, HN-*CH*$_2$Ar (major)), 3.58 (0.5H, s, HN-*CH*$_2$Ar (minor)), 3.58-3.62 (1H, m, C*H*$_2$-O (major and minor)), 3.71-3.77 (1H, m, C*H*$_2$-O (major and minor)), 6.47-6.49 (1H, m, Ar-H (major and minor)), 7.10-7.12 (2H, m, Ar-H (major and minor)), 7.15-7.18 (1H, m, Ar-H (major and minor)), 7.24-7.27 (2H, m, Ar-H (major and minor)), 7.41-7.44 (1H, m, Ar-H (major and minor)), 8.01-8.03 (1H, m, Ar-H (major and minor)); ^{13}C δ/ppm (125 MHz, $CDCl_3$) 21.8, 29.4, 29.6, 29.9, 31.9, 33.0, 33.2, 37.2, 37.3, 38.2, 39.4, 39.8, 42.8, 43.0, 46.7, 50.3, 61.8, 71.8, 105.7, 125.8, 128.3, 129.0, 129.1, 137.8, 141.3, 147.8, 158.9; LC-MS (ESI+) *m/z* = 396.5 $[M+H]^+$; HRMS calcd. for $C_{26}H_{39}N_2O$ $[M+H]^+$ 396.3009, found 396.3011; Analytical HPLC: 97.6%

***(±)*-*N*,*N*-Dimethyl-4-(((4-phenyl-3-(tetrahydro-2*H*-pyran-4-yl)butyl)amino)methyl)aniline (68a)[79]**

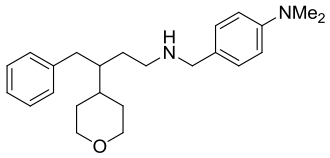

General Procedure A: Using amine **67** (200 mg, 0.86 mmol) and 4-(*N*,*N*-dimethylamino)benzaldehyde (154 mg, 1.03 mmol), chromatography (silica, 20% EtOAc, DCM followed by 2% $NH_{3(aq)}$, MeOH) afforded **68a** as a yellow oil (299 mg, 95%); R_f = 0.54 (silica, 2% $NH_{3(aq)}$, MeOH); UV λ_{max} (EtOH/nm) 302.0 and 263.0; IR ν_{max}/cm^{-1} 3024 (C-H), 2928 (C-H), 2840 (C-H), 1614, 1521, 1443, 1342, 1228, 1091, 1014, 946, 804, 740, 699 ^{1}H δ/ppm (500 MHz, $CDCl_3$) 1.36-1.65 (9H, m, Alk-H and N*H*), 2.44 (1H, dd, Alk-H, *J* = 7.72 and 13.7 Hz), 2.53-2.63 (2H, m, CH_2CH_2NH), 2.67 (1H, dd, Alk-H, *J* = 6.2 and 13.7 Hz), 2.93 (6H, s, N(CH_3)$_2$), 3.29-3.35 (2H, m, Alk-H), 3.61 (2H, s, NHCH_2Ar), 3.95-4.02 (2H, m, Alk-H), 6.70 (2H, d, Ar-H, *J* = 8.7 Hz) 7.10-7.15 (4H, m, Ar-H), 7.18 (1H, t, Ar-H, *J* = 7.4 Hz), 7.24-7.29 (2H, m, Ar-H); ^{13}C δ/ppm (125 MHz, $CDCl_3$) 29.5, 29.8, 30.5, 37.3, 37.4, 40.8, 43.0, 47.4, 53.5, 68.5, 112.7, 125.8, 128.3, 128.5, 129.0, 129.1, 141.5, 149.8; LC-MS (ESI+) *m/z* = 367.4 $[M+H]^+$; HRMS calcd. for $C_{24}H_{35}N_2O$ $[M+H]^+$ 367.2744, found 367.2743; Analytical HPLC: 97.9%

(*R*)- and (*S*)-*N*,*N*-Dimethyl-4-(((4-phenyl-3-(tetrahydro-2*H*-pyran-4-yl)butyl)amino)methyl)aniline ((*R*)- and (*S*)-68a)

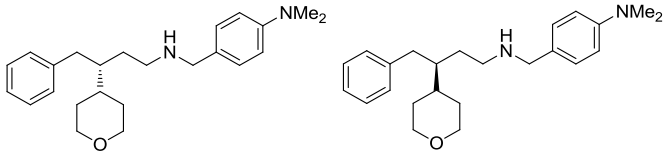

General Procedure A: Using either (*R*)- or (*S*)-amine **(*R*)-67** or **(*S*)-67** (115 mg, 0.49 mmol and 133 mg, 0.57 mmol respectively), chromatography (silica, 5-15% MeOH, DCM) afforded **(*R*)-** and **(*S*)-68** as yellow oils (29 mg, 16% and 137 mg, 65% respectively). Analytical data equivalent to ***(±)*-68**; $[\alpha]_D^{26.5}$ +11.4^o (*R*) (*c* 1.97 in EtOH), $[\alpha]_D^{26.5}$ -11.0^o (*S*) (*c* 1.97 in EtOH)

4-Phenyl-*N*-(4-(pyrrolidin-1-yl)benzyl)-3-(tetrahydro-2*H*-pyran-4-yl)butan-1-amine (68b)

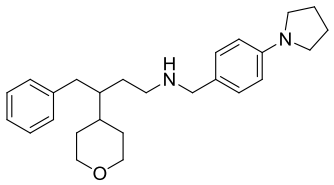

General Procedure A: Using amine **67** (50 mg, 0.21 mmol) and 4-(1-pyrrolidinyl)benzaldehyde (45.6 mg, 0.26 mmol), chromatography (silica, 20% EtOAc, DCM followed by 5-10% MeOH, DCM) afforded **68b** as a yellow oil (392 mg, 77%); R_f = 0.35 (silica, 10% MeOH, DCM); UV λ_{max} (EtOH/nm) 262.0; IR ν_{max}/cm^{-1} 2930 (C-H), 2838 (C-H), 1614, 1521, 1488, 1454, 1368, 1181, 1092, 1014, 963, 802, 738, 700; ^{1}H δ/ppm (500 MHz, $CDCl_3$) 1.42-1.59 (9.5H, m, Alk-H, N*H* and H_2O), 1.97-2.00 (4H, m, (C*H*$_2$)$_2$, pyrrolidino ring), 2.42 (1H, dd, PhC*H*$_2$, *J* = 7.5 and 13.6 Hz), 2.53-2.61 (2H, m, AlkC*H*$_2$-NH), 2.66 (1H, dd, PhC*H*$_2$, *J* = 5.7 and 13.6 Hz), 3.25-3.27 (4H, m, (C*H*$_2$)$_2$, pyrrolidino ring), 3.28-3.35 (2H, m, C*H*$_2$-O), 3.61 (2H, s, HN-C*H*$_2$Ar), 3.95-4.00 (2H, m, C*H*$_2$-O), 6.50-6.52 (2H, m, Ar-H), 7.11-7.13 (4H, m, Ar-H), 7.16-7.19 (1H, m, Ar-H), 7.25-7.28 (2H, m, Ar-H); ^{13}C δ/ppm (125 MHz, $CDCl_3$) 25.5, 29.5, 29.7, 37.2, 37.4, 43.0, 47.7, 68.5, 111.6, 125.8, 128.3, 129.1, 129.4, 141.4, 147.3; LC-MS (ESI+) *m/z* = 393.3 $[M+H]^+$; HRMS calcd. for $C_{26}H_{37}ON_2$ $[M+H]^+$ 393.2900, found 393.2901; Analytical HPLC: 97.9%

4-Phenyl-3-(tetrahydro-2*H*-pyran-4-yl)-*N*-(4-(trifluoromethyl)benzyl)butan-1-amine (68c)

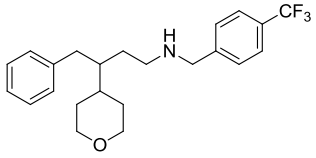

General Procedure A: Using amine **67** (50 mg, 0.21 mmol) and 4-(trifluoromethyl)benzaldehyde (35 µL, 44.6 mg, 0.25 mmol), chromatography (silica, 0-10% MeOH, DCM) afforded **68c** as a yellow oil (73 mg, 85%); R_f = 0.36 (silica, 5% MeOH, DCM); UV λ_{max} (EtOH/nm) 258.5; IR ν_{max}/cm^{-1} 2928 (C-H), 2843 (C-H), 1619, 1454, 1323 (sharp), 1161, 1117, 1065, 1017, 822, 739, 699; ^{1}H δ/ppm (500 MHz, $CDCl_3$) 1.37-1.63 (11.5H, m, Alk-H, N*H* and H_2O), 2.41 (1H, dd, PhC*H*$_2$, *J* = 8.1 and

13.6 Hz), 2.50-2.60 (2H, m, AlkCH_2-NH), 2.70 (1H, dd, PhCH_2, J = 5.9 and 13.6 Hz), 3.29-3.36 (2H, m, CH_2-O), 3.74 (2H, s, HN-CH_2Ar), 3.96-4.01 (2H, m, CH_2-O), 7.12 (2H, d, Ar-H, J = 7.6 Hz), 7.17-7.19 (1H, m, Ar-H), 7.25-7.28 (2H, m, Ar-H), 7.37 (2H, d, Ar-H, J = 8.0 Hz), 7.56 (2H, d, Ar-H, J = 8.1 Hz); ^{13}C δ/ppm (125 MHz, $CDCl_3$) 29.5, 29.8, 30.5, 37.5, 42.9, 47.6, 53.4, 68.4, 125.18, 125.24, 125.9, 128.2, 128.3, 129.0, 129.3, 141.4, 144.5; LC-MS (ESI+) *m/z* = 392.1 $[M+H]^+$; HRMS calcd. for $C_{23}H_{29}ONF_3$ $[M+H]^+$ 392.2196, found 392.2195; Analytical HPLC: 95.4%

***N*-(4-(Methylthio)benzyl)-4-phenyl-3-(tetrahydro-2*H*-pyran-4-yl)butan-1-amine (68d)**

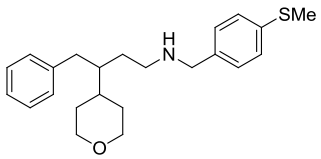

General Procedure A: Using amine **67** (100 mg, 0.43 mmol) and 4-(thiomethyl)benzaldehyde (70 µL, 80.1 mg, 0.52 mmol), chromatography (silica, 0-10% MeOH, DCM) afforded **68d** as a yellow oil (127 mg, 77%); R_f = 0.27 (silica, 5% MeOH, DCM); UV λ_{max} (EtOH/nm) 257.5; IR ν_{max}/cm^{-1} 2924 (C-H), 2838 (C-H), 1601, 1493, 1453, 1090, 1014, 800, 739, 699; ^{1}H δ/ppm (500 MHz, $CDCl_3$) 1.37-1.61 (11.5H, m, Alk-H, N*H* and H_2O), 2.42 (1H, dd, PhCH_2, J = 7.9 and 13.6 Hz), 2.47 (3H, s, SCH_3), 2.50-2.61 (2H, m, AlkCH_2-NH), 2.68 (1H, dd, PhCH_2, J = 6.1 and 13.8 Hz), 3.29-3.35 (2H, m, CH_2-O), 3.65 (2H, s, HN-CH_2Ar), 3.96-4.01 (2H, m, CH_2-O), 7.12 (2H, d, Ar-H, J = 7.1 Hz), 7.17-7.22 (5H, m, Ar-H), 7.25-7.28 (2H, m, Ar-H); ^{13}C δ/ppm (125 MHz, $CDCl_3$) 16.1, 29.5, 29.7, 30.4, 37.4, 43.0, 47.4, 53.4, 68.4, 125.8, 126.9, 128.3, 128.7, 129.1, 136.8, 141.4; LC-MS (ESI+) *m/z* = 370.4 $[M+H]^+$; HRMS calcd. for $C_{23}H_{32}ONS$ $[M+H]^+$ 370.2199, found 370.2202; Analytical HPLC: 96.3%

***N*-(4-Chlorobenzyl)-4-phenyl-3-(tetrahydro-2*H*-pyran-4-yl)butan-1-amine (68e)[79]**

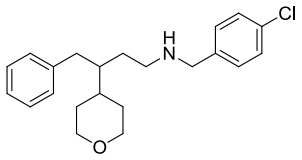

General Procedure A: Using amine **67** (100 mg, 0.43 mmol) and 4-chlorobenzaldehyde (74 mg, 0.52 mmol), chromatography (silica, 0-10% MeOH, DCM) afforded **68e** as a yellow oil (116 mg, 72%); R_f = 0.38 (silica, 5% MeOH, DCM); UV λ_{max} (EtOH/nm) 260.0; IR ν_{max}/cm^{-1} 2928 (C-H), 2841 (C-H), 1601, 1490, 1453, 1242, 1089, 1014, 982, 801, 739, 699; ^{1}H δ/ppm (500 MHz, $CDCl_3$) 1.36-1.61 (12H, m, Alk-H, N*H* and H_2O), 2.41 (1H, dd, PhC*H*$_2$, *J* = 7.8 and 13.8 Hz), 2.49-2.59 (2H, m, AlkC*H*$_2$-NH), 2.69 (1H, dd, PhC*H*$_2$, *J* = 5.4 and 13.2 Hz), 3.29-3.36 (2H, m, C*H*$_2$-O), 3.66 (2H, s, HN-C*H*$_2$Ar), 3.96-4.01 (2H, m, C*H*$_2$-O), 7.12 (2H, d, Ar-H, *J* = 7.5 Hz), 7.17-7.20 (3H, m, Ar-H), 7.25-7.28 (4H, m, Ar-H); ^{13}C δ/ppm (125 MHz, $CDCl_3$) 29.5, 29.7, 30.5, 37.5, 43.0, 47.5, 53.2, 68.4, 125.8, 128.3, 128.5, 129.0, 129.4, 132.6, 138.9, 141.4; LC-MS (ESI+) *m/z* = 358.4 $[M+H]^+$; HRMS calcd. for $C_{22}H_{29}ON^{35}Cl$ $[M+H]^+$ 358.1932, found 358.1936; Analytical HPLC: 93.8%

***N*-(4-Fluorobenzyl)-4-phenyl-3-(tetrahydro-2*H*-pyran-4-yl)butan-1-amine (68f)[79]**

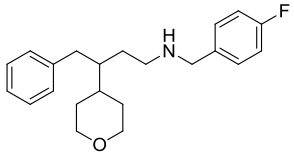

General Procedure A: Using amine **67** (50 mg, 0.21 mmol) and 4-fluorobenzaldehyde (27 μL, 31.2 mg, 0.25 mmol), chromatography (silica, 0-10% MeOH, DCM) afforded **68f** as a yellow oil (43 mg, 58%); R_f = 0.30 (silica, 5% MeOH, DCM); UV λ_{max} (EtOH/nm) 264.0; IR ν_{max}/cm^{-1} 2928 (C-H), 2842 (C-H), 1602, 1508, 1454, 1387, 1219, 1091, 1014, 822, 739, 699; ^{1}H δ/ppm (500 MHz, $CDCl_3$) 1.37-1.62 (11H, m, Alk-H, N*H* and H_2O), 2.42 (1H, dd, PhC*H*$_2$, *J* = 8.0 and 13.6 Hz), 2.50-2.60 (2H, m, AlkC*H*$_2$-NH), 2.69 (1H, dd, PhC*H*$_2$, *J* = 5.8 and 13.7 Hz), 3.29-3.36 (2H, m, C*H*$_2$-O), 3.66 (2H, s, HN-C*H*$_2$Ar), 3.96-4.01 (2H, m, C*H*$_2$-O), 6.97-7.00 (2H, m, Ar-H), 7.12 (2H, d, Ar-H, *J* = 7.4 Hz), 7.17-7.22 (3H, m, Ar-H), 7.25-7.28 (2H, m, Ar-H); ^{13}C δ/ppm (125 MHz, $CDCl_3$) 29.5, 29.7, 30.4, 37.4, 43.0, 47.5, 53.1, 68.4, 115.1, 125.8, 128.3, 129.0, 129.6, 141.4,

160.9, 162.9; LC-MS (ESI+) *m/z* = 342.1 $[M+H]^+$; HRMS calcd. for $C_{22}H_{29}ONF$ $[M+H]^+$ 342.2228, found 342.2230; Analytical HPLC: 95.4%

_N_-(4-Nitrobenzyl)-4-phenyl-3-(tetrahydro-2*H*-pyran-4-yl)butan-1-amine (68g)

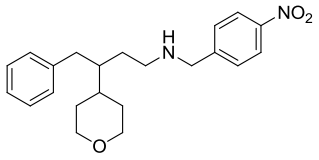

General Procedure A: Using amine **67** (450 mg, 1.93 mmol) and 4-nitrobenzaldehyde (351 mg, 2.32 mmol), chromatography (silica, 5% EtOAc, DCM followed by 10% MeOH, DCM) afforded **68g** as a yellow gum (467 mg, 66%); R_f = 0.38 (silica, 2% MeOH, DCM); m.p. 39-45 ^oC; UV λ_{max} (EtOH/nm) 266.5; IR ν_{max}/cm^{-1} 3409 (N-H), 2932 (C-H), 2845 (C-H), 2752 (C-H), 1605, 1519, 1454, 1344, 1090, 1014, 982, 856, 739, 698; ^1H δ/ppm (500 MHz, $CDCl_3$) 1.42-1.69 (8H, m, Alk-H), 1.80-1.87 (1H, m, N*H*), 2.31 (1H, dd, PhC*H*$_2$, *J* = 9.0 and 13.8 Hz), 2.41-2.47 (1H, m, AlkC*H*$_2$-NH), 2.54-2.60 (1H, m, AlkC*H*$_2$-NH), 2.76 (1H, dd, PhC*H*$_2$, *J* = 4.9 and 13.8 Hz), 3.27-3.32 (2H, m, C*H*$_2$-O), 3.89 (2H, s, HN-C*H*$_2$Ar), 3.94-3.97 (2H, m, C*H*$_2$-O), 7.09 (2H, d, Ar-H, *J* = 7.0 Hz), 7.17 (1H, t, Ar-H, *J* = 7.4 Hz), 7.22-7.25 (2H, m, Ar-H), 7.56 (2H, d, Ar-H, *J* = 8.7 Hz), 8.17 (2H, d, Ar-H, *J* = 8.8 Hz); ^{13}C δ/ppm (125 MHz, $CDCl_3$) 27.4, 29.5, 29.7, 37.5, 38.2, 42.9, 45.2, 49.7, 68.2, 124.1, 126.3, 128.6, 128.9, 130.7, 140.5, 148.2; LC-MS (ESI+) *m/z* = 369.7 $[M+H]^+$; HRMS calcd. for $C_{22}H_{29}O_3N_2$ $[M+H]^+$ 369.2173, found 369.2175; Analytical HPLC: 98.7%

2-(Methyl-(4-(((4-phenyl-3-(tetrahydro-2*H*-pyran-4-yl)butyl)amino)methyl)phenyl)amino)ethanol (68j)

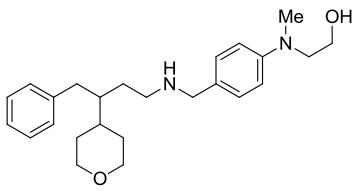

General Procedure A: Using amine **67** (100 mg, 0.43 mmol) and 4-(*N*-methyl-*N*-(2-hydroxyethyl)amino)benzaldehyde (93.2 mg, 0.52 mmol), chromatography (silica, 5-20% MeOH, Et_2O) afforded **68j** as a yellow gum (93 mg, 55%); R_f = 0.14 (silica, 20%

MeOH, DCM); UV λ_{max} (EtOH/nm) 262.5; IR ν_{max}/cm^{-1} 3368 (br) (N-H and O-H), 2929 (C-H), 2846 (C-H), 1613, 1521, 1453, 1369, 1189, 1091, 1051, 803, 740, 700; ^{1}H δ/ppm (500 MHz, $CDCl_3$) 1.42-1.61 (9H, m, Alk-H and N*H*), 1.94 (1H, s, br, O*H*), 2.42 (1H, dd, PhC*H*$_2$, *J* = 7.6 and 13.7 Hz), 2.53-2.63 (2H, m, AlkC*H*$_2$-NH), 2.67 (1H, dd, PhC*H*$_2$, *J* = 5.8 and 13.7 Hz), 2.94 (3H, s, NC*H*$_3$), 3.28-3.34 (2H, m, C*H*$_2$-O), 3.44 (2H, t, MeN-C*H*$_2$, *J* = 5.6 Hz), 3.61 (2H, s, HN-C*H*$_2$Ar), 3.79 (2H, t, C*H*$_2$OH, *J* = 5.7 Hz), 3.95-3.99 (2H, m, C*H*$_2$-O), 6.73-6.75 (2H, m, Ar-H), 7.11-7.15 (4H, m, Ar-H), 7.17-7.20 (1H, m, Ar-H), 7.25-7.28 (2H, m, Ar-H); ^{13}C δ/ppm (125 MHz, $CDCl_3$) 29.4, 29.7, 29.9, 37.3, 37.4, 38.9, 43.0, 47.0, 52.9, 55.6, 60.1, 68.4, 113.1, 125.9, 128.4, 129.1, 129.5, 141.4, 149.4; LC-MS (ESI+) *m/z* = 397.4 $[M+H]^+$; HRMS calcd. for $C_{25}H_{37}O_2N_2$ $[M+H]^+$ 397.2850, found 397.2852; Analytical HPLC: 96.8%

_N_-(4-(Methylsulfonyl)benzyl)-4-phenyl-3-(tetrahydro-2*H*-pyran-4-yl)butan-1-amine (68k)

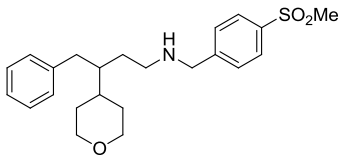

General Procedure A: Using amine **67** (50 mg, 0.21 mmol) and 4-(methanesulfonyl)benzaldehyde (47.9 mg, 0.26 mmol), chromatography (silica, 17% EtOAc, DCM followed by 20% MeOH, DCM) afforded **68k** as a blue/green oil (63 mg, 75%); R_f = 0.22 (silica, 5% MeOH, DCM); UV λ_{max} (EtOH/nm) No distinguishable peak; IR ν_{max}/cm^{-1} 2929 (C-H), 2843 (C-H), 1600, 1454, 1408, 1304 (S=O asym. stretch), 1148 (S=O sym. stretch), 1089, 1016, 956, 735, 701; ^{1}H δ/ppm (500 MHz, $CDCl_3$) 1.39-1.66 (10.5H, m, Alk-H, N*H* and H_2O), 2.41 (1H, dd, PhC*H*$_2$, *J* = 8.1 and 13.6 Hz), 2.49-2.60 (2H, m, AlkC*H*$_2$-NH), 2.71 (1H, dd, PhC*H*$_2$, *J* = 5.8 and 13.7 Hz), 3.04 (3H, s, SO_2C*H*$_3$), 3.29-3.36 (2H, m, C*H*$_2$-O), 3.78 (2H, s, HN-C*H*$_2$Ar), 3.97-4.03 (2H, m, C*H*$_2$-O), 7.12-7.13 (2H, m, Ar-H), 7.17-7.20 (1H, m, Ar-H), 7.25-7.28 (2H, m, Ar-H), 7.46-7.47 (2H, m, Ar-H), 7.86-7.89 (2H, m, Ar-H); ^{13}C δ/ppm (125 MHz, $CDCl_3$) 29.5, 29.7, 30.3, 37.4, 37.6, 42.9, 44.6, 47.6, 50.9, 53.0, 53.4, 68.4, 125.9, 127.5, 128.4, 128.9, 129.0, 139.2, 141.3; LC-MS (ESI+) *m/z* = 402.7 $[M+H]^+$; HRMS calcd. for $C_{23}H_{32}O_3NS$ $[M+H]^+$ 402.2097, found 402.2098; Analytical HPLC: 97.4%

***N*-(4-Chlorobenzyl)-3-methyl-4-phenylbutan-1-amine (109)**

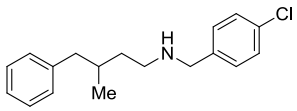

General Procedure A: Using amine **108** (43 mg, 0.26 mmol) and 4-chlorobenzaldehyde (43 mg, 0.31 mmol), chromatography (silica, 5% MeOH, DCM) afforded **109** as a yellow oil (20 mg, 27%); R_f = 0.33 (silica, 5% MeOH, DCM); UV λ_{max} (EtOH/nm) No distinguishable peak; IR ν_{max}/cm^{-1} 3026 (C-H), 2918 (C-H), 1598, 1490, 1453, 1089, 1015, 803, 738, 699; ^{1}H δ/ppm (500 MHz, $CDCl_3$) 0.90 (3H, d, C*H*$_3$, *J* = 6.6 Hz), 1.29-1.41 (2H, m, Alk-H and N*H*), 1.57-1.64 (1H, m, Alk-H), 1.79-1.89 (1H, m, Alk-H), 2.45 (1H, dd, PhC*H*$_2$, *J* = 7.9 and 13.4 Hz), 2.60-2.65 (2H, m, AlkC*H*$_2$-NH), 2.71 (1H, dd, PhC*H*$_2$, *J* = 5.6 and 9.4 Hz), 3.75 (2H, s, HN-C*H*$_2$Ar), 7.15-7.17 (2H, m, Ar-H), 7.19-7.22 (1H, m, Ar-H), 7.25-7.32 (6H, m, Ar-H); ^{13}C δ/ppm (125 MHz, $CDCl_3$) 19.6, 33.2, 36.8, 43.9, 47.3, 53.3, 125.8, 128.2, 128.5, 129.2, 129.5, 132.6, 138.9, 141.2; LC-MS (ESI+) *m/z* = 288.3 [M+H]$^+$; HRMS calcd. for $C_{18}H_{23}N^{35}Cl$ [M+H]$^+$ 288.1514, found 288.1518; Analytical HPLC: 95.2%

***N*-(4-Chlorobenzyl)-3-methylbutan-1-amine (111)**

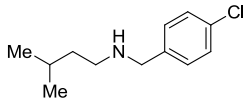

General Procedure A: Using isopentylamine (267 µL, 200 mg, 2.29 mmol) (**110**) and 4-chlorobenzaldehyde (394 mg, 2.80 mmol), chromatography (silica, 33% Et_2O, hexane) afforded **111** as a yellow oil (231 mg, 48%); R_f = 0.36 (silica, 5% MeOH, DCM); UV λ_{max} (EtOH/nm) 218.0; IR ν_{max}/cm^{-1} 2955 (C-H), 2923 (C-H), 2869 (C-H), 2822 (C-H), 1597, 1490, 1461, 1407, 1366, 1091, 1015, 806, 745; ^{1}H δ/ppm (500 MHz, $CDCl_3$) 0.89 (6H, d, CH(C*H*$_3$)$_2$, *J* = 6.6 Hz), 1.37-1.43 (3H, m, C*H*$_2$-CH$_2$-N*H*), 1.62 (1H, sep, C*H*(CH$_3$)$_2$, *J* = 6.7 Hz), 2.60-2.63 (2H, m, C*H*$_2$-NH), 3.75 (2H, s, HN-C*H*$_2$Ar), 7.25-7.30 (4H, m, Ar-H); ^{13}C δ/ppm (125 MHz, $CDCl_3$) 22.7, 26.2, 39.2, 47.6, 53.4, 128.5, 129.4, 132.5, 139.0; LC-MS (ESI+) *m/z* = 213.2 [M+H]$^+$; HRMS calcd. for $C_{12}H_{19}N^{35}Cl$ [M+H]$^+$ 212.1201, found 212.1202; Analytical HPLC: 98.1%

4-Chloro-*N*-(4-phenyl-3-(tetrahydro-2*H*-pyran-4-yl)butyl)benzamide (68l)

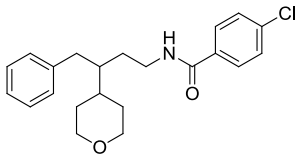

General Procedure B: Using amine **67** (50 mg, 0.21 mmol) and 4-chlorobenzoyl chloride (54 µL, 73.7 mg, 0.42 mmol), chromatography (silica, 10% EtOAc, DCM) afforded **68l** as a brown solid (73 mg, 94%); R_f = 0.23 (silica, 10% EtOAc, DCM); m.p. 110-112 ^oC; UV λ_{max} (EtOH/nm) 235.0; IR ν_{max}/cm^{-1} 3304 (N-H), 2956 (C-H), 2837 (C-H), 1627 (C=O), 1595, 1530, 1484, 1271, 1145, 1093, 1015, 844, 748, 702; ^1H δ/ppm (500 MHz, $CDCl_3$) 1.45-1.73 (14H, m, Alk-H and H_2O), 2.43 (1H, dd, PhCH_2, *J* = 8.9 and 13.7 Hz), 2.80 (1H, dd, PhCH_2, *J* = 5.1 and 13.7 Hz), 3.34-3.40 (4H, m, CH_2-O and AlkCH_2-NH), 3.99-4.03 (2H, m, CH_2-O), 5.72 (1H, m, N*H*), 7.17 (2H, d, Ar-H, *J* = 7.5 Hz), 7.19-7.22 (1H, m, Ar-H), 7.27-7.30 (2H, m, Ar-H), 7.37-7.38 (2H, m, Ar-H), 7.55-7.56 (2H, m, Ar-H); ^{13}C δ/ppm (125 MHz, $CDCl_3$) 29.6, 29.8, 30.0, 30.9, 37.2, 37.8, 38.5, 43.0, 68.4, 126.1, 128.2, 128.6, 128.8, 129.1, 132.9, 137.6, 141.3, 166.3; LC-MS (ESI+) *m/z* = 372.4 $[M+H]^+$; HRMS calcd. for $C_{22}H_{27}O_2N^{35}Cl$ $[M+H]^+$ 372.1725, found 372.1728; Analytical HPLC: 97.3%

4-(Dimethylamino)-*N*-(3-(2,2dimethyltetrahydro-2*H*-pyran-4-yl)-4-phenylbutyl)benzenesulfonamide (16j)

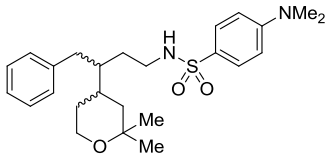

General Procedure B: Using amine **28** (100 mg, 0.38 mmol) and 4-(*N*,*N*-dimethylamino)benzenesulfonyl chloride (**71**) (101 mg, 0.46 mmol), chromatography (silica, 0-10% EtOAc, DCM) afforded **16j**, as an inseparable mixture of diastereoisomers (*dr* = 5:2), as a white solid (134 mg, 89%); R_f = 0.57 (silica, 10% MeOH, DCM); UV λ_{max} (EtOH/nm) 278.0; IR ν_{max}/cm^{-1} 3268 (N-H), 2930 (C-H), 2863 (C-H), 1596, 1516, 1446, 1365 (S=O asym. stretch), 1311, 1229, 1144 (S=O sym. stretch), 1093, 1000, 944, 858, 815, 772, 737, 700; ^1H δ/ppm (500 MHz, $CDCl_3$) 1.10 (2.3H, s, Alk-CH_3 (major)), 1.11 (0.8H, s, Alk-CH_3 (minor)), 1.14-1.20 (1H, m, Alk-H

(major and minor)), 1.19 (2.4H, s, Alk-C*H*$_3$ (major)), 1.20 (0.8H, s, Alk-C*H*$_3$ (minor)), 1.24-1.54 (6H, m, Alk-H (major and minor)), 1.64-1.69 (1H, m, Alk-H (major and minor)), 2.32 (1H, dd, PhC*H*$_2$, *J* = 8.8 and 13.7 Hz (major and minor)), 2.65 (1H, dd, PhC*H*$_2$, *J* = 5.5 and 13.7 Hz (major and minor)), 2.78-2.87 (2H, m, AlkC*H*$_2$-NH (major and minor)), 3.04 (6H, s, Ar-N(C*H*$_3$)$_2$ (major and minor)), 3.52-3.58 (1H, m, *CH*$_2$-O (major and minor)), 3.68-3.73 (1H, m, *CH*$_2$-O (major and minor)), 4.02 (1H, dt, N*H*, *J* = 6.1 and 17.0 Hz (major and minor)), 6.66 (2H, dd, Ar-H, *J* = 2.8 and 9.0 Hz (major and minor)), 7.06 (2H, d, Ar-H *J* = 7.3 Hz (major and minor)), 7.16-7.19 (1H, m, Ar-H (major and minor)), 7.23-7.26 (2H, m, Ar-H (major and minor)), 7.62-7.64 (2H, m, Ar-H (major and minor)); ^{13}C δ/ppm (125 MHz, $CDCl_3$) 21.8, 29.3, 29.5, 29.9, 30.0, 31.9, 32.8, 33.0, 36.9, 39.3, 39.7, 40.1, 41.2, 41.3, 41.9, 42.1, 61.7, 71.7, 110.9, 111.0, 125.0, 126.0, 128.4, 128.9, 129.0, 140.9, 152.8; LC-MS (ESI+) *m/z* = 445.5 $[M+H]^+$; HRMS calcd. for $C_{25}H_{36}N_2O_3S$ $[M+H]^+$ 445.2519, found 445.2519; Analytical HPLC: 96.6%

4-Chloro-*N*-(4-phenyl-3-(tetrahydro-2*H*-pyran-4-yl)butyl)benzenesulfonamide (68m)

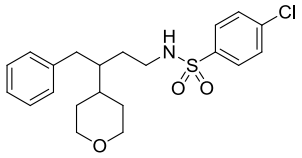

General Procedure B: Using amine **67** (50 mg, 0.21 mmol) and 4-chlorobenzenesulfonyl chloride (89 mg, 0.42 mmol), chromatography (silica, 5% EtOAc, DCM) afforded **68m** as a colourless oil (67 mg, 79%); R_f = 0.45 (silica, 10% EtOAc, DCM); UV λ_{max} (EtOH/nm) 230.5; IR ν_{max}/cm^{-1} 3280 (N-H), 2934 (C-H), 2849 (C-H), 1586, 1328 (S=O asym. stretch), 1159 (S=O sym. stretch), 1084, 1014, 827, 751, 700; ^{1}H δ/ppm (500 MHz, $CDCl_3$) 1.30-1.56 (13.5H, m, Alk-H and H_2O), 2.32 (1H, dd, PhC*H*$_2$, *J* = 8.6 and 13.6 Hz), 2.71 (1H, dd, PhC*H*$_2$, *J* = 5.2 and 13.6 Hz), 2.79-2.88 (2H, m, AlkC*H*$_2$-NH), 3.29-3.35 (2H, m, C*H*$_2$-O), 3.96-4.00 (2H, m, C*H*$_2$-O), 4.08-4.10 (1H, m, N*H*), 7.07 (2H, d, Ar-H, *J* = 7.1 Hz), 7.18-7.21 (1H, m, Ar-H), 7.25-7.28 (2H, m, Ar-H), 7.45-7.47 (2H, m, Ar-H), 7.69-7.70 (2H, m, Ar-H); ^{13}C δ/ppm (125 MHz, $CDCl_3$) 29.46, 29.54, 30.4, 37.2, 37.7, 41.6, 42.2, 68.3, 126.2, 128.46, 128.54, 128.9, 129.4, 138.4, 139.1, 140.7; LC-MS (ESI+) *m/z* = 408.3 $[M+H]^+$; HRMS calcd. for $C_{21}H_{27}O_3N^{35}ClS$ $[M+H]^+$ 408.1395, found 408.1397; Analytical HPLC: 99.2%

***N*-(4-Chlorobenzyl)-*N*-methyl-4-phenyl-3-(tetrahydro-2*H*-pyran-4-yl)butan-1-amine (74b)**

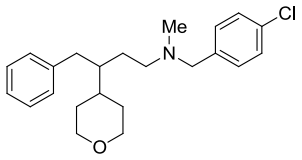

General Procedure C: Using amine **68e** (100 mg, 0.28 mmol), chromatography (silica, 3% MeOH, DCM) afforded **74b** as a yellow oil (75 mg, 69%); R_f = 0.42 (silica, 5% MeOH, DCM); UV λ_{max} (EtOH/nm) No distinguishable peak; IR ν_{max}/cm^{-1} 2933 (C-H), 2840 (C-H), 2789 (C-H), 1681, 1600, 1490, 1451, 1364, 1243, 1087, 1014, 841, 803, 739, 700; ^{1}H δ/ppm (500 MHz, $CDCl_3$) 1.43-1.65 (8H, m, Alk-H), 2.11 (3H, s, N-C*H*$_3$), 2.30-2.31 (2H, m, Alk-C*H*$_2$-NMe), 2.43 (1H, dd, PhC*H*$_2$, *J* = 8.1 and 13.6 Hz), 2.69 (1H, dd, PhC*H*$_2$, *J* = 5.8 and 13.3 Hz), 3.30-3.38 (4H, m, C*H*$_2$-O and MeN-C*H*$_2$Ar), 3.98-4.03 (2H, m, C*H*$_2$-O), 7.14 (2H, d, Ar-H, *J* = 7.5 Hz), 7.21-7.22 (3H, m, Ar-H), 7.28-7.31 (4H, m, Ar-H); ^{13}C δ/ppm (125 MHz, $CDCl_3$) 27.3, 29.5, 29.8, 37.3, 42.1, 42.7, 53.4, 55.2, 61.6, 68.4, 125.8, 128.3, 129.1, 130.3, 141.4; LC-MS (ESI+) *m/z* = 372.4 $[M+H]^+$; HRMS calcd. for $C_{23}H_{31}ON^{35}Cl$ $[M+H]^+$ 372.2089, found 372.2092; Analytical HPLC: 92.4%

***Tert*-butyl-(3-(2,2-dimethyltetrahydro-2*H*-pyran-4-yl)-4-phenylbutyl)carbamate (101)**

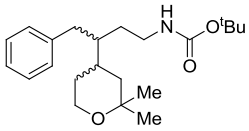

General Procedure G i: Using amine **28** (291 mg, 1.11 mmol) and Boc_2O (255 mg, 1.17 mmol) at room temperature overnight, chromatography (silica, 0-5% EtOAc, hexane) afforded **101**, as an inseparable mixture of diastereoisomers (*dr* = 5:2), as a yellow oil (243 mg, 65%); R_f = 0.25 (silica, 10% EtOAc, DCM); UV λ_{max} (EtOH/nm) 259.5; IR ν_{max}/cm^{-1} 3338 (N-H), 2973 (C-H), 2930 (C-H), 2868 (C-H), 1698 (C=O), 1521, 1454, 1365, 1250, 1169, 1086, 739, 700; ^{1}H δ/ppm (500 MHz, $CDCl_3$) 1.15 (3H, s, Alk-C*H*$_3$ (major and minor)), 1.22 (2.3H, s, Alk-C*H*$_3$ (major)), 1.23 (0.9H, s, Alk-C*H*$_3$ (minor)), 1.23-1.39 (4H, m, Alk-H (major and minor)), 1.42 (9H, s, C(C*H*$_3$)$_3$ (major and minor)), 1.47-1.53 (3H, m, Alk-H (major and minor)), 1.76-1.81 (1H, m,

Alk-H (major and minor)), 2.39-2.49 (1H, m, PhC*H*$_2$ (major and minor)), 2.69 (1H, dd, PhC*H*$_2$, *J* = 5.2 and 13.5 Hz (major and minor)), 3.01-3.12 (2H, m, AlkC*H*$_2$-NH (major and minor)), 3.56-3.65 (1H, m, C*H*$_2$-O (major and minor)), 3.72-3.79 (1H, m, C*H*$_2$-O (major and minor)), 4.24-4.34 (1H, m, N*H* (major and minor)), 7.13 (2H, d, Ar-H, *J* = 7.2 Hz (major and minor)), 7.17-7.20 (1H, m, Ar-H, *J* = 7.3 Hz (major and minor)), 7.26-7.29 (2H, m, Ar-H (major and minor)); ^{13}C δ/ppm (125 MHz, $CDCl_3$) 21.8, 28.4, 29.2, 29.5, 30.1, 31.9, 33.0, 37.0, 38.8, 39.3, 40.0, 42.6, 61.8, 71.8, 125.9, 128.4, 129.0, 141.2, 155.9; LC-MS (ESI+) *m/z* = mass not observed; HRMS calcd. for $C_{22}H_{36}O_3N$ $[M+H]^+$ 362.2690, found 362.2693; Analytical HPLC: 99.5%

(E)- and (Z)-Methyl 2-(2,2-dimethyldihydro-2*H*-pyran-4-(3*H*)-ylidene) acetate (22)[79]

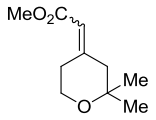

General Procedure M: Using pyranone **21** (600 mg, 4.68 mmol) and trimethyl phosphonoacetate (0.91 mL, 1.02 g, 5.62 mmol), chromatography (silica, 20% EtOAc, petrol) eluted **22** as a pale yellow oil (707 mg, 80%, E:Z ratio 3:2); R_f = 0.23 (silica, 5% EtOAc, petrol); UV λ_{max} (EtOH/nm) 228.0; IR ν/cm^{-1} 2974 (C-H), 2950 (C-H), 2871 (C-H), 1715 (C=O), 1653, 1435, 1367, 1245, 1183, 1149, 1127, 1080, 1049, 1024, 847, 756; ^{1}H δ/ppm (500 MHz, $CDCl_3$) 1.21 (6H, s, *gem*-C*H*$_3$ *(E)*), 1.23 (4H, s *gem*-C*H*$_3$ *(Z)*), 2.19 (2H, s, Alk-H *(E)*), 2.25-2.27 (1.4H, m, Alk-H *(Z)*), 2.88 (1.4H, s, Alk-H *(Z)*), 2.93-2.96 (2H, m, Alk-H *(E)*), 3.69 (2H, s, CO_2C*H*$_3$ *(Z)*), 3.70 (3H, s, CO_2C*H*$_3$ *(E)*), 3.77 (2H, t, C*H*$_2$-O, *(E), J* = 5.8 Hz), 3.81 (1.4H, t, C*H*$_2$-O, *(Z), J* = 5.8 Hz), 5.65 (1H, s, C*H*CO_2Me, *(E)*), 5.77 (0.66H, m, C*H*CO_2Me, *(Z)*); ^{13}C δ/ppm (125 MHz, $CDCl_3$) 26.4, 26.5, 30.3, 37.2, 41.4, 48.3, 50.9, 51.0, 61.8, 62.5, 74.1, 74.3, 115.1, 115.2, 157.2, 157.4, 166.76, 166.84; LC-MS (ESI+) *m/z* = 185.1 $[M+H]^+$; HRMS calcd. for $C_{10}H_{17}O_3$ $[M+H]^+$ 185.1172, found 185.1170

(E)-Ethyl 2-methyl-3-phenylacrylate (103)

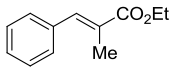

General Procedure M: Using benzaldehyde (0.67 mL, 700 mg, 6.60 mmol) (**102**) and triethyl 2-phosphonopropionate (1.70 mL, 1.89 g, 7.92 mmol) at 40 ^{o}C, chromatography (silica, 5% EtOAc, hexane) afforded **103** as a pale yellow oil (417 mg, 33%); R_f = 0.33 (silica, 5% EtOAc, hexane); UV λ_{max} (EtOH/nm) 268.0; IR ν_{max}/cm^{-1} 2937 (C-H), 1704 (C=O), 1635, 1447, 1366, 1248, 1200, 1110, 1032, 763, 703; ^{1}H δ/ppm (500 MHz, $CDCl_3$) 1.36 (3H, t, $CO_2CH_2CH_3$, *J* = 7.2 Hz), 2.12 (3H, d, CH_3CCO_2Et, *J* = 1.5 Hz), 4.28 (2H, q, $CO_2CH_2CH_3$, *J* = 7.1 Hz), 7.30-7.35 (1H, m, Ar-H), 7.37-7.41 (4H, m, Ar-H), 7.69 (1H, m, C*H*=C); ^{13}C δ/ppm (125 MHz, $CDCl_3$) 14.1, 14.4, 60.9, 128.3, 128.4, 128.7, 129.6, 136.0, 138.7, 168.7; LC-MS (ESI+) *m/z* = 191.2 $[M+H]^+$

Methyl 2-(2,2-dimethyltetrahydro-2*H*-pyran-4-yl) acetate (23)[79]

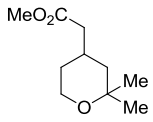

General Procedure N: Using ester **22** (700 mg, 3.80 mmol, E:Z ratio 3:2), partitioning with distilled water (10 mL) and EtOAc (2 × 10 mL), washing with brine (10 mL), drying ($MgSO_4$), filtration and concentration *in vacuo* afforded **23** as a pale yellow oil (646 mg, 90%); R_f = 0.28 (silica, 10% EtOAc, petrol); UV λ_{max} (EtOH/nm) No distinguishable peak; IR ν/cm^{-1} 2973 (C-H), 2926 (C-H), 2859 (C-H), 1736 (C=O), 1437, 1366, 1283, 1259, 1196, 1167, 1139, 1087, 1057, 1001, 691, 916, 856, 734; ^{1}H δ/ppm (500 MHz, $CDCl_3$) 1.12 (1H, t, C*H*, *J* = 12.4 Hz), 1.16-1.19 (1H, m, Alk-H), 1.20 (3H, s, Alk-CH_3), 1.22 (3H, s, Alk-CH_3), 1.54-1.62 (2H, m, Alk-H), 2.16-2.21 (3H, m, C*H*C$H_2$$CO_2$Me), 3.66 (1H, td, C$H_2$-O, *J* = 2.4 and 12.1 Hz), 3.67 (3H, s, CO_2CH_3), 3.72 (1H, qd, CH_2-O, *J* = 1.6 and 5.3 Hz); ^{13}C δ/ppm (125 MHz, $CDCl_3$) 21.8, 28.6, 31.6, 32.4, 41.6, 43.1, 51.5, 61.3, 71.6, 172.9; LC-MS (ESI+) *m/z* = mass not found; HRMS calcd. for $C_{10}H_{19}O_3$ $[M+H]^+$ 187.1329, found 187.1329

Ethyl 2-methyl-3-phenylpropanoate (104)

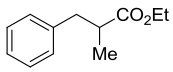

General Procedure N: Using (*E*)-ester **103** (400 mg, 2.10 mmol), partitioning with distilled water (10 mL) and EtOAc (2 × 10 mL), washing with brine (10 mL), drying ($MgSO_4$), filtration and concentration *in vacuo* afforded **104** as a pale yellow oil (375 mg, 93%); R_f = No spot seen by UV or stains; UV λ_{max} (EtOH/nm) 258.5; IR ν_{max}/cm^{-1} 2978 (C-H), 2937 (C-H), 1730 (C=O), 1454, 1376, 1283, 1251, 1163, 1117, 1029, 744, 699; ^{1}H δ/ppm (500 MHz, $CDCl_3$) 1.16 (3H, d, C*H*$_3$CHCO$_2$Et, *J* = 6.8 Hz), 1.19 (3H, t, CO$_2$CH$_2$C*H*$_3$, *J* = 7.2 Hz), 2.64-2.76 (2H, m, C*H* and PhC*H*$_2$), 3.02 (1H, dd, PhC*H*$_2$, *J* = 6.6 and 13.0 Hz), 4.09 (2H, q, CO$_2$C*H*$_2$CH$_3$, *J* = 7.2 Hz), 7.16-7.21 (3H, m, Ar-H), 7.26-7.29 (2H, m, Ar-H); ^{13}C δ/ppm (125 MHz, $CDCl_3$) 14.2, 16.8, 39.8, 41.5, 60.3, 126.3, 128.3, 129.0, 139.5, 176.2; LC-MS (ESI+) *m/z* = 193.2 $[M+H]^+$; HRMS calcd. for $C_{12}H_{17}O_2$ $[M+H]^+$ 193.1223, found 193.1223

Methyl 2-(2,2-dimethyltetrahydro-2*H*-pyran-4-yl)-3-phenylpropanoate (24)[79]

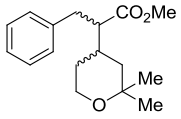

General Procedure O: Using ester **23** (640 mg, 3.44 mmol) and benzyl bromide (491 µL, 706 mg, 4.13 mmol), chromatography (silica, 5-15% EtOAc, petrol) eluted **24**, as an inseparable mixture of diastereoisomers (*dr* = 5:2), as a pale, yellow solid (1.18 g, 86%); R_f = 0.30 (silica, 10% EtOAc, petrol); m.p. 56-62 ^{o}C; UV λ_{max} (EtOH/nm) 206.0; IR ν/cm^{-1} 2934 (C-H), 2859 (C-H), 1732 (C=O), 1603, 1496, 1366, 1202, 1162, 1089, 1031, 960, 840, 745, 699; ^{1}H δ/ppm (500 MHz, $CDCl_3$) 1.18-1.23 (2H, m, Alk-H), 1.22 (3H, s, *gem*-C*H*$_3$ (major and minor)), 1.25 (3H, s, *gem*-C*H*$_3$ (major and minor)), 1.30-1.39 (1H, m, Alk-H (major and minor)), 1.43-1.49 (1H, m, Alk-H (major and minor)), 1.68-1.72 (1H, m, Alk-H (major and minor)), 1.98-2.06 (1H, m, Alk-H (major and minor)), 2.43-2.49 (1H, m, Alk-H (major and minor)), 2.78-2.85 (1H, m, PhC*H*$_2$ (major and minor)), 2.88-2.93 (1H, m, PhC*H*$_2$ (major and minor)), 3.51 (2.2H, s CO$_2$C*H*$_3$ (major)), 3.52 (0.7H, s CO$_2$C*H*$_3$ (minor)), 3.61-3.69 (1H, m, C*H*$_2$-O (major and minor)), 3.72-3.80 (1H, m, C*H*$_2$-O (major and minor)), 7.13 (2H, d, Ar-H, *J* = 7.3 Hz (major and minor)), 7.19 (1H, t, Ar-H, *J* = 7.4 Hz (major and minor)), 7.24-7.27 (2H, m, Ar-H

(major and minor)); ^{13}C δ/ppm (125 MHz, $CDCl_3$) 21.8, 21.9, 30.4, 30.5, 31.7, 31.9, 33.9, 34.1, 35.5, 41.1, 51.2, 53.9, 54.1, 61.3, 61.4, 71.6, 71.7, 126.3, 128.4, 128.7, 139.3, 174.9; LC-MS (ESI+) *m/z* = 277.3 $[M+H]^+$; HRMS Calcd. for $C_{17}H_{25}O_3$ $[M+H]^+$ 277.1798, found 277.1797

(*R*,*R*)- and (*S*,*S*)-4-Benzyl-3-(3-phenyl-2-(tetrahydro-2*H*-pyran-4-yl)propanoyl)oxazolidin-2-one ((*R*,*R*)- and (*S*,*S*)-114)

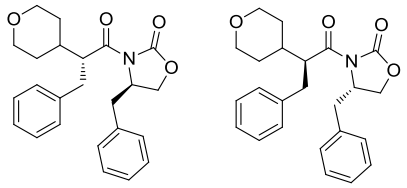

General Procedure O: Using either (*R*)- or (*S*)-oxazolidin-2-one **(*R*)-113** or **(*S*)-113** (1.70 g, 5.60 mmol and 1.54 g, 5.08 mmol respectively), deprotonation was achieved using diisopropylamine (1.1 equiv.) and *n*-butyllithium (2.5 M in hexanes, 1.1 equiv.) in THF (17.1 and 15.5 mL respectively) and HMPA (1.8 equiv.) before addition of benzyl bromide (4.0 equiv.). Partitioning with diethyl ether (20 mL) and 0.5 M HCl (20 mL) and washing the organic layer with 1 M HCl (3 × 10 mL), isolated **(*R*,*R*)-114** and **(*S*,*S*)-114** as white solids following filtration (1.87 g, ≥ 96% *d.e*, 81% and 1.59 g, ≥ 98% *d.e*, 79% respectively); R_f = 0.14 (silica, 50% EtOAc, petrol); m.p. 153-156 ^{o}C; $[\alpha]_D^{24.3}$ -38.1^o (*R*,*R*) (*c* 0.10 in THF), $[\alpha]_D^{24.1}$ +29.5^o (*S*,*S*) (*c* 0.10 in THF); UV λ_{max} (EtOH/nm) 206.2; IR ν_{max}/cm^{-1} 2942 (C-H), 2835 (C-H), 1758 (C=O), 1691 (C=O), 1494, 1454, 1395, 1350, 1224 (C-O), 1188, 1089, 1015, 996, 951, 868, 747, 701; ^{1}H δ/ppm (500 MHz, DMSO-d_6) 1.36 (1H, qd, OCH_2CH_2CH, *J* = 4.4 and 12.4 Hz), 1.42-1.53 (2H, m, OCH_2CH_2CH), 1.67-1.69 (1H, m, OCH_2CH_2CH), 1.85-1.91 (1H, m, OCH_2CH_2CH), 2.44 (1H, dd, $PhCH_2$, *J* = 7.0 and 13.6 Hz), 2.63 (1H, dd, $PhCH_2$, *J* = 3.3 and 13.7 Hz), 2.88-2.98 (2H, m, $PhCH_2$), 3.23-3.31 (2H, m, O-CH_2), 3.84-3.90 (2H, m, O-CH_2), 4.03 (1H, dd, CHCO, *J* = 2.5 and 8.9 Hz), 4.19-4.27 (2H, m, CH_2OCON), 4.62-4.66 (1H, m, CHN), 6.70 (2H, d, Ar-H, *J* = 6.9 Hz), 7.11-7.25 (6H, m, Ar-H), 7.32 (2H, t, Ar-H, *J* = 7.5 Hz); ^{13}C δ/ppm (125 MHz, DMSO-d_6) 29.4, 30.1, 34.1, 36.0, 37.8, 48.6, 54.1, 65.3, 67.0, 126.2, 126.7, 128.3, 128.4, 129.2, 129.3, 135.1, 139.5, 153.0, 173.8; LC-MS (ESI+) *m/z* = 394.5 $[M+H]^+$; HRMS calcd. for $C_{24}H_{28}O_4N$ $[M+H]^+$ 394.2013, found 394.2014

2-(2,2-Dimethyltetrahydro-2*H*-pyran-4-yl)-3-phenylpropan-1-ol (25)[79]

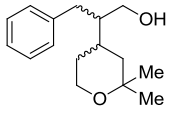

General Procedure P: Using ester **24** (850 mg, 3.08 mmol), partitioning with EtOAc (2 × 10 mL), washing with brine (10 mL), drying ($MgSO_4$), filtering and concentrating *in vacuo* afforded **25**, as an inseparable mixture of diastereoisomers (*dr* = 5:2), as a pale yellow oil (787 mg, 93%); R_f = 0.45 (silica, 40% EtOAc, petrol); UV λ_{max} (EtOH/nm) 207.0; IR ν/cm^{-1} 3392 (O-H), 2933 (C-H), 2845 (C-H), 1495, 1454, 1388, 1244, 1142, 1087, 1031, 921, 870, 838, 742, 699; ^{1}H δ/ppm (500 MHz, $CDCl_3$) 1.07 (1H, t, Alk-H, *J* = 5.3 Hz (major and minor)), 1.20 (0.9H, s, Alk-C*H*$_3$ (minor)), 1.21 (2.1H, s, Alk-C*H*$_3$ (major)), 1.24 (0.8H, s, Alk-C*H*$_3$ (minor)), 1.25 (2.3H, s, Alk-C*H*$_3$ (major)), 1.25-1.30 (1H, m, Alk-H (major and minor)), 1.32-1.40 (1H, m, Alk-H (major and minor)), 1.56-1.65 (3H, m, Alk-H (major and minor)), 1.90-1.98 (1H, m, O*H* (major and minor)), 2.50-2.57 (1H, m, PhC*H*$_2$ (major and minor)), 2.74-2.81 (1H, m, PhC*H*$_2$ (major and minor)), 3.50-3.56 (1H, m, C*H*$_2$-OH (major and minor)), 3.56-3.61 (1H, m, C*H*$_2$-OH (major and minor)), 3.62-3.69 (1H, m, C*H*$_2$-O (major and minor)), 3.76-3.80 (1H, m, C*H*$_2$-O (major and minor)), 7.18-7.21 (3H, m, Ar-H (major and minor)), 7.29 (2H, t, Ar-H, *J* = 7.4 Hz (major and minor)); ^{13}C δ/ppm (125 MHz, $CDCl_3$) 30.3, 34.3, 35.7, 47.6, 61.8, 68.4, 126.0, 128.5, 129.1, 141.0; LC-MS (ESI+) *m/z* = mass not found; HRMS calcd. for $C_{16}H_{25}O_2$ $[M+H]^+$ 249.1849, found 249.1851

2-Methyl-3-phenylpropan-1-ol (105)

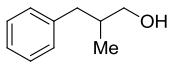

General Procedure P: Using ester **104** (440 mg, 2.47 mmol), partitioning with EtOAc (2 × 10 mL), washing with brine (10 mL), drying ($MgSO_4$), filtering and concentrating *in vacuo* afforded **105** as a pale yellow oil (339 mg, 87%); R_f = 0.27 (silica, 20% EtOAc, hexane); UV λ_{max} (EtOH/nm) 209.0; IR ν_{max}/cm^{-1} 3330 (O-H), 2955 (C-H), 2919 (C-H), 1495, 1453, 1030, 986, 738, 698; ^{1}H δ/ppm (500 MHz, $CDCl_3$) 0.93 (3H, d, C*H*$_3$, *J* = 6.7 Hz), 1.35 (1H, s, br, O*H*), 1.91-2.00 (1H, m, C*H*), 2.43 (1H, dd, PhC*H*$_2$, *J* = 8.0 and 13.5 Hz), 2.76 (1H, dd, PhC*H*$_2$, *J* = 6.4 and 13.5 Hz), 3.49 (1H, dd, C*H*$_2$OH, *J* = 6.0 and 10.6 Hz), 3.55 (1H, dd, C*H*$_2$OH, *J* = 5.9 and 10.5 Hz), 7.17-7.21 (3H, m,

Ar-H), 7.27-7.30 (2H, m, Ar-H); ^{13}C δ/ppm (125 MHz, $CDCl_3$) 16.5, 37.8, 39.7, 67.7, 125.9, 128.3, 129.2, 140.6; LC-MS (ESI+) *m/z* = 151.2 $[M+H]^+$; HRMS calcd. for $C_{10}H_{15}O$ $[M+H]^+$ 151.1117, found 151.1113

2-(2,2-Dimethyltetrahydro-2*H*-pyran-4-yl)-3-phenylpropyl methanesulfonate (26)[79]

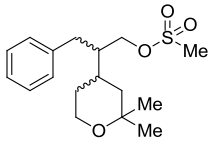

General Procedure Q: Using alcohol **25** (760 mg, 3.06 mmol), partitioning with distilled water (2 × 10 mL) and 1 M HCl (2 × 10 mL), washing with brine (10 mL) drying ($MgSO_4$), filtering and concentration *in vacuo* afforded **26**, as an inseparable mixture of diastereoisomers (*dr* = 5:2), as a brown solid (1.010 g, 96%); R_f = 0.32 (silica, 30% EtOAc, petrol); m.p. 66-68 ^oC; UV λ_{max} (EtOH/nm) 205.5; IR ν/cm^{-1} 3018 (C-H), 2900 (C-H), 2841 (C-H), 1602, 1468, 1345, 1248, 1173, 1089, 973, 925, 821, 747, 699; ^{1}H δ/ppm (500 MHz, $CDCl_3$) 1.20 (0.9H, s, Alk-C*H*$_3$ (minor)), 1.21 (2.3H, s, Alk-C*H*$_3$ (major)), 1.24-1.27 (1H, m, Alk-H (major and minor)), 1.24 (0.9H, s, Alk-C*H*$_3$ (minor)), 1.25 (2.1H, s, Alk-C*H*$_3$ (major)), 1.31-1.40 (1H, m, Alk-H (major and minor)), 1.60-1.69 (2H, m, Alk-H (major and minor)), 1.77-1.84 (1H, m, Alk-H (major and minor)), 1.90-1.97 (1H, m, Alk-H (major and minor)), 2.50 (0.8H, dd, PhC*H*$_2$, *J* = 10.2 and 13.8 Hz (major)), 2.56 (0.2H, dd, PhC*H*$_2$, *J* = 10.2 and 13.8 Hz (minor)), 2.87 (1H, dd, PhC*H*$_2$, *J* = 4.8 and 12.3 Hz (major and minor)), 2.90 (2.2H, s, SO_2C*H*$_3$ (major)), 2.91 (0.7H, s, SO_2C*H*$_3$ (minor)), 3.63-3.69 (1H, m, C*H*$_2$-O (major and minor)), 3.77-3.81 (1H, m, C*H*$_2$-O (major and minor)), 4.03-4.07 (1H, m, C*H*$_2$-OMs (major and minor)), 4.13-4.16 (1H, m, C*H*$_2$-OMs (major and minor)), 7.17 (2H, d, Ar-H, *J* = 7.4 Hz (major and minor)), 7.22 (1H, t, Ar-H, *J* = 7.4 Hz (major and minor)), 7.31 (2H, t, Ar-H, *J* = 7.3 Hz (major and minor)); ^{13}C δ/ppm (125 MHz, $CDCl_3$) 30.2, 30.3, 33.9, 35.6, 37.0, 45.0, 68.1, 68.7, 126.5, 128.7, 129.0, 139.6; LC-MS (ESI+) *m/z* = 299.2 $[M+H]^+$; HRMS mass not observed

2-Methyl-3-phenylpropyl methanesulfonate (106)

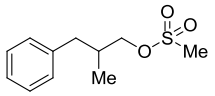

General Procedure Q: Using alcohol **105** (330 mg, 2.20 mmol), partitioning with distilled water (2 × 10 mL) and 1 M HCl (2 × 10 mL), washing with brine (10 mL) drying ($MgSO_4$), filtering and concentration *in vacuo* afforded **106** as a brown oil (508 mg, 96%); R_f = 0.30 (silica, 20% EtOAc, hexane); UV λ_{max} (EtOH/nm) No distinguishable peak; IR ν_{max}/cm^{-1} 3028 (C-H), 2968 (C-H), 1455, 1350, 1171, 959, 832, 740, 701; ^{1}H δ/ppm (500 MHz, $CDCl_3$) 1.01 (3H, d, C*H*$_3$, *J* = 6.7 Hz), 2.21 (1H, oct, C*H*, *J* = 6.6 Hz), 2.53 (1H, dd, PhCH_2, *J* = 7.7 and 13.6 Hz), 2.76 (1H, dd, PhCH_2, *J* = 6.7 and 13.6 Hz), 2.99 (3H, s, SO_2C*H*$_3$), 4.05 (1H, dd, C*H*$_2$OMs, *J* = 5.9 and 9.4 Hz), 4.09 (1H, dd, C*H*$_2$OMs, *J* = 5.6 and 9.5 Hz), 7.15-7.17 (2H, m, Ar-H), 7.20-7.23 (1H, m, Ar-H), 7.28-7.31 (2H, m, Ar-H); ^{13}C δ/ppm (125 MHz, $CDCl_3$) 16.4, 35.0, 37.2, 39.2, 73.7, 126.4, 128.5, 129.1, 139.2; LC-MS (ESI+) *m/z* = mass peak not observed; HRMS mass not observed

3-(2,2-Dimethyltetrahydro-2*H*-pyran-4-yl)-4-phenylbutanenitrile (27)[79]

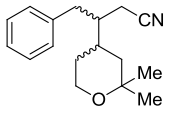

General Procedure R: Using sulfonate **26** (1.00 g, 3.06 mmol), the reaction was partitioned with diethyl ether (10 mL) and saturated aqueous K_2CO_3 (40 mL) with brine (10 mL). The aqueous layer was extracted with diethyl ether (3 × 10 mL) and the organic layer was washed with 50% distilled water, brine (6 × 10 mL), brine (10 mL), dried ($MgSO_4$), filtered and concentrated *in vacuo* to afford **27**, as an inseparable mixture of diastereoisomers (*dr* = 5:2), as a brown solid (652 mg, 83%); R_f = 0.40 (silica, 20% EtOAc, petrol); m.p. 62-64 ^{o}C; UV λ_{max} (EtOH/nm) 207.0; IR ν/cm^{-1} 2945 (C-H), 2915 (C-H), 2855 (C-H), 2242 (C≡N), 1676, 1600, 1493, 1452, 1420, 1247, 1138, 1095, 1023, 984, 887, 855, 805, 748, 703; ^{1}H δ/ppm (500 MHz, $CDCl_3$) 1.21-1.26 (1H, m, Alk-H (major and minor)), 1.23 (1H, s, Alk-C*H*$_3$ (minor)), 1.24 (2.2H, s, Alk-C*H*$_3$ (major)), 1.25 (1H, s, Alk-C*H*$_3$ (minor)), 1.27 (2.3H, s, Alk-C*H*$_3$ (major)), 1.30-1.36 (1H, m, Alk-H (major and minor)), 1.58-1.65 (1H, m, C*H* (major and minor)),

1.70-1.76 (2H, m, Alk-H (major and minor)), 1.89-1.97 (1H, m, Alk-H (major and minor)), 2.19 (1H, dd, PhCH_2, J = 5.5 and 17.1 Hz (major and minor)), 2.30 (1H, dd, PhCH_2, J = 5.1 and 17.2 Hz (major and minor)), 2.46 (0.8H, dd, CH_2CN, J = 10.6 and 13.8 Hz (major)), 2.49 (0.2H, dd, CH_2CN, J = 10.6 and 13.8 Hz (minor)), 3.00 (1H, dd, CH_2CN, J = 4.4 and 13.8 Hz (major and minor)), 3.69 (1H, td, CH_2-O, J = 2.3 and 12.3 Hz (major and minor)), 3.79-3.83 (1H, m, CH_2-O (major and minor)), 7.18 (2H, d, Ar-H, J = 7.3 Hz (major and minor)), 7.24 (1H, t, Ar-H, J = 7.5 Hz (major and minor)), 7.30-7.33 (2H, m, Ar-H, J = 7.2 Hz (major and minor)); ^{13}C δ/ppm (125 MHz, $CDCl_3$) 18.1, 30.2, 30.3, 36.4, 37.4, 42.6, 67.9, 118.5, 126.7, 128.8, 129.0, 139.1; LC-MS (ESI) *m/z* = 230.2 $[M+H]^+$; HRMS mass not observed

3-Methyl-4-phenylbutanenitrile (107)

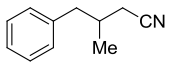

General Procedure R: Using methanesulfonate **106** (500 mg, 2.19 mmol), the reaction was partitioned with diethyl ether (10 mL) and saturated aqueous K_2CO_3 (20 mL) with brine (10 mL). The aqueous layer was extracted with diethyl ether (3 × 10 mL) and the organic layer was washed with 50% distilled water, brine (6 × 10 mL), brine (10 mL), dried ($MgSO_4$), filtered and concentrated *in vacuo* to afford **107** as a brown oil (283 mg, 81%); R_f = 0.33 (silica, 10% EtOAc, hexane); ^{1}H δ/ppm (500 MHz, $CDCl_3$) 1.13 (3H, d, CH_3, 6.7 Hz), 2.12-2.17 (1H, m, CH), 2.20 (1H, dd, PhCH_2, J = 6.6 and 16.5 Hz), 2.30 (1H, dd, PhCH_2, J = 4.9 and 16.2 Hz), 2.67 (2H, dd, CH_2CN, J = 2.7 and 6.8 Hz), 7.16-7.18 (2H, m, Ar-H), 7.21-7.25 (1H, m, Ar-H), 7.28-7.33 (2H, m, Ar-H); ^{13}C δ/ppm (125 MHz, $CDCl_3$) 19.5, 23.7, 32.5, 42.1, 118.7, 126.6, 128.6, 129.0, 139.0; LC-MS (ESI+) *m/z* = 160.2 $[M+H]^+$; HRMS calcd. for $C_{11}H_{14}N$ $[M+H]^+$ 160.1121, found 160.1119

3-Methyl-4-phenylbutan-1-amine (108)

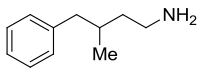

General Procedure T: Using nitrile **107** (310 mg, 1.95 mmol), the crude material was partitioned with EtOAc (30 mL) and 1 M HCl (4 × 10 mL). The aqueous layer was neutralised with 2 M NaOH and partitioned with EtOAc (2 × 20 mL). The organic layer was washed with brine (20 mL), dried ($MgSO_4$), filtered and concentrated *in vacuo* to

give **108** as a yellow oil (145 mg, 43%); R_f = 0.10 (silica, 20% MeOH, DCM); UV λ_{max} (EtOH/nm) 205.0; IR ν_{max}/cm^{-1} 3400 (N-H), 3282 (N-H), 2922 (C-H), 1668, 1603, 1494, 1454, 1377, 737, 699; ^{1}H δ/ppm (500 MHz, $CDCl_3$) 0.88 (3H, d, C*H*$_3$, *J* = 6.7 Hz), 1.24-1.57 (4H, m, CHC*H*$_2$CH_2N*H*$_2$), 1.78-1.85 (1H, m, C*H*), 2.42 (1H, dd, PhC*H*$_2$, *J* = 8.0 and 13.4 Hz), 2.61 (1H, dd, PhC*H*$_2$, *J* = 6.5 and 13.4 Hz), 2.71-2.80 (2H, m, C*H*$_2$NH_2), 7.14-7.15 (2H, m, Ar-H), 7.16-7.19 (1H, m, Ar-H), 7.25-7.28 (2H, m, Ar-H); ^{13}C δ/ppm (125 MHz, $CDCl_3$) 19.5, 32.8, 32.9, 33.2, 43.9, 125.7, 128.2, 129.2, 141.2; LC-MS (ESI+) *m/z* = 164.2 $[M+H]^+$; HRMS calcd. for $C_{11}H_{18}N$ $[M+H]^+$ 164.1434, found 164.1431

7.12.2 MDMX

A) 3'-Amino-[1,1'-biphenyl]-4-ol (117a)

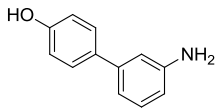

Bromophenol (100 mg, 0.58 mmol), boronic acid **116** (108 mg, 0.79 mmol) and $Pd(PPh_3)_4$ (20.1 mg, 0.02 mmol) were dissolved in 2 M Na_2CO_3 (0.3 mL, 0.6 mmol), ethanol (0.4 mL) and toluene (5.8 mL) and heated to 100 ^oC. After 22 h, the reaction was partitioned with EtOAc (20 mL) and distilled water (10 mL). The organic layer was filtered through celite, washing with EtOAc (10 mL) and distilled water (10 mL). The aqueous layer was extracted with EtOAc (10 mL) and the organic layer was washed with brine (15 mL), dried ($MgSO_4$), filtered and concentrated *in vacuo*. Chromatography (silica, 0-40% EtOAc, hexane) afforded **117a** as a brown solid (27.6 mg, 26%); R_f = 0.22 (silica, 40% EtOAc, hexane); m.p. 190 ^oC (decomposed); UV λ_{max} (EtOH/nm) 239.0; IR ν_{max}/cm^{-1} 3357 (N-H), 3292 (N-H), 2595 (br) (O-H), 1588, 1523, 1481, 1461, 1425, 1378, 1270, 1240, 1210, 931, 834, 782, 690; ^1H δ/ppm (500 MHz, DMSO-d_6) 5.07 (2H, s, N*H*$_2$), 6.48 (1H, d, Ar-H, *J* = 8.0 Hz), 6.69 (1H, d, Ar-H, *J* = 7.8 Hz), 6.75 (1H, s, Ar-H), 6.80-6.82 (2H, m, Ar-H), 7.04 (1H, t, Ar-H, *J* = 7.7 Hz), 7.35-7.37 (2H, m, Ar-H), 9.46 (1H, s, O*H*); ^{13}C δ/ppm (125 MHz, DMSO-d_6) 111.6, 112.2, 113.8, 115.5, 127.4, 129.2, 131.8, 140.9, 148.9, 156.7; LC-MS (ESI+) *m/z* = 186.1 $[M+H]^+$; HRMS calcd. for $C_{12}H_{12}ON$ $[M+H]^+$ 186.0913, found 186.0913; HRMS calcd. for $C_{12}H_{10}ON$ $[M-H]^-$ 184.0768, found 184.0767

B) 3'-Amino-[1,1'-biphenyl]-3-ol (117b)

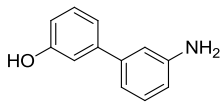

3-Bromophenol (61 µL, 100 mg, 0.58 mmol), boronic acid **116** (112 mg, 0.81 mmol) and $Pd(dtbpf)Cl_2$ (19.0 mg, 0.03 mmol) were dissolved in 2 M Na_2CO_3 (0.58 mL, 1.16 mmol) and 1,2-DME (3.5 mL) and irradiated at 120 ^oC. After 30 min, the reaction was partitioned with EtOAc (20 mL) and saturated aqueous NH_4Cl (20 mL). The organic layer was washed with distilled water (20 mL) and the aqueous layer was extracted with

EtOAc (2 × 10 mL). The organic layer was washed with brine (15 mL), dried ($MgSO_4$), filtered and concentrated *in vacuo*. Chromatography (silica, 40% EtOAc, hexane) afforded **117b** as a light brown solid (101 mg, 94%); R_f = 0.23 (silica, 40% EtOAc, hexane); m.p. 156-159 ^oC; UV λ_{max} (EtOH/nm) 292.5 and 216.5; IR ν_{max}/cm^{-1} 3389 (N-H), 3307 (N-H), 2590 (br) (O-H), 1585, 1484, 1433, 1313, 1259, 1196, 1166, 857, 771, 691; ^1H δ/ppm (500 MHz, MeOH-d_4) 6.74 (2H, qd, Ar-H, *J* = 0.9 and 2.5 Hz), 6.91-6.93 (1H, m, Ar-H), 6.97 (1H, t, Ar-H, *J* = 1.9 Hz), 7.01 (1H, t, Ar-H, *J* = 2.1 Hz), 7.04-7.06 (1H, m, Ar-H), 7.17 (1H, t, Ar-H, *J* = 7.8 Hz), 7.23 (1H, t, Ar-H, *J* = 7.8 Hz); ^{13}C δ/ppm (125 MHz, MeOH-d_4) 114.8, 115.0, 115.2, 115.7, 118.1, 119.3, 130.4, 130.6, 143.5, 144.5, 149.0, 158.7; LC-MS (ESI+) *m/z* = 186.1 $[M+H]^+$; HRMS calcd. for $C_{12}H_{12}ON$ $[M+H]^+$ 186.0913, found 186.0913; HRMS calcd. for $C_{12}H_{10}ON$ $[M-H]^-$ 184.0768, found 184.0767

C) 3'-((4-Fluorobenzyl)amino)-[1,1'-biphenyl]-4-ol (118a)

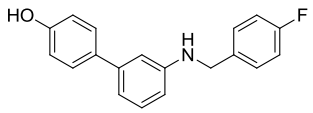

4-Fluorobenzaldehyde (17.4 µL, 20.1 mg, 0.17 mmol) was added to a mixture of aniline **117a** (26 mg, 0.14 mmol) and anhydrous magnesium sulfate in THF (0.8 mL) and stirred at room temperature. After 16 h, the reaction was filtered and concentrated *in vacuo*, then dissolved in methanol (1.0 mL) and mixed with sodium borohydride (15.3 mg, 0.42 mmol) at room temperature. After 1 h, the reaction was quenched with distilled water (10 mL) and partitioned with EtOAc (10 mL) and distilled water (2 × 10 mL). The aqueous layer was extracted with EtOAc (10 mL) and the organic layer was washed with brine (10 mL), dried ($MgSO_4$), filtered and concentrated *in vacuo*. Chromatography (silica, 20% EtOAc, hexane) afforded **118a** as a brown gum (27.7 mg, 68%); R_f = 0.39 (silica, 30% EtOAc, hexane); m.p. 75-82 ^oC; UV λ_{max} (EtOH/nm) 252.0; IR ν_{max}/cm^{-1} 3402 (br) (N-H and O-H), 3035 (C-H), 1604, 1489, 1443, 1329, 1265, 1219, 1190, 1159, 825, 772, 690; ^1H δ/ppm (500 MHz, $CDCl_3$) 4.35 (2H, s, C*H*$_2$), 4.68 (1H, s, O*H*), 4.73 (1H, s, br, N*H*), 6.58-6.60 (1H, m, Ar-H), 6.79-6.80 (1H, m, Ar-H), 6.85-6.88 (2H, m, Ar-H), 6.91-6.93 (1H, m, Ar-H), 7.02-7.07 (2H, m, Ar-H), 7.20-7.23 (1H, m, Ar-H), 7.33-7.37 (2H, m, Ar-H), 7.41-7.44 (2H, m, Ar-H); ^{13}C δ/ppm (125 MHz, $CDCl_3$) 47.9, 111.6, 115.4, 115.6, 116.8, 128.4, 129.1, 129.7, 134.3, 134.8, 142.0, 148.0, 155.0, 161.1, 163.1; LC-MS (ESI+) *m/z* = 294.3 $[M+H]^+$; HRMS calcd. for

$C_{19}H_{17}ONF$ $[M+H]^+$ 294.1289, found 294.1294; HRMS calcd. for $C_{19}H_{15}ONF$ $[M-H]^-$ 292.1143, found 292.1136; Analytical HPLC: 99.2%

D) *N*-(4-Fluorobenzyl)-4'-methoxy-[1,1'-biphenyl]-3-amine (118i)

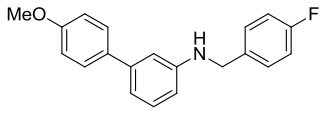

3-Amino-4'-methoxybiphenyl hydrochloride (200 mg, 0.85 mmol) (**117f**) and sodium triacetoxyborohydride (180 mg, 0.85 mmol) were dissolved in DMF (4.26 mL) and glacial acetic acid (42.6 µL). After 10 min, 4-fluorobenzaldehyde (46.2 µL, 53.4 mg, 0.43 mmol) was added at room temperature. After 20 h, the reaction was partitioned with diethyl ether (10 mL), distilled water (20 mL) and brine (10 mL). The aqueous layer was extracted with diethyl ether (2 × 10 mL) and the organic layer was washed with brine (10 mL), dried ($MgSO_4$), filtered and concentrated *in vacuo*. Chromatography (silica, 0-5% EtOAc, petrol) eluted **118i** as a yellow solid (100 mg, 74%); R_f = 0.16 (silica, 5% EtOAc, petrol); m.p. 93-96 ^oC; UV λ_{max} (EtOH/nm) 252.0; IR ν_{max}/cm^{-1} 3416 (N-H), 2932 (C-H), 2837 (C-H), 1602, 1488, 1437, 1329, 1298, 1232, 1214, 1184, 1146, 1080, 1028, 988, 830, 821, 778, 695; ^1H δ/ppm (500 MHz, $CDCl_3$) 3.84 (3H, s, OC*H*$_3$), 4.14, (1H, s, br, N*H*), 4.35 (2H, s, C*H*$_2$), 6.58 (1H, dd, Ar-H, *J* = 2.2 and 8.0 Hz), 6.80-6.81 (1H, m, Ar-H), 6.91-6.97 (3H, m, Ar-H), 7.01-7.06 (2H, m, Ar-H), 7.23 (1H, t, Ar-H, *J* = 7.8 Hz), 7.35-7.37 (2H, m, Ar-H), 7.46-7.49 (2H, m, Ar-H); ^{13}C δ/ppm (125 MHz, $CDCl_3$) 47.8, 55.3, 111.5, 114.1, 115.4, 115.6, 116.8, 128.1, 129.1, 129.6, 134.1, 134.9, 142.1, 148.1, 159.1, 161.1, 163.1; LC-MS (ESI+) *m/z* = 308.3 $[M+H]^+$; HRMS calcd. for $C_{20}H_{19}ONF$ $[M+H]^+$ 308.1445, found 308.1445; Analytical HPLC: 98.0%

E) *N*-(4-(((2-(4-Chlorophenoxy)-4'-fluoro-[1,1'biphenyl]-3-yl)amino)methyl)phenyl)-1,1,1-trifluoromethanesulfonamide (138n)

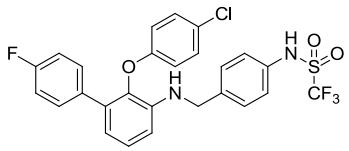

Aniline **137f** (40 mg, 0.13 mmol) and aldehyde **155** (59.5 mg, 0.24 mmol) were dissolved in TFE (0.7 mL) at room temperature and heated to 40 ^{o}C. After 24 h, the solution was cooled to room temperature before addition of sodium borohydride (15 mg, 0.39 mmol). After 1 h, the reaction was quenched with distilled water (10 mL) and the layers were separated. The aqueous layer was extracted with DCM (2 × 10 mL) and the organic layer was washed with brine (10 mL), dried ($MgSO_4$), filtered and concentrated *in vacuo*. Chromatography (silica, 10-15% EtOAc, petrol) eluted **138n** as a yellow oil (45 mg, 64%); R_f = 0.26 (silica, 20% EtOAc, petrol); UV λ_{max} (EtOH/nm) 231.2; IR ν_{max}/cm^{-1} 3401 (N-H), 3272 (N-H), 3048 (C-H), 2858 (C-H), 1607, 1513, 1484, 1416, 1365, 1338, 1280, 1212 (C-O), 1160, 1135, 1092, 1020, 939, 820, 782, 749; ^{1}H δ/ppm (500 MHz, $CDCl_3$) 4.38 (2H, d, C*H*$_2$, *J* = 3.9 Hz), 4.55 (1H, s, br, amino N*H*), 6.61-6.64 (4H, m, Ar-H and sulfonamido N*H*), 6.74 (1H, dd, Ar-H, *J* = 1.2 and 7.7 Hz), 6.93-6.96 (2H, m, Ar-H), 7.06-7.09 (2H, m, Ar-H), 7.13 (1H, t, Ar-H, *J* = 7.9 Hz), 7.21-7.22 (2H, m, Ar-H), 7.26-7.29 (2H, m, Ar-H), 7.35-7.38 (2H, m, Ar-H); ^{13}C δ/ppm (125 MHz, $CDCl_3$) 47.0, 111.2, 114.9, 115.1, 116.3, 119.2, 124.2, 126.5, 126.8, 128.2, 129.4, 130.5, 130.6, 132.5, 133.5, 133.6, 134.6, 137.9, 139.0, 141.2, 155.8, 161.1, 163.1; ^{19}F δ/ppm (470 MHz, $CDCl_3$) -75.3, -115.4; LC-MS (ESI+) *m/z* = 549.2 $[M-H]^+$; HRMS calcd. for $C_{26}H_{18}O_3N_2{}^{35}ClF_4S$ $[M-H]^-$ 549.0668, found 549.0659; Analytical HPLC: 95.5%

F) 1-Bromo-2-(4-chlorophenoxy)-3-nitrobenzene (135a)

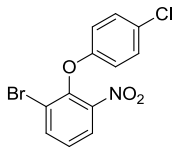

4-Chlorophenol (116 mg, 0.90 mmol), aryl fluoride **139** (100 mg, 0.45 mmol) and anhydrous K_2CO_3 (124 mg, 0.90 mmol) were dissolved in DMF (2.25 mL) and

irradiated at 120 ^{o}C for 20 min. The reaction was partitioned with distilled water (40 mL), brine (10 mL) and diethyl ether (3 × 10 mL). The organic layer was washed with 2 M NaOH (2 × 10 mL), brine (10 mL), dried ($MgSO_4$), filtered and concentrated *in vacuo* to afford **135a** as a brown oil (135 mg, 92%); R_f = 0.48 (silica, 20% EtOAc, hexane); UV λ_{max} (EtOH/nm) 221.0; IR ν_{max}/cm^{-1} 3086 (C-H), 1581, 1527, 1483, 1445, 1347, 1247 (C-O), 1194, 1163, 1090, 1010, 824, 789, 747, 708; ^{1}H δ/ppm (500 MHz, DMSO-d_6) 6.89-6.93 (2H, m, Ar-H), 7.40-7.43 (2H, m, Ar-H), 7.55 (1H, t, Ar-H, *J* = 8.1 Hz), 8.16-8.19 (2H, m, Ar-H); ^{13}C δ/ppm (125 MHz, DMSO-d_6) 116.9, 118.9, 125.4, 126.9, 128.1, 129.7, 138.9, 143.5, 144.4, 155.4; LC-MS (ESI+) *m/z* = Mass not observed; HRMS calcd. for $C_{12}H_8O_3N^{79}Br^{35}Cl$ $[M+H]^+$ 327.9371, found 327.9370

G) 3'-Amino-2'-(4-chlorophenoxy)-[1,1'-biphenyl]-4-ol (137a)

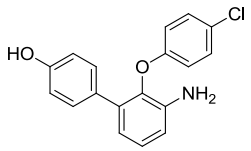

Iron powder (324 mg, 5.8 mmol) was added to a solution of nitro **136a** (197 mg, 0.58 mmol) in glacial acetic acid (5.8 mL) and heated to 50 ^{o}C. After 45 min, the reaction was filtered, washing with EtOAc (15 mL), and concentrated *in vacuo*. The oil was partitioned with distilled water (2 × 10 mL) and EtOAc (15 mL). The aqueous layer was extracted with EtOAc (4 × 10 mL) and the organic layer was washed with brine (10 mL), dried ($MgSO_4$), filtered and concentrated *in vacuo*. Chromatography (silica, 0-20% EtOAc, hexane) afforded **137a** as a white solid (134 mg, 78%); R_f = 0.20 (silica, 20% EtOAc, hexane); m.p. 58 ^{o}C (decomposed); UV λ_{max} (EtOH/nm) 231.5; IR ν_{max}/cm^{-1} 3658 (N-H), 3381 (br) (N-H and O-H), 2981 (C-H), 2889 (C-H), 1612, 1518, 1470, 1430, 1381, 1217 (C-O), 1173, 1087, 954, 825, 783, 748; ^{1}H δ/ppm (500 MHz, DMSO-d_6) 4.92 (2H, s, br, N*H*$_2$), 6.59 (1H, dd, Ar-H, *J* = 1.6 and 7.6 Hz), 6.64-6.68 (2H, m, Ar-H), 6.77 (1H, dd, Ar-H, *J* = 1.5 and 8.0 Hz), 7.03 (1H, t, Ar-H, *J* = 7.8 Hz), 7.18-7.24 (4H, m, Ar-H), 9.38 (1H, s, O*H*); ^{13}C δ/ppm (125 MHz, DMSO-d_6) 114.4, 114.9, 116.5, 117.5, 124.7, 126.1, 128.2, 129.0, 129.7, 135.0, 136.6, 141.7, 155.9, 156.4; LC-MS (ESI+) *m/z* = 312.2 $[M+H]^+$; HRMS calcd. for $C_{18}H_{15}O_2NCl$ $[M+H]^+$ 312.0786, found 312.0789; HRMS calcd. for $C_{18}H_{13}O_2N^{35}Cl$ $[M-H]^-$ 310.0640, found 310.0632

H) *N*-(2-Bromopyridin-4-yl)-4-fluorobenzamide (130)

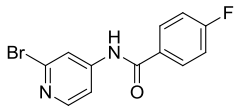

4-Fluorobenzoyl chloride (206 µL, 276 mg, 1.74 mmol) was added to a solution of aminopyridine **126c** (200 mg, 1.16 mmol) and pyridine (282 µL, 275 mg, 3.48 mmol) in acetonitrile (12.8 mL) and stirred at room temperature. After 15 h, the reaction was quenched with 2.5 M NaOH (2.32 mL) in methanol (6.96 mL). After 15 min, the reaction was partitioned with 60% distilled water, brine (50 mL) and EtOAc (3 × 10 mL). The organic layer was washed with distilled water (3 × 10 mL) and the aqueous layer was extracted with EtOAc (10 mL). The organic layer was washed with brine (10 mL), dried ($MgSO_4$), filtered and concentrated *in vacuo*. Chromatography (silica, 0-5%, EtOAc, DCM) afforded **130** as a yellow/white solid (293 mg, 86%); R_f = 0.34 (silica, 10% EtOAc, DCM); m.p. 129-131 ^oC; UV λ_{max} (EtOH/nm) 262.5; IR ν_{max}/cm^{-1} 3305 (N-H), 3137 (C-H), 3070 (C-H), 2963 (C-H), 1670 (C=O), 1575, 1490, 1372, 1303, 1275, 1222, 1159, 1094, 1073, 988, 914, 845, 809, 758, 706; ^1H δ/ppm (500 MHz, $CDCl_3$) 7.16-7.20 (2H, m, Ar-H), 7.55 (1H, dd, Ar-H, *J* = 1.9 and 5.6 Hz), 7.87-7.91 (3H, m, Ar-H), 8.12 (1H, s, br, N*H*), 8.28 (1H, d, Ar-H, *J* = 5.6 Hz); ^{13}C δ/ppm (125 MHz, $CDCl_3$) 113.1, 116.1, 116.3, 117.5, 129.8, 143.0, 146.7, 150.7, 165.0; LC-MS (ESI+) *m/z* = 297.2 $[M+H]^+$; HRMS calcd. for $C_{12}H_9ON_2BrF$ $[M+H]^+$ 294.9877, found 294.9884; HRMS calcd. for $C_{12}H_7ON_2{}^{79}BrF$ $[M-H]^-$ 292.9731, found 292.9724

I) *N*-(4-Bromophenyl)-1,1,1-trifluoromethanesulfonamide (120)

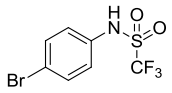

Trifluoromethanesulfonic anhydride (429 µL, 719 mg, 2.55 mmol) in DCM (2.55 mL, 1 M) was added dropwise to a solution of 4-bromoaniline (200 mg, 1.16 mmol) (**119**) and diisopropylethylamine (606 µL, 450 mg, 3.48 mmol) in DCM (4.64 mL) at 0 ^oC and stirred at room temperature. After 30 min, the reaction was quenched with 2.5 M NaOH (2.32 mL) in methanol (4.64 mL) at room temperature. After 22 h, the reaction was partitioned with DCM (2 × 10 mL) and 1 M HCl (10 mL). The organic layer was washed with 1 M HCl (10 mL), brine (15 mL), dried ($MgSO_4$), filtered and concentrated

in vacuo. Chromatography (silica, 0-10% EtOAc, hexane) afforded **120** as a yellow/white solid (268 mg, 76%); R_f = 0.30 (silica, 14% EtOAc, hexane); UV λ_{max} (EtOH/nm) 230.0; IR ν_{max}/cm^{-1} 3283 (N-H), 1610, 1488, 1404, 1361 (S=O asym. stretch), 1201, 1136 (S=O sym. stretch), 1013, 935, 818, 709; ^{1}H δ/ppm (500 MHz, $CDCl_3$) 6.68 (1H, s, br, N*H*), 7.15-7.18 (2H, m, Ar-H), 7.51-7.54 (2H, m, Ar-H); ^{13}C δ/ppm (125 MHz, $CDCl_3$) 121.5, 125.4, 132.7, 132.9; LC-MS (ESI+) *m/z* = 302.0 and 304.0 $[M-H]^-$; HRMS calcd. for $C_7H_4O_2N^{79}BrF_3S$ $[M-H]^-$ 301.9104, found 301.9094

J) 4-(4-((4-Fluorobenzyl)amino)pyridin-2-yl)phenol (128c)

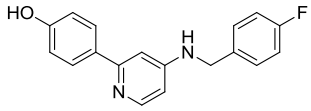

Lithium aluminium hydride (2 M in THF, 0.64 mL, 1.28 mmol) was added dropwise to a solution of benzamide **131** (80 mg, 0.26 mmol) in THF (10.5 mL) at 0 °C and stirred at room temperature. After 72 h, saturated aqueous Rochelle salt (5 mL) was added and the reaction was partitioned with distilled water (10 mL) and EtOAc (10 mL). The organic layer was washed with brine (10 mL), dried ($MgSO_4$), filtered and concentrated *in vacuo*. Trituration with diethyl ether (8 × 5 mL), followed by semi-preparative HPLC (C18, 80% H_2O with 0.1% (v/v) HCO_2H, MeCN at 21.2 mL/min) eluted **128c** as a red/brown solid (59 mg, 79%); R_f = 0.44 (silica, 20% MeOH, DCM); m.p. 192 °C (decomposed); UV λ_{max} (EtOH/nm) 259.5; IR ν_{max}/cm^{-1} 3239 (N-H), 2919 (br) (O-H), 2802 (C-H), 1631, 1567, 1508, 1344, 1223, 817, 758; ^{1}H δ/ppm (500 MHz, DMSO-d_6) 4.39 (2H, d, C*H*$_2$, *J* = 5.8 Hz), 6.42 (1H, dd, Ar-H, *J* = 1.7 and 5.5 Hz), 6.79-6.81 (2H, m, Ar-H), 6.91 (1H, m, Ar-H), 7.07-7.10 (1H, m, Ar-H), 7.15-7.19 (2H, m, Ar-H), 7.40-7.43 (2H, m, Ar-H), 7.75-7.76 (2H, m, Ar-H), 8.03-8.05 (1H, m, Ar-H), 8.27 (1H, s, br, O*H*); ^{13}C δ/ppm (125 MHz, DMSO-d_6) 44.5, 115.0, 115.1, 115.2, 127.6, 129.07, 129.14, 130.4, 135.43, 135.46, 148.9, 154.3, 156.1, 158.1, 160.2, 162.2); LC-MS (ESI+) *m/z* = 295.3 $[M+H]^+$; HRMS calcd. for $C_{18}H_{16}ON_2F$ $[M+H]^+$ 295.1241, found 295.1246; HRMS calcd. for $C_{18}H_{14}ON_2F$ $[M-H]^-$ 293.1096, found 293.1088; Analytical HPLC: 94.9%

K) 2'-(4-Chlorophenoxy)-3'-((4-fluorophenyl)amino)-[1,1'-biphenyl]-4-ol (138c)

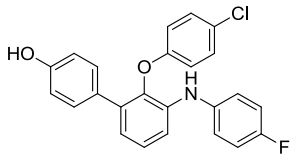

Pd_2dba_3 (14.7 mg, 0.016 mmol), XPhos (7.63 mg, 0.02 mmol), anhydrous K_2CO_3 (44.2 mg, 0.32 mmol), 1-bromo-4-fluorobenzene (35.2 µL, 56 mg, 0.32 mmol) and aniline **137a** (50 mg, 0.16 mmol) were dissolved in acetonitrile (2 mL), purged with nitrogen for 5 min and irradiated at 120 ^oC for 3 h. The reaction was partitioned with EtOAc (10 mL) and 83% distilled water, brine (4 × 12 mL) and the aqueous layer was extracted with EtOAc (3 × 10 mL). The organic layer was washed with brine (10 mL), dried ($MgSO_4$), filtered and concentrated *in vacuo*. Chromatography (silica, 0-15% EtOAc, petrol) eluted **138n** as a grey solid (56 mg, 82%); R_f = 0.31 (silica, 20% EtOAc, petrol); m.p. 132-135 ^oC; UV λ_{max} (EtOH/nm) 271.0; IR ν_{max}/cm^{-1} 3418 (N-H), 3330 (O-H), 1598, 1509, 1470, 1335, 1214, 1090, 1006, 922, 824, 775, 747; ^1H δ/ppm (500 MHz, DMSO-d_6) 6.60-6.63 (2H, m, Ar-H), 6.69-6.72 (2H, m, Ar-H), 6.93 (1H, dd, Ar-H, *J* = 1.7 and 7.4 Hz), 7.00-7.06 (4H, m, Ar-H), 7.14-7.22 (4H, m, Ar-H), 7.26-7.28 (2H, m, Ar-H), 7.61 (1H, s, N*H*), 9.46 (1H, s, O*H*); ^{13}C δ/ppm (125 MHz, DMSO-d_6) 115.0, 115.3, 115.4, 116.2, 116.6, 119.8, 119.9, 121.9, 124.9, 126.2, 127.7, 128.9, 129.8, 135.8, 137.6, 139.3, 140.3, 155.7, 156.0, 156.7; LC-MS (ESI+) *m/z* = 406.3 $[M+H]^+$; HRMS calcd. for $C_{24}H_{18}O_2NClF$ $[M+H]^+$ 406.1005, found 406.1007; HRMS calcd. for $C_{24}H_{16}O_2N^{35}ClF$ $[M-H]^-$ 404.0859, found 404.0847; Analytical HPLC: 94.7%

L) 1-Bromo-2-((4-chlorobenzyl)oxy)-3-nitrobenzene (135b)

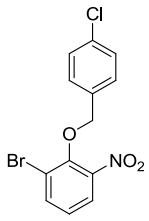

Phenol **134** (240 mg, 1.10 mmol), 4-chlorobenzyl bromide (189 mg, 0.92 mmol) and anhydrous K_2CO_3 (254 mg, 1.84 mmol) were dissolved in acetonitrile (2 mL) and irradiated at 100 ^oC for 90 min. The reaction was partitioned with EtOAc (10 mL) and 3 M NaOH (3 × 10 mL). The organic layer was washed with brine (10 mL), dried

($MgSO_4$), filtered and concentrated *in vacuo*. Chromatography (silica, 0-5% EtOAc, petrol) eluted **135b** as a yellow/white solid (304.6 mg, 97%); R_f = 0.37 (silica, 5% EtOAc, petrol); m.p. 113-116 ^oC; UV λ_{max} (EtOH/nm) 220.5; IR ν_{max}/cm^{-1} 3079 (Ar C-H), 2944, 2894 1589, 1522 (N=O asym. stretch), 1493, 1451, 1362 (N=O sym. stretch), 1245 (C-O), 1103, 934, 879, 814, 791, 747, 705; ^1H δ/ppm (500 MHz, $CDCl_3$) 5.16 (2H, s, C*H*$_2$), 7.17 (1H, t, Ar-H, *J* = 8.1 Hz), 7.37-7.40 (2H, m, Ar-H), 7.47-7.50 (2H, m, Ar-H), 7.80 (1H, dd, Ar-H, *J* = 1.6 and 8.2 Hz), 7.84 (1H, dd, Ar-H, *J* = 1.6 and 8.1 Hz); ^{13}C δ/ppm (125 MHz, $CDCl_3$) 75.7, 120.2, 124.6, 125.5, 128.8, 130.1, 134.0, 134.6, 138.0, 149.1; LC-MS (ESI+) *m/z* = mass not observed; HRMS calcd. for $C_{13}H_8O_3N^{35}Cl^{79}Br$ $[M-H]^-$ 339.9371, found 339.9365

M) 3-Bromo-5-((4-fluorobenzyl)amino)pyridine-1-oxide (133)

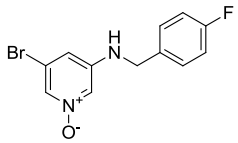

Meta-chloroperbenzoic acid (≥ 77%, 47.7 mg, 0.21 mmol) was added to a solution of aniline **132** (20 mg, 0.07 mmol) in DCM (1.56 mL) at room temperature. After 45 min, the reaction was quenched with 3 M NaOH (5 mL) and the layers were separated. The organic layer was washed with 3 M NaOH (4 × 5 mL), brine (10 mL), dried ($MgSO_4$), filtered and concentrated *in vacuo* to give **133** as a yellow solid (12 mg, 49%), which was taken forward without further purification; R_f = 0.22 (silica, 20% MeOH, DCM); ^1H δ/ppm (500 MHz, $CDCl_3$) 4.25 (2H, d, C*H*$_2$, *J* = 5.4 Hz), 4.82 (1H, m, N*H*), 6.72 (1H, s, Ar-H), 7.03-7.06 (2H, m, Ar-H), 7.26-7.28 (2H, m, Ar-H), 7.62 (1H, m, Ar-H), 7.70 (1H, m, Ar-H); LC-MS (ESI+) *m/z* = 297.1 and 299.2 $[M+H]^+$

N) 4-Ethynylanisole (159)

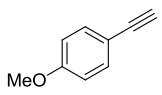

Zinc dichloride (21.9 mg, 0.160 mmol), $(PhCN)_2PdCl_2$ (30.8 mg, 0.080 mmol) and $^tBu_3P$ (33.5 mg, 0.170 mmol) were dissolved in THF (4.5 mL), mixed with diisopropylamine (564 µL, 407 mg, 4.02 mmol) and the solution was degassed with nitrogen for 30 min. Anisole **156** (201 µL, 300 mg, 1.61 mmol) and

trimethylsilylacetylene (454 µL, 316 mg, 3.22 mmol) were added and the reaction was heated to 50 ^{o}C. After 3 h, the reaction was partitioned with EtOAc (20 mL) and 1 M HCl (10 mL). The organic layer was washed with 1 M HCl (2 × 10 mL) and the aqueous layer was extracted with EtOAc (10 mL). The organic layer was washed with brine (10 mL), dried ($MgSO_4$), filtered and concentrated *in vacuo*, then dissolved in THF (2 mL) and mixed with TBAF (1 M in THF, 4.83 mL, 4.83 mmol) at room temperature. After 1 h, the reaction was concentrated to a low volume *in vacuo*. Chromatography (silica, 10% DCM, petrol) eluted **159** as a yellow oil (172 mg, 80%); R_f = 0.26 (silica, 10% DCM, petrol); UV λ_{max} (EtOH/nm) 247.5; IR ν_{max}/cm^{-1} 3285 (alkyne C-H), 2960 (C-H), 2838 (C-H), 2106 (C≡C), 1606, 1506, 1290, 1246 (C-O), 1170, 1030, 832 ; ^{1}H δ/ppm (500 MHz, $CDCl_3$) 3.00 (1H, s, CC*H*), 3.82 (3H, s, OC*H*$_3$), 6.83-6.86 (2H, m, Ar-H), 7.42-7.45 (2H, m, Ar-H); ^{13}C δ/ppm (125 MHz, $CDCl_3$) 55.3, 75.8, 83.7, 113.9, 114.2, 133.6, 159.9; LC-MS (ESI+) *m/z* = mass not observed; HRMS calcd. for C_9H_8O $[M+H]^+$ 132.0570, found 132.0567

O) Methyl 3-(4-methoxyphenyl)propiolate (157)

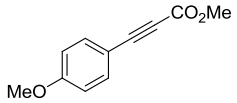

n-Butyllithium (1.5 M in hexanes, 1.28 mL, 1.95 mmol) was added dropwise to a solution of diisopropylamine (273 µL, 197 mg, 1.95 mmol) in THF (4.4 mL) at -78 ^{o}C. After 40 min, 4-ethynylanisole (230 µL, 234 mg, 1.77 mmol) (**159**), as a solution in THF (1 mL, 1.8 M), was added dropwise. After 30 min, methyl chloroformate (206 µL, 251 mg, 2.66 mmol), as a solution in THF (1 mL, 2.7 M), was added dropwise and the reaction was warmed to room temperature. After 30 min, the reaction was quenched with saturated aqueous $NaHCO_3$ (5 mL) and partitioned with EtOAc (10 mL) and distilled water (10 mL). The organic layer was washed with distilled water (2 × 10 mL) and the aqueous layer was extracted with EtOAc (10 mL). The organic layer was washed with brine (10 mL), dried ($MgSO_4$), filtered and concentrated *in vacuo*. Chromatography (silica, 20-35% DCM, petrol) eluted **157** as a yellow solid (285 mg, 85%); R_f = 0.36 (silica, 5% EtOAc, petrol); m.p. 55-58 ^{o}C; UV λ_{max} (EtOH/nm) 253.0; IR ν_{max}/cm^{-1} 3074 (C-H), 2963 (C-H), 2226 (C≡C), 1700 (C=O), 1619, 1440, 1247 (C-O), 1157, 1098, 972, 831, 747, 718; ^{1}H δ/ppm (500 MHz, $CDCl_3$) 3.79 (3H, s, CO_2CH_3), 3.83 (3H, s, OC*H*$_3$), 6.48 (2H, d, Ar-H, *J* = 16.1 Hz), 6.79 (2H, d, Ar-H, *J* =

16.0 Hz); ^{13}C δ/ppm (125 MHz, $CDCl_3$) 52.3, 53.1, 81.8, 86.8, 121.7, 135.1, 153.6, 165.1; LC-MS (ESI+) *m/z* = mass not observed; HRMS mass not observed

P) 3-Hydroxy-5-(4-methoxyphenyl)isoxazole (162a)

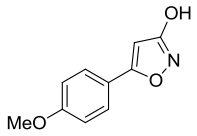

Ester **157** (20 mg, 0.11 mmol), as a solution in methanol (0.5 mL, 0.2 M), was added dropwise to a solution of hydroxylamine hydrochloride (23 mg, 0.33 mmol) in 3 M NaOH (0.28 mL, 33.2 mg, 0.83 mmol) at 0 °C. After 30 min, the reaction was heated to 70 °C for 30 min then cooled back to 0 °C, quenched with *conc.* HCl (1 mL) and partitioned with EtOAc (10 mL) and 1 M HCl (10 mL). The organic layer was washed with 1 M HCl (2 × 10 mL) and the aqueous layer was extracted with EtOAc (2 × 10 mL). The organic layer was washed with brine (10 mL), dried ($MgSO_4$), filtered and concentrated *in vacuo* to afford **162a** as a light brown solid (18.6 mg, 93%); R_f = 0.25 (silica, 40% EtOAc, petrol); m.p. 199 °C (decomposed); UV λ_{max} (EtOH/nm) 273.5; IR ν_{max}/cm^{-1} 2953 (C-H), 2774 (C-H) and 2612 (br) (O-H), 1629, 1536, 1498, 1358, 1302, 1253 (C-O), 1179, 956, 829, 775, 726; ^{1}H δ/ppm (500 MHz, DMSO-d_6) 3.82 (3H, s, OC*H*$_3$), 6.40 (1H, s, isoxazole C$_4$-H), 7.06 (2H, d, Ar-H, *J* = 8.7 Hz), 7.74 (2H, d, Ar-H, *J* = 8.7 Hz), 11.30 (1H, s, br, O*H*); ^{13}C δ/ppm (125 MHz, DMSO-d_6) 55.3, 90.2, 114.5, 120.1, 126.9, 160.7, 169.0, 170.9; LC-MS (ESI+) *m/z* = 192.2 [M-H]$^-$; HRMS calcd. for $C_{10}H_8O_3N$ [M-H]$^-$ 190.0510, found 190.0511

Q) *N*-(3-Bromo-2-methylphenyl)-4-methoxybenzamide (147a)

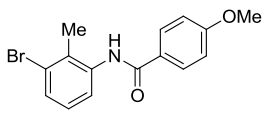

Isopropylmagnesium chloride lithium chloride solution (1.3 M in THF, 4.96 mL, 6.45 mmol) was added dropwise to a solution of aniline **146** (265 µL, 400 mg, 2.15 mmol) and methyl 4-methoxybenzoate (358 mg, 2.15 mmol) in 1,2-DME (10.8 mL) at room temperature. After 3 h, the reaction was quenched with saturated aqueous NH_4Cl (5 mL) and partitioned with EtOAc (10 mL) and distilled water (10 mL). The aqueous layer

was extracted with EtOAc (10 mL) and the organic layer was washed with brine (10 mL), dried ($MgSO_4$), filtered and concentrated *in vacuo* to give **147a** as a light brown solid (635 mg, 92%); R_f = 0.22 (silica, 20% EtOAc, petrol); m.p. 164-167 ^oC; UV λ_{max} (EtOH/nm) 258.8; IR ν_{max}/cm^{-1} 3275 (N-H), 1642, 1606, 1568, 1504, 1458, 1299, 1253 (C-O), 1176, 1106, 1024, 915, 843, 774, 688; ^1H δ/ppm (500 MHz, DMSO-d_6) 2.27 (3H, s, Ar-C*H*$_3$), 3.85 (3H, s, OC*H*$_3$), 7.06-7.08 (2H, m, Ar-H), 7.18 (1H, t, Ar-H, *J* = 7.9 Hz), 7.33 (1H, d, Ar-H, *J* = 7.8 Hz), 7.53 (1H, d, Ar-H, *J* = 8.0 Hz), 7.96-7.98 (2H, m, Ar-H), 10.01 (1H, s, N*H*); ^{13}C δ/ppm (125 MHz, DMSO-d_6) 18.4, 55.4, 113.6, 117.4, 124.6, 126.6, 127.3, 129.6, 129.9, 138.1; LC-MS (ESI+) *m/z* = 320.3 and 322.3 $[M+H]^+$; HRMS calcd. for $C_{15}H_{15}O_2N^{79}Br$ $[M+H]^+$ 320.0281, found 320.0283

R) 4-((2-(4-Chlorophenoxy)-4'-fluoro-[1,1'-biphenyl]-3-yl)amino)phenol (138o)

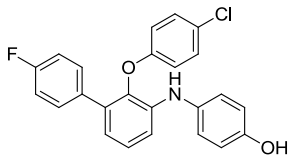

Boron tribromide (1 M in DCM, 0.4 mL, 0.4 mmol) was added dropwise to a solution of anisole **137f** (20 mg, 0.05 mmol) in DCM (1.4 mL) at 0 ^oC and stirred at room temperature. After 24 h, the reaction was quenched with distilled water (5 mL) and partitioned with DCM (10 mL). The organic layer was washed with brine (10 mL), dried ($MgSO_4$), filtered and concentrated *in vacuo* to give **138o** as a magenta solid (12.9 mg, 66%); R_f = 0.30 (20% EtOAc, petrol); m.p. 148 ^oC (decomposed); UV λ_{max} (EtOH/nm) 230.8; IR ν_{max}/cm^{-1} 3427 (N-H), 3115 (br) (O-H), 3031 (C-H), 2924 (C-H), 2855 (C-H), 1605, 1517, 1469, 1453, 1390, 1335, 1274, 1215 (C-O), 1159, 1084, 1009, 923, 869, 825, 773, 743, 722; ^1H δ/ppm (500 MHz, $CDCl_3$) 4.55 (1H, s, br, N*H*), 5.72 (1H, s, br, O*H*), 6.65-6.68 (2H, m, Ar-H), 6.79-6.81 (3H, m, Ar-H), 6.94-6.98 (2H, m, Ar-H), 7.01-7.04 (2H, m, Ar-H), 7.04-7.09 (3H, m, Ar-H), 7.11-7.14 (1H, m, Ar-H), 7.37-7.40 (2H, m, Ar-H); ^{13}C δ/ppm (125 MHz, $CDCl_3$) 113.4, 114.9, 115.1, 116.1, 116.3, 120.5, 124.3, 126.2, 126.8, 129.4, 130.5, 130.6, 134.5, 135.0, 138.5, 139.6, 151.9, 155.8; LC-MS (ESI+) *m/z* = 406.3 $[M+H]^+$; HRMS calcd. for $C_{24}H_{16}O_2N^{35}ClF$ $[M-H]^-$ 404.0859, found 404.0862; Analytical HPLC: 96.3%

S) 4-(2-((4-Fluorophenyl)amino)thiazol-4-yl)phenol (44r)

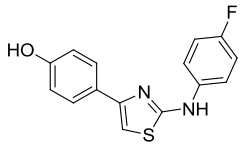

Phenacyl bromide **260** (153 mg, 0.71 mmol) and thiourea **261** (100 mg, 0.59 mmol) were dissolved in ethanol (2.6 mL) and irradiated at 70 ^{o}C for 10 min. The mixture was filtered through filter paper and the solid was washed with ice-cooled ethanol (10 mL) to give **44r** as an off-white solid (115 mg, 68%); R_f = 0.26 (silica, 30% EtOAc, petrol); m.p. 238 ^{o}C (decomposed); UV λ_{max} (EtOH/nm) 281.6 and 264.2; IR ν_{max}/cm^{-1} 3251 (N-H), 3080 (C-H), 3022 (br) (O-H), 2923 (C-H), 2761 (C-H), 1613, 1585, 1503, 1443, 1331, 1271, 1210 (C-O), 1179, 1159, 1104, 924, 871, 831, 775, 737, 710, 680; ^{1}H δ/ppm (500 MHz, DMSO-d_6) 6.24 (1H, s, br, N*H*), 6.80-6.83 (2H, m, Ar-H), 7.06 (1H, s, thiazole C_5-H), 7.17-7.20 (2H, m, Ar-H), 7.71-7.76 (4H, m, Ar-H), 10.23 (1H, s, br, O*H*); ^{13}C δ/ppm (125 MHz, DMSO-d_6) 99.8, 115.3, 115.4, 115.6, 118.2, 118.3, 125.8, 127.0, 150.2, 155.8, 157.1, 162.9; ^{19}F δ/ppm (470 MHz, DMSO-d_6) -122.2; LC-MS (ESI+) *m/z* = 287.2 $[M+H]^+$ and 285.2 $[M-H]^-$; HRMS calcd. for $C_{15}H_{10}ON_2FS$ $[M-H]^-$ 285.0503, found 285.0501; Analytical HPLC: 97.9%

T) 1,1,1-Trifluoro-*N*-(4-formylphenyl)methanesulfonamide (155)

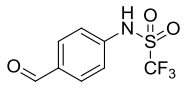

Dess-Martin periodinane (0.3 M in DCM, 3.4 mL, 1.01 mmol) was added dropwise to a solution of benzyl alcohol **154** (170 mg, 0.67 mmol) in DCM (3.3 mL) at room temperature. After 2 h, the reaction was quenched with sodium thiosulfate (800 mg, 5.06 mmol) in distilled water (10 mL, 0.5 M) and the layers were separated. The aqueous layer was acidified to pH 1 with 1 M HCl and extracted with DCM (10 × 10 mL). The organic layer was washed with brine (10 mL), dried ($MgSO_4$), filtered and concentrated *in vacuo*, then triturated with ice-cooled DCM (8 × 5 mL). Chromatography (silica, 0-15% EtOAc, petrol) afforded **155** as a white solid (71 mg, 42%); R_f = 0.34 (20% EtOAc, petrol); m.p. 91-95 ^{o}C; UV λ_{max} (EtOH/nm) 264.8; IR ν_{max}/cm^{-1} 3151 (N-H), 3071 (C-H), 2960 (C-H), 2855 (C-H), 1679 (C=O), 1601, 1512,

1492, 1422, 1378 (S=O asym. stretch), 1295, 1196, 1170, 1137 (S=O sym. stretch), 1015, 939, 830, 791, 736; ^{1}H δ/ppm (500 MHz, $CDCl_3$) 7.21 (1H, s, br, N*H*), 7.43-7.45 (2H, m, Ar-H), 7.92-7.94 (2H, m, Ar-H), 10.00 (1H, s, C*H*O); ^{13}C δ/ppm (125 MHz, $CDCl_3$) 121.5, 131.4, 134.4, 139.5, 190.7; LC-MS (ESI+) *m/z* = 252.0 $[M-H]^-$; HRMS calcd. for $C_8H_5O_3NF_3S$ $[M-H]^-$ 251.9948, found 251.9942

U) 4-Bromopyridine-*N*-oxide (125)

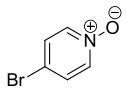

4-Bromopyridine hydrochloride (715 mg, 3.68 mmol) (**124**) was dissolved in minimal distilled water (~ 1 mL) and mixed with 3 M NaOH (1.23 mL, 147 mg, 3.68 mmol). After 20 min, the reaction was partitioned with diethyl ether (10 mL) and the aqueous layer was extracted with diethyl ether (2 × 10 mL). The organic layer was washed with brine (10 mL), dried ($MgSO_4$), filtered and concentrated *in vacuo*, then dissolved in diethyl ether (4.6 mL) and mixed with *m*CPBA (70%, 1.36 g, 5.52 mmol) at room temperature. After 24 h, the reaction was partitioned with 3 M NaOH solution (10 mL) and the organic layer was dried ($MgSO_4$), filtered and concentrated *in vacuo* to give **125** as a white solid (552 mg, 86%); R_f = 0.41 (silica, 10% MeOH, DCM); m.p. 122 ^{o}C (decomposed); UV λ_{max} (EtOH/nm) 276.2 and 213.8; IR ν_{max}/cm^{-1} 3076 (C-H), 3022 (C-H), 2998 (C-H), 1469, 1445, 1242 (N-O), 1187, 1094, 1038, 863, 696; ^{1}H δ/ppm (500 MHz, DMSO-d_6) 7.64-7.66 (2H, m, Ar-H), 8.13-8.16 (2H, m, Ar-H); ^{13}C δ/ppm (125 MHz, DMSO-d_6) 117.0, 129.5, 140.1; LC-MS (ESI+) *m/z* = 173.9 and 176.0 $[M+H]^+$; HRMS calcd. for $C_5H_5NO^{79}Br$ $[M+H]^+$ 173.9549, found 173.9547

V) 2-(2-Fluoro-3-nitrophenyl)-4,4,5,5-tetramethyl-1,3,2-dioxaborolane (142)

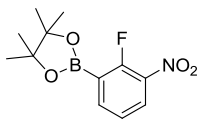

Aryl fluoride **139** (937 mg, 4.26 mg), $B_2(pin)_2$ (1.62 g, 6.39 mmol), $(PPh_3)_2PdCl_2$ (91 mg, 0.13 mmol) and potassium acetate (836 mg, 8.52 mmol) were dissolved in 1,4-dioxane (18 mL) and DMSO (0.4 mL), degassed with nitrogen for 35 min and stirred at

90 °C. After 17 h, the reaction was partitioned with EtOAc (10 mL) and distilled water (20 mL). The aqueous layer was extracted with EtOAc (8 × 8 mL) and the organic layer was washed with brine (20 mL), dried ($MgSO_4$), filtered and concentrated *in vacuo*. Chromatography (silica, 0-20% EtOAc, petrol) afforded **142** as a sand-coloured solid (699 mg, 61%); R_f = 0.18 (silica, 50% EtOAc, petrol stained with ammonium molybdate); m.p. 84-87 °C; UV λ_{max} (EtOH/nm) 252.4 and 210.4; IR ν_{max}/cm^{-1} 2979 (C-H), 2933 (C-H), 1615, 1582, 1533, 1474, 1446, 1395, 1365, 1336 (C-O), 1293, 1271, 1240, 1214, 1170, 1145, 1121, 1082, 966, 900, 855, 839, 815, 748, 692; ^{1}H δ/ppm (500 MHz, $CDCl_3$) 1.37 (12H, s, $(CH_3)_4$), 7.28 (1H, t, Ar-H, *J* = 7.8 Hz), 7.99-8.01 (1H, m, Ar-H), 8.08-8.12 (1H, m, Ar-H); ^{13}C δ/ppm (125 MHz, $CDCl_3$) 24.8, 84.7, 124.0, 128.8, 142.2, 158.2, 160.3; ^{19}F δ/ppm (470 MHz, $CDCl_3$) -108.4; LC-MS (ESI+) *m/z* = mass not observed;

W) *N*-(4-Bromothiazol-2-yl)-4-fluorobenzamide (268)

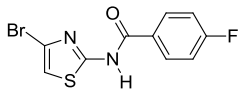

n-Butyllithium (2.7 M in hexanes, 0.21 mL, 0.56 mmol) was added dropwise to a solution of diisopropylamine (78.5 µL, 56.7 mg, 0.56 mmol) in THF (1.5 mL) at -78 °C and stirred at 0 °C for 30 min before addition of bromothiazole **267** (50 mg, 0.17 mmol). After 30 min, the reaction was quenched with distilled water (10 mL), then warmed to room temperature and stirred overnight. The reaction was partitioned with EtOAc (10 mL) and the organic layer was washed with 2 M HCl (10 mL). The aqueous layer was extracted with EtOAc (10 mL) and the organic layer was washed with brine (10 mL), dried ($MgSO_4$), filtered and concentrated *in vacuo*. Chromatography (silica, 0-10% EtOAc, petrol) afforded **268** as a white solid (30 mg, 60%); R_f = 0.29 (silica, 10% EtOAc, petrol); m.p. 150-153 °C; UV λ_{max} (EtOH/nm) 292.2 and 229.4; IR ν_{max}/cm^{-1} 3132 (N-H), 2980 (C-H), 2934 (C-H), 1669 (C=O), 1615, 1535, 1509, 1479, 1446, 1366, 1343, 1292, 1239, 1158, 1123, 1083, 1016, 967, 902, 845, 815, 750, 692; ^{1}H δ/ppm (500 MHz, DMSO-d_6) 7.39 (1H, s, thiazole C_5-H), 7.40-7.43 (2H, m, Ar-H), 8.16-8.20 (2H, m, Ar-H), 12.98 (1H, s, N*H*); ^{13}C δ/ppm (125 MHz, DMSO-d_6) 111.9, 115.7, 115.8, 120.3, 128.0, 128.1, 131.0, 131.1, 159.6, 163.8, 164.3, 165.8; ^{19}F δ/ppm (470 MHz, DMSO-d_6) -106.5; LC-MS (ESI+) *m/z* = 303.1 and 301.0 $[M+H]^+$; HRMS

calcd. for $C_{10}H_7ON_2{}^{79}BrFS$ $[M+H]^+$ 300.9441, found 300.9444; Analytical HPLC: 96.8%

X) *N*-(4-Fluorobenzyl)-4-(1*H*-indazol-5-yl)thiazol-2-amine (44t)

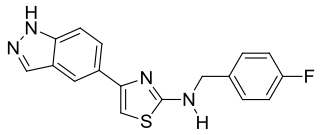

Dilute HCl (1 M, 1.0 mL) was added to a solution of thiazole **276** (40 mg, 0.10 mmol) in methanol (1.0 mL, 0.1 M) at room temperature in air and stirred at 50 ^oC. After 24 h, the reaction was quenched with saturated aqueous $NaHCO_3$ (10 mL) and partitioned with EtOAc (10 mL). The organic layer was washed with brine (10 mL), dried ($MgSO_4$), filtered and concentrated *in vacuo*. Chromatography (silica, 20-50% EtOAc, petrol) followed by semi-preparative HPLC (35% H_2O with 0.1% (v/v) HCO_2H, methanol) afforded **44t** as an off-white solid (12 mg, 37%); R_f = 0.28 (silica, 50% EtOAc, petrol); m.p. 224-227 ^oC (decomposed); UV λ_{max} (EtOH/nm) 233.2; IR ν_{max}/cm^{-1} 3225 (N-H), 3097 (N-H), 3002 (C-H), 2839 (C-H), 2780 (C-H), 1555, 1504, 1465, 1412, 1346, 1299, 1201, 1154, 1091, 1046, 942, 894, 813, 783, 745, 696, 670; ^1H δ/ppm (500 MHz, DMSO-d_6) 4.53 (2H, d, C*H*$_2$, *J* = 5.8 Hz), 7.00 (1H, s, thiazole C_5-H), 7.17-7.20 (2H, m, Ar-*H*), 7.45-7.48 (2H, m, Ar-H), 7.52 (1H, d, indazole C_7-H, *J* = 8.8 Hz), 7.84 (1H, dd, indazole C_6-H, *J* = 1.2 and 8.7 Hz), 8.09 (1H, s, Ar-H), 8.14-8.16 (1H, m, amino-N*H*), 8.22 (1H, s, Ar-H), 13.06 (1H, s, indazole-N*H*); ^{13}C δ/ppm (125 MHz, DMSO-d_6) 47.0, 99.6, 110.0, 114.9, 115.1, 117.3, 123.0, 124.6, 127.7, 129.46, 129.52, 134.0, 135.5, 139.3, 150.3, 160.3, 162.2, 168.0; ^{19}F δ/ppm (470 MHz, DMSO-d_6) -116.0; LC-MS (ESI+) *m/z* = 325.3 $[M+H]^+$ and 323.2 $[M-H]^-$; HRMS calcd. for $C_{17}H_{14}N_4FS$ $[M+H]^+$ 325.0918, found 325.0919; Analytical HPLC: 99.3%

Y) 2-(4-Chlorophenoxy)-3-ethynyl-*N*-(4-fluorophenyl)aniline (167)

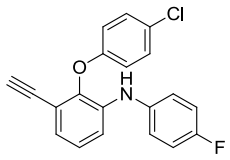

TBAF (1 M in THF, 1.31 mL, 1.31 mmol) was added to a solution of acetylene **178** (499 mg, 1.01 mmol) in THF (5 mL) and stirred at room temperature for 20 min, then concentrated to a low volume *in vacuo*. Chromatography (silica, 0-10% DCM, petrol) afforded **167** as a yellow oil (296 mg, 87%); R_f = 0.30 (silica, 20% DCM, petrol); UV λ_{max} (EtOH/nm) 280.0 and 230.0; IR ν_{max}/cm^{-1} 3408 (N-H), 3290 (C-H), 3062 (C-H), 2923 (C-H), 2107 (C≡C), 1593, 1506, 1481, 1435, 1389, 1327, 1278, 1208 (C-O), 1091, 1008, 871, 824, 778, 746; ^{1}H δ/ppm (500 MHz, $CDCl_3$) 3.06 (1H, s, CC*H*), 5.79 (1H, s, br, N*H*), 6.84-6.88 (2H, m, Ar-H), 6.97-7.02 (3H, m, Ar-H), 7.04-7.07 (3H, m, Ar-H), 7.15 (1H, dd, Ar-H, *J* = 1.6 and 8.0 Hz), 7.22-7.25 (2H, m, Ar-H; ^{13}C δ/ppm (125 MHz, $CDCl_3$) 78.8, 82.6, 115.4, 116.0, 116.2, 116.6, 117.3, 123.07, 123.13, 124.3, 125.8, 127.3, 129.6, 137.1, 138.5, 143.2, 156.1, 158.0, 160.0; ^{19}F δ/ppm (470 MHz, $CDCl_3$) -119.6; LC-MS (ESI+) *m/z* = 338.3 $[M+H]^+$ and 336.3 $[M-H]^-$; HRMS calcd. for $C_{20}H_{14}ON^{35}ClF$ $[M+H]^+$ 338.0742, found 338.0743; Analytical HPLC: 99.0%

Z) *Tert*-butyl-(2-(4-chlorophenoxy)-3-(1*H*-1,2,3-triazol-4-yl)phenyl)(4-fluorophenyl)carbamate (184)

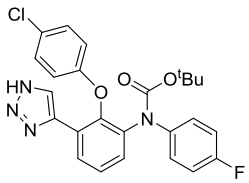

TMS-azide (61 µL, 52.5 mg, 0.46 mmol) was added to a solution of acetylene **181** (100 mg, 0.23 mmol) in ethanol (2.8 mL) and distilled water (1.0 mL) followed by sodium ascrobate (136 mg, 0.68 mmol), as a solution in distilled water (0.45 mL, 1.5 M), and then copper(II) sulfate pentahydrate (114 mg, 0.46 mmol), as a solution in distilled water (0.45 mL, 1 M) at room temperature and heated to 50 ^{o}C. After 24 h, the reaction was quenched with saturated aqueous $NaHCO_3$ (5 mL) and distilled water (15 mL) and partitioned with EtOAc (10 mL). The organic layer was washed with saturated aqueous $NaHCO_3$ (10 mL) and the aqueous layer was extracted with EtOAc (10 mL). The

organic layer was washed with brine (10 mL), dried ($MgSO_4$), filtered and concentrated *in vacuo*, then suspended in ethanol (8 mL) and treated with a homogeneous solution of EDTA (613 mg, 2.1 mmol) in ethanol (4 mL) and 3 M NaOH (4 mL) and heated to 40 ^oC. After 16 h, the solution was cooled to room temperature, concentrated *in vacuo* and partitioned with EtOAc (10 mL). The organic layer was washed with brine (10 mL), dried ($MgSO_4$), filtered and concentrated *in vacuo* to give **184** as a pale green solid (109 mg, 100%); R_f = 0.25 (silica, 5% MeOH, DCM); m.p. 90-92 ^oC; UV λ_{max} (EtOH/nm) 231.4; IR ν_{max}/cm^{-1} 3167 (br) (N-H), 2935 (C-H), 2862 (C-H), 1709 (C=O), 1684, 1505, 1483, 1461, 1326, 1289, 1219 (C-O), 1152, 1089, 1065, 1009, 824, 755; ^1H δ/ppm (500 MHz, DMSO-d_6) 1.15 (9H, s, C(C*H*$_3$)$_3$), 6.61-6.63 (2H, m, Ar-H), 6.91-6.94 (2H, m, Ar-H), 7.00-7.04 (2H, m, Ar-H), 7.21-7.23 (2H, m, Ar-H), 7.42 (1H, t, Ar-H, *J* = 7.9 Hz), 7.54 (1H, d, br, Ar-H, *J* = 7.4 Hz), 7.76 (1H, s, br, Ar-H), 8.00 (1H, s, br, Ar-H), 15.10 (1H, s, N*H*); ^{13}C δ/ppm (125 MHz, DMSO-d_6) 27.5, 80.8, 115.0, 115.2, 116.7, 125.9, 126.6, 127.5, 129.3, 131.4, 136.1, 137.8, 152.2, 155.0, 158.4, 160.4; ^{19}F δ/ppm (470 MHz, DMSO-d_6) -117.1; LC-MS (ESI+) *m/z* = 479.3 $[M-H]^-$; HRMS calcd. for $C_{25}H_{23}O_3N_4{}^{35}ClF$ $[M+H]^+$ 481.1437, found 481.1432; Analytical HPLC: 97.3%

A') 2-(4-Chlorophenoxy)-*N*-(4-fluorophenyl)-3-(1*H*-1,2,3-triazol-4-yl)aniline (185)

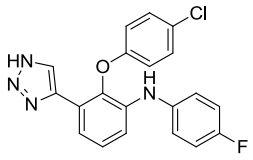

Trifluoroacetic acid (0.15 mL) was added to a solution of carbamate **184** (72 mg, 0.15 mmol) in DCM (1.5 mL) in air at room temperature. After 1 h, the reaction was partitioned with DCM (10 mL) and 1.5 M NaOH (10 mL). The aqueous layer was extracted with DCM (2 × 10 mL) and organic layers were washed with 3 M NaOH (2 × 10 mL), 1 M HCl (10 mL), brine (10 mL), dried ($MgSO_4$), filtered and concentrated *in vacuo* to give **185** as a red solid (43 mg, 75%); R_f = 0.22 (silica, 5% MeOH, DCM); m.p. 158-160 ^oC; UV λ_{max} (EtOH/nm) 230.0; IR ν_{max}/cm^{-1} 3413 (N-H), 3128 (br) (triazolo N-H), 2939 (C-H), 2863 (C-H), 1582, 1507, 1482, 1460, 1211 (C-O), 1160, 1089, 1009, 820, 748; ^1H δ/ppm (500 MHz, DMSO-d_6) 6.79-6.81 (2H, m, Ar-H), 7.01-7.06 (4H, m, Ar-H), 7.19-7.32 (4H, m, Ar-H), 7.52-7.85 (2H, m, Ar-H) (when heated to 130 ^oC, this signal converges to a broad singlet at 7.60), 7.90-8.11 (2 singlets, 1H, aniline N*H*) (when heated to 130 ^oC, this signal converges to a broad singlet at 7.90),

15.01-15.64 (3 singlets, 1H, triazole N*H*), (when heated to 130 ^{o}C, this signal converges to a broad singlet at 14.75); ^{13}C δ/ppm (125 MHz, DMSO-d_6) 115.3, 115.5, 116.5, 117.0, 117.2, 119.2, 119.6, 120.07, 120.13, 120.29, 120.35, 121.7, 125.2, 125.5, 126.5, 126.6, 129.3, 132.8, 137.9, 138.1, 139.0, 139.6, 140.1, 142.1, 155.1, 155.4; ^{19}F δ/ppm (470 MHz, DMSO-d_6) -122.3, -122.8 and -123.0 (height ratio, 1:7:4). Heating the solution to 130 ^{o}C causes coalescence into a single peak at -122.8 to -123.0; LC-MS (ESI+) *m/z* = 381.3 $[M+H]^+$ and 379.3 $[M-H]^-$; HRMS calcd. for $C_{20}H_{13}ON_4{}^{35}ClF$ $[M-H]^-$ 379.0767, found 379.0754; Analytical HPLC: 94.2%

B') 3-(3-((*tert*-butoxycarbonyl)(4-fluorophenyl)amino)-2-(4-chlorophenoxy)phenyl)propiolic acid (186)

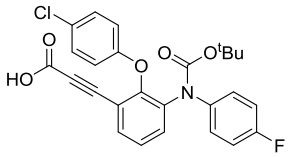

Lithium hydroxide monohydrate (269 mg, 6.40 mmol), as a solution in distilled water (3.4 mL, 1.9 M) was added to a solution of propiolate ester **182** (160 mg, 0.32 mmol) in THF (3.4 mL) in air at room temperature and stirred at 60 ^{o}C. After 2 h, the reaction was cooled to room temperature, acidified to pH 0 with 1 M HCl and extracted with EtOAc (2 × 10 mL). The organic layer was washed with distilled water (10 mL), brine (10 mL), dried ($MgSO_4$), filtered and concentrated *in vacuo* to give **186** as a white solid (153 mg, 99%); R_f = 0.30 (silica, 15% MeOH, DCM); m.p. 109-112 ^{o}C; UV λ_{max} (EtOH/nm) 229.4; IR ν_{max}/cm^{-1} 3071 (C-H), 2977 (C-H), 2615 (br) (O-H), 2223 (C≡C), 1706 and 1684 (C=O), 1506, 1483, 1452, 1333, 1228, 1151 (C-O), 1088, 1008, 926, 825, 752, 730; ^{1}H δ/ppm (500 MHz, DMSO-d_6) 1.26 (9H, s, C(C*H*$_3$)$_3$), 6.73-6.75 (2H, m, Ar-H), 7.04-7.07 (2H, m, Ar-H), 7.10-7.14 (2H, m, Ar-H), 7.36-7.38 (2H, m, Ar-H), 7.47 (1H, t, Ar-H, *J* = 7.8 Hz), 7.72 (1H, dd, Ar-H, *J* = 1.5 and 7.8 Hz), 7.80 (1H, dd, Ar-H, *J* = 1.0 and 8.1 Hz), 13.80 (1H, s, br, CO_2*H*); ^{13}C δ/ppm (125 MHz, DMSO-d_6) 27.5, 54.9, 81.1, 86.5, 115.1, 115.3, 115.4, 117.1, 126.3, 126.6, 127.6, 129.3, 133.7, 134.5, 135.1, 136.0, 137.5, 152.1, 153.8, 155.7, 158.7; ^{19}F δ/ppm (470 MHz, DMSO-d_6) -116.6; LC-MS (ESI+) *m/z* = mass not observed; HRMS mass not observed; Analytical HPLC: 99.2%

C') 5-(2-(4-Chlorophenoxy)-3-((4-fluorophenyl)amino)phenyl)-1*H*-pyrazol-3-ol (183b)

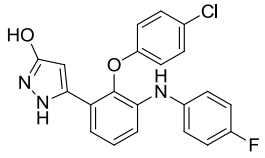

Hydrazine hydrate (15 µL, 15 mg, 0.30 mmol) was added to a solution of propiolate ester **182** (50 mg, 0.10 mmol) in methanol (1.0 mL) at 0 ^{o}C and stirred at room temperature for 45 min, before heating to 60 ^{o}C for 20 min. The reaction was cooled to 0 ^{o}C and quenched with *conc.* HCl (2.0 mL), then heated to 50 ^{o}C for 90 min. The reacton was cooled to room temperature and partitioned with EtOAc (10 mL) and 1 M HCl (10 mL). The organic layer was washed with 1 M HCl (2 × 10 mL) and the aqueous layer was extracted with EtOAc (2 × 10 mL). The organic layer was washed with brine (10 mL), dried ($MgSO_4$), filtered and concentrated *in vacuo*. Preparative HPLC (5-100% MeCN, H_2O + 0.1% (v/v) HCO_2H) afforded **183b** as a dark brown solid (15 mg, 38%); R_f = 0.36 (silica, 5% MeOH, DCM); m.p. 187-188 ^{o}C (decomposed); UV λ_{max} (EtOH/nm) 263.8 and 229.6; IR ν_{max}/cm^{-1} 3406 (amino N-H), 3038 (pyrazolo N-H), 2921 (C-H), 2653 (br) (O-H), 1585, 1504, 1480, 1322, 1205 (C-O), 1158, 1089, 1007, 904, 860, 822, 772, 743; ^{1}H δ/ppm (500 MHz, DMSO-d_6) 5.71 (1H, s, pyrazole C_4-*H*), 6.74-6.76 (2H, m, Ar-H), 6.98-7.07 (4H, m, Ar-H), 7.16-7.33 (5H, m, Ar-H), 7.61 (1H, s, amine N*H*), 9.73 (1H, s, br, pyrazole N*H*), 12.00 (1H, s, br, O*H*); ^{13}C δ/ppm (125 MHz, DMSO-d_6) 115.3, 115.5, 116.5, 117.0, 118.6, 120.15, 120.21, 125.4, 126.3, 129.2, 138.1, 139.0, 155.6, 155.9, 157.8, 166.7, 168.7; ^{19}F δ/ppm (470 MHz, DMSO-d_6) -122.9; LC-MS (ESI+) *m/z* = 396.3 $[M+H]^+$ and 394.2 $[M-H]^-$; HRMS calcd. for $C_{21}H_{14}O_2N_3{}^{35}ClF$ $[M-H]^-$ 394.0764, found 394.0756; Analytical HPLC: 97.0%

D') 2'-(4-Chlorophenoxy)-3'-((4-fluorophenyl)amino)-5'-(hydroxymethyl)-[1,1'-biphenyl]-4-ol (231)

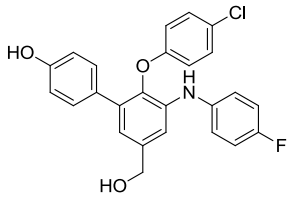

DIBAL-H (1 M in cyclohexane, 1.85 mL, 1.85 mmol) was added dropwise to a solution of ester **230** (190 mg, 0.41 mmol) in THF (3.0 mL) at -78 ^{o}C and stirred for 30 min, then warmed to 0 ^{o}C. After 4 h, the reaction was quenched with saturated aqueous Rochelle salt (3 mL), warmed to room temperature and stirred overnight. The reaction was partitioned with EtOAc (10 mL) and distilled water (2 × 10 mL) and the aqueous layer was extracted with EtOAc (2 × 10 mL). The organic layer was washed with brine (10 mL), dried ($MgSO_4$), filtered and concentrated *in vacuo*. Chromatography (silica, 20-75% EtOAc, petrol) afforded **231** as a brown solid (165 mg, 93%); R_f = 0.40 (silica, 50% EtOAc, petrol); m.p. 192-194 ^{o}C; UV λ_{max} (EtOH/nm) 271.2 and 230.0; IR ν_{max}/cm^{-1} 3601 (benzyl O-H), 3398 (N-H), 3307 (br) (phenol O-H), 3037 (C-H), 2942 (C-H), 1589, 1502, 1445, 1376, 1215 (C-O), 1166, 1104, 1029, 825, 739; ^{1}H δ/ppm (500 MHz, DMSO-d_6) 4.49 (2H, d, C*H*$_2$, *J* = 5.5 Hz), 5.19 (1H, t, CH$_2$O*H*, *J* = 5.8 Hz), 6.61-6.64 (2H, m, Ar-H), 6.71 (2H, d, Ar-H, *J* = 8.5 Hz), 6.87 (1H, d, Ar-H, *J* = 1.7 Hz), 7.01-7.07 (4H, m, Ar-H), 7.14-7.17 (3H, m, Ar-H), 7.26-7.27 (2H, m, Ar-H), 7.58 (1H, s, amino N*H*), 9.45 (1H, s, O*H*); ^{13}C δ/ppm (125 MHz, DMSO-d_6) 62.6, 114.0, 115.0, 115.3, 115.4, 116.6, 119.8, 119.9, 124.8, 127.9, 128.9, 129.7, 135.2, 137.3, 139.0, 139.4, 140.4, 155.7, 156.1, 156.7, 157.6; ^{19}F δ/ppm (470 MHz, DMSO-d_6) -123.3; LC-MS (ESI+) *m/z* = 436.3 $[M+H]^+$ and 434.2 $[M-H]^-$; HRMS calcd. for $C_{25}H_{18}O_3N^{35}ClF$ $[M-H]^-$ 434.0965, found 434.0956; Analytical HPLC: 96.1%

E') Ethyl 5-(4-chlorobenzyl)-1-(4-chlorophenyl)-2-(4-fluorophenyl)-1*H*-pyrrole-3-carboxylate (283b)

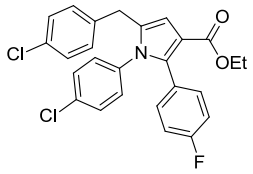

A solution of 1,4-diketone **282b** (160 mg, 0.42 mmol) and 4-chloroaniline (268 mg, 2.10 mmol) in glacial acetic acid (1.4 mL) was irradiated at 170 ^{o}C for 12 min. The reaction was partitioned with EtOAc (10 mL) and saturated aqueous NH_4Cl (30 mL). The organic layer was washed with saturated aqueous $NaHCO_3$ (10 mL) and the aqueous layer was extracted with EtOAc (2 × 10 mL). The organic layer was washed with brine (10 mL), dried ($MgSO_4$), filtered and concentrated *in vacuo*. Chromatography (silica, 0-15% EtOAc, petrol) afforded **283b** as a yellow solid (165 mg, 83%); R_f = 0.30 (silica, 10% EtOAc, petrol); m.p. 132-134 ^{o}C; UV λ_{max} (EtOH/nm) 223.0; IR ν_{max}/cm^{-1} 3104 (C-H), 2979 (C-H), 2931 (C-H), 1684 (C=O), 1527, 1490, 1431, 1341, 1295, 1220 (C-O), 1155, 1090, 1016, 835, 776; ^{1}H δ/ppm (500 MHz, $CDCl_3$) 1.18 (3H, t, $CO_2CH_2CH_3$, *J* = 7.1 Hz), 3.71 (2H, s, 4-ClPhCH_2), 4.15 (2H, q, $CO_2CH_2CH_3$, *J* = 7.1 Hz), 6.54 (1H, s, pyrrole C_4-H), 6.79-6.81 (2H, m, Ar-H), 6.86-6.91 (4H, m, Ar-H), 7.08-7.11 (2H, m, Ar-H), 7.17-7.20 (4H, m, Ar-H); ^{13}C δ/ppm (125 MHz, $CDCl_3$) 14.2, 32.7, 59.7, 110.1, 113.8, 114.5, 114.7, 127.26, 127.29, 128.5, 129.1, 129.9, 130.0, 132.2, 132.78, 132.84, 132.9, 134.3, 135.9, 136.9, 138.1, 161.3, 163.3, 164.6; ^{19}F δ/ppm (470 MHz, $CDCl_3$) -113.4; LC-MS (ESI+) *m/z* = 468.3 $[M+H]^+$; HRMS calcd. for $C_{26}H_{21}O_2N^{35}Cl_2F$ $[M+H]^+$ 468.0928, found 468.0929; Analytical HPLC: 99.2%

F') 2-(6-(4-Chlorophenoxy)-5-((4-fluorophenyl)amino)-4'-hydroxy-[1,1'-biphenyl]-3-yl)acetic acid (244)

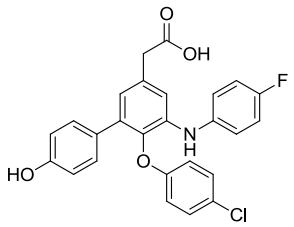

Nitrile **243** (20 mg, 0.045 mmol) was refluxed in 15% NaOH (2 mL) at 130 ^{o}C. After 17 h, the flask was cooled to room temperature and washed with diethyl ether (2 × 10 mL). The aqueous layer was acidified to pH 0 with 2 M HCl (20 mL) and extracted with diethyl ether (2 × 10 mL). The organic layer was washed with brine (10 mL), dried ($MgSO_4$), filtered and concentrated *in vacuo*. Preparative HPLC (25% H_2O with 0.1% (v/v) HCO_2H, MeCN) afforded **244** as a brown solid (7 mg, 33%); R_f = 0.42 (silica, 5% MeOH, DCM); UV λ_{max} (EtOH/nm) 273.4 and 231.8; IR ν_{max}/cm^{-1} 3405 (N-H), 3033 (C-H), 2955 (C-H), 2921 (C-H), 2852 (C-H), 2614 (br) (O-H), 1701 (C=O), 1585, 1504, 1482, 1445, 1420, 1390, 1361, 1262, 1210 (C-O), 1172, 1088, 1008, 823; ^{1}H δ/ppm (500 MHz, $CDCl_3$) 3.61 (2H, s, C*H*$_2$), 5.80 (1H, s, br, phenol O*H*), 6.67 (2H, d, Ar-H, *J* = 8.9 Hz), 6.72 (2H, d, Ar-H, *J* = 8.6 Hz), 6.79-6.80 (1H, m, Ar-H), 6.97-7.00 (2H, m, Ar-H), 7.04-7.07 (5H, m, Ar-H), 7.26 (1H, s, N*H*), 7.29 (2H, d, Ar-H, *J* = 8.4 Hz) - The CO_2H proton was not observed; ^{13}C δ/ppm (125 MHz, $CDCl_3$) 40.7, 114.5, 115.1, 116.0, 116.2, 116.3, 122.3, 122.7, 122.8, 126.8, 129.4, 129.6, 130.3, 131.1, 135.8, 137.4, 138.4, 138.5, 155.0, 155.8, 157.9, 159.8, 176.3; ^{19}F δ/ppm (470 MHz, $CDCl_3$) -120.0; LC-MS (ESI+) *m/z* = 464.2 $[M+H]^+$ and 462.2 $[M-H]^-$; HRMS calcd. for $C_{26}H_{18}O_4N^{35}ClF$ $[M-H]^-$ 462.0914, found 462.0908; Analytical HPLC: 99.2%

G') 6-Chloro-1-(triisopropylsilyl)-1*H*-indole (200)

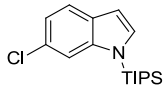

n-Butyllithium (2.7 M in hexanes, 0.52 mL, 1.39 mmol) was added dropwise to a solution of indole **199** (200 mg, 1.32 mmol) in THF (4.4 mL) at -78 ^{o}C. After 1 h, TIPS-chloride (368 µL, 332 mg, 1.72 mmol) was added and the reaction was warmed to room temperature. After 1 h, the reaction was quenched with saturated aqueous NH_4Cl (5 mL)

and the layers were separated. The organic layer was washed with distilled water (10 mL) and the aqueous layer was extracted with EtOAc (10 mL). The organic layer was washed with brine (10 mL), dried ($MgSO_4$), filtered and concentrated *in vacuo*. Chromatography (silica, 0-10% EtOAc, petrol) afforded **200** as a colourless solid (384 mg, 95%); R_f = 0.75 (silica, 5% EtOAc, petrol); m.p. 50-53 ^oC; UV λ_{max} (EtOH/nm) 275.4 and 226.8; IR ν_{max}/cm^{-1} 2948 (C-H), 2868 (C-H), 1603, 1509, 1457, 1429, 1319, 1274, 1143, 1072, 1016, 979, 901, 882, 805, 721, 689; ^1H δ/ppm (500 MHz, $CDCl_3$) 1.15 (18H, d, $Si(CH(CH_3)_2)_3$, *J* = 7.6 Hz), 1.69 (3H, sep, $Si(CH(CH_3)_2)_3$, *J* = 7.6 Hz), 6.60 (1H, dd, C_3-*H*, *J* = 0.8 and 3.2 Hz), 7.08 (1H, dd, C_5-H, *J* = 1.7 and 8.4 Hz), 7.24 (1H, d, C_2-H, *J* = 3.2 Hz), 7.47 (1H, s, C_7-H), 7.52 (1H, d, C_4-H, *J* = 8.4 Hz); ^{13}C δ/ppm (125 MHz, $CDCl_3$) 12.8, 18.1, 104.8, 113.7, 120.4, 121.2, 127.2, 130.0, 131.9, 141.2; LC-MS (ESI+) *m/z* = 308.3 $[M+H]^+$; HRMS mass not observed

H') 1-(Tetrahydro-2*H*-pyran-2-yl)-5-(4,4,5,5-tetramethyl-1,3,2-dioxaborolan-2-yl)-1*H*-indazole (273)

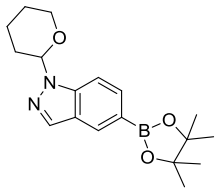

3,4-Dihydro-2*H*-pyran (608 µL, 560 mg, 6.66 mmol) was added to a solution of indazole **272** (270 mg, 1.11 mmol) and *p*TSA (42.2 mg, 0.22 mmol) in DCM (4.5 mL) at room temperature. After 2 h, the reaction was diluted with DCM (10 mL) and washed with saturated aqueous $NaHCO_3$ (3 × 10 mL). The aqueous layer was extracted with DCM (2 × 10 mL) and the organic layer was washed with brine (10 mL), dried ($MgSO_4$), filtered and concentrated *in vacuo*. Chromatography (silica, 0-30% Et_2O, petrol followed by 0-10% EtOAc, petrol) afforded **273** as a colourless oil (252 mg, 65%); R_f = 0.31 (silica, 20% EtOAc, petrol); UV λ_{max} (EtOH/nm) 225.4; IR ν_{max}/cm^{-1} 2975 (C-H), 2940 (C-H), 2863 (C-H), 1614, 1364, 1302, 1269, 1211, 1142, 1071, 1042, 994, 964, 912, 858, 813, 758, 684; ^1H δ/ppm (500 MHz, DMSO-d_6) 1.32 (12H, s, $(CH_3)_4$), 1.57-1.60 (2H, m, CH_2-CH_2-O), 1.70-1.80 (1H, m, CH_2-CH_2-CH_2-O), 1.95-1.98 (1H, m, CH_2-CH_2-CH_2-O), 2.03-2.05 (1H, m, CH_2-CH-O), 2.38-2.48 (1H, m, CH_2-CH-O), 3.72-3.77 (1H, m, CH_2-O), 3.88-3.91 (1H, m, CH_2-O), 5.87 (1H, dd, N-C*H*-O, *J* = 2.4 and 9.7 Hz), 7.67 (1H, dd, C_6-H, *J* = 0.7 and 8.5 Hz), 7.72 (1H, d, C_7-H, *J* = 8.5 Hz), 8.16-8.17 (2H, two singlets, C_3-H and C_4-H); ^{13}C δ/ppm (125 MHz, DMSO-d_6)

22.2, 24.7, 24.8, 28.9, 66.6, 83.6, 84.0, 109.8, 124.0, 128.8, 131.4, 134.2, 140.7; LC-MS (ESI+) *m/z* = 329.5 $[M+H]^+$; HRMS calcd. for $C_{18}H_{26}O_3N_2{}^{10}B$ $[M+H]^+$ 329.2031, found 329.2037

I') 3-Bromo-6-chloro-1-(triisopropylsilyl)-1*H*-indole (202)

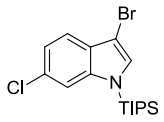

N-bromosuccinimide (909 mg, 5.11 mmol), as a solution in THF (10 mL, 0.5 M) was added to a solution of indole **200** (1.50 g, 4.87 mmol) in THF (10 mL, 0.5 M) at -78 ^oC in air. After 3 h, the reaction was quenched with distilled water (20 mL), warmed to room temperature and partitioned with diethyl ether (10 mL). The aqueous layer was extracted with diethyl ether (10 mL) and the organic layer was washed with brine (10 mL), dried ($MgSO_4$), filtered and concentrated *in vacuo*. Chromatography (silica, 0-10% DCM, petrol) afforded **202** as a colourless solid (1.75 g, 93%); R_f = 0.72 (silica, 20% DCM, petrol); m.p. 59-60 ^oC; UV λ_{max} (EtOH/nm) 285.2 and 231.2; IR ν_{max}/cm^{-1} 2948 (C-H), 2868 (C-H), 1606, 1559, 1459, 1426, 1319, 1281, 1194, 1136, 1069, 1017, 937, 882, 844, 799, 735, 692; ^1H δ/ppm (500 MHz, $CDCl_3$) 1.15 (18H, d, $Si(CH(CH_3)_2)_3$, *J* = 7.6 Hz), 1.66 (3H, sep, $Si(CH(CH_3)_2)_3$, *J* = 7.5 Hz), 7.17 (1H, dd, C_5-*H*, *J* = 1.6 and 8.4 Hz), 7.21 (1H, s, C_2-H), 7.45 (1H, d, C_7-H, *J* = 1.6 Hz), 7.47 (1H, d, C_4-H, *J* = 8.5 Hz); ^{13}C δ/ppm (125 MHz, $CDCl_3$) 12.8, 18.0, 93.6, 113.9, 120.0, 121.3, 128.6, 128.7, 130.5, 140.4; LC-MS (ESI+) *m/z* = 386.3 and 388.3 $[M+H]^+$; HRMS mass not observed

J') ((2-Fluoro-3-nitrophenyl)ethynyl)triisopropylsilane (164)

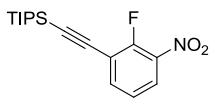

Diisopropylamine (82 µL, 59 mg, 0.58 mmol) was added to a solution of aryl bromide **139** (50 mg, 0.23 mmol), $(PPh_3)_2PdCl_2$ (4.8 mg, 0.007 mmol) and CuI (1.3 mg, 0.007 mmol) in THF (2.3 mL). The solution was degassed with nitrogen for 5 min, mixed with TIPS-acetylene (79 µL, 64 mg, 0.35 mmol) and heated to 70 ^oC for 1 h. The

reaction was partitioned with EtOAc (10 mL) and 66% distilled water, 1 M HCl (15 mL). The organic layer was washed with 66% distilled water, 1 M HCl (15 mL) and the aqueous layer was extracted with EtOAc (5 × 8 mL). The organic layer was washed with brine (10 mL), dried ($MgSO_4$), filtered and concentrated *in vacuo*. Chromatography (silica, 0-10% DCM, petrol) afforded **164** as a yellow solid (62 mg, 85%); R_f = 0.32 (silica, 20% DCM, petrol); m.p. 39-41 ^oC; UV λ_{max} (EtOH/nm) 245.4; IR ν_{max}/cm^{-1} 3088 (C-H), 2939 (C-H), 2864 (C-H), 2160 (C≡C), 1609, 1580, 1542, 1454, 1346, 1289, 1269, 1192, 1075, 1017, 993, 944, 882, 841, 797, 734, 674; ^1H δ/ppm (500 MHz, $CDCl_3$) 1.12-1.15 (21H, m, Si(C*H*(CH_3)$_2$)$_3$), 7.23 (1H, dd, C_5-H, *J* = 1.1 and 7.8 Hz), 7.71-7.74 (1H, m, C_6-H), 7.95-7.99 (1H, m, C_4-H); ^{13}C δ/ppm (125 MHz, $CDCl_3$) 11.2, 18.6, 97.0, 100.90, 100.94, 115.6, 115.7, 123.8, 123.9, 125.45, 125.47, 137.8, 138.77, 138.79, 155.2, 157.3; ^{19}F δ/ppm (470 MHz, $CDCl_3$) -114.4; LC-MS (ESI+) *m/z* = 320.3 $[M-H]^-$; HRMS calcd. for $C_{17}H_{25}O_2NFSi$ $[M+H]^+$ 322.1633, found 322.1630

K') 2-(4-Chlorophenoxy)-3-ethynylaniline (166)

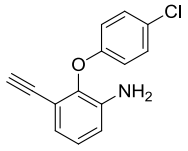

Tin(II) chloride dihydrate (2.89 g, 12.8 mmol) was added to a solution of nitro **165** (439 mg, 1.60 mmol) in ethanol (4.0 mL) room temperature and stirred at 70 ^oC for 30 min. The reaction was cooled to room temperatature, quenched with saturated aqueous $NaHCO_3$ (10 mL), filtered through celite and partitioned with EtOAc (10 mL) and distilled water (10 mL). The organic layer was dried ($MgSO_4$), filtered and concentrated *in vacuo* to give **166** as a brown solid (390 mg, 100%); R_f = 0.28 (silica, 10% EtOAc, petrol); m.p. 73-75 ^oC; UV λ_{max} (EtOH/nm) 226.8; IR ν_{max}/cm^{-1} 3486 (N-H), 3394 (N-H), 3286 (alkyne C-H), 1614, 1471, 1324, 1276, 1219 (C-O), 1163, 1095, 1056, 1009, 965, 869, 832, 790, 750, 700 (C≡C bond not observed); ^1H δ/ppm (500 MHz, $CDCl_3$) 3.04 (1H, s, CC*H*), 3.97 (2H, s, br, NH_2), 6.82-6.85 (3H, m, 1-H_2NPh C_6-H, 4-ClPh C_3-H and C_5-H), 6.95 (1H, dd, 1-H_2NPh C_4-H, *J* = 1.6 and 7.7 Hz), 7.02 (1H, t, 1-H_2NPh C_5-H, *J* = 7.8 Hz), 7.23 (2H, d, 4-ClPh C_2-H and C_6-H, *J* = 8.9 Hz); ^{13}C δ/ppm (125 MHz, $CDCl_3$) 79.0, 82.1, 116.5, 117.2, 117.4, 123.8, 126.0, 127.1, 129.5, 139.7, 142.3, 156.0; LC-MS (ESI+) *m/z* = 244.3 $[M+H]^+$; HRMS mass not observed

L') *Tert*-butyl (2-(4-chlorophenoxy)-3-ethynylphenyl)(4-fluorophenyl)carbamate (181)

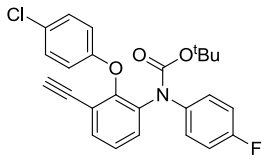

Boc_2O (262 mg, 1.20 mmol), as a solution in acetonitrile (0.3 mL, 4 M) was added dropwise to a solultion of aniline **167** (201 mg, 0.60 mmol) and DMAP (37 mg, 0.30 mmol) in acetonitrile (3.6 mL) at room temperature in a sealed vial in air and heated to 50 ^oC for 1 h. The reaction was cooled to room temperature, concentrated to a low volume *in vacuo* and partitioned with EtOAc (10 mL) and saturated aqueous $NaHCO_3$ (3 × 10 mL). The organic layer was washed with brine (10 mL), dried ($MgSO_4$), filtered and concentrated *in vacuo*. Chromatography (silica, 0-10% Et_2O, petrol) afforded **181** as a yellow oil (62 mg, 85%); R_f = 0.25 (silica, 10% Et_2O, petrol); UV λ_{max} (EtOH/nm) 230.0; IR ν_{max}/cm^{-1} 3295 (alkyne C-H), 3071 (C-H), 2975 (C-H), 2324 (C≡C), 1706 (C=O), 1588, 1506, 1484, 1449, 1328, 1227 (C-O), 1152, 1081, 1009, 876, 827, 754; ^1H δ/ppm (500 MHz, $CDCl_3$) 1.32 (9H, s, C(C*H*$_3$)$_3$) 3.08 (1H, s, CC*H*), 6.70 (2H, d, 4-ClPh C_3-H and C_5-H, *J* = 8.9 Hz), 6.90 (2H, t, 4-FPh C_3-H and C_5-H, *J* = 8.4 Hz), 6.98-7.01 (2H, m, 4-FPh C_2-H and C_6-H), 7.19 (2H, d, 4-ClPh C_2-H and C_6-H, *J* = 8.9 Hz), 7.25 (1H, t, C_5-H, *J* = 7.9 Hz), 7.45 (1H, d, br, C_6-H, *J* = 7.9 Hz), 7.50 (1H, dd, C_4-H, *J* = 1.5 and 7.8 Hz); ^{13}C δ/ppm (125 MHz, $CDCl_3$) 28.0, 78.1, 81.7, 83.3, 115.1, 115.3, 117.0, 118.6, 125.5, 127.1, 127.5, 129.1, 131.9, 133.2, 136.3, 151.7, 153.1, 156.0, 159.3, 161.3; ^{19}F δ/ppm (470 MHz, $CDCl_3$) -116.7; LC-MS (ESI+) *m/z* = mass not observed; HRMS mass not observed

M') 6-Chloro-1-(4-methoxybenzyl)-1*H*-indole (206)

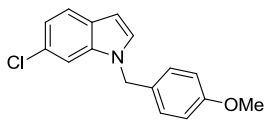

Indole **199** (100 mg, 0.66 mmol), as a solution in DMF (0.5 mL, 1.3 M), was added dropwise to a suspension of sodium hydride (60% in mineral oil, 53 mg, 1.32 mmol) in DMF (2.5 mL), followed by *p*-methoxybenzyl chloride (134 µL, 155 mg, 0.99 mmol) at room temperature and then heated to 80 ^oC. After 2 h, the reaction was cooled to room temperature, quenched with saturated aqueous NH_4Cl (3 mL) and partitioned with diethyl ether (10 mL) and distilled water (30 mL). The organic layer was washed with

distilled water (30 mL) and the aqueous layer was extracted with diethyl ether (2 × 10 mL). The organic layer was washed with brine (10 mL), dried ($MgSO_4$), filtered and concentrated *in vacuo*. Chromatography (silica, 0-10% DCM, petrol) afforded **206** as a yellow oil (147 mg, 85%); R_f = 0.49 (silica, 20% DCM, petrol); UV λ_{max} (EtOH/nm) 278.2 and 227.0; IR ν_{max}/cm^{-1} 3099 (C-H), 2999 (C-H), 2930 (C-H), 2834 (C-H), 1609, 1509, 1460, 1314, 1243 (C-O), 1173, 1098, 1030, 898, 800, 757, 715, 660; ^{1}H δ/ppm (500 MHz, $CDCl_3$) 3.78 (3H, s, OC*H*$_3$), 5.21 (2H, s, NC*H*$_2$Ar), 6.50 (1H, dd, C_3-H, *J* = 0.7 and 3.2 Hz), 6.85 (2H, d, 4-MeOPh C_2-H and C_6-H, *J* = 8.7 Hz), 7.06 (2H, d, 4-MeOPh C_3-H and C_5-H, *J* = 8.7 Hz), 7.07 (1H, dd, C_5-H, *J* = 1.8 and 8.4 Hz), 7.09 (1H, d, C_2-H, *J* = 3.2 Hz), 7.29 (1H, s, br, C_7-H), 7.53 (1H, d, C_4-H, *J* = 8.4 Hz); ^{13}C δ/ppm (125 MHz, $CDCl_3$) 49.7, 55.3, 101.8, 109.7, 114.3, 120.2, 121.8, 127.3, 127.6, 128.2, 128.8, 128.9, 136.6, 159.2; LC-MS (ESI+) *m/z* = mass not observed

N') 6-Chloro-1-(4-methoxybenzyl)-3-(2-nitrophenyl)-1*H*-indole (211)

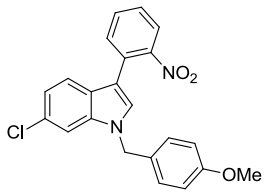

n-Butyllithium (2.5 M in hexanes, 0.13 mL, 0.32 mmol) was added dropwise to a solution of indole **210** (100 mg, 0.29 mmol) in THF (2.2 mL, 0.1 M) at 0 ^oC. After 15 min, aryl fluoride **207** (61 µL, 81.8 mg, 0.58 mmol) was added. After 30 min, the reaction was quenched with distilled water (10 mL), warmed to room temperature and partitioned with EtOAc (10 mL). The organic layer was washed with brine (10 mL), dried ($MgSO_4$), filtered and concentrated *in vacuo*. Chromatography (silica, 0-30% Et_2O, petrol) afforded **211** as a brown solid (64 mg, 53%); R_f = 0.22 (silica, 20% Et_2O, petrol); m.p. 106-108 ^oC; UV λ_{max} (EtOH/nm) 228.0; IR ν_{max}/cm^{-1} 3126 (C-H), 3014 (C-H), 2932 (C-H), 2833 (C-H), 1606, 1509, 1440, 1377, 1342, 1224 (C-O), 1172, 1089, 1029, 939, 804; ^{1}H δ/ppm (500 MHz, $CDCl_3$) 3.79 (3H, s, OC*H*$_3$), 5.25 (2H, s, NC*H*$_2$), 6.88 (2H, d, 4-MeOPh C_2-H and C_6-H, *J* = 8.7 Hz), 7.09-7.11 (3H, m, 4-MeOPh C_3-H, C_5-H and indole C_5-H), 7.23 (1H, s, indole C_2-H), 7.33 (1H, d, indole C_7-H, *J* = 1.6 Hz), 7.39 (1H, d, indole C_4-H, *J* = 8.5 Hz), 7.42-7.45 (1H, m, 2-NO_2Ph C_4-H), 7.58-7.62 (2H, m, 2-NO_2Ph C_5-H and C_6-H), 7.84 (1H, d, 2-NO_2Ph C_3-H, *J* = 8.1 Hz); ^{13}C δ/ppm (125 MHz, $CDCl_3$) 50.0, 55.3, 110.3, 111.8, 114.1, 114.4, 120.0, 121.2, 124.2, 125.6,

127.3, 127.8, 128.2, 128.3, 128.5, 128.6, 132.0, 132.5, 136.8, 159.4; LC-MS (ESI+) *m/z* = 393.0 $[M+H]^+$; HRMS calcd. for $C_{22}H_{18}O_3N_2{}^{35}Cl$ $[M+H]^+$ 393.1000, found 393.0999

O') 3-Bromo-4-fluoro-5-nitrobenzoic acid (222)

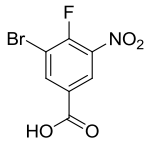

Conc. H_2SO_4 (6.5 mL) was added to a mixture of aryl fluoride **221** (1.00 g, 5.40 mmol) and NBS (1.44 g, 8.10 mmol) at room temperature and heated to 80 ^oC. After 1 h, the reaction was cooled to room temperature, poured into a beaker of ice-cooled 1 M HCl (20 mL) and filtered, washing with ice-cooled 1 M HCl (3 × 10 mL). The solid was dissolved in EtOAc (10 mL) and partitioned with distilled water (10 mL). The organic layer was washed with brine (10 mL), dried ($MgSO_4$), filtered and concentrated *in vacuo* to give **222** as a yellow solid (1.35 g, 95%); R_f = 0.39 (silica, 20% MeOH, DCM); m.p. 164-166 ^oC; UV λ_{max} (EtOH/nm) 220.0; IR ν_{max}/cm^{-1} 3081 (C-H), 2965 (C-H), 2810 (C-H), 2643 (br) (O-H), 1688 (C=O), 1604, 1538, 1482, 1415, 1341, 1274, 1162, 1083, 912, 749, 729; ^1H δ/ppm (500 MHz, $CDCl_3$) 6.85 (1H, s, br, CO_2H), 8.59 (1H, dd, Ar-H, *J* = 2.1 and 5.5 Hz), 8.73 (1H, dd, Ar-H, *J* = 2.1 and 6.4 Hz); ^{13}C δ/ppm (125 MHz, $CDCl_3$) 112.7, 112.9, 126.47, 126.51, 127.2, 138.2, 138.3, 140.1, 154.6, 156.8, 167.1; ^{19}F δ/ppm (470 MHz, $CDCl_3$) -101.2; LC-MS (ESI+) *m/z* = 262.0 and 264.0 $[M-H]^-$; HRMS calcd. for $C_7H_2O_4N^{79}BrF$ $[M-H]^-$ 261.9157, found 261.9148

P') Methyl 3-bromo-4-(4-chlorophenoxy)-5-nitrobenzoate (227)

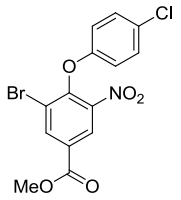

Conc. H_2SO_4 (0.70 mL) was added to a solution of carboxylic acid **223** (500 mg, 1.34 mmol) in methanol (3.5 mL) at room temperature in air and heated to 80 ^oC for 2 h. The reaction was cooled to room temperature, concentrated to a low volume *in vacuo*, dissolved in EtOAc (10 mL) and washed with saturated aqueous $NaHCO_3$ (2 × 10 mL). The aqueous layer was extracted with EtOAc (2 × 10 mL) and the organic layer was washed with brine (10 mL), dried ($MgSO_4$), filtered and concentrated *in vacuo* to give

227 as a brown solid (498 mg, 96%); R_f = 0.27 (silica, 10% EtOAc, petrol); m.p. 111-113 ^{o}C; UV λ_{max} (EtOH/nm) 228.0; IR ν_{max}/cm^{-1} 3066 (C-H), 2948 (C-H), 1725 (C=O), 1586, 1532, 1483, 1428, 1344, 1289 (C-O), 1192, 1136, 1083, 983, 911, 819, 757, 726, 688; ^{1}H δ/ppm (500 MHz, DMSO-d_6) 3.95 (3H, s, CO_2CH_3), 6.99 (2H, d, 4-MeOPh C_3-H and C_5-H, J = 9.0 Hz), 7.43 (2H, d, 4-MeOPh C_2-H and C_6-H, J = 9.0 Hz), 8.57 (1H, d, 3-BrPh C_2-H, J = 2.0 Hz), 8.59 (1H, d, 3-BrPh C_6-H, J = 2.0 Hz); ^{13}C δ/ppm (125 MHz, DMSO-d_6) 53.1, 117.1, 119.6, 126.1, 127.3, 128.8, 129.8, 138.7, 144.2, 147.2, 155.0, 163.2; LC-MS (ESI+) *m/z* = mass not observed; HRMS calcd. for $C_{14}H_{10}O_5N^{79}Br^{35}Cl$ $[M+H]^+$ 385.9425, found 385.9424

Q') 1-(4-Chlorophenyl)propan-2-one (284)

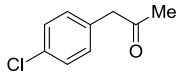

Methyllithium (1.6 M in diethyl ether, 5.96 mL, 9.54 mmol) was added dropwise to a suspension of CuI (908 mg, 4.77 mmol) in diethyl ether (12.7 mL) at 0 ^{o}C. After 10 min, the solution was cooled to -78 ^{o}C and mixed with acyl chloride **280** (232 µL, 300 mg, 1.59 mmol), as a solution in diethyl ether (1.59 mL, 1 M). After 45 min, the reaction was quenched with methanol (1.0 mL) and warmed to room temperature. After 2 h, the reaction was partitioned with 66% saturated aqueous NH_4Cl and distilled water (15 mL) and the organic layer was washed with distilled water (3 × 10 mL). The organic layer was washed with brine (10 mL), dried ($MgSO_4$), filtered and concentrated *in vacuo*. Chromatography (silica, 0-10% EtOAc, petrol) afforded **284** as a yellow oil (268 mg, 100%); R_f = 0.26 (silica, 10% EtOAc, petrol); UV λ_{max} (EtOH/nm) 222.0; IR ν_{max}/cm^{-1} 2900 (C-H), 1709 (C=O), 1490, 1409, 1356, 1323, 1225, 1159, 1087, 1015, 831, 781, 713, 672; ^{1}H δ/ppm (500 MHz, $CDCl_3$) 2.17 (3H, s, CH_3), 3.68 (2H, s, CH_2), 7.13 (2H, d, C_2-H and C_6-H, J = 8.3 Hz), 7.31 (2H, d, C_3-H and C_5-H, J = 8.4 Hz); ^{13}C δ/ppm (125 MHz, $CDCl_3$) 29.4, 50.1, 128.9, 130.8, 132.6, 133.1, 205.7; LC-MS (ESI+) *m/z* = 169.1 $[M+H]^+$; HRMS calcd. for $C_9H_{10}O^{35}Cl$ $[M+H]^+$ 169.0415, found 169.0412

R') Ethyl 4-(4-chlorophenyl)-3-oxobutanoate (281)

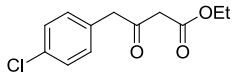

Pyridine (1.10 mL, 1.08 g, 13.6 mmol) was added dropwise over 5-7 min to a solution of Meldrum's acid (1.00 g, 6.94 mmol) in DCM (6 mL) at 0 ^{o}C, followed by dropwise addition over 5-7 min of acyl chloride **280** (1.01 mL, 1.31 g, 6.93 mmol). After 1 h, the solution was warmed to room temperature and stirred for 2 h, then partitioned with 2 M HCl (20 mL). The aqueous layer was extracted with DCM (4 × 10 mL) and organic layers were washed with brine (10 mL), dried ($MgSO_4$), filtered and concentrated *in vacuo*, then dissolved in ethanol (22 mL) and heated to 100 ^{o}C. After 2 h, the reaction was cooled to room temperature and concentrated *in vacuo*. Chromatography (silica, 0-20% EtOAc, petrol) afforded **281** as a yellow oil (1.268 g, 76%); R_f = 0.50 (silica, 20% EtOAc, petrol); UV λ_{max} (EtOH/nm) 221.4; IR ν_{max}/cm^{-1} 2982 (C-H), 2935 (C-H), 1739 (C=O), 1715 (C=O), 1651, 1491, 1408, 1313, 1231, 1193, 1149, 1088, 1028, 1016, 936, 823, 793, 677; ^{1}H δ/ppm (500 MHz, $CDCl_3$) 1.27 (3H, t, $CO_2CH_2CH_3$), 3.46 (1.6H, s, keto ArCH_2), 3.47 (0.3H, s, enol ArCH_2), 3.82 (1.7H, s, keto $COCH_2CO_2Et$), 4.18 (2H, q, $CO_2CH_2CH_3$, J = 7.1 Hz), 4.90 (0.1H, s, enol $COHCHCO_2Et$), 7.14 (1.6H, d, keto C_2-H and C_6-H, J = 8.4 Hz), 7.19 (0.3H, d, enol C_2-H and C_6-H, J = 8.3 Hz), 7.29 (0.3H, d, enol C_3-H and C_5-H, J = 8.5 Hz), 7.33 (1.6H, d, keto C_3-H and C_5-H, J = 8.4 Hz); ^{13}C δ/ppm (125 MHz, $CDCl_3$) 14.1, 14.2, 40.7, 48.5, 49.1, 60.2, 61.6, 90.4, 128.8, 129.0, 130.6, 131.0, 131.6, 133.0, 133.4, 134.1, 167.0, 172.6, 176.3, 199.9; LC-MS (ESI+) *m/z* = 241.2 $[M+H]^+$ and 239.1 $[M-H]^-$; HRMS calcd. for $C_{12}H_{14}O_3{}^{35}Cl$ $[M+H]^+$ 241.0626, found 241.0624

S') Ethyl 4-(4-chlorophenyl)-2-(2-(4'-fluorophenyl)-2-oxoethyl)-3-oxobutanoate (282a)

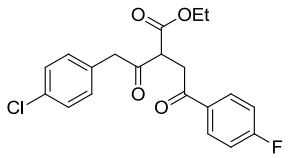

Sodium hydride (60% in mineral oil, 108 mg, 2.70 mmol) was added to a solution of β-keto ester **281** (500 mg, 2.08 mmol) in THF (1.3 mL) at 0 ^{o}C. After 20 min, 2'-bromo-4-fluoroacetophenone (497 mg, 2.29 mmol), as a solution in THF (1.0 mL, 2.3 M), was added dropwise over 5 min and the reaction was stirred at 0 ^{o}C for 10 min, then warmed to room temperature. After 3 h, the reaction was cooled to 0 ^{o}C, quenched with distilled water (3 mL) and partitioned with EtOAc (10 mL). The organic layer was washed with brine (10 mL), dried ($MgSO_4$), filtered and concentrated *in vacuo*. Chromatography (silica, 0-20% EtOAc, petrol) afforded **282a** as a colourless solid (395 mg, 51%); R_f =

0.17 (silica, 10% EtOAc, petrol); m.p. 53-56 ^{o}C; UV λ_{max} (EtOH/nm) 244.8 and 226.0; IR ν_{max}/cm^{-1} 3070 (C-H), 2980 (C-H), 2931 (C-H), 2904 (C-H), 1730 (C=O), 1712 (C=O), 1679 (C=O), 1594, 1507, 1491, 1406, 1342, 1300, 1249, 1229, 1190, 1157, 1089, 1039, 1014, 985, 837, 808, 735, 683; ^{1}H δ/ppm (500 MHz, $CDCl_3$) 1.29 (3H, t, $CO_2CH_2CH_3$, 7.2 Hz), 3.51 (1H, dd, CH_2COAr, *J* = 4.8 and 18.4 Hz), 3.73 (1H, dd, CH_2COAr, *J* = 9.0 and 18.4 Hz), 4.06 (1H, d, $ArCH_2CO$, *J* = 17.0 Hz), 4.12 (1H, d, $ArCH_2CO$, *J* = 17.0 Hz), 4.22 (2H, q, $CO_2CH_2CH_3$, *J* = 7.2 Hz), 4.29 (1H, dd, $COCHCO_2Et$, *J* = 4.7 and 9.0 Hz), 7.13 (2H, t, 4-ClPh C_3-H and C_5-H, *J* = 8.6 Hz), 7.18 (2H, d, 4-FPh C_2-H and C_6-H, *J* = 8.5 Hz), 7.32 (2H, d, 4-FPh C_3-H and C_5-H, *J* = 8.5 Hz), 7.99 (2H, dd, 4-ClPh C_2-H and C_6-H, *J* = 5.4 and 9.0 Hz); ^{13}C δ/ppm (125 MHz, $CDCl_3$) 14.0, 14.1, 37.7, 49.2, 52.6, 62.0, 62.1, 115.8, 115.9, 128.7, 129.0, 130.6, 130.8, 130.9, 131.2, 132.0, 132.4, 133.1, 165.0, 167.1, 168.6, 195.6, 201.8; ^{19}F δ/ppm (470 MHz, $CDCl_3$) -104.2, -108.3; LC-MS (ESI+) *m/z* = 375.2 $[M-H]^-$; HRMS calcd. for $C_{20}H_{19}O_4{}^{35}ClF$ $[M+H]^+$ 377.0950, found 377.0951

T') 3-Bromo-4-(4-chlorophenoxy)-5-nitrobenzylmethanesulfonate (233)

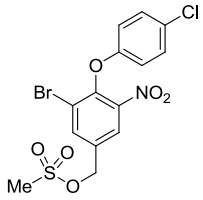

Methanesulfonic anhydride (73.2 mg, 0.42 mmol), as a solution in DCM (0.5 mL, 0.84 M), was added to a solution of alcohol **232** (100 mg, 0.28 mmol) and triethylamine (59 µL, 42.5 mg, 0.42 mmol) in DCM (0.5 mL) at 0 ^{o}C and warmed to room temperature. After 1 h, the reaction was washed with 20% 1 M HCl, distilled water (2 × 10 mL) and the aqueous layer was extracted with EtOAc (8 mL). The organic layer was washed with brine (10 mL), dried ($MgSO_4$), filtered and concentrated *in vacuo*. Chromatography (silica, 10-30% EtOAc, petrol) afforded **233** as a brown solid (66 mg, 54%); R_f = 0.17 (silica, 30% EtOAc, petrol); m.p. 112-114 ^{o}C; UV λ_{max} (EtOH/nm) 222.4; IR ν_{max}/cm^{-1} 3077 (C-H), 2936 (C-H), 1589, 1536, 1484, 1341 (S=O asym. stretch), 1262, 1166 (S=O sym. stretch), 1088, 972, 902, 816, 752, 727; ^{1}H δ/ppm (500 MHz, $CDCl_3$) 3.13 (3H, s, SO_2CH_3), 5.27 (2H, s, $ArCH_2$), 6.77 (2H, d, 4-ClPh C_3-H and C_5-H, *J* = 9.0 Hz), 7.28 (2H, d, 4-ClPh C_2-H and C_6-H, *J* = 9.1 Hz), 7.96-7.97 (2H, m, 3-BrPh C_2-H and C_6-H); ^{13}C δ/ppm (125 MHz, $CDCl_3$) 38.3, 67.5, 116.7, 120.8, 124.5,

128.5, 129.8, 133.2, 137.8, 144.8, 145.6, 155.2; LC-MS (ESI+) *m/z* = mass not observed; HRMS mass not observed

U') 1-Bromo-5-(chloromethyl)-2-(4-chlorophenoxy)-3-nitrobenzene (235)

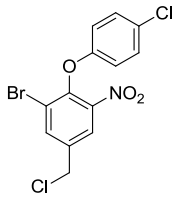

Methanesulfonyl chloride (48 µL, 71 mg, 0.62 mmol) was added to a solution of alcohol **232** (200 mg, 0.56 mmol) and triethylamine (117 µL, 85 mg, 0.84 mmol) in DCM (2.0 mL) at 0 ^{o}C and warmed to room temperature. After 30 min, the reaction was washed with 0.3 M HCl (15 mL) and the aqueous layer was extracted with DCM (4 × 6 mL). The organic layer was dried ($MgSO_4$), filtered and concentrated *in vacuo*. Chromatography (silica, 0-30% DCM, petrol) afforded **235** as a yellow solid (102 mg, 48%); R_f = 0.26 (silica, 30% DCM, petrol); m.p. 77-79 ^{o}C; UV λ_{max} (EtOH/nm) 223.2; IR ν_{max}/cm^{-1} 3072 (C-H), 2964 (C-H), 2922 (C-H), 2873 (C-H), 1523, 1483, 1461, 1352, 1259, 1193, 1164, 1088, 1009, 953, 891, 826, 795, 704; ^{1}H δ/ppm (500 MHz, $CDCl_3$) 4.61 (2H, s, C*H*$_2$Cl), 6.78 (2H, d, 4-ClPh C_3-H and C_5-H, *J* = 9.1 Hz), 7.27 (2H, d, 4-ClPh C_2-H and C_6-H, *J* = 9.1 Hz), 7.94-7.97 (2H, m, 1-BrPh C_2-H and C_6-H); ^{13}C δ/ppm (125 MHz, $CDCl_3$) 43.4, 116.7, 120.5, 124.7, 128.4, 129.8, 136.7, 138.1, 144.6, 144.9, 155.3; LC-MS (ESI+) *m/z* = mass not observed; HRMS calcd. for $C_{13}H_9O_3N^{79}Br^{35}Cl_2$ $[M+H]^+$ 375.9137, found 375.9140

V') 2-(3-Bromo-4-(4-chlorophenoxy)-5-nitrophenyl)acetonitrile (234)

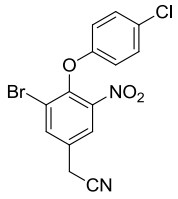

TMS-cyanide (53 µL, 42 mg, 0.42 mmol) was added to a solution of mesylate **233** (122 mg, 0.28 mmol) in acetonitrile (2.2 mL) at 0 ^{o}C, followed by dropwise addition of TBAF (1 M in THF, 0.42 mL, 0.42 mmol) and the reaction was warmed to room temperature. After 90 min, the reaction was quenched with distilled water (10 mL), partitioned with EtOAc (10 mL) and the organic layer was washed with brine (10 mL),

dried ($MgSO_4$), filtered and concentrated *in vacuo*. Chromatography (silica, 0-50% Et_2O, petrol) afforded **234** as a brown solid (29.5 mg, 29%); R_f = 0.40 (silica, 30% EtOAc, petrol); m.p. 112-114 ^oC; UV λ_{max} (EtOH/nm) 222.6; IR ν_{max}/cm^{-1} 3090 (C-H), 2919 (C-H), 2854 (C-H), 2253 (C≡N), 1529, 1483, 1349, 1258, 1200 (C-O), 1162, 1087, 1008, 824, 794, 725; ^1H δ/ppm (500 MHz, $CDCl_3$) 3.87 (2H, s, CH_2CN), 6.77 (2H, d, 4-ClPh C_3-H and C_5-H, J = 9.1 Hz), 7.29 (2H, d, 4-ClPh C_2-H and C_6-H, J = 9.1 Hz), 7.91-7.93 (2H, m, 3-BrPh C_2-H and C_6-H); ^{13}C δ/ppm (125 MHz, $CDCl_3$) 22.8, 115.8, 116.7, 121.2, 124.3, 128.6, 129.3, 129.8, 137.6, 144.8, 145.1, 155.2; LC-MS (ESI+) *m/z* = -365.0 and -367.0 $[M-H]^-$; HRMS calcd. for $C_{14}H_9O_3N_2{}^{79}Br^{35}Cl$ $[M+H]^+$ 366.9480, found 366.9480

W') 1-Bromo-3-(4-chlorophenyl)propan-2-one (286)

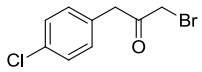

N-bromosuccinimide (683 mg, 3.84 mmol) was added portionwise to a solution of ketone **284** (216 mg, 1.28 mmol) and *p*TSA (365 mg, 1.92 mmol) in acetonitrile (12.8 mL) at room temperature and heated to 100 ^oC. After 3 h, the reaction was concentrated *in vacuo*, dissolved with EtOAc (10 mL) and washed with distilled water (2 × 10 mL) and 1 M HCl (10 mL). The aqueous layer was extracted with EtOAc (10 mL) and the organic layer was washed with brine (10 mL), dried ($MgSO_4$), filtered and concentrated *in vacuo*. Crude material was taken up in glacial acetic acid (0.6 mL) and acetone (1.0 mL) before addition of HBr (45% in acetic acid, 0.1 mL) at room temperature. After 18 h, the reaction was quenched with saturated aqueous $NaHCO_3$ (10 mL) and partitioned with EtOAc (10 mL). The organic layer was washed with saturated aqueous $NaHCO_3$ (2 × 10 mL) and the aqueous layer was extracted with EtOAc (10 mL). The organic layer was dried ($MgSO_4$), filtered and concentrated *in vacuo*. Chromatography (silica, 0-10% EtOAc, petrol) afforded **286** as a brown solid (175 mg, 55%); R_f = 0.30 (silica, 10% EtOAc, petrol); m.p. 44-46 ^oC; UV λ_{max} (EtOH/nm) 220.4; IR ν_{max}/cm^{-1} 3431 (enol O-H), 2990 (C-H), 2942 (C-H), 2881 (C-H), 1720 (C=O), 1487, 1381, 1337, 1261, 1178, 1088, 1047, 1014, 807, 718, 700; ^1H δ/ppm (500 MHz, $CDCl_3$) 3.91 (2H, s, COCH_2Br), 3.94 (2H, s, ArCH_2), 7.17 (2H, d, C_2-H and C_6-H, J = 8.5 Hz), 7.33 (2H, d, C_3-H and C_5-H, J = 8.5 Hz); ^{13}C δ/ppm (125 MHz, $CDCl_3$) 33.4, 45.8, 129.1, 130.8, 131.5, 133.5, 199.0; LC-MS (ESI+) *m/z* = mass not observed; HRMS calcd. for $C_9H_9O^{35}Cl^{79}Br$ $[M+H]^+$ 246.9520, found 246.9519

X') Methyl 2-(3-nitrophenyl)acetate (240)

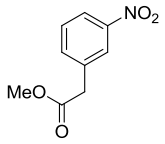

Thionyl chloride (440 µL, 715 mg, 6.00 mmol) was added dropwise to a solution of 3-nitrobenzoic acid (200 mg, 1.20 mmol) (**238**) in THF (1.2 mL, 1 M) and DMF (2 drops) at 0 ^{o}C and warmed to room temperature. After 5 h, the reaction was concentrated *in vacuo*, dissolved in 60% THF, acetonitrile (1.9 mL), mixed with triethylamine (251 µL, 182 mg, 1.80 mmol) and cooled to 0 ^{o}C before treating with TMS-diazomethane (2 M in hexanes, 0.6 mL, 1.20 mmol). After 2 h, the reaction was quenched with glacial acetic acid (0.5 mL) and distilled water (2.0 mL) and partitioned with diethyl ether (8 mL) and distilled water (8 mL). The aqueous layer was extracted with diethyl ether (10 mL) and the organic layer was washed with saturated aqueous $NaHCO_3$ (10 mL), brine (10 mL), dried ($MgSO_4$), filtered and concentrated *in vacuo*. Crude material was dissolved in methanol (4.5 mL) and treated with a solution of $PhCO_2Ag$ (212 mg, 0.92 mmol) in triethylamine (377 µL, 273 mg, 2.7 mmol, 2.4 M) dropwise at room temperature. After 24 h, the reaction was concentrated *in vacuo*, dissolved in EtOAc (10 mL), filtered through celite and washed with saturated aqueous $NaHCO_3$ (10 mL), 1 M HCl (10 mL), brine (10 mL), dried ($MgSO_4$), filtered and concentrated *in vacuo*. Chromatography (silica, 0-20% EtOAc, petrol) afforded **240** as a yellow oil (50 mg, 27%); R_f = 0.26 (silica, 20% EtOAc, petrol); UV λ_{max} (EtOH/nm) 258.8; IR ν_{max}/cm^{-1} 2954 (C-H), 1733 (C=O), 1524, 1435, 1346, 1224, 1159, 1098, 1006, 900, 805, 712, 672; ^{1}H δ/ppm (500 MHz, $CDCl_3$) 3.73 (3H, s, CO_2CH_3), 3.75 (2H, s, $ArCH_2$), 7.52 (1H, t, C_5-H, J = 7.9 Hz), 7.63 (1H, d, C_6-H, J = 7.6 Hz), 8.15 (1H, d, C_4-H, J = 8.4 Hz), 8.17 (1H, s, C_2-H); ^{13}C δ/ppm (125 MHz, $CDCl_3$) 40.5, 52.4, 122.3, 122.4, 129.5, 135.6, 135.8, 148.4, 170.8; LC-MS (ESI+) *m/z* = -194.0 $[M-H]^-$; HRMS calcd. for $C_9H_{10}O_4N$ $[M+H]^+$ 196.0604, found 196.0603

Y') Di-*tert*-butyl (2-(4-chlorophenoxy)-4'-methoxy-[1,1'-biphenyl]-3-yl)dicarbamate (259)

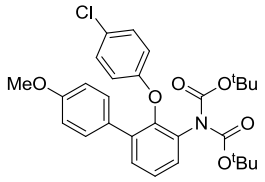

Tin(II) chloride dihydrate (882 mg, 3.91 mmol) was added to a solution of nitro **251** (278 mg, 0.78 mmol) in ethanol (7.8 mL, 0.1 M) at room temperature and heated to 70 ^{o}C for 20 min. The reaction was quenched with saturated aqueous $NaHCO_3$ (10 mL), filtered through celite and partitioned with EtOAc (20 mL). The organic layer was washed with brine (10 mL), dried ($MgSO_4$), filtered and concentrated *in vacuo*, then dissolved in acetonitrile (1.6 mL), mixed with DMAP (48 mg, 0.39 mmol) followed by Boc_2O (504 mg, 2.31 mmol) in a sealed vial at room temperature and heated to 50 ^{o}C. After 3 h, the reaction was quenched with saturated aqueous $NaHCO_3$ (10 mL), partitioned with EtOAc (10 mL) and the organic layer was washed with saturated aqueous $NaHCO_3$ (2 × 10 mL). The aqueous layer was extracted with EtOAc (10 mL) and the organic layer was washed with brine (10 mL), dried ($MgSO_4$), filtered and concentrated *in vacuo*. Chromatography (silica, 0-20% EtOAc, petrol) afforded **259** as a white solid (289 mg, 70%); R_f = 0.17 (silica, 70% DCM, petrol); m.p. 120-122 ^{o}C; UV λ_{max} (EtOH/nm) 262.6 and 228.4; IR ν_{max}/cm^{-1} 3075 (C-H), 2973 (C-H), 2936 (C-H), 2851 (C-H), 1777 (C=O), 1707, 1608, 1516, 1484, 1454, 1366, 1279, 1249 (C-O), 1152, 1099, 1033, 826, 780; ^{1}H δ/ppm (500 MHz, $CDCl_3$) 1.36 (18H, s, (C(C*H*$_3$)$_3$)$_2$), 3.78 (3H, s, OC*H*$_3$), 6.60 (2H, d, Ar-H, *J* = 9.0 Hz), 6.83 (2H, d, Ar-H, *J* = 8.8 Hz), 7.02 (2H, d, Ar-H, *J* = 9.0 Hz), 7.18 (1H, dd, Ar-H, *J* = 1.6 and 7.8 Hz), 7.29 (1H, t, 3-(Boc)$_2$NPh C_5-H, *J* = 7.9 Hz), 7.36-7.39 (3H, m, Ar-H); ^{13}C δ/ppm (125 MHz, $CDCl_3$) 27.8, 55.2, 82.6, 113.7, 117.2, 125.5, 126.7, 128.6, 128.9, 129.3, 130.0, 130.2, 133.9, 136.1, 147.4, 150.9, 156.0, 159.1; LC-MS (ESI+) *m/z* = mass not observed; HRMS mass not observed

Z') *Tert*-butyl (2-(4-chlorophenoxy)-4'-methoxy-[1,1'-biphenyl]-3-yl)carbamate (253)

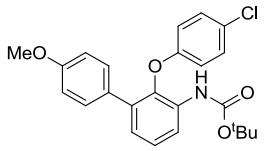

Sodium hydroxide (200 mg, 5.00 mmol) was added to a solution of dicarbamate **259** (270 mg, 0.51 mmol) in 33% THF, methanol (2.7 mL) at room temperature. After 1 h, the reaction was partitioned with distilled water (8 mL) and EtOAc (8 mL) and the organic layer was washed with distilled water (10 mL). The aqueous layer was extracted with EtOAc (10 mL) and the organic layer was washed with brine (10 mL), dried ($MgSO_4$), filtered and concentrated *in vacuo* to give **253** as a white solid (170 mg, 78%); R_f = 0.39 (silica, 10% EtOAc, petrol); m.p. 150-152 ^oC; UV λ_{max} (EtOH/nm) 233.8; IR ν_{max}/cm^{-1} 3439 (N-H), 2976 (C-H), 2932 (C-H), 2835 (C-H), 1728 (C=O), 1608, 1522, 1482, 1427, 1401, 1367, 1275, 1222 (C-O), 1147, 1089, 1046, 861, 825, 786, 750; ^1H δ/ppm (500 MHz, $CDCl_3$) 1.50 (9H, s, C(CH_3)$_3$), 3.79 (3H, s, OCH_3), 6.62 (2H, d, 4-ClPh C_3-H and C_5-H, *J* = 9.0 Hz), 6.81 (3H, d, Ar-H, *J* = 8.8 Hz), 7.06-7.09 (3H, m, 4-ClPh C_2-H, C_6-H and Ar-H), 7.30 (1H, t, 3-BocHNPh C_5-H, *J* = 8.1 Hz), 7.33 (2H, d, Ar-H, *J* = 8.9 Hz); ^{13}C δ/ppm (125 MHz, $CDCl_3$) 28.3, 55.2, 80.9, 113.6, 116.6, 118.6, 124.7, 126.2, 127.0, 129.3, 129.4, 130.0, 132.6, 135.0, 139.9, 152.7, 155.8, 158.9; LC-MS (ESI+) *m/z* = 424.3 $[M-H]^-$; HRMS calcd. for $C_{24}H_{25}O_4N^{35}Cl$ $[M+H]^+$ 426.1467, found 426.1468

A'') *N*-((4-Fluorobenzyl)carbamothioyl)benzamide (278)

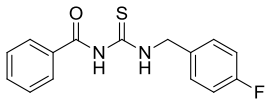

Benzylamine **277** (350 µL, 383 mg, 3.06 mmol) was added dropwise over 1 min to a solution of benzoyl isothiocyanate (412 µL, 500 mg, 3.06 mmol) in DCM (6.0 mL, 0.5 M) at 0 ^oC and warmed to room temperature. After 1 h, the reaction was cooled to 0 ^oC, quenched with distilled water (10 mL) and the layers were separated. The aqueous layer was extracted with DCM (2 × 10 mL) and the organic layer was washed with brine (10 mL), dried ($MgSO_4$), filtered and concentrated *in vacuo*. Chromatography (silica, 0-20% EtOAc, petrol) afforded **278** as a yellow solid (464 mg, 53%); R_f = 0.32 (silica, 20% EtOAc, petrol); m.p. 99-102 ^oC; UV λ_{max} (EtOH/nm) 242.4; IR ν_{max}/cm^{-1} 3271 (N-

H), 3173 (N-H), 3035 (C-H), 2936 (C-H), 1677 (C=O), 1599, 1501 (C=S), 1427, 1307 (C=S), 1242, 1215, 1151, 1082, 1019, 953, 934, 885, 839, 766, 738, 701; ^{1}H δ/ppm (500 MHz, DMSO-d_6) 4.87 (2H, d, ArC*H*$_2$, *J* = 5.7 Hz), 7.20 (2H, t, 4-FPh C_2-H and C_6-H, *J* = 8.9 Hz), 7.46 (2H, dd, 4-FPh C_3-H and C_5-H, *J* = 5.7 and 8.4 Hz), 7.52 (2H, t, Ph C_3-H and C_5-H, *J* = 7.8 Hz), 7.65 (1H, t, Ph C_4-H, *J* = 7.4 Hz), 7.94 (2H, d, Ph C_2-H and C_6-H, *J* = 7.7 Hz), 11.20 (1H, t, CSN*H*CH$_2$, *J* = 5.1 Hz), 11.40 (1H, s, CON*H*CS); ^{13}C δ/ppm (125 MHz, DMSO-d_6) 47.8, 115.6, 115.8, 128.9, 129.0, 130.2, 130.3, 132.7, 133.5, 134.12, 134.15, 160.9, 162.9, 168.5, 181.0; ^{19}F δ/ppm (470 MHz, DMSO-d_6) -115.4; LC-MS (ESI+) *m/z* = 289.2 $[M+H]^+$ and 287.1 $[M-H]^-$; HRMS calcd. for $C_{15}H_{12}ON_2FS$ $[M-H]^-$ 287.0660, found 287.0653

B'') 1-(4-Fluorobenzyl)thiourea (279)

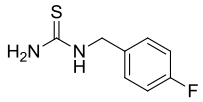

Anhydrous K_2CO_3 (449 mg, 3.25 mmol) was added to a solution of benzamide **278** (468 mg, 1.62 mmol) in methanol (21 mL) at room temperature. After 18 h, the reaction was concentrated *in vacuo*, partitioned with EtOAc (10 mL) and distilled water (2 × 20 mL) and the aqueous layer was extracted with EtOAc (10 mL). The organic layer was washed with brine (10 mL), dried ($MgSO_4$), filtered and concentrated *in vacuo*. Chromatography (silica, 0-20% EtOAc, DCM) afforded **279** as a white solid (143 mg, 48%); R_f = 0.22 (silica, 20% EtOAc, petrol); m.p. 119-121 ^{o}C; UV λ_{max} (EtOH/nm) 244.2; IR ν_{max}/cm^{-1} 3411 (secondary N-H), 3274 (primary N-H), 3177 (primary N-H), 3057 (C-H), 3016 (C-H), 1623, 1603, 1539, 1505 (C=S), 1440, 1417, 1355, 1314 (C=S), 1217, 1154, 1114, 1090, 1016, 960, 930, 845, 820, 730; ^{1}H δ/ppm (500 MHz, DMSO-d_6) 4.61 (2H, s, br, C*H*$_2$), 7.10 (2H, s, br, N*H*$_2$), 7.17 (2H, t, C_3-H and C_5-H, *J* = 8.9 Hz), 7.32-7.35 (2H, m, C_2-H and C_6-H), 7.98 (1H, s, br, N*H*); ^{13}C δ/ppm (125 MHz, DMSO-d_6) 47.1, 115.4, 115.5, 129.8, 136.0, 160.7, 162.7, 183.9; ^{19}F δ/ppm (470 MHz, DMSO-d_6) -116.0; LC-MS (ESI+) *m/z* = 185.1 $[M+H]^+$ and 183.1 $[M-H]^-$; HRMS calcd. for $C_8H_{10}N_2FS$ $[M+H]^+$ 185.0543, found 185.0542

C'') Methyl 5-amino-6-(4-chlorophenoxy)-4'-methoxy-[1,1'-biphenyl]-3-carboxylate (246)

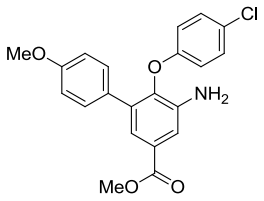

Zinc powder (316 mg, 4.8 mmol) was added to a solution of nitro **245** (200 mg, 0.48 mmol) in glacial acetic acid (10 mL, 0.05 M) at room temperature and stirred in air for 1 h. The reaction was filtered through celite, washing with methanol (20 mL) and concentrated *in vacuo*, then partitioned with EtOAc (10 mL) and 2 M NaOH (2 × 10 mL). The aqueous layer was extracted with EtOAc (10 mL) and the organic layer was washed with brine (10 mL), dried ($MgSO_4$), filtered and concentrated *in vacuo* to give **246** as a brown solid (193 mg, 99%); R_f = 0.15 (silica, 20% EtOAc, petrol); m.p. 60-62 ^oC; UV λ_{max} (EtOH/nm) 327.4, 249.6 and 227.2; IR ν_{max}/cm^{-1} 3463 (N-H), 3369 (N-H), 2950 (C-H), 2836 (C-H), 1709 (C=O), 1609, 1513, 1478, 1434, 1358, 1210 (C-O), 1179, 1088, 1006, 929, 874, 824, 768; ^1H δ/ppm (500 MHz, DMSO-d_6) 3.72 (3H, s, ArOCH_3), 3.84 (3H, s, CO_2CH_3), 5.33 (2H, s, NH_2), 6.69 (2H, d, 4-ClPh C_3-H and C_5-H, J = 9.0 Hz), 6.88 (2H, d, 4-MeOPh C_2-H and C_6-H, J = 8.7 Hz), 7.18 (1H, d, Ar-H, 2.1 Hz), 7.21 (2H, d, 4-ClPh C_2-H and C_6-H, J = 9.0 Hz), 7.36 (2H, d, 4-MeOPh C_3-H and C_5-H, J = 8.7 Hz), 7.45 (1H, d, Ar-H, J = 2.1 Hz); ^{13}C δ/ppm (125 MHz, $CDCl_3$) 52.2, 55.2, 113.6, 116.1, 116.3, 121.9, 127.0, 128.0, 129.1, 129.5, 130.0, 135.8, 140.3, 141.6, 155.2, 159.1, 166.8; LC-MS (ESI+) *m/z* = 384.3 $[M+H]^+$; HRMS calcd. for $C_{21}H_{19}O_4N^{35}Cl$ $[M+H]^+$ 384.0997, found 384.1000

3'-Amino-[1,1'-biphenyl]-3,4-diol (117c)

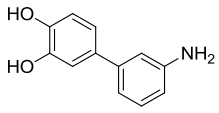

General Procedure B: Using 4-bromocatechol (110 mg, 0.58 mmol) and boronic acid **116** (112 mg, 0.81 mmol), chromatography (silica, 60% EtOAc, hexane) afforded **117c** as a dark brown solid (55 mg, 47%); R_f = 0.24 (silica, 60% EtOAc, hexane); m.p. 143 ^oC (decomposed); UV λ_{max} (EtOH/nm) 295.0 and 215.0; IR ν_{max}/cm^{-1} 3366 (N-H), 3301 (N-H), 3054 (C-H), 2934 (C-H), 2552 (br) (O-H), 1584, 1532, 1489, 1426, 1392, 1310,

1263, 1206, 1117, 773, 694; ^{1}H δ/ppm (500 MHz, MeOH-d_4) 6.66 (1H, dd, Ar-H, *J* = 0.9 and 2.3 Hz), 6.81 (1H, d, Ar-H, *J* = 8.2 Hz), 6.87-6.89 (1H, m, Ar-H), 6.91-6.93 (2H, m, Ar-H), 7.03 (1H, d, Ar-H, *J* = 2.2 Hz), 7.13 (1H, t, Ar-H, 7.8 Hz); ^{13}C δ/ppm (125 MHz, MeOH-d_4) 114.8, 115.0, 115.2, 115.6, 116.5, 117.8, 118.2, 119.4, 130.3, 135.0, 143.5, 145.9, 146.4, 148.8; LC-MS (ESI+) *m/z* = 202.2 $[M+H]^+$

***N*-(3'-Amino-[1,1'-biphenyl]-4-yl)-1,1,1-trifluoromethanesulfonamide (117d)**

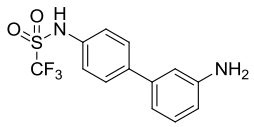

General Procedure B: Using aryl bromide **120** and boronic acid **116** (89 mg, 0.65 mmol), chromatography (silica, 40% EtOAc, hexane) afforded **117d** as a brown solid (93 mg, 64%); R_f = 0.22 (silica, 40% EtOAc, hexane); m.p. 165-170 ^{o}C; UV λ_{max} (EtOH/nm) 243.0; IR ν_{max}/cm^{-1} 3414 (aniline N-H), 3345 (aniline N-H), 2655 (br) (sulfonamido N-H), 1515, 1449, 1365, 1225, 1193, 1140, 969, 795, 731, 700; ^{1}H δ/ppm (500 MHz, MeOH-d_4) 6.73-6.75 (1H, m, Ar-H), 6.95-6.97 (1H, m, Ar-H), 6.99-7.00 (1H, m, Ar-H), 7.20 (1H, t, Ar-H, *J* = 7.7 Hz), 7.32-7.35 (2H, m, Ar-H), 7.59-7.62 (2H, m, Ar-H); ^{13}C δ/ppm (125 MHz, MeOH-d_4) 115.0, 115.9, 118.0, 124.2, 128.8, 130.6, 136.0, 141.2, 149.1; LC-MS (ESI+) *m/z* = 317.2 $[M+H]^+$

***N*-(4'-Amino-[1,1'-biphenyl]-4-yl)-1,1,1-trifluoromethanesulfonamide (117e)**

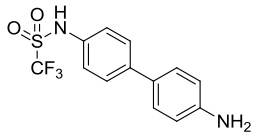

General Procedure B: Using aryl bromide **120** and 4-aminophenylboronic acid pinacol ester (143 mg, 0.65 mmol), chromatography (silica, 30-50% EtOAc, hexane) afforded **117e** as a yellow/brown solid (104 mg, 75%); R_f = 0.26 (silica, 40% EtOAc, hexane); m.p. 136 ^{o}C (decomposed); UV λ_{max} (EtOH/nm) 287.5; IR ν_{max}/cm^{-1} 3443 (amino N-H), 3361 (amino N-H), 3034 (C-H), 2798 (br) (sulfonamido N-H), 1626, 1500, 1378, 1198, 1184, 1140, 1009, 955, 817; ^{1}H δ/ppm (500 MHz, MeOH-d_4) 6.80-6.82 (2H, m, Ar-H), 7.29-7.30 (2H, m, Ar-H), 7.39-7.41 (2H, m, Ar-H), 7.55-7.56 (2H, m, Ar-H); ^{13}C δ/ppm (125 MHz, MeOH-d_4) 25.0, 116.8, 124.5, 127.9, 128.6, 141.1; LC-MS (ESI+) *m/z* = 317.2 $[M+H]^+$

***N*-(3'-((4-Fluorobenzyl)amino)-[1,1'-biphenyl]-4-yl)methanesulfonamide (118f)**

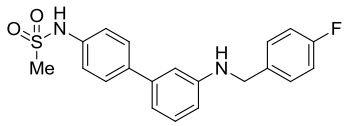

General procedure B: Using boronic ester **123** (40 mg, 0.12 mmol) and *N*-(4-bromophenyl)methanesulfonamide (46 mg, 0.18 mmol), chromatography (silica, 20-40% EtOAc, hexane) yielded **118f** as a brown solid (43 mg, 95%); R_f = 0.28 (silica, 40% EtOAc, hexane); m.p. 117-119 ^oC; UV λ_{max} (EtOH/nm) 316.5 and 254.0; IR ν_{max}/cm^{-1} 3413 (secondary amine N-H), 3240 (sulfonamide N-H), 2932 (C-H), 1604, 1509, 1315 (S=O asym. stretch), 1222, 1146 (S=O sym. stretch), 980, 829, 766, 698; ^1H δ/ppm (500 MHz, $CDCl_3$) 3.04 (3H, s, $NHSO_2CH_3$), 4.36 (3H, m, CH_2 and amino N*H*), 6.44 (1H, s, sulfonamido N*H*), 6.63 (1H, dd, Ar-H, *J* = 1.8 and 8.0 Hz), 6.80 (1H, m, Ar-H), 6.92 (1H, m, Ar-H), 7.02-7.06 (2H, m, Ar-H), 7.23-7.26 (3H, m, Ar-H), 7.34-7.37 (2H, m, Ar-H), 7.51-7.53 (2H, m, Ar-H); ^{13}C δ/ppm (125 MHz, $CDCl_3$) 39.5, 48.4, 113.1, 115.5, 115.7, 121.1, 128.4, 129.4, 129.5, 129.9, 134.0, 135.8, 138.7, 141.3; LC-MS (ESI+) *m/z* = 371.3 $[M+H]^+$; HRMS calcd. for $C_{20}H_{20}O_2N_2FS$ $[M+H]^+$ 371.1224, found 371.1227; Analytical HPLC: 99.7%

***N*-(4-Fluorobenzyl)-[1,1'-biphenyl]-3,4'-diamine (118g)**

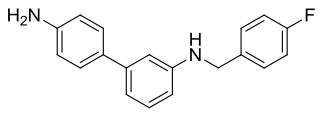

General procedure B: Using boronic ester **123** (44 mg, 0.13 mmol) and aniline **119** (33 mg, 0.190 mmol), chromatography (silica, 15-30% EtOAc, hexane) yielded **118g** as a yellow solid (30 mg, 76%); R_f = 0.22 (silica, 30% EtOAc, hexane); m.p. 94-97 ^oC; UV λ_{max} (EtOH/nm) 258.5; IR ν_{max}/cm^{-1} 3411 (primary N-H), 3371 (primary N-H), 3028 (secondary N-H), 2852 (C-H), 1599, 1503, 1327, 1279, 1218, 1183, 1154, 824, 774, 695; ^1H δ/ppm (500 MHz, $CDCl_3$) 3.87 (3H, s, br, N*H*), 4.35 (2H, s, CH_2), 6.55(1H, dd, Ar-H, *J* = 2.2 and 8.0 Hz), 6.71-6.74 (2H, m, Ar-H), 6.79-6.80 (1H, m, Ar-H), 6.90-6.92 (1H, m, Ar-H), 6.99-7.06 (2H, m, Ar-H), 7.20 (1H, t, Ar-H, *J* = 7.8 Hz), 7.34-7.37 (4H, m, Ar-H); ^{13}C δ/ppm (125 MHz, $CDCl_3$) 47.8, 111.1, 111.2, 115.3, 115.4, 115.6, 116.4, 128.0, 129.1, 129.2, 129.6, 132.0, 135.1, 142.4, 145.8, 148.1, 161.1, 163.1; LC-MS

(ESI+) *m/z* = 293.3 $[M+H]^+$; HRMS calcd. for $C_{19}H_{18}N_2F$ $[M+H]^+$ 293.1449, found 293.1451; Analytical HPLC: 98.0%

***N*-(4-Fluorobenzyl)-[1,1'-biphenyl]-3,3'-diamine (118h)**

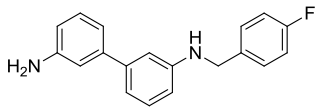

General procedure B: Using boronic ester **123** (40 mg, 0.12 mmol) and 3-bromoaniline (20.0 µL, 31.5 mg, 0.18 mmol), chromatography (silica, 20-30% EtOAc, hexane) yielded **118h** as a dark yellow oil (28 mg, 78%); R_f = 0.21 (silica, 30% EtOAc, petrol); UV λ_{max} (EtOH/nm) 308.5 and 232.0; IR ν_{max}/cm^{-1} 3413 (br) (primary and secondary N-H), 3372 (primary N-H), 3042 (C-H), 2848 (C-H), 1597, 1577, 1507, 1486, 1216, 1154, 856, 826, 771, 695; ^1H δ/ppm (500 MHz, $CDCl_3$) 3.88 (3H, s, br, N*H*), 4.35 (2H, s, C*H*$_2$), 6.60 (1H, dd, Ar-H, *J* = 2.4 and 8.1 Hz), 6.66 (1H, dd, Ar-H, *J* = 2.3 and 7.9 Hz), 6.81-6.82 (1H, m, Ar-H), 6.85-6.86 (1H, m, Ar-H), 6.92-6.95 (2H, m, Ar-H), 7.02-7.05 (2H, m, Ar-H), 7.20 (1H, t, Ar-H, *J* = 7.8 Hz), 7.22 (1H, t, Ar-H, *J* = 7.8 Hz), 7.34-7.37 (2H, m, Ar-H); ^{13}C δ/ppm (125 MHz, $CDCl_3$) 47.8, 111.9, 112.0, 114.1, 114.2, 115.4, 115.6, 117.1, 117.8, 129.1, 129.2, 129.55, 129.56, 134.91, 134.94, 142.6, 142.9, 146.4, 148.0, 161.1, 163.1; LC-MS (ESI+) *m/z* = 293.3 $[M+H]^+$; HRMS calcd. for $C_{19}H_{18}N_2F$ $[M+H]^+$ 293.1449, found 293.1451; Analytical HPLC: 97.9%

***N*-(4-Fluorobenzyl)-3'-methoxy-[1,1'-biphenyl]-3-amine (118j)**

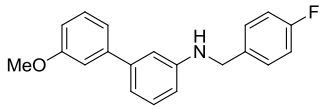

General procedure B: Using boronic ester **123** (40 mg, 0.12 mmol) and 3-bromoanisole (23.2 µL, 34 mg, 0.18 mmol), chromatography (silica, 5% EtOAc, hexane) yielded **118j** as a brown oil (25 mg, 77%); R_f = 0.22 (silica, 10% EtOAc, petrol); UV λ_{max} (EtOH/nm) 241.5; IR ν_{max}/cm^{-1} 3416 (N-H), 2835 (C-H), 1599, 1576, 1508, 1486, 1221, 1163, 1038, 824, 773, 697; ^1H δ/ppm (500 MHz, $CDCl_3$) 3.84 (3H, s, OC*H*$_3$), 4.36 (2H, s, C*H*$_2$), 6.63 (1H, dd, Ar-H, *J* = 2.0 and 8.1 Hz), 6.83-6.84 (1H, m, Ar-H), 6.87-6.89 (1H, m, Ar-H, *J* = 2.3 and 8.1 Hz), 6.95-6.97 (1H, m, Ar-H), 7.02-7.07 (3H, m, Ar-H), 7.12-7.13 (1H, m, Ar-H), 7.24 (1H, t, Ar-H, *J* = 7.9 Hz), 7.33 (1H, t, Ar-

H, *J* = 7.8 Hz), 7.35-7.38 (2H, m, Ar-H); ^{13}C δ/ppm (125 MHz, $CDCl_3$) 47.8, 55.3, 111.9, 112.2, 112.7, 112.8, 115.4, 115.6, 117.1, 119.7, 129.1, 129.2, 129.62, 129.65, 142.4, 143.2, 159.8, 161.1, 163.1; LC-MS (ESI+) *m/z* = 308.3 $[M+H]^+$; HRMS calcd. for $C_{20}H_{19}ONF$ $[M+H]^+$ 308.1445, found 308.1445; Analytical HPLC: 97.7%

_N_-(3'-((4-Fluorobenzyl)amino)-[1,1'-biphenyl]-4-yl)acetamide (118k)

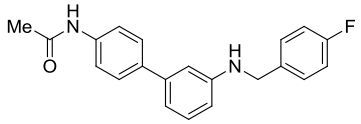

General procedure B: Using boronic ester **123** (40 mg, 0.12 mmol) and 4'-bromoacetanilide (39 mg, 0.18 mmol), chromatography (silica, 5% EtOAc, DCM followed by 50-80% Et_2O, petrol) yielded **118k** as a pale solid (17 mg, 41%); R_f = 0.31 (silica, 80% Et_2O, petrol); m.p. 99-101 ^oC; UV λ_{max} (EtOH/nm) 262.5; IR ν_{max}/cm^{-1} 3395 (secondary amine N-H), 3255 (amide N-H), 1661, 1601, 1506, 1323, 1221, 829, 777, 697; ^{1}H δ/ppm (500 MHz, $CDCl_3$) 2.20 (3H, s, NHCOC*H*$_3$), 4.35 (3H, m, C*H*$_2$ and amino N*H*), 6.60 (1H, dd, Ar-H, *J* = 1.5 and 7.9 Hz), 6.81 (1H, m, Ar-H), 6.92-6.94 (1H, m, Ar-H), 7.02-7.05 (2H, m, Ar-H), 7.19 (1H, s, br, amido N*H*), 7.23 (1H, t, Ar-H, *J* = 7.6 Hz), 7.34-7.37 (2H, m, Ar-H), 7.48-7.54 (4H, m, Ar-H); ^{13}C δ/ppm (125 MHz, $CDCl_3$) 47.8, 111.1, 111.2, 115.3, 115.4, 115.6, 116.4, 128.0, 129.1, 129.2, 129.6, 132.0, 135.1, 142.4, 145.8, 148.1, 161.1, 163.1; LC-MS (ESI+) *m/z* = 335.3 $[M+H]^+$; HRMS calcd. for $C_{21}H_{20}ON_2F$ $[M+H]^+$ 335.1554, found 335.1558; Analytical HPLC: 95.9%

4-(3-((4-Fluorobenzyl)amino)phenyl)pyridine-1-oxide (118n)

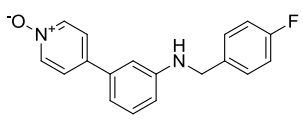

General procedure B: Using aniline **123** (100 mg, 0.31 mmol) and bromopyridine **125** (97.5 mg, 0.56 mmol), chromatography (silica, 0-5% MeOH, DCM) yielded **118n** as a brown solid (5.8 mg, 6%); R_f = 0.21 (silica, 5% MeOH, DCM); m.p. 189 ^oC (decomposed); UV λ_{max} (EtOH/nm) 295.0 and 244.2; IR ν_{max}/cm^{-1} 3235 (N-H), 3106 (C-H), 3060 (C-H), 2923 (C-H), 2853 (C-H), 1601, 1545, 1508, 1467, 1419, 1343, 1230

(C-O), 1173, 1104, 1037, 1014, 987, 833, 783, 701; ^{1}H δ/ppm (500 MHz, DMSO-d_6) 4.34 (2H, d, CH_2, *J* = 6.0 Hz), 5.77 (1H, s, N*H*), 6.43-6.46 (1H, m, Ar-H), 6.63-6.65 (1H, m, Ar-H), 6.90-6.91 (2H, m, Ar-H), 7.14-7.18 (3H, m, Ar-H), 7.41-7.44 (2H, m, Ar-H), 7.61-7.63 (2H, m, Ar-H), 8.21-8.23 (2H, m, Ar-H); ^{13}C δ/ppm (125 MHz, DMSO-d_6) 45.5, 109.5, 113.0, 113.9, 114.9, 115.1, 123.4, 129.06, 129.13, 129.7, 136.1, 136.3, 136.9, 138.7, 149.2, 161.9; ^{19}F δ/ppm (470 MHz, DMSO-d_6) -116.4; LC-MS (ESI+) *m/z* = 295.4 $[M+H]^+$; HRMS calcd. for $C_{18}H_{16}ON_2F$ $[M+H]^+$ 295.1241, found 295.1243; Analytical HPLC: 96.2%

4-(2-Aminopyridin-4-yl)phenol (127a)

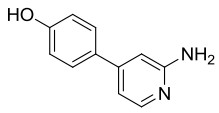

General Procedure B: Using 4-hydroxybenzeneboronic acid (97 mg, 0.70 mmol) and aminopyridine **126a** (100 mg, 0.58 mmol), chromatography (silica, 10% MeOH, DCM) afforded **127a** as a brown solid (81.7 mg, 76%); R_f = 0.28 (silica, 10% MeOH, DCM); m.p. 220 ^{o}C (decomposed); UV λ_{max} (EtOH/nm) 276.5 and 240.5; IR ν_{max}/cm^{-1} 3477 (N-H), 3383 (N-H), 2925 (C-H), 2583 (br) (O-H), 1582, 1541, 1519, 1438, 1290, 1235, 1185, 1115, 999, 903, 832, 802, 734, 661; ^{1}H δ/ppm (500 MHz, DMSO-d_6) 5.86 (2H, s, br, NH_2), 6.63 (1H, m, Ar-H), 6.72 (1H, dd, Ar-H, *J* = 1.6 and 5.4 Hz), 6.84-6.87 (2H, m, Ar-H), 7.47-7.50 (2H, m, Ar-H), 7.90 (1H, d, Ar-H, *J* = 5.2 Hz), 9.70 (1H, s, O*H*); ^{13}C δ/ppm (125 MHz, DMSO-d_6) 104.0, 109.5, 115.7, 127.5, 128.8, 148.0, 148.2, 158.1, 160.3; LC-MS (ESI+) *m/z* = 187.1 $[M+H]^+$; HRMS calcd. for $C_{11}H_{11}ON_2$ $[M+H]^+$ 187.0866, found 187.0863; HRMS calcd. for $C_{11}H_9ON_2$ $[M-H]^-$ 185.0720, found 185.0720

4-(5-Aminopyridin-3-yl)phenol (127b)

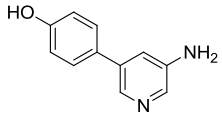

General Procedure B: Using 4-hydroxybenzeneboronic acid (97 mg, 0.70 mmol) and aminopyridine **126b** (100 mg, 0.58 mmol), chromatography (silica, 2% MeOH, EtOAc) afforded **127b** as a dark yellow solid (69.4 mg, 64%); R_f = 0.31 (silica, 2% MeOH,

EtOAc); m.p. 204 ^{o}C (decomposed); UV λ_{max} (EtOH/nm) 316.0, 243.5; IR ν_{max}/cm^{-1} 3447 (N-H), 3361 (N-H), 2487 (br) (O-H), 1594, 1489, 1461, 1249, 1162, 1108, 909, 864, 835, 709; ^{1}H δ/ppm (500 MHz, DMSO-d_6) 5.32 (2H, s, br, N*H*$_2$), 6.84-6.86 (2H, m, Ar-H), 7.05-7.06 (1H, m, Ar-H), 7.41-7.42 (2H, m, Ar-H), 7.86 (1H, d, Ar-H, *J* = 2.5 Hz), 7.96 (1H, d, Ar-H, *J* = 1.9 Hz), 9.57 (1H, s, O*H*); ^{13}C δ/ppm (125 MHz, DMSO-d_6) 115.8, 116.9, 127.7, 128.6, 134.6, 134.8, 135.6, 144.7, 157.3; LC-MS (ESI+) *m/z* = 187.2 $[M+H]^+$; HRMS calcd. for $C_{11}H_{11}ON_2$ $[M+H]^+$ 187.0866, found 187.0865; HRMS calcd. for $C_{11}H_9ON_2$ $[M-H]^-$ 185.0720, found 185.0721; LC-MS (*m/z*) 187.2 [M+H]

4-(4-Aminopyridin-2-yl)phenol (127c)

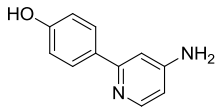

General Procedure B: Using 4-hydroxybenzeneboronic acid (97 mg, 0.70 mmol) and aminopyridine **126c** (100 mg, 0.58 mmol), irradiation for 2.5 h and chromatography (silica, 2-25% MeOH, EtOAc) afforded **127c** as a dark brown solid (45.6 mg, 42%); R_f = 0.20 (silica, 20% MeOH, EtOAc); m.p. 250 ^{o}C (decomposed); UV λ_{max} (EtOH/nm) 250.0; IR ν_{max}/cm^{-1} 3478 (N-H), 3380 (N-H), 3208 (C-H), 2965 (C-H), 2487 (br) (O-H), 1600, 1556, 1482, 1429, 1282, 1250, 1127, 1001, 950, 842, 816, 724, 659; ^{1}H δ/ppm (500 MHz, DMSO-d_6) 5.98 (2H, s, br, N*H*$_2$), 6.38 (1H, dd, Ar-H, *J* = 2.0 and 5.6 Hz), 6.80-6.82 (2H, m, Ar-H), 6.88 (1H, d, Ar-H, *J* = 1.8 Hz), 7.74-7.76 (2H, m, Ar-H), 8.02 (1H, d, Ar-H, *J* = 5.6 Hz), 9.60 (1H, s, O*H*); ^{13}C δ/ppm (125 MHz, DMSO-d_6) 103.8, 107.1, 115.1, 127.4, 130.5, 149.1, 155.0, 156.2, 157.9; LC-MS (ESI+) *m/z* = 187.1 $[M+H]^+$; HRMS calcd. for $C_{11}H_{11}ON_2$ $[M+H]^+$ 187.0866, found 187.0865; HRMS calcd. for $C_{11}H_9ON_2$ $[M-H]^-$ 185.0720, found 185.0721

3-((4-Fluorobenzyl)amino)-5-(4-hydroxyphenyl)pyridine-1-oxide (128d)

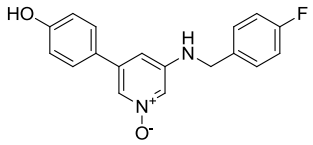

General procedure B: Using bromopyridine **133** (19 mg, 0.06 mmol) and 4-hydroxybenzeneboronic acid (13.2 mg, 0.10 mmol), chromatography (silica, 70-80% EtOAc, DCM) yielded **128d** as a brown gum (11 mg, 67%); R_f = 0.39 (silica, 10% MeOH, DCM); m.p. 116 ^oC (decomposed); UV λ_{max} (EtOH/nm) 345.0 and 261.5; IR ν_{max}/cm^{-1} 3336 (N-H), 3061 (br) (O-H), 2922 (C-H), 1581, 1507, 1224 (C-O), 1154 (N-O), 1091, 816; ^1H δ/ppm (500 MHz, DMSO-d_6) 4.33(2H, d, C*H*$_2$, *J* = 5.8 Hz), 6.79-6.86 (4H, m, Ar-H), 7.16-7.19 (2H, m, Ar-H), 7.39-7.43 (4H, m, Ar-H), 7.50 (1H, m, Ar-H), 7.70 (1H, m, N*H*), 9.75 (1H, s, O*H*); ^{13}C δ/ppm (125 MHz, DMSO-d_6) 45.1, 107.4, 115.1, 115.3, 115.8, 121.7, 124.7, 126.2, 127.9, 129.18, 129.24, 135.0, 138.4, 146.7, 158.2, 160.3, 162.2; LC-MS (ESI+) *m/z* = 311.3 $[M+H]^+$; HRMS calcd. for $C_{18}H_{14}O_2N_2F$ $[M-H]^-$ 309.1045, found 309.1048; Analytical HPLC: 97.1%

4-Fluoro-*N*-(2-(4-hydroxyphenyl)pyridine-4-yl)benzamide (131)

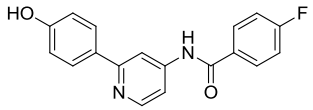

General procedure B: Using aryl bromide **130** (280 mg, 0.95 mmol) and 4-hydroxybenzeneboronic acid (270 mg, 1.96 mmol), chromatography (silica, 40-70% EtOAc, hexane) yielded a beige solid (163 mg). The solid was dissolved in methanol (5 mL) and distilled water (2 mL), mixed with sodium methoxide (705 mg, 13.1 mmol) and stirred in air at room temperature. After 48 h, the reaction was partitioned with 2 M NaOH (20 mL) and diethyl ether (20 mL). The aqueous layer was extracted with diethylether (20 mL) and filtered, neutralised with 1 M HCl (30 mL) and extracted with EtOAc (3 × 10 mL). The organic layer was washed with brine (10 mL), dried ($MgSO_4$), filtered and concentrated *in vacuo* to give **131** as a beige solid (110 mg, 38%); R_f = 0.15 (silica, 50% EtOAc, hexane); m.p. 258-260 ^oC; UV λ_{max} (EtOH/nm) 265.5; IR ν_{max}/cm^{-1} 3349 (N-H), 2480 (br) (O-H), 1692 (C=O), 1588, 1497, 1447, 1384, 1319, 1272, 1238, 1212, 1157, 1089, 1010, 839, 809, 760, 654; ^1H δ/ppm (500 MHz, DMSO-d_6) 6.88-6.90 (2H, m, Ar-H), 7.40-7.45 (2H, m, Ar-H), 7.69 (1H, dd, Ar-H, *J* = 1.9 and 5.5 Hz), 7.85-

7.87 (2H, m, Ar-H), 8.07-8.11 (2H, m, Ar-H), 8.21 (1H, d, Ar-H, *J* = 1.7 Hz), 8.51 (1H, d, Ar-H, *J* = 5.5 Hz), 9.75 (1H, s, O*H*), 10.60 (1H, s, N*H*); ^{13}C δ/ppm (125 MHz, DMSO-d_6) 109.1, 111.9, 115.4, 115.5, 115.6, 127.7, 129.8, 130.6, 130.68, 130.71, 146.7, 150.1, 157.0, 158.5, 163.4, 165.3; LC-MS (ESI+) *m/z* = 309.3 $[M+H]^+$; Analytical HPLC: 98.9%

2'-(4-Chlorophenoxy)-3'-nitro-[1,1'-biphenyl]-4-ol (136a)

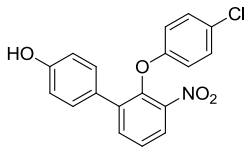

General Procedure B: Using 4-hydroxybenzeneboronic acid (66.2 mg, 0.48 mmol) and aryl bromide **135a** (130 mg, 0.40 mmol), chromatography (silica, 1% EtOAc, DCM) afforded **136a** as a dark brown solid (101 mg, 74%); R_f = 0.42 (silica, 1% EtOAc, DCM); m.p. 125-130 ^{o}C; UV λ_{max} (EtOH/nm) 263.0; IR ν_{max}/cm^{-1} 3228 (O-H), 1593, 1515, 1483, 1345, 1230, 1195, 1090, 1008, 887, 813, 794, 756; ^{1}H δ/ppm (500 MHz, DMSO-d_6) 6.68-6.74 (4H, m, Ar-H), 7.21-7.24 (2H, m, Ar-H), 7.29-7.32 (2H, m, Ar-H), 7.60 (1H, t, Ar-H, *J* = 8.0 Hz), 7.81 (1H, dd, Ar-H, *J* = 1.6 and 7.8 Hz), 8.03 (1H, dd, Ar-H, *J* = 1.6 and 8.2 Hz), 9.63 (1H, s, O*H*); ^{13}C δ/ppm (125 MHz, DMSO-d_6) 115.3, 116.8, 123.8, 125.4, 126.1, 126.7, 129.3, 130.1, 135.8, 137.3, 142.8, 144.2, 155.7, 157.5; LC-MS (ESI+) *m/z* = 340.2 $[M-H]^-$

2-(4-Chlorophenoxy)-3-nitro-1,1'-biphenyl (136b)

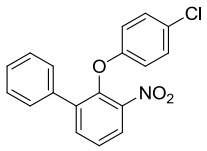

General Procedure B: Using benzeneboronic acid (196 mg, 1.61 mmol) and aryl bromide **135a** (440 mg, 1.34 mmol), chromatography (silica, 0-5% EtOAc, petrol) afforded **136b** as a yellow oil (382 mg, 79%); R_f = 0.33 (silica, 10% EtOAc, petrol); UV λ_{max} (EtOH/nm) 225.5; IR ν_{max}/cm^{-1} 3069 (C-H), 1583, 1529 (N=O asym. stretch), 1483, 1352 (N=O sym. stretch), 1237 (C-O), 1091, 827, 761, 699; ^{1}H δ/ppm (500 MHz, $CDCl_3$) 6.57-6.60 (2H, m, Ar-H), 7.04-7.07 (2H, m, Ar-H), 7.27-7.33 (3H, m, Ar-H),

7.37-7.40 (2H, m, Ar-H), 7.45 (1H, t, Ar-H, *J* = 8.0 Hz), 7.68 (1H, dd, Ar-H, *J* = 1.7 and 7.8 Hz), 7.92 (1H, dd, Ar-H, *J* = 1.6 and 8.1 Hz); ^{13}C δ/ppm (125 MHz, $CDCl_3$) 116.69, 116.74, 124.5, 125.8, 127.4, 128.37, 128.44, 129.0, 129.3, 129.7, 135.3, 135.9, 138.7, 144.5, 144.7, 155.9; LC-MS (ESI+) *m/z* = mass not observe

2'-((4-Chlorobenzyl)oxy)-3'-nitro-[1,1'-biphenyl]-4-ol (136c)

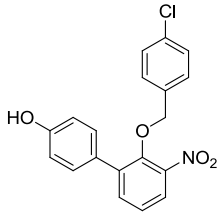

General Procedure B: Using 4-hydroxybenzeneboronic acid (149 mg, 1.08 mmol) and aryl bromide **135b** (310 mg, 0.90 mmol), chromatography (silica, 10-20% EtOAc, petrol) afforded **136c** as a yellow/brown solid (290 mg, 86%); R_f = 0.19 (silica, 20% EtOAc, petrol); m.p. 129-131 ^{o}C; UV λ_{max} (EtOH/nm) 262.0; IR ν_{max}/cm^{-1} 3263 (O-H), 1600, 1512 (N=O asym. stretch), 1349 (N=O sym. stretch), 1230 (C-O), 1082, 966, 836, 803; ^{1}H δ/ppm (500 MHz, DMSO-d_6) 4.56 (2H, s, C*H*$_2$), 6.87-6.90 (2H, m, Ar-H), 7.11-7.13 (2H, m, Ar-H), 7.37-7.39 (2H, m, Ar-H), 7.42 (1H, t, Ar-H, *J* = 7.9 Hz), 7.43-7.45 (2H, m, Ar-H), 7.67 (1H, dd, Ar-H, *J* = 1.7 and 7.8 Hz), 7.83 (1H, dd, Ar-H, *J* = 1.6 and 8.0 Hz); ^{13}C δ/ppm (125 MHz, DMSO-d_6) 74.1, 115.5, 122.9, 125.1, 126.3, 128.3, 129.9, 130.1, 132.9, 134.7, 134.9, 137.1, 145.3, 147.4, 157.6; LC-MS (ESI+) *m/z* = 354.1 [M-H]$^{-}$; HRMS calcd. for $C_{19}H_{13}O_4N^{35}Cl$ [M-H]$^{-}$ 354.0539, found 354.0530

2-(4-Chlorophenoxy)-4'-fluoro-3-nitro-1,1'-biphenyl (136f)

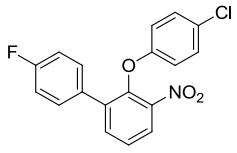

General procedure B: Using aryl bromide **135a** (700 mg, 2.13 mmol) and 4-fluorobenzeneboronic acid (448 mg, 3.20 mmol), chromatography (silica, 10% Et_2O, petrol) yielded **136f** as a dark yellow oil (627 mg, 86%); R_f = 0.31 (silica, 20% Et_2O, petrol); UV λ_{max} (EtOH/nm) 226.2; IR ν_{max}/cm^{-1} 3077 (C-H), 1604, 1532, 1510, 1483, 1448, 1403, 1351, 1235 (C-O), 1195, 1160, 1091, 1010, 887, 813, 754; ^{1}H δ/ppm (500

MHz, $CDCl_3$) 6.56-6.59 (2H, m, Ar-H), 6.98-7.03 (2H, m, Ar-H), 7.06-7.09 (2H, m, Ar-H), 7.35-7.39 (2H, m, Ar-H), 7.46 (1H, t, Ar-H, *J* = 8.0 Hz), 7.66 (1H, dd, Ar-H, *J* = 1.7 and 7.8 Hz), 7.93 (1H, dd, Ar-H, *J* = 1.7 and 8.2 Hz); ^{13}C δ/ppm (125 MHz, $CDCl_3$) 115.5, 115.7, 116.6, 124.7, 125.9, 127.6, 129.4, 130.7, 130.8, 131.27, 131.30, 135.7, 137.6, 144.5, 144.6, 155.8, 161.7, 163.7; LC-MS (ESI+) *m/z* = mass not observed

2'-Fluoro-2-methyl-3'-nitro-[1,1'-biphenyl]-4-ol (144a)

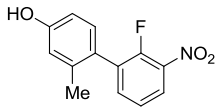

General procedure B: Using boronic ester **142** (230 mg, 0.86 mmol) and 4-bromo-3-methylboronic acid (322 mg, 1.72 mmol), chromatography (silica, 5-15% EtOAc, petrol) yielded **144a** as a dark brown solid (183 mg, 79%); R_f = 0.28 (silica, 20% EtOAc, petrol); m.p. 127-129 ^{o}C; UV λ_{max} (EtOH/nm) 252.8; IR ν_{max}/cm^{-1} 3261 (O-H), 3093 (C-H), 2924 (C-H), 2858 (C-H), 1613, 1581, 1532, 1504, 1466, 1447, 1344 (C-O), 1294, 1234, 1162, 1124, 1083, 951, 880, 806, 734; ^{1}H δ/ppm (500 MHz, $CDCl_3$) 2.16 (3H, s, ArC*H*$_3$), 4.89 (1H, s, br, O*H*), 6.74 (1H, dd, Ar-H, *J* = 2.5 and 8.1 Hz), 6.80 (1H, d, Ar-H, *J* = 2.4 Hz), 7.07 (1H, d, Ar-H, *J* = 8.4 Hz), 7.30-7.33 (1H, m, Ar-H), 7.50-7.53 (1H, m, Ar-H), 8.00-8.03 (1H, m, Ar-H); ^{13}C δ/ppm (125 MHz, $CDCl_3$) 113.0, 117.1, 123.87, 123.92, 124.8, 124.86, 125.90, 131.4, 132.1, 132.3, 137.2, 137.3, 138.2, 138.4, 151.6, 153.7, 156.0; ^{19}F δ/ppm (470 MHz, $CDCl_3$) -119.8; LC-MS (ESI+) *m/z* = 246.2 [M-H]$^{-}$; HRMS calcd. for $C_{13}H_9O_3NF$ [M-H]$^{-}$ 246.0572, found 246.0571

2-Chloro-2'-fluoro-3'-nitro-[1,1'-biphenyl]-4-ol (144b)

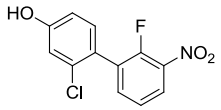

General procedure B: Using boronic ester **142** (230 mg, 0.86 mmol) and 4-bromo-3-chloroboronic acid (357 mg, 1.72 mmol), chromatography (silica, 10-25% EtOAc, petrol) yielded **144b** as a light brown solid (192 mg, 76%); R_f = 0.50 (silica, 40% EtOAc, petrol); m.p. 120-123 ^{o}C; UV λ_{max} (EtOH/nm) 249.4; IR ν_{max}/cm^{-1} 3442 (O-H), 3098 (C-H), 1605, 1586, 1525, 1499, 1421, 1346 (C-O), 1300, 1269, 1243, 1213, 1078, 1029, 909, 879, 863, 809, 739, 692; ^{1}H δ/ppm (500 MHz, $CDCl_3$) 5.63 (1H, s, br, O*H*),

6.85 (1H, dd, Ar-H, *J* = 2.6 and 8.4 Hz), 7.04 (1H, d, Ar-H, *J* = 2.5 Hz), 7.19 (1H, d, Ar-H, 8.5 Hz), 7.31-7.35 (1H, m, Ar-H), 7.57-7.60 (1H, m, Ar-H), 8.04-8.07 (1H, m, Ar-H); ^{13}C δ/ppm (125 MHz, $CDCl_3$) 114.3, 114.4, 116.3, 116.8, 116.9, 123.7, 123.8, 124.7, 125.5, 129.9, 130.0, 132.3, 134.2, 137.4, 151.8, 153.9, 157.0; ^{19}F δ/ppm (470 MHz, $CDCl_3$) -119.0; LC-MS (ESI+) *m/z* = 266.2 $[M-H]^-$; HRMS calcd. for $C_{12}H_6O_3N^{35}ClF$ $[M-H]^-$ 266.0026, found 266.0025

***N*-(4'-Fluoro-2-methyl-[1,1'-biphenyl]-3-yl)-4-methoxybenzamide (148a)**

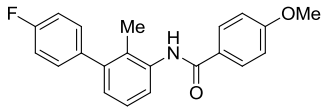

General procedure B: Using aryl bromide **147a** (650 mg, 2.03 mmol) and 4-fluorobenzeneboronic acid (511 mg, 3.65 mmol), chromatography (silica, 20-50% EtOAc, petrol) yielded **148a** as a brown solid (590 mg, 87%); R_f = 0.32 (silica, 30% EtOAc, petrol); m.p. 158-160 ^oC; UV λ_{max} (EtOH/nm) 253.4; IR ν_{max}/cm^{-1} 3200 (N-H), 3006 (C-H), 2848 (C-H), 1638 (C=O), 1605, 1577, 1529, 1495, 1450, 1299, 1242 (C-O), 1179, 1030, 935, 905, 851, 803, 766, 665; ^{1}H δ/ppm (500 MHz, $CDCl_3$) 2.19 (3H, s, Ar*CH*$_3$), 3.88 (3H, s, O*CH*$_3$), 6.98-7.01 (2H, m, Ar-H), 7.08-7.13 (3H, m, Ar-H), 7.25-7.31 (3H, m, Ar-H), 7.65 (1H, s, br, N*H*), 7.86-7.90 (3H, m, Ar-H); ^{13}C δ/ppm (125 MHz, $CDCl_3$) 15.2, 55.5, 114.1, 115.0, 115.2, 122.9, 126.2, 127.08, 127.12, 127.6, 129.0, 130.86, 130.93, 136.3, 137.66, 137.69, 142.1, 161.1, 162.6, 163.0, 165.3; LC-MS (ESI+) *m/z* = 336.4 $[M+H]^+$; HRMS calcd. for $C_{21}H_{17}O_2NF$ $[M-H]^-$ 334.1249, found 334.1246; Analytical HPLC: 100.0%

***N*-(4'-Fluoro-2-methyl-[1,1'-biphenyl]-3-yl)-4-hydroxybenzamide (148b)**

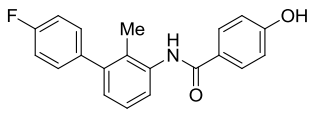

General procedure B: Using aryl bromide **147b** (500 mg, 1.63 mmol) and 4-fluorobenzeneboronic acid (410 mg, 2.93 mmol), chromatography (silica, 30-45% EtOAc, petrol) yielded **148b** as a brown solid (486 mg, 93%); R_f = 0.23 (silica, 30% EtOAc, petrol); m.p. 104-106 ^oC; UV λ_{max} (EtOH/nm) 256.2; IR ν_{max}/cm^{-1} 3198 (O-H), 1641 (C=O), 1605, 1497, 1440, 1375, 1280, 1220 (C-O), 1171, 1108, 1039, 996, 931,

838, 785, 765, 727; ^{1}H δ/ppm (500 MHz, $CDCl_3$) 2.19 (3H, s, ArC*H*$_3$), 5.67 (1H, s, br, O*H*), 6.92-6.94 (2H, m, Ar-H), 7.09-7.13 (3H, m, Ar-H), 7.25-7.31 (3H, m, Ar-H), 7.64 (1H, s, br, N*H*), 7.81-7.86 (3H, m, Ar-H); ^{13}C δ/ppm (125 MHz, $CDCl_3$) 15.2, 115.0, 115.2, 115.7, 123.1, 126.3, 127.1, 127.3, 127.8, 129.2, 130.86, 130.92, 136.1, 142.2, 159.1; LC-MS (ESI+) *m/z* = 322.4 $[M+H]^+$; HRMS calcd. for $C_{20}H_{15}O_2NF$ $[M-H]^-$ 320.1092, found 320.1092; Analytical HPLC: 97.0%

2-Fluoro-4'-methoxy-3-nitro-1,1'-biphenyl (216)

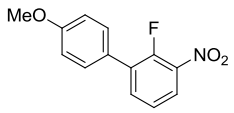

General Procedure B: Using aryl bromide **139** (200 mg, 0.91 mmol) and 4-methoxybenzeneboronic acid (277 mg, 1.82 mmol), chromatography (silica, 0-40% DCM, petrol) afforded **216** as a white solid (197 mg, 88%); R_f = 0.34 (silica, 40% DCM, petrol); m.p. 106-108 ^{o}C; UV λ_{max} (EtOH/nm) 257.0; IR ν_{max}/cm^{-1} 3086 (C-H), 2972 (C-H), 2935 (C-H), 2840 (C-H), 1605, 1583, 1510, 1454, 1344, 1297, 1251 (C-O), 1178, 1115, 1022, 882, 837, 799, 733; ^{1}H δ/ppm (500 MHz, MeOH-d_4) 3.86 (3H, s, OC*H*$_3$), 7.06 (2H, d, 4-MeOPh C_3-H and C_5-H, *J* = 8.8 Hz), 7.42 (1H, t, 2-FPh C_5-H, *J* = 7.9 Hz), 7.51 (2H, dd, 4-MeOPh C_2-H and C_6-H, *J* = 1.7 and 8.8 Hz), 7.76-7.80 (1H, m, Ar-H), 7.97-8.00 (1H, m, Ar-H); ^{13}C δ/ppm (125 MHz, MeOH-d_4) 54.4, 113.9, 123.89, 123.91, 124.2, 124.3, 125.8, 130.0, 130.1, 131.6, 131.7, 135.51, 135.54, 151.0, 153.0, 160.2; ^{19}F δ/ppm (470 MHz, MeOH-d_4) -127.5; LC-MS (ESI+) *m/z* = 248.2 $[M+H]^+$; HRMS calcd. for $C_{13}H_{11}O_3NF$ $[M+H]^+$ 248.0717, found 248.0716

6-(4-Chlorophenoxy)-4'-hydroxy-5-nitro-[1,1'-biphenyl]-3-carboxylic acid (224)

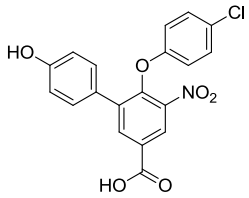

General Procedure B: Using aryl bromide **223** (110 mg, 0.30 mmol) and 4-hydroxybenzeneboronic acid (83 mg, 0.60 mmol), chromatography (C18, 50-70% MeOH + 0.1% (v/v) HCO_2H, H_2O) afforded **224** as a yellow solid (64 mg, 56%); R_f = 0.18 (silica, 10% MeOH, DCM); m.p. 201-203 ^{o}C; UV λ_{max} (EtOH/nm) 225.2; IR ν_{max}/cm^{-1} 3294 (phenol O-H), 3071 (C-H), 2650 (carboxyl O-H), 1695 (C=O), 1609,

1536, 1482, 1420, 1347, 1304, 1232 (C-O), 1189, 1090, 1009, 927, 820, 736, 667; ^{1}H δ/ppm (500 MHz, DMSO-d_6) 6.74 (2H, d, 4-HOPh C_2-H and C_6-H, *J* = 8.7 Hz), 6.78 (2H, d, 4-ClPh C_3-H and C_5-H, *J* = 9.1 Hz), 7.24 (2H, d, 4-ClPh C_2-H and C_6-H, *J* = 9.1 Hz), 7.33 (2H, d, 4-HOPh C_3-H and C_5-H, *J* = 8.7 Hz), 8.21 (1H, dd, Ar-H, *J* = 2.1 Hz), 8.46 (1H, dd, Ar-H, *J* = 2.2 Hz), 9.70 (1H, s, br, ArO*H*), 13.74 (1H, s, br, CO_2*H*); ^{13}C δ/ppm (125 MHz, DMSO-d_6) 115.4, 117.1, 124.6, 124.8, 126.5, 129.4, 130.2, 135.8, 137.7, 144.1, 146.2, 155.3, 157.7, 165.1; LC-MS (ESI+) *m/z* = 384.2 $[M-H]^-$; HRMS calcd. for $C_{19}H_{11}O_6N^{35}Cl$ $[M-H]^-$384.0280, found 384.0272

Methyl 6-(4-chlorophenoxy)-4'-hydroxy-5-nitro-[1,1'-biphenyl]-3-carboxylate (228)

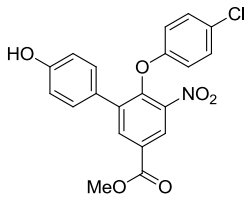

General Procedure B: Using aryl bromide **227** (492 mg, 1.27 mmol) and 4-hydroxybenzeneboronic acid (350 mg, 2.54 mmol), chromatography (silica, 0-20% EtOAc, petrol followed by 45-80% DCM, petrol) afforded **228** as a yellow solid (255 mg, 50%); R_f = 0.23 (silica, 30% EtOAc, petrol); m.p. 76-78 ^{o}C; UV λ_{max} (EtOH/nm) 226.2; IR ν_{max}/cm^{-1} 3389 (phenol O-H), 3085 (C-H), 2953 (C-H), 1723 (C=O), 1610, 1537, 1483, 1433, 1352, 1312, 1235 (C-O), 1193, 1114, 1075, 1009, 981, 913, 821, 762, 695; ^{1}H δ/ppm (500 MHz, $CDCl_3$) 3.99 (3H, s, CO_2C*H*$_3$), 4.84 (1H, s, br, ArO*H*), 6.60 (2H, d, Ar-H, *J* = 9.0 Hz), 6.79 (2H, d, Ar-H, *J* = 8.7 Hz), 7.09 (2H, d, Ar-H, *J* = 9.0 Hz), 7.32 (2H, d, Ar-H, *J* = 8.7 Hz), 8.32 (1H, d, Ar-H, *J* = 2.1 Hz), 8.51 (1H, d, Ar-H, *J* = 2.1 Hz); ^{13}C δ/ppm (125 MHz, $CDCl_3$) 52.9, 115.6, 116.8, 125.2, 127.1, 127.8, 128.0, 129.5, 130.5, 136.3, 138.4, 144.5, 147.9, 155.4, 156.0, 164.6; LC-MS (ESI+) *m/z* = 400.3 $[M+H]^+$ and 398.2 $[M-H]^-$; HRMS calcd. for $C_{20}H_{13}O_6N^{35}Cl$ $[M-H]^-$ 398.0437, found 398.0426

2-(6-(4-Chlorophenoxy)-4'-hydroxy-5-nitro-[1,1'-biphenyl]-3-yl)acetonitrile (241)

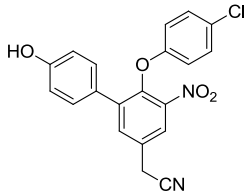

General Procedure B: Using aryl bromide **234** (595 mg, 1.62 mmol) and 4-hydroxybenzeneboronic acid (446 mg, 3.24 mmol) and irradiating at 120 ^{o}C for 22 min, chromatography (silica, 0-10% EtOAc, DCM) afforded **241** as a yellow solid (374 mg, 61%); R_f = 0.21 (silica, 40% EtOAc, petrol); m.p. 159-161 ^{o}C; UV λ_{max} (EtOH/nm) 270.0; IR ν_{max}/cm^{-1} 3367 (O-H), 3069 (C-H), 2924 (C-H), 2250 (C≡N), 1610, 1588, 1535, 1515, 1482, 1412, 1346, 1266, 1235 (C-O), 1196, 1174, 1090, 1042, 1009, 936, 822, 744; ^{1}H δ/ppm (500 MHz, $CDCl_3$) 3.88 (2H, s, ArC*H*$_2$), 4.87 (1H, s, br, ArO*H*), 6.59 (2H, d, Ar-H, *J* = 9.0 Hz), 6.78 (2H, d, Ar-H, *J* = 8.7 Hz), 7.08 (2H, d, Ar-H, *J* = 9.0 Hz), 7.29 (2H, d, Ar-H, *J* = 8.7 Hz), 7.64 (1H, d, Ar-H, *J* = 2.2 Hz), 7.85 (1H, d, Ar-H, *J* = 2.2 Hz); ^{13}C δ/ppm (125 MHz, $CDCl_3$) 23.1, 115.6, 116.4, 116.7, 123.4, 127.0, 127.8, 128.0, 129.4, 130.4, 134.8, 139.4, 144.4, 144.7, 155.6, 156.0; LC-MS (ESI+) *m/z* = 379.1 [M-H]$^{-}$; HRMS calcd. for $C_{20}H_{12}O_4N_2{}^{35}Cl$ [M-H]$^{-}$ 379.0491, found 379.0483

Methyl 6-(4-chlorophenoxy)-4'-methoxy-5-nitro-[1,1'-biphenyl]-3-carboxylate (245)

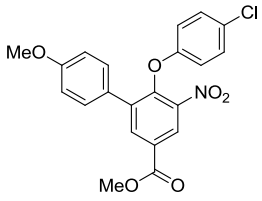

General Procedure B: Using aryl bromide **227** (250 mg, 0.65 mmol) and 4-methxybenzeneboronic acid (198 mg, 1.30 mmol) and irradiating at 120 ^{o}C for 19 min, chromatography (silica, 0-20% Et_2O, petrol) afforded **245** as a yellow oil (160 mg, 60%); R_f = 0.26 (silica, 30% Et_2O, petrol); UV λ_{max} (EtOH/nm) 225.8; IR ν_{max}/cm^{-1} 3237 (C-H), 3086 (C-H), 2954 (C-H), 2839 (C-H), 1724 (C=O), 1609, 1538, 1513, 1483, 1464, 1434, 1356, 1306, 1230 (C-O), 1197, 1112, 1091, 1029, 1009, 983, 910, 824, 799, 762, 733, 694; ^{1}H δ/ppm (500 MHz, $CDCl_3$) 3.79 (3H, s, ArOC*H*$_3$), 3.99 (3H, s, CO_2C*H*$_3$), 6.60 (2H, d, 4-ClPh C_3-H and C_5-H, *J* = 9.0 Hz), 6.85 (2H, d, 4-MeOPh C_2-H and C_6-H, *J* = 8.8 Hz), 7.08 (2H, d, 4-ClPh C_2-H and C_6-H, *J* = 9.0 Hz), 7.36 (2H,

d, 4-MeOPh C_3-H and C_5-H, *J* = 8.8 Hz), 8.33 (1H, d, Ar-H, 2.1 Hz), 8.50 (1H, d, Ar-H, *J* = 2.1 Hz); ^{13}C δ/ppm (125 MHz, $CDCl_3$) 52.9, 55.3, 114.1, 116.8, 125.2, 126.8, 127.8, 128.0, 129.5, 130.2, 136.3, 138.5, 144.4, 147.9, 155.4, 159.9, 164.6; LC-MS (ESI+) *m/z* = 414.3 $[M+H]^+$; HRMS calcd. for $C_{21}H_{17}O_6N^{35}Cl$ $[M+H]^+$ 414.0739, found 414.0741

4-Fluoro-*N*-(4-(1-(tetrahydro-2*H*-pyran-2-yl)-1*H*-indazol-5-yl)thiazol-2-yl)benzamide (274)

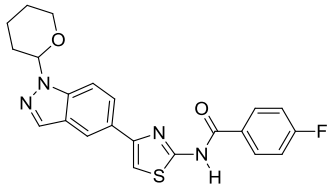

General Procedure B: Using boronic ester **273** (230 mg, 0.70 mmol) and bromothiazole **268** (142 mg, 0.47 mmol) and irradiating for 40 min, chromatography (silica, 10-60% EtOAc, petrol) afforded **274** as a brown solid (155 mg, 78%); R_f = 0.25 (silica, 10% EtOAc, petrol); m.p. 215-217 ^{o}C; UV λ_{max} (EtOH/nm) 245.4 and 222.8; IR ν_{max}/cm^{-1} 3333 (N-H), 3088 (C-H), 2927 (C-H), 2857 (C-H), 1668 (C=O), 1600, 1532, 1511, 1483, 1446, 1420, 1372, 1341, 1315, 1272, 1226, 1208, 1164, 1079, 1040, 994, 911, 891, 848, 791, 752, 716, 684; ^{1}H δ/ppm (500 MHz, DMSO-d_6) 1.61 (2H, m, Alk-H), 1.98-2.07 (2H, m, Alk-H), 2.37-2.47 (2H, m, Alk-H), 3.74-3.79 (1H, m, Alk-H), 3.91-3.94 (1H, m, Alk-H), 5.87-5.89 (1H, m, Alk-H), 7.40-7.43 (2H, m, Ar-H), 7.69 (1H, s, thiazole C_5-H), 7.80 (1H, d, Ar-H, *J* = 8.8 Hz), 8.04 (1H, dd, Ar-H, *J* = 1.2 and 8.8 Hz), 8.20 (1H, s, Ar-H), 8.22-8.25 (2H, m, Ar-H), 8.35 (1H, s, Ar-H), 12.82 (1H, s, N*H*); ^{13}C δ/ppm (125 MHz, DMSO-d_6) 22.2, 24.8, 29.0, 66.6, 84.1, 107.5, 110.6, 115.6, 115.7, 117.7, 124.5, 125.0, 128.0, 128.6, 131.1, 134.1, 139.0, 139.3, 150.9, 158.4, 164.2, 185.5; ^{19}F δ/ppm (470 MHz, DMSO-d_6) -107.0; LC-MS (ESI+) *m/z* = 423.4 $[M+H]^+$ and 421.3 $[M-H]^-$; HRMS calcd. for $C_{22}H_{20}O_2N_4FS$ $[M+H]^+$ 423.1286, found 423.1285; Analytical HPLC: 94.9%

3'-((4-Fluorobenzyl)amino)-[1,1'-biphenyl]-3-ol (118b)

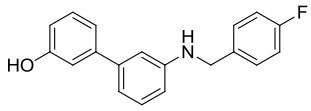

General Procedure C: Using aniline **117b** (97 mg, 0.52 mmol) and 4-fluorobenzaldehyde (67 µL, 77 mg, 0.62 mmol), chromatography (silica, 20% EtOAc, hexane) afforded **118b** as a light brown solid (130 mg, 85%); R_f = 0.43 (silica, 30% EtOAc, hexane); m.p. 106-109 ^oC; UV λ_{max} (EtOH/nm) 239.0; IR ν_{max}/cm^{-1} 3323 (N-H), 3048 (C-H), 2856 (br) (O-H), 1602, 1574, 1508, 1483, 1456, 1416, 1349, 1315, 1226, 1189, 1157, 1072, 1046, 1014, 933, 875, 836, 777, 695; ^1H δ/ppm (500 MHz, $CDCl_3$) 4.35 (2H, s, C*H*$_2$), 4.68 (1H, s, O*H*), 4.79 (1H, s, br, N*H*), 6.61-6.63 (1H, m, Ar-H), 6.78-6.81 (1H, m, Ar-H), 6.82-6.83 (1H, m, Ar-H), 6.93-6.94 (1H, m, Ar-H), 7.00-7.07 (3H, m, Ar-H), 7.10-7.12 (1H, m, Ar-H), 7.23 (1H, t, Ar-H, *J* = 7.9 Hz), 7.28 (1H, t, Ar-H, *J* = 7.9 Hz), 7.33-7.37 (2H, m, Ar-H); ^{13}C δ/ppm (125 MHz, $CDCl_3$) 47.9, 111.9, 112.4, 114.1, 115.4, 115.6, 117.2, 119.8, 128.8, 129.1, 129.2, 129.7, 129.9, 134.7, 142.0, 143.4, 147.9, 155.7, 161.2, 163.1; LC-MS (ESI+) *m/z* = 294.3 $[M+H]^+$; HRMS calcd. for $C_{19}H_{17}ONF$ $[M+H]^+$ 294.1289, found 294.1294; HRMS calcd. for $C_{19}H_{15}ONF$ $[M-H]^-$ 292.1143, found 292.1136; Analytical HPLC: 99.1%

3'-((4-Fluorobenzyl)amino)-[1,1'-biphenyl]-3,4-diol (118c)

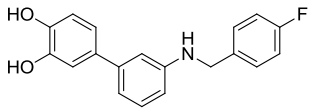

General Procedure C: Using aniline **117c** (60 mg, 0.30 mmol) and 4-fluorobenzaldehyde (39 µL, 45 mg, 0.36 mmol), chromatography (silica, 10-50% EtOAc, hexane) afforded **118c** as a dark brown oil (56.6 mg, 61%); R_f = 0.44 (silica, 50% EtOAc, hexane); UV λ_{max} (EtOH/nm) 252.5 and 214.5; IR ν_{max}/cm^{-1} 3414 (N-H), 3047 (C-H), 2948 (C-H), 2846 (br) (O-H), 1601, 1507, 1439, 1261, 1218, 1113, 1043, 814, 773, 697; ^1H δ/ppm (500 MHz, $CDCl_3$) 4.34 (2H, s, C*H*$_2$), 5.15 (3H, s, br, O*H* and N*H*), 6.57-6.59 (1H, m, Ar-H), 6.77-6.78 (1H, m, Ar-H), 6.88-6.90 (2H, m, Ar-H), 6.98-7.06 (4H, m, Ar-H), 7.21 (1H, t, Ar-H, *J* = 7.8 Hz), 7.34-7.36 (2H, m, Ar-H); ^{13}C δ/ppm (125 MHz, $CDCl_3$) 47.8, 111.5, 111.7, 114.3, 115.4, 115.6, 116.8, 119.9, 129.1, 129.6, 134.9, 135.1, 141.9, 143.1, 143.6, 148.0, 161.1, 163.1; LC-MS (ESI+) *m/z* =

310.3 $[M+H]^+$; HRMS calcd. for $C_{19}H_{17}O_2NF$ $[M+H]^+$ 310.1238, found 310.1241; HRMS calcd. for $C_{19}H_{15}O_2NF$ $[M-H]^-$ 308.1092, found 308.1084; Analytical HPLC: 97.5%

1,1,1-Trifluoro-*N*-(3'-((4-fluorobenzyl)amino)-[1,1'-biphenyl]-4-yl)methanesulfonamide (118d)

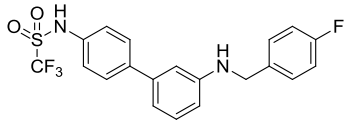

General Procedure C: Using aniline **117d** (89 mg, 0.28 mmol) and 4-fluorobenzaldehyde (36 µL, 42 mg, 0.34 mmol), chromatography (silica, 25% EtOAc, hexane) afforded **118d** as a light brown solid (105.2 mg, 90%); R_f = 0.41 (silica, 30% EtOAc, hexane); m.p. 106-109 ^oC; UV λ_{max} (EtOH/nm) 251.5; IR ν_{max}/cm^{-1} 3459 (amino N-H), 3265 (sulfonamido N-H), 3049 (C-H), 1606, 1507, 1449, 1416, 1364, 1331 (S=O asym. stretch), 1216, 1188, 1137 (S=O sym. stretch), 1014, 990, 819, 772, 728, 684; ^1H δ/ppm (500 MHz, $CDCl_3$) 4.36 (2H, s, C*H*$_2$), 4.67 (1H, s, N*H*), 6.64-6.66 (1H, m, Ar-H), 6.79-6.80 (1H, m, Ar-H), 6.91-6.93 (1H, m, Ar-H), 7.02-7.07 (2H, m, Ar-H), 7.25 (2H, t, Ar-H, *J* = 7.8 Hz), 7.29-7.32 (2H, m, Ar-H), 7.34-7.37 (2H, m, Ar-H), 7.52-7.55 (2H, m, Ar-H); ^{13}C δ/ppm (125 MHz, $CDCl_3$) 48.1, 115.5, 115.7, 121.1, 124.0, 128.3, 129.3, 129.9, 132.7, 140.9, 161.2; LC-MS (ESI+) *m/z* = 425.3 $[M+H]^+$; HRMS calcd. for $C_{20}H_{17}O_2N_2F_4S$ $[M+H]^+$ 425.0941, found 425.0943; HRMS calcd. for $C_{20}H_{15}O_2N_2F_4S$ $[M-H]^-$ 423.0796, found 423.0782; Analytical HPLC: 95.6%

1,1,1-Trifluoro-*N*-(4'-((4-fluorobenzyl)amino)-[1,1'-biphenyl]-4-yl)methanesulfonamide (118e)

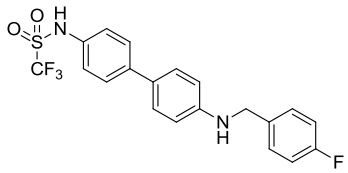

General Procedure C: Using aniline **117e** (103 mg, 0.33 mmol) and 4-fluorobenzaldehyde (43 µL, 50 mg, 0.40 mmol), chromatography (silica, 25% EtOAc, hexane) afforded **118e** as a light brown solid (75.6 mg, 54%); R_f = 0.45 (silica, 30%

EtOAc, hexane); m.p. 144-146 ^{o}C; UV λ_{max} (EtOH/nm) 298.5; IR ν_{max}/cm^{-1} 3403 (amino N-H), 3277 (sulfonamido N-H), 3033 (C-H), 2841 (C-H), 1615, 1501, 1467, 1413, 1364, 1330 (S=O asym. stretch), 1198, 1137 (S=O sym. stretch), 936, 821, 769; ^{1}H δ/ppm (500 MHz, $CDCl_3$) 4.19 (1H, s, br, N*H*), 4.35 (2H, s, C*H*$_2$), 6.67-6.70 (3H, m, Ar-H and sulfonamido N*H*), 7.03-7.07 (2H, m, Ar-H), 7.27-7.30 (2H, m, Ar-H), 7.33-7.36 (2H, m, Ar-H), 7.39-7.42 (2H, m, Ar-H), 7.52-7.54 (2H, m, Ar-H); ^{13}C δ/ppm (125 MHz, $CDCl_3$) 47.5, 113.2, 115.5, 115.6, 124.5, 127.3, 127.9, 128.9, 129.0, 131.4, 140.9, 147.7; LC-MS (ESI+) *m/z* = 425.3 $[M+H]^+$; HRMS calcd. for $C_{20}H_{17}O_2N_2F_4S$ $[M+H]^+$ 425.0941, found 425.0944; HRMS calcd. for $C_{20}H_{15}O_2N_2F_4S$ $[M-H]^-$ 423.0796, found 423.0795; Analytical HPLC: 98.2%

***N*-(4-Fluorobenzyl)-[1,1'-biphenyl]-3-amine (118l)**

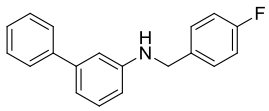

General Procedure C: Using aniline **117g** (100 mg, 0.59 mmol) and 4-fluorobenzaldehyde (76.1 µL, 88.1 mg, 0.71 mmol), chromatography (silica, 0-5% EtOAc, petrol) afforded **118l** as a yellow oil (148 mg, 91%); R_f = 0.24 (silica, 5% EtOAc, petrol); UV λ_{max} (EtOH/nm) 316.5 and 241.0; IR ν_{max}/cm^{-1} 3419 (N-H), 3032 (C-H), 1599, 1509, 1486, 1328, 1223, 1155, 756, 699; ^{1}H δ/ppm (500 MHz, $CDCl_3$) 4.20 (1H, s, br, N*H*), 4.36 (2H, s, C*H*$_2$), 6.62 (1H, dd, Ar-H, *J* = 2.2 and 8.0 Hz), 6.84-6.85 (1H, m, Ar-H), 6.96-6.98 (1H, m, Ar-H), 7.03-7.06 (2H, m, Ar-H), 7.25 (1H, t, Ar-H, *J* = 7.8 Hz), 7.31-7.35 (1H, m, Ar-H), 7.35-7.38 (2H, m, Ar-H), 7.40-7.43 (2H, m, Ar-H), 7.54-7.55 (2H, m, Ar-H); ^{13}C δ/ppm (125 MHz, $CDCl_3$) 47.9, 112.0, 112.2, 115.4, 115.6, 117.3, 127.17, 127.24, 128.7, 129.16, 129.21, 129.7, 134.8, 141.6, 142.5, 147.9, 161.2, 163.1; LC-MS (ESI+) *m/z* = 278.3 $[M+H]^+$; HRMS calcd. for $C_{19}H_{17}NF$ $[M+H]^+$ 278.1340, found 278.1345; Analytical HPLC: 99.9%

***N*-(4-Fluorobenzyl)-3-(pyridin-4-yl)aniline (118m)**

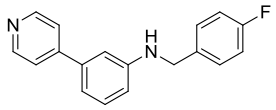

General Procedure C: Using aniline **117i** (100 mg, 0.59 mmol) and 4-fluorobenzaldehyde (76.1 µL, 88.1 mg, 0.71 mmol), trituration with EtOAc (5 × 2 mL) afforded **118m** as a pale yellow solid (86 mg, 52%); R_f = 0.28 (silica, 50% EtOAc, petrol); m.p. 160-162 ^oC; UV λ_{max} (EtOH/nm) 340.5 and 248.0; IR ν_{max}/cm^{-1} 3228 (N-H), 3037 (C-H), 1594, 1551, 1507, 1405, 1217, 823, 775, 694; ^1H δ/ppm (500 MHz, $CDCl_3$) 4.20 (1H, s, br, N*H*), 4.37 (2H, d, C*H*$_2$, *J* = 3.7 Hz), 6.69 (1H, dd, Ar-H, *J* = 2.3 and 8.1 Hz), 6.85 (1H, m, Ar-H), 6.98-6.99 (1H, m, Ar-H), 7.03-7.07 (2H, m, Ar-H), 7.29 (1H, t, Ar-H, *J* = 7.8 Hz), 7.35-7.37 (2H, m, Ar-H), 7.44-7.45 (2H, m, Ar-H), 8.63 (2H, s, br, Ar-H); ^{13}C δ/ppm (125 MHz, $CDCl_3$) 47.6, 111.2, 113.7, 115.5, 115.7, 116.5, 121.9, 129.0, 129.1, 130.1, 134.6, 134.7, 139.1, 148.5, 149.4, 149.5, 161.2, 163.1; LC-MS (ESI+) *m/z* = 279.3 $[M+H]^+$; Analytical HPLC: 98.0%

***N*-(4-Fluorobenzyl)-3-(pyridin-3-yl)aniline (118o)**

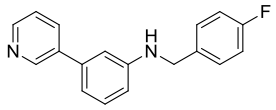

General Procedure C: Using aniline **117h** (100 mg, 0.59 mmol) and 4-fluorobenzaldehyde (76.1 µL, 88.1 mg, 0.71 mmol), chromatography (silica, 30-40% EtOAc, petrol) afforded **118o** as a white solid (144 mg, 86%); R_f = 0.40 (silica, 50% EtOAc, petrol); m.p. 81-84 ^oC; UV λ_{max} (EtOH/nm) 324.5 and 241.0; IR ν_{max}/cm^{-1} 3280 (N-H), 3042 (C-H), 1599, 1507, 1477, 1426, 1336, 1223, 1154, 1018, 831, 766, 707; ^1H δ/ppm (500 MHz, $CDCl_3$) 4.20 (1H, s, br, N*H*), 4.37 (2H, s, C*H*$_2$), 6.66 (1H, dd, Ar-H, *J* = 0.7 and 8.1 Hz), 6.80 (1H, m, Ar-H), 6.92-6.94 (1H, m, Ar-H), 7.02-7.07 (2H, m, Ar-H), 7.28 (1H, t, Ar-H, *J* = 7.9 Hz), 7.32-7.37 (3H, m, Ar-H), 7.81-7.83 (1H, m, Ar-H), 8.57 (1H, dd, Ar-H, *J* = 1.5 and 4.8 Hz), 8.80 (1H, d, Ar-H, *J* = 1.9 Hz); ^{13}C δ/ppm (125 MHz, $CDCl_3$) 47.6, 111.4, 112.7, 115.5, 115.7, 116.7, 123.6, 129.0, 129.1, 130.1, 134.72, 134.74, 134.8, 137.3, 138.8, 147.88, 147.90, 148.5, 161.2, 163.1; LC-MS (ESI+) *m/z* = 279.3 $[M+H]^+$; HRMS calcd. for $C_{18}H_{16}N_2F$ $[M+H]^+$ 279.1292, found 279.1297; Analytical HPLC: 98.3%

***N*-(4-Fluorobenzyl)-3-(4,4,5,5-tetramethyl-1,3,2-dioxaborolan-2-yl)aniline (123)**

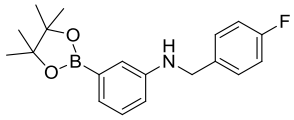

General Procedure C: Using aniline **122** (50 mg, 0.23 mmol) and 4-fluorobenzaldehyde (30 µL, 34.8 mg, 0.28 mmol), chromatography (silica, 0-30% EtOAc, hexane) afforded **123** as a white solid (52.4 mg, 70%); R_f = 0.72 (silica, 30% EtOAc, hexane); m.p. 68-72 ^oC; UV λ_{max} (EtOH/nm) 318.0 and 254.0; IR ν_{max}/cm^{-1} 3362 (N-H), 2983 (C-H), 2855 (C-H), 1605, 1578, 1508, 1468, 1362, 1318, 1240, 1220, 1141, 1089, 965, 908, 852, 827, 789, 764, 706, 677; ^1H δ/ppm (500 MHz, $CDCl_3$) 1.33 (12H, s, $(CH_3)_4$), 4.32 (2H, s, CH_2), 6.69-6.72 (1H, m, Ar-H), 6.99-7.04 (2H, m, Ar-H), 7.13 (1H, m, Ar-H), 7.19 (2H, d, Ar-H, *J* = 4.7 Hz), 7.31-7.34 (2H, m, Ar-H); ^{13}C δ/ppm (125 MHz, $CDCl_3$) 24.9, 47.8, 83.7, 115.3, 115.5, 115.7, 119.5, 124.5, 128.8, 129.2, 161.1, 163.1; LC-MS (ESI+) *m/z* = 328.3 $[M+H]^+$; HRMS calcd. for $C_{19}H_{24}O_2N^{10}BF$ $[M+H]^+$ 328.1879, found 328.1886

4-(2-((4-Fluorobenzyl)amino)pyridin-4-yl)phenol (128a)

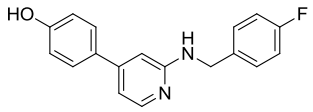

General Procedure C: Using aniline **127a** (80 mg, 0.43 mmol) and 4-fluorobenzaldehyde (246 µL, 285 mg, 2.30 mmol), chromatography (silica, 30% EtOAc, DCM followed by 0-3% MeOH, DCM) afforded **128a** as a white solid (15.5 mg, 12%); R_f = 0.40 (silica, 50% EtOAc, DCM); m.p. 68 ^oC (decomposed); UV λ_{max} (EtOH/nm) 253.0; IR ν_{max}/cm^{-1} 3421 (N-H), 3027 (C-H), 2575 (br) (O-H), 1604, 1553, 1506, 1467, 1220, 1175, 1103, 996, 879, 809; ^1H δ/ppm (500 MHz, DMSO-d_6) 4.50 (2H, d, CH_2, *J* = 6.1 Hz), 6.68-6.69 (1H, m, NH), 6.74 (1H, dd, Ar-H, *J* = 5.4 and 1.6 Hz), 6.84-6.87 (2H, m, Ar-H), 7.03 (1H, t, Ar-H, *J* = 6.1 Hz), 7.11-7.16 (2H, m, Ar-H), 7.37-7.40 (2H, m, Ar-H), 7.47-7.49 (2H, m, Ar-H), 7.96 (1H, d, Ar-H, *J* = 5.4 Hz), 9.71 (1H, s, OH); ^{13}C δ/ppm (125 MHz, DMSO-d_6) 43.5, 104.1, 109.7, 114.7, 114.9, 115.7, 127.6, 128.8, 129.0, 129.1, 136.9, 147.7, 148.0, 158.2, 159.2, 161.9; LC-MS (ESI+) *m/z* = 295.3 $[M+H]^+$; HRMS calcd. for $C_{18}H_{16}ON_2F$ $[M+H]^+$ 295.1241, found 295.1243;

HRMS calcd. for $C_{18}H_{14}ON_2F$ $[M-H]^-$ 293.1096, found 293.1086; Analytical HPLC: 97.5%

4-(5-((4-Fluorobenzyl)amino)pyridin-3-yl)phenol (128b)

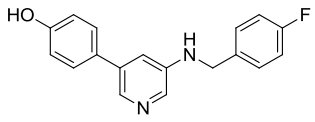

General Procedure C: Using aniline **127b** (70 mg, 0.38 mmol) and 4-fluorobenzaldehyde (167 µL, 193 mg, 1.56 mmol), chromatography (silica, 50% EtOAc, DCM) afforded **128b** as a white solid (67.6 mg, 61%); R_f = 0.19 (silica, 50% EtOAc, DCM); m.p. 73 ^oC (decomposed); UV λ_{max} (EtOH/nm) 325.0 and 257.5; IR ν_{max}/cm^{-1} 3350 (N-H), 3030 (C-H), 2582 (br) (O-H), 1591, 1507, 1464, 1431, 1333, 1223, 1155, 1106, 1014, 828, 707; ^1H δ/ppm (500 MHz, DMSO-d_6) 4.36 (2H, d, C*H*$_2$, *J* = 6.0 Hz), 6.54 (1H, t, N*H*, *J* = 6.1 Hz), 6.82-6.85 (2H, m, Ar-H), 7.03 (1H, t, Ar-H, *J* = 2.3 Hz), 7.14-7.19 (2H, m, Ar-H), 7.39-7.44 (4H, m, Ar-H), 7.90 (1H, d, Ar-H, *J* = 2.6 Hz), 7.97 (1H, d, Ar-H, *J* = 1.90 Hz), 9.59 (1H, s, OH); ^{13}C δ/ppm (125 MHz, DMSO-d_6) 45.2, 115.0, 115.1, 115.7, 127.8, 128.5, 129.1, 129.2, 133.8, 134.9, 135.6, 135.8, 144.4, 157.4, 160.2; LC-MS (ESI+) *m/z* = 295.3 $[M+H]^+$; HRMS calcd. for $C_{18}H_{16}ON_2F$ $[M+H]^+$ 295.1241, found 295.1246; HRMS calcd. for $C_{18}H_{14}ON_2F$ $[M-H]^-$ 293.1096, found 293.1087; Analytical HPLC: 98.4%

5-Bromo-*N*-(4-fluorobenzyl)pyridin-3-amine (132)

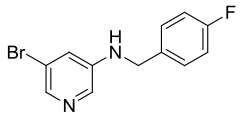

General Procedure C: Using pyridine **126b** (400 mg, 2.31 mmol) and 4-fluorobenzaldehyde (743 µL, 860 mg, 6.93 mmol) at 50 ^oC, chromatography (silica, 0-7% EtOAc, DCM) eluted **132** as a beige solid (533 mg, 82%); R_f = 0.25 (silica, 10% EtOAc, DCM); m.p. 92-94 ^oC; UV λ_{max} (EtOH/nm) 319.5 and 258.0; IR ν_{max}/cm^{-1} 3256 (N-H), 3052 (C-H), 1579, 1507, 1447, 1412, 1335, 1224, 1156, 1085, 1004, 829, 778, 690; ^1H δ/ppm (500 MHz, DMSO-d_6) 4.31 (2H, d, C*H*$_2$, *J* = 6.1 Hz), 6.82-6.85 (1H, m, N*H*), 7.09-7.10 (1H, m, Ar-H), 7.15-7.20 (2H, m, Ar-H), 7.38-7.42 (2H, m, Ar-H), 7.81 (1H, d, Ar-H, *J* = 2.0 Hz), 7.97 (1H, d, Ar-H, *J* = 2.5 Hz); ^{13}C δ/ppm (125 MHz,

DMSO-d_6) 44.9, 115.1, 115.2, 119.4, 120.4, 129.18, 129.24, 134.2, 135.03, 135.05, 136.7, 145.8, 160.3, 162.2; LC-MS (ESI+) *m/z* = 281.2 and 283.2 $[M+H]^+$; HRMS calcd. for $C_{12}H_{11}N_2{}^{79}BrF$ $[M+H]^+$ 281.0084, found 281.0086; Analytical HPLC: 97.6%

2'-(4-Chlorophenoxy)-3'-((4-fluorobenzyl)amino)-[1,1'-biphenyl]-4-ol (138a)

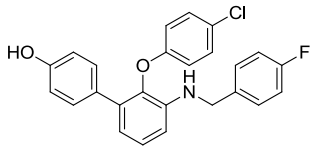

General Procedure C: Using aniline **137a** (50 mg, 0.16 mmol) and 4-fluorobenzaldehyde (42 µL, 47.2 mg, 0.38 mmol), chromatography (silica, 80% DCM, hexane) afforded **138a** as a white solid (22.5 mg, 34%); R_f = 0.33 (silica, 80% DCM, hexane); m.p. 126-129 ^oC; UV λ_{max} (EtOH/nm) 246.0 and 232.0; IR ν_{max}/cm^{-1} 3426 (N-H), 3235 (br) (O-H), 1603, 1509, 1484, 1413, 1333, 1278, 1215, 1126, 1097, 1009, 869, 830, 782, 747; ^1H δ/ppm (500 MHz, DMSO-d_6) 4.31 (2H, d, C*H*$_2$, *J* = 6.1 Hz), 5.89-5.92 (1H, m, N*H*), 6.54 (1H, d, Ar-H, *J* = 8.1 Hz), 6.58 (1H, d, Ar-H, *J* = 7.7 Hz), 6.65-6.68 (4H, m, Ar-H), 7.03 (1H, t, Ar-H, *J* = 8.0 Hz), 7.11 (1H, t, Ar-H, *J* = 8.9 Hz), 7.20-7.23 (4H, m, Ar-H), 7.30 (2H, dd, Ar-H, *J* = 5.6 and 8.3 Hz), 9.38 (1H, s, O*H*); ^{13}C δ/ppm (125 MHz, DMSO-d_6) 45.1, 110.4, 114.8, 114.9, 115.0, 116.7, 117.3, 124.9, 126.2, 128.0, 128.6, 128.7, 128.9, 129.7, 134.6, 136.2, 137.0, 141.3, 155.9, 156.5, 160.0; LC-MS (ESI+) *m/z* = 420.3 $[M+H]^+$; HRMS calcd. for $C_{25}H_{20}O_2NClF$ $[M+H]^+$ 420.1161, found 420.1171; HRMS calcd. for $C_{25}H_{18}O_2N^{35}ClF$ $[M-H]^-$ 418.1016, found 418.1005; Analytical HPLC: 98.2%

2-(4-Chlorophenoxy)-*N*-(4-fluorobenzyl)-[1,1'-biphenyl]-3-amine (138b)

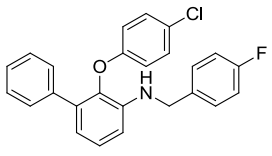

General Procedure C: Using aniline **137b** (150 mg, 0.51 mmol) and 4-fluorobenzaldehyde (164 µL, 190 mg, 1.53 mmol) at 70 ^oC, chromatography (silica, 10-30% DCM, petrol) eluted **138b** as a yellow oil (23 mg, 11%); R_f = 0.72 (silica, 20% EtOAc, petrol); m.p. 103-105 ^oC; UV λ_{max} (EtOH/nm) 259.5; IR ν_{max}/cm^{-1} 3444 (N-H),

2920 (C-H), 2850 (C-H), 1602, 1507, 1482, 1335, 1214 (C-O), 1090, 1008, 810, 756, 699; ^{1}H δ/ppm (500 MHz, DMSO-d_6) 4.33 (2H, d, C*H*$_2$, *J* = 6.1 Hz), 5.99-6.01 (1H, m, N*H*), 6.60-6.63 (2H, m, Ar-H), 6.66-6.68 (2H, m, Ar-H), 7.06-7.13 (3H, m, Ar-H), 7.20-7.23 (3H, m, Ar-H), 7.27-7.32 (4H, m, Ar-H), 7.38-7.39 (2H, m, Ar-H); ^{13}C δ/ppm (125 MHz, DMSO-d_6) 45.1, 111.1, 114.9, 115.0, 116.7, 117.5, 125.0, 126.4, 127.1, 128.0, 128.6, 128.7, 129.0, 134.7, 136.2, 137.1, 137.5, 141.3, 155.9, 160.0, 162.0; LC-MS (ESI+) *m/z* = 404.3 $[M+H]^+$; HRMS calcd. for $C_{25}H_{20}ON^{35}ClF$ $[M+H]^+$ 404.1212, found 404.1212; Analytical HPLC: 94.3%

2'-((4-Chlorobenzyl)oxy)-3'-((4-fluorobenzyl)amino)-[1,1'-biphenyl]-4-ol (138h)

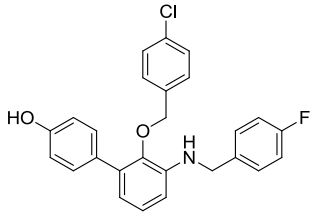

General Procedure C: Using aniline **137c** (100 mg, 0.31 mmol) and 4-fluorobenzaldehyde (101 µL, 116 mg, 0.93 mmol) at 70 ^{o}C, chromatography (silica, 10-30% Et_2O, petrol) eluted **138h** as a yellow oil (35 mg, 26%); R_f = 0.27 (silica, 30% Et_2O, petrol); UV λ_{max} (EtOH/nm) 246.0; IR ν_{max}/cm^{-1} 3411 (br) (O-H and N-H), 3033 (C-H), 2927 (C-H), 2860 (C-H), 1598, 1509, 1469, 1336, 1218 (C-O), 1172, 1084, 972, 810, 781, 743; ^{1}H δ/ppm (500 MHz, DMSO-d_6) 4.33 (2H, d, HN-C*H*$_2$, *J* = 6.0 Hz), 4.43 (2H, s, O-C*H*$_2$), 5.80 (1H, t, N*H*, *J* = 5.9 Hz), 6.40-6.41 (1H, m, Ar-H), 6.49-6.50 (1H, m, Ar-H), 6.80-6.81 (2H, m, Ar-H), 6.86-6.89 (1H, m, Ar-H), 7.12-7.15 (2H, m, Ar-H), 7.21-7.23 (2H, m, Ar-H), 7.34-7.36 (6H, m, Ar-H); ^{13}C δ/ppm (125 MHz, DMSO-d_6) 45.2, 71.8, 109.7, 114.9, 115.0, 117.4, 124.7, 128.0, 128.67, 128.74, 128.9, 129.8, 130.0, 132.3, 134.0, 136.1, 136.4, 141.6, 141.9, 156.5, 160.0, 162.0; LC-MS (ESI+) *m/z* = 434.4 $[M+H]^+$; HRMS calcd. for $C_{26}H_{20}O_2N^{35}ClF$ $[M-H]^-$ 432.1172, found 432.1161; Analytical HPLC: 97.1%

2-(4-Chlorophenoxy)-4'-fluoro-*N*-(4-methoxybenzyl)-[1,1'-biphenyl]-3-amine (138q)

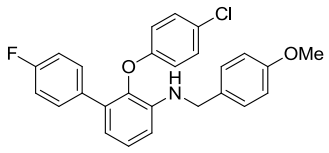

General procedure E: Using aniline **137f** (40 mg, 0.13 mmol) and 4-anisaldehyde (20 µL, 21.8 mg, 0.16 mmol), chromatography (silica, 2-10% Et_2O, petrol) eluted **138q** as a yellow oil (23.8 mg, 42%); R_f = 0.21 (silica, 10% EtOAc, petrol); UV λ_{max} (EtOH/nm) 230.6; IR ν_{max}/cm^{-1} 3434 (N-H), 3064 (C-H), 3002 (C-H), 2932 (C-H), 2836 (C-H), 1604, 1576, 1512, 1483, 1423, 1400, 1337, 1284, 1246, 1216 (C-O), 1174, 1159, 1129, 1089, 1034, 1009, 824, 778, 744; ^{1}H δ/ppm (500 MHz, $CDCl_3$) 3.79 (3H, s, OC*H*$_3$), 4.29 (2H, d, C*H*$_2$, *J* = 4.9 Hz), 4.43 (1H, s, br, N*H*), 6.60-6.63 (2H, m, Ar-H), 6.70-6.73 (2H, m, Ar-H), 6.82-6.85 (2H, m, Ar-H), 6.91-6.96 (2H, m, Ar-H), 7.04-7.08 (2H, m, Ar-H), 7.12-7.16 (3H, m, Ar-H), 7.34-7.38 (2H, m, Ar-H); ^{13}C δ/ppm (125 MHz, $CDCl_3$) 47.2, 55.3, 111.3, 114.0, 114.8, 115.0, 116.4, 118.7, 126.4, 126.6, 128.4, 129.3, 130.5, 130.6, 131.0, 137.8, 141.6, 155.9, 157.8, 158.8; ^{19}F δ/ppm (470 MHz, $CDCl_3$) -115.3; LC-MS (ESI+) *m/z* = 434.1 $[M+H]^+$; HRMS calcd. for $C_{26}H_{22}O_2N^{35}ClF$ $[M+H]^+$ 434.1318, found 434.1317; Analytical HPLC: 99.4%

2'-(4-Chlorophenoxy)-2-methyl-3'-nitro-[1,1'-biphenyl]-4-ol (136d)

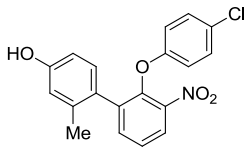

General procedure F: Using aryl fluoride **144a** (164 mg, 0.66 mmol) and 4-chlorophenol (509 mg, 3.96 mmol), chromatography (silica, 0-10% EtOAc, petrol) eluted **136d** as a yellow oil (194 mg, 83%); R_f = 0.24 (silica, 20% EtOAc, petrol); UV λ_{max} (EtOH/nm) 256.4; IR ν_{max}/cm^{-1} 3466 (O-H), 2925 (C-H), 1607, 1585, 1531, 1484, 1438, 1351, 1292, 1235 (C-O), 1197, 1162, 1090, 1045, 1010, 951, 885, 863, 818, 794, 755; ^{1}H δ/ppm (500 MHz, $CDCl_3$) 2.07 (3H, s, C*H*$_3$), 4.74 (1H, s, br, O*H*), 6.49-6.53 (3H, m, Ar-H), 6.60-6.61 (1H, m, Ar-H), 6.84 (1H, d, Ar-H, *J* = 8.3 Hz), 7.01-7.04 (2H, m, Ar-H), 7.41 (1H, t, Ar-H, *J* = 7.8 Hz), 7.50 (1H, dd, Ar-H, *J* = 1.7 and 7.7 Hz), 7.93

(1H, dd, Ar-H), 1.7 and 8.2 Hz); ^{13}C δ/ppm (125 MHz, $CDCl_3$) 20.0, 112.5, 112.6, 116.6, 116.7, 117.1, 124.3, 125.4, 127.5, 129.0, 131.1, 136.7, 137.9, 138.3, 144.4, 145.7, 155.4, 155.5, 156.0; LC-MS (ESI+) *m/z* = 354.2 $[M-H]^-$; HRMS calcd. for $C_{19}H_{13}O_4N^{35}Cl$ $[M-H]^-$ 354.0539, found 354.0540; Analytical HPLC: 97.7%

2-Chloro-2'-(4-chlorophenoxy)-3'-nitro-[1,1'-biphenyl]-4-ol (136e)

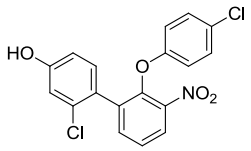

General procedure F: Using aryl fluoride **144b** (152 mg, 0.57 mmol) and 4-chlorophenol (440 mg, 3.42 mmol), chromatography (silica, 0-10% EtOAc, petrol) eluted **136e** as a yellow oil (198 mg, 82%); R_f = 0.24 (silica, 20% EtOAc, petrol); UV λ_{max} (EtOH/nm) 250.6; IR ν_{max}/cm^{-1} 3411 (O-H), 3088 (C-H), 1605, 1531, 1504, 1484, 1445, 1350, 1279, 1236 (C-O), 1196, 1163, 1089, 1030, 910, 883, 863, 821, 793, 755; ^{1}H δ/ppm (500 MHz, $CDCl_3$) 5.02 (1H, s, O*H*), 6.56-6.60 (2H, m, Ar-H), 6.65 (1H, dd, Ar-H, *J* = 2.5 and 8.4 Hz), 6.83 (1H, d, Ar-H, *J* = 2.5 Hz), 7.04-7.07 (3H, m, Ar-H), 7.42 (1H, t, Ar-H, *J* = 8.0 Hz), 7.59 (1H, dd, Ar-H, *J* = 1.7 and 7.7 Hz), 7.96 (1H, dd, Ar-H, *J* = 1.7 and 8.2 Hz); ^{13}C δ/ppm (125 MHz, $CDCl_3$) 113.9, 114.0, 116.5, 116.6, 117.0, 125.0, 125.1, 126.3, 127.6, 129.2, 132.2, 133.8, 135.7, 137.2, 144.3, 145.7, 155.9, 156.2; LC-MS (ESI+) *m/z* = 374.2 $[M-H]^-$; HRMS calcd. for $C_{18}H_{10}O_4N^{35}Cl_2$ $[M-H]^-$ 373.9992, found 373.9992; Analytical HPLC: 97.4%

2-(4-Chlorophenoxy)-1-ethynyl-3-nitrobenzene (165)

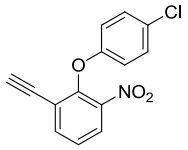

General procedure F: Using aryl fluoride **164** (1.83 g, 5.68 mmol) and 4-chlorophenol (1.46 g, 11.4 mmol), the crude material was dissolved in THF (5 mL) and mixed with TBAF (1 M in THF, 5.68 mL, 5.68 mmol) at room temperature for 30 min, then concentrated to a low volume *in vacuo*. Chromatography (silica, 10-30% Et_2O, petrol) eluted **165** as a yellow solid (1.47 g, 94%); R_f = 0.24 (silica, 30% DCM, petrol); m.p. 68-70 ^oC; UV λ_{max} (EtOH/nm) 227.0; IR ν_{max}/cm^{-1} 3287 (alkyne C-H), 3081 (C-H),

2873 (C-H), 1885 (C≡C), 1588, 1526, 1487, 1445, 1354, 1283, 1237 (C-O), 1196, 1170, 1093, 1011, 874, 828, 799, 750, 670; ^{1}H δ/ppm (500 MHz, $CDCl_3$) 3.20 (1H, s, CC*H*), 6.81 (2H, d, 4-ClPh C_3-H and C_5-H, *J* = 9.1 Hz), 7.26 (2H, d, 4-ClPh C_2-H and C_6-H, *J* = 8.9 Hz), 7.36 (1H, t, 3- NO_2Ar C_5-H, *J* = 8.1 Hz), 7.78 (1H, dd, Ar-H, *J* = 1.6 and 7.8 Hz), 7.95 (1H, dd, Ar-H, 1.6 and 8.2 Hz); ^{13}C δ/ppm (125 MHz, $CDCl_3$) 85.5, 117.1, 120.4, 125.5, 125.9, 128.0, 129.5, 138.7, 144.1, 149.1, 156.2; LC-MS (ESI+) *m/z* = mass not observed

3-Bromo-4-(4-chlorophenoxy)-5-nitrobenzoic acid (223)

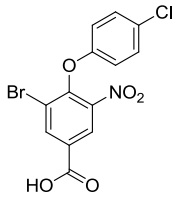

General procedure F: Using aryl fluoride **222** (970 mg, 3.67 mmol) and 4-chlorophenol (944 mg, 7.34 mmol), chromatography (C18, 50-80% MeOH, H_2O) eluted **223** as a white solid (1.15 g, 84%); R_f = 0.42 (C18, 70% MeOH, H_2O); m.p. 219-221 ^{o}C; UV λ_{max} (EtOH/nm) 226.0; IR ν_{max}/cm^{-1} 3085 (C-H), 2959 (C-H), 2814 (C-H), 2654 (O-H), 1687 (C=O), 1609, 1585, 1536, 1481, 1414, 1352, 1280 (C-O), 1192, 1159, 1085, 1007, 905, 823, 753, 723, 675; ^{1}H δ/ppm (500 MHz, DMSO-d_6) 6.99 (2H, d, 4-ClPh C_3-H and C_5-H, *J* = 9.0 Hz), 7.43 (2H, d, 4-ClPh C_2-H and C_6-H, *J* = 9.0 Hz), 8.53 (1H, dd, Ar-H, *J* = 2.0 Hz), 8.56 (1H, dd, Ar-H, *J* = 2.0 Hz), 14.00 (1H, s, br, CO_2H); ^{13}C δ/ppm (125 MHz, DMSO-d_6) 117.1, 119.4, 126.1, 127.2, 129.8, 130.2, 138.8, 144.1, 146.9, 155.1, 164.1; LC-MS (ESI+) *m/z* = 371.0 and 373.3 $[M+H]^+$ and 370.1 and 372.1 $[M-H]^-$; HRMS calcd. for $C_{13}H_6O_5N^{79}Br^{35}Cl$ $[M-H]^-$ 369.9123, found 369.9110

2-(4-Chlorophenoxy)-4'-methoxy-3-nitro-1,1'-biphenyl (251)

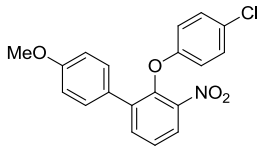

General procedure F: Using aryl fluoride **216** (190 mg, 0.77 mmol) and 4-chlorophenol (149 mg, 1.16 mmol), chromatography (silica, 0-40% DCM, petrol) eluted **251** as a green oil (264 mg, 96%); R_f = 0.25 (silica, 40% DCM, petrol); UV λ_{max}

(EtOH/nm) 261.6; IR ν_{max}/cm^{-1} 3072 (C-H), 2932 (C-H), 2836 (C-H), 1607, 1521, 1512, 1482, 1442, 1348, 1233 (C-O), 1177, 1089, 1027, 886, 823, 803, 751; ^{1}H δ/ppm (500 MHz, $CDCl_3$) 3.79 (3H, s, OC*H*$_3$), 6.60 (2H, d, 4-ClPh C_3-H and C_5-H, *J* = 9.1 Hz), 6.84 (2H, d, 4-MeOPh C_2-H and C_6-H, *J* = 8.8 Hz), 7.07 (2H, d, 4-ClPh C_2-H and C_6-H, *J* = 9.0 Hz), 7.36 (2H, d, 4-MeOPh C_3-H and C_5-H, *J* = 8.8 Hz), 7.43 (1H, t, 3-NO_2Ar C_5-H, *J* = 8.0 Hz), 7.66 (1H, dd, Ar-H, *J* = 1.6 and 7.7 Hz), 7.88 (1H, dd, Ar-H, *J* = 1.6 and 8.1 Hz); ^{13}C δ/ppm (125 MHz, $CDCl_3$) 55.2, 113.9, 116.6, 124.1, 125.8, 127.4, 127.6, 129.3, 130.2, 135.7, 138.3, 144.4, 144.5, 155.9, 159.6; LC-MS (ESI+) *m/z* = mass not observed; HRMS calcd. for $C_{19}H_{15}O_4N^{35}Cl$ $[M+H]^+$ 356.0684, found 356.0677

2-(4-Chlorophenoxy)-[1,1'-biphenyl]-3-amine (137b)

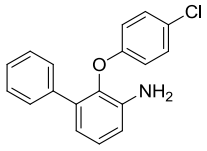

General Procedure G: Using **136b** (374 mg, 1.15 mmol), chromatography (silica, 0-10% EtOAc, petrol) eluted **137b** as a yellow solid (309 mg, 96%); R_f = 0.40 (silica, 20% EtOAc, petrol); m.p. 98-101 ^{o}C; UV λ_{max} (EtOH/nm) 229.0; IR ν_{max}/cm^{-1} 3484 and 3388 (N-H), 3057 (C-H), 2925 (C-H), 1616, 1467, 1434, 1219 (C-O), 1086, 822, 756, 697; ^{1}H δ/ppm (500 MHz, DMSO-d_6) 4.99 (2H, s, N*H*), 6.63 (1H, dd, Ar-H, *J* = 1.5 and 7.6 Hz), 6.64-6.68 (2H, m, Ar-H), 6.84 (1H, dd, Ar-H, *J* = 1.6 and 8.0 Hz), 7.08 (1H, t, Ar-H, *J* = 7.8 Hz), 7.17-7.23 (3H, m, Ar-H), 7.27-7.30 (2H, m, Ar-H), 7.38-7.40 (2H, m, Ar-H); ^{13}C δ/ppm (125 MHz, DMSO-d_6) 115.2, 116.6, 117.7, 124.8, 126.3, 127.0, 128.0, 128.5, 129.0, 135.1, 136.6, 141.8, 155.9; LC-MS (ESI+) *m/z* = 296.3 $[M+H]^+$; HRMS calcd. for $C_{18}H_{15}ON^{35}Cl$ $[M+H]^+$ 296.0837, found 296.0843; Analytical HPLC: 96.9%

3'-Amino-2'-((4-chlorobenzyl)oxy)-[1,1'-biphenyl]-4-ol (137c)

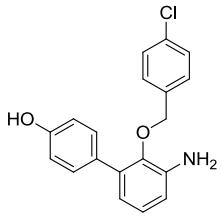

General Procedure G: Using **136c** (250 mg, 0.70 mmol), chromatography (silica, 0-20% EtOAc, petrol) eluted **137c** as a brown solid (208 mg, 92%); R_f = 0.17 (silica, 20% EtOAc, petrol); m.p. 160-163 ^oC; UV λ_{max} (EtOH/nm) 208.0; IR ν_{max}/cm^{-1} 3386 (N-H), 3268 (br) (O-H and N-H), 1591, 1516, 1467, 1246 (C-O), 1204, 989, 874, 831, 804, 746; ^1H δ/ppm (500 MHz, DMSO-d_6) 4.40 (2H, s, CH_2), 4.92 (2H, s, br, NH_2), 6.53 (1H, m, Ar-H), 6.71 (1H, m, Ar-H), 6.78-6.80 (2H, m, Ar-H), 6.88-6.89 (1H, m, Ar-H), 7.20-7.22 (2H, m, Ar-H), 7.34 (4H, m, Ar-H), 9.45 (1H, s, O*H*); ^{13}C δ/ppm (125 MHz, DMSO-d_6) 71.5, 115.0, 115.2, 115.3, 117.8, 124.5, 127.8, 128.0, 128.4, 129.5, 129.8, 135.1, 135.3, 156.0; LC-MS (ESI+) *m/z* = 326.3 $[M+H]^+$; HRMS calcd. for $C_{19}H_{17}O_2NCl$ $[M+H]^+$ 326.0942, found 326.0944; HRMS calcd. for $C_{19}H_{15}O_2N^{35}Cl$ $[M-H]^-$ 324.0797, found 324.0788

3'-Amino-2'-(4-chlorophenoxy)-2-methyl-[1,1'-biphenyl]-4-ol (137d)

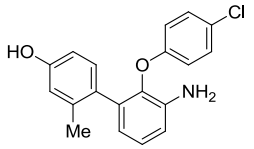

General Procedure G: Using **136d** (191 mg, 0.54 mmol), chromatography (silica, 0-20% EtOAc, petrol) eluted **137d** as a yellow oil (131 mg, 75%); R_f = 0.26 (silica, 20% EtOAc, petrol); UV λ_{max} (EtOH/nm) 228.6; IR ν_{max}/cm^{-1} 3384 and 3323 (N-H), 3196 (br) (O-H), 3028 (C-H), 2919 (C-H), 1610, 1583, 1508, 1483, 1467, 1281, 1217 (C-O), 1161, 1087, 1008, 953, 859, 823, 785, 735; ^1H δ/ppm (500 MHz, DMSO-d_6) 2.02 (3H, s, CH_3), 4.93 (2H, s, br, NH_2), 6.40 (2H, ddd, Ar-H, *J* = 2.5, 8.2 and 12.9 Hz), 6.52 (1H, d, Ar-H, *J* = 2.4 Hz), 6.55-6.58 (2H, m, Ar-H), 6.77 (1H, d, Ar-H, *J* = 8.3 Hz), 6.80 (1H, dd, Ar-H, *J* = 1.5 and 8.0 Hz), 7.01 (1H, t, Ar-H, *J* = 7.9 Hz), 7.13-7.16 (2H, m, Ar-H), 9.15 (1H, s, O*H*); ^{13}C δ/ppm (125 MHz, DMSO-d_6) 19.9, 112.0, 114.5, 116.1, 116.6, 118.6, 124.6, 125.7, 128.2, 128.8, 130.5, 135.3, 136.6, 137.7, 141.5, 156.1,

156.2; LC-MS (ESI+) *m/z* = 326.3 $[M+H]^+$ and 324.2 $[M-H]^-$; HRMS calcd. for $C_{19}H_{15}O_2N^{35}Cl$ $[M-H]^-$324.0797, found 324.0794; Analytical HPLC: 99.0 %

3'-Amino-2-chloro-2'-(4-chlorophenoxy)-[1,1'-biphenyl]-4-ol (137e)

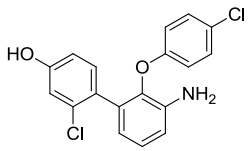

General Procedure G: Using **136e** (199 mg, 0.53 mmol), chromatography (silica, 0-20% EtOAc, petrol) eluted **137e** as a yellow oil (149 mg, 81%); R_f = 0.23 (silica, 20% EtOAc, petrol); UV λ_{max} (EtOH/nm) 280.6 and 228.8; IR ν_{max}/cm^{-1} 3384 and 3323 (N-H), 3066 (br) (O-H), 2971 (C-H), 2919 (C-H), 1609, 1583, 1507, 1483, 1466, 1278, 1215 (C-O), 1161, 1088, 1035, 1008, 953, 919, 859, 823, 784, 748; ^{1}H δ/ppm (500 MHz, DMSO-d_6) 4.98 (1H, s, br, N*H*$_2$), 6.45 (1H, dd, Ar-H, *J* = 1.4 and 7.5 Hz), 6.57-6.62 (3H, m, Ar-H), 6.75 (1H, d, Ar-H, *J* = 2.4 Hz), *J* = 6.83 (1H, dd, Ar-H, *J* = 1.5 and 8.0 Hz), 6.95 (1H, d, Ar-H, *J* = 8.4 Hz), 7.02 (1H, t, Ar-H, *J* = 7.8 Hz), 7.15-7.18 (2H, m, Ar-H), 9.78 (1H, s, O*H*); ^{13}C δ/ppm (125 MHz, DMSO-d_6) 113.8, 115.2, 115.5, 116.7, 118.6, 124.8, 125.5, 126.9, 128.8, 132.0, 132.4, 133.0, 137.7, 141.5, 156.1, 157.2; LC-MS (ESI+) *m/z* = 346.2 $[M+H]^+$ and 344.1 $[M-H]^-$; HRMS calcd. for $C_{18}H_{12}O_2N^{35}Cl_2$ $[M-H]^-$ 344.0251, found 344.0252 Analytical HPLC: 98.6 %

2-(4-Chlorophenoxy)-4'-fluoro-[1,1'-biphenyl]-3-amine (137f)

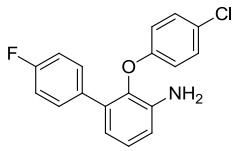

General Procedure G: Using **136f** (617 mg, 1.79 mmol), chromatography (silica, 10-20% Et_2O, petrol) eluted **137f** as a dark orange solid (440 mg, 78%); R_f = 0.40 (silica, 20% Et_2O, petrol); m.p. 87-91 ^oC; UV λ_{max} (EtOH/nm) 229.2; IR ν_{max}/cm^{-1} 3485 and 3389 (N-H), 3070 (C-H), 1617, 1511, 1468, 1402, 1335, 1278, 1217 (C-O), 1157, 1085, 1007, 905, 867, 815, 778, 746, 659; ^{1}H δ/ppm (500 MHz, $CDCl_3$) 4.59 (2H, s, br, N*H*$_2$), 6.60-6.66 (2H, m, Ar-H), 6.84-6.88 (2H, m, Ar-H) 6.93-6.97 (2H, m, Ar-H), 7.06-7.09 (2H, m, Ar-H), 7.13-7.16 (1H, m, Ar-H), 7.35-7.38 (2H, m, Ar-H); ^{13}C δ/ppm (125

MHz, $CDCl_3$) 114.9, 115.1, 116.3, 126.4, 126.7, 129.4, 130.5, 130.6, 135.2, 144.9, 155.7, 161.2; LC-MS (ESI+) *m/z* = 314.3 $[M+H]^+$; HRMS calcd. for $C_{18}H_{14}ON^{35}ClF$ $[M+H]^+$ 314.0742, found 314.0747

N^1-(2-(4-Chlorophenoxy)-4'-fluoro-[1,1'-biphenyl]-3-yl)benzene-1,4-diamine (138t)

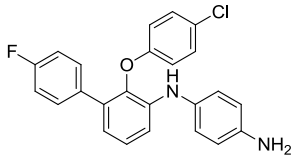

General Procedure G: Using **138s** (280 mg, 0.64 mmol), heating at 50 °C for 48 h, chromatography (silica, 0-30% EtOAc, petrol) eluted **138t** as a dark red solid (162 mg, 63%); R_f = 0.20 (silica, 90% DCM, petrol); m.p. 146-150 °C; UV λ_{max} (EtOH/nm) 261.0; IR ν_{max}/cm^{-1} 3731 (secondary N-H), 3427 and 3347 (primary N-H), 2926 (C-H), 1592, 1488, 1464, 1399, 1300, 1259, 1217 (C-O), 1160, 1097, 1062, 824; ^1H δ/ppm (500 MHz, $CDCl_3$) 5.55 (2H, s, br, N*H*$_2$), 5.83 (1H, s, N*H*), 6.79-6.81 (2H, m, Ar-H), 6.83-6.85 (2H, m, Ar-H), 6.95-7.00 (3H, m, Ar-H), 7.05-7.08 (1H, m, Ar-H), 7.08-7.13 (2H, m, Ar-H), 7.15-7.17 (2H, m, Ar-H), 7.20-7.21 (1H, m, Ar-H), 7.53-7.57 (2H, m, Ar-H); ^{13}C δ/ppm (125 MHz, $CDCl_3$) 115.1, 115.3, 118.2, 118.5, 121.2, 124.9, 126.7, 127.4, 128.1, 128.6, 129.3, 130.86, 130.92, 133.6, 146.3, 149.2; ^{19}F δ/ppm (470 MHz, $CDCl_3$) -115.1; LC-MS (ESI+) *m/z* = 405.4 $[M+H]^+$ and 403.3 $[M-H]^-$; HRMS calcd. for $C_{24}H_{19}ON_2{}^{35}ClF$ $[M+H]^+$ 405.1164, found 405.1165; Analytical HPLC: 98.7 %

***N*-(5-Bromothiazol-2-yl)-4-fluorobenzamide (267)**

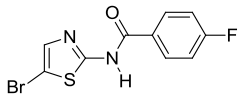

General Procedure H: Using thiazole hydrobromide **266** (500 mg, 1.92 mmol) and 4-fluorobenzoyl chloride (272 µL, 365 mg, 2.30 mmol), chromatography (silica, 10-30% THF, petrol) eluted **267** as a brown solid (511 mg, 88%); R_f = 0.29 (silica, 20% EtOAc, petrol); m.p. 224 °C (decomposed); UV λ_{max} (EtOH/nm) 293.8 and 230.0; IR ν_{max}/cm^{-1} 3647 (N-H), 3141 (C-H), 3080 (C-H), 2953 (C-H), 2916 (C-H), 2874 (C-H), 1667 (C=O), 1602, 1550, 1509, 1448, 1307, 1291, 1222, 1150, 1114, 1094, 994, 900, 847, 815, 753, 695; ^1H δ/ppm (500 MHz, DMSO-d_6) 7.39-7.42 (2H, m, Ar-H), 7.67 (1H, s,

thiazole C_4-H), 8.16-8.19 (2H, m, Ar-H), 12.95 (1H, s, N*H*); ^{13}C δ/ppm (125 MHz, DMSO-d_6) 102.2, 115.6, 115.8, 124.9, 128.0, 131.1, 131.2, 138.8, 163.8, 165.8, 189.0; LC-MS (ESI+) *m/z* = 301.2 and 303.1 $[M+H]^+$ and 299.0 and 301.1 $[M-H]^-$; HRMS calcd. for $C_{10}H_7ON_2{}^{79}BrFS$ $[M+H]^+$ 300.9441, found 300.9444 and calcd. for $C_{10}H_5ON_2BrFS$ $[M-H]^-$ 298.9295, found 298.9294

_N_-(4-((2-(4-Chlorophenoxy)-4'-fluoro-[1,1'-biphenyl]-3-yl)amino)phenyl)-1,1,1-trifluoromethanesulfonamide (138p)

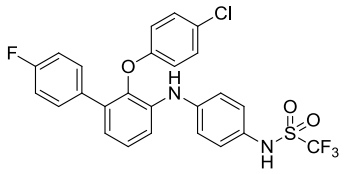

General procedure I: Using aniline **138t** (40 mg, 0.10 mmol) and trifluoromethanesulfonic anhydride (16.6 µL, 27.9 mg, 0.10 mmol) with no base at 0 °C, chromatography (silica, 0-30% EtOAc, petrol) eluted **138p** as a dark red oil (18.8 mg, 35%); R_f = 0.23 (silica, 20% EtOAc, petrol); UV λ_{max} (EtOH/nm) 288.4 and 231.4; IR ν_{max}/cm^{-1} 3409 (N-H), 3280 (N-H), 2962 (C-H), 2925 (C-H), 1604, 1576, 1513, 1484, 1422, 1368, 1334, 1278, 1206 (C-O), 1139, 1089, 1009, 949, 825, 781, 751; ^{1}H δ/ppm (500 MHz, $CDCl_3$) 5.93 (1H, s, br, N*H*), 6.58 (1H, s, br, N*H*), 6.59-6.62 (2H, m, Ar-H), 6.95-7.00 (3H, m, Ar-H), 7.03-7.07 (4H, m, Ar-H), 7.17-7.19 (2H, m, Ar-H), 7.24 (1H, t, Ar-H, *J* = 7.8 Hz), 7.36-7.40 (3H, m, Ar-H); ^{13}C δ/ppm (125 MHz, $CDCl_3$) 109.4, 115.1, 115.2, 116.3, 116.6, 119.0, 123.3, 126.2, 126.9, 127.0, 129.5, 130.5, 130.6, 133.1, 135.6, 142.3, 152.1, 155.7; ^{19}F δ/ppm (470 MHz, $CDCl_3$) -75.1 and -114.7; LC-MS (ESI+) *m/z* = 537.3 $[M+H]^+$ and 535.2 $[M-H]^-$; HRMS calcd. for $C_{25}H_{16}O_3N_2{}^{35}ClF_4S$ $[M-H]^-$ 535.0512, found 535.0504; Analytical HPLC: 96.3%

Methyl 4-(trifluoromethylsulfonamido)benzoate (153)

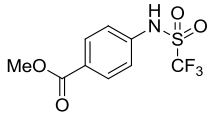

General procedure I: Using methyl aniline **152** (500 mg, 3.31 mmol) and trifluoromethanesulfonic anhydride (1.22 mL, 2.05 g, 7.28 mmol), chromatography (silica, 5-10% Et_2O, DCM) eluted **153** as a light brown solid (682 mg, 74%); R_f = 0.17

(silica, 5% Et_2O, DCM); m.p. 149-151 ^oC; UV λ_{max} (EtOH/nm) 250.4; IR ν_{max}/cm^{-1} 3151 (N-H), 3069 (C-H), 2957 (C-H), 2854 (C-H), 1688 (C=O), 1608, 1513, 1421, 1380, 1300 (S=O asym. stretch), 1183 (C-O), 1137 (S=O sym. stretch), 1020, 944, 855, 766, 695; ^1H δ/ppm (500 MHz, $CDCl_3$) 3.93 (3H, s, CO_2CH_3), 6.94 (1H, s, br, N*H*), 7.32-7.34 (2H, m, Ar-H), 8.06-8.08 (2H, m, Ar-H); ^{13}C δ/ppm (125 MHz, $CDCl_3$) 52.4, 121.4, 128.8 131.3, 135.5, 166.0; ^{19}F δ/ppm (470 MHz, $CDCl_3$) -75.5; LC-MS (ESI+) *m/z* = 282.2 $[M-H]^-$; HRMS calcd. for $C_9H_7O_4NF_3S$ $[M-H]^-$ 282.0053, found 282.0046; Analytical HPLC: 97.5%

_N_-(4-Acetylphenyl)-1,1,1-trifluoromethanesulfonamide (263)

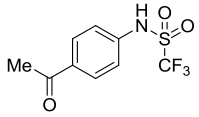

General procedure I: Using aniline **262** (500 mg, 3.70 mmol) and trifluoromethanesulfonic anhydride (1.37 mL, 2.30 g, 8.14 mmol), washing the reaction mixture with 1 M HCl (50 mL) and distilled water (8 × 10 mL), brine (10 mL), drying ($MgSO_4$), filtering and concentration *in vacuo* afforded **263** as a brown solid (887 mg, 90%); R_f = 0.21 (silica, 20% EtOAc, petrol); m.p. 114-118 ^oC; UV λ_{max} (EtOH/nm) 260.0; IR ν_{max}/cm^{-1} 3146 (N-H), 3065 (C-H), 2948 (C-H), 2856 (C-H), 1666 (C=O), 1601, 1513, 1485, 1414, 1376 (S=O asym. stretch), 1275, 1181, 1136 (S=O sym. stretch), 1017, 941, 841, 670; ^1H δ/ppm (500 MHz, $CDCl_3$) 2.61 (3H, s, C*H*$_3$), 7.35-7.38 (2H, m, Ar-H), 7.98-8.01 (2H, m, Ar-H); ^{13}C δ/ppm (125 MHz, $CDCl_3$) 26.6, 121.5, 130.1, 135.4, 138.4, 196.6; ^{19}F δ/ppm (470 MHz, $CDCl_3$) -75.5; LC-MS (ESI+) *m/z* = 268.3 $[M+H]^+$ and 266.2 $[M-H]^-$; HRMS calcd. for $C_9H_7O_3NF_3S$ $[M-H]^-$ 266.0104, found 266.0101

4'-Fluoro-_N_-(4-methoxybenzyl)-2-methyl-[1,1'-biphenyl]-3-amine (149a)

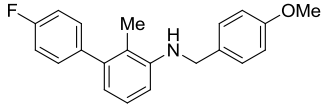

General Procedure J: Using benzamide **148a** (150 mg, 0.45 mmol), chromatography (silica, 90% EtOAc, petrol followed by C18, 80-90% MeOH + 0.1% (v/v) HCO_2H, H_2O) eluted **149a** as a brown solid (81 mg, 56%); R_f = 0.26 (C18, 90% MeOH, H_2O);

m.p. 87-89 ^{o}C; UV λ_{max} (EtOH/nm) 228.6; IR ν_{max}/cm^{-1} 3421 (N-H), 2985 (C-H), 2933 (C-H), 2845 (C-H), 1582, 1510, 1463, 1420, 1322, 1281, 1251 (C-O), 1211, 1185, 1154, 1110, 1088, 1067, 1037, 992, 887, 828, 782, 722, 669; ^{1}H δ/ppm (500 MHz, $CDCl_3$) 2.02 (3H, s, ArC*H*$_3$), 3.82 (3H, s, OC*H*$_3$), 3.90 (1H, s, br, N*H*), 4.34 (2H, s, C*H*$_2$), 6.66 (2H, dd, Ar-H, *J* = 7.9 and 15.4 Hz), 6.90-6.92 (2H, m, Ar-H), 7.06-7.10 (2H, m, Ar-H), 7.15 (1H, t, Ar-H, *J* = 7.9 Hz), 7.23-7.28 (2H, m, Ar-H), 7.33-7.35 (2H, m, Ar-H); ^{13}C δ/ppm (125 MHz, $CDCl_3$) 14.3, 48.1, 55.3, 109.1, 114.1, 114.7, 114.9, 119.2, 119.4, 126.4, 128.9, 130.88, 130.94, 138.6, 141.6, 159.0, 160.9, 162.8; LC-MS (ESI+) *m/z* = mass not observed

_N_-(4-Fluorobenzyl)-4-(1-(tetrahydro-2_H_-pyran-2-yl)-1_H_-indazol-5-yl)thiazol-2-amine (276)

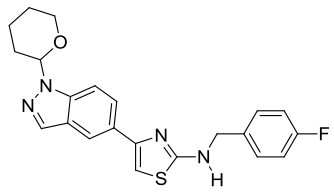

General Procedure J: Using benzamide **274** (266 mg, 0.63 mmol), and lithium aluminium hydride (1 M in THF, 5.0 mL, 5.0 mmol) at 60 ^{o}C for 24 h, chromatography (silica, 0-30% EtOAc, petrol followed by 0-10% EtOAc, DCM) eluted **276** as a yellow oil (131 mg, 51%); R_f = 0.25 (silica, 30% EtOAc, petrol); ^{1}H δ/ppm (500 MHz, $CDCl_3$) 1.64-1.69 (1H, m, Alk-H), 1.72-1.82 (2H, m, Alk-H), 2.08-2.11 (1H, m, Alk-H), 2.15-2.18 (1H, m, Alk-H), 2.54-2.62 (1H, m, Alk-H), 3.73-3.78 (1H, m, C*H*$_2$-O), 4.03-4.05 (1H, m, C*H*$_2$-O), 4.53 (2H, d, NHC*H*$_2$Ar, *J* = 5.3 Hz), 5.52 (1H, s, br, N*H*), 5.72 (1H, dd, NC*H*O, *J* = 2.7 and 9.4 Hz), 6.69 (1H, s, thiazole C_5-H), 7.06 (2H, t, 4-FPh C_2-H and C_6-H, *J* = 8.8 Hz), 7.36-7.43 (2H, m, 4-FPh C_3-H and C_5-H), 7.57 (1H, d, indazole C_7-H, *J* = 8.8 Hz), 7.83 (1H, dd, indazole C_6-H, *J* = 1.5 and 8.8 Hz), 8.03 (1H, s, indazole C_3-H), 8.20 (1H, m, indazole C_4-H); ^{13}C δ/ppm (125 MHz, $CDCl_3$) 22.6, 25.1, 29.5, 49.2, 67.5, 85.4, 99.9, 110.2, 115.6, 115.8, 118.6, 125.1, 125.2, 127.7, 127.9, 128.8, 129.4, 129.5, 134.6, 139.2; ^{19}F δ/ppm (470 MHz, $CDCl_3$) -114.4; LC-MS (ESI+) *m/z* = 409.3 $[M+H]^+$ and 407.3 $[M-H]^-$; Analytical HPLC: 93.8%

2-(4-Chlorophenoxy)-*N*-(4-fluorophenyl)-[1,1'-biphenyl]-3-amine (138d)

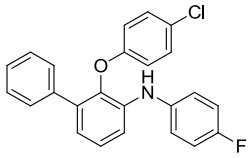

General Procedure K: Using aniline **137b** (150 mg, 0.51 mmol) and 1-bromo-4-fluorobenzene (112 µL, 179 mg, 1.02 mmol), chromatography (silica, 0-10% DCM, petrol) eluted **138d** as a white solid (113 mg, 56%); R_f = 0.25 (silica, 20% DCM, petrol); m.p. 123-126 ^oC; UV λ_{max} (EtOH/nm) 279.5 and 231.5; IR ν_{max}/cm^{-1} 3408 (N-H), 3064 (C-H), 1594, 1510, 1484, 1428, 1213 (C-O), 1087, 820, 756, 698; ^1H δ/ppm (500 MHz, DMSO-d_6) 6.60-6.64 (2H, m, Ar-H), 6.98 (1H, dd, Ar-H, *J* = 2.1 and 7.0 Hz), 7.02-7.08 (4H, m, Ar-H), 7.13-7.17 (2H, m, Ar-H), 7.22-7.28 (3H, m, Ar-H), 7.32-7.35 (2H, m, Ar-H), 7.43-7.44 (2H, m, Ar-H), 7.67 (1H, s, N*H*); ^{13}C δ/ppm (125 MHz, DMSO-d_6) 115.3, 115.5, 116.7, 117.0, 119.96, 120.02, 122.0, 125.0, 126.3, 127.3, 128.1, 128.7, 128.9, 135.8, 137.2, 137.7, 139.2, 140.3, 156.0; LC-MS (ESI+) *m/z* = 390.3 $[M+H]^+$; Analytical HPLC: 98.5%

2'-(4-Chlorophenoxy)-3'-(phenylamino)-[1,1'-biphenyl]-4-ol (138e)

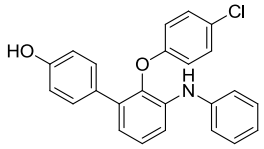

General Procedure K: Using aniline **137a** (50 mg, 0.16 mmol) and bromobenzene (51.2 µL, 75.4 mg, 0.48 mmol), chromatography (silica, 5-20% EtOAc, petrol) eluted **138e** as a brown solid (49.3 mg, 79%); R_f = 0.29 (silica, 20% EtOAc, petrol); m.p. 105-108 ^oC; UV λ_{max} (EtOH/nm) 277.4 and 230.8; IR ν_{max}/cm^{-1} 3517 (N-H), 3388 (br) (O-H), 3036 (C-H), 2926 (C-H), 1594, 1519, 1483, 1470, 1399, 1332, 1265, 1216 (C-O), 1172, 1086, 1007, 921, 868, 819, 779, 746, 713, 690; ^1H δ/ppm (500 MHz, $CDCl_3$) 4.60 (1H, s, N*H*), 5.90 (1H, s, O*H*), 6.65-6.68 (2H, m, Ar-H), 6.72-6.75 (2H, m, Ar-H), 6.91 (1H, dd, Ar-H, *J* = 1.5 and 7.6 Hz), 6.96-6.99 (1H, m, Ar-H), 7.04-7.07 (2H, m, Ar-H), 7.08-7.10 (2H, m, Ar-H), 7.18 (1H, t, Ar-H, *J* = 7.9 Hz), 7.26-7.29 (2H, m, Ar-H), 7.30-7.35 (3H, m, Ar-H); ^{13}C δ/ppm (125 MHz, $CDCl_3$) 114.7, 115.0, 116.3, 119.6, 121.9, 122.1, 126.0, 126.7, 129.3, 130.3, 135.8, 137.6, 139.7, 141.9, 154.9, 155.9; LC-MS

(ESI+) *m/z* = 386.3 $[M+H]^+$; HRMS calcd. for $C_{24}H_{17}O_2N^{35}Cl$ $[M-H]^-$ 386.0953, found 386.0952; Analytical HPLC: 98.2%

2'-(4-Chlorophenoxy)-3'-((4-chlorophenyl)amino)-[1,1'-biphenyl]-4-ol (138f)

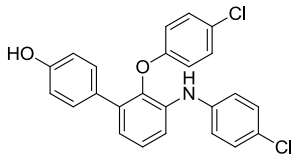

General Procedure K: Using aniline **137a** (30 mg, 0.10 mmol) and 1-bromo-4-chlorobenzene (55.1 mg, 0.29 mmol), chromatography (silica, 5-20% EtOAc, petrol) eluted **138f** as a brown solid (38 mg, 94%); R_f = 0.28 (silica, 20% EtOAc, petrol); m.p. 65-68 ^oC; UV λ_{max} (EtOH/nm) 280.6; IR ν_{max}/cm^{-1} 3533 (N-H), 3408 (br) (O-H), 3032 (C-H), 2927 (C-H), 1594, 1519, 1429, 1420, 1384, 1332, 1263, 1215 (C-O), 1173, 1088, 1008, 921, 867, 822, 781, 750; ^1H δ/ppm (500 MHz, $CDCl_3$) 4.62 (1H, s, N*H*), 5.85 (1H, s, O*H*), 6.62-6.66 (2H, m, Ar-H), 6.72-6.75 (2H, m, Ar-H), 6.94 (1H, dd, Ar-H, *J* = 1.6 and 7.6 Hz), 6.99-7.02 (2H, m, Ar-H), 7.04-7.07 (2H, m, Ar-H), 7.19 (1H, t, Ar-H, *J* = 7.8 Hz), 7.20-7.23 (2H, m, Ar-H), 7.26 (1H, dd, Ar-H, *J* = 1.5 and 8.1 Hz), 7.29-7.32 (2H, m, Ar-H); ^{13}C δ/ppm (125 MHz, $CDCl_3$) 115.08, 115.13, 116.3, 126.0, 126.77, 126.80, 129.3, 129.4, 129.9, 130.3, 135.9, 137.1, 140.0, 140.6, 154.9, 155.9; LC-MS (ESI+) *m/z* = 422.4 $[M+H]^+$; HRMS calcd. for $C_{24}H_{16}O_2N^{35}Cl_2$ $[M-H]^-$ 420.0564, found 420.0562; Analytical HPLC: 98.0%

2'-((4-Chlorobenzyl)oxy)-3'-((4-fluorophenyl)amino)-[1,1'-biphenyl]-4-ol (138g)

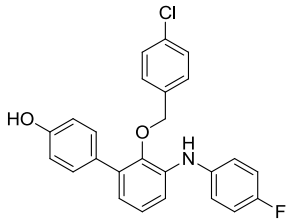

General Procedure K: Using aniline **137c** (100 mg, 0.31 mmol) and 1-bromo-4-fluorobenzene (68 µL, 109 mg, 0.62 mmol), chromatography (silica, 10-15% EtOAc, petrol) eluted **138g** as a brown gum (90 mg, 69%); R_f = 0.34 (silica, 20% EtOAc, petrol); UV λ_{max} (EtOH/nm) 267.5; IR ν_{max}/cm^{-1} 3403 (br) (O-H and N-H), 3038 (C-H), 2926 (C-H), 1597, 1506, 1469, 1334, 1211 (C-O), 1090, 968, 834, 783; ^1H δ/ppm (500

MHz, DMSO-d_6) 4.47 (2H, s, C*H*$_2$), 6.81-6.83 (3H, m, Ar-H), 7.03-7.08 (8H, m, Ar-H), 7.23-7.25 (2H, m, Ar-H), 7.35-7.37 (2H, m, Ar-H), 7.52 (1H, s, N*H*), 9.50 (1H, s, O*H*); ^{13}C δ/ppm (125 MHz, DMSO-d_6) 72.2, 115.0, 115.3, 115.4, 119.2, 119.3, 124.6, 127.8, 129.9, 130.0, 132.3, 135.5, 135.8, 137.5, 145.3; LC-MS (ESI+) *m/z* = 420.3 $[M+H]^+$; HRMS calcd. for $C_{25}H_{20}O_2NClF$ $[M+H]^+$ 420.1161, found 420.1164; HRMS calcd. for $C_{25}H_{18}O_2N^{35}ClF$ $[M-H]^-$ 418.1016, found 418.1006; Analytical HPLC: 93.3%

2'-(4-Chlorophenoxy)-3'-((4-fluoro-2-methylphenyl)amino)-[1,1'-biphenyl]-4-ol (138i)

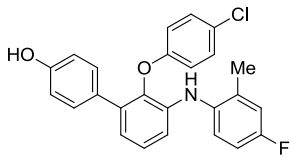

General Procedure K: Using aniline **137a** (50 mg, 0.16 mmol) and 2-bromo-5-fluorotoluene (60.7 µL, 90.7 mg, 0.48 mmol), chromatography (silica, 5-20% EtOAc, petrol) eluted **138i** as a dark brown oil (67 mg, 100%); R_f = 0.31 (silica, 20% EtOAc, petrol); UV λ_{max} (EtOH/nm) 263.6 and 232.2; IR ν_{max}/cm^{-1} 3400 (br) (N-H and O-H), 2977 (C-H), 1602, 1519, 1483, 1375, 1333, 1265, 1213 (C-O), 1173, 1088, 1043, 1008, 956, 913 868, 824, 780, 748; ^{1}H δ/ppm (500 MHz, $CDCl_3$) 2.09 (3H, s, ArC*H*$_3$), 4.62 (1H, s, N*H*), 5.47 (1H, s, O*H*), 6.69-6.72 (3H, m, Ar-H), 6.73-6.76 (2H, m, Ar-H), 6.84 (1H, dd, Ar-H, *J* = 1.5 and 7.7 Hz), 6.87 (1H, td, Ar-H, *J* = 3.0, 8.4 and 16.7 Hz), 6.92 (1H, dd, Ar-H, *J* = 2.9 and 9.2 Hz), 7.07-7.10 (2H, m, Ar-H), 7.11 (1H, t, Ar-H, *J* = 7.8 Hz), 7.15 (1H, dd, Ar-H, *J* = 5.3 and 8.6 Hz), 7.32-7.35 (2H, m, Ar-H); ^{13}C δ/ppm (125 MHz, $CDCl_3$) 18.0, 113.1, 113.3, 113.5, 115.0, 116.3, 117.4, 117.5, 120.6, 125.17, 125.24, 126.1, 129.4, 130.1, 130.3, 135.6, 138.5, 139.2, 154.8, 155.9; LC-MS (ESI+) *m/z* = 420.4 $[M+H]^+$; HRMS calcd. for $C_{25}H_{18}O_2N^{35}ClF$ $[M-H]^-$ 418.1016, found 418.1012; Analytical HPLC: 99.1%

3'-((2-Chloro-4-fluorophenyl)amino)-2'-(4-chlorophenoxy)-[1,1'-biphenyl]-4-ol (138j)

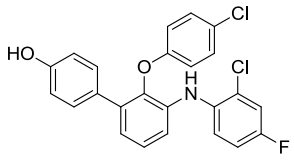

General Procedure K: Using aniline **137a** (50 mg, 0.16 mmol) and 1-bromo-2-chloro-4-fluorobenzene (101 mg, 0.48 mmol), chromatography (silica, 5-20% EtOAc, petrol) eluted **138j** as a brown oil (70 mg, 100%); R_f = 0.32 (silica, 20% EtOAc, petrol); UV λ_{max} (EtOH/nm) 272.4 and 232.0; IR ν_{max}/cm^{-1} 3407 (br) (N-H and O-H), 3068 (C-H), 2928 (C-H), 1605, 1520, 1481, 1419, 1333, 1256, 1214 (C-O), 1184, 1090, 1041, 1008, 930, 893, 859, 823, 779, 749; ^{1}H δ/ppm (500 MHz, $CDCl_3$) 4.68 (1H, s, N*H*), 6.00 (1H, s, O*H*), 6.64-6.67 (2H, m, Ar-H), 6.73-6.77 (2H, m, Ar-H), 6.90-6.94 (1H, m, Ar-H), 7.00 (1H, dd, Ar-H, *J* = 1.8 and 7.5 Hz), 7.05-7.08 (2H, m, Ar-H), 7.11 (1H, dd, Ar-H, *J* = 2.9 and 8.3 Hz), 7.15-7.22 (2H, m, Ar-H), 7.29 (1H, dd, Ar-H, *J* = 5.3 and 9.1 Hz), 7.32-7.34 (2H, m, Ar-H); ^{13}C δ/ppm (125 MHz, $CDCl_3$) 114.3, 114.5, 115.1, 115.8, 116.4, 116.9, 117.1, 119.7, 119.8, 123.1, 126.0, 129.4, 130.3, 136.2, 136.5, 154.9, 155.9; LC-MS (ESI+) *m/z* = 440.4 $[M+H]^+$; HRMS calcd. for $C_{24}H_{15}O_2N^{35}Cl_2F$ $[M-H]^-$ 438.0469, found 438.0469; Analytical HPLC: 99.2%

2'-(4-Chlorophenoxy)-3'-((4-fluorophenyl)amino)-2-methyl-[1,1'-biphenyl]-4-ol (138k)

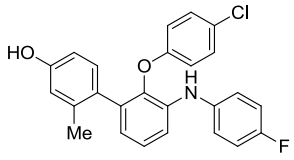

General Procedure K: Using aniline **137d** (50 mg, 0.15 mmol) and 1-bromo-4-fluorobenzene (50.0 µL, 79 mg, 0.45 mmol), chromatography (silica, 0-15% EtOAc, petrol) eluted **138k** as a yellow oil (49.8 mg, 80%); R_f = 0.24 (silica, 20% EtOAc, petrol); UV λ_{max} (EtOH/nm) 278.8; IR ν_{max}/cm^{-1} 3534 (N-H), 3410 (br) (O-H), 3029 (C-H), 2924 (C-H), 1607, 1576, 1507, 1483, 1434, 1387, 1333, 1290, 1211 (C-O), 1159, 1091, 1043, 1009, 954, 913, 864, 823, 783, 750; ^{1}H δ/ppm (500 MHz, $CDCl_3$) 2.11 (3H, s, ArC*H*$_3$), 4.53 (1H, s, br, O*H*), 6.50 (1H, dd, Ar-H, *J* = 2.7 and 8.2 Hz), 6.54-6.58 (2H,

m, Ar-H), 6.60 (1H, d, Ar-H, *J* = 2.6 Hz), 6.72 (1H, dd, Ar-H, *J* = 1.7 and 7.4 Hz), 6.87 (1H, d, Ar-H, 8.2 Hz), 6.98-7.04 (4H, m, Ar-H), 7.08-7.11 (2H, m, Ar-H), 7.13-7.14 (1H, m, Ar-H), 7.18 (1H, dd, Ar-H, *J* = 1.7 and 8.2 Hz); ^{13}C δ/ppm (125 MHz, $CDCl_3$) 20.1, 112.1, 113.7, 115.9, 116.1, 116.3, 116.7, 122.3, 122.36, 122.41, 125.6, 126.8, 129.1, 131.1, 135.7, 137.9, 138.1, 140.5, 156.2; ^{19}F δ/ppm (470 MHz, $CDCl_3$) -120.5; LC-MS (ESI+) *m/z* = 420.4 $[M+H]^+$ and 418.3 $[M-H]^-$; HRMS calcd. for $C_{25}H_{18}O_2N^{35}ClF$ $[M-H]^-$ 418.1016, found 418.1014; Analytical HPLC: 99.6%

2-Chloro-2'-(4-chlorophenoxy)-3'-((4-fluorophenyl)amino)-[1,1'-biphenyl]-4-ol (138l)

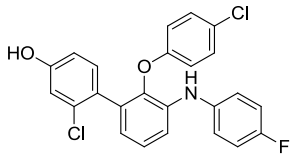

General Procedure K: Using aniline **137e** (50 mg, 0.14 mmol) and 1-bromo-4-fluorobenzene (46.0 µL, 74 mg, 0.42 mmol), chromatography (silica, 0-15% EtOAc, petrol) eluted **138l** as a yellow oil (51.5 mg, 84%); R_f = 0.35 (silica, 20% EtOAc, petrol); UV λ_{max} (EtOH/nm) 279.4; IR ν_{max}/cm^{-1} 3535 (N-H), 3405 (br) (O-H), 3041 (C-H), 2934 (C-H), 1608, 1577, 1507, 1483, 1439, 1388, 1335, 1275, 1211 (C-O), 1160, 1091, 1039, 1009, 930, 894, 824, 782, 748; ^{1}H δ/ppm (500 MHz, $CDCl_3$) 4.95 (1H, s, br, O*H*), 6.60 (1H, dd, Ar-H, *J* = 2.6 and 8.4 Hz), 6.61-6.64 (2H, m, Ar-H), 6.80 (1H, dd, Ar-H, *J* = 1.6 and 7.5 Hz), 6.83 (1H, d, Ar-H, *J* = 2.5 Hz), 6.97-7.07 (5H, m, Ar-H), 7.07-7.12 (2H, m, Ar-H), 7.15 (1H, t, Ar-H, *J* = 7.6 Hz), 7.21 (1H, dd, Ar-H, *J* = 1.6 and 8.2 Hz); ^{13}C δ/ppm (125 MHz, $CDCl_3$) 113.6, 114.4, 115.9, 116.1, 116.3, 116.6, 122.4, 122.50, 122.53, 125.5, 126.9, 128.6, 129.2, 132.2, 133.3, 133.8, 137.6, 138.2, 140.3, 155.4, 156.0; ^{19}F δ/ppm (470 MHz, $CDCl_3$) -120.4; LC-MS (ESI+) *m/z* = 440.3 $[M+H]^+$ and 438.2 $[M-H]^-$; HRMS calcd. for $C_{24}H_{15}O_2N^{35}Cl_2F$ $[M-H]^-$ 438.0469, found 438.0472; Analytical HPLC: 98.8%

2-(4-Chlorophenoxy)-4'-fluoro-*N*-(4-methoxyphenyl)-[1,1'-biphenyl]-3-amine (138r)

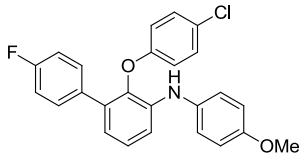

General Procedure K: Using aniline **137f** (50 mg, 0.16 mmol) and 4-bromoanisole (60.1 µL, 89.8 mg, 0.48 mmol), chromatography (silica, 5% Et_2O, petrol) eluted **138r** as an off-white solid (24.8 mg, 37%); R_f = 0.41 (silica, 10% Et_2O, petrol); m.p. 76-79 ^oC; UV λ_{max} (EtOH/nm) 279.8 and 230.2; IR ν_{max}/cm^{-1} 3405 (N-H), 2956 (C-H), 2926 (C-H), 1603, 1514, 1483, 1439, 1389, 1335, 1276, 1217 (C-O), 1161, 1089, 1040, 923, 867, 826, 781, 749, 721; ^1H δ/ppm (500 MHz, $CDCl_3$) 3.80 (3H, s, OC*H*$_3$), 5.74 (1H, s, br, N*H*), 6.66-6.69 (2H, m, Ar-H), 6.80 (1H, dd, Ar-H, *J* = 1.6 and 7.5 Hz), 6.85-6.88 (2H, m, Ar-H), 6.94-6.98 (2H, m, Ar-H), 7.06-7.09 (5H, m, Ar-H), 7.13 (1H, t, Ar-H, *J* = 8.0 Hz), 7.37-7.41 (2H, m, Ar-H); ^{13}C δ/ppm (125 MHz, $CDCl_3$) 55.6, 113.4, 114.7, 114.9, 115.1, 116.3, 120.5, 124.1, 126.2, 126.8, 129.4, 130.5, 130.6, 133.6, 134.3, 135.0, 138.5, 139.7, 155.8, 156.1; LC-MS (ESI+) *m/z* = 420.4 $[M+H]^+$; HRMS calcd. for $C_{25}H_{20}O_2N^{35}ClF$ $[M+H]^+$ 420.1161, found 420.1160; Analytical HPLC: 99.0%

2-(4-Chlorophenoxy)-*N*-(4-fluorophenyl)-3-((triisopropylsilyl)ethynyl)aniline (178)

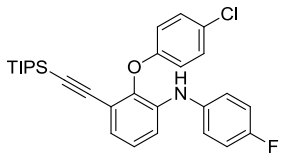

General Procedure K: Using aniline **177** (30 mg, 0.075 mmol), 1-bromo-4-fluorobenzene (41.2 µL, 66 mg, 0.38 mmol) and NaO^{t}Bu (18 mg, 0.19 mmol) chromatography (silica, 0-10% DCM, petrol) eluted **178** as a colourless gum (25 mg, 70%); R_f = 0.29 (silica, 10% DCM, petrol); UV λ_{max} (EtOH/nm) 264.2 and 253.0; IR ν_{max}/cm^{-1} 3419 (N-H), 2941 (C-H), 2862 (C-H), 2154 (C≡C), 1595, 1509, 1468, 1387, 1330, 1279, 1212 (C-O), 1158, 1091, 1002, 919, 879, 824, 769, 739; ^1H δ/ppm (500 MHz, $CDCl_3$) 0.96 (21H, s, Si(C*H*(C*H*$_3$)$_2$)$_3$), 5.81 (1H, s, br, N*H*), 6.83-6.84 (2H, m, Ar-H), 6.97-7.07 (6H, m, Ar-H), 7.11-7.12 (1H, m, Ar-H), 7.19-7.21 (2H, m, Ar-H); ^{13}C δ/ppm (125 MHz, $CDCl_3$) 11.1, 18.5, 97.1, 101.6, 114.8, 116.0, 116.2, 116.4, 118.6,

123.0, 123.1, 124.4, 125.7, 127.1, 129.4, 137.2, 137.3, 138.5, 142.6, 156.1, 158.0, 159.9; ^{19}F δ/ppm (470 MHz, $CDCl_3$) -119.8; LC-MS (ESI+) *m/z* = 492.5 and 494.5 $[M-H]^-$; HRMS calcd. for $C_{29}H_{34}ON^{35}ClFSi$ $[M+H]^+$ 494.2077, found 494.2067; Analytical HPLC: 93.8%

Methyl-6-(4-chlorophenoxy)-5-((4-fluorophenyl)amino)-4'-hydroxy-[1,1'-biphenyl]-3-carboxylate (230)

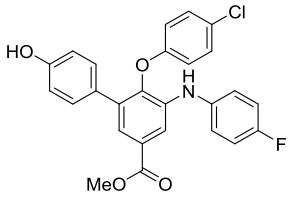

General Procedure K: Using aniline **229** (40 mg, 0.11 mmol) and 1-bromo-4-fluorobenzene (72 µL, 113 mg, 0.65 mmol), chromatography (silica, 0-20% EtOAc, petrol) eluted **230** as a white solid (35 mg, 70%); R_f = 0.36 (silica, 30% EtOAc, petrol); m.p. 216-218 ^oC; UV λ_{max} (EtOH/nm) 277.0 and 228.2; IR ν_{max}/cm^{-1} 3422 (br) (N-H and O-H), 2957 (C-H), 1699 (C=O), 1610, 1499, 1436, 1359, 1211 (C-O), 1096, 1009, 937, 886, 824, 770, 734; ^{1}H δ/ppm (500 MHz, $CDCl_3$) 3.89 (3H, s, O*CH$_3$*), 4.74 (1H, s, br, N*H*), 5.87 (1H, s, br, O*H*), 6.64-6.67 (2H, m, Ar-H), 6.74-6.76 (2H, m, Ar-H), 7.00-7.05 (2H, m, Ar-H), 7.06-7.11 (4H, m, Ar-H), 7.31-7.33 (2H, m, Ar-H), 7.58 (1H, d, Ar-H, *J* = 2.0 Hz), 7.76 (1H, d, Ar-H, *J* = 2.0 Hz); ^{13}C δ/ppm (125 MHz, $CDCl_3$) 52.3, 114.1, 115.2, 116.2, 116.4, 122.8, 123.1, 123.2, 127.2, 127.9, 129.1, 129.5, 130.3, 135.7, 136.4, 136.9, 138.8, 142.5, 155.2, 155.3, 158.2, 166.7; ^{19}F δ/ppm (470 MHz, $CDCl_3$) -119.3; LC-MS (ESI+) *m/z* = 464.4 $[M+H]^+$ and 462.3 $[M-H]^-$; HRMS calcd. for $C_{26}H_{18}O_4N^{35}ClF$ $[M-H]^-$ 462.0914, found 462.0903; Analytical HPLC: 97.3%

Methyl-6-(4-chlorophenoxy)-5-((4-fluorophenyl)amino)-4'-methoxy-[1,1'-biphenyl]-3-carboxylate (247)

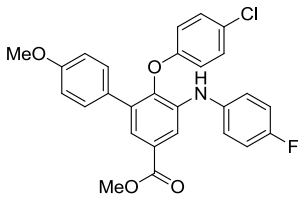

General Procedure K: Using aniline **246** (480 mg, 1.25 mmol) and 1-bromo-4-fluorobenzene (824 µL, 1.31 g, 7.50 mmol), chromatography (silica, 0-10% EtOAc, petrol) eluted **247** as a beige solid (454 mg, 76%); R_f = 0.17 (silica, 10% EtOAc, petrol); m.p. 152-155 ^{o}C; UV λ_{max} (EtOH/nm) 275.0; IR ν_{max}/cm^{-1} 3417 (N-H), 3073 (C-H), 2953 (C-H), 2842 (C-H), 1720 (C=O), 1606, 1504, 1433, 1358, 1290, 1212 (C-O), 1090, 1010, 942, 820, 768; ^{1}H δ/ppm (500 MHz, $CDCl_3$) 3.78 (3H, s, OC*H*$_3$), 3.89 (3H, s, CO_2C*H*$_3$), 5.87 (1H, s, N*H*), 6.67 (2H, d, 4-ClPh C_3-H and C_5-H, *J* = 9.0 Hz), 6.82 (2H, d, 4-MeOPh, C_2-H and C_6-H, *J* = 8.8 Hz), 7.01-7.05 (2H, m, Ar-H), 7.06-7.10 (4H, m, 4-ClPh C_2-H and C_6-H and Ar-H), 7.37 (2H, d, 4-MeOPh, C_3-H and C_5-H, *J* = 8.8 Hz), 7.60 (1H, d, Ar-H, *J* = 2.0 Hz), 7.76 (1H, d, Ar-H, *J* = 2.0 Hz); ^{13}C δ/ppm (125 MHz, $CDCl_3$) 52.3, 55.2, 113.7, 114.1, 116.2, 116.4, 122.9, 123.1, 123.2, 127.2, 128.0, 128.9, 129.3, 129.5, 130.1, 130.3, 135.8, 136.97, 136.99, 138.8, 142.5, 155.3, 159.2, 166.7; ^{19}F δ/ppm (470 MHz, $CDCl_3$) -119.4; LC-MS (ESI+) *m/z* = 478.3 $[M+H]^+$; HRMS calcd. for $C_{27}H_{22}O_4N^{35}ClF$ $[M+H]^+$ 478.1216, found 478.1209

Methyl 3-(2-(4-chlorophenoxy)-3-nitrophenyl)propiolate (168)

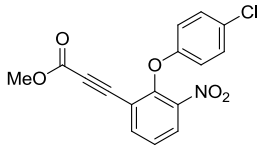

General Procedure O: Using acetylene **165** (600 mg, 2.22 mmol), diisopropylamine (404 µL, 292 mg, 2.89 mmol), *n*-butyllithium (2.5 M in hexanes, 1.16 mL, 2.89 mmol) and methyl chloroformate (343 µL, 420 mg, 4.44 mmol) and transferring the $^{i}Pr_2NH$/*n*-BuLi, as a solution in THF (1.16 mL, 1 M) to a solution of **165** in THF (12.4 mL) at -78 ^{o}C, chromatography (silica, 0-40% Et_2O, petrol) eluted **168** as a dark yellow solid (596 mg, 81%); R_f = 0.30 (silica, 20% EtOAc, petrol); m.p. 94-97 ^{o}C; UV λ_{max} (EtOH/nm) 225.8; IR ν_{max}/cm^{-1} 3086 (C-H), 2955 (C-H), 2223 (C≡C), 1712 (C=O), 1588, 1533,

1484, 1445, 1351, 1301, 1220, 1195, 1090, 1010, 931, 879, 854, 829, 796, 746, 664; ^{1}H δ/ppm (500 MHz, $CDCl_3$) 3.76 (3H, s, CO_2CH_3), 6.85 (2H, d, 4-ClPh C_3-H and C_5-H, *J* = 9.1 Hz), 7.27 (2H, d, 4-ClPh C_2-H and C_6-H, *J* = 8.9 Hz), 7.40 (1H, t, 3-NO_2Ar C_5-H, *J* = 8.0 Hz), 7.84 (1H, dd, Ar-H, *J* = 1.7 and 7.8 Hz), 8.03 (1H, dd, Ar-H, *J* = 1.7 and 8.2 Hz); ^{13}C δ/ppm (125 MHz, $CDCl_3$) 53.0, 78.7, 87.1, 117.6, 117.8, 125.5, 127.6, 128.6, 129.7, 139.2, 144.0, 150.2, 153.3, 156.1; LC-MS (ESI+) *m/z* = mass not observed; HRMS calcd. for $C_{16}H_{11}O_5N^{35}Cl$ $[M+H]^+$ 332.0320, found 332.0317

Methyl 3-(2-(4-Chlorophenoxy)-3-((4-fluorophenyl)(methoxycarbonyl)amino)phenyl)propiolate (179)

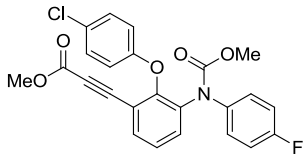

General Procedure O: Using aniline **167** (20 mg, 0.06 mmol), diisopropylamine (9.1 µL, 6.6 mg, 0.07 mmol), *n*-butyllithium (2.5 M in hexanes, 26 µL, 0.07 mmol) and methyl chloroformate (5.3 µL, 6.5 mg, 0.07 mmol) and transferring the $^{i}Pr_2NH$/*n*-BuLi, as a solution in THF (0.5 mL, 0.1 M) to a solution of **167** in THF (1.4 mL) at -78 ^{o}C, chromatography (silica, 0-80% DCM, petrol) eluted **179** as a brown gum (15 mg, 56%); R_f = 0.32 (silica, 40% DCM, petrol); UV λ_{max} (EtOH/nm) 227.4; IR ν_{max}/cm^{-1} 2953 (C-H), 2225 (C≡C), 1707 (C=O), 1588, 1505, 1437, 1292, 1211 (C-O), 1087, 1045, 956, 866, 824, 745; ^{1}H δ/ppm (500 MHz, $CDCl_3$) 3.60 (3H, s, OCH_3), 3.71 (3H, s, OCH_3), 6.71-6.73 (2H, m, Ar-H), 6.92-6.97 (2H, m, Ar-H), 7.07-7.10 (2H, m, Ar-H), 7.18-7.21 (2H, m, Ar-H), 7.28 (1H, t, Ar-H, *J* = 7.9 Hz), 7.53 (1H, d, Ar-H, *J* = 7.7 Hz), 7.57 (1H, dd, Ar-H, *J* = 1.5 and 7.8 Hz); ^{13}C δ/ppm (125 MHz, $CDCl_3$) 52.8, 53.4, 80.5, 86.1, 115.5, 115.7, 115.9, 117.4, 125.7, 127.8, 129.3, 133.4, 134.3, 136.1, 137.2, 153.1, 153.7, 154.8, 155.9; ^{19}F δ/ppm (470 MHz, $CDCl_3$) -115.3; LC-MS (ESI+) *m/z* = mass not observed; HRMS mass not observed; Analytical HPLC: 98.8%

Methyl 3-(3-((*tert*-butoxycarbonyl)(4-fluorophenyl)amino)-2-(4-chlorophenoxy)phenyl)propiolate (182)

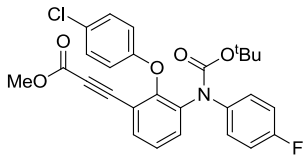

General Procedure O: Using aniline **181** (130 mg, 0.30 mmol), diisopropylamine (51 µL, 36.4 mg, 0.36 mmol), *n*-butyllithium (2.5 M in hexanes, 144 µL, 0.36 mmol) and methyl chloroformate (70 µL, 85 mg, 0.90 mmol), chromatography (silica, 0-20% Et_2O, petrol) eluted **182** as a yellow oil (98 mg, 67%); R_f = 0.23 (silica, 20% Et_2O, petrol); UV λ_{max} (EtOH/nm) 224.2; IR ν_{max}/cm^{-1} 2976 (C-H), 2227 (C≡C), 1707 (C=O), 1588, 1506, 1484, 1452, 1314, 1291, 1212 (C-O), 1152, 1087, 1010, 978, 901, 871, 827, 747, 703; ^{1}H δ/ppm (500 MHz, $CDCl_3$) 1.34 (9H, s, C(CH_3)$_3$), 3.71 (3H, s, CO_2CH_3), 6.71 (2H, d, 4-ClPh, C_3-H and C_5-H, *J* = 8.7 Hz), 6.92 (2H, t, 4-FPh C_3-H and C_5-H, *J* = 8.1 Hz), 6.99-7.00 (2H, m, 4-FPh C_2-H and C_6-H), 7.20 (2H, d, 4-ClPh C_2-H and C_6-H, *J* = 8.9 Hz), 7.29 (1H, t, C_5-H, *J* = 7.8 Hz), 7.53-7.56 (2H, m, Ar-H); ^{13}C δ/ppm (125 MHz, $CDCl_3$) 28.0, 52.8, 80.8, 82.0, 85.6, 115.2, 115.4, 116.1, 117.3, 125.6, 127.6, 129.2, 133.80, 133.82, 136.5, 153.1, 153.8, 155.9; ^{19}F δ/ppm (470 MHz, $CDCl_3$) -116.3; LC-MS (ESI+) *m/z* = mass not observed; HRMS mass not observed

5-(2-(4-Chlorophenoxy)-3-nitrophenyl)isoxazol-3-ol (169)

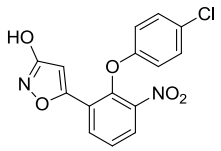

General Procedure P: Using propiolate ester **168** (100 mg, 0.30 mmol) and hydroxylamine hydrochloride (21 mg, 0.30 mmol) in 3 M NaOH (0.1 mL, 0.30 mmol) and ethanol (3 mL), chromatography (silica, 20-80% EtOAc, petrol) eluted **169** as a brown solid (28 mg, 28%); R_f = 0.24 (silica, 50% EtOAc, petrol); m.p. 204-207 ^{o}C; UV λ_{max} (EtOH/nm) 253.2 and 223.0; IR ν_{max}/cm^{-1} 2997 (C-H), 2776 (C-H), 2626 (br) (O-H), 1619, 1578, 1535, 1483, 1449, 1335, 1290, 1237, 1185, 1088, 1009, 951, 879, 828, 790, 745, 689; ^{1}H δ/ppm (500 MHz, DMSO-d_6) 6.30 (1H, s, isoxazole C_4-H), 6.91-6.94 (2H, m, 4-ClPh, C_3-H and C_5-H), 7.37-7.40 (2H, m, 4-ClPh C_2-H and C_6-H), 7.74 (1H, t, Ar-H, *J* = 8.3 Hz), 8.27 (1H, dd, Ar-H, 1.6 and 8.2 Hz), 8.31 (1H, dd, Ar-H, *J* = 1.6

and 7.9 Hz), 11.52 (1H, s, O*H*); ^{13}C δ/ppm (125 MHz, DMSO-d_6) 96.8, 116.6, 123.8, 127.0, 127.4, 127.6, 129.9, 132.8, 142.5, 143.9, 155.3, 162.4, 170.8; LC-MS (ESI+) *m/z* = 333.3 $[M+H]^+$ and 331.2 $[M-H]^-$; HRMS calcd. for $C_{15}H_8O_5N_2{}^{35}Cl$ $[M-H]^-$ 331.0127, found 331.0117; Analytical HPLC: 94.6%

5-(2-(4-Chlorophenoxy)-3-((4-fluorophenyl)amino)phenyl)isoxazol-3-ol (183a)

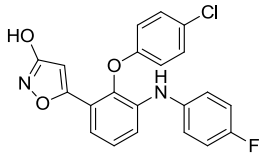

General Procedure P: Using propiolate ester **182** (50 mg, 0.10 mmol) and hydroxylamine hydrochloride (21 mg, 0.30 mmol) in 3 M NaOH (0.3 mL, 0.90 mmol) and methanol (1 mL), semi-preparative HPLC (5-100% MeCN, H_2O + 0.1% (v/v) HCO_2H) eluted **183a** as a white powder (21.7 mg, 56%); R_f = 0.25 (silica, 5% MeOH, DCM); m.p. 217-219 ^oC; UV λ_{max} (EtOH/nm) 270.0 and 226.6; IR ν_{max}/cm^{-1} 3425 (N-H), 2923 (C-H), 2848 (C-H), 2773 (C-H), 2628 (br) (O-H), 1594, 1512, 1482, 1445, 1338, 1278, 1202 (C-O), 1158, 1087, 1007, 961, 864, 824, 780, 744; ^{1}H δ/ppm (500 MHz, DMSO-d_6) 6.14 (1H, s, isoxazole C_4-H), 6.79-6.82 (2H, m, Ar-H), 7.00-7.03 (2H, m, Ar-H), 7.05-7.09 (2H, m, Ar-H), 7.29-7.34 (4H, m, Ar-H), 7.39-7.43 (1H, m, Ar-H), 7.76 (1H, s, br, N*H*), 11.30 (1H, s, br, O*H*); ^{13}C δ/ppm (125 MHz, DMSO-d_6) 95.2, 115.4, 115.6, 116.4, 118.1, 119.2, 120.6, 120.7, 122.2, 125.8, 126.8, 129.4, 138.4, 138.6, 139.3, 155.0, 158.0, 164.5, 170.7; ^{19}F δ/ppm (470 MHz, DMSO-d_6) -122.3; LC-MS (ESI+) *m/z* = 397.3 $[M+H]^+$ and 395.3 $[M-H]^-$; HRMS calcd. for $C_{21}H_{13}O_3N_2{}^{35}ClF$ $[M-H]^-$ 395.0604, found 395.0593; Analytical HPLC: 99.6%

***N*-(2-(4-Chlorophenoxy)-4'-fluoro-[1,1'-biphenyl]-3-yl)-4-hydroxybenzamide (151a)**

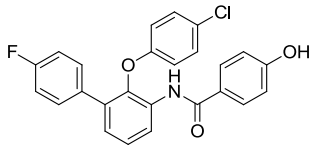

General procedure Q: Using aniline **137f** (40 mg, 0.13 mmol) and ethyl 4-hydroxybenzoate (26 mg, 0.16 mmol), chromatography (silica, 15-80% EtOAc, petrol)

eluted **151a** as a white solid (51 mg, 91%); R_f = 0.22 (silica, 30% EtOAc, petrol); m.p. 87 ^oC (decomposed); UV λ_{max} (EtOH/nm) 229.8; IR ν_{max}/cm^{-1} 3417 (N-H), 3280 (br) (O-H), 3076 (C-H), 3023 (C-H), 1650 (C=O), 1607, 1534, 1505, 1483, 1427, 1397, 1273, 1244, 1217 (C-O), 1160, 1091, 1009, 868, 826, 786, 753, 659; ^1H δ/ppm (500 MHz, DMSO-d_6) 6.66-6.69 (2H, m, Ar-H), 6.73-6.75 (2H, m, Ar-H), 7.16-7.22 (4H, m, Ar-H), 7.35 (1H, dd, Ar-H, *J* = 1.7 and 7.7 Hz), 7.42 (1H, t, Ar-H, *J* = 7.9 Hz), 7.47-7.50 (2H, m, Ar-H), 7.52-7.54 (2H, m, Ar-H), 7.79 (1H, dd, Ar-H, *J* = 1.7 and 7.9 Hz), 9.54 (1H, s, N*H*), 10.05 (1H, s, O*H*); ^{13}C δ/ppm (125 MHz, DMSO-d_6) 114.7, 115.1, 115.2, 116.7, 124.6, 125.5, 125.8, 126.4, 127.4, 129.2, 129.5, 130.7, 130.8, 132.0, 133.1, 134.3, 144.1, 155.9, 160.5, 164.9; ^{19}F δ/ppm (470 MHz, DMSO-d_6) -114.7; LC-MS (ESI+) *m/z* = 434.1 $[M+H]^+$ and 432.1 $[M-H]^-$; HRMS calcd. for $C_{25}H_{16}O_3N^{35}ClF$ $[M-H]^-$ 432.0808, found 432.0807; Analytical HPLC: 97.8%

N-(2-(4-Chlorophenoxy)-4'-fluoro-[1,1'-biphenyl]-3-yl)-4-(trifluoromethylsulfonamido)benzamide (151b)

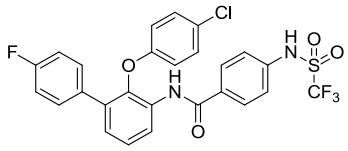

General procedure Q: Using aniline **137f** (50 mg, 0.16 mmol) and ester **153** (45.3 mg, 0.16 mmol), chromatography (silica, 0-70% EtOAc, petrol) eluted **151b** as an off-white solid (19 mg, 21%); R_f = 0.21 (silica, 50% EtOAc, petrol); m.p. 163-166 ^oC; UV λ_{max} (EtOH/nm) 230.8; IR ν_{max}/cm^{-1} 3428 (sulfonamido N-H), 3081 (amido N-H), 3038 (C-H), 2921 (C-H), 2829 (C-H), 1662 (C=O), 1607, 1535, 1508, 1473, 1431, 1376, 1330 (S=O asym. stretch), 1275, 1211 (C-O), 1192 (C-O), 1135 (S=O sym. stretch), 1090, 1017, 951, 828, 784, 751, 698; ^1H δ/ppm (500 MHz, $CDCl_3$) 6.64-6.66 (2H, m, Ar-H), 6.96-7.00 (3H, m, Ar-H), 7.09-7.11 (2H, m, Ar-H), 7.20 (1H, dd, Ar-H, *J* = 1.4 and 7.7 Hz), 7.30-7.32 (2H, m, Ar-H), 7.35-7.41 (3H, m, Ar-H), 7.65-7.67 (2H, m, Ar-H), 8.20 (1H, s, br, amido N*H*), 8.56-8.57 (1H, m, sulfonamido N*H*); ^{13}C δ/ppm (125 MHz, $CDCl_3$) 115.2, 115.4, 116.4, 120.7, 122.2, 126.5, 126.6, 127.7, 128.6, 129.8, 130.56, 130.63, 131.9, 133.1, 134.6, 137.3, 140.6, 155.4, 164.1; LC-MS (ESI+) *m/z* = 563.2 $[M-H]^-$; HRMS calcd. for $C_{26}H_{16}O_4N_2{}^{35}ClF_4S$ $[M-H]^-$ 563.0461, found 563.0450; Analytical HPLC: 99.4%

***N*-(2-(4-Chlorophenoxy)-4'-fluoro-[1,1'-biphenyl]-3-yl)-4-methoxybenzamide (151c)**

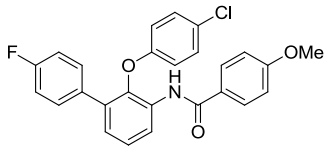

General procedure Q: Using aniline **137f** (100 mg, 0.32 mmol) and methyl 4-methoxybenzoate (53.2 mg, 0.32 mmol), chromatography (silica, 0-20% EtOAc, petrol) eluted **151c** as a white solid (117.4 mg, 82%); R_f = 0.34 (silica, 20% EtOAc, petrol); m.p. 120-123 ^oC; UV λ_{max} (EtOH/nm) 230.6; IR ν_{max}/cm^{-1} 3289 (N-H), 2933 (C-H), 2839 (C-H), 1648, 1606, 1531, 1504, 1482, 1430, 1395, 1316, 1293, 1251, 1221 (C-O), 1175, 1092, 1031, 894, 827, 779, 749; ^1H δ/ppm (500 MHz, $CDCl_3$) 3.84 (3H, s, OC*H*$_3$), 6.64-6.67 (2H, m, Ar-H), 6.88-6.91 (2H, m, Ar-H), 6.95-7.00 (2H, m, Ar-H), 7.08-7.11 (2H, m, Ar-H), 7.16 (1H, dd, Ar-H, *J* = 1.6 and 7.7 Hz), 7.35-7.39 (3H, m, Ar-H), 7.59-7.62 (2H, m, Ar-H), 8.18 (1H, s, br, N*H*), 8.61 (1H, dd, Ar-H, *J* = 1.6 and 8.3 Hz); ^{13}C δ/ppm (125 MHz, $CDCl_3$) 55.5, 114.1, 115.1, 115.3, 116.4, 120.5, 125.8, 126.6, 126.8, 127.6, 128.8, 129.7, 130.58, 130.64, 132.5, 132.9, 134.5, 140.3, 155.5, 161.3, 162.6, 163.3, 164.9; LC-MS (ESI+) *m/z* = 448.4 $[M+H]^+$; HRMS calcd. for $C_{26}H_{20}O_3N^{35}ClF$ $[M+H]^+$ 448.1110, found 448.1105 Analytical HPLC: 97.3%

1,1,1-Trifluoro-*N*-(4-(2-((4-fluorophenyl)amino)thiazol-4-yl)phenyl)methanesulfonamide (44s)

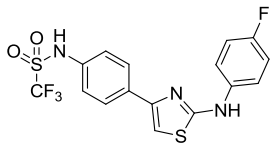

General procedure S: Using phenacyl bromide **264** (120 mg, 0.35 mmol) and thiourea **261** (49.4 mg, 0.29 mmol), preparative HPLC (C18, 15% H_2O + 0.1% (v/v) HCO_2H, MeCN) eluted **44s** as a white solid (44.6 mg, 37%); R_f = 0.25 (silica, 30% EtOAc, petrol); m.p. 198-201 ^oC; UV λ_{max} (EtOH/nm) 281.8; IR ν_{max}/cm^{-1} 3330 (amino N-H), 3121 (C-H), 3018 (C-H), 2653 (br) (sulfonamido N-H), 1611, 1551, 1501, 1430, 1411, 1370, 1329, 1211, 1186, 1141, 1064, 964, 833, 807, 745, 721, 671; ^1H δ/ppm (500 MHz, DMSO-d_6) 7.17-7.21 (2H, m, Ar-H), 7.31-7.32 (2H, m, Ar-H), 7.34 (1H, s,

thiazole C_5-H), 7.74-7.77 (2H, m, Ar-H), 7.94-7.96 (2H, m, Ar-H), 10.31 (1H, s, amino N*H*), 11.96 (1H, s, br, sulfonamido N*H*); ^{13}C δ/ppm (125 MHz, DMSO-d_6) 103.3, 115.4, 115.6, 118.3, 118.4, 123.0, 126.7, 137.7, 149.0, 155.9, 157.8, 163.2; ^{19}F δ/ppm (470 MHz, DMSO-d_6) -75.3, -121.9; LC-MS (ESI+) *m/z* = 418.3 $[M+H]^+$ and 416.2 $[M-H]^-$; HRMS calcd. for $C_{16}H_{10}O_2N_3F_4S_2$ $[M-H]^-$ 416.0156, found 416.0147; Analytical HPLC: 98.7%

1,1,1-Trifluoro-*N*-(4-(2-((4-fluorobenzyl)amino)thiazol-4-yl)phenyl)methanesulfonamide (44j)

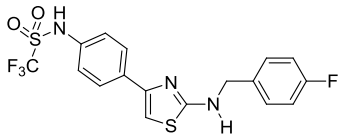

General procedure S: Using phenacyl bromide **264** (4:1 mixture with **265**, 337 mg, 0.78 mmol) and thiourea **279** (116 mg, 0.63 mmol), chromatography (silica, 0-30% EtOAc, petrol) eluted **44j** as a yellow solid (168 mg, 62%); R_f = 0.29 (silica, 30% EtOAc, petrol); m.p. 181-183 ^{o}C; UV λ_{max} (EtOH/nm) 295.2 and 248.8; IR ν_{max}/cm^{-1} 3386 (amino N-H), 3281 (sulfonamido N-H), 3115 (C-H), 2919 (C-H), 1561, 1510, 1442, 1408, 1359, 1289, 1192, 1137, 1047, 958, 821, 753, 688; ^{1}H δ/ppm (500 MHz, DMSO-d_6) 4.49 (2H, d, C*H*$_2$, *J* = 5.5 Hz), 7.07 (1H, s, thiazole C_5-H), 7.16-7.19 (2H, m, Ar-H), 7.25-7.27 (2H, m, Ar-H), 7.43-7.45 (2H, m, Ar-H), 7.83-7.85 (2H, m, Ar-H), 8.21 (1H, t, amino N*H*, *J* = 4.9 Hz), 11.90 (1H, s, sulfonamido N*H*); ^{13}C δ/ppm (125 MHz, DMSO-d_6) 47.5, 102.2, 115.4, 115.6, 123.5, 127.1, 130.0, 130.1, 133.6, 134.5, 135.9, 149.3, 160.8, 162.8, 168.7; ^{19}F δ/ppm (470 MHz, DMSO-d_6) -75.5, -115.9; LC-MS (ESI+) *m/z* = 432.2 $[M+H]^+$ and 430.2 $[M-H]^-$; HRMS calcd. for $C_{17}H_{12}O_2N_3F_4S$ $[M-H]^-$ 430.0313, found 430.0301; Analytical HPLC 99.1%

2-(2-Methoxy-6-nitrophenyl)-4,4,5,5-tetramethyl-1,3,2-dioxaborolane (204)

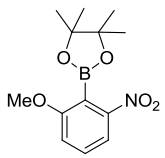

General procedure V: Using aryl bromide **189** (2.40 g, 10.3 mmol) and $B_2(pin)_2$ (5.78 g, 22.8 mmol) at 90 ^{o}C for 20 h, chromatography (silica, 0-20%, Et_2O, petrol), afforded **204** as a brown solid (2.76 g, 78%); R_f = 0.17 (silica, 20% Et_2O, petrol); m.p. 94-97 ^{o}C;

UV λ_{max} (EtOH/nm) 332.2, 271.4 and 233.0; IR ν_{max}/cm^{-1} 3288 (C-H), 3083 (C-H), 2979 (C-H), 2939 (C-H), 1620, 1528, 1478, 1349, 1303, 1261, 1182, 1142, 1102, 1054, 962, 908, 856, 827, 796, 738, 658; ^{1}H δ/ppm (500 MHz, $CDCl_3$) 1.44 (12H, s, $(CH_3)_4$), 3.86 (3H, s, OCH_3), 7.13 (1H, d, C_3-H, *J* = 8.2 Hz), 7.46 (1H, t, C_4-H, *J* = 8.2 Hz), 7.79 (1H, dd, C_5-H, *J* = 0.6 and 8.2 Hz); ^{13}C δ/ppm (125 MHz, $CDCl_3$) 24.7, 56.3, 84.6, 115.2, 115.8, 131.1, 151.3, 163.0; LC-MS (ESI+) *m/z* = mass not observed; HRMS calcd. for $C_{13}H_{19}O_5N^{10}B$ $[M+H]^+$ 279.1387, found 279.1389

5-(4,4,5,5-tetramethyl-1,3,2-dioxaborolan-2-yl)-1*H*-indazole (272)

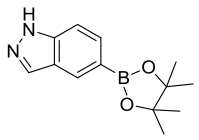

General procedure V: Using indazole **271** (100 mg, 0.51 mmol) in DMF (5.7 mL) at 90 ^{o}C for 15 h, chromatography (silica, 0-20%, EtOAc, petrol), afforded **272** as a white solid (75 mg, 61%); R_f = 0.25 (silica, 30% EtOAc, petrol); m.p. 166-168 ^{o}C; UV λ_{max} (EtOH/nm) 222.4; IR ν_{max}/cm^{-1} 3332 (N-H), 2978 (C-H), 2941 (C-H), 1616, 1536, 1511, 1473, 1447, 1363, 1339, 1309, 1271, 1139, 1077, 948, 857, 819, 748, 667; ^{1}H δ/ppm (500 MHz, $CDCl_3$) 1.37 (12H, s, $(CH_3)_4$), 7.56 (1H, d, C_6-H, *J* = 8.5 Hz), 7.87 (1H, d, C_7-H, *J* = 8.5 Hz), 8.16 (1H, s, C_4-H), 8.33 (1H, s, C_3-H) - N*H* proton was not observed; ^{13}C δ/ppm (125 MHz, $CDCl_3$) 24.9, 83.9, 109.2, 123.0, 129.3, 132.9, 135.1, 141.5; LC-MS (ESI+) *m/z* = 245.3 $[M+H]^+$ and 243.2 $[M-H]^-$; HRMS calcd. for $C_{13}H_{16}O_2N_2{}^{10}B$ $[M-H]^-$ 243.1310, found 243.1311

***N*-(4-(1*H*-indazol-5-yl)thiazol-2-yl)-4-fluorobenzamide (275)**

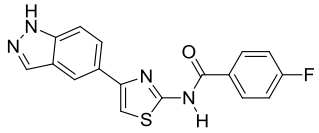

Poor solubility meant a suitable ^{13}C and ^{19}F NMR could not be obtained for this compound.

General procedure X: Using indazole **274** (140 mg, 0.33 mg) at 55 ^{o}C for 24 h, trituration with ice-cooled DCM (5 × 10 mL) isolated **275** as a light brown solid (54 mg, 45%); R_f = 0.20 (silica, 20% EtOAc, petrol); m.p. > 400 ^{o}C; UV λ_{max} (EtOH/nm) 242.6 and 220.2; IR ν_{max}/cm^{-1} 3197 (br) indazolo and amino N-H), 2978 (C-H), 2921 (C-H), 1681 (C=O), 1605, 1564, 1512, 1453, 1343, 1312, 1295, 1236, 1159, 1056, 1004, 949,

834, 702; ^{1}H δ/ppm (500 MHz, DMSO-d_6) 5.61 (1H, s, br, thiazole C_5-H), 7.04 (1H, s, br, Ar-H), 7.16 (2H, s, br, Ar-H), 7.50 (1H, s, br, Ar-H), 7.94 (1H, s, br, Ar-H), 8.07 (1H, s, br, Ar-H), 8.20 (2H, s, br, Ar-H), 8.30 (1H, s, br, Ar-H), 13.10 (1H, s, br, N*H*); LC-MS (ESI+) *m/z* = 339.3 $[M+H]^+$ and 337.2 $[M-H]^-$; HRMS mass not observed; Analytical HPLC 94.2%

3-(2-(4-Chlorophenoxy)-3-((4-fluorophenyl)amino)phenyl)propiolic acid (187)

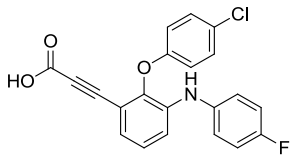

General Procedure A': Using carbamate **186** (100 mg, 0.21 mmol) and TFA (322 µL) in DCM (2.1 mL), partitioning with diethyl ether and saturated aqueous $NaHCO_3$ afforded **187** as a brown solid (74 mg, 93%); R_f = 0.40 (silica, 15% MeOH, DCM); m.p. 149-151 ^{o}C; UV λ_{max} (EtOH/nm) 271.4 and 227.0; IR ν_{max}/cm^{-1} 3428 (N-H), 2923 (C-H), 2822 (br) (O-H), 2217 (C≡C), 1669 (C=O), 1593, 1513, 1473, 1441, 1407, 1337, 1285, 1204 (C-O), 1162, 1088, 825, 779, 742; ^{1}H δ/ppm (500 MHz, DMSO-d_6) 6.78-6.81 (2H, m, Ar-H), 7.02-7.09 (4H, m, Ar-H), 7.13 (1H, dd, Ar-H, *J* = 1.3 and 7.6 Hz), 7.21 (1H, t, Ar-H, *J* = 7.9 Hz), 7.31-7.33 (3H, m, Ar-H), 7.84 (1H, s, N*H*) - CO_2*H* peak not observed); ^{13}C δ/ppm (125 MHz, DMSO-d_6) 78.4, 87.3, 115.4, 115.6, 117.1, 119.3, 120.8, 120.9, 124.8, 125.8, 126.5, 129.2, 138.1, 138.39, 138.41, 144.6, 154.3, 156.1, 156.2, 158.1; ^{19}F δ/ppm (470 MHz, DMSO-d_6) -122.1; LC-MS (ESI+) *m/z* = mass not observed; HRMS calcd. for $C_{21}H_{12}O_3N^{35}ClF$ $[M-H]^-$ 380.0495, found 380.0483; Analytical HPLC: 93.5%

Methyl 3-(2-(4-chlorophenoxy)-3-((4-fluorophenyl)amino)phenyl)propiolate (188)

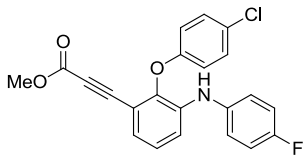

General Procedure A': Using carbamate **182** (49 mg, 0.10 mmol) and TFA (155 µL) in DCM (1.0 mL), partitioning with diethyl ether and saturated aqueous $NaHCO_3$

afforded **188** as a brown oil (33 mg, 85%); R_f = 0.43 (silica, 10% EtOAc, petrol); UV λ_{max} (EtOH/nm) 272.2 and 224.8; IR ν_{max}/cm^{-1} 3383 (N-H), 2952 (C-H), 2220 (C≡C), 1704 (C=O), 1594, 1507, 1482, 1434, 1391, 1337, 1283, 1205 (C-O), 1088, 1040, 1009, 961, 824, 778, 743; ^{1}H δ/ppm (500 MHz, $CDCl_3$) 3.74 (3H, s, CO_2CH_3), 5.88 (1H, s, N*H*), 6.86-6.89 (2H, m, Ar-H), 6.99-7.03 (2H, m, Ar-H), 7.04-7.10 (4H, m, Ar-H), 7.22 (1H, dd, Ar-H, *J* = 2.1 and 8.0 Hz), 7.24-7.26 (2H, m, Ar-H); ^{13}C δ/ppm (125 MHz, $CDCl_3$) 52.7, 81.7, 85.1, 114.7, 116.1, 116.3, 116.9, 117.0, 123.38, 123.44, 124.7, 126.0, 127.8, 129.7, 136.7, 138.8, 144.2, 154.0, 156.0, 158.2, 160.2; ^{19}F δ/ppm (470 MHz, $CDCl_3$) -119.0; LC-MS (ESI+) *m/z* = 396.3 $[M+H]^+$ and 394.2 $[M-H]^-$; HRMS calcd. for $C_{22}H_{16}O_3N^{35}ClF$ $[M+H]^+$ 396.0797, found 396.0800; Analytical HPLC: 94.9%

6-(4-Chlorophenoxy)-5-((4-fluorophenyl)amino)-4'-hydroxy-[1,1'-biphenyl]-3-carboxylic acid (226)

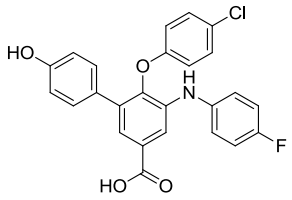

General Procedure B': Using ester **230** (30 mg, 0.07 mmol) and lithium hydroxide monohydrate (55 mg, 1.30 mmol) in 50% THF, H_2O (2.8 mL), chromatography (silica, 0-5%, MeOH, DCM), afforded **226** as a light red solid (22.5 mg, 78%); R_f = 0.30 (silica, 5% MeOH, DCM); m.p. 245-248 ^{o}C; UV λ_{max} (EtOH/nm) 276.6 and 228.0; IR ν_{max}/cm^{-1} 3564 (N-H), 3420 (phenol O-H), 2919 (C-H), 2850 (C-H), 2607 (br) (carboxyl O-H), 1682 (C=O), 1581, 1510, 1413, 1353, 1260, 1214 (C-O), 1186, 1088, 1008, 943, 890, 823, 773; ^{1}H δ/ppm (500 MHz, DMSO-d_6) 6.66-6.68 (2H, m, Ar-H), 6.72-6.73 (2H, m, Ar-H), 7.06-7.13 (4H, m, Ar-H), 7.17-7.19 (2H, m, Ar-H), 7.28-7.29 (2H, m, Ar-H), 7.45 (1H, d, Ar-H, *J* = 1.8 Hz), 7.68 (1H, d, Ar-H, *J* = 1.7 Hz), 7.80 (1H, s, N*H*), 9.54 (1H, s, br, ArO*H*), 13.00 (1H, s, br, CO_2H); ^{13}C δ/ppm (125 MHz, DMSO-d_6) 115.1, 115.5, 115.7, 115.8, 116.8, 121.16, 121.23, 122.4, 125.3, 127.0, 129.0, 129.8, 135.7, 138.3, 138.6, 143.2, 155.4, 156.3, 157.0, 167.0; ^{19}F δ/ppm (470 MHz, DMSO-d_6) -121.9; LC-MS (ESI+) *m/z* = 450.4 $[M+H]^+$ and 448.3 $[M-H]^-$; HRMS calcd. for $C_{25}H_{16}O_4N^{35}ClF$ $[M-H]^-$ 448.0757, found 448.0749; Analytical HPLC: 97.0%

2-(4-Chlorobenzyl)-1-(4-chlorophenyl)-5-(4-fluorophenyl)-1*H*-pyrrole-3-carboxylic acid (220c)

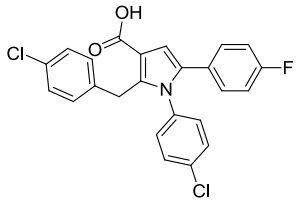

General Procedure B': Using ester **283a** (239 mg, 0.51 mmol) and NaOH (518 mg, 13.0 mmol) in 75% MeOH, H_2O (4.3 mL) at 90 ^oC for 4 h, chromatography (silica, 10-40%, EtOAc, petrol), afforded **220c** as a white solid (182 mg, 81%); R_f = 0.39 (silica, 50% EtOAc, petrol); m.p. 186-187 ^oC; UV λ_{max} (EtOH/nm) 221.4; IR ν_{max}/cm^{-1} 3044 (C-H), 2938 (C-H), 2851 (C-H), 2582 (br) (O-H), 1670 (C=O), 1654, 1560, 1526, 1490, 1458, 1429, 1255, 1234 (C-O), 1152, 1089, 1074, 1015, 938, 835, 774; ^1H δ/ppm (500 MHz, DMSO-d_6) 4.25 (2H, s, C*H*$_2$), 6.76 (1H, s, pyrrole C_4-H), 6.79-6.81 (2H, m, Ar-H), 7.04-7.12 (6H, m, Ar-H), 7.20-7.21 (2H, m, Ar-H), 7.41-7.43 (2H, m, Ar-H), 12.20 (1H, s, br, CO_2*H*); ^{13}C δ/ppm (125 MHz, DMSO-d_6) 29.8, 110.3, 114.0, 115.1, 115.3, 128.0, 129.2, 129.5, 130.1, 130.2, 130.5, 132.9, 133.2, 135.9, 137.7, 138.4, 160.1, 162.1, 165.8; ^{19}F δ/ppm (470 MHz, DMSO-d_6) -114.9; LC-MS (ESI+) *m/z* = 440.2, 442.2, 444.2 $[M+H]^+$ and 438.2, 440.2, 442.1 $[M-H]^-$; HRMS calcd. for $C_{24}H_{15}O_2N^{35}Cl_2F$ $[M-H]^-$ 438.0469, found 438.0462; Analytical HPLC: 96.9%

5-(4-Chlorobenzyl)-1-(4-chlorophenyl)-2-(4-fluorophenyl)-1*H*-pyrrole-3-carboxylic acid (220g)

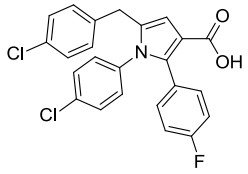

General Procedure B': Using ester **283b** (149 mg, 0.32 mmol) and NaOH (390 mg, 9.75 mmol) in 75% MeOH, H_2O (3.2 mL) at 90 ^oC for 4 h, chromatography (silica, 10-40%, EtOAc, petrol), afforded **220g** as a white solid (124 mg, 88%); R_f = 0.29 (silica, 40% EtOAc, petrol); m.p. 229-231 ^oC; UV λ_{max} (EtOH/nm) 223.0; IR ν_{max}/cm^{-1} 2919 (C-H), 2849 (C-H), 2587 (br) (O-H), 1653 (C=O), 1594, 1527, 1490, 1338, 1259, 1221 (C-O), 1161, 1091, 1013, 987, 842, 797, 739; ^1H δ/ppm (500 MHz, DMSO-d_6) 3.74

(2H, s, ArC*H*$_2$), 6.32 (1H, s, pyrrole C_4-H), 7.01-7.04 (4H, m, Ar-H), 7.10-7.12 (2H, m, Ar-H), 7.17-7.20 (2H, m, Ar-H), 7.28-7.29 (2H, m, Ar-H), 7.35-7.37 (2H, m, Ar-H), 11.74 (1H, s, br, CO_2*H*); ^{13}C δ/ppm (125 MHz, DMSO-d_6) 32.2, 110.3, 114.1, 114.6, 114.8, 128.2, 128.3, 128.6, 129.4, 130.9, 131.1, 131.3, 133.3, 133.5, 133.6, 133.7, 136.3, 137.5, 138.0, 160.9, 162.9, 165.6; ^{19}F δ/ppm (470 MHz, DMSO-d_6) -114.1; LC-MS (ESI+) *m/z* = 440.3 $[M+H]^+$ and 438.2 $[M-H]^-$; HRMS calcd. for $C_{24}H_{15}O_2N^{35}Cl_2F$ $[M-H]^-$ 438.0469, found 438.0462; Analytical HPLC: 97.5%

(3-Bromo-4-(4-chlorophenoxy)-5-nitrophenyl)methanol (232)

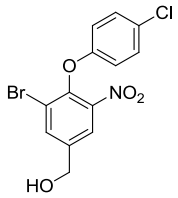

General Procedure D': Using ester **227** (1.92 g, 4.97 mmol) and DIBAL-H (1 M in hexanes, 10.9 mL, 10.9 mmol), the reaction was quenched at 0 ^{o}C with distilled water (0.44 mL), 15% NaOH (0.44 mL) and more distilled water (1.09 mL), filtered through celite and worked up with EtOAc. Chromatography (silica, 50-100%, DCM, petrol), afforded **232** as a yellow solid (1.13 g, 64%); R_f = 0.22 (silica, 100% DCM); m.p. 85-87 ^{o}C; UV λ_{max} (EtOH/nm) 222.2; IR ν_{max}/cm^{-1} 3339 (O-H), 3075 (C-H), 2927 (C-H), 2868 (C-H), 1531, 1482, 1341, 1251 (C-O), 1189, 1087, 1058, 1009, 945, 865, 821, 729; ^{1}H δ/ppm (500 MHz, $CDCl_3$) 1.97 (1H, t, O*H*, *J* = 5.6 Hz), 4.82 (2H, d, ArC*H*$_2$, *J* = 5.6 Hz), 6.77 (2H, d, 4-ClPh C_3-H and C_5-H, *J* = 9.0 Hz), 7.27 (2H, d, 4-ClPh C_2-H and C_6-H, *J* = 9.0 Hz), 7.93-7.94 (2H, m, 3-BrPh C_2-H and C_6-H); ^{13}C δ/ppm (125 MHz, $CDCl_3$) 63.0, 116.7, 120.2, 122.6, 128.2, 129.7, 136.1, 140.3, 144.0, 144.7, 155.5; LC-MS (ESI+) *m/z* = 358.2 $[M+H]^+$; HRMS calcd. for $C_{13}H_{10}O_4N^{79}Br^{35}Cl$ $[M+H]^+$ 357.9476, found 357.9480

***Tert*-butyl (2-(4-chlorophenoxy)-5-(hydroxymethyl)-4'-methoxy-[1,1'-biphenyl]-3-yl)(4-fluorophenyl)carbamate (249)**

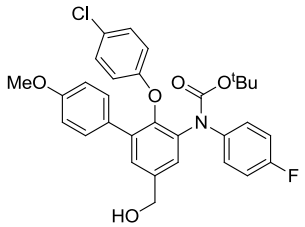

General Procedure D': Using ester **248** (180 mg, 0.31 mmol) and DIBAL-H (1 M in hexanes, 0.69 mL, 0.69 mmol), the reaction was quenched at 0 ^{o}C with distilled water (12 µL), 15% NaOH (12 µL) and more distilled water (31 µL), filtered through celite and worked up with EtOAc. Chromatography (silica, 0-10%, EtOAc, DCM), afforded **249** as a colourless solid (124 mg, 73%); R_f = 0.29 (silica, 100% DCM); m.p. 99-101 ^{o}C; UV λ_{max} (EtOH/nm) 233.8; IR ν_{max}/cm^{-1} 3421 (O-H), 2978 (C-H), 2933 (C-H), 2906 (C-H), 2874 (C-H), 2837 (C-H), 1708 (C=O), 1608, 1506, 1484, 1460, 1436, 1368, 1320, 1228 (C-O), 1158, 1146, 1089, 1042, 1008, 827, 764, 727; ^{1}H δ/ppm (500 MHz, $CDCl_3$) 1.35 (9H, s, $CO_2C(CH_3)_3$), 1.83 (1H, t, O*H*, *J* = 5.8 Hz), 3.75 (3H, s, OCH_3), 4.78 (2H, d, CH_2OH, *J* = 5.9 Hz), 6.56 (2H, d, 4-ClPh C_3-H and C_5-H, *J* = 8.8 Hz), 6.79 (2H, d, 4-MeOPh C_2-H and C_6-H, *J* = 8.8 Hz), 6.88-6.91 (2H, m, 4-FPh C_3-H and C_5-H, *J* = 8.4 Hz), 6.96-6.97 (2H, m, 4-FPh, C_2-H and C_6-H), 7.07 (2H, d, 4-ClPh C_2-H and C_6-H, *J* = 9.1 Hz), 7.30 (2H, d, 4-MeOPh C_3-H and C_5-H, *J* = 8.8 Hz), 7.38 (1H, d, Ar-H, *J* = 2.1 Hz), 7.41 (1H, s, br, Ar-H); ^{13}C δ/ppm (125 MHz, $CDCl_3$) 28.1, 55.2, 64.5, 81.5, 113.7, 114.9, 115.1, 116.7, 126.5, 127.5, 128.0, 128.3, 129.0, 129.1, 130.0, 136.9, 137.9, 138.5, 146.4, 153.3, 156.0, 159.15, 159.20, 171.2; ^{19}F δ/ppm (470 MHz, $CDCl_3$) -117.0; LC-MS (ESI+) *m/z* = mass not observed; HRMS mass not observed

(6-(4-Chlorophenoxy)-4'-methoxy-5-nitro-[1,1'-biphenyl]-3-yl)methanol (250)

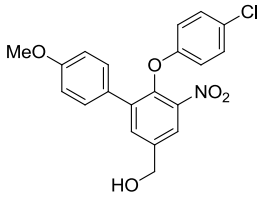

General Procedure D': Using ester **245** (540 mg, 1.30 mmol) and DIBAL-H (1 M in hexanes, 2.86 mL, 2.86 mmol), the reaction was quenched at 0 ^{o}C with distilled water

(52 µL), 15% NaOH (52 µL) and more distilled water (0.13 mL), filtered through celite and worked up with EtOAc. Chromatography (silica, 0-10%, EtOAc, DCM), afforded **250** as a yellow oil (321 mg, 64%); R_f = 0.14 (silica, 100% DCM); UV λ_{max} (EtOH/nm) 260.6; IR ν_{max}/cm^{-1} 3417 (O-H), 3268 (C-H), 3067 (C-H), 1506, 1483, 1305, 1241, 1215 (C-O), 1152, 1082, 1023, 823, 765, 736, 701; ^{1}H δ/ppm (500 MHz, $CDCl_3$) 1.94 (1H, t, O*H*, *J* = 5.7 Hz), 3.78 (3H, s, OC*H*$_3$), 4.84 (2H, d, C*H*$_2$OH, *J* = 5.7 Hz), 6.60 (2H, d, 4-ClPh C_3-H and C_5-H, *J* = 9.0 Hz), 6.84 (2H, d, 4-MeOPh C_2-H and C_6-H, *J* = 8.8 Hz), 7.07 (2H, d, 4-ClPh C_2-H and C_6-H, *J* = 9.1 Hz), 7.35 (2H, d, 4-MeOPh C_3-H and C_5-H, *J* = 8.8 Hz), 7.66 (1H, d, Ar-H, 2.2 Hz), 7.90 (1H, d, Ar-H, *J* = 2.1 Hz); ^{13}C δ/ppm (125 MHz, $CDCl_3$) 55.3, 63.7, 113.9, 116.6, 122.0, 127.4, 127.6, 129.3, 130.2, 133.6, 138.3, 139.0, 143.6, 144.4, 155.9, 159.7; LC-MS (ESI+) *m/z* = 386.3 $[M+H]^+$; HRMS calcd. for $C_{20}H_{17}O_5N^{35}Cl$ $[M+H]^+$ 386.0790, found 386.0795

Ethyl 2-(4-chlorobenzyl)-1-(4-chlorophenyl)-5-(4-fluorophenyl)-1*H*-pyrrole-3-carboxylate (283a)

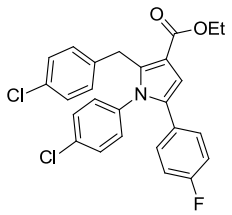

General Procedure E': Using 1,4-diketone **282a** (400 mg, 1.07 mmol) and 4-chloroaniline (682 mg, 5.35 mmol), chromatography (silica, 0-20% Et_2O, petrol) afforded **283a** as a yellow solid (252 mg, 50%); R_f = 0.39 (silica, 20% Et_2O, petrol); m.p. 115-117 ^oC; UV λ_{max} (EtOH/nm) 223.4; IR ν_{max}/cm^{-1} 3050 (C-H), 2972 (C-H), 1693 (C=O), 1565, 1526, 1489, 1420, 1376, 1222 (C-O), 1158, 1067, 1013, 960, 833; ^{1}H δ/ppm (500 MHz, $CDCl_3$) 1.33 (3H, t, $CO_2CH_2CH_3$, *J* = 7.1 Hz), 4.23 (2H, s, Ar*CH*$_2$), 4.32 (2H, q, $CO_2CH_2CH_3$, *J* = 7.1 Hz), 6.79-6.83 (4H, m, Ar-H), 6.86 (2H, t, Ar-H, *J* = 8.6 Hz), 6.97-7.00 (2H, m, Ar-H), 7.13 (2H, d, Ar-H, *J* = 8.3 Hz), 7.24-7.26 (3H, m, Ar-H); ^{13}C δ/ppm (125 MHz, $CDCl_3$) 14.5, 30.8, 59.9, 110.4, 114.2, 115.2, 115.4, 128.4, 129.3, 129.4, 129.97, 130.03, 130.1, 131.8, 133.8, 134.6, 136.0, 137.4, 138.8, 165.1; ^{19}F δ/ppm (470 MHz, $CDCl_3$) -114.6; LC-MS (ESI+) *m/z* = 468.3 $[M+H]^+$; HRMS calcd. for $C_{26}H_{21}O_2N^{35}Cl_2F$ $[M+H]^+$ 468.0928, found 468.0924

3-Bromo-6-chloro-1-(4-methoxybenzyl)-1*H*-indole (210)

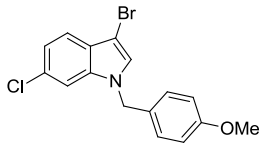

General Procedure I': Using indole **206** (480 mg, 1.77 mmol) and NBS (377 mg, 2.12 mmol) at -78 ^{o}C for 1 h, chromatography (silica, 10-20%, DCM, petrol), afforded **210** as a brown solid (598 mg, 84%); R_f = 0.25 (silica, 20% DCM, petrol); m.p. 53-55 ^{o}C; UV λ_{max} (EtOH/nm) 284.0 and 230.6; IR ν_{max}/cm^{-1} 3114 (C-H), 3000 (C-H), 2929 (C-H), 2834 (C-H), 1609, 1510, 1459, 1321, 1244 (C-O), 1173, 1111, 1030, 947, 798, 761; ^{1}H δ/ppm (500 MHz, $CDCl_3$) 3.79 (3H, s, OC*H*$_3$), 5.16 (2H, s, NC*H*$_2$Ar), 6.86 (2H, d, 4-ClPh C_3-H and C_5-H, *J* = 8.7 Hz), 7.08 (2H, d, 4-ClPh C_2-H and C_6-H, *J* = 8.2 Hz), 7.09 (1H, s, indole C_2-H), 7.15 (1H, dd, indole C_5-H, *J* = 1.8 and 8.5 Hz), 7.30 (1H, d, indole C_7-H, *J* = 1.5 Hz), 7.47 (1H, d, indole C_4-H, *J* = 8.5 Hz); ^{13}C δ/ppm (125 MHz, $CDCl_3$) 50.0, 55.3, 90.3, 109.9, 114.4, 120.5, 121.1, 126.2, 127.6, 128.1, 128.5, 129.0, 136.1, 159.5; LC-MS (ESI+) *m/z* = mass not observed; HRMS mass not observed

***Tert*-butyl 3-bromo-6-chloro-1*H*-indole-1-carboxylate (213)**

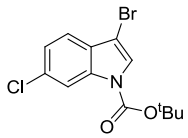

General Procedure I': Using indole **212** (731 mg, 2.90 mmol) and NBS (570 mg, 3.20 mmol) in DMF (6.7 mL) at 60 ^{o}C for 1 h, chromatography (silica, 0-10%, DCM, petrol), afforded **213** as a white solid (827 mg, 86%); R_f = 0.49 (silica, 10% DCM, petrol); m.p. 124-126 ^{o}C; UV λ_{max} (EtOH/nm) 271.8 and 231.4; IR ν_{max}/cm^{-1} 3149 (C-H), 2987 (C-H), 2938 (C-H), 1732 (C=O), 1605, 1572, 1540, 1450, 1430, 1366, 1320, 1281, 1243, 1210, 1152, 1085, 953, 842, 805, 761, 729; ^{1}H δ/ppm (500 MHz, $CDCl_3$) 1.67 (9H, s, C(C*H*$_3$)$_3$), 7.29 (1H, dd, C_5-H, *J* = 1.8 and 8.4 Hz), 7.44 (1H, d, C_4-H, 8.4 Hz), 7.61 (1H, s, C_2-H), 8.21 (1H, s, br, C_7-H); ^{13}C δ/ppm (125 MHz, $CDCl_3$) 28.1, 84.9, 97.6, 115.5, 120.4, 123.9, 125.3, 128.0, 131.6, 134.9, 148.5; LC-MS (ESI+) *m/z* = mass not observed; HRMS mass not observed

((2-(4-Chlorophenoxy)-3-nitrophenyl)ethynyl)triisopropylsilane (176)

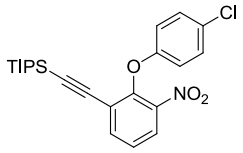

General Procedure J': Using aryl bromide **135a** (100 mg, 0.30 mmol) and TIPS-acetylene (0.1 mL, 82 mg, 0.45 mmol), chromatography (silica, 10-20%, DCM, petrol), afforded **176** as a yellow oil (109 mg, 84%); R_f = 0.22 (silica, 20% DCM, petrol); UV λ_{max} (EtOH/nm) 249.8 and 226.0; IR ν_{max}/cm^{-1} 2942 (C-H), 2864 (C-H), 2150 (C≡C), 1533, 1484, 1462, 1352, 1240 (C-O), 1197, 1091, 1010, 942, 879, 822, 807, 749, 675; ^{1}H δ/ppm (500 MHz, $CDCl_3$) 0.95 (21H, s, Si((C*H*(C*H*$_3$)$_2$)$_3$), 6.75-6.79 (2H, m, Ar-H), 7.20-7.23 (2H, m, Ar-H), 7.33 (1H, t, C_5-H, *J* = 7.8 Hz), 7.76 (1H, dd, C_6-H, *J* = 1.6 and 7.8 Hz), 7.90(1H, dd, C_4-H, *J* = 1.6 and 8.2 Hz); ^{13}C δ/ppm (125 MHz, $CDCl_3$) 11.0, 18.4, 99.2, 101.2, 116.7, 121.7, 125.1, 125.4, 127.7, 129.4, 138.6, 144.3, 148.3, 156.2; LC-MS (ESI+) *m/z* = mass not observed; HRMS calcd. for $C_{23}H_{29}O_3N^{35}ClSi$ $[M+H]^+$ 430.1600, found 430.1595

3-Bromo-2-(4-chlorophenoxy)aniline (171)

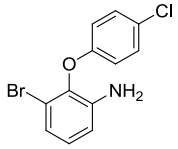

General Procedure K': Using **135a** (1.40 g, 4.26 mmol) and $SnCl_2.2H_2O$ (5.77 g, 25.6 mmol), filtration through celite, work-up with EtOAc and distilled water and concentration *in vacuo* isolated **171** as a brown solid (1.26 g, 93%); R_f = 0.43 (silica, 20% EtOAc, petrol); m.p. 62-64 ^{o}C; UV λ_{max} (EtOH/nm) 286.6; IR ν_{max}/cm^{-1} 3485 and 3392 (N-H), 3185 (C-H), 3081 (C-H), 1609, 1586, 1473, 1315, 1223 (C-O), 1201, 1161, 1093, 1039, 1009, 888, 860, 828, 772, 737; ^{1}H δ/ppm (500 MHz, $CDCl_3$) 4.14 (2H, s, br, N*H*$_2$), 6.78 (1H, dd, Ar-H, *J* = 1.4 and 8.0 Hz), 6.82 (2H, d, 4-ClPh C_3-H and C_5-H, *J* = 9.0 Hz), 6.95 (1H, t, 3-BrPh C_5-H, *J* = 8.0 Hz), 7.02 (1H, dd, Ar-H, *J* = 1.3 and 8.0 Hz), 7.24 (2H, d, 4-ClPh C_2-H and C_6-H, *J* = 9.0 Hz); ^{13}C δ/ppm (125 MHz, $CDCl_3$) 116.2, 116.3, 117.8, 123.7, 127.3, 127.4, 129.7, 138.7, 140.0, 155.2; LC-MS (ESI+) *m/z* = 298.2, 300.2 and 302.2 $[M+H]^+$; HRMS mass not observed

2-(4-Chlorophenoxy)-3-((triisopropylsilyl)ethynyl)aniline (177)

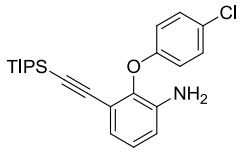

General Procedure K': Using **176** (970 mg, 2.26 mmol) and $SnCl_2.2H_2O$ (3.06 g, 13.6 mmol), filtration through celite, work-up with EtOAc and distilled water and concentration *in vacuo* isolated **177** as a yellow oil (897 mg, 99.5%); R_f = 0.35 (silica, 30% DCM, petrol); UV λ_{max} (EtOH/nm) 265.2 and 230.4; IR ν_{max}/cm^{-1} 3481 and 3389 (N-H), 2941 (C-H), 2863 (C-H), 2152 (C≡C), 1613, 1464, 1320, 1220 (C-O), 1161, 1090, 1059, 989, 880, 824, 756, 726, 656; ^{1}H δ/ppm (500 MHz, $CDCl_3$) 0.94-0.95 (21H, m, Si((C*H*(C*H*$_3$)$_2$)$_3$), 4.56 (2H, s, br, N*H*$_2$), 6.80 (2H, d, 4-ClPh C_3-H and C_5-H, *J* = 9.0 Hz), 6.84 (1H, dd, Ar-H, *J* = 2.0 and 7.5 Hz), 6.97-7.03 (2H, m, Ar-H), 7.18 (2H, d, 4-ClPh C_2-H and C_6-H, *J* = 9.0 Hz); ^{13}C δ/ppm (125 MHz, $CDCl_3$) 11.1, 18.4, 96.8, 101.7, 116.4, 117.3, 118.6, 123.1, 124.5, 125.8, 126.8, 129.3, 142.2, 156.0; LC-MS (ESI+) *m/z* = 400.5 and 402.5 $[M+H]^+$; HRMS calcd. for $C_{23}H_{31}ON^{35}ClSi$ $[M+H]^+$ 400.1858, found 400.1858

5-Amino-6-(4-chlorophenoxy)-4'-hydroxy-[1,1'-biphenyl]-3-carboxylic acid (225)

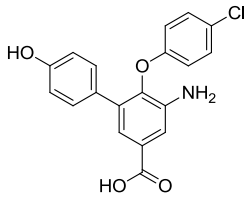

General Procedure K': Using **224** (60 mg, 0.16 mmol) and $SnCl_2.2H_2O$ (211 mg, 0.94 mmol), filtration through celite, work-up with EtOAc and 0.5 M HCl, H_2O and concentration *in vacuo* isolated **225** as a brown solid (46 mg, 84%); R_f = 0.26 (silica, 10% MeOH, DCM); m.p. 235-237 ^{o}C; UV λ_{max} (EtOH/nm) 246.8 and 228.2; IR ν_{max}/cm^{-1} 3351 and 3282 (N-H), 3067 (phenol O-H), 3058 (C-H), 2631 (carboxyl O-H), 1700 (C=O), 1596, 1519, 1481, 1401, 1333, 1260, 1205 (C-O), 1171, 1089, 1008, 928, 873, 824, 812, 678; ^{1}H δ/ppm (500 MHz, DMSO-d_6) 5.23 (2H, s, br, N*H*$_2$), 6.67 (2H, d, 4-ClPh C_3-H and C_5-H, *J* = 9.0 Hz), 6.68 (2H, d, 4-HOPh C_2-H and C_6-H, *J* = 8.5 Hz), 7.16 (1H, d, Ar-H, *J* = 2.1 Hz), 7.20 (2H, d, 4-ClPh, C_2-H and C_6-H, *J* = 8.9 Hz), 7.24 (2H, d, 4-HOPh, C_3-H and C_5-H, *J* = 8.5 Hz), 7.40 (1H, d, Ar-H, *J* = 2.1 Hz), 9.46 (1H,

s, ArO*H*), 12.73 (1H, s, br, CO_2H); ^{13}C δ/ppm (125 MHz, DMSO-d_6) 115.0, 115.1, 116.7, 118.6, 125.1, 127.5, 128.4, 129.1, 129.7, 135.0, 139.8, 142.0, 155.3, 156.7, 167.3; LC-MS (ESI+) *m/z* = 356.3 $[M+H]^+$ and 354.2 $[M-H]^-$; HRMS calcd. for $C_{19}H_{13}O_4N^{35}Cl$ $[M-H]^-$ 354.0539, found 354.0533

Methyl 5-amino-6-(4-chlorophenoxy)-4'-hydroxy-[1,1'-biphenyl]-3-carboxylate (229)

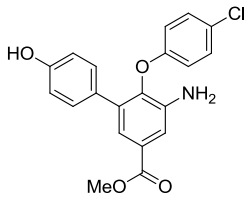

General Procedure K': Using **228** (249 mg, 0.62 mmol) and $SnCl_2.2H_2O$ (844 mg, 3.74 mmol), filtration through celite, work-up with EtOAc and distilled water and concentration *in vacuo* isolated **229** as a brown solid (217 mg, 94%); R_f = 0.36 (silica, 40% EtOAc, petrol); m.p. 175-177 ^oC; UV λ_{max} (EtOH/nm) 328.4, 251.0 and 227.4; IR ν_{max}/cm^{-1} 3472 (N-H), 3382 (N-H and phenol O-H), 3027 (C-H), 2951 (C-H), 1681 (C=O), 1612, 1519, 1481, 1439, 1361, 1256, 1212 (C-O), 1163, 1092, 1006, 930, 882, 819, 772; ^{1}H δ/ppm (500 MHz, $CDCl_3$) 3.91 (3H, s, CO_2CH_3), 3.97 (2H, s, br, NH_2), 4.80 (1H, s, br, ArO*H*), 6.65 (2H, d, Ar-H, *J* = 9.1 Hz), 6.74(2H, d, Ar-H, *J* = 8.7 Hz), 7.09 (2H, d, Ar-H, *J* = 9.0 Hz), 7.30 (2H, d, Ar-H, *J* = 8.6 Hz), 7.48 (1H, d, Ar-H, *J* = 2.0 Hz), 7.51 (1H, d, Ar-H, *J* = 2.0 Hz); ^{13}C δ/ppm (125 MHz, $CDCl_3$) 52.2, 115.1, 116.1, 116.3, 121.9, 127.0, 128.0, 129.3, 129.5, 130.3, 135.7, 140.3, 141.6, 155.1, 155.2, 166.8; LC-MS (ESI+) *m/z* = 370.3 $[M+H]^+$ and 368.2 $[M-H]^-$; HRMS calcd. for $C_{20}H_{15}O_4N^{35}Cl$ $[M-H]^-$ 368.0695, found 368.0682

2-(5-Amino-6-(4-chlorophenoxy)-4'-hydroxy-[1,1'-biphenyl]-3-yl)acetonitrile (242)

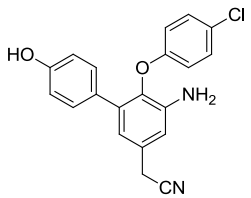

General Procedure K': Using **241** (63 mg, 0.17 mmol) and $SnCl_2.2H_2O$ (325 mg, 1.44 mmol), filtration through celite, work-up with EtOAc and distilled water and chromatography (0-70% Et_2O, petrol) isolated **242** as a yellow solid (38.8 mg, 67%); R_f

= 0.34 (silica, 40% EtOAc, petrol); m.p. 50-52 ^{o}C; UV λ_{max} (EtOH/nm) 232.6; IR ν_{max}/cm^{-1} 3446 and 3368 (N-H), 3201 (br) (O-H), 3032 (C-H), 2956 (C-H), 2924 (C-H), 2855 (C-H), 2254 (C≡N), 1611, 1588, 1478, 1444, 1424, 1355, 1260, 1214 (C-O), 1159, 1089, 1006, 926, 822; ^{1}H δ/ppm (500 MHz, DMSO-d_6) 3.96 (2H, s, ArC*H*$_2$), 5.14 (2H, s, N*H*$_2$), 6.53 (1H, s, br, Ar-H), 6.66-6.68 (4H, m, 4-ClPh C_3-H, C_5-H and 4-HOPh C_2-H and C_6-H), 6.76 (1H, s, br, Ar-H), 7.18-7.23 (4H, m, 4-ClPh C_2-H, C_6-H and 4-HOPh C_3-H and C_5-H), 9.43 (1H, s, ArO*H*); ^{13}C δ/ppm (125 MHz, DMSO-d_6) 22.6, 114.0, 115.5, 117.1, 117.4, 119.9, 125.4, 128.2, 129.3, 129.5, 130.1, 135.8, 136.4, 142.7, 156.3, 157.2; LC-MS (ESI+) *m/z* = 351.1 $[M+H]^+$ and 349.2 $[M-H]^-$; HRMS calcd. for $C_{20}H_{14}O_2N_2{}^{35}Cl$ $[M-H]^-$ 349.0749, found 349.0743; Analytical HPLC: 96.2%

tert-Butyl 6-chloro-1*H*-indole-1-carboxylate (212)

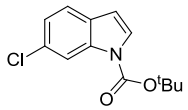

General Procedure L': Using indole **199** (200 mg, 1.32 mmol), Boc_2O (607 µL, 576 mg, 2.64 mmol) and DMAP (322 mg, 2.64 mmol) at room temperature for 1 h, chromatography (silica, 0-10%, DCM, petrol), afforded **212** as a colourless solid (306 mg, 95%); R_f = 0.18 (silica, 10% DCM, petrol); m.p. 97-100 ^{o}C; UV λ_{max} (EtOH/nm) 258.4 and 228.8; IR ν_{max}/cm^{-1} 2978 (C-H), 1732 (C=O), 1606, 1528, 1434, 1371, 1333, 1247, 1204, 1150, 1120, 1092, 1021, 896, 851, 809, 760, 718; ^{1}H δ/ppm (500 MHz, $CDCl_3$) 1.67 (9H, s, C(C*H*$_3$)$_3$), 6.54 (1H, d, C_3-H, *J* = 3.5 Hz), 7.20 (1H, dd, C_5-H, *J* = 1.9 and 8.3 Hz), 7.46 (1H, d, C_4-H, *J* = 8.3 Hz), 7.57 (1H, dd, C_2-H, *J* = 3.3 Hz), 8.19 (1H, s, br, C_7-H); ^{13}C δ/ppm (125 MHz, $CDCl_3$) 28.2, 84.2, 107.0, 115.5, 121.6, 123.2, 126.4, 129.0, 130.2, 135.6, 149.4; LC-MS (ESI+) *m/z* = mass not observed; HRMS mass not observed

Methyl 5-((*tert*-butoxycarbonyl)(4-fluorophenyl)amino)-6-(4-chlorophenoxy)-4'-methoxy-[1,1'-biphenyl]-3-carboxylate (248)

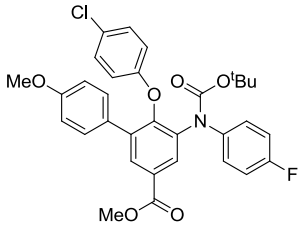

General Procedure L': Using aniline **247** (200 mg, 0.42 mmol), Boc_2O (183 mg, 0.84 mmol) and DMAP (10.3 mg, 0.084 mmol) at 60 ^oC for 2 h, chromatography (silica, 50-80%, DCM, petrol), afforded **248** as a yellow solid (202 mg, 93%); R_f = 0.20 (silica, 80% DCM, petrol); m.p. 92-95 ^oC; UV λ_{max} (EtOH/nm) 256.8 and 227.0; IR ν_{max}/cm^{-1} 3071 (C-H), 2953 (C-H), 2839 (C-H), 1713 (C=O), 1609, 1507, 1485, 1458, 1434, 1349, 1320, 1293, 1217 (C-O), 1159, 1091, 1056, 1033, 1007, 827, 798, 766 ; ^1H δ/ppm (500 MHz, $CDCl_3$) 1.36 (9H, s, $C(CH_3)_3$), 3.76 (3H, s, $ArOCH_3$), 3.96 (3H, s, CO_2CH_3), 6.55 (2H, d, 4-ClPh C_3-H and C_5-H, *J* = 8.8 Hz), 6.80 (2H, d, 4-MeOPh C_2-H and C_6-H, *J* = 8.8 Hz), 6.89-6.93 (2H, m, 4-FPh C_3-H and C_5-H, *J* = 8.4 Hz), 6.96-6.99 (2H, m, 4-FPh, C_2-H and C_6-H), 7.07 (2H, d, 4-ClPh C_2-H and C_6-H, *J* = 9.0 Hz), 7.31 (2H, d, 4-MeOPh C_3-H and C_5-H, *J* = 8.8 Hz), 8.07 (1H, s, br, Ar-H), 8.08 (1H, d, Ar-H, *J* = 2.2 Hz); ^{13}C δ/ppm (125 MHz, $CDCl_3$) 28.1, 52.5, 55.2, 81.8, 113.8, 115.1, 115.3, 116.8, 127.0, 127.5, 127.7, 128.3, 129.1, 130.1, 131.0, 131.2, 136.5, 137.1, 137.5, 151.0, 153.1, 155.5, 159.3, 159.4, 161.3, 165.9; ^{19}F δ/ppm (470 MHz, $CDCl_3$) -116.7; LC-MS (ESI+) *m/z* = mass not observed; HRMS mass not observed

Ethyl 5-(4-chlorophenyl)-2-(4-fluorobenzoyl)-4-oxopentanoate (282b)

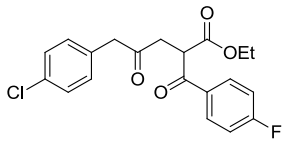

General Procedure S': Using ethyl 3-(4-fluorophenyl)-3-oxopropanoate (201 µL, 235 mg, 1.12 mmol), α-bromoketone **286** (233 mg, 0.94 mmol) and sodium hydride (60% in mineral oil, 56 mg, 1.40 mmol), chromatography (silica, 10-20%, EtOAc, petrol), afforded **282b** as a yellow oil (165 mg, 47%); R_f = 0.38 (silica, 20% EtOAc, petrol); UV λ_{max} (EtOH/nm) 247.8; IR ν_{max}/cm^{-1} 3071 (C-H), 2982 (C-H), 2908 (C-H), 1719 (C=O), 1681 (C=O), 1595 (C=O), 1491, 1408, 1329, 1232 (C-O), 1156, 1090, 1014, 956, 846,

811; ^{1}H δ/ppm (500 MHz, $CDCl_3$) 1.14 (3H, t, $CO_2CH_2CH_3$, *J* = 7.2 Hz), 3.14 (1H, dd, CH_2COCH_2Ar, *J* = 5.8 and 18.3 Hz), 3.28 (1H, dd, CH_2COCH_2Ar, *J* = 8.0 and 18.3 Hz), 3.77 (2H, d, $ArCH_2$, *J* = 1.5 Hz), 4.11 (2H, q, $CO_2CH_2CH_3$, *J* = 7.2 Hz), 4.83 (1H, dd, $COCHCO_2Et$, *J* = 5.08 and 8.0 Hz), 7.12-7.16 (4H, m, Ar-H), 7.29-7.30 (2H, m, Ar-H), 8.02-8.05 (2H, m, Ar-H); ^{13}C δ/ppm (125 MHz, $CDCl_3$) 13.9, 41.0, 48.8, 48.9, 61.9, 115.8, 115.9, 128.9, 130.9, 131.6, 131.7, 131.9, 132.37, 132.40, 133.2, 165.1, 167.1, 168.8, 192.8, 204.8; ^{19}F δ/ppm (470 MHz, $CDCl_3$) -104.0; LC-MS (ESI+) *m/z* = 375.1 $[M-H]^-$; HRMS calcd. for $C_{20}H_{19}O_4{}^{35}ClF$ $[M+H]^+$ 377.0950, found 377.0952

2-(6-(4-Chlorophenoxy)-4'-methoxy-5-nitro-[1,1'-biphenyl]-3-yl)acetonitrile (250a)

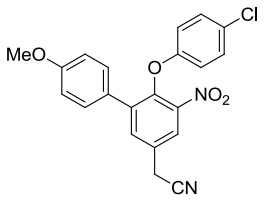

General Procedures T' and V': Using alcohol **250** (327 mg, 0.85 mmol) and methanesulfonic anhydride (223 mg, 1.28 mmol), the crude mesylate was dissolved in acetonitrile (3.4 mL) and mixed with TMS-cyanide (160 µL, 127 mg, 1.28 mmol) and TBAF (1 M in THF, 1.28 mL, 1.28 mmol). Chromatography (silica, 10-30%, EtOAc, petrol), afforded **250a** as a yellow oil (69 mg, 21%); R_f = 0.25 (silica, 30% EtOAc, petrol); UV λ_{max} (EtOH/nm) 263.0; IR ν_{max}/cm^{-1} 3069 (C-H), 2932 (C-H), 2837 (C-H), 2254 (C≡N), 1607, 1535, 1513, 1483, 1408, 1348, 1297, 1236 (C-O), 1179, 1090, 1027, 825, 793, 736; ^{1}H δ/ppm (500 MHz, $CDCl_3$) 3.79 (3H, s, OCH_3), 3.88 (2H, s, CH_2CN), 6.58 (2H, d, 4-ClPh C_3-H and C_5-H, *J* = 8.8 Hz), 6.84 (2H, d, 4-MeOPh C_2-H and C_6-H, *J* = 8.6 Hz), 7.08 (2H, d, 4-ClPh C_2-H and C_6-H, *J* = 8.8 Hz), 7.34 (2H, d, 4-MeOPh C_3-H and C_5-H, *J* = 8.6 Hz), 7.65 (1H, s, Ar-H), 7.84 (1H, s, Ar-H); ^{13}C δ/ppm (125 MHz, $CDCl_3$) 23.1, 55.3, 114.1, 116.4, 116.6, 123.3, 126.8, 127.7, 128.0, 129.4, 130.2, 134.8, 139.5, 144.4, 144.7, 155.6, 160.0; LC-MS (ESI+) *m/z* = 393.1 $[M-H]^-$; HRMS calcd. for $C_{21}H_{15}O_4N_2{}^{35}Cl$ $[M+H]^+$ 394.0715, found 394.0715

Chapter Eight: Bibliography

1. Jemal, A.; Bray, F.; Center, M. M.; Ferlay, J.; Ward, E.; Forman, D., Global Cancer Statistics. *CA: Cancer J. Clin.* **2011,** *61*, 69-90.
2. Zimonjic, D.; Brooks, M. W.; Popescu, N., Derivation of Human Tumor Cells in Vitro without Widespread Genomic Instability. *Cancer Res.* **2001,** *61*, 8838-8844.
3. Hanahan, D.; Weinberg, R. A., The Hallmarks of Cancer. *Cell* **2000,** *100*, 57-70.
4. Hanahan, D.; Weinberg, R. A., Hallmarks of Cancer: The Next Generation. *Cell* **2011,** *144*, 646-674.
5. Kerr, J. F.; Wyllie, A. H.; Currie, A. R., Apoptosis: a Basic Biological Phenomenon with Wide-Ranging Implications in Tissue Kinetics. *Br. J. Cancer* **1972,** *26*, 239-257.
6. Symonds, H.; Krall, L.; Remington, L.; Saenz-Robels, M.; Lowe, S.; Jacks, T.; Van Dyke, T., P53-Dependent Apoptosis Suppresses Tumour Growth and Progression In Vivo. *Cell* **1994,** *78*, 703-711.
7. Wyllie, A. H.; Kerr, J. F.; Currie, A. R., Cell Death: the Significance of Apoptosis. *Int. Rev. Cytol.* **1980,** *68*, 251-306.
8. Harris, C. C., P53 Tumour Suppressor Gene: from the Basic Research Laboratory to the Clinic - an Abridged Historical Perspective. *Carcinogenesis* **1996,** *17*, 1187-1198.
9. Kamal, A.; Mohammed, A. A.; Shaik, T. B., p53–MDM2 Inhibitors: Patent Review (2009 – 2010). *Expert Opin. Ther. Pat.* **2012,** *22*, 95-105.
10. Hu, B.; Gilkes, D. M.; Farooqi, B.; Sebti, S. M.; Chen, J., MDMX Overexpression Prevents p53 Activation by the MDM2 Inhibitor Nutlin. *J. Biol. Chem.* **2006,** *281*, 33030-33035.
11. Hayflick, L., Mortality and Immortality at the Cellular Level. A Review. *Biochem.* **1997,** *62*, 1180-1190.
12. Wright, W. E.; Pereira-Smith, O. M.; Shay, J. W., Reversible Cellular Senescence: Implications for Immortalisation of Normal Human Diploid Fibroblasts. *Mol. Cell. Biol.* **1989,** *9*, 3088-3092.
13. Bouck, N.; Stellmach, V.; Hsu, S. C., How Tumours Become Angiogenic. *Adv. Cancer Res.* **1996,** *69*, 135-174.
14. Hanahan, D.; Folkman, J., Patterns and Emerging Mechanisms of the Angiogenic Switch During Tumorigenesis. *Cell* **1996,** *86*, 353-364.
15. Saaristo, A.; Karpanen, T.; Alitalo, K., Mechanisms of Angiogenesis and Their Use in the Inhibition of Tumor Growth and Metastasis. *Nature* **2000,** *19*, 6122-6129.
16. Frixen, U. H.; Behrens, J.; Sachs, M.; Eberle, G.; Voss, B.; Warda, A.; Ltehner, D.; Bircluneier, W., E-Cadherin-Mediated Cell-Cell Adhesion Prevents Invasiveness of Human Carcinoma Cells. *J. Cell Biol.* **1991,** *113*, 173-185.
17. Sporn, M. B., The War on Cancer. *Lancet* **1996,** *347*, 1377-1381.
18. Christofori, G.; Semb, H., The Role of the Cell-Adhesion Molecule E-cadherin as a Tumour-Suppressor Gene. *Trends Biochem. Sci.* **1999,** *24*, 73-76.
19. Pleasance, E. D.; Stephens, P. J.; O'Meara, S.; McBride, D. J.; Meynert, A.; Jones, D.; Lin, M.-L.; Beare, D.; Lau, K. W.; Greenman, C.; Varela, I.; Nik-Zainal, S.; Davies, H. R.; Ordonez, G. R.; Mudie, L. J.; Latimer, C.; Edkins, S.; Stebbings, L.; Chen, L.; Jia, M.; Leroy, C.; Marshall, J.; Menzies, A.; Butler, A.; Teague, J. W.; Mangion, J.; Sun, Y. A.; McLaughlin, S. F.; Peckham, H. E.; Tsung, E. F.; Costa, G. L.; Lee, C. C.; Minna, J. D.; Gazdar, A.; Birney, E.; Rhodes, M. D.; McKernan, K. J.; Stratton, M. R.; Futreal, P. A.; Campbell, P. J., A Small-Cell Lung Cancer Genome with Complex Signatures of Tobacco Exposure. *Nature* **2010,** *463*, 184-190.

20. Secretan, B.; Straif, K.; Baan, R.; Grosse, Y.; El Ghissassi, F.; Bouvard, V.; Benbrahim-Tallaa, L.; Guha, N.; Freeman, C.; Galichet, L.; Cogliano, V., A Review of Human Carcinogens—Part E: Tobacco, Areca Nut, Alcohol, Coal Smoke, and Salted Fish. *Lancet Oncol.* **2009,** *10*, 1033-1034.
21. Wells, A. J., Breast Cancer, Cigarette Smoking, and Passive Smoking. *Am. J. Epidemiol.* **1991,** *133*, 208-210.
22. Lange, S. S.; Takata, K.-i.; Wood, R. D., DNA Polymerases and Cancer. *Nat. Rev. Cancer* **2011,** *11*, 96-110.
23. Fong, P. C.; Boss, D. S.; Yap, T. A.; Tutt, A.; Wu, P.; Mergui-Roelvink, M.; Mortimer, P. S., H.; Lau, A.; O'Connor, M. J.; Ashworth, A.; Carmichael, J.; Kaye, S. B.; Schellens, J.; de Bono, J. S., Inhibition of Poly(ADP-Ribose) Polymerase in Tumors from BRCA Mutation Carriers. *N. Engl. J. Med.* **2009,** *361*, 123-134.
24. Pan, A.; Sun, Q.; Bernstein, A. M.; Schulze, M. B.; Manson, J. E.; Stampfer, M. J.; Willett, W. C.; Hu, F. B., Red Meat Consumption and Mortality: Results from 2 Prospective Cohort Studies. *Arch. Intern. Med.* **2012,** *172*, 555-563.
25. Narayanan, D. L.; Saladi, R. N.; Fox, J. L., Review: Ultraviolet Radiation and Skin Cancer. *Int. J. Dermatol.* **2010,** *49*, 978-986.
26. de Sanjose, S.; Quint, W. G. V.; Alemany, L.; Geraets, D. T.; Klaustermeier, J. E.; Lloveras, B.; Tous, S.; Felix, A.; Bravo, L. E.; Shin, H.-R.; Vallejos, C. S.; de Ruiz, P. A.; Lima, M. A.; Guimera, N.; Clavero, O.; Alejo, M.; Llombart-Bosch, A.; Cheng-Yang, C.; Tatti, S. A.; Kasamatsu, E.; Iljazovic, E.; Odida, M.; Prado, R.; Seoud, M.; Grce, M.; Usubutun, A.; Jain, A.; Suarez, G. A. H.; Lombardi, L. E.; Banjo, A.; Menéndez, C.; Domingo, E. J.; Velasco, J.; Nessa, A.; Chichareon, S. C. B.; Qiao, Y. L.; Lerma, E.; Garland, S. M.; Sasagawa, T.; Ferrera, A.; Hammouda, D.; Mariani, L.; Pelayo, A.; Steiner, I.; Oliva, E.; Meijer, C. J. L. M.; Al-Jassar, W. F.; Cruz, E.; Wright, T. C.; Puras, A.; Llave, C. L.; Tzardi, M.; Agorastos, T.; Garcia-Barriola, V.; Clavel, C.; Ordi, J.; Andújar, M.; Castellsagué, X.; Sánchez, G. I.; Nowakowski, A. M.; Bornstein, J.; Muñoz, N.; Bosch, F. X., Human Papillomavirus Genotype Attribution in Invasive Cervical Cancer: a Retrospective Cross-Sectional Worldwide Study. *Lancet Oncol.* **2010,** *11*, 1048-1056.
27. Polk, D. B.; Peek, R. M., Helicobacter Pylori: Gastric Cancer and Beyond. *Nat. Rev. Cancer* **2010,** *10*, 403-414.
28. Povirk, L. F.; Shuker, D. E., DNA Damage and Mutagenesis Induced by Nitrogen Mustards. *Mutat. Res-Rev. Genet.* **1994,** *318*, 205-226.
29. Chabner, B. A.; Roberts, T. G., Chemotherapy and the War on Cancer. *Nat. Rev. Cancer* **2005,** *5*, 65-72.
30. Karran, P., Thiopurines, DNA Damage, DNA Repair and Therapy-Related Cancer. *Br. Med. Bull.* **2006,** *79-80*, 153-170.
31. Longley, D. B.; Harkin, D. P.; Johnston, P. G., 5-Fluorouracil: Mechanisms of Action and Clinical Strategies. *Nat. Rev. Cancer* **2003,** *3*, 330-338.
32. Johnson, I. S.; Armstrong, J. G.; Gorman, M.; Burnett, J. P. J., The Vinca Alkaloids: a New Class of Oncolytic Agents. *Cancer Res.* **1963,** *23*, 1390-1427.
33. Bensch, K. G.; Malawista, S. E., Microtubule Crystals: a New Biophysical Phenomenon Induced by Vinca Alkaloids. *Nature* **1968,** *218*, 1176-1177.
34. Cragg, G. M.; Newman, D. J., Plants as a Source of Anti-Cancer Agents. *J. Ethnopharmacol.* **2005,** *100*, 72-79.
35. Rozencweig, M.; Von Hoff, D. D.; Slavik, M.; Muggia, F. M., *Cis*-diamminedichloroplatinum(II): a New Anticancer Drug. *Ann. Intern. Med.* **1977,** *86*, 803-812.
36. Eastman, A., Reevaluation of Interaction of *cis*-dichloro(ethylenediamine) Platinum(II) (Cisplatin) to DNA. *Biochem.* **1986,** *25*, 3912.

37. Rice, J. A.; Crothers, D. M.; Pinto, A. L.; Lippard, S. J., The Major Adduct of the Antitumor Drug *cis*-Diamminedichloroplatinum(II) with DNA Bends the Duplex by ~ 40^{o} Toward the Major Groove. *Proc. Natl. Acad. Sci. USA* **1988,** *85*, 4158-4161.
38. Wu, H.; Chang, D.; Huang, C., Targeted Therapy for Cancer. *J. Cancer Mol.* **2006,** *2*, 57-66.
39. Allen, T. M., Ligand-Targeted Therapeutics in Anticancer Therapy. *Nat. Rev. Cancer* **2002,** *2*, 750-763.
40. Gamble, L. J.; Borovjagin, A. V.; Matthews, Q. L., Role of RGD-Containing Ligands in Targeting Cellular Integrins: Applications for Ovarian Cancer Virotherapy (Review) *Exp. Ther. Med.* **2010,** *1*, 233-240.
41. Rosa, D. D.; Ismael, G.; Lago, L. D.; Awada, A., Molecular-Targeted Therapies: Lessons from Years of Clinical Development. *Cancer Treat. Rev.* **2008,** *34*, 61-80.
42. Verweij, J.; Casali, P. G.; Zalcberg, J.; LeCesne, A.; Reichardt, P.; Blay, J.-Y.; Issels, R.; van Oosterom, A.; Hogendoorn, P. C. W.; Van Glabbeke, M.; Bertulli, R.; Judson, I., Progression-free Survival in Gastrointestinal Stromal Tumours with High-dose Imatinib: Randomised Trial. *Lancet* **2004,** *364*, 1127-1134.
43. Paez, J. G.; Jänne, P. A.; Lee, J. C.; Tracy, S.; Greulich, H.; Gabriel, S.; Herman, P.; Kaye, F. J.; Lindeman, N.; Boggon, T. J.; Naoki, K.; Sasaki, H.; Fujii, Y.; Eck, M. J.; Sellers, W. R.; Johnson, B. E.; Meyerson, M., EGFR Mutations in Lung Cancer: Correlation with Clinical Response to Gefitinib Therapy. *Science* **2004,** *304*, 1497-1500.
44. Shepherd, F. A.; Rodrigues, P. J.; Ciuleanu, T.; Tan, E. H.; Hirsh, V.; Thongprasert, S.; Campos, D.; Maoleekoonpiroj, S.; Smylie, M.; Martins, R.; van Kooten, M.; Dediu, M.; Findlay, B.; Tu, D.; Johnston, D.; Bezjak, A.; Clark, G.; Santabarbara, P.; Seymour, L., Erlotinib in Previously Treated Non-Small-Cell Lung Cancer. *N. Engl. J. Med.* **2005,** *353*, 123-132.
45. Blackwell, K. L.; Burstein, H. J.; Storniolo, A. M.; Rugo, H.; Sledge, G.; Koehler, M.; Ellis, C.; Casey, M.; Vukelja, S.; Bischoff, J.; Baselga, J.; O'Shaughnessy, J., Randomized Study of Lapatinib Alone or in Combination With Trastuzumab in Women With ErbB2-Positive, Trastuzumab-Refractory Metastatic Breast Cancer. *J. Clin. Oncol.* **2010,** *28*, 1124-1130.
46. Paramore, A.; Frantz, S., Bortezomib. *Nat. Rev. Drug Discov.* **2003,** *2*, 611-612.
47. Llovet, J. M.; Ricci, S.; Mazzaferro, V.; Hilgard, P.; Gane, E.; Blanc, F.; de Oliveira, A. C.; Santoro, A.; Raoul, J.; Forner, A.; Schwartz, M.; Porta, C.; Zeuzem, S.; Bolondi, L.; Greten, T. F.; Galle, P. R.; Seitz, J.; Borbath, I.; Haussinger, D.; Giannaris, T.; Shan, M.; Moscovici, M.; Voliotis, D.; Bruix, J., Sorafenib in Advanced Hepatocellular Carcinoma. *N. Engl. J. Med.* **2008,** *359*, 378-390.
48. Wells, S. A.; Gosnell, J. E.; Gagel, R. F.; Moley, J.; Pfister, D.; Sosa, J. A.; Skinner, M.; Krebs, A.; Vasselli, J.; Schlumberger, M., Vandetanib for the Treatment of Patients With Locally Advanced or Metastatic Hereditary Medullary Thyroid Cancer. *J. Clin. Oncol.* **2010,** *28*, 767-772.
49. Marks, P. A.; Breslow, R., Dimethyl Sulfoxide to Vorinostat: Development of this Histone Deacetylase Inhibitor as an Anticancer Drug. *Nat. Biotech.* **2007,** *25*, 84-90.
50. Mann, B. S.; Johnson, J. R.; Cohen, M. H.; Justice, R.; Pazdur, R., FDA Approval Summary: Vorinostat for Treatment of Advanced Primary Cutaneous T-Cell Lymphoma. *Oncologist* **2007,** *12*, 1247-1252.
51. Wilson, A. J., Inhibition of Protein-Protein Interactions using Designed Molecules. *Chem. Soc. Rev.* **2009,** *38*, 3289-3300.
52. Vassilev, L. T.; Vu, B. T.; Graves, B.; Carvajal, D.; Podlaski, F.; Filipovic, Z.; Kong, N.; Kammlott, U.; Lukacs, C.; Klein, C.; Fotouhi, N.; Liu, E. A., In Vivo

Activation of the p53 Pathway by Small-Molecule Antagonists of MDM2. *Science* **2004,** *303*, 844-848.
53. Vu, B.; Wovkulich, P.; Pizzolato, G.; Lovey, A.; Ding, Q.; Jiang, N.; Liu, J.-J.; Zhao, C.; Glenn, K.; Wen, Y.; Tovar, C.; Packman, K.; Vassilev, L.; Graves, B., Discovery of RG7112: A Small-Molecule MDM2 Inhibitor in Clinical Development. *ACS Med. Chem. Lett.* **2013,** *4*, 466-469.
54. Dorr, P.; Westby, M.; Dobbs, S.; Griffin, P.; Irvine, B.; Macartney, M.; Mori, J.; Rickett, G.; Smith-Burchnell, C.; Napier, C.; Webster, R.; Armour, D.; Price, D.; Stammen, B.; Wood, A.; Perros, M., Maraviroc (UK-427,857), a Potent, Orally Bioavailable, and Selective Small-Molecule Inhibitor of Chemokine Receptor CCR5 with Broad-Spectrum Anti-Human Immunodeficiency Virus Type 1 Activity. *Antimicrob. Agents Chemother.* **2005,** *49*, 4721-4732.
55. Lipinski, C. A.; Lombardo, F.; Dominy, B. W.; Feeney, P. J., Experimental and Computational Approaches to Estimate Solubility and Permeability in Drug Discovery and Development Settings. *Adv. Drug Deliv. Rev.* **1997,** *23*, 3-25.
56. Walters, W. P., Going Further than Lipinski's Rule in Drug Design. *Expert Opin. Drug Discov.* **2012,** *7*, 99-107.
57. Page, C. P.; Hofmann, B.; Curtis, M.; Walker, M., *Integrated Pharmacology*. 3rd ed.; Elsevier Mosby: Edinburgh, 2006.
58. Lipinski, C. A., Drug-like Properties and the Causes of Poor Solubility and Poor Permeability. *J. Pharmacol. Toxicol. Methods* **2000,** *44*, 235-249.
59. Jia, L.; Sun, Y., SCF E3 Ubiquitin Ligases as Anticancer Targets. *Curr. Cancer Drug Targets* **2011,** *11*, 347-356.
60. Jacobson, A. D.; Zhang, N.-Y.; Xu, P.; Han, K.-J.; Noone, S.; Peng, J.; Liu, C.-W., The Lysine 48 and Lysine 63 Ubiquitin Conjugates Are Processed Differently by the 26 S Proteasome. *J. Biol. Chem.* **2009,** *284*, 35485-35494.
61. Wei, D.; Sun, Y., Small RING Finger Proteins RBX1 and RBX2 of SCF E3 Ubiquitin Ligases: The Role in Cancer and as Cancer Targets. *Genes & Cancer* **2010,** *1*, 700-707.
62. Wang, Z.; Gao, D.; Fukushima, H.; Inuzuka, H.; Liu, P.; Wan, L.; Sarkar, F. H.; Wei, W., SKP2: A Novel Potential Therapeutic Target for Prostate Cancer. *Biochim. Biophys. Acta (BBA) - Rev. Cancer* **2012,** *1825*, 11-17.
63. Wang, Z.; Liu, P.; Inuzuka, H.; Wei, W., Roles of F-box Proteins in Cancer. *Nat. Rev. Cancer* **2014,** *14*, 233-247.
64. Fujii, Y.; Yada, M.; Nishiyama, M.; Kamura, T.; Takahashi, H.; Tsunematsu, R.; Susaki, E.; Nakagawa, T.; Matsumoto, A.; Nakayama, K. I., Fbxw7 Contributes to Tumor Suppression by Targeting Multiple Proteins for Ubiquitin-Dependent Degradation. *Cancer Sci.* **2006,** *97*, 729-736.
65. Frescas, D.; Pagano, M., Deregulated Proteolysis by the F-box Proteins SKP2 and [beta]-TrCP: Tipping the Scales of Cancer. *Nat. Rev. Cancer* **2008,** *8*, 438-449.
66. Nakayama, K. I.; Nakayama, K., Ubiquitin Ligases: Cell-Cycle Control and Cancer. *Nat. Rev. Cancer* **2006,** *6*, 369-381.
67. Pan, Z.-Q.; Kentsis, A.; Dias, D. C.; Yamoah, K.; Wu, K., Nedd8 on Cullin: Building an Expressway to Protein Destruction. *Oncogene* **2004,** *23*, 1985-1997.
68. Shapira, M. a.; Ben–Izhak, O.; Linn, S.; Futerman, B.; Minkov, I.; Hershko, D. D., The Prognostic Impact of the Ubiquitin Ligase Subunits SKP2 and Cks1 in Colorectal Carcinoma. *Cancer* **2005,** *103*, 1336-1346.
69. Wang, D.; Qin, H.; Du, W.; Shen, Y.-W.; Lee, W.-H.; Riggs, A. D.; Liu, C.-P., Inhibition of S-phase Kinase-associated Protein 2 (SKP2) Reprograms and Converts Diabetogenic T Cells to Foxp3+ Regulatory T Cells. *Proc. Nat. Acad. Sci.* **2012,** *109*, 9493-9498.

70. Masciullo, V.; Ferrandina, G.; Pucci, B.; Fanfani, F.; Lovergine, S.; Palazzo, J.; Zannoni, G.; Mancuso, S.; Scambia, G.; Giordano, A., P27Kip1 Expression is Associated with Clinical Outcome in Advanced Epithelial Ovarian Cancer: Multivariate Analysis. *Clin. Cancer Res.* **2000,** *6*, 4816-4822.
71. Esposito, V.; Baldi, A.; de Luca, A.; Groger, A. M.; Loda, M.; Giordano, G. G.; Caputi, M.; Baldi, F.; Pagano, M.; Giordano, A., Prognostic Role of the Cyclin-Dependent Kinase Inhibitor P27 in Non-Small Cell Lung Cancer. *Cancer Res.* **1997,** *57*, 3381-3385.
72. Shaughnessy, J., Amplification and Overexpression of CKS1B at Chromosome Band 1q21 is Associated with Reduced Levels of p27Kip1 and an Aggressive Clinical Course in Multiple Myeloma. *Hematology* **2005,** *10*, 117-126.
73. Chan, C.-H.; Morrow, J. K.; Zhang, S.; Lin, H.-K., SKP2: A Dream Target in the Coming Age of Cancer Therapy. *Cell Cycle* **2014,** *13*, 679-680.
74. Weiss, W. A.; Aldape, K.; Mohapatra, G.; Feuerstein, B. G.; Bishop, J. M., *Targeted Expression of MYCN Causes Neuroblastoma in Transgenic Mice*. 1997; Vol. 16, p 2985-2995.
75. Bretones, G.; Acosta, J. C.; Caraballo, J.; Ferrandiz, N.; Gomez-Casares, M. T.; Albajar, M.; Blanco, R.; Ruiz, P.; Hung, W.; Albero, M. P.; Perez-Roger, I.; Leon, J., SKP2 Oncogene is a Direct MYC Target Gene and MYC Downregulates p27KIP1 Through SKP2 in Human Leukemia Cells. *J. Biol. Chem.* **2011,** *286*, 9815-9825.
76. Muth, D.; Ghazaryan, S.; Eckerle, I.; Beckett, E.; Pöhler, C.; Batzler, J.; Beisel, C.; Gogolin, S.; Fischer, M.; Henrich, K.-O.; Ehemann, V.; Gillespie, P.; Schwab, M.; Westermann, F., Transcriptional Repression of SKP2 Is Impaired in MYCN-Amplified Neuroblastoma. *Cancer Res.* **2010,** *70*, 3791-3802.
77. Barnes, P. J.; Larin, M., Mechanisms of Disease - Nuclear Factor-Kappa b - A Pivotal Transcription Factor in Chronic Inflammatory Diseases *N. Engl. J. Med.* **1997,** *336*, 1066-1071.
78. Chen, Q.; Xie, W.; Kuhn, D. J.; Voorhees, P. M.; Lopez-Girona, A.; Mendy, D.; Corral, L. G.; Krenitski, V. P.; Xu, W.; Parseval, L. M.; Webb, D. R.; Mercurio, F.; Nakayama, K. I.; Nakayama, K.; Orlowski, R. Z., Targeting the p27 E3 Ligase SCFSKP2 Results in p27- and SKP2-Mediated Cell-Cycle Arrest and Activation of Autophagy. *Blood* **2008,** *111*, 4690-4699.
79. McKenna, J.; Mercurio, F.; Plantevin, V.; Xie, W. Compounds Useful for the Treatment of Cancer, Compositions Thereof and Methods Therewith. WO03105774 (A2) **2003**.
80. Wu, L.; Grigoryan, Arsen V.; Li, Y.; Hao, B.; Pagano, M.; Cardozo, Timothy J., Specific Small Molecule Inhibitors of Skp2-Mediated p27 Degradation. *Chem. Biol.* **2012,** *19*, 1515-1524.
81. Zhang, S., Computer-Aided Drug Discovery and Development. In *Drug Design and Discovery*, Satyanarayanajois, S. D., Ed. Humana Press: 2011; Vol. 716, pp 23-38.
82. Chan, C.-H.; Morrow, John K.; Li, C.-F.; Gao, Y.; Jin, G.; Moten, A.; Stagg, Loren J.; Ladbury, John E.; Cai, Z.; Xu, D.; Logothetis, Christopher J.; Hung, M.-C.; Zhang, S.; Lin, H.-K., Pharmacological Inactivation of SKP2 SCF Ubiquitin Ligase Restricts Cancer Stem Cell Traits and Cancer Progression. *Cell* **2013,** *154*, 556-568.
83. Zheng, N.; Schulman, B. A.; Song, L.; Miller, J. J.; Jeffrey, P. D.; Wang, P.; Chu, C.; Koepp, D. M.; Elledge, S. J.; Pagano, M.; Conaway, R. C.; Conaway, J. W.; Harper, J. W.; Pavletich, N. P., Structure of the Cul1-Rbx1-SKP1-F boxSKP2 SCF Ubiquitin Ligase Complex. *Nature* **2002,** *416*, 703-709.
84. Ungermannova, D.; Lee, J.; Zhang, G.; Dallmann, H. G.; McHenry, C. S.; Liu, X., High-Throughput Screening AlphaScreen Assay for Identification of Small-Molecule Inhibitors of Ubiquitin E3 Ligase SCFSkp2-Cks1. *J. Biomol. Screen.* **2013,** *18*, 910-920.

85. Kaur, G.; Narayanan, V. L.; Risbood, P. A.; Hollingshead, M. G.; Stinson, S. F.; Varma, R. K.; Sausville, E. A., Synthesis, Structure–Activity Relationship, and p210bcr-abl Protein Tyrosine Kinase Activity of Novel AG 957 Analogs. *Bioorg. Med. Chem.* **2005,** *13*, 1749-1761.
86. Koo, K. H.; Kim, H.; Bae, Y. K.; Kim, K.; Park, B. K.; Lee, C. H.; Kim, Y. N., Salinomycin Induces Cell Death via Inactivation of STAT3 and Downregulation of SKP2. *Cell Death Dis.* **2013,** *4*, e693.
87. Siddiquee, K.; Zhang, S.; Guida, W. C.; Blaskovich, M. A.; Greedy, B.; Lawrence, H. R.; Yip, M. L. R.; Jove, R.; McLaughlin, M. M.; Lawrence, N. J.; Sebti, S. M.; Turkson, J., Selective Chemical Probe Inhibitor of STAT3, Identified Through Structure-based Virtual Screening, Induces Antitumor Activity. *Proc. Nat. Acad. Sci.* **2007,** *104*, 7391-7396.
88. Shvarts, A.; Steegenga, W. T.; Riteco, N.; van Laar, T.; Dekker, P.; Bazuine, M.; vanHam, R. C. A.; vanOordt, W. V.; Hateboer, G.; vanderEb, A. J.; Jochemsen, A. G., MDMX: A Novel p53-Binding Protein with some Functional Properties of MDM2. *Embo J.* **1996,** *15*, 5349-5357.
89. Wang, H.; Ma, X.; Ren, S.; Yan, C., Small Molecules Inhibitory for MDMX Expression Activate p53 and Induce Apoptosis. *Proc. Annu. Meet. Am. Assoc. Cancer Res.* **2010,** *51*, 1098-1099.
90. Phan, J.; Li, Z.; Kasprzak, A.; Li, B.; Sebti, S.; Guida, W.; Schoenbrunn, E.; Chen, J., Structure-based Design of High Affinity Peptides Inhibiting the Interaction of p53 with MDM2 and MDMX. *J. Biol. Chem.* **2010,** *285*, 2174-2183.
91. Reed, D.; Shen, Y.; Shelat, A. A.; Arnold, L. A.; Ferreira, A. M.; Zhu, F.; Mills, N.; Smithson, D. C.; Regni, C. A.; Bashford, D.; Cicero, S. A.; Schulman, B. A.; Jochemsen, A. G.; Guy, R. K.; Dyer, M. A., Identification and Characterization of the First Small Molecule Inhibitor of MDMX. *J. Biol. Chem.* **2010,** *285*, 10786-10796.
92. Wade, M.; Wahl, G. M., Targeting MDM2 and MDMX in Cancer Therapy: Better Living through Medicinal Chemistry? *Mol. Cancer Res.* **2009,** *7*, 1-11.
93. Toledo, F.; Wahl, G. M., MDM2 and MDM4: p53 Regulators as Targets in Anticancer Therapy. *Int. J. Biochem. Cell Biol.* **2007,** *39*, 1476-1482.
94. Chi, S.-W.; Lee, S.-H.; Kim, D.-H.; Ahn, M.-J.; Kim, J.-S.; Woo, J.-Y.; Torizawa, T.; Kainosho, M.; Han, K.-H., Structural Details on MDM2-p53 Interaction. *J. Biol. Chem.* **2005,** *280*, 38795-38802.
95. Kussie, P. H.; Gorina, S.; Marechal, V.; Elenbaas, B.; Moreau, J.; Levine, A. J.; Pavletich, N. P., Structure of the MDM2 Oncoprotein Bound to the p53 Tumor Suppressor Transactivation Domain. *Science* **1996,** *274*, 948-953.
96. Klein, C.; Vassilev, L. T., Targeting the p53-MDM2 Interaction to Treat Cancer. *Br. J. Cancer* **2004,** *91*, 1415-1419.
97. Kallen, J.; Goepfert, A.; Blechschmidt, A.; Izaac, A.; Geiser, M.; Tavares, G.; Ramage, P.; Furet, P.; Masuya, K.; Lisztwan, J., Crystal Structures of Human MDMX (HDMX) in Complex with p53 Peptide Analogues Reveal Surprising Conformational Changes. *J. Biol. Chem.* **2009,** *284*, 8812-21.
98. Hu, B.; Gilkes, D. M.; Chen, J., Efficient p53 Activation and Apoptosis by Simultaneous Disruption of Binding to MDM2 and MDMX. *Cancer Res.* **2007,** *67*, 8810-8817.
99. Xiong, S.; Pant, V.; Suh, Y.-A.; Van Pelt, C. S.; Wang, Y.; Valentin-Vega, Y. A.; Post, S. M.; Lozano, G., Spontaneous Tumorigenesis in Mice Overexpressing the p53-Negative Regulator MDM4. *Cancer Res.* **2010,** *70*, 7148-7154.
100. Popowicz, G. M.; Czarna, A.; Holak, T. A., Structure of the Human MDMX Protein Bound to the p53 Tumor Suppressor Transactivation Domain. *Cell Cycle* **2008,** *7*, 2441-2443.

101. Gilkes, D. M.; Pan, Y.; Coppola, D.; Yeatman, T.; Reuther, G. W.; Chen, J., Regulation of MDMX Expression by Mitogenic Signaling. *Mol. Cell. Biol.* **2008,** *28*, 1999-2010.
102. Linke, K.; Mace, P. D.; Smith, C. A.; Vaux, D. L.; Silke, J.; Day, C. L., Structure of the MDM2/MDMX RING Domain Heterodimer Reveals Dimerization is Required for their Ubiquitylation in Trans. *Cell Death Differ.* **2008,** *15*, 841-848.
103. Bista, M.; Smithson, D.; Pecak, A.; Salinas, G.; Pustelny, K.; Min, J.; Pirog, A.; Finch, K.; Zdzalik, M.; Waddell, B.; Wladyka, B.; Kedracka-Krok, S.; Dyer, M. A.; Dubin, G.; K., G. R., On the Mechanism of Action of SJ-172550 in Inhibiting the Interaction of MDM4 and p53. *PLoS ONE* **2012,** *7*.
104. Furet, P.; Chène, P.; De Pover, A.; Valat, T. S.; Lisztwan, J. H.; Kallen, J.; Masuya, K., The Central Valine Concept Provides an Entry in a New Class of Non-Peptide Inhibitors of the p53–MDM2 Interaction. *Bioorg. Med. Chem. Lett.* **2012,** *22*, 3498-3502.
105. García-Echeverría, C.; Chène, P.; Blommers, M. J. J.; Furet, P., Discovery of Potent Antagonists of the Interaction between Human Double Minute 2 and Tumor Suppressor p53. *J. Med. Chem.* **2000,** *43*, 3205-3208.
106. Popowicz, G. M.; Czarna, A.; Wolf, S.; Wang, K.; Wang, W.; Dömling, A.; Holak, T. A., Structures of Low Molecular Weight Inhibitors Bound to MDMX and MDM2 Reveal New Approaches for p53-MDMX/MDM2 Antagonist Drug Discovery. *Cell Cycle* **2010,** *9*, 1104-1111.
107. Blackburn, T. J.; Ahmed, S.; Coxon, C. R.; Liu, J.; Lu, X.; Golding, B. T.; Griffin, R. J.; Hutton, C.; Newell, D. R.; Ojo, S.; Watson, A. F.; Zaytzev, A.; Zhao, Y.; Lunec, J.; Hardcastle, I. R., Diaryl- and Triaryl-Pyrrole Derivatives: Inhibitors of the MDM2-p53 and MDMX-p53 Protein-Protein Interactions. *Med. Chem. Comm* **2013,** *4*, 1297-1304.
108. Zhuang, C.; Miao, Z.; Zhu, L.; Dong, G.; Guo, Z.; Wang, S.; Zhang, Y.; Wu, Y.; Yao, J.; Sheng, C.; Zhang, W., Discovery, Synthesis, and Biological Evaluation of Orally Active Pyrrolidone Derivatives as Novel Inhibitors of p53–MDM2 Protein–Protein Interaction. *J. Med. Chem.* **2012,** *55*, 9630-9642.
109. Graves, B.; Thompson, T.; Xia, M.; Janson, C.; Lukacs, C.; Deo, D.; Di Lello, P.; Fry, D.; Garvie, C.; Huang, K.-S.; Gao, L.; Tovar, C.; Lovey, A.; Wanner, J.; Vassilev, L. T., Activation of the p53 Pathway by Small-Molecule-Induced MDM2 and MDMX Dimerization. *Proc. Nat. Acad. Sci.* **2012,** *109*, 11788-11793.
110. Chang, Y. S.; Graves, B.; Guerlavais, V.; Tovar, C.; Packman, K.; To, K.-H.; Olson, K. A.; Kesavan, K.; Gangurde, P.; Mukherjee, A.; Baker, T.; Darlak, K.; Elkin, C.; Filipovic, Z.; Qureshi, F. Z.; Cai, H.; Berry, P.; Feyfant, E.; Shi, X. E.; Horstick, J.; Annis, D. A.; Manning, A. M.; Fotouhi, N.; Nash, H.; Vassilev, L. T.; Sawyer, T. K., Stapled α−Helical Peptide Drug Development: A Potent Dual Inhibitor of MDM2 and MDMX for p53-Dependent Cancer Therapy. *Proc. Nat. Acad. Sci.* **2013,** *110*, E3445-E3454.
111. Bernal, F.; Tyler, A. F.; Korsmeyer, S. J.; Walensky, L. D.; Verdine, G. L., Reactivation of the p53 Tumor Suppressor Pathway by a Stapled p53 Peptide. *J. Am. Chem. Soc.* **2007,** *129*, 2456-2457.
112. Subramanian, R.; Lee, M. R.; Allen, J. G.; Bourbeau, M. P.; Fotsch, C.; Hong, F.-T.; Tadesse, S.; Yao, G.; Yuan, C. C.; Surapaneni, S.; Skiles, G. L.; Wang, X.; Wohlhieter, G. E.; Zeng, Q.; Zhou, Y.; Zhu, X.; Li, C., Cytochrome P450-Mediated Epoxidation of 2-Aminothiazole-Based AKT Inhibitors: Identification of Novel GSH Adducts and Reduction of Metabolic Activation through Structural Changes Guided by in Silico and in Vitro Screening. *Chem. Res. Toxicol.* **2010,** *23*, 653-663.
113. Haynes, N.-E.; Corbett, W. L.; Bizzarro, F. T.; Guertin, K. R.; Hilliard, D. W.; Holland, G. W.; Kester, R. F.; Mahaney, P. E.; Qi, L.; Spence, C. L.; Tengi, J.;

Dvorozniak, M. T.; Railkar, A.; Matschinsky, F. M.; Grippo, J. F.; Grimsby, J.; Sarabu, R., Discovery, Structure−Activity Relationships, Pharmacokinetics, and Efficacy of Glucokinase Activator (2R)-3-Cyclopentyl-2-(4-methanesulfonylphenyl)-N-thiazol-2-yl-propionamide (RO0281675). *J. Med. Chem.* **2010,** *53*, 3618-3625.
114. Bulatov, E. Identification and Validation of a Series of p53-MDM2 and p53-MDMX Protein-Protein Interaction Inhibitors. Newcastle University, Newcastle-upon-Tyne, UK, **2010**.
115. Imamoto, T.; Takiyama, N.; Nakamura, K.; Hatajima, T.; Kamiya, Y., Reactions of Carbonyl Compounds with Grignard Reagents in the Presence of Cerium Chloride. *J. Am. Chem. Soc.* **1989,** *111*, 4392-4398.
116. Katritzky, A. R.; Fan, W. Q.; Fu, C., A Novel Method for the Synthesis of Symmetrical Vicinal Tertiary and Secondary Diamines. *J. Org. Chem.* **1990,** *55*, 3209-3213.
117. Katritzky, A. R.; Qiu, G. F.; Yang, B. Z., Preparations of Trisubstituted Hydrazines and Pyrazolidines from N-(1-Benzotriazolylalkyl)hydrazines. *J. Org. Chem.* **1997,** *62*, 8210-8214.
118. Colonge, J.; Varagnat, A., *Bull. Soc. Chim. Fr.* **1964,** *10*, 2499-2504.
119. Kosower, E. M.; Sorensen, T. S., 5-Methyl-2,3,4-hexatrienal and Related Compounds. *J. Org. Chem.* **1963,** *28*, 687-692.
120. Maruoka, K.; Concepcion, A. B.; Murase, N.; Oishi, M.; Hirayama, N.; Yamamoto, H., Stabilization of Reactive Aldehydes by Complexation with Methylaluminum Bis(2,6-diphenylphenoxide) and their Synthetic Application. *J. Am. Chem. Soc.* **1993,** *115*, 3943-3949.
121. Mass, O.; Lindsey, J. S., A trans-AB-Bacteriochlorin Building Block. *J. Org. Chem.* **2011,** *76*, 9478-9487.
122. Fry, J. L.; Ott, R. A., Aldehydes from Nitriles. Formation of *N*-Alkylnitrilium Ions and their Reduction to *N*-Alkylaldimines by Organosilicon Hydrides. *J. Org. Chem.* **1981,** *46*, 602-607.
123. Huang, Y.; Rawal, V. H., Hydrogen-Bond-Promoted Hetero-Diels-Alder Reactions of Unactivated Ketones. *J. Am. Chem. Soc.* **2002,** *124*, 9662-9663.
124. Evans, D. A.; Ng, H. P.; Rieger, D. L., Total Synthesis of the Macrolide Antibiotic Rutamycin B. *J. Am. Chem. Soc.* **1993,** *115*, 11446-11459.
125. Palomo, C.; Oiarbide, M.; Dias, F.; Ortiz, A.; Linden, A., Asymmetric Synthesis of β-Mercapto Carboxylic Acid Derivatives by Intramolecular Sulfur Transfer in N-Enoyl Oxazolidine-2-thiones Promoted by Lewis Acids. *J. Am. Chem. Soc.* **2001,** *123*, 5602-5603.
126. Kanomata, N.; Maruyama, S.; Tomono, K.; Anada, S., A Simple Method Removing 2-Oxazolidinone and 2-Hydroxyethylamine Auxiliaries in Methoxide–Carbonate Systems for Synthesis of Planar-Chiral Nicotinate. *Tet. Lett.* **2003,** *44*, 3599-3603.
127. Walker, E. R. H., The Functional Group Selectivity of Complex Hydride Reducing Agents. *Chem. Soc. Rev.* **1976,** *5*, 23-50.
128. Maiti, D.; Buchwald, S. L., Cu-Catalyzed Arylation of Phenols: Synthesis of Sterically Hindered and Heteroaryl Diaryl Ethers. *J. Org. Chem.* **2010,** *75*, 1791-1794.
129. Tajbakhsh, M.; Hosseinzadeha, R.; Alinezhada, H.; Ghaharia, S.; Heydarib, A.; Khaksarca, S., Catalyst-Free One-Pot Reductive Alkylation of Primary and Secondary Amines and N,N-Dimethylation of Amino Acids Using Sodium Borohydride in 2,2,2-Trifluoroethanol. *Synthesis-Stuttgart* **2011,** *3*, 490-496.
130. Imanishi, M.; Tomishima, Y.; Itou, S.; Hamashima, H.; Nakajima, Y.; Washizuka, K.; Sakurai, M.; Matsui, S.; Imamura, E.; Ueshima, K.; Yamamoto, T.; Yamamoto, N.; Ishikawa, H.; Nakano, K.; Unami, N.; Hamada, K.; Matsumura, Y.; Takamura, F.; Hattori, K., Discovery of a Novel Series of Biphenyl Benzoic Acid

Derivatives as Potent and Selective Human β3-Adrenergic Receptor Agonists with Good Oral Bioavailability. Part I. *J. Med. Chem.* **2008,** *51*, 1925-1944.
131. Matos, K.; Burkhardt, E. R., Aryl Boronates from Bis(pinacolato)diboron and Pinacolborane. *Chim. Oggi.* **2005,** *23*, 12-17.
132. Goodacre, S. C.; Street, L. J.; Hallett, D. J.; Crawforth, J. M.; Kelly, S.; Owens, A. P.; Blackaby, W. P.; Lewis, R. T.; Stanley, J.; Smith, A. J.; Ferris, P.; Sohal, B.; Cook, S. M.; Pike, A.; Brown, N.; Wafford, K. A.; Marshall, G.; Castro, J. L.; Atack, J. R., Imidazo[1,2-a]pyrimidines as Functionally Selective and Orally Bioavailable GABAAα2/α3 Binding Site Agonists for the Treatment of Anxiety Disorders. *J. Med. Chem.* **2005,** *49*, 35-38.
, 133. Verkade, J. G.; Urgaonkar, S., Palladium/Proazaphosphatrane-Catalyzed Amination of Aryl Halides Possessing a Phenol, Alcohol, Acetanilide, Amide or an Enolizable Ketone Functional Group: Efficacy of Lithium Bis(trimethylsilyl)amide as the Base *Adv. Synth. Catal.* **2004,** *346*, 611-616.
134. Merişor, E.; Beifuss, U., From the Study of Naturally Occurring N-allylated Phenazines Towards New Pd-Mediated Transformations. *Tet. Lett.* **2007,** *48*, 8383-8387.
135. Schlummer, B.; Scholz, U., Palladium-Catalyzed C□N and C□O Coupling–A Practical Guide from an Industrial Vantage Point. *Adv. Synth. Catal.* **2004,** *346*, 1599-1626.
136. Brehm, L.; Krogsgaard-Larsen, P., Organic Hydroxylamine Derivatives. XI. Structural Analogues of Gamma-Aminobutyric Acid (GABA) of the Isoxazole Enol-betaine Type. Synthesis and the Crystal Structure of 3-Hydroxy-5-(3-aminopropyl)isoxazole Zwitterion. *Acta Chem. Scand.* **1974,** *B 28*, 625-635.
137. Jørgensen, L.; Nielsen, B.; Pickering, D. S.; Kristensen, A. S.; Frydenvang, K.; Madsen, U.; Clausen, R. P., Analogues of 3-Hydroxyisoxazole-Containing Glutamate Receptor Ligands Based on the 3-Hydroxypyrazole-Moiety: Design, Synthesis and Pharmacological Characterization. *Neurochem. Res.* **2014,** *39*, 1895-1905.
138. Iwai, I.; Kishida, Y.; Hiraoka, T.; Nakamura, N. Certain 5-Alkyl-3-Hydroxyisoxazoles. 3,544,584, **1970**.
139. Sonogashira, K., Development of Pd–Cu Catalyzed Cross-Coupling of Terminal Acetylenes with sp2-Carbon Halides. *J. Organomet. Chem.* **2002,** *653*, 46-49.
140. Finke, A. D.; Elleby, E. C.; Boyd, M. J.; Weissman, H.; Moore, J. S., Zinc Chloride-Promoted Aryl Bromide−Alkyne Cross-Coupling Reactions at Room Temperature. *J. Org. Chem.* **2009,** *74*, 8897-8900.
141. Elangovan, A.; Wang, Y.-H.; Ho, T.-I., Sonogashira Coupling Reaction with Diminished Homocoupling. *Org. Lett.* **2003,** *5*, 1841-1844.
142. Woodcock, S.; Green, D. V. S.; Vincent, M. A.; Hillier, I. H.; Guest, M. F.; Sherwood, P., Tautomeric Equilibria in 3- and 5-Hydroxyisoxazole in the Gas Phase and in Aqueous Solution: a Test of Molecular Dynamics and Continuum Models of Solvation. *J. Chem. Soc. Perkin Trans. 2* **1992**, 2151-2154.
143. Shimada, T.; Mukaide, K.; Shinohara, A.; Han, J. W.; Hayashi, T., Asymmetric Synthesis of 1-Aryl-1,2-ethanediols from Arylacetylenes by Palladium-Catalyzed Asymmetric Hydrosilylation as a Key Step. *J. Am. Chem. Soc.* **2002,** *124*, 1584-1585.
144. Del Grosso, A.; Singleton, P. J.; Muryn, C. A.; Ingleson, M. J., Pinacol Boronates by Direct Arene Borylation with Borenium Cations. *Angew. Chem. Int. Ed.* **2011,** *50*, 2102-2106.
145. Yang, C.-G.; Liu, G.; Jiang, B., Preparing Functional Bis(indole) Pyrazine by Stepwise Cross-coupling Reactions: An Efficient Method to Construct the Skeleton of Dragmacidin D. *J. Org. Chem.* **2002,** *67*, 9392-9396.

146. Selvakumar, N.; Yadi Reddy, B.; Sunil Kumar, G.; Iqbal, J., Dimethyl Malonate as a One-Carbon Source: a Novel Method of Introducing Carbon Substituents onto Aromatic Nitro Compounds. *Tet. Lett.* **2001,** *42*, 8395-8398.
147. Bella, M.; Kobbelgaard, S.; Jørgensen, K. A., Organocatalytic Regio- and Asymmetric C-Selective SNAr Reactions Stereoselective Synthesis of Optically Active Spiro-pyrrolidone-3,3‘-oxoindoles. *J. Am. Chem. Soc.* **2005,** *127*, 3670-3671.
148. Bordwell, F. G.; Hughes, D. L., Nucleophilic Aromatic Substitution Reactions with Carbanions and Nitranions in Dimethyl Sulfoxide Solution. *J. Am. Chem. Soc.* **1986,** *108*, 5991-5997.
149. Gribble, G. W.; Saulnier, M. G., Generation and Ring-Opening of 2,3-Dilithio-1-(phenylsulfonyl)indole. *J. Org. Chem.* **1983,** *48*, 607-609.
150. Periasamy, M.; Thirumalaikumar, M., Methods of Enhancement of Reactivity and Selectivity of Sodium borohydride for Applications in Organic Synthesis. *J. Organomet. Chem.* **2000,** *609*, 137-151.
151. Molander, G. A.; Pack, S. K., Determining the Scope of the Lanthanide Mediated, Sequential Hydroamination/C–C Cyclization Reaction: Formation of Tricyclic and Tetracyclic Aromatic Nitrogen Heterocycles. *Tetrahedron* **2003,** *59*, 10581-10591.
152. Soli, E. D.; Manoso, A. S.; Patterson, M. C.; DeShong, P.; Favor, D. A.; Hirschmann, R.; Smith, A. B., Azide and Cyanide Displacements via Hypervalent Silicate Intermediates. *J. Org. Chem.* **1999,** *64*, 3171-3177.
153. Snieckus, V., Directed Ortho Metalation. Tertiary Amide and O-Carbamate Directors in Synthetic Strategies for Polysubstituted Aromatics. *Chem. Rev.* **1990,** *90*, 879-933.
154. Meanwell, N. A., Synopsis of Some Recent Tactical Application of Bioisosteres in Drug Design. *J. Med. Chem.* **2011,** *54*, 2529-2591.
155. Stanetty, P.; Schnürch, M.; Mereiter, K.; Mihovilovic, M. D., Investigations of the Halogen Dance Reaction on N-Substituted 2-Thiazolamines. *J. Org. Chem.* **2004,** *70*, 567-574.
156. Schnurch, M.; Spina, M.; Khan, A. F.; Mihovilovic, M. D.; Stanetty, P., Halogen Dance Reactions-A Review. *Chem. Soc. Rev.* **2007,** *36*, 1046-1057.
157. Lee, J. C.; Bae, Y. H.; Chang, S. K., Efficient Alpha-Halogenation of Carbonyl Compounds by N-Bromosuccinimide and N-Chlorosuccinimde. *Bull. Korean Chem. Soc.* **2003,** *24*, 407-408.
158. Choi, H. Y.; Chi, D. Y., Nonselective Bromination−Selective Debromination Strategy: Selective Bromination of Unsymmetrical Ketones on Singly Activated Carbon against Doubly Activated Carbon. *Org. Lett.* **2003,** *5*, 411-414.
159. Cully, S. J. Design and Synthesis of Isoindolinone MDM2-p53 Inhibitors. Newcastle University, Newcastle-upon-Tyne, UK, **2013**.
160. Iwakuma, T.; Lozano, G., MDM2, An Introduction. *Mol. Cancer Res.* **2003,** *1*, 993-1000.
161. https://www.gelifesciences.com/pgex (accessed 04-07-2014).
162. www.studyblue.com (accessed 05-07-2014).
163. Kanovsky, M.; Raffo, A.; Drew, L.; Rosal, R.; Do, T.; Friedman, F. K.; Rubinstein, P.; Visser, J.; Robinson, R.; Brandt-Rauf, P. W.; Michl, J.; Fine, R. L.; Pincus, M. R., Peptides from the Amino Terminal MDM2-Binding Domain of p53, Designed from Conformational Analysis, are Selectively Cytotoxic to Transformed Cells. *Proc. Nat. Acad. Sci.* **2001,** *98*, 12438-12443.
164. Böttger, V.; Böttger, A.; Howard, S. F.; Picksley, S. M.; Chène, P.; Garcia-Echeverria, C.; Hochkeppel, H. K.; Lane, D. P., Identification of Novel MDM2 Binding Peptides by Phage Display. *Oncogene* **1996,** *13*, 2141-2147.

165. http://www.hybrigenics-services.com/contents/our-services/validate/1-by-1-with-htrf (accessed 12-07-2014).
166. http://www.htrf.com/other/tr-fret-basics (accessed 13-07-2014).
167. Niesen, F. H.; Berglund, H.; Vedadi, M., The Use of Differential Scanning Fluorimetry to Detect Ligand Interactions that Promote Protein Stability. *Nat. Protocols* **2007,** *2*, 2212-2221.
168. Lo, M.-C.; Aulabaugh, A.; Jin, G.; Cowling, R.; Bard, J.; Malamas, M.; Ellestad, G., Evaluation of Fluorescence-based Thermal Shift Assays for Hit Identification in Drug Discovery. *Anal. Biochem.* **2004,** *332*, 153-159.
169. http://www.bio.anl.gov/molecular_and_systems_biology/Sensor/sensor2.html (accessed 15-07-2014).
170. Ding, Q.; Zhang, Z.; Liu, J.-J.; Jiang, N.; Zhang, J.; Ross, T. M.; Chu, X.-J.; Bartkovitz, D.; Podlaski, F.; Janson, C.; Tovar, C.; Filipovic, Z. M.; Higgins, B.; Glenn, K.; Packman, K.; Vassilev, L. T.; Graves, B., Discovery of RG7388, a Potent and Selective p53–MDM2 Inhibitor in Clinical Development. *J. Med. Chem.* **2013,** *56*, 5979-5983.
171. Skehan, P.; Storeng, R.; Scudiero, D.; Monks, A.; McMahon, J.; Vistica, D.; Warren, J. T.; Bokesch, H.; Kenney, S.; Boyd, M. R., New Colorimetric Cytotoxicity Assay for Anticancer-Drug Screening. *J. Natl. Cancer Inst.* **1990,** *82*, 1107-1112.